SHELF-TO-SLOPE SEDIMENTATION ON THE NORTH KAIPARA CONTINENTAL MARGIN, NORTHWESTERN NORTH ISLAND, NEW ZEALAND

A thesis

submitted in partial fulfilment

of the requirements for the degree of

Master of Science in Earth and Ocean Sciences

at the

University of Waikato

by

Danielle Sarah Payne

University of Waikato

2008

“It was an exquisite day. It was one of those days so clear, so still, so silent, you almost feel the Earth has stopped in astonishment at its own beauty.”

- Katherine Mansfield 1888-1923

ABSTRACT

Temperate mixed carbonate-siliciclastic sediments and authigenic minerals are the current surficial deposits at shelf and slope depths (30-1015 m water depth) on the north Kaipara continental margin (NKCM) in northern New Zealand. This is the first detailed study of these NKCM deposits which are described and mapped from the analysis of 54 surficial sediment samples collected along seven shore-normal transects and from three short piston cores. Five surficial sediment facies are defined from the textural and compositional characteristics of this sediment involving relict, modern or mixed relict-modern components. Facies 1 (siliciclastic sand) forms a modern sand prism that extends out to outer shelf depths and contains three subfacies. Subfacies 1a (quartzofeldspathic sand) is an extensive North Island volcanic and basement rock derived sand deposit that occurs at less than 100-200 m water depth across the entire NKCM. Subfacies 1b (heavy mineral sand) occurs at less than 50 m water depth along only two transects and consists of predominantly local basaltic to basaltic andesite derived heavy mineral rich (>30%) deposits. Subfacies 1c (mica rich sand) occurs at one sample site at 300 m water depth and contains 20-30% mica grains, probably sourced from South Island schists and granites. Facies 2 (glauconitic sand) comprises medium to fine sand with over 30% and up to 95% authigenic glauconite grains occurring in areas of low sedimentation on the outer shelf and upper slope (150-400 m water depth) in central NKCM. Facies 3 (mixed bryozoan-siliciclastic sand) consists of greater than 40% bryozoan skeletal material and occurs only in the northern half of the NKCM. Facies 4 (pelletal mud) occurs on the mid shelf (100-150 m water depth) in northern NKCM and comprises muddy sediment dominated by greater than c. 30% mixed carbonate-siliciclastic pellets. Facies 5 (foraminiferal mud and sand) contains at least 30% foraminifera tests and comprises two subfacies. Subfacies 5a consists of at least 50% mud sized sediment and occurs at >400 m water depth in southern NKCM while subfacies 5b comprises >70% sand sized sediment and occurs at mid to outer shelf and slope depths in the northern NKCM.

A number of environmental controls affect the composition and distribution of NKCM sediments and these include: (1) variable sediment inputs to the NKCM dominated by inshore bedload sources from the south; (2) northerly directed nearshore littoral and combined storm-current sediment transport on the beach and shelf, respectively; (3) offshore suspended sediment bypassing allowing deposition of authigenic minerals and skeletal grains; (4) exchange between the beach and shelf producing similar compositions and grain sizes at less than 150 m water depth; and (5) the episodic rise of sea level since the Last Glaciation maximum approximately 20 000 years ago which has resulted in much sediment being left stranded at greater depths than would otherwise be anticipated.

Sedimentation models developed from other wave-dominated shelves generally do not appear to apply to the NKCM sediments due to their overall relative coarseness and their mosaic textural characteristics. In particular, the NKCM sediments do not show the expected fining offshore trends of most wave-dominated shelf models. Consequently, sandy sediments (both siliciclastic and authigenic) are most typical with mud becoming a dominant component in southern NKCM sediments only at greater than 400 m water depth, over 350 m deeper than most models suggest, a situation accentuated by the very low mud sediment supply to the NKCM from the bordering Northland landmass.

ACKNOWLEDGEMENTS

First and foremost, to my wonderful partner, Jesse, thank you for all of your support, for giving me an ear to bash when necessary, for forcing me to take time off and for the pick me ups when things hit rock bottom (more than once!). To my marvellous parents, George and Marie, for supporting me through my university years, for cooking me dinner every night and for just being there for me through all the ups and downs along the way. To my fantastic friends, Brenda, Nicole and Orla, thanks for all the laughter and the discussions about the inadequacies of the male sex when university work was too touchy to discuss. And to my second parents, Bernice and Roger, the other volunteers at Cambridge RDA and everyone else for providing me with light entertainment throughout the last two years and being understanding when my mind was elsewhere and I couldn't participate fully in events.

Secondly, I would like to thank my supervisors, Professor Cam Nelson and Dr Steven Hood. Steve is especially thanked for all the time, energy, technical help (even though you're not a technician!) and encouragement you have given me through the duration of this thesis. Most of all I want to thank you for being the friendliest face in the department. Many could learn from your example. Specific thanks to Cam for setting up this project and for all the knowledge, wisdom and direction you have imparted to me, not forgetting all the time dedicated to editing my thesis!

Thirdly, thank you to the New Zealand Oceanographic Institute (now NIWA) for logistical support, to B.J. Wardle (Captain) and the other officers and crew of the R.V. Tangaroa on Cruise No. 1077, and to Neville Day (NZOI) and Peter Kamp, Graeme Hancock, Richard Sutherland and Alan Devcich (University of Waikato) for collecting, sorting and some initial work on the sediment samples used in this thesis. Also, thank you to Scott Nodder and Miles Dunkin at NIWA for help in accessing data and especially to Alan Beu at GNS for his skilful assistance with all the shell identifications. Thank you to Rochelle Hansen for the many hours spent pouring over my forams and to Adam Vonk for the help with using ArcGIS. Your effort to save me time is very much appreciated. Thank you also to all the technical and other staff at both Waikato (Annette, Chris, Dirk, Xu and Renat) and the University of Otago (Lorraine Paterson, Brent Pooley, Daphne Lee) for the help with sample preparation and use of equipment.

And finally I want to say a big thank you to all the organisations that provided me with funding: University of Waikato, AusIMM, Freemasons NZ, Cambridge Altrusa Club, Broad Memorial Fund, Waikato Graduate Women and the Bank of New Zealand. And not forgetting Eagle Technologies Ltd. who happily provided me with two ArcView licences.

TABLE OF CONTENTS

LIST OF FIGURES

LIST OF PLATES

following page

LIST OF TABLES

Chapter 1

INTRODUCTION

1.1 INTRODUCTION

The distribution of continental margin sediments around portions of the northern and western North Island of New Zealand has been broadly mapped in previous studies by McDougall and Brodie (1967), Summerhayes (1969) and McDougall (1972). However, some parts of this margin have largely been neglected and one such area is the continental shelf and slope off western Northland. Very little research has been conducted in this area apart from a study of the coastal sand deposits by Schofield (1970) and of the slope sediments off southwestern Northland by McDougall (1972). This thesis research addresses this shortcoming by focussing attention on the nature and distribution of the surficial sediments on the western Northland shelf and slope, hereafter referred to as the north Kaipara continental margin (NKCM).

This chapter introduces the reader to the location of the study area (Section 1.2), the types of continental margin sediments occurring around New Zealand (Section 1.3), the specific aims of this study (Section 1.4) and the thesis format (Section 1.5).

1.2 STUDY AREA

This study of continental margin sedimentation is located immediately off the west coast of northern New Zealand in the Tasman Sea, and stretches from Cape Reinga in the north (34º27.3S, 172º38.9E) to the vicinity of Kaipara Harbour entrance in the south (36º23.4S, 174º05.5E) out to slope depths of up to 1050 m (Fig. 1-1). It focuses on the continental shelf but also beyond out onto the upper slope as well as onshore to include the coastal sedimentary system (dune, beach and harbour). This north Kaipara continental margin (NKCM) is bounded to the north by the carbonate-rich Three Kings platform (Nelson et al., 1982), and to the

south by the titanomagnetite-rich black sands, which stretch from the south Taranaki coast to the south Kaipara region (McDougall and Brodie, 1967). The offshore sample sites occur in seven transects (A-G) extending from shallow shelfal depths (c. 30 m) to upper slope depths (c. 1000 m). The three northernmost transects occur in an east-west direction while the other four transects are aligned northeast-southwest (Fig. 1-1).

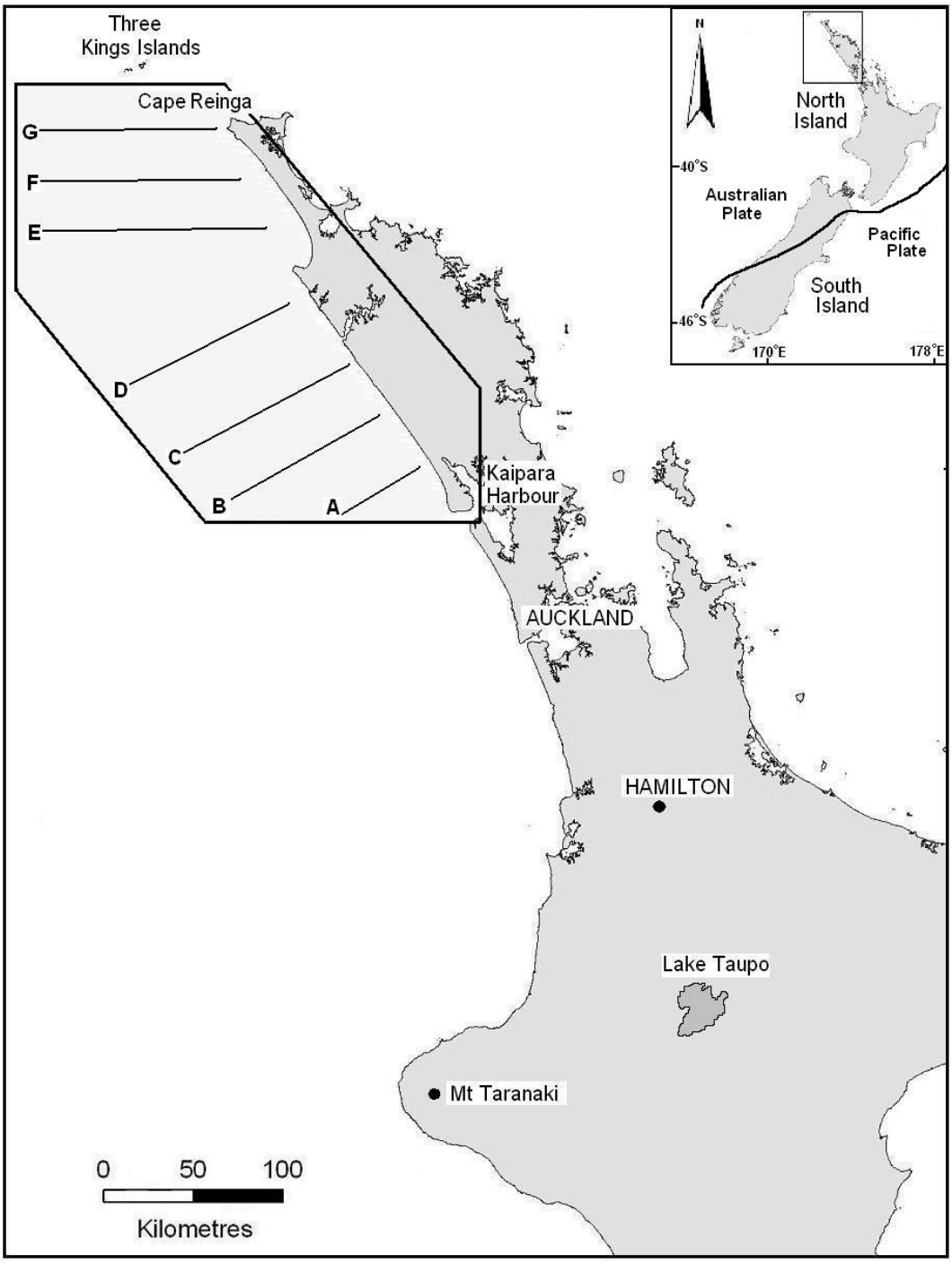

Figure 1-1. Location of the north Kaipara continental margin (NKCM) and the seven transects within New Zealand (inset) and the North Island.

1.3 CONTINENTAL MARGIN SEDIMENT TYPES

Shelf sediment off the western North Island consists predominantly of both modern and relict terrigenous and biogenic deposits, but also includes locally important authigenic and volcanogenic sediment (Fig. 1-2) (Carter, 1975; Carter and Heath, 1975; Nelson et al., 1982). The main sediment types are mentioned below in order of decreasing abundance on the western shelf (based on Fig. 1-2).

1.3.1 Terrigenous sediment

Terrigenous sediment may be relict, modern or palimpsest in nature and is derived from land mainly via rivers and coastal erosion (Carter, 1975). Relict sediments generally occur where modern sedimentation rates are low, but may also occur on those shelf sectors with moderate sedimentation rates where they are restricted to the middle and outer shelf depths, such as off the west coast of Auckland, Waikato and Taranaki (Fig. 1-2) (Carter, 1975; Griffiths and Glasby, 1985). Most relict sediment was deposited during the low sea levels associated with the Last Glacial maximum (Marine Isotope Stage 2), mainly between about 20 000 to 15 000 years ago (Carter, 1975).

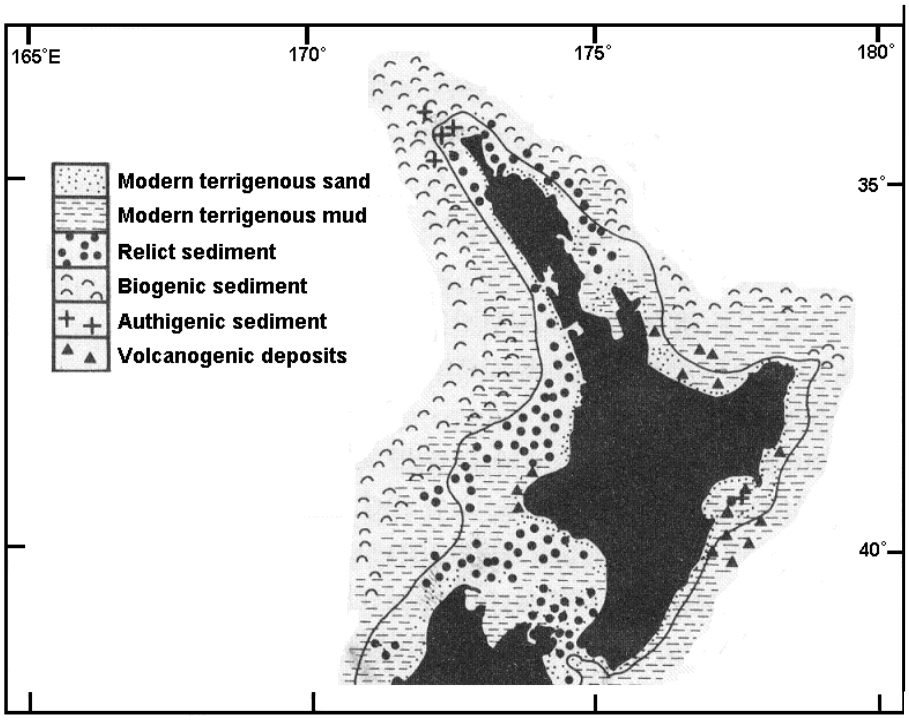

Figure 1-2. Generalised distribution of terrigenous, biogenic, authigenic, relict and volcanogenic sediment around the North Island (adapted from Carter, 1975).

Modern terrigenous sedimentation is often restricted to a nearshore modern sand prism, which generally consists of very fine and fine sand sizes (Fig. 1-3). Muddy terrigenous sediment may bypass the shelf or accumulate in low energy areas to cover older relict or biogenic sediments (Carter, 1975). The western North Island rivers transport large amounts of terrigenous material (approximately 12.9 x 10^6 tonnes per year) onto the shelf (Griffiths and Glasby, 1985) and generally drain either volcanic or sedimentary rock catchments (Churchman et al., 1988). As a result, terrigenous sediment typically consists of quartz, plagioclase feldspar and

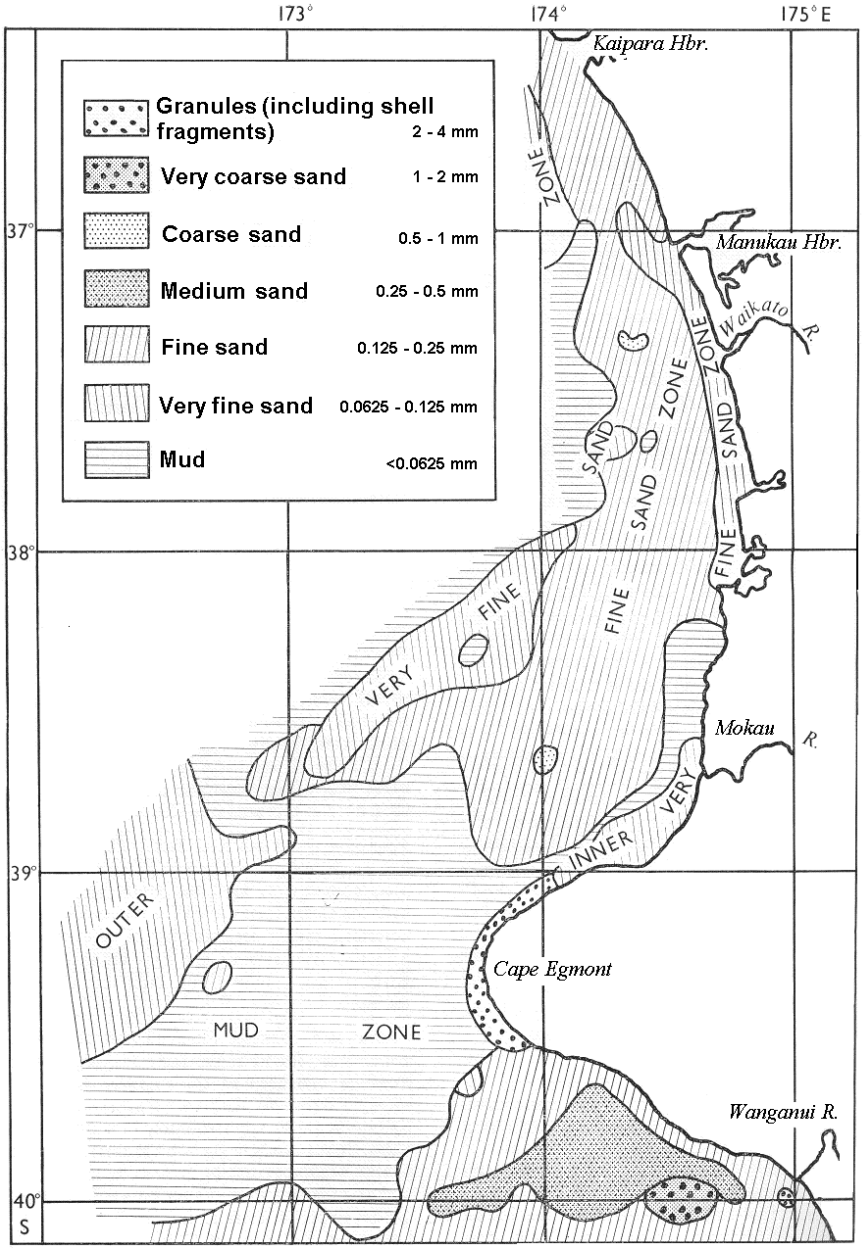

Figure 1-3. Distribution of modal grain sizes along the western shelf of central North Island between Kaipara Harbour and Wanganui River (adapted from McDougall and Brodie, 1967).

clay minerals as the predominant components with smaller amounts of volcanic glass, allophane, biosiliceous material and rare opaque minerals (Hume and Nelson, 1986).

The clay fraction on the central western North Island shelf consists mainly of illite and smectite with chlorite, mixed layer clays and kaolinite occurring in variable amounts (Hume and Nelson, 1986). The amount of clay in the shelf sediments depends on the type and availability of clay-bearing source materials in the catchment areas of the main rivers. The main source of clay for the western shelf is the voluminous Cenozoic mudstone formations in inland western North Island (Hume and Nelson, 1986). The clay mineral assemblages on the shelf are very similar to the clay mineral assemblages observed in the rivers and estuaries of the western North Island, suggesting a likely source of clay (Hume and Nelson, 1986). Smectite, being a major component, is most likely to have originated from sedimentary, basaltic volcanic or calcareous rocks (Churchman et al., 1988).

Titanomagnetite is an important heavy mineral in the terrigenous fraction of shelf sediment from Cape Egmont in the south to north of Manukau Harbour (McDougall and Brodie, 1967). The titanomagnetite occurs on average as c. 2% of the total sediment and ranges from silt to fine sand grain sizes (McDougall and Brodie, 1967). It generally occurs as very fine sand on the inner shelf, silt and very fine sand across the mid shelf, and silt sizes on the outer shelf (McDougall and Brodie, 1967).

1.3.2 Biogenic sediment

Biogenic sediment is the accumulated skeletons and hard parts of benthic and pelagic organisms and is predominantly of calcareous composition in New Zealand (Carter, 1975). The main components of biogenic sediments off the western North Island are bryozoan and molluscan bivalve fragments, but gastropod remains, foraminiferal tests, algal nodules, echinoid fragments, brachiopod valves, arthropod plates, polychaete tubes, solitary corals and siliceous sponge spicules may also occur in varying quantities (Carter, 1975). Biogenic

sediments include both relict and modern biological material and occur in areas where modern terrigenous sedimentation is low (Carter, 1975; Carter and Heath, 1975; Griffiths and Glasby, 1985; Gillespie and Nelson, 1996). Biogenic sediments occur in the highest concentrations (>70% $CaCO_3$) on the western shelf off northernmost North Island, merging into the Three Kings platform. There are localised areas of skeletal carbonate sediment with over 70% $CaCO_3$ elsewhere, such as off Wanganui (Fig. 1-4) (Nelson et al., 1988; Gillespie and Nelson, 1996).

1.3.3 Glauconite

Glauconite is the main authigenic mineral in shelf sediments off the western North Island (Carter, 1975). It forms less than 5% of most sediment but locally may reach up to 40 to 45%. It mainly occurs where there is a low input of modern terrigenous sediment to the shelf and slope and has primarily formed *in situ* on the sea floor (Summerhayes, 1969; Carter, 1975). There are two main forms of glauconite in New Zealand. The first comprises green or green-brown rounded or

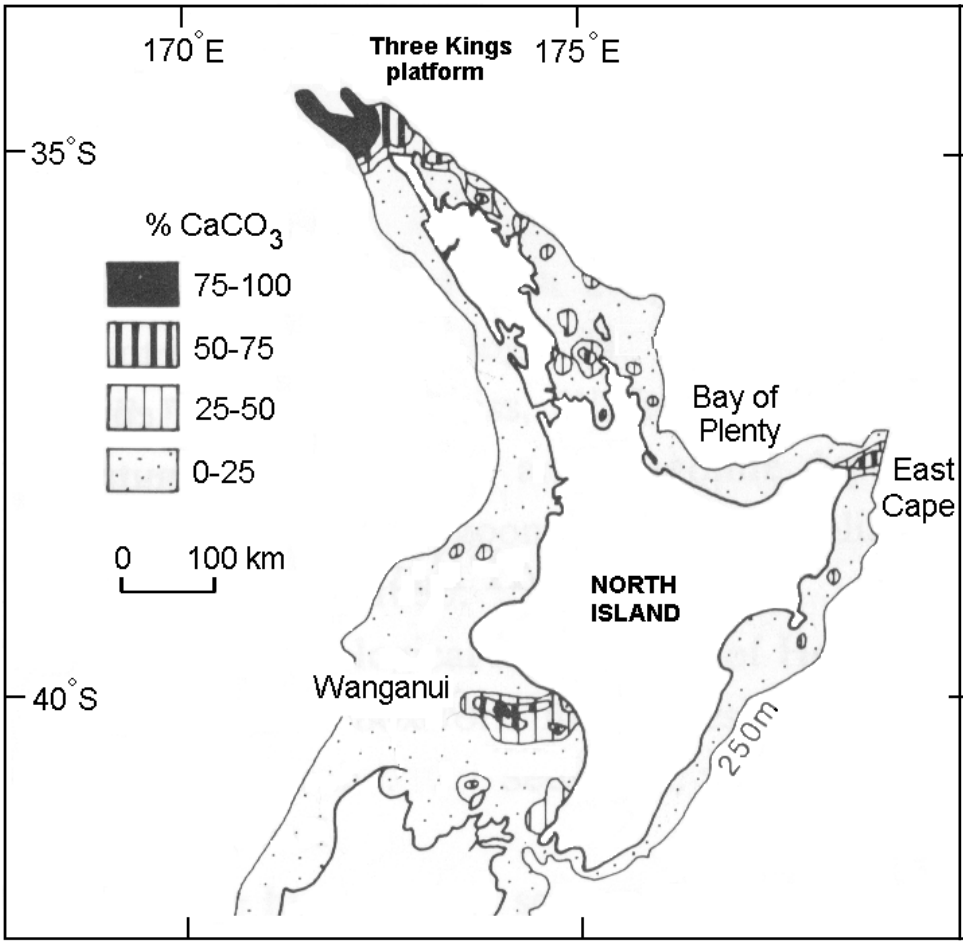

Figure 1-4. Distribution of $CaCO_3$ over the North Island shelf (adapted from Nelson et al., 1988).

botryoidal grains which occur as replaced faecal pellets and sedimentary rock fragments (Carter, 1975). The second form of glauconite occurs as the infilling of foraminiferal tests, while echinoid spines and pumice fragments may also form hosts for glauconite formation (Carter, 1975).

1.3.4 Slope sediment

Slope sediments along the western North Island continental margin include the types of sediments mentioned above. They generally show an increase in carbonate and decrease in grain size with depth and distance from the shore (McDougall, 1972; Carter, 1975). Mud makes up the main type of terrigenous sediment on the western slope (Fig. 1-2) and the amount of mud present correlates with the rate of modern sediment input onto the shelf (Carter, 1975). The amount of terrigenous sediment on the slope is low where the shelf is wide (i.e. near Taranaki) and modern sedimentation rates are low to moderate (Carter, 1975). In these areas the slope sediments are generally dominated by biogenic sediment (Carter, 1975). Glauconite also occurs in the slope sediments, most commonly as the internal casts of echinoid spines and foraminifera (Carter, 1975).

1.4 AIMS OF THIS STUDY

The general aims of this thesis project are to:

1) Determine the texture, composition and distribution of surficial sediments across the NKCM and to interpret the environments of sediment deposition, the provenance of the sediment types present and the possible transport mechanisms occurring to produce these distributions.

2) Catalogue the main faunal species present on the NKCM, determine their distribution and compare the species present with those found both north and south of the study area.

3) Determine the difference in sediment texture and composition between the onland beach and dune sediments and the shelf sediments of the NKCM.

4) Determine the presence and distribution of quartz-rich sand, glauconite and phosphate minerals in deposits as potential industrial mineral resources.

5) Investigate the glauconite-phosphate association across the NKCM and compare and interpret with similar kinds of associations observed in the Tertiary rock record at selected onland sites.

6) Generate an integrated sedimentation model and history for the NKCM.

1.5 THESIS FORMAT

Chapter Two of this thesis discusses the physical setting and geology of the Northland Peninsula and the western North Island continental margin. Chapter Three describes the sample locations and the methods of sample collection and laboratory analysis. Chapters Four, Five, Six and Seven discuss the main sediment types, skeletal taxa (their preservation and mineralogy), glauconite-phosphate association and composition of onshore beach and dune sediments, respectively. The interpretation of these descriptions occurs in Chapter Eight with the determination of provenance, development of facies and discussion of sedimentation models, while Chapter 9 develops a late Quaternary sedimentary history for the NKCM based partly on some sediment cores.

The localities mentioned in the text of this thesis can be found in maps A and B in Appendix A.

SHELF-TO-SLOPE SEDIMENTATION ON THE NORTH KAIPARA CONTINENTAL MARGIN, NORTHWESTERN NORTH ISLAND, NEW ZEALAND

A thesis

submitted in partial fulfilment

of the requirements for the degree of

Master of Science in Earth and Ocean Sciences

at the

University of Waikato

by

Danielle Sarah Payne

University of Waikato

2008

“It was an exquisite day. It was one of those days so clear, so still, so silent, you almost feel the Earth has stopped in astonishment at its own beauty.”

- Katherine Mansfield 1888-1923

ABSTRACT

Temperate mixed carbonate-siliciclastic sediments and authigenic minerals are the current surficial deposits at shelf and slope depths (30-1015 m water depth) on the north Kaipara continental margin (NKCM) in northern New Zealand. This is the first detailed study of these NKCM deposits which are described and mapped from the analysis of 54 surficial sediment samples collected along seven shore-normal transects and from three short piston cores. Five surficial sediment facies are defined from the textural and compositional characteristics of this sediment involving relict, modern or mixed relict-modern components. Facies 1 (siliciclastic sand) forms a modern sand prism that extends out to outer shelf depths and contains three subfacies. Subfacies 1a (quartzofeldspathic sand) is an extensive North Island volcanic and basement rock derived sand deposit that occurs at less than 100-200 m water depth across the entire NKCM. Subfacies 1b (heavy mineral sand) occurs at less than 50 m water depth along only two transects and consists of predominantly local basaltic to basaltic andesite derived heavy mineral rich (>30%) deposits. Subfacies 1c (mica rich sand) occurs at one sample site at 300 m water depth and contains 20-30% mica grains, probably sourced from South Island schists and granites. Facies 2 (glauconitic sand) comprises medium to fine sand with over 30% and up to 95% authigenic glauconite grains occurring in areas of low sedimentation on the outer shelf and upper slope (150-400 m water depth) in central NKCM. Facies 3 (mixed bryozoan-siliciclastic sand) consists of greater than 40% bryozoan skeletal material and occurs only in the northern half of the NKCM. Facies 4 (pelletal mud) occurs on the mid shelf (100-150 m water depth) in northern NKCM and comprises muddy sediment dominated by greater than c. 30% mixed carbonate-siliciclastic pellets. Facies 5 (foraminiferal mud and sand) contains at least 30% foraminifera tests and comprises two subfacies. Subfacies 5a consists of at least 50% mud sized sediment and occurs at >400 m water depth in southern NKCM while subfacies 5b comprises >70% sand sized sediment and occurs at mid to outer shelf and slope depths in the northern NKCM.

A number of environmental controls affect the composition and distribution of NKCM sediments and these include: (1) variable sediment inputs to the NKCM dominated by inshore bedload sources from the south; (2) northerly directed nearshore littoral and combined storm-current sediment transport on the beach and shelf, respectively; (3) offshore suspended sediment bypassing allowing deposition of authigenic minerals and skeletal grains; (4) exchange between the beach and shelf producing similar compositions and grain sizes at less than 150 m water depth; and (5) the episodic rise of sea level since the Last Glaciation maximum approximately 20 000 years ago which has resulted in much sediment being left stranded at greater depths than would otherwise be anticipated.

Sedimentation models developed from other wave-dominated shelves generally do not appear to apply to the NKCM sediments due to their overall relative coarseness and their mosaic textural characteristics. In particular, the NKCM sediments do not show the expected fining offshore trends of most wave-dominated shelf models. Consequently, sandy sediments (both siliciclastic and authigenic) are most typical with mud becoming a dominant component in southern NKCM sediments only at greater than 400 m water depth, over 350 m deeper than most models suggest, a situation accentuated by the very low mud sediment supply to the NKCM from the bordering Northland landmass.

ACKNOWLEDGEMENTS

First and foremost, to my wonderful partner, Jesse, thank you for all of your support, for giving me an ear to bash when necessary, for forcing me to take time off and for the pick me ups when things hit rock bottom (more than once!). To my marvellous parents, George and Marie, for supporting me through my university years, for cooking me dinner every night and for just being there for me through all the ups and downs along the way. To my fantastic friends, Brenda, Nicole and Orla, thanks for all the laughter and the discussions about the inadequacies of the male sex when university work was too touchy to discuss. And to my second parents, Bernice and Roger, the other volunteers at Cambridge RDA and everyone else for providing me with light entertainment throughout the last two years and being understanding when my mind was elsewhere and I couldn't participate fully in events.

Secondly, I would like to thank my supervisors, Professor Cam Nelson and Dr Steven Hood. Steve is especially thanked for all the time, energy, technical help (even though you're not a technician!) and encouragement you have given me through the duration of this thesis. Most of all I want to thank you for being the friendliest face in the department. Many could learn from your example. Specific thanks to Cam for setting up this project and for all the knowledge, wisdom and direction you have imparted to me, not forgetting all the time dedicated to editing my thesis!

Thirdly, thank you to the New Zealand Oceanographic Institute (now NIWA) for logistical support, to B.J. Wardle (Captain) and the other officers and crew of the R.V. Tangaroa on Cruise No. 1077, and to Neville Day (NZOI) and Peter Kamp, Graeme Hancock, Richard Sutherland and Alan Devcich (University of Waikato) for collecting, sorting and some initial work on the sediment samples used in this thesis. Also, thank you to Scott Nodder and Miles Dunkin at NIWA for help in accessing data and especially to Alan Beu at GNS for his skilful assistance with all the shell identifications. Thank you to Rochelle Hansen for the many hours spent pouring over my forams and to Adam Vonk for the help with using ArcGIS. Your effort to save me time is very much appreciated. Thank you also to all the technical and other staff at both Waikato (Annette, Chris, Dirk, Xu and Renat) and the University of Otago (Lorraine Paterson, Brent Pooley, Daphne Lee) for the help with sample preparation and use of equipment.

And finally I want to say a big thank you to all the organisations that provided me with funding: University of Waikato, AusIMM, Freemasons NZ, Cambridge Altrusa Club, Broad Memorial Fund, Waikato Graduate Women and the Bank of New Zealand. And not forgetting Eagle Technologies Ltd. who happily provided me with two ArcView licences.

TABLE OF CONTENTS

LIST OF FIGURES

LIST OF PLATES

following page

LIST OF TABLES

Chapter 1

INTRODUCTION

1.1 INTRODUCTION

The distribution of continental margin sediments around portions of the northern and western North Island of New Zealand has been broadly mapped in previous studies by McDougall and Brodie (1967), Summerhayes (1969) and McDougall (1972). However, some parts of this margin have largely been neglected and one such area is the continental shelf and slope off western Northland. Very little research has been conducted in this area apart from a study of the coastal sand deposits by Schofield (1970) and of the slope sediments off southwestern Northland by McDougall (1972). This thesis research addresses this shortcoming by focussing attention on the nature and distribution of the surficial sediments on the western Northland shelf and slope, hereafter referred to as the north Kaipara continental margin (NKCM).

This chapter introduces the reader to the location of the study area (Section 1.2), the types of continental margin sediments occurring around New Zealand (Section 1.3), the specific aims of this study (Section 1.4) and the thesis format (Section 1.5).

1.2 STUDY AREA

This study of continental margin sedimentation is located immediately off the west coast of northern New Zealand in the Tasman Sea, and stretches from Cape Reinga in the north (34º27.3S, 172º38.9E) to the vicinity of Kaipara Harbour entrance in the south (36º23.4S, 174º05.5E) out to slope depths of up to 1050 m (Fig. 1-1). It focuses on the continental shelf but also beyond out onto the upper slope as well as onshore to include the coastal sedimentary system (dune, beach and harbour). This north Kaipara continental margin (NKCM) is bounded to the north by the carbonate-rich Three Kings platform (Nelson et al., 1982), and to the

south by the titanomagnetite-rich black sands, which stretch from the south Taranaki coast to the south Kaipara region (McDougall and Brodie, 1967). The offshore sample sites occur in seven transects (A-G) extending from shallow shelfal depths (c. 30 m) to upper slope depths (c. 1000 m). The three northernmost transects occur in an east-west direction while the other four transects are aligned northeast-southwest (Fig. 1-1).

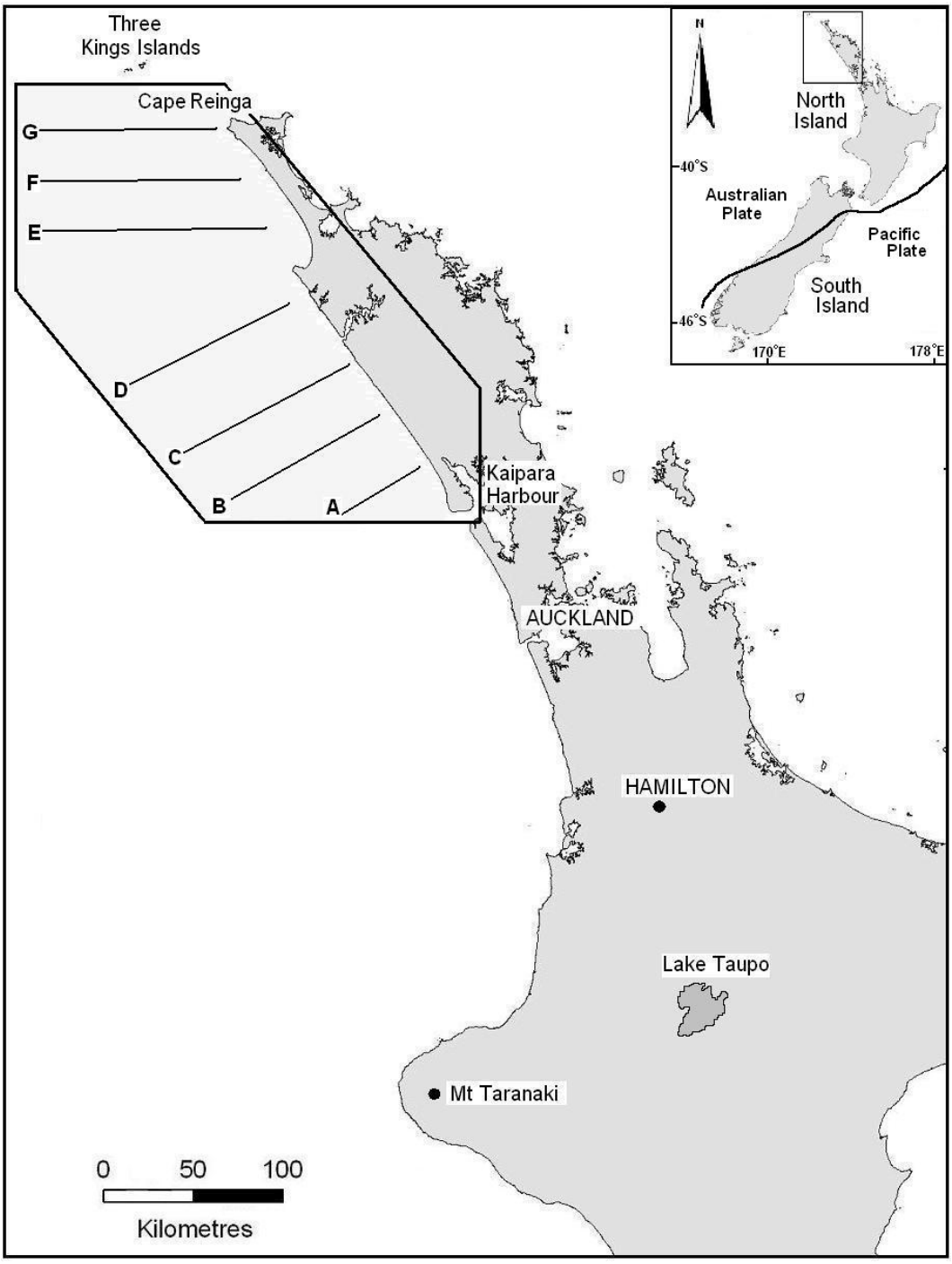

Figure 1-1. Location of the north Kaipara continental margin (NKCM) and the seven transects within New Zealand (inset) and the North Island.

1.3 CONTINENTAL MARGIN SEDIMENT TYPES

Shelf sediment off the western North Island consists predominantly of both modern and relict terrigenous and biogenic deposits, but also includes locally important authigenic and volcanogenic sediment (Fig. 1-2) (Carter, 1975; Carter and Heath, 1975; Nelson et al., 1982). The main sediment types are mentioned below in order of decreasing abundance on the western shelf (based on Fig. 1-2).

1.3.1 Terrigenous sediment

Terrigenous sediment may be relict, modern or palimpsest in nature and is derived from land mainly via rivers and coastal erosion (Carter, 1975). Relict sediments generally occur where modern sedimentation rates are low, but may also occur on those shelf sectors with moderate sedimentation rates where they are restricted to the middle and outer shelf depths, such as off the west coast of Auckland, Waikato and Taranaki (Fig. 1-2) (Carter, 1975; Griffiths and Glasby, 1985). Most relict sediment was deposited during the low sea levels associated with the Last Glacial maximum (Marine Isotope Stage 2), mainly between about 20 000 to 15 000 years ago (Carter, 1975).

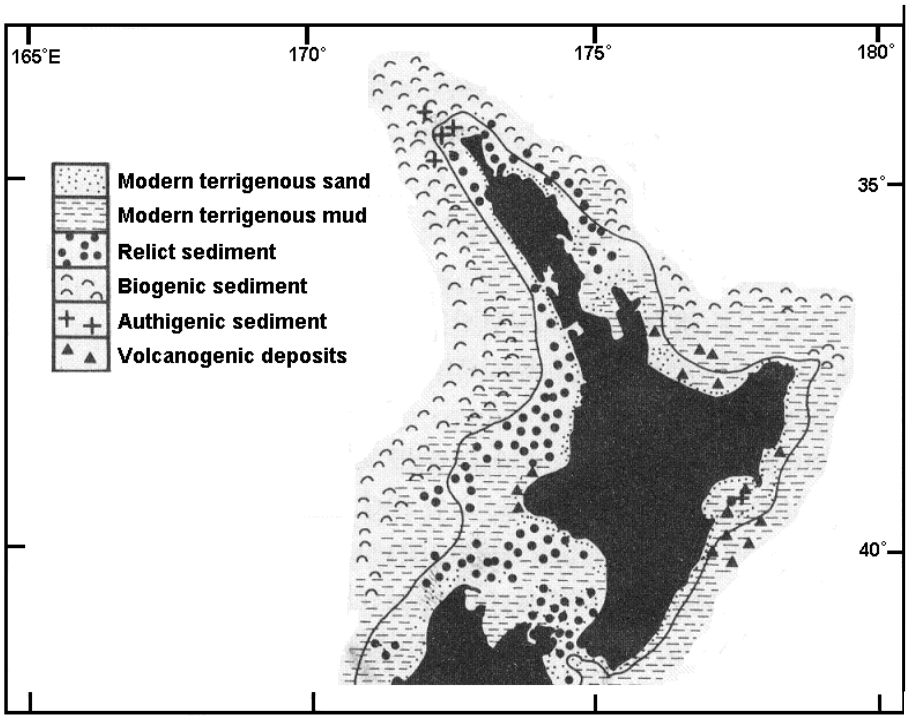

Figure 1-2. Generalised distribution of terrigenous, biogenic, authigenic, relict and volcanogenic sediment around the North Island (adapted from Carter, 1975).

Modern terrigenous sedimentation is often restricted to a nearshore modern sand prism, which generally consists of very fine and fine sand sizes (Fig. 1-3). Muddy terrigenous sediment may bypass the shelf or accumulate in low energy areas to cover older relict or biogenic sediments (Carter, 1975). The western North Island rivers transport large amounts of terrigenous material (approximately 12.9 x 10^6 tonnes per year) onto the shelf (Griffiths and Glasby, 1985) and generally drain either volcanic or sedimentary rock catchments (Churchman et al., 1988). As a result, terrigenous sediment typically consists of quartz, plagioclase feldspar and

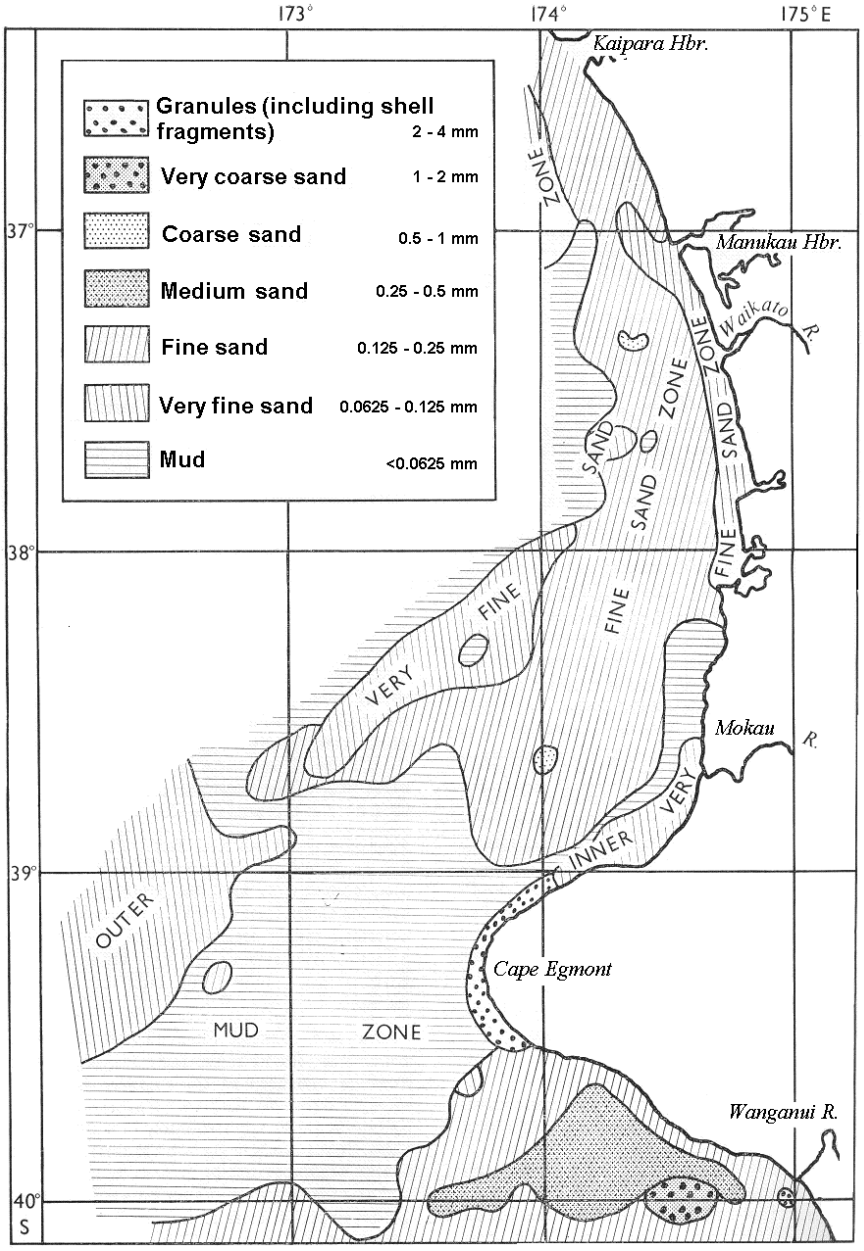

Figure 1-3. Distribution of modal grain sizes along the western shelf of central North Island between Kaipara Harbour and Wanganui River (adapted from McDougall and Brodie, 1967).

clay minerals as the predominant components with smaller amounts of volcanic glass, allophane, biosiliceous material and rare opaque minerals (Hume and Nelson, 1986).

The clay fraction on the central western North Island shelf consists mainly of illite and smectite with chlorite, mixed layer clays and kaolinite occurring in variable amounts (Hume and Nelson, 1986). The amount of clay in the shelf sediments depends on the type and availability of clay-bearing source materials in the catchment areas of the main rivers. The main source of clay for the western shelf is the voluminous Cenozoic mudstone formations in inland western North Island (Hume and Nelson, 1986). The clay mineral assemblages on the shelf are very similar to the clay mineral assemblages observed in the rivers and estuaries of the western North Island, suggesting a likely source of clay (Hume and Nelson, 1986). Smectite, being a major component, is most likely to have originated from sedimentary, basaltic volcanic or calcareous rocks (Churchman et al., 1988).

Titanomagnetite is an important heavy mineral in the terrigenous fraction of shelf sediment from Cape Egmont in the south to north of Manukau Harbour (McDougall and Brodie, 1967). The titanomagnetite occurs on average as c. 2% of the total sediment and ranges from silt to fine sand grain sizes (McDougall and Brodie, 1967). It generally occurs as very fine sand on the inner shelf, silt and very fine sand across the mid shelf, and silt sizes on the outer shelf (McDougall and Brodie, 1967).

1.3.2 Biogenic sediment

Biogenic sediment is the accumulated skeletons and hard parts of benthic and pelagic organisms and is predominantly of calcareous composition in New Zealand (Carter, 1975). The main components of biogenic sediments off the western North Island are bryozoan and molluscan bivalve fragments, but gastropod remains, foraminiferal tests, algal nodules, echinoid fragments, brachiopod valves, arthropod plates, polychaete tubes, solitary corals and siliceous sponge spicules may also occur in varying quantities (Carter, 1975). Biogenic

sediments include both relict and modern biological material and occur in areas where modern terrigenous sedimentation is low (Carter, 1975; Carter and Heath, 1975; Griffiths and Glasby, 1985; Gillespie and Nelson, 1996). Biogenic sediments occur in the highest concentrations (>70% $CaCO_3$) on the western shelf off northernmost North Island, merging into the Three Kings platform. There are localised areas of skeletal carbonate sediment with over 70% $CaCO_3$ elsewhere, such as off Wanganui (Fig. 1-4) (Nelson et al., 1988; Gillespie and Nelson, 1996).

1.3.3 Glauconite

Glauconite is the main authigenic mineral in shelf sediments off the western North Island (Carter, 1975). It forms less than 5% of most sediment but locally may reach up to 40 to 45%. It mainly occurs where there is a low input of modern terrigenous sediment to the shelf and slope and has primarily formed *in situ* on the sea floor (Summerhayes, 1969; Carter, 1975). There are two main forms of glauconite in New Zealand. The first comprises green or green-brown rounded or

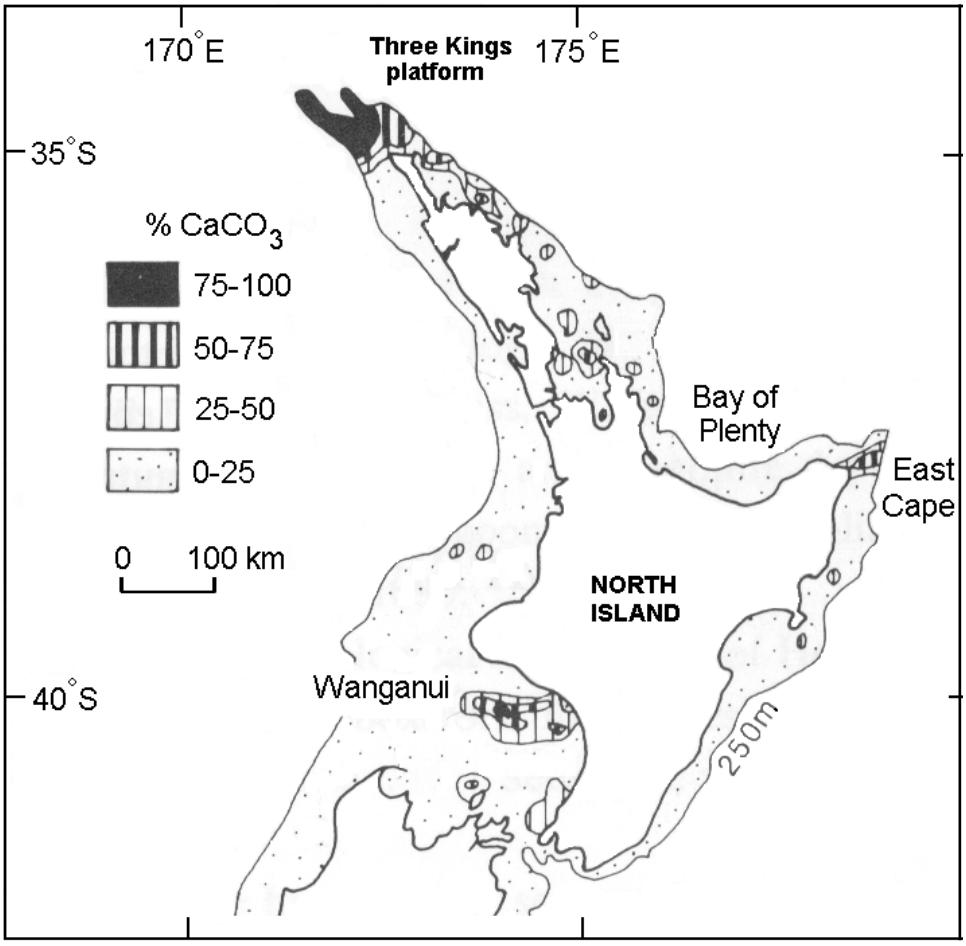

Figure 1-4. Distribution of $CaCO_3$ over the North Island shelf (adapted from Nelson et al., 1988).

botryoidal grains which occur as replaced faecal pellets and sedimentary rock fragments (Carter, 1975). The second form of glauconite occurs as the infilling of foraminiferal tests, while echinoid spines and pumice fragments may also form hosts for glauconite formation (Carter, 1975).

1.3.4 Slope sediment

Slope sediments along the western North Island continental margin include the types of sediments mentioned above. They generally show an increase in carbonate and decrease in grain size with depth and distance from the shore (McDougall, 1972; Carter, 1975). Mud makes up the main type of terrigenous sediment on the western slope (Fig. 1-2) and the amount of mud present correlates with the rate of modern sediment input onto the shelf (Carter, 1975). The amount of terrigenous sediment on the slope is low where the shelf is wide (i.e. near Taranaki) and modern sedimentation rates are low to moderate (Carter, 1975). In these areas the slope sediments are generally dominated by biogenic sediment (Carter, 1975). Glauconite also occurs in the slope sediments, most commonly as the internal casts of echinoid spines and foraminifera (Carter, 1975).

1.4 AIMS OF THIS STUDY

The general aims of this thesis project are to:

1) Determine the texture, composition and distribution of surficial sediments across the NKCM and to interpret the environments of sediment deposition, the provenance of the sediment types present and the possible transport mechanisms occurring to produce these distributions.

2) Catalogue the main faunal species present on the NKCM, determine their distribution and compare the species present with those found both north and south of the study area.

3) Determine the difference in sediment texture and composition between the onland beach and dune sediments and the shelf sediments of the NKCM.

4) Determine the presence and distribution of quartz-rich sand, glauconite and phosphate minerals in deposits as potential industrial mineral resources.

5) Investigate the glauconite-phosphate association across the NKCM and compare and interpret with similar kinds of associations observed in the Tertiary rock record at selected onland sites.

6) Generate an integrated sedimentation model and history for the NKCM.

1.5 THESIS FORMAT

Chapter Two of this thesis discusses the physical setting and geology of the Northland Peninsula and the western North Island continental margin. Chapter Three describes the sample locations and the methods of sample collection and laboratory analysis. Chapters Four, Five, Six and Seven discuss the main sediment types, skeletal taxa (their preservation and mineralogy), glauconite-phosphate association and composition of onshore beach and dune sediments, respectively. The interpretation of these descriptions occurs in Chapter Eight with the determination of provenance, development of facies and discussion of sedimentation models, while Chapter 9 develops a late Quaternary sedimentary history for the NKCM based partly on some sediment cores.

The localities mentioned in the text of this thesis can be found in maps A and B in Appendix A.

Chapter 2

PHYSICAL SETTING

2.1 INTRODUCTION

The Northland region lies 400-700 km northwest of the present-day active plate boundary off eastern North Island and is situated entirely on the continental Australian Plate (Fig. 1-1 inset) (Issac, 1996). Northland consists of several tombolos that join together islands of varying geological make-up. The Aupouri Peninsula is the only tombolo within the study area and consists of Pleistocene and Holocene dune and beach sands and alluvial, lacustrine, swamp and estuarine sediments (Appendix A, Map B and Fig. 2-5) (Issac, 1996; Kasper-Zubillaga et al., 2005). The North and South Kaipara Barriers form prograding spits across the mouth of Kaipara Harbour and are the only other major sand-dominated features within the study area (Appendix A, Map B and Fig. 2-5).

This chapter aims to introduce the reader to the geology of the Northland region (Section 2.2), the morphology and bathymetry of offshore western Northland (Section 2.3), climatic and oceanographic setting (Sections 2.4-2.7) and the shelf sectors present along the western shelf of North Island, New Zealand (Section 2.9).

2.2 GEOLOGY

The geology of the Northland Peninsula and associated north Kaipara continental margin (NKCM) varies considerably across the study area and includes Mesozoic basement rocks, autochthonous Eocene-Oligocene sedimentary rocks, sedimentary and igneous rocks of the Cretaceous-early Miocene Northland Allochthon, Miocene volcanic rocks, Miocene sedimentary rocks and Pleistocene and Holocene sediments (Fig. 2-1). The basic geological history of the region and the rock units relevant to the study area are briefly discussed here.

2.2.1 Mid-Cretaceous to Recent geological history

Pre-rifting and rifting characterise the early history of western Northland with the deposition of a passive margin sequence during the Early Cretaceous alongside eastern Gondwanaland (Herzer et al., 1997). Rifting began during the mid-Cretaceous (110-90 Ma) along with the deposition of terrestrial and coal measure deposits (Herzer et al., 1997). Rifting continued into the Late Cretaceous with extensional faulting resulting in the subsidence of the area and the subsequent deposition of a marine sandstone and mudstone sequence (Issac et al., 1994;

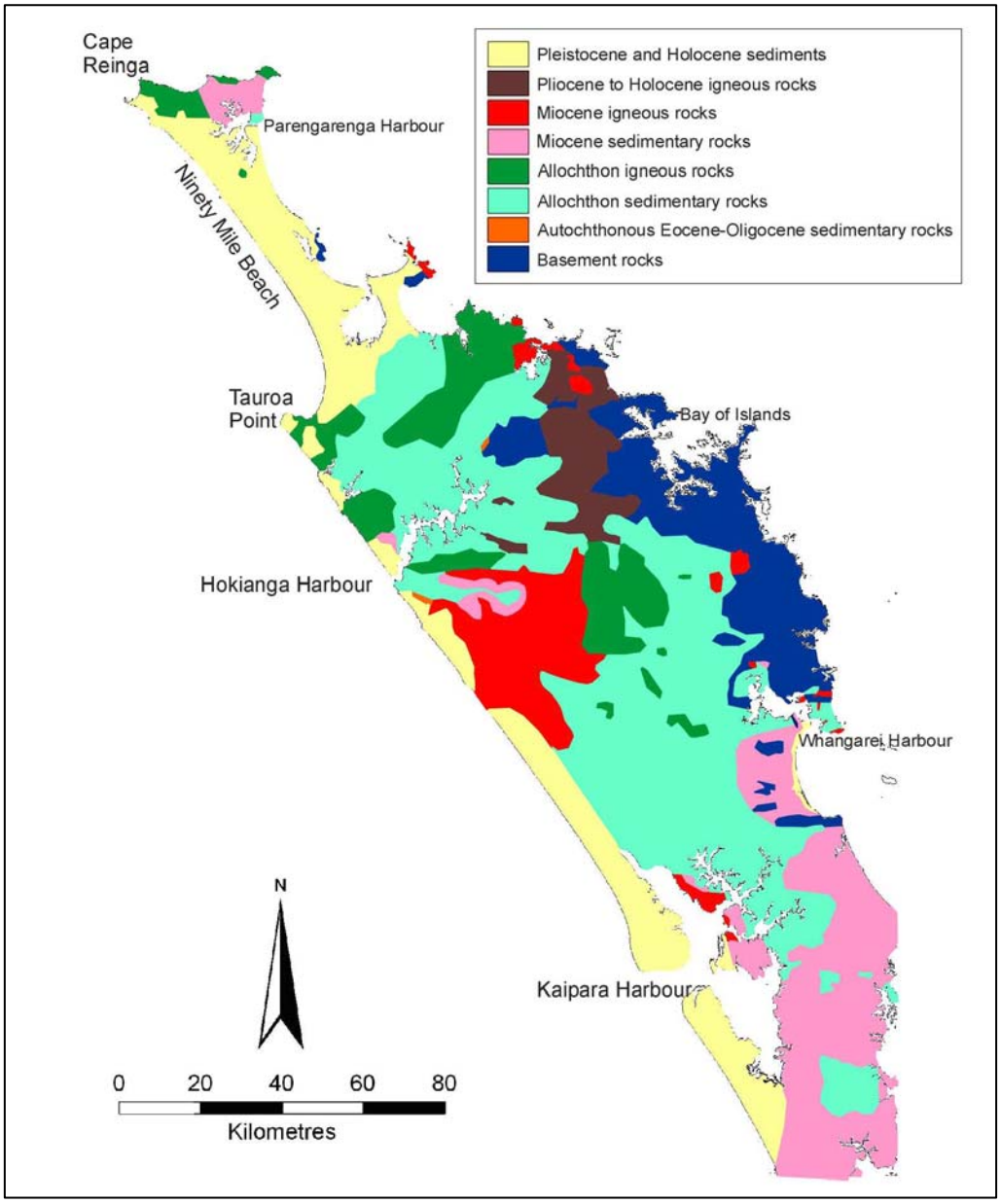

Figure 2-1. Generalised geology of Northland (from Issac, 1994, 1996; Rait, 2000; Edbrooke, 2001; Spörli and Harrison, 2004). Boundaries are only approximate.

Herzer et al., 1997). Thin paralic to bathyal sedimentary and calcareous sediments were deposited on the margin during the Paleocene to Late Oligocene with regional limestone deposition (Herzer et al., 1997). The development of a convergent plate boundary and subduction between the Australian and Pacific plates to the northeast during the Late Oligocene resulted in rapid foreland subsidence and a change in sediment character from shelf and shallow bathyal to deep-water carbonates (Herzer et al., 1997). Emplacement of the Northland Allochthon onto the Northland Peninsula occurred from the northeast during the Late Oligocene to Early Miocene followed by the commencement of andesitic arc volcanism, both onshore and offshore, during the Early Miocene (Issac et al., 1994; Herzer et al., 1997). Sedimentary and volcaniclastic turbidites were deposited in subsiding basins in southern Northland during the Early Miocene. Arc volcanism waned in Northland during the Middle Miocene and was followed by deposition of a primarily offshore sedimentary infill throughout the Middle and Late Miocene and the Pliocene-Pleistocene (Herzer et al., 1997). This sediment was supplied by erosion of the Northland Allochthon when the Northland Peninsula was tilted during the Early Miocene and subduction under Northland ceased (Issac et al., 1994; Herzer et al., 1997).

2.2.2 Mesozoic basement rocks

Basement rocks, loosely referred to as Mesozoic basement rocks, comprise three terranes (Murihiku, Waipapa and Mount Camel, Fig. 2-2 and Table 2-1), only two of which crop out in Northland (Issac et al., 1994; Issac, 1996; Herzer et al., 1997). The terranes consist of Late Triassic to Late Cretaceous sandstone, siltstone, argillite, greywacke and submarine basalt and basaltic andesite lavas (Hayward, 1993; Issac et al., 1994; Herzer et al., 1997). Waipapa and Mount Camel terrane rocks crop out in northeastern and northern Northland, respectively (Fig. 2-1).

2.2.3 Autochthonous Eocene-Oligocene sedimentary rocks

Autochthonous rock is relatively rare within western Northland with only the Late Eocene Ruatangata Sandstone and Mangapa Mudstone and Oligocene Whangarei

Limestone of the Te Kuiti Group represented (Fig. 2-1 and Table 2-1). The Ruatangata Sandstone comprises shelfal glauconitic sandstone that unconformably overlies Mesozoic basement rocks (Issac et al., 1994; Issac, 1996). The Mangapa Mudstone conformably overlies the Ruatangata Sandstone and consists of calcareous mudstone. The Whangarei Limestone is exposed mainly in eastern Northland and overlies the Ruatangata Sandstone and comprises glauconitic bryozoan-molluscan-algal-foraminiferal limestone (Issac, 1996).

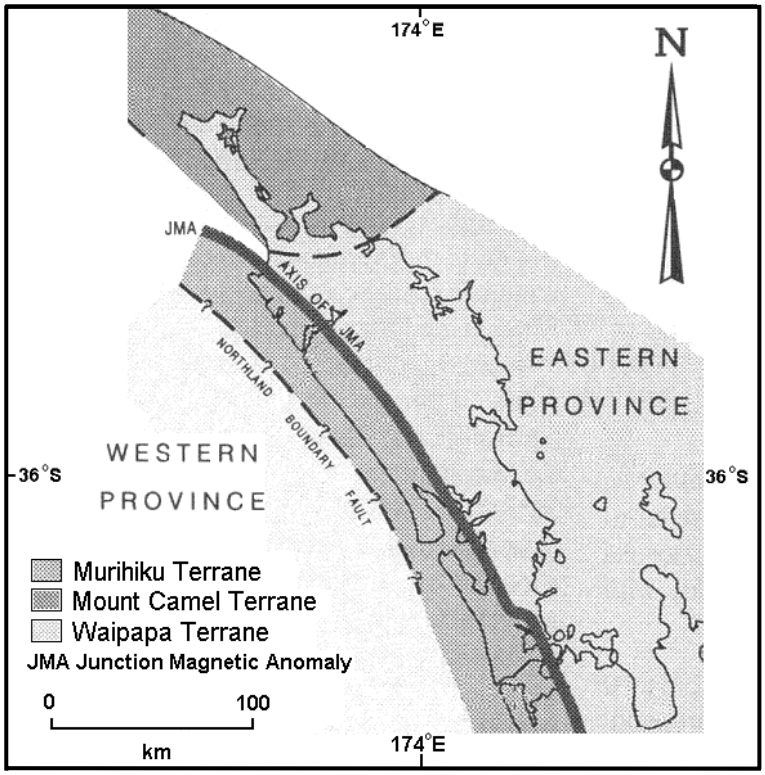

Figure 2-2. Location of basement terranes in Northland (adapted from Issac et al., 1994).

2.2.4 Northland Allochthon

The Northland Allochthon extends across the Northland Peninsula with seismic evidence suggesting its western limit lies 80 km west of Cape Maria Van Diemen in the north but only 25 km west of the coastline south of Hokianga Harbour (Fig. 2-1 and 2-3A) (Issac et al., 1994). The rocks of the Northland Allochthon range in age from Early Cretaceous to earliest Miocene and are divided into four complexes: the Tupoa, Mangakahia, Motatau and Tangihua Complexes (Table 2-1) (Issac et al., 1994). The Early Cretaceous Tupoa Complex consists of

Table 2-1. Distribution and ages of stratigraphic units that crop out in Northland (from Ballance, 1993; Issac et al., 1994; Herzer, 1995; Issac, 1996; Edbrooke, 2001). sst = sandstone, mst = mudstone, slst = siltstone, lst = limestone.

PERIOD	GEOLOGICAL UNITS	
Holocene	Monogenetic scoria cones and lava flows Coastal dune, swamp, fluvial and lacustrine deposits	KERIKERI VOLC. KARIOITAHI GP
Pliocene	Moderately to poorly consolidated quartzofeldspathic sandstone	AWHITU GP
Middle Miocene	**OFFSHORE** / **ONSHORE** Ninety Mile Volcano Ahipara Volcano Herekino Whangape Volcano Hokianga Waipoua Subgroup Tokatoka Volcano Hukatere Volcano Kaipara Volcano Manukau Volcano Conglomerate and sst = Matapia Hemipelagic sst and conglomerate = Paratoetoe Channelised cobble conglomerate = Kaurahoupo Conglomerate Bathyal mst, sst =Tom Bowling Fm Conglomerate with mst beds = Omapere Conglomerate Mst, muddy sst = Waitiiti Fm Mst, sandy slst, muddy sst = Waihangaru Fm Matapoura Conglomerate Mst, slst, muddy sst = Timber Bay Fm } = Timber Bay Facies Sst and slst turbidite beds = Pakiri Facies	WAITAKERE VOLCANIC ARC PARENGA-RENGA GP OTAUA GP WAITEMATA GP
Early Miocene	Sst and slst turbidites = Cornwallis Facies	
	WEST / **EAST** Basaltic pillow lava, mud interbeds, hypabyssal intrusions = TANGIHUA COMPLEX Taipa Mst, Omahuta Sst, Mahurangi Lst, Puriri Mst = MOTATAU COMPLEX Motukaraka Sst, Punakitere Sst, Waikaraka Mst = MANGAKAHIA COMPLEX Whangai Fm = MANGAKAHIA COMPLEX Hukerenui Mst and Taikirau Greensand = MANGAKAHIA COMPLEX Waipawa Black Shale = MANGAKAHIA COMPLEX Conglomerate, pebbly sst and mst = TUPOA COMPLEX	NORTHLAND ALLOCHTHON
Oligocene	**WEST** / **EAST** Glauconitic lst = Whangarei Lst Calcareous mst = Mangapa Mst Glauconitic sst = Ruatangata Sst	TE KUITI GP
Eocene		
Cretaceous Triassic	Conglomerate, sst, siltstone, argillite, greywacke, basaltic/basaltic andesite lavas = Murihiku, Waipapa and Mount Camel Suspect Terranes	BASEMENT

conglomerate, pebbly sandstone, sandstone and mudstone which is restricted to exposures along the northeastern Northland coastline (Hayward, 1993; Issac et al., 1994; Issac, 1996). The Mangakahia Complex consists of Late Cretaceous to Eocene terrigenous sedimentary facies with minor amounts of limestone and chert (Fig. 2-3B) (Hayward, 1993; Issac et al., 1994). The Motatau Complex consists of Early Eocene to earliest Miocene carbonate-rich rocks while the Tangihua Complex consists of Early Cretaceous to Paleocene submarine basaltic lava as well as basalt, dolerite and gabbro intrusives (Fig. 2-3C) (Issac et al., 1994; Issac, 1996; Edbrooke, 2001). These units are highly deformed and faulted compared to the surrounding autochthonous sediments (Issac et al., 1994).

2.2.5 Miocene igneous rocks

During the Early Miocene a 350 km long NW–SE trending volcanic arc was active along western Northland known as the Waitakere volcanic arc (Fig. 2-4) (Hayward, 1993; Issac et al., 1994; Herzer, 1995; Edbrooke, 2001). The arc represented initiation of an active convergent margin created by subduction of the

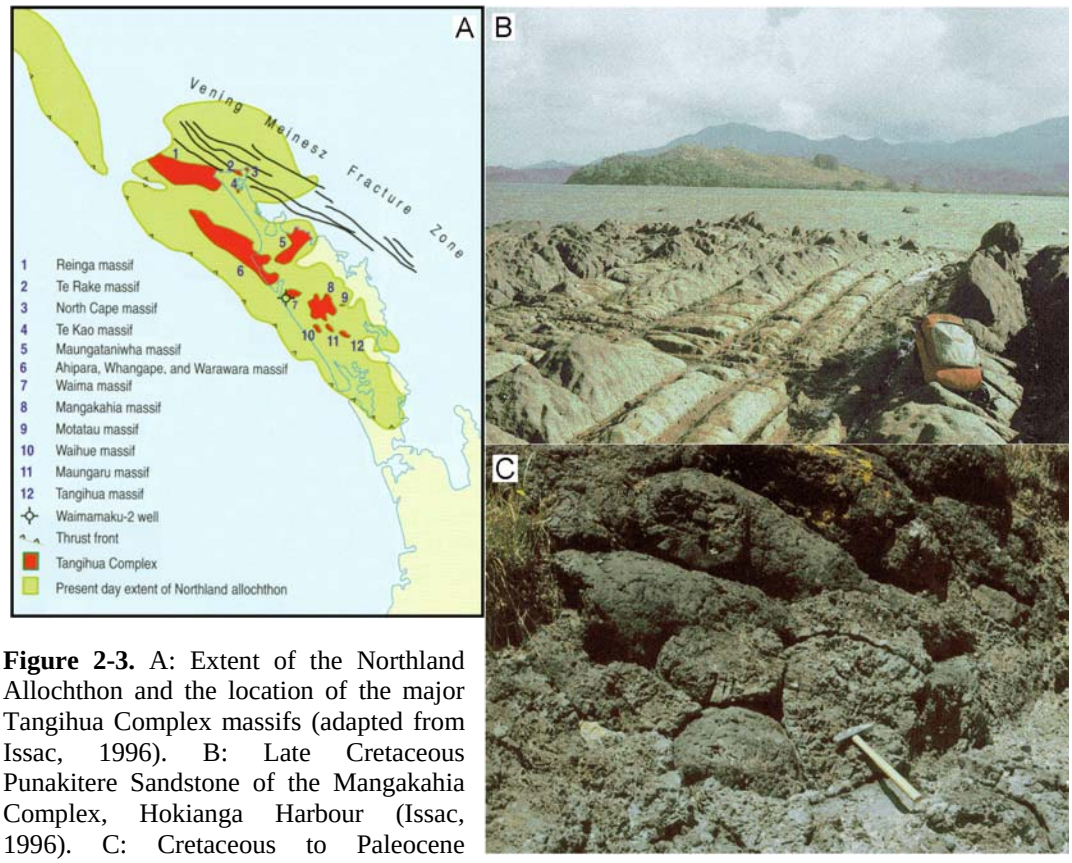

Figure 2-3. A: Extent of the Northland Allochthon and the location of the major Tangihua Complex massifs (adapted from Issac, 1996). B: Late Cretaceous Punakitere Sandstone of the Mangakahia Complex, Hokianga Harbour (Issac, 1996). C: Cretaceous to Paleocene Tangihua Complex basalt pillow lavas, Whangape Harbour (Issac, 1996).

Pacific Plate beneath the Australian Plate (Wright and Black, 1981; Hayward, 1993; Issac et al., 1994). The majority of the Waitakere arc volcanoes occur offshore, west of the present day Northland Peninsula (Fig. 2-4) (Issac et al., 1994).

Over 50 separate volcanic centres have been identified along the shelf and slope of offshore western Northland between Manukau Harbour in the south and Ninety Mile Beach in the north (Issac et al., 1994; Herzer, 1995). Seven large 30–80 km across, volcanic massifs are evident along with another five smaller 10-16 km wide volcanoes. A cluster of three large massifs occurs in the north, named the Ninety Mile, Ahipara and Whangape massifs (Fig. 2-4) (Issac et al., 1994; Herzer, 1995). Further to the south there are two large massifs, the Hokianga and Waipoua, along with two intermediate-sized volcanoes. The Kaipara massif occurs in the southern part of the study area, while the large Manukau massif lies further south (Fig. 2-4) (Issac et al., 1994; Herzer, 1995).

The massifs have varying morphologies with broad, flat-topped, steep-sided tables or rugged-peaked pedestals being the most common. Terracing also occurs on the Ahipara, Whangape and Hokianga massifs (Issac et al., 1994; Herzer, 1995). The Hokianga and Kaipara massifs are the oldest of the seven. The Hokianga massif formed a volcano 3 km high while the Kaipara massif was much smaller at 1.6 km high (Issac et al., 1994; Herzer, 1995). The wave cut summit of the Hokianga massif forms the Hokianga Terrace southwest of Hokianga Harbour (Fig. 2-6B) (Issac, 1996). The Whangape and Ahipara massifs were active at the same time as Hokianga and Kaipara but their volcanic activity continued after the extinction of the latter massifs. The Whangape massif has an uneven, terraced pedestal with a flat-topped cone that gives the massif a height of 2.5 km (Issac et al., 1994; Herzer, 1995). The Ahipara massif to the north is less complicated morphologically, forming a volcano 2.3 km high. The offshore section of the Ahipara massif forms the North and South Ahipara Banks (Fig. 2-6B) (Issac, 1996). The Herekino and Ninety Mile volcanoes are not well known but are thought to have reached 1.6 km and 1.2 km, respectively, and have wave planed tops (Issac et al., 1994). The Whangape and Herekino massifs form the Whangape and Herekino Banks, respectively (Fig. 2-6B) (Issac, 1996). The Waipoua massif is the youngest and largest massif within the study area and formed a large 40 km wide and 60 km long flat-topped shield with a height of 2.5 km. The Waipoua massif occurs south of Hokianga Harbour (Fig. 2-4) with a third of its area on land (Herzer, 1995). The summits of the Herekino, Whangape and Hokianga massifs have not been buried by younger sediments and remain exposed on the sea floor (Issac, 1996).

2.2.6 Miocene sedimentary rocks

Miocene sedimentary rocks within the study area include the Waitemata, Otaua and Parengarenga Groups (Fig. 2-1 and Table 2-1).

The Early Miocene Waitemata Group is found only in southern Northland with the Pakiri, Cornwallis and Timber Bay facies present within the study area at Kaipara Harbour (Table 2-1). The Pakiri and Cornwallis facies comprise

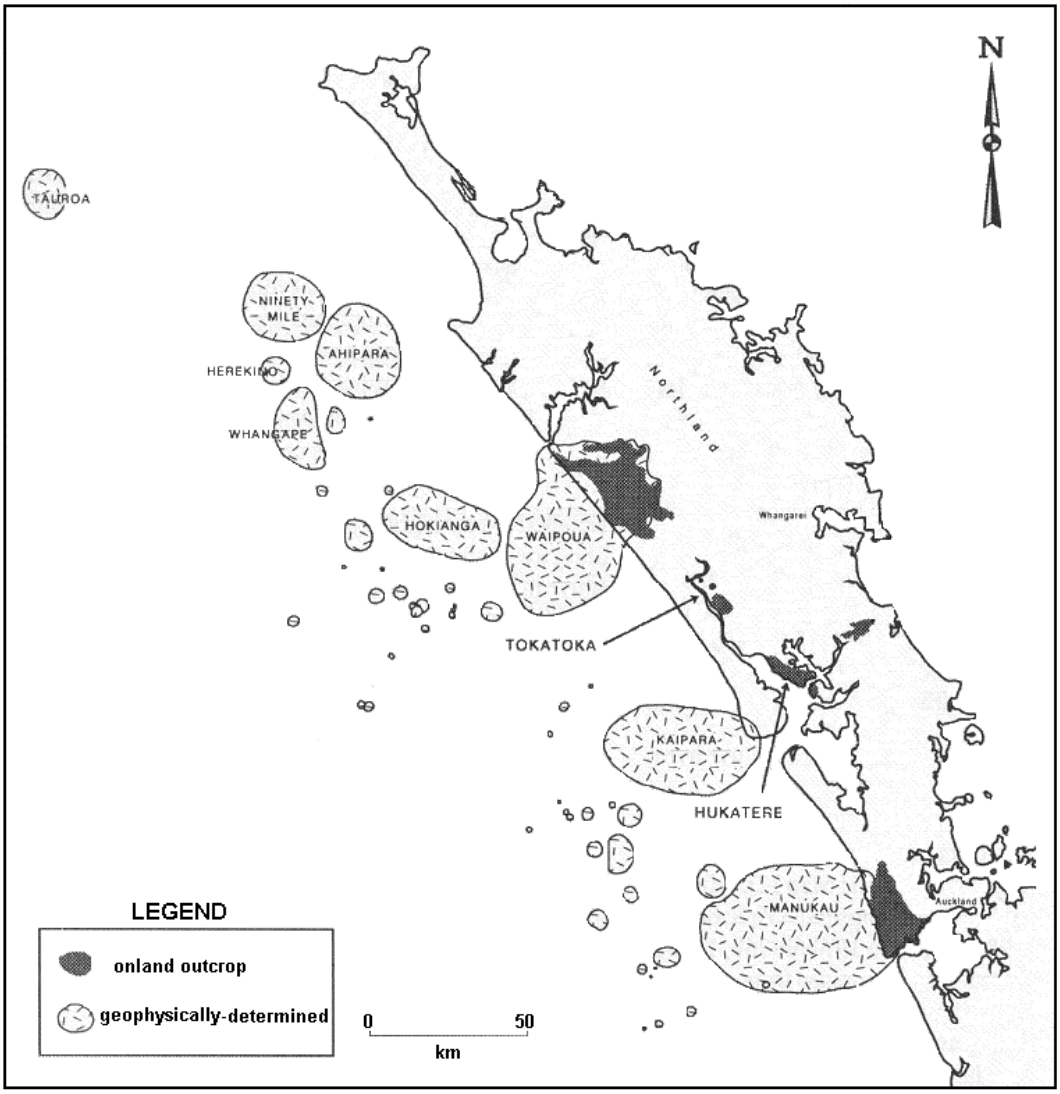

Figure 2-4. Location of the large massifs and smaller associated intermediate sized volcanoes of the Early Miocene Waitakere Group (adapted from Issac et al., 1994).

sandstone and siltstone turbidite beds sourced from Northland Allochthon and Waitakere volcanic arc sediments (Hayward, 1993; Issac et al., 1994; Edbrooke, 2001). The Timber Bay facies includes the Timber Bay Formation, Matapoura Conglomerate and the Waihangaru Formation (Hayward, 1993; Issac et al., 1994). These formations include volcanic-rich mudstone, siltstone, sandstone and conglomerate sourced from the Kaipara volcano (Waitakere volcanic arc) and the Northland Allochthon (Hayward, 1993; Issac et al., 1994; Edbrooke, 2001).

The Early Miocene Otaua Group is found primarily on both sides of the mouth of Hokianga Harbour, but also within the Waimamaku Valley (Table 2-1) (Hayward, 1993; Issac et al., 1994; Issac, 1996). The Otaua Group was deposited over the

Northland Allochthon and Oligocene Whangarei Limestone and includes the Waitiiti Formation, Waiwhatawhata Conglomerate and the Omapere Conglomerate (Issac et al., 1994; Issac, 1996). These formations consist of mudstone, muddy or pebbly sandstone and cobble conglomerate derived from the Motatau and Tangihua complexes of the Northland Allochthon (Hayward, 1993; Issac et al., 1994).

The Parengarenga Group is an Early Miocene terrigenous sedimentary sequence found only in northern Northland and includes the Tom Bowling Formation, Kaurahoupo Conglomerate, Paratoetoe Formation and the Matapia Formation (Hayward, 1993; Issac et al., 1994). These formations comprise bathyal calcareous mudstone and muddy sandstone, conglomerate and pebbly sandstone. The rocks are sourced from Northland Allochthon, Mount Camel Terrane and Waitakere volcanic arc sediments (Hayward, 1993; Issac et al., 1994).

2.2.7 Pleistocene and Holocene units

The Pleistocene and Holocene units within the study area include the Awhitu Group, Karioitahi Group and the Kerikeri Volcanics (Table 2-1). The Pliocene to Early Pleistocene Awhitu Group consists of moderately to poorly consolidated quartzofeldspathic sandstone found along the west coast from south Auckland to Aupouri Peninsula (Issac et al., 1994; Issac, 1996; Edbrooke, 2001). The Pleistocene to Holocene aged Karioitahi Group comprises moderately consolidated to unconsolidated coastal dune and swamp, fluvial and lacustrine deposits (Issac et al., 1994; Issac, 1996; Edbrooke, 2001). The Kerikeri Volcanics consist of Pliocene to Holocene monogenetic scoria cones and their related lava flows within the Kaikohe-Bay of Islands and Puhipuhi-Whangarei fields (Issac et al., 1994; Edbrooke, 2001). Only the Taheke Basalt from the Kaikohe-Bay of Islands field is present within the study area, comprising a third of this field and commonly forming steep sided cones (Issac et al., 1994).

2.3 PHYSICAL FEATURES OF OFFSHORE WESTERN NORTHLAND

2.3.1 Morphology of coastline

The coastal morphology shows significant variation along the NKCM. Overall, the coastline is long (c. 292 km between Cape Reinga and Kaipara Harbour mouth) and straight, lacking the numerous coastal embayments that characterise the east coast of Northland (Fig. 2-5). It is dominated by sandy beaches which comprise c. 75% of the coastline (c. 220 km), with coastal rocky outcrops forming the remainder. The sandy beaches dominate the southern and northern parts of the NKCM coastline and may be backed by coastal cliffs or terraces. Sandy barriers formed through nearshore wave processes (e.g. longshore or littoral drift) are also common, with the North Kaipara Barrier and Northland Peninsula tombolo (Aupouri Peninsula) being the most significant (Fig. 2-5). Areas of active dune fields occur at the southern end of North Kaipara Barrier, the mouth of Hokianga Harbour, south Tauroa Point and surrounding Cape Reinga and Cape Maria van Diemen (Fig. 2-5).

Four harbours of varying sizes are present along the NKCM coastline, the largest and southernmost being Kaipara Harbour (Fig. 2-5). The largest river discharging into the NKCM is the Wairoa River (suspended sediment yield of 1.1 million tonnes per year; Hume et al., 2003) which feeds into the northern arm of Kaipara Harbour and drains a catchment area to the north and east with many tributary streams, including the more significant Kaihu and Manganui Rivers (Fig. 2-5) (Irwin and Eade, 1984b). Further north, three smaller harbours occur clustered along the coastline. These are the Herekino, Whangape and Hokianga Harbours (Fig. 2-5). The Hokianga Harbour is the largest of the three and extends 34 km inland (Issac, 1996) draining a number of small rivers and streams (Irwin and Eade, 1984a). The four harbours comprise drowned river valley systems formed when the sea flooded the lower valleys during sea level rise following the Last Glaciation (Hume et al., 2003).

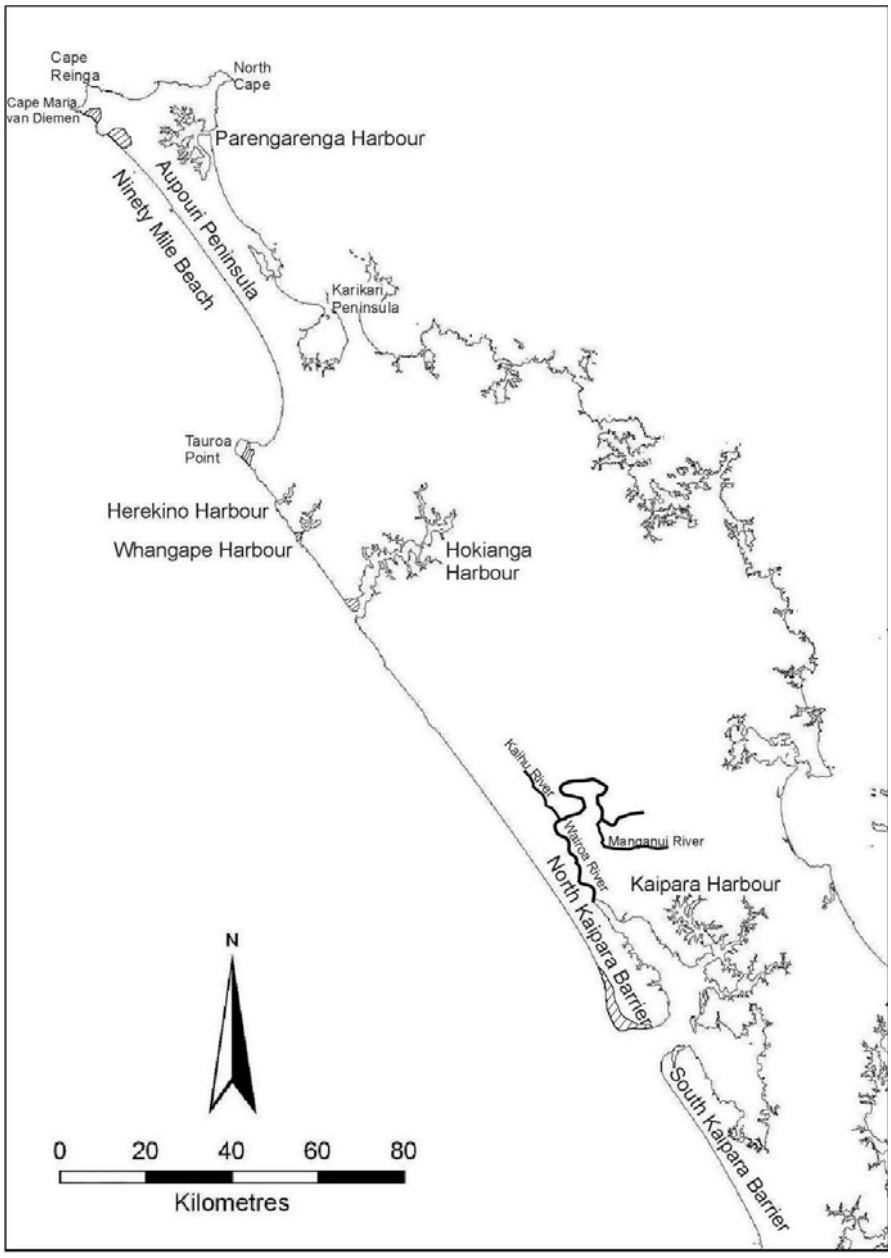

Figure 2-5. Location of the main onland morphologic features along the NKCM. Hatched areas are active dune fields.

2.3.2 Bathymetry

The bathymetry of the NKCM varies across the margin with both the shelf and slope width increasing northwards between Kaipara Harbour and Cape Maria Van Diemen (Fig. 2-6A) (Irwin and Eade, 1984 a,b). The narrower southern shelf is c. 25 km wide compared to the c. 50 km wide shelf off Ninety Mile Beach, north of Tauroa Point. The shelf edge is located between c. 150 and 175 m water depth and primarily follows the smooth shape of the coastline; however, north of Tauroa

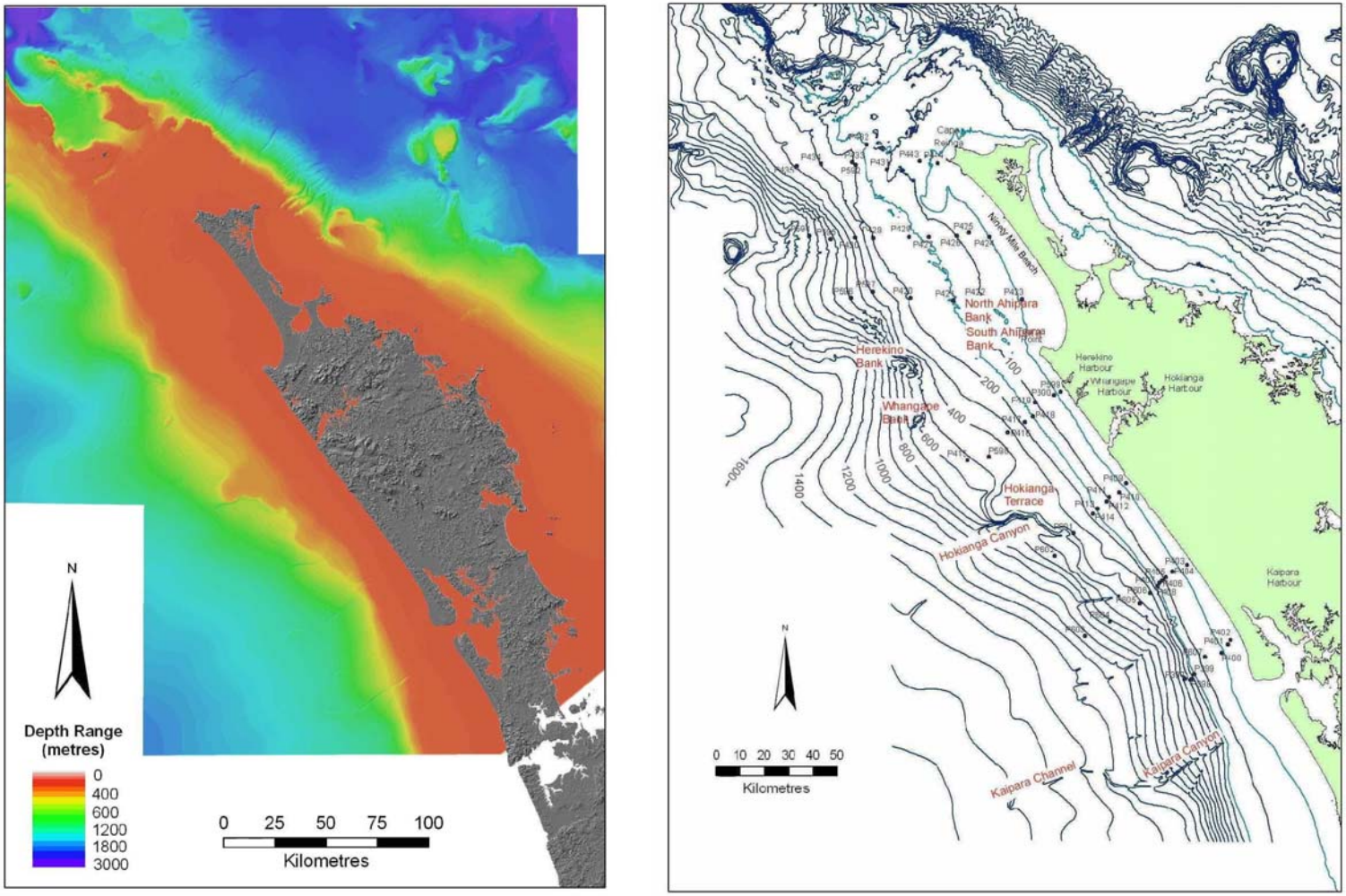

Figure 2-6. Bathymetry maps showing bathymetry in (A) grading colours and (B) contour lines.

Point, along Ninety Mile Beach, its morphology becomes more complex with an irregular nature and a series of higher elevation (shallower depth) features along the shelf edge (Fig. 2-6B).

The bathymetry of the southern half of the NKCM is more complex with a series of submarine canyons and significant bathymetric features (Fig. 2-6). Offshore from Kaipara Harbour is the Kaipara Canyon which extends from the shelf edge (c. 150 m water depth) to a depth of c. 1200 m where it continues as the Kaipara Channel (Fig. 2-6B) (Irwin and Eade, 1984b). These two features are the most significant submarine conduits within the NKCM although there are several smaller canyons on the continental slope between Kaipara and Hokianga harbours. The largest of these smaller canyons is the Hokianga Canyon, which extends between 700 and 1000 m water depth on the southern flank of Hokianga Terrace. The Hokianga Terrace occurs directly offshore from Hokianga Harbour between 350 and 800 m water depth and extends to 50 km from the coastline (Fig. 2-6A) (Irwin and Eade, 1984a); it is underpinned by the Hokianga basaltic massif (Fig. 2-4).

Two smaller banks occur further north between 500 and 700 m water depth, called the Whangape and Herekino Banks (Irwin and Eade, 1984a). These banks are located c. 40 and 60 km north of the Hokianga Terrace, respectively. West and northwest of Tauroa Point, at the southern end of Ninety Mile Beach, is another pair of much smaller banks known as the North and South Ahipara Banks that are located between 50 and 100 m depth (Irwin and Eade, 1984a). All of these banks also sit above basaltic volcanoes (Fig. 2-4).

In Figure 2-7 bathymetric profiles for each of the transects (A-G) are shown. Transect A has a flat, gently sloping shelf with a sharp shelf-slope break at c. 25 km from the coastline in c. 145 m of water (Fig. 2-7A and Table 2-2). The slope is relatively steep when compared to the shelf with an increase of 550 m water depth (150-700 m) out to 40 km from the coastline. Five of the seven sample sites are on the shelf with one at the shelf edge and the other on the upper slope.

Transect B also has a flat, gently sloping shelf with the shelf break at 145 m depth some 18 km from the coastline and a steeply inclined section of slope between 18 and 22 km where the water depth increases from c. 160-250 m (Fig. 2-7B and Table 2-2). The rest of the slope has a less accentuated increase in depth. At 40 km from the coastline (the extent of transect A's profile) the slope is at 600 m water depth compared to a slightly deeper 700 m along transect A (Table 2-2). The slope decreases in gradient further at >1100 m water depth. Four of the ten samples occur on the shelf with five on the slope and the tenth sample near the shelf-slope break.

The shelf along transect C has a steeper slope and is more uneven than transects A and B with a sharper increase in depth from the shore out to 50 m water depth. The shelf edge is c. 21 km from the coastline and is not as well defined with a less apparent break in gradient (Fig. 2-7C and Table 2-2). At 40 km from the coastline the slope is at c. 400 m water depth (Table 2-2). This shows a steady northwards decrease in the water depth that occurs 40 km from the coastline. Four of the eight samples occur on the shelf, three on the slope and another near the shelf-slope break.

Along transect D the shelf is still relatively gently sloping although it has a reasonably uneven surface when compared to transects A and B (Fig. 2-7D and Table 2-2). The shelf edge is slightly further offshore at c. 22 km from the coastline with a less distinct change in gradient and less steeply inclined slope than transects A-C (Table 2-2). At 40 km from the coastline the slope depth is c. 400 m and four of the eight samples occur on the shelf, three on the slope and one at the shelf-slope break.

Transect E has a very wide and relatively flat shelf with a shelf edge which occurs at c. 54 km from the coastline and is not defined by a sharp increase in water depth (Fig. 2-7E). At 40 km from the coastline the water depth is c. 150 m, considerably shallower than at the same distance from the coastline along transects A-D (Table 2-2). There are three samples on the shelf, two on the slope and one at the shelf-slope break.

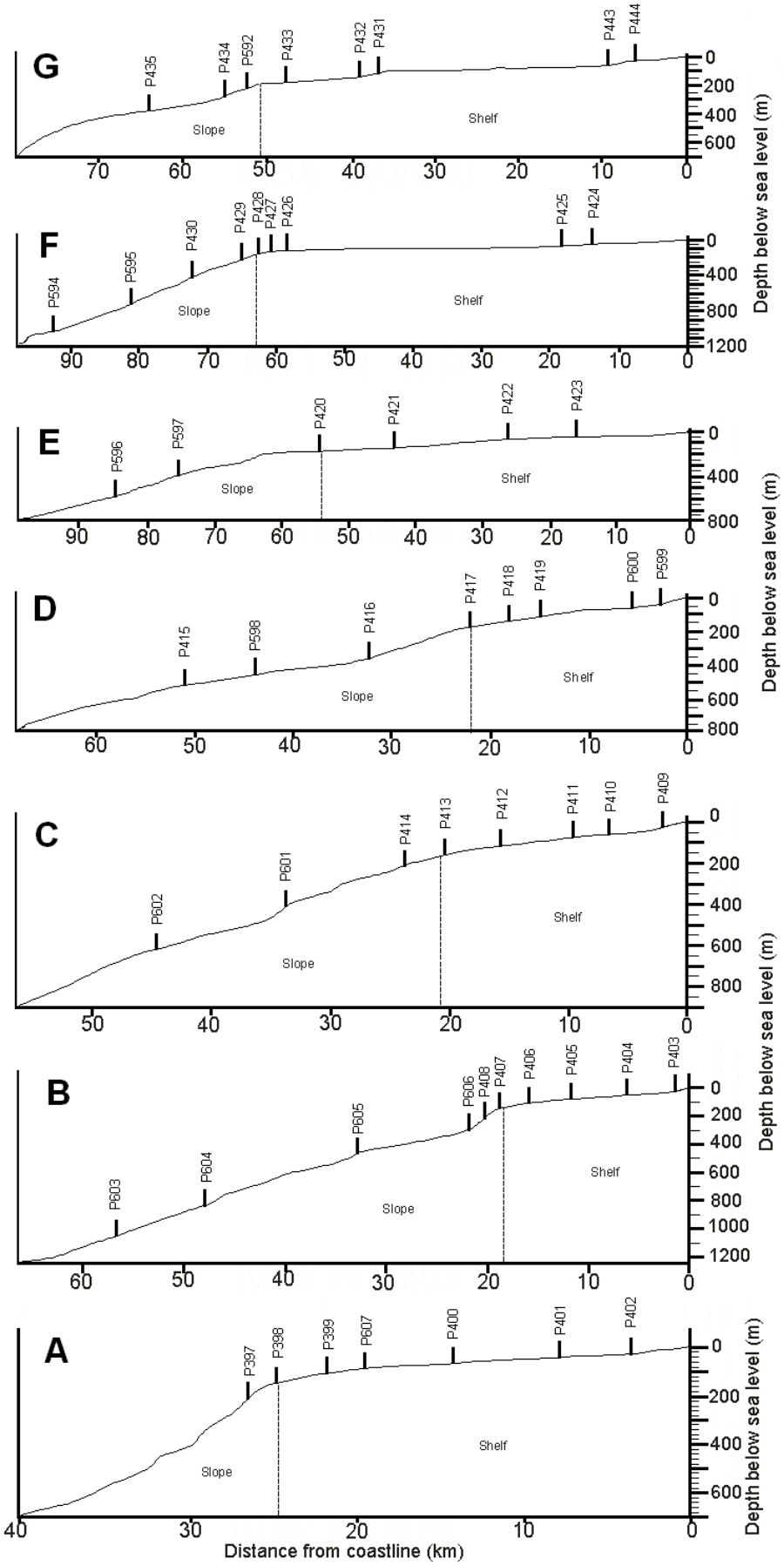

Figure 2-7. Bathymetric profiles for the seven transects (A-G) along the NKCM. Location of transects shown in Fig. 1-1 and 3-1.

Transect F also has a very wide and flat shelf with a relatively gentle transition to the slope at 63 km from the coastline (Fig. 2-7E and Table 2-2). The shelf is wider and the slope slightly steeper than transect E, which has a similar overall profile. At 40 km from the coastline the water depth is c. 200 m (Table 2-2) with four samples on both the shelf and slope and one at the shelf-slope break.

Transect G also has a wide shelf but is considerably more uneven when compared to transects E and F, with sizeable increases in water depth (c. 50 m) between 5 and 10 km and between 35 and 40 km from the coastline, while the shelf in between these areas of increase is relatively flat (Fig. 2-7G). The shelf edge is not as well defined as in transect F and the slope has an unusual profile at >300 m water depth where the gradient increases significantly. At 40 km from the coastline the water depth is 150 m (Table 2-2) with four samples on each of the shelf and slope.

Table 2-2. Summary of the shelf-slope boundary depths and distances as well as water depth at 40 km from the coastline for the seven NKCM transects.

Transect	Shelf-slope depth (m)	Shelf-slope distance from coastline (km)	Water depth at 40 km from coastline (m)
A	145	25	700
B	145	18	600
C	160	21	400
D	180	22	400
E	180	54	150
F	175	63	200
G	185	50	150

2.4 CLIMATE

New Zealand has a temperate climate and the dominant winds across the country are from the west and southwest (Fig. 2-8) (Schofield, 1970; Carter, 1975; Heath, 1985). Northern New Zealand has a maximum annual temperature of 24-28˚C and a mean annual wind speed of 5.2 ms^{-1}, although speeds are significantly higher at Cape Reinga where they reach between 8 and 10 ms^{-1}. Gale force winds occur on an average of 5 days per year with most between May and August, but have occurred up to 61 days per year (1964). The mean sea level pressure in northern

New Zealand is 1016 hpa (at 9 am) and the mean annual rainfall is 1399 mm (obtained from raw data from National Climate Database, NIWA website).

2.5 WAVE CLIMATE

The westerly winds which dominate New Zealand mean that the southern and western continental margins are the most exposed and experience a high-energy wave environment dominated by swell waves from the south and southwest and

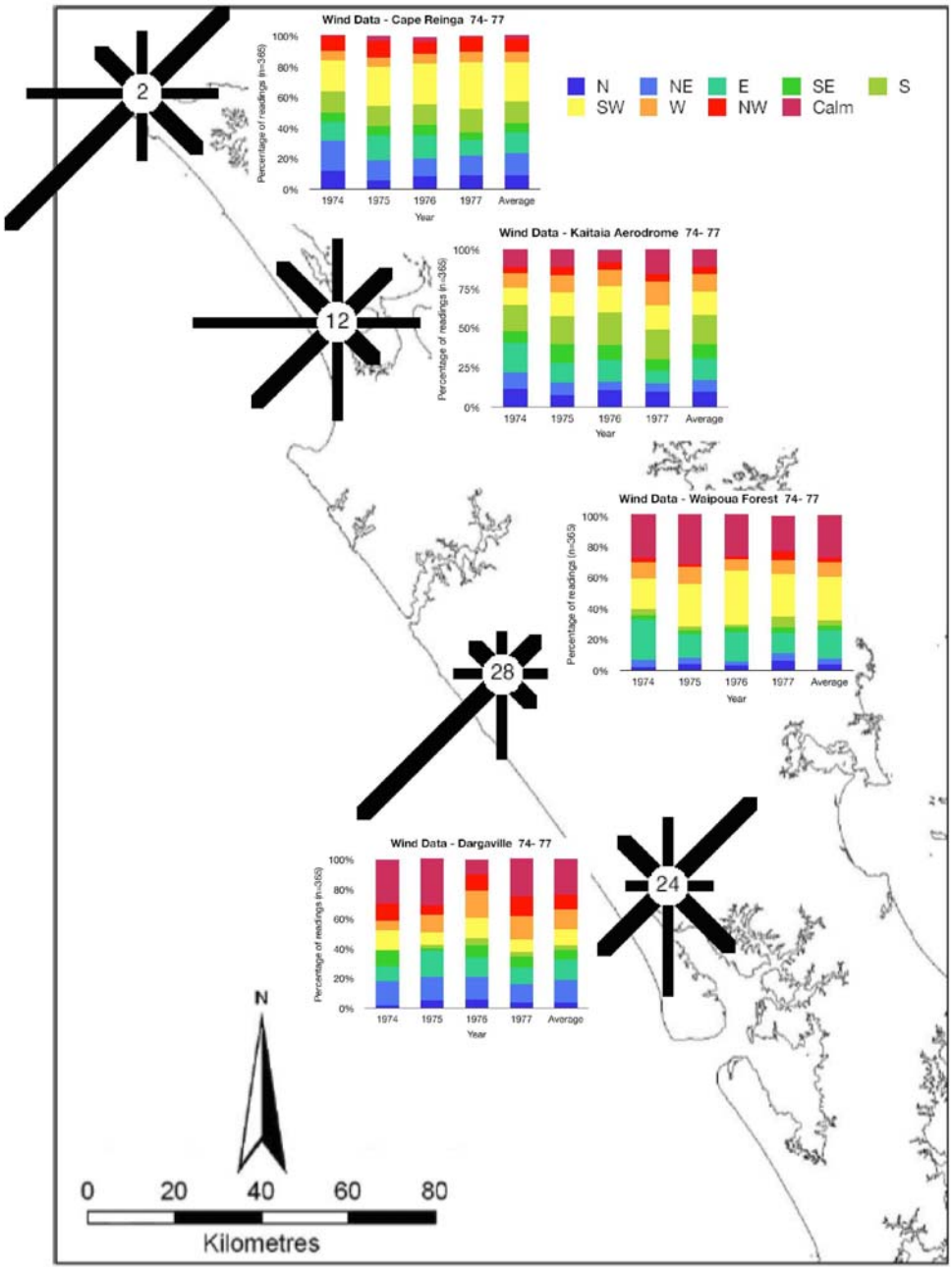

Figure 2-8. Percent frequency of surface wind directions at four sites in Northland (Cape Reinga, Kaitaia, Waipoua Forest and Dargaville) from 1974-1977. Wind rose bars illustrate the direction the wind came from and the number in the centre of each rose is the number of calm days per year (made using raw data from National Climate Database, NIWA website).

locally generated storm waves generated from north of New Zealand (Carter, 1975; Heath, 1982, 1985; Nelson et al., 1988). The deep-water swell waves originating from the south of New Zealand have wave heights of 3.5-4.5 m and wave periods of 10-12 s compared with 1.0-3.0 m and 4-8 s respectively for storm waves generated from the northeast (Heath, 1982). The swell waves increase slightly in wave height during winter although no significant seasonal variation is observed in the storm waves generated from the northeast. Southern generated swell waves do not reach the northern coastline between North Cape and East Cape and this area is instead exposed to waves from the northeast with wave heights of 0.5-1.5 m and wave periods of 5-7 s (Heath, 1982).

2.6 TIDAL CURRENTS

Tidal currents, induced by the gravitational attraction of the moon and sun on water, travel around New Zealand anticlockwise at high tide and clockwise at low tide (Heath, 1982). They consist primarily of a M_2 tide that propagates as a trapped wave along the New Zealand continental shelf with a period of 12.42 hours and a S_2 tide that travels as a standing wave on the west coast of New Zealand with a period of 12 hours (Stanton, 1973; Heath, 1982). As a result, tidal currents along the west coast move southwards on a rising tide and northwards on a falling tide (Stanton, 1973).

The tidal currents around the New Zealand continental shelf are significant enough that changes in the direction and speed of the water flow can be observed over a tidal cycle (Heath, 1982). However, these currents are mainly incapable of transporting sediments across the open shelf (Carter and Heath, 1975; Heath, 1982). In areas where the tidal currents are restricted or where the phase changes occur rapidly as a result of the low and high tide occurring simultaneously on either side of New Zealand, these currents are strong enough to transport sediment (Heath, 1982). The speed of the tidal flow on the central western shelf at Taranaki reaches c. 20 cms^{-1}, although this area of the western shelf is affected by strong tidal currents through Cook Strait (50 cms^{-1}) (Carter and Heath, 1975). The

average tidal current through the entrances of Kaipara and Hokianga harbours reaches 1.12 and 0.81 ms^{-1}, respectively (Hicks and Hume, 1996).

2.7 OCEANOGRAPHIC SETTING

New Zealand is located in the convergence zone of two main surface current systems, namely the Trade Wind Drift from the northeast and the West Wind Drift from the southwest (Brodie, 1960; Stanton, 1969; Carter, 1975). The Trade Wind Drift comprises subtropical southwest Pacific water that is moving southwestwards towards northern New Zealand while the West Wind Drift involves cold sub-Antarctic water that is moving northeast towards southern New Zealand (Fig. 2-9) (Carter, 1975).

The Trade Wind Drift is deflected off the eastern side of the Australian continent in the Coral Sea to form a southward moving current called the East Australian Current (Fig. 2-9) (Stanton, 1969, 1972; Carter, 1975; Heath, 1985). This current forms anticyclonic eddies along eastern Australia until it meets the northeastwards flowing West Wind Drift at the Subtropical Convergence Zone off the east coast of Tasmania (Heath, 1985). This convergence results in formation of the northeastward moving Tasman Current which is present offshore of the west coast of both North and South Islands (Fig. 2-9) (Brodie, 1960; Stanton, 1969, 1972; Carter, 1975). A section of the East Australian Current separates at about 34ºS and moves eastwards towards northern New Zealand (Stanton, 1969, 1972).

The Tasman Current separates west of New Zealand at 44ºS to form a southern component called the Southland Current that flows south of New Zealand and a northern component called the Westland Current that flows northwards along the west coast of New Zealand (Fig. 2-9) (Stanton, 1972; Carter, 1975; Heath, 1982, 1985). The Southland Current flows around the bottom of the South Island and up the east coast while the Westland Current flows up the west coast of the South Island (Brodie, 1960; Carter, 1975; Heath, 1985; Hume and Nelson, 1986). At the northern end of the South Island the Westland Current splits into the D'Urville Current which flows southeastwards into Cook Strait and a lesser northward

flowing current (Fig. 2-9) (Brodie, 1960; Carter, 1975; Heath, 1982). This northward flowing current is still termed the Westland Current and continues up the west coast of the North Island (Carter, 1975; Schofield, 1975; Heath, 1982). The Westland Current likely extends as far north as Kaipara Harbour, although its extent has probably shifted up and down the coast over time with changing weather patterns altering the strength of the current (Schofield, 1975).

The Trade Wind Drift and the East Australian Current interact with the northernmost tip of New Zealand to form the southwards flowing West Auckland Current, East Auckland Current and East Cape Current (Fig. 2-9) (Carter, 1975; Heath, 1985). The West Auckland Current flows from the north and west of Cape Reinga down the west coast of northernmost New Zealand (Brodie, 1960; Carter, 1975). The southernmost extent of the West Auckland Current coincides roughly with the entrance to Kaipara Harbour, beyond which a mixing zone with the

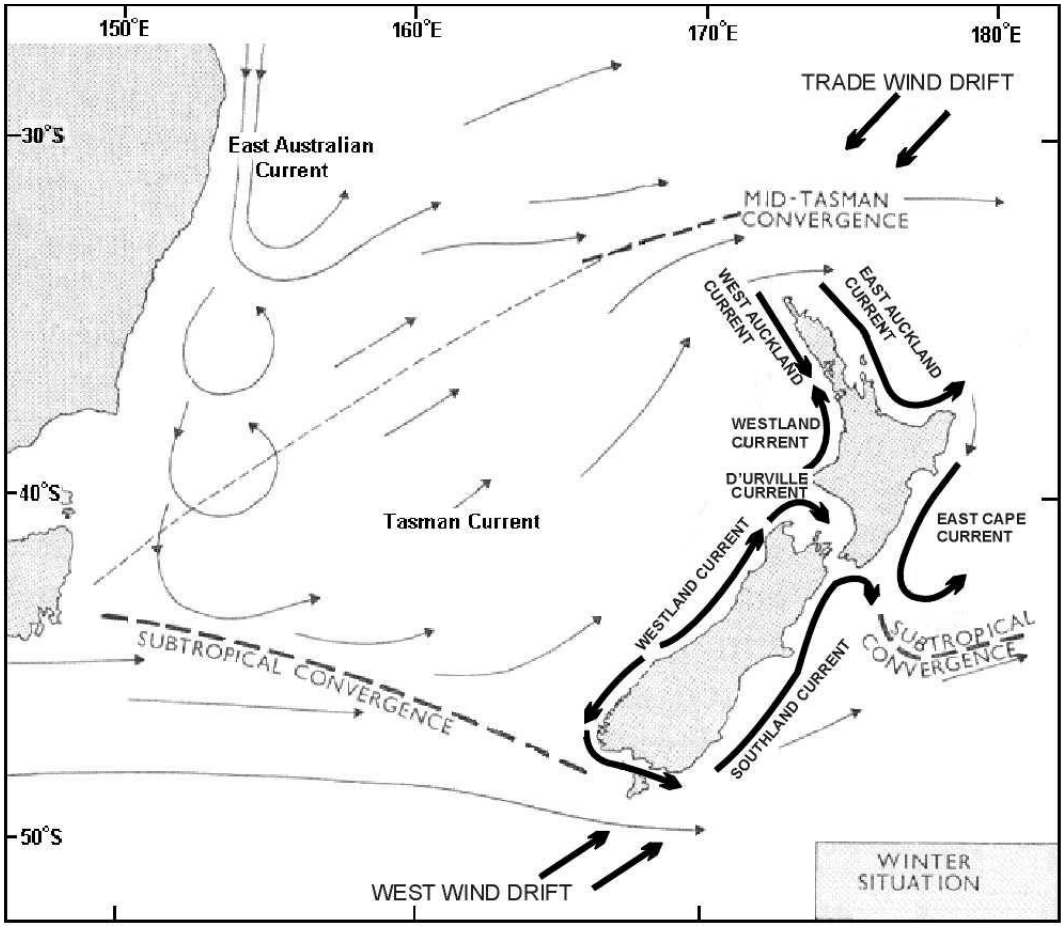

Figure 2-9. Surface circulation in the Tasman region showing the position of the Subtropical Convergence, the main regional currents (West Wind and Trade Wind drifts) and the local currents around New Zealand (adapted from Stanton, 1972 and Carter, 1975).

Westland Current extends as far south as Raglan Harbour (Summerhayes, 1969; Hume and Nelson, 1986), and at times may even reach as far south as Cape Egmont (Stanton, 1972). Both the East Auckland Current and the East Cape Current move down the east coast of the North Island (Carter, 1975).

The location of the converging Westland and West Auckland Currents varies along the coastline and this variation reflects changes in the local weather conditions (Brodie, 1960; Schofield, 1975). For example, stronger southerly winds allow the Westland Current to extend further north as less of the current is deflected into the Cook Strait as the D'Urville Current (Brodie, 1960). The coastal profile of the western North Island, particularly north of Cape Egmont, along with the distribution of heavy minerals sourced from Mount Taranaki and its deposits, support sediment transport northwards along the west coast (Summerhayes, 1969). However, under normal coastal conditions the Westland and West Auckland Currents do not reach velocities capable of transporting sediment (Carter, 1975). When combined with storm conditions and tidal currents these oceanic currents become capable of moving fine sand and often coarser grain sizes at most shelf depths (Carter, 1975).

Locally, upwelling currents as suggested by lower surface temperatures and salinities, occurs along the west coast of the North Island as westerly winds are deflected northeastwards by the ranges which extend along sections of the west coast (Stanton, 1972, 1973). Upwelling is particularly strong at Cape Reinga and over parts of the Three Kings platform where it is intensified by strong tidal currents (Stanton, 1972). At Three Kings platform the upwelling is also produced when the coastal currents strike the southwestern edge of the platform forcing nutrient-rich water into shallow water from water depths greater than 100 m (Stanton, 1972). Weak upwelling along the Northland coast near Tauroa Point is documented by Stanton (1973) where the 19 and 20˚C isotherms and the 35.5‰ isohaline show an upward trend over the shelf with inshore waters generally cooler than those offshore.

2.8 SEAWATER PROPERTIES AND PLANKTON BIOMASS

Off Northland the annual summer (February) sea surface temperature varies between 20 and 25˚C while the summer surface salinity ranges from 35.5-35.8‰ (Fig. 2-10A) (Garner, 1969; Heath, 1982; Chiswell, 1994). Surface salinity may be reduced in some coastal areas by freshwater dilution, such as where the Waikato River enters the coast west of Auckland (Garner, 1969). A well-defined thermocline forms during summer with a c. 20 m thick upper mixed layer and a bottom layer that rapidly decreases in temperature to reach an average bottom

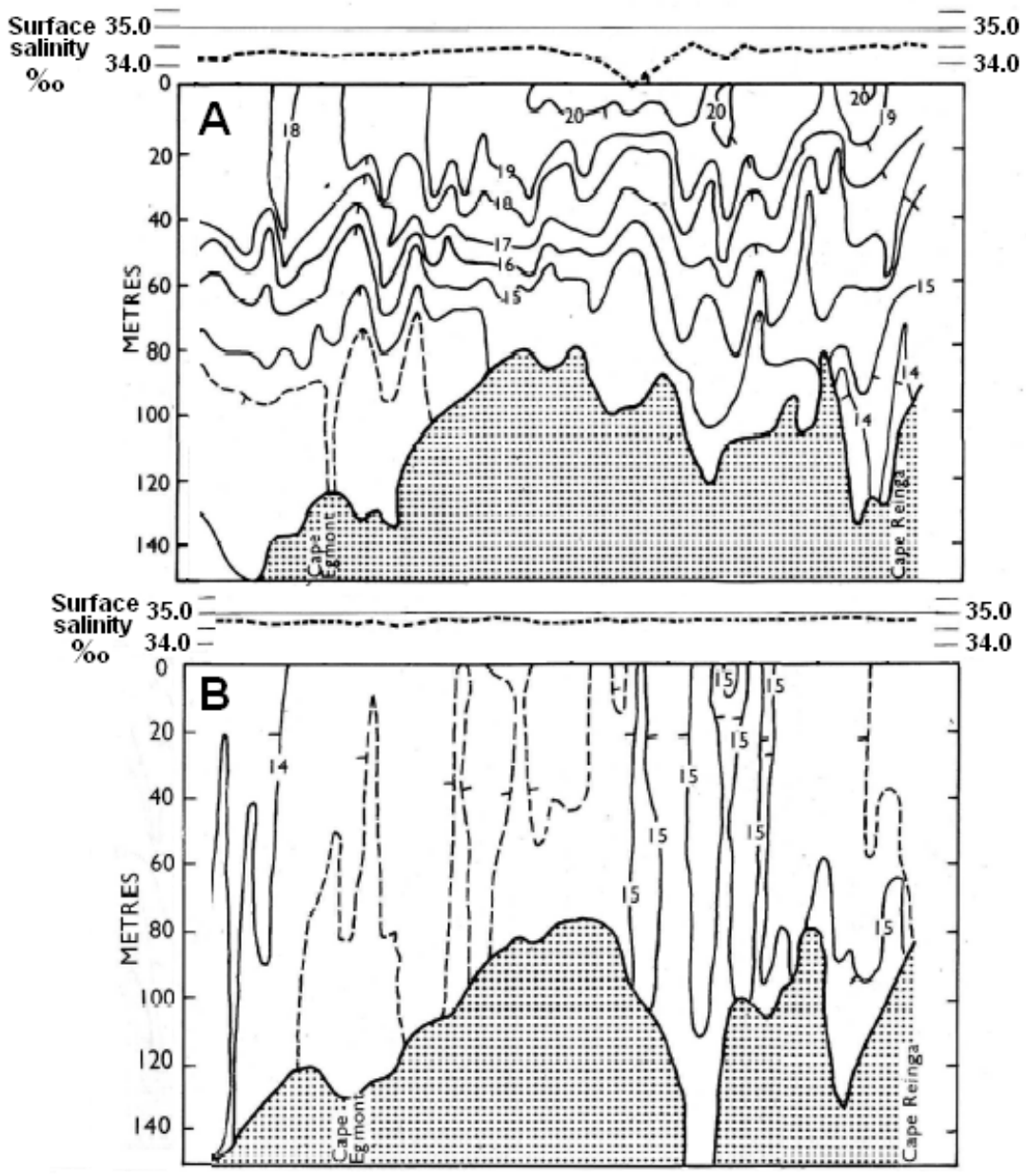

Figure 2-10. Vertical cross sections of temperature (˚C) and salinity (**‰**) in (A) summer and (B) winter in roughly south to north profiles between Cape Egmont and Cape Reinga (adapted from Garner, 1969). Dotted area is sea floor bottom and dashed lines represent half a ˚C.

temperature of 13.5-15.0˚C (Fig. 2-10A) (Garner, 1969). The winter (August) sea surface temperature is approximately 16-18˚C off Northland while the surface salinity shows little seasonal change (Garner, 1969; Chiswell, 1994). A vertical isothermal structure dominates the water column as a result of convective overturn destroying the summer thermocline (Fig. 2-10B) (Garner, 1969; Chiswell, 1994). The winter bottom temperature is on average 0.5˚C warmer than the summer bottom temperature (Garner, 1969).

Phytoplankton and zooplankton form the base of the food chain in the marine environment. In general, their biomasses are relatively low in the seas along western Northland, certainly in comparison with areas of upwelling in eastern and southern New Zealand. The spring bloom of phytoplankton in New Zealand occurs between late August and October with chlorophyll *a* (measure of phytoplankton biomass) concentrations reaching c. 0.50-1.00 $mg.m^{-3}$ in very shallow water (<30 m) off Northland (Fig. 2-11A) (Bradford and Roberts, 1978). The chlorophyll *a* concentration decreases offshore to 0.25-0.50 $mg.m^{-3}$ between c. 30 and 200 m water depth and to 0-0.24 $mg.m^{-3}$ at greater than c. 200 m water depth (Fig. 2-11A). The zooplankton biomass is much larger with between 25 and greater than 300 $mg.m^{-3}$ along western Northland, then decreasing offshore as the phytoplankton biomass does (Fig. 2-11A). The highest concentration of zooplankton biomass is offshore from Kaipara Harbour (>300 $mg.m^{-3}$).

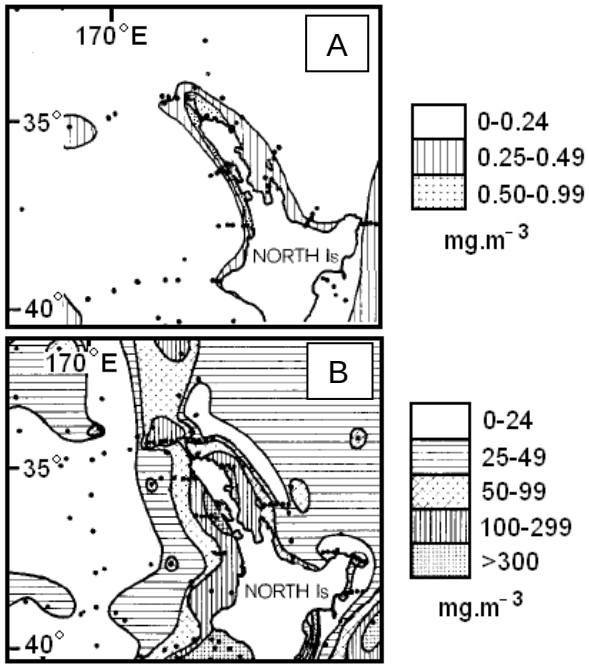

Figure 2-11. Distribution of (A) chlorophyll *a* and (B) zooplankton biomass ($mg.m^{-3}$) off North Island, New Zealand (Bradford and Roberts, 1978).

2.9 SEDIMENTATION ON WESTERN SHELF OF NORTH ISLAND

The western continental margin of the North Island is an area of active modern sedimentation dominated by terrigenous sediments, but locally including biogenic sediments. Terrigenous sedimentation is high due to the active plate boundary through New Zealand resulting in considerable uplift and erosion and volcanism (Nelson et al., 1988; Gillespie and Nelson, 1996). Biogenic sedimentation becomes prominent (>70% $CaCO_3$) where terrigenous sedimentation rates are low as occurs off northernmost New Zealand on the Three Kings platform and more locally on Wanganui shelf (Nelson et al., 1982; Nelson et al., 1988; Gillespie and Nelson, 1997).

The western continental margin of the North Island consists of a gently seaward dipping continental shelf out to the shelf break at about 130 m water depth (McDougall and Brodie, 1967; Norris, 1972; Carter, 1975; Hume and Nelson, 1986). The shelf width varies considerably from 16 to 64 km, while locally, as off Wanganui, it can reach over 160 km wide (Carter, 1975). The western North Island shelf covers an area of 250 000 km^2 to a depth of 200 m (Griffiths and Glasby, 1985). The continental slope steepens to slopes of 2 to 10º and is diversified by canyons and terraces intersecting the slope margins (Carter, 1975). The base of the slope along the western margin terminates between 500 and 4000 m water depth (Carter, 1975).

The North Island supplies some 13-14 million tonnes of river-derived sediment to the western continental shelf of the North Island from a total catchment area of approximately 44 000 km^2 (Fig. 2-12) (Griffiths and Glasby, 1985). The western shelf is bordered along much of the coastline by Mesozoic basement rocks, Cenozoic terrigenous-dominated sedimentary formations and Quaternary basaltic/andesitic volcanoes (Hume and Nelson, 1986). There are four major rivers that supply the western shelf along with several smaller, but nevertheless significant, rivers (Griffiths and Glasby, 1985). The four main rivers are the Waikato, Waitara, Mokau and Wanganui Rivers, while the Wairoa, Awakino and Patea Rivers are more locally important (Fig. 2-12) (Griffiths and Glasby, 1985).

Modern sedimentation on the western continental margin of the North Island is dependent on the shelf hydraulic regime and the rate of supply of sediment to the shelf (McDougall and Brodie, 1967; Carter, 1975). Terrigenous sands and muds generally dominate along this margin with relatively small amounts of included carbonate (shell) material (McDougall and Brodie, 1967; Carter, 1975; Hume and Nelson, 1986; Nelson et al., 1988). Across the western margin the carbonate content of bottom sediments shows an overall increase with increasing water depth beyond the shelf, where terrigenous mud is replaced by foraminiferal-nannoplankton-rich oozes (Nelson et al., 1988).

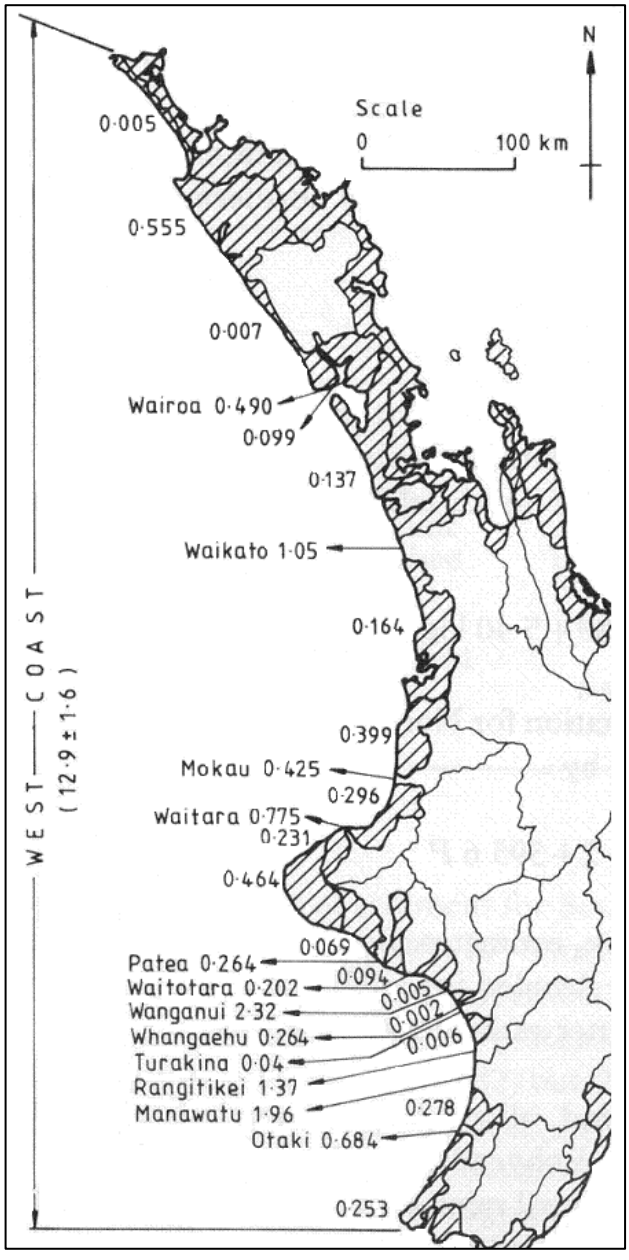

Figure 2-12. River-derived suspended sediment input to the western continental shelf, North Island (adapted from Griffiths and Glasby, 1985). All sediment loads multiplied by 10^6 tonnes per year. Bedload quantity calculated as 3% of the suspended sediment amount.

2.9.1 Shelf sectors

For convenience of discussion the western continental margin can be divided into five main shelf sectors as defined by Hume and Nelson (1986): Three Kings Shelf, West Auckland Shelf, Waikato Shelf, Taranaki Shelf (includes three subdivisions) and Wanganui Shelf (Fig. 2-13).

2.9.1.1 Three Kings Shelf

The Three Kings Shelf (or platform), at 34ºS off northern New Zealand (Fig. 2-13), consists of shallow marine platforms covering 10 000 km^2 in area in less than 500 m water depth (Nelson et al., 1982, 1988). The platform consists of the mainland shelf as well as submarine ridges and banks centred about the Three Kings Islands (Fig. 2-14) (Nelson et al., 1982). Modern sedimentation rates are extremely low on the Three Kings Shelf and the shelf is starved of sediment input as no major rivers discharge onto the coast and river sediment is trapped within coastal embayments or in the nearshore sand prism (Summerhayes, 1969; Carter, 1975; Nelson et al., 1982; Griffiths and Glasby, 1985; Nelson et al., 1988).

Active upwelling and a high-energy wind and wave environment exist on the Three Kings Shelf and as a result the area is relatively high in nutrients and essentially lacks carbonate mud to a depth of 1500 to 3000 m (Nelson et al., 1982, 1988). The shelf is subjected to significant swell wave and storm conditions (Nelson et al., 1988), and the tidal currents across the platform are strong as the offshore banks and islands act to constrict the flow of water to reach speeds of 50 to 200 cm/sec (Nelson et al., 1982). The West Auckland Current moves southeast along Ninety Mile Beach influencing sedimentation on the platform while between Cape Reinga and North Cape the predominant currents move from west to east (Summerhayes, 1969). Sediment transport on the western shelf of the platform is mainly north to northwest (Summerhayes, 1969).

Coarse grained biogenic sands and gravels dominate the sediments in this area and consist primarily of molluscan bivalve, bryozoan and foraminiferal fragments on the shelf and foraminifera and calcareous nannoplankton on the slope

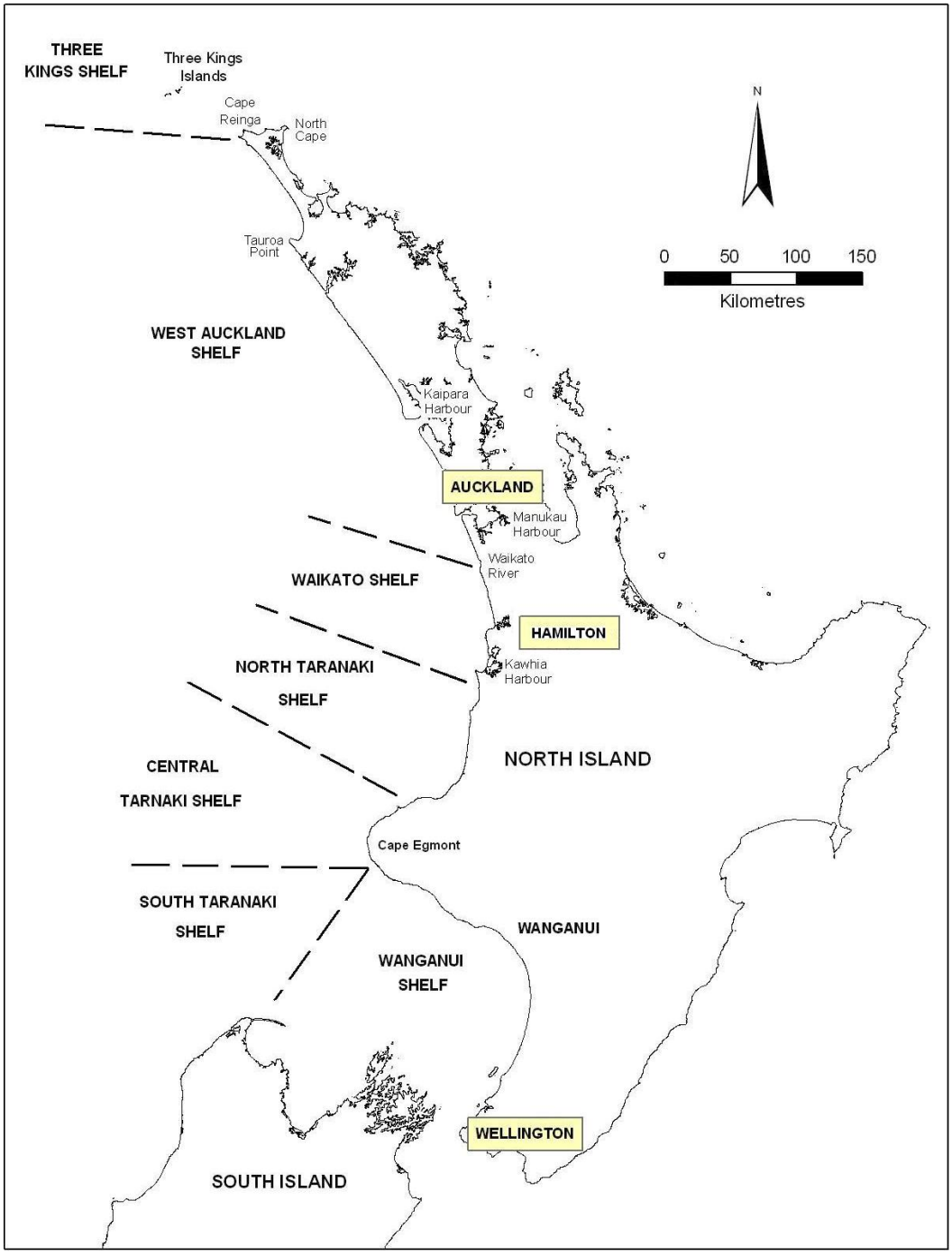

Figure 2-13. Location of the five shelf sectors off western North Island (adapted from Hume and Nelson, 1986). Note that the Taranaki Shelf is divided into three subsections: north, central and south.

(Summerhayes, 1969; Carter, 1975; Nelson et al., 1982; Griffiths and Glasby, 1985; Nelson et al., 1988). Smaller proportions of ahermatypic corals, calcareous red algae, gastropods, benthic foraminifera, serpulids, barnacles, echinoderms, brachiopods, sponges and pteropods are present on the platform (Summerhayes, 1969; Nelson et al., 1982). There is little to no grading in grain size with depth

and medium to very coarse sand sizes predominate across the platform (Nelson et al., 1982).

The sediments are skeletal carbonates which typically exceed 70% $CaCO_3$. They range in age from 20 000 years old to modern (Fig. 2-14) and consist primarily of a high to low-Mg calcite mineralogy (Summerhayes, 1969; Nelson et al., 1982, 1988). Active production of skeletal material appears to be restricted to less than 10% of the total platform area, mainly associated with hard or very coarse substrates and occurs in water depths from 50 to 200 m depth (Nelson et al., 1982).

The maximum $CaCO_3$ concentrations on Three Kings Shelf occur in the north and west although there is much local variation across the region (Fig. 2-14; Nelson et

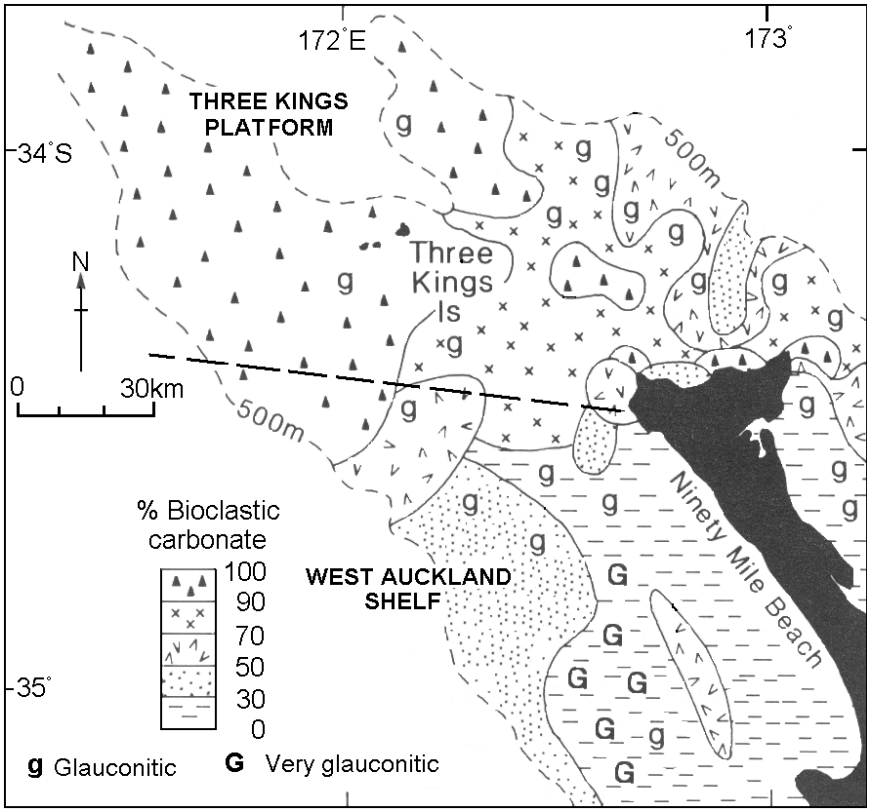

Figure 2-14. Distribution of $CaCO_3$ and glauconite across the Three Kings platform and northern West Auckland Shelf (adapted from Nelson et al., 1988).

al., 1982). To the south, the carbonate content of the sediments decreases rapidly into the terrigenous-rich Kaipara shelf and slope sediments offshore from Ninety Mile Beach (Nelson et al., 1982). The outer shelf of the platform below 80 m water depth consists of 50 to 75% $CaCO_3$ decreasing to 25 to 50% near the shelf edge (Fig. 2-14) (Summerhayes, 1969). The shallow nearshore environment involves predominantly terrigenous sediments with less than 25% $CaCO_3$.

The minor terrigenous component at Three Kings Shelf is dominated by quartz and plagioclase feldspar sourced from Ninety Mile Beach on the west coast and Parengarenga Harbour on the east coast (Nelson et al., 1982). Both these sources consist of quartzofeldspathic sand belts (Nelson et al., 1982). Heavy minerals make up less than 10% of the terrigenous sediment with hornblende, hypersthene and epidote being the most common (Summerhayes, 1969). Hornblende and epidote are relatively enriched on the western side of the platform (Summerhayes, 1969). Authigenic glauconite also occurs on the platform in small quantities as pellets and infills below 100 m water depth, while basalt and greywacke residual gravels are also present and locally important (Summerhayes, 1969; Nelson et al., 1982).

2.9.1.2 West Auckland Shelf

The West Auckland Shelf (as defined by Hume and Nelson, 1986) extends from the Waikato River mouth to the tip of Ninety Mile Beach and includes the north Kaipara continental margin (NKCM), the focus of this thesis study (Fig. 2-13 and 2-14). The shelf sediments are dominated by terrigenous and biogenic components with only two significant onland catchments from which new terrigenous sediment is supplied (Schofield, 1975). The first is the Waikato River catchment which drains 14 200 km^2 of land and the other is the Kaipara Harbour catchment including the Wairoa River which drains approximately 12 500 km^2 of land (Schofield, 1975). Despite the large volumes of sediment supplied to the coastline by the Waikato River (c. 1 million tonnes per year) only about 5% of this sediment occurs in coastal sand deposits. The remaining sediment is sourced from higher volume alongshore sources including black sand derived from Mount Taranaki over 200 km to the south (Schofield, 1970, 1975). Heavy minerals

comprise 1 to 9% of the Waikato River sediment while residual sediment consisting primarily of rhyolitic rock fragments, ranges from 28 to 48% (Schofield, 1970, 1975).

Along the West Auckland Shelf from the Waikato River mouth to the Manukau Harbour the sediment is primarily terrigenous with a characteristic increase in the quartz content but decrease in plagioclase feldspar northwards (Carter, 1975). The plagioclase feldspar is sourced from calc-alkaline volcanic rocks or reworked from volcanic-rich sediments such as those of the central North Island or Mount Taranaki (Carter, 1975). Glauconite is common on the outer northern section of this part of the shelf (Fig. 2-11). Biogenic sediments are also common with foraminifera, molluscan shells and bryozoan fragments dominating on the shelf edge while bryozoans dominate on the middle and inner shelf (Carter, 1975). Titanomagnetite, hornblende, clinopyroxene and orthopyroxene are the most common heavy minerals present across this section of the West Auckland Shelf and have also been sourced predominantly from the Mount Taranaki volcanic deposits (Carter, 1975; Churchman et al., 1988).

The Manukau Barrier forms a spit 40 km long across the Manukau Harbour and consists of well-sorted, coarse-grained sand which is dominated by titanomagnetite (Schofield, 1970). The proportion of heavy minerals on the seaward side of the barrier ranges from 64 to 100% compared with 0 to 11% on the landward harbour side (Schofield, 1970). The landward side of the barrier consists primarily of feldspar and quartz ranging from 30 to 65% of the sediment, strongly supporting a coastal source for the heavy mineral content of the sand (Schofield, 1970).

Further north along the West Auckland Shelf, between Manukau Harbour and Tauroa Point, is the Kaipara and Hokianga section of the shelf and slope. The predominant movement of sand occurs between 50 m water depth and the shore (Schofield, 1975) and as a result the mineralogy of the shelf sediment is considered identical to that of the terrigenous beach and dune sands along the Kaipara barriers due to a lack of information available on the shelf sediments (to be addressed by this thesis study).

The South Kaipara Barrier forms a 48 km long spit across southern Kaipara Harbour. The quartz content of the beach sand is relatively constant along the barrier, ranging from 50-62%, but the total feldspar content decreases from an average of 44% at the southern end of the barrier to 18% at the northern end (Schofield, 1970). The decrease in the total feldspar content may be the result of mixing with more quartz-rich sediment from Kaipara Harbour or the higher susceptibility of feldspar to being broken down during transport (Schofield, 1970, 1975). The heavy mineral content decreases from an average proportion of 60% in the south to less than 10% at the northern end of the barrier (Schofield, 1970). This considerable decrease in heavy mineral content is significant as it may delineate the northernmost extent of the black sands sourced from the erosion of the Mount Taranaki volcanic deposits. Within the Kaipara Harbour the quartz content is very high at 76%, with a heavy mineral content of only 3%, suggesting the Kaipara Harbour and Wairoa River catchment supply considerable volumes of quartz-rich sediment to the harbour (Schofield, 1975).

The North Kaipara Barrier forms an 80 km long spit across the northern half of the Kaipara Harbour. This barrier separates the Wairoa River from the open ocean, directing its sediment load into the Kaipara Harbour (Schofield, 1970). Along the barrier the quartz content ranges from 30-60% while the total feldspar content ranges from 26-52% (Schofield, 1970). The heavy mineral content is considerably lower than on the South Kaipara Barrier, being generally less than 10%, but it may range from 2-32% (Schofield, 1970).

The Kaipara slope occurs at water depths from 128-1670 m (McDougall, 1972). Calcareous biogenic sediment comprises a considerable proportion of the slope sediment and this proportion increases with depth (McDougall, 1972). At 128 to 300 m water depth the carbonate content ranges from 5-15% and this increases to 10-47% at 300-1400 m water depth. Between 1400 and 1670 m water depth the carbonate content has increased to 41-57% of the total sediment (McDougall, 1972). The calcareous biogenic sediment consists of molluscan shell fragments, echinoid spines, worm tubes, foraminifera and coccoliths (McDougall, 1972). The molluscan shell material occurs only on the outermost shelf and upper slope and is absent along the lower Kaipara slope (McDougall, 1972). Both benthic and

planktic foraminifera occur on the slope with the proportion of planktic to benthic foraminifera increasing with depth and distance from the shelf edge (McDougall, 1972).

Ninety Mile Beach extends from Tauroa Point in the south to Cape Maria van Diemen in the north and consists of brownish pink fine sands which include up to 90% quartz (Summerhayes, 1969; Carter, 1975). Along the shelf, well sorted fine to medium sized terrigenous sand occurs in parallel belts with authigenic glauconite present at depths greater than 100 m (Summerhayes, 1969). The quartz content along the shelf and beach is on average 60% while the total feldspar content ranges from 21-33% and heavy minerals are about 1% (Schofield, 1970). The beach profiles along Ninety Mile Beach suggest that longshore drift is to the north to Cape Reinga, but a low westerly trending ridge blocks this northward transport of sediment at the northern end of the beach (Summerhayes, 1969).

2.9.1.3 Waikato Shelf

The Waikato Shelf extends from the Waikato River to south of Kawhia Harbour (Fig. 2-13) (Hume and Nelson, 1986). The shelf has moderate rates of river sediment input at approximately 1 million tonnes per year (Griffiths and Glasby, 1985) and consists of a nearshore modern sand prism on the inner shelf which merges with relict terrigenous and biogenic sediments on the middle shelf and coarse sand on the outer shelf (Carter, 1975). The terrigenous sediment consists mainly of quartz and plagioclase feldspar but contains locally important proportions of volcanic and sedimentary rock fragments, including andesitic rock fragments sourced from Mount Taranaki to the south (Carter, 1975; Churchman et al., 1988). Mud comprises a minor fraction of the modern terrigenous sedimentation onto the Waikato Shelf as many of the main rivers discharge into harbours such as Raglan, Aotea and Kawhia Harbours where mud can be trapped. Nevertheless, plumes of suspended sediment may extend up to 20 km offshore from these harbours (Carter, 1975; Hume and Nelson, 1986). The clay fraction on the shelf has similar mineralogy to the clay in these harbours, implying a terrigenous source for the clay (Hume and Nelson, 1986). Kaolinite is a noticeable component of the clay fraction and is sourced from erosion of the Te Kuiti Group

coal measures and soils on Mesozoic rocks, while smectite is derived from erosion of Oligocene mudstones which consist of up to 80 to 90% smectite (Hume and Nelson, 1986). Biogenic sediment on the Waikato Shelf consists primarily of foraminiferal and coccolith tests which occur on the outer shelf to produce a carbonate proportion of 20-30% (Hume and Nelson, 1986).

2.9.1.4 Taranaki Shelf

The Taranaki Shelf extends from south of Kawhia Harbour to Cape Egmont and for the purpose of discussion may be divided into northern, central and southern regions (Fig. 2-13) (Hume and Nelson, 1986). The Taranaki Shelf is very wide (up to 160 km) and the shelf edge extends out to 250 to 300 m water depth (Carter, 1975). Terrigenous and biogenic sediments dominate the Taranaki Shelf with the terrigenous sediments composed mainly of quartz and plagioclase feldspar and locally important volcanic and sedimentary rock fragments (Carter, 1975). Modern terrigenous sedimentation on the Taranaki Shelf occurs generally at moderate rates, but locally high rates occur where large rivers discharge onto the shelf (Carter, 1975). Modern terrigenous sedimentation north of Cape Egmont is generally restricted to the inner shelf, primarily involving very fine sand (McDougall and Brodie, 1967; Hume and Nelson, 1986).

The middle shelf comprises mainly relict terrigenous sediment due to the wide nature of the Taranaki Shelf and the decreased capacity to transport large volumes of sediment out to the middle shelf (Carter, 1975; Hume and Nelson, 1986). This is accentuated on the southern Taranaki Shelf where little terrigenous sediment is deposited directly onto the shelf from North Island rivers (Hume and Nelson, 1986). Modern terrigenous mud deposition occurs across the Taranaki Shelf with suspended sediment plumes extending up to 40 km from the major rivers (Hume and Nelson, 1986). Clay minerals on the northern Taranaki Shelf are similar to those found in the onland catchment areas which consist of non-calcareous Miocene sandstones and mudstones that contain illite, chlorite and mixed layer clay minerals (Hume and Nelson, 1986). There are elevated levels of smectite present on the northern Taranaki Shelf which are thought to have been sourced from the onland Mahoenui Group (Hume and Nelson, 1986). On the central

Taranaki Shelf the major rivers supply volcanogenic material to the shelf as they drain andesitic volcanic rocks and tephra from Mount Taranaki (Hume and Nelson, 1986). Smectite is also common in this area, derived from the alteration of glassy volcanic material (Hume and Nelson, 1986).

The southern Taranaki Shelf is considerably different to its northern and central sectors as the terrigenous sediment is derived from both North and South Island sources (Hume and Nelson, 1986). Modern fine-grained terrigenous sands from North Island sources occur on the inner shelf with relict mud occurring further offshore on the middle shelf and fine sand on the outer shelf (Hume and Nelson, 1986). Andesitic gravels dominate in the nearshore zone surrounding Cape Egmont (Hume and Nelson, 1986). Clay on the southern Taranaki Shelf is predominantly sourced from the western South Island where the Westland Current has transported highly crystalline mica and chlorite northwards (Hume and Nelson, 1986). Large-scale erosion of the granites and schists of the Southern Alps has produced these large volumes of mica and chlorite (Hume and Nelson, 1986). Smectite is also present in the clay fraction and may be both terrigenous and authigenic, with the latter forming from the alteration of volcanic sediments (Hume and Nelson, 1986).

Biogenic sediment on the Taranaki Shelf consists of coarse-grained carbonate skeletal fragments, mainly of molluscs, bryozoans and benthic foraminifera (Hume and Nelson, 1986). The shelf generally has a carbonate content less than 15%, however on the middle shelf on the northern Taranaki Shelf, and outer shelf on the southern Taranaki Shelf, carbonate concentrations increase to 20-30% (Hume and Nelson, 1986). On the northern Taranaki Shelf molluscan and bryozoan fragments dominate while foraminifera and coccolith tests dominate on the southern Taranaki Shelf (Hume and Nelson, 1986).

2.9.1.5 Wanganui Shelf

The Wanganui Shelf is located south of Cape Egmont over an area of 5300 km^2 and consists of mixed terrigenous and carbonate sediment (Fig. 2-13) (Hume and Nelson, 1986; Gillespie and Nelson, 1996, 1997; Gillespie et al., 1998). The shelf

is relatively shallow and flat with water depths less than 125 m and a gradient less than 1º (Hume and Nelson, 1986; Gillespie and Nelson, 1996; Gillespie et al., 1998). The Wanganui Shelf is subjected to a mixed swell and locally generated wave environment and is influenced by the Westland and D'Urville Currents which transport upwelled water and sediment onto the shelf (Gillespie and Nelson, 1996; Gillespie et al., 1998). It includes localised areas of carbonate deposits which occur in close association with terrigenous sedimentary deposits (Nelson et al., 1988; Gillespie and Nelson, 1997). The inner shelf generally comprises a modern terrigenous sand prism which changes to terrigenous sand and gravelly muddy sand on the middle to outer shelf with a mud belt present off the south Wanganui coast (McDougall and Brodie, 1967; Gillespie and Nelson, 1996, 1997). Mud generally occurs on the deeper areas of the shelf at greater than 90 m water depth while coarse gravels dominate at middle shelf depths from 50 to 90 m water depth (McDougall and Brodie, 1967; Gillespie and Nelson, 1996).

Molluscan bivalve and bryozoan fragments dominate the carbonate deposits on Wanganui Shelf where they form a deposit approximately 2000 km^2 in area (Gillespie and Nelson, 1996, 1997; Gillespie et al., 1998). Bryozoans are only abundant at 50 to 80 m water depth on the middle shelf (Gillespie and Nelson, 1996). The carbonate content is on average about 50% but may be as high as 70% on the middle shelf where terrigenous sedimentation is low (Gillespie and Nelson, 1996; Gillespie et al., 1998). The terrigenous component of the Wanganui Shelf sediments has a high total mud content of up to 50% and a composition similar to the onland catchment geology (Gillespie and Nelson, 1997; Gillespie et al., 1998). Rock fragments make up an important component of the terrigenous sediment and are sourced from Mount Taranaki and the associated ancestral weathered volcanic cones (Gillespie and Nelson, 1996). The terrigenous sediment is derived from both North and South Island sources and is dominated by quartz and plagioclase feldspar (Gillespie and Nelson, 1996, 1997; Gillespie et al., 1998). Clay material is dominated by illite supplied from erosion of upper Miocene and Quaternary mudstones from the North Island and western South Island schists (Gillespie and Nelson, 1996, 1997). The sediment is dispersed across the shelf primarily during storms when the waves and tidal and oceanic currents combine to produce strong

currents which can erode and transport large volumes of sediment (Gillespie and Nelson, 1996, 1997; Gillespie et al., 1998).

2.10 SUMMARY OF PHYSICAL SETTING

Northland has a highly complex and varied geology which consists primarily of sedimentary and igneous Northland Allochthon rocks and Pleistocene and Holocene sediments with lesser outcrops of autochthonous Eocene-Oligocene sedimentary rocks, Miocene igneous and sedimentary rocks and Mesozoic basement rocks. The geological history of the Northland area is complex with rifting from Gondwanaland during the Cretaceous resulting in marine sedimentation followed by the development of the Australian-Pacific Plate boundary during the Late Oligocene. This was followed by the emplacement of the Northland Allochthon during the Late Oligocene and the commencement of basaltic arc volcanism during the Early Miocene. Marine sedimentation followed the culmination of this volcanism from the Middle Miocene until the Pliocene-Pleistocene.

The Westland Current dominates the oceanographic setting of the western continental margin of New Zealand, originating from the Tasman Current west of New Zealand. The West Auckland Current derived from the East Australian Current forms a much smaller and less regionally significant flow. These oceanic currents alone do not reach flow velocities great enough to induce sediment transport and must be combined with storm waves and tidal currents in order to achieve this at shelf depths. The western New Zealand continental margin is a high-energy wave environment dominated by swell waves from the south and southwest and locally generated storm waves from north of New Zealand. Tidal currents are also an important flow component and consist primarily of a M_2 tide that propagates as a trapped wave along the New Zealand continental shelf and a S_2 tide that travels as a standing wave on the west coast of New Zealand. These currents are also not capable of transporting sediment on the open shelf. However, where they are constricted or where low and high tides occur simultaneously on

either side of New Zealand, then these currents can become strong enough to transport sediment.

The western North Island continental margin is dominated by terrigenous sands and muds and more localised biogenic sediments and can be divided into five main sectors. These sectors consist of the carbonate dominated Three Kings Shelf, the terrigenous dominated West Auckland, Waikato and Taranaki Shelves and the mixed terrigenous-carbonate dominated Wanganui Shelf. The West Auckland Shelf contains the NKCM which is the focus of this thesis study.

Chapter 3

STUDY AREA, SAMPLE COLLECTION AND LABORATORY METHODS

3.1 INTRODUCTION

The north Kaipara continental margin (NKCM), bordering the eastern side of the Tasman Sea off western Northland between Kaipara Harbour and Cape Reinga, comprises a highly varied coastline and shelf-slope bathymetry (see Section 2.3). 54 surficial sediment samples and three piston cores were collected from the shelf and slope margin (Fig. 3-1) in June-July 1978 when a joint University of Waikato and New Zealand Oceanographic Institute (NZOI) cruise (No. 1077) on the old *Tangaroa* (Fig. 3-4A) was conducted to the Three Kings platform off northernmost New Zealand. The location of the sample and core sites was determined using a satellite navigation system on the vessel with an accuracy of approximately ± 500 m (Appendix B).

This chapter discusses the sample collection (Section 3.2) and laboratory methods (Section 3.3) used to gather and analyse the sediment samples from the NKCM.

3.2 SAMPLE COLLECTION

The RV *Tangaroa* commenced sediment sampling from the southern end of the study area and moved northwards in a zigzag pattern collecting samples P397 to P435 in chronological order until the cruise continued north onto the Three Kings platform (Fig. 3-2). Samples P592 to P607 were collected on return from the Three Kings platform.

Sediment samples were collected from the NKCM by four methods: orange peel grab, pipe dredge, a modified biological dredge and piston corer (Fig. 3-3, 3-4, Appendix B). The orange peel grab was used initially but with decreasing success as the vessel moved to the north because shell material prevented the jaws from

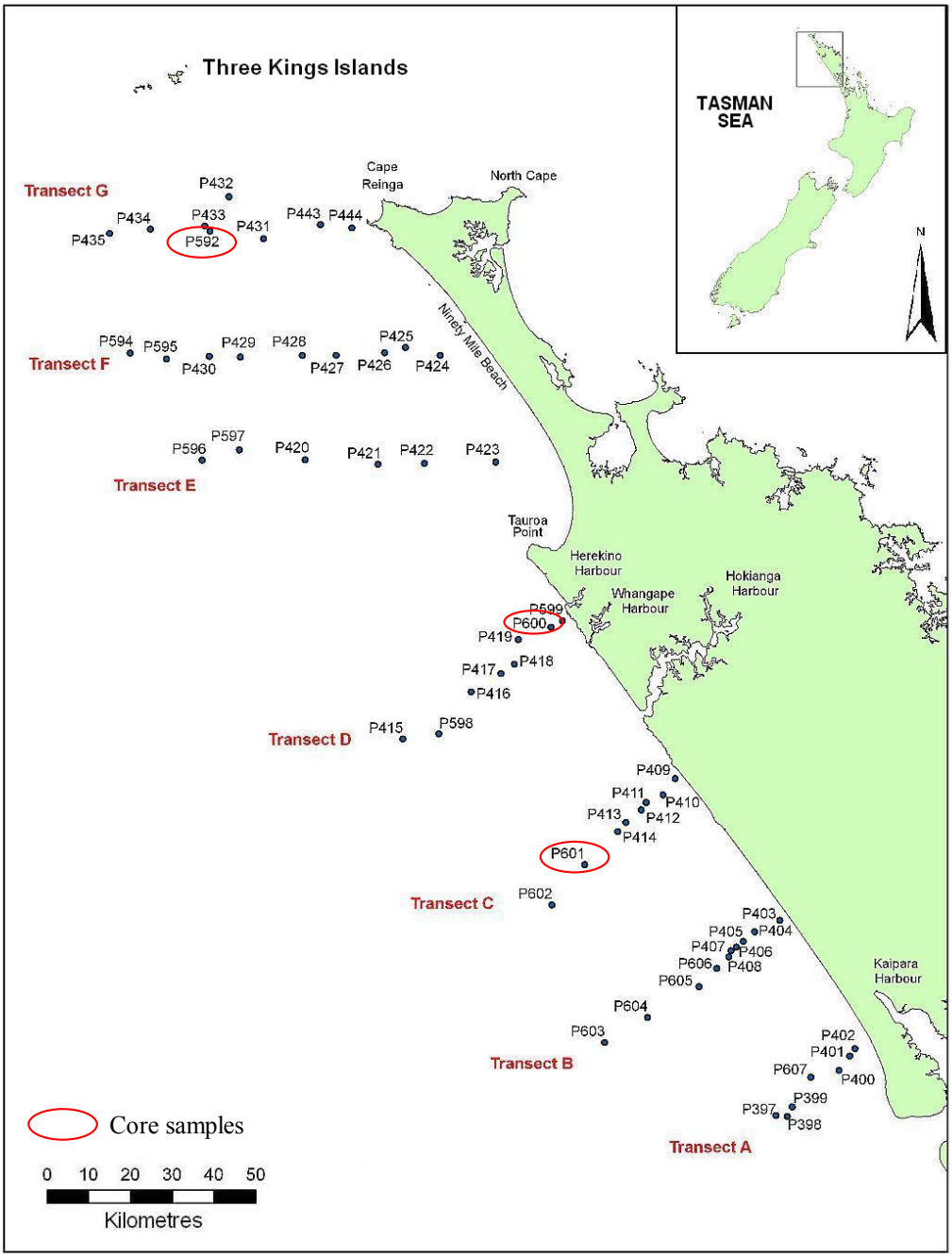

Figure 3-1. Location of sampling sites (surface and core) on the NKCM.

complete closure and some sediment washing occurred. The use of a pipe dredge became increasingly common from transect C (Fig. 3-3) as repeated attempts to retrieve representative sediment using the orange peel grab failed. The pipe dredge was used to collect sediment across transect G before it was lost on the Three Kings platform. A biological dredge was then modified, by incorporating a canvas liner, to successfully collect sediment from the remaining sample sites

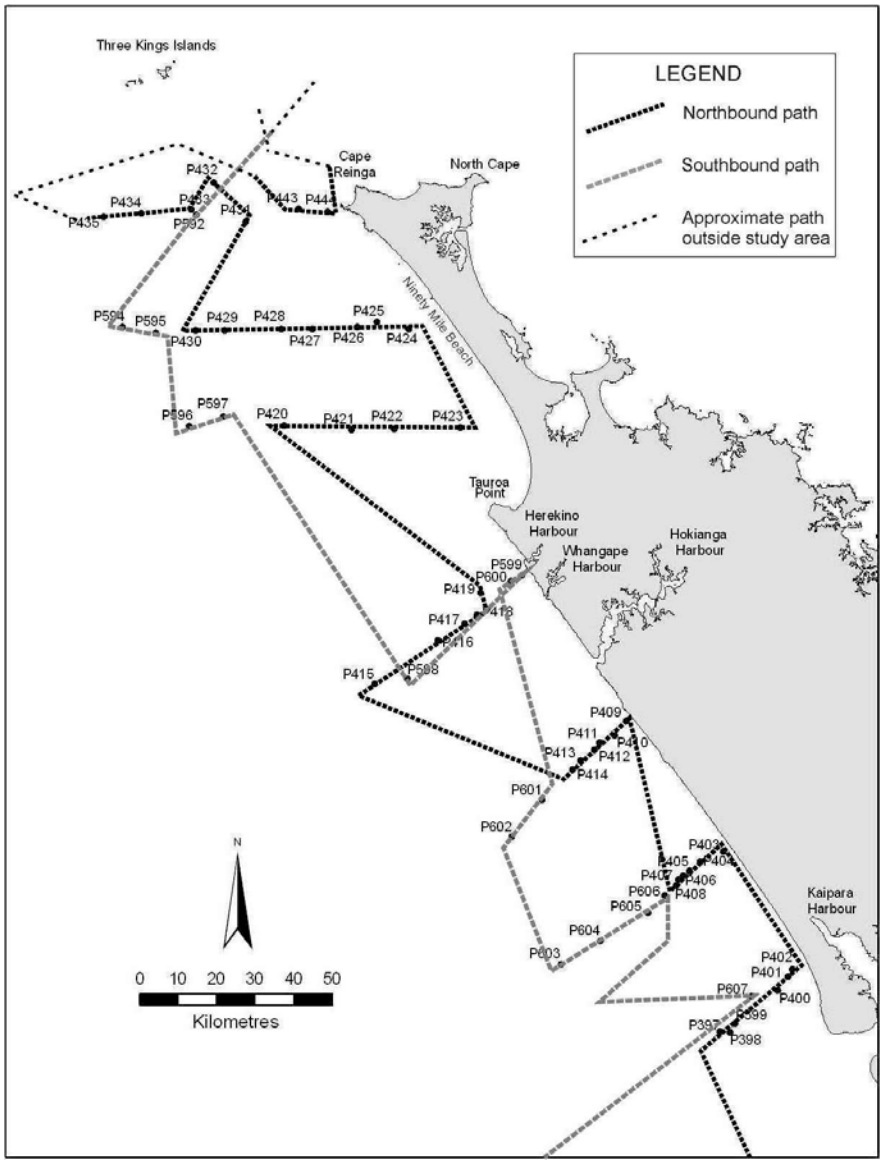

Figure 3-2. The path of the RV *Tangaroa* across the north Kaipara continental margin for NZOI cruise No. 1077 (adapted from Nelson, 1982).

(Fig. 3-4D). Three sediment cores (P592, P600, P601) were collected using a piston corer (Fig. 3-3) with three unsuccessful attempts to collect other cores from the NKCM., mainly because of their coarse texture.

The surface sediment samples were split into three: one for the NZOI (now NIWA) archives and the other two for the University of Waikato (Fig. 3-4C). Any excess sediment remaining after making these splits was sieved over a 2 mm mesh with the >2 mm gravel fraction retained and the rest of the sediment discarded (Nelson, 1982).

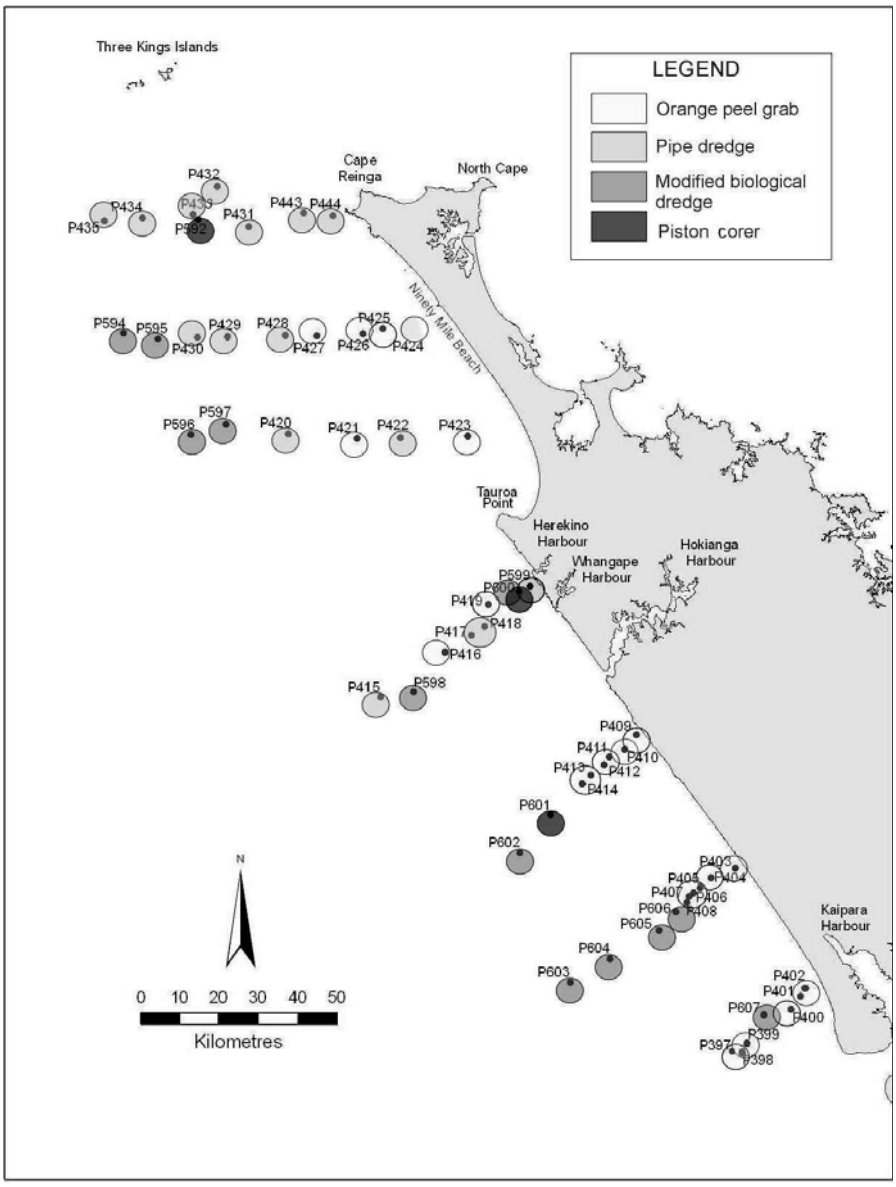

Figure 3-3. The four different sediment collection methods used at each of the sample sites within the study area.

3.3 MAIN LABORATORY METHODS

Laboratory methods were used to determine the weight percentages of gravel, sand and mud (Section 3.3.1), carbonate content (Section 3.3.2), sediment sorting (Section 3.3.3), heavy mineral fraction (Section 3.3.4), glauconite fraction (Section 3.3.5), mineralogy through x-ray diffraction (XRD) (Section 3.3.6) and grain mount petrography (Section 3.3.7). The methods used in thin section

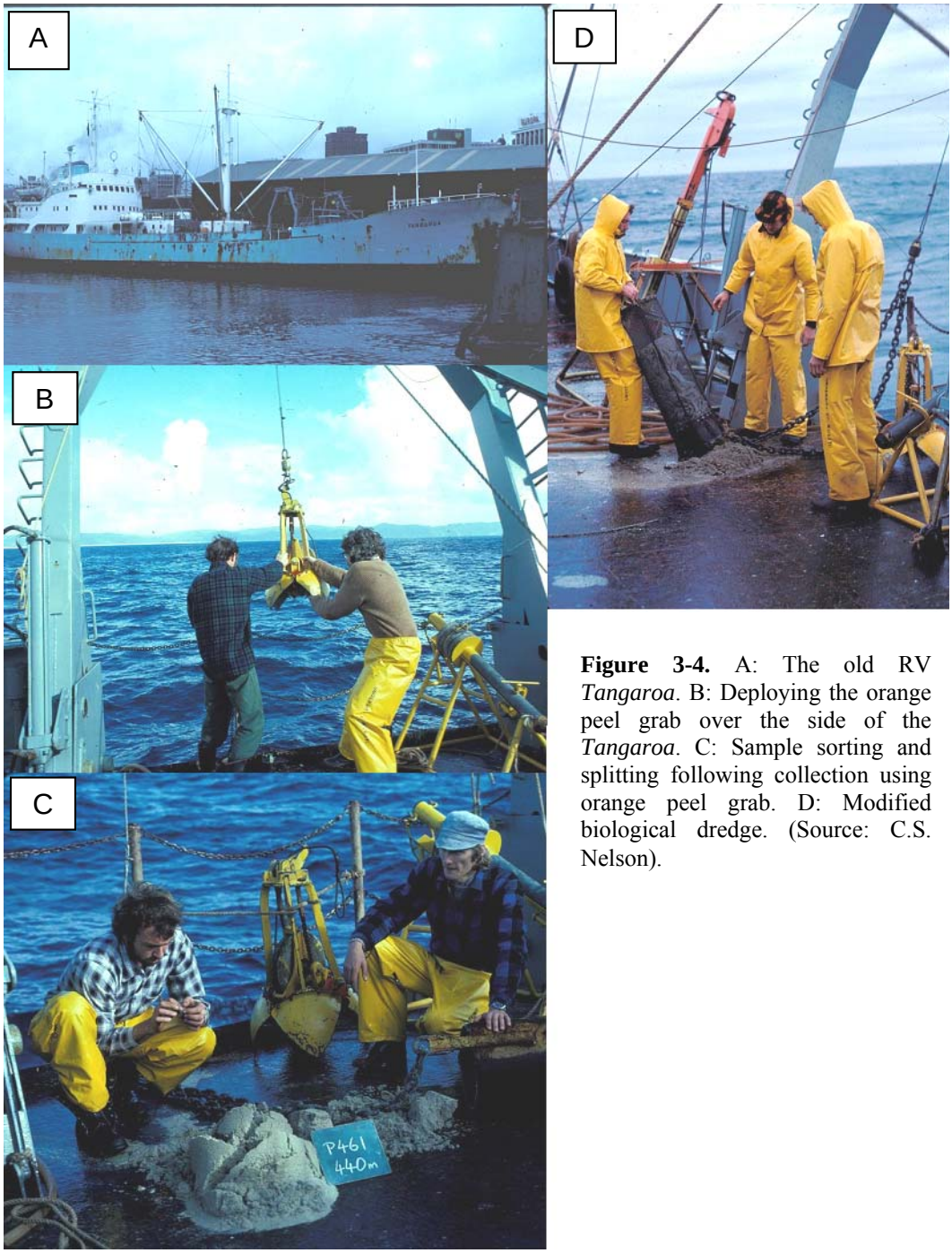

Figure 3-4. A: The old RV *Tangaroa*. B: Deploying the orange peel grab over the side of the *Tangaroa*. C: Sample sorting and splitting following collection using orange peel grab. D: Modified biological dredge. (Source: C.S. Nelson).

petrography (Section 3.3.8), cathodoluminescence (CL) petrography (Section 3.3.9) and microprobe analysis (Section 3.3.10) are also discussed.

3.3.1 Separation of gravel, sand and mud fractions

Washing of the surficial sediment samples with tap water to remove salt was conducted over a bucket with 2 and 0.063 mm sieves separating the sediment into the gravel (>2 mm), sand (0.063 to 2 mm) and mud (<0.063 mm) fractions

(Nelson, 1982). The gravel and sand fraction was dried on a labelled tray at between 50 and 60ºC in a drying cabinet before weighing to an accuracy of 0.01 g. The fraction was then stored in clear plastic screw top jars. The modal grain size classes were determined by sieving the gravel and sand fraction on an Endecott sieve shaker for 5 minutes using 0.5-1Φ interval sieves. In the small number of samples that contained mud, the mixture of water and mud from the bucket was transferred into a 1-litre cylinder where it was briskly stirred (Nelson, 1982). After 20 seconds of stirring, 20 ml of the suspension was removed at a depth of 20 cm using a pipette and was placed in a pre-weighed (±0.001 g) 50 ml beaker then dried and weighed to determine the weight of the mud fraction. The weight of mud in the original sample was determined by multiplying the weighed mud by 50 (Nelson, 1982). The separate weights of the gravel, sand and mud fractions were then converted to percentages.

3.3.2 Carbonate content

The percentage of carbonate in NKCM sediments was determined by removing the large carbonates (through sieving) and small carbonates (through acid digestion) from the total sediment. The weight of each of these fractions was combined to provide the total carbonate weight, which was divided by the weight of the total sediment to determine the carbonate percentage.

3.3.3 Sorting

The sorting values for the NKCM sediment were determined from logarithmic cumulative percent curves produced by plotting the grain size results from the sediment sieving. Following Folk (1968), the 5, 16, 84 and 95Φ percentiles were measured from these curves and used to calculate the sorting values and their classification using the equation below and Table 3-1:

$$\frac{84\Phi - 16\Phi}{4} + \frac{95\Phi - 5\Phi}{6.6}$$

Table 3-1. The sorting value ranges and their classifications used for NKCM bottom sediments.

Sorting Value	Classification
<0.35Φ	Very well sorted
0.35-0.50Φ	Well sorted
0.50-0.71Φ	Moderately well sorted
0.71-1.00Φ	Moderately sorted
1.00-2.00Φ	Poorly sorted
>2.00Φ	Very poorly sorted

3.3.4 Separation of heavy mineral fraction

After weighing, the fine and very fine heavy mineral sand fraction was separated from the light sand-sized minerals by sedimentation using tetrabromoethane (specific gravity of 2.94) in a steep-sided funnel. The tetrabromoethane was poured into the funnel, which was clamped tightly at the base, until three-quarters fill and covered with a glass plate. The bulk sediment samples were placed into the tetrabromoethane and stirred vertically several times with periods of settling in between. Once satisfied the darker heavy mineral fraction had settled at the base of the funnel, the clamp was released and the heavy minerals fed via a tube into a beaker before being washed with acetone on filter paper and dried. The process was repeated for the light minerals floating at the top of the tetrabromoethane and the percentage of light vs. heavy minerals was determined as a proportion of the bulk sample.

3.3.5 Separation of glauconite

Glauconite concentrates from five samples (P399, P416, P417, P420, P421) were separated initially to determine their chemical composition using X-ray fluorescence (XRF). In the event an electron microprobe became available and was used instead (Section 3.3.10). The glauconite was separated using a Frantz magnetic separator set at a 15˚ sideways and 30˚ forward tilt. The machine was set at 0.5 amps. A small portion of the sediment was poured into the chute and released down the tray to separate predominantly glauconite from non-magnetic light minerals. The light minerals were discarded while the more concentrated glauconite was run through again. This process was repeated until the glauconite was sufficiently concentrated.

3.3.6 X-ray diffraction (XRD)

X-ray diffraction (XRD) was used to determine the bulk mineralogy of the NKCM sediments. The mineralogy was determined separately for the sand-gravel and mud fractions and this was then combined to obtain the total sediment mineralogy. The XRD scans were run from 3-40˚2θ and the different minerals identified from their characteristic peak positions (Hume and Nelson, 1986). In-house calibration charts relating peak heights to mineral abundances were used to semi-quantify the mineralogy (Nelson and Cochrane, 1970; Hume and Nelson, 1986).

XRD was also used to determine the clay mineralogy of the NKCM sediments using dropper-on-glass-slide orientated slide mounts (Hume and Nelson, 1986).

3.3.7 Grain thin section mounts

Thin sections of the loose sand and gravel sediment were made for each of the sample sites across the NKCM. Small moulds of aluminium foil (45 mm by 25 mm by 20 mm deep) were made for each of the samples and labelled appropriately. 15 g of sand and gravel was split from each sample and placed on a hotplate to warm while 24 g of Araldite K42 resin was prepared. The resin was poured into the mould with enough to cover the bottom. Approximately 1/3 of the sample was sprinkled into the mould and then followed by enough resin to cover the sediment. The sediment within the resin was pushed slowly back and forth to spread it evenly across the mould and ensure no pockets of sediment remained. This process was repeated until all the sediment was in the mould. The remaining resin was poured on top before a paper label was pushed into the resin and the sample mould was then placed into a vacuum for 5 minutes. The sample was then left to set for 24 hours.

Once the block of sediment had set, the aluminium foil was removed and the sample number written on top. The base of the resin block was ground on a glass plate with 600-grade carborundum and/or a diamond lap wheel. The blocks were glued to frosted glass slides with Hillquist Thin Section Epoxy and left 24 hours

to harden. The resin blocks were then cut off the slides using a discoplane saw and ground down to the correct thickness using a discoplan.

The thin sections were polished for cathodoluminescence (CL) petrography using 500-grade silicon carbide paper and 0.3 μm alumina polishing powder dispersed with distilled water. Nine slides were polished further for microprobe analysis using diamond paste and a felt cloth. The grains identified for analysis were then marked and scanned to produce a slide map before carbon coating.

3.3.8 Thin section petrography

The percentage of each mineral or skeletal component (e.g. quartz, feldspar, bivalve, bryozoan fragment) was obtained by estimating the proportion that the component comprised of the total sediment using the comparative percentage circles in Figure 3-5. The component proportion was classified using a percentage

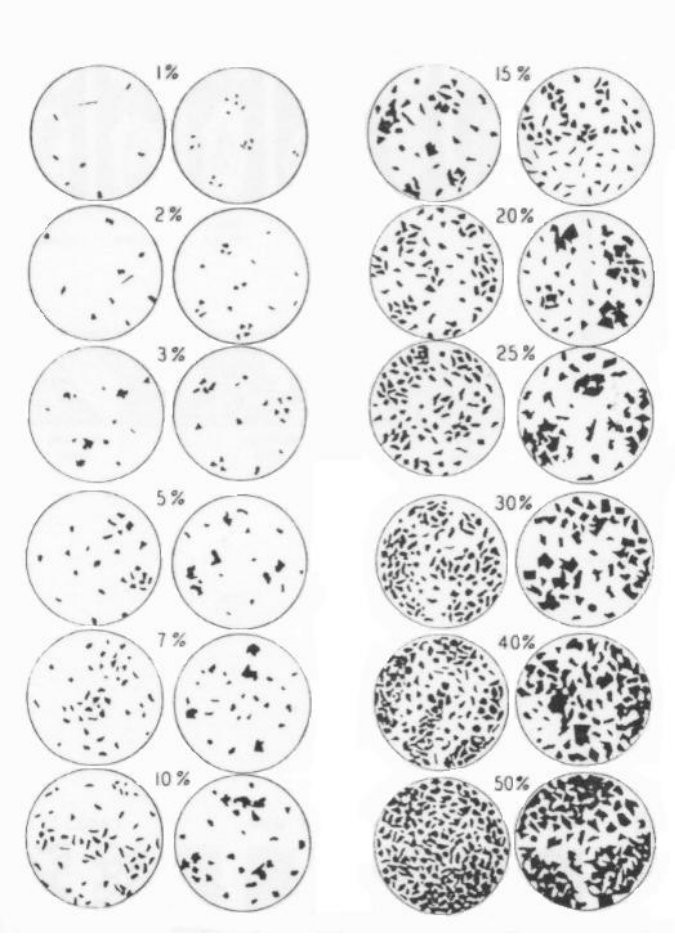

Figure 3-5. Percentage circles used to estimate the proportion of each component of the total sediment (Jones and Bloss, 1980).

Table 3-2. Percentage ranges used to describe the NKCM bottom sediments in thin section.

Classification	Percentage of component
Rare	<5%
Some	5-10%
Common-lower	10-20%
Common-upper	20-30%
Abundant-lower	30-40%
Abundant-upper	40-50%
Very abundant	>50%

range scale as described in Table 3-2. The sorting and rounding of the mineral or skeletal grains was also determined using Figure 3-6A and B, respectively, with five grades used for each (Table 3-3).

3.3.9 Cathodoluminescence (CL) petrography

Cathodoluminescence (CL) petrography was conducted at the University of Waikato using a CITL MK5-1 cathodoluminescence microscope with a gun voltage of 20 kV and gun current of 450-500 µA. The images were captured on a Nikon digital camera DXM1200 using Nikon ACT-1 software.

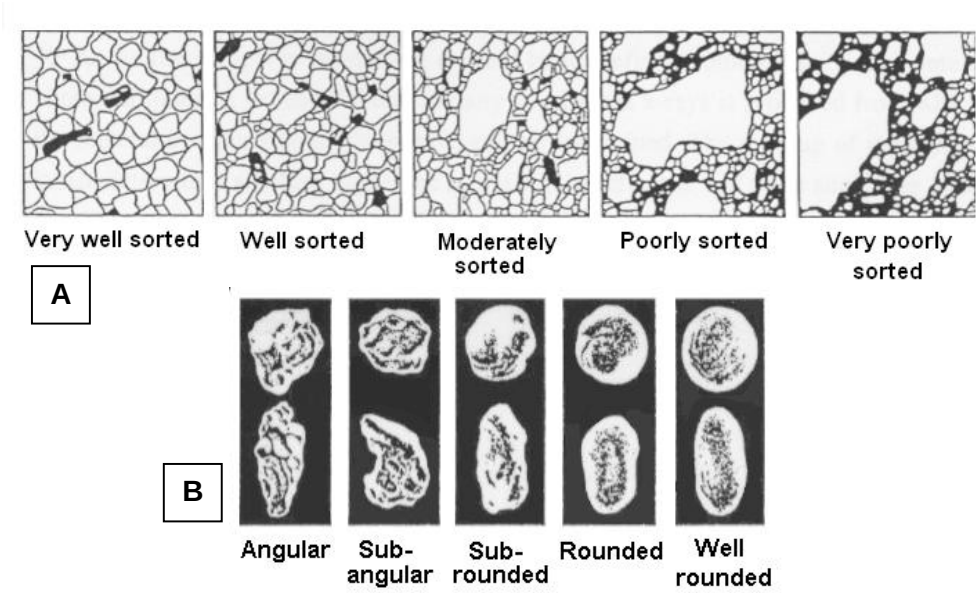

Figure 3-6. The sorting (A) and rounding (B) scales used to classify the NKCM sediments (Powers, 1953; Prothero and Schwab, 1996).

Table 3-3. Sorting and rounding classifications used to describe the NKCM bottom sediments in thin section.

Sorting		**Rounding**	
Grade	Classification	Grade	Classification
1	Very poorly sorted	1	Angular
2	Poorly sorted	2	Subangular
3	Moderately sorted	3	Subrounded
4	Well sorted	4	Rounded
5	Very well sorted	5	Well rounded

3.3.10 Microprobe analysis

Microprobe analysis was carried out at the University of Otago on a semi-automated JEOL JXA-8600 electron microprobe analyser using energy dispersive x-ray spectroscopy (EDS) with a 20 μm electron beam. The grains and analysis points were chosen using backscatter electron images and the location of each sample point in grain images is shown in Appendix E.

Chapter 4

SHELF AND SLOPE SEDIMENTS

4.1 INTRODUCTION

The shelf on the north Kaipara continental margin (NKCM) extends from the coastline out to the shelf edge, which is between c. 150 and 175 m water depth (Fig. 4-1). That part of the slope considered within this thesis study continues from the shelf edge out to a maximum depth of c. 1200 m. The nature of the sediments across the NKCM varies considerably both onshore to offshore and north to south. The variation in sediment texture (Section 4.2), carbonate content

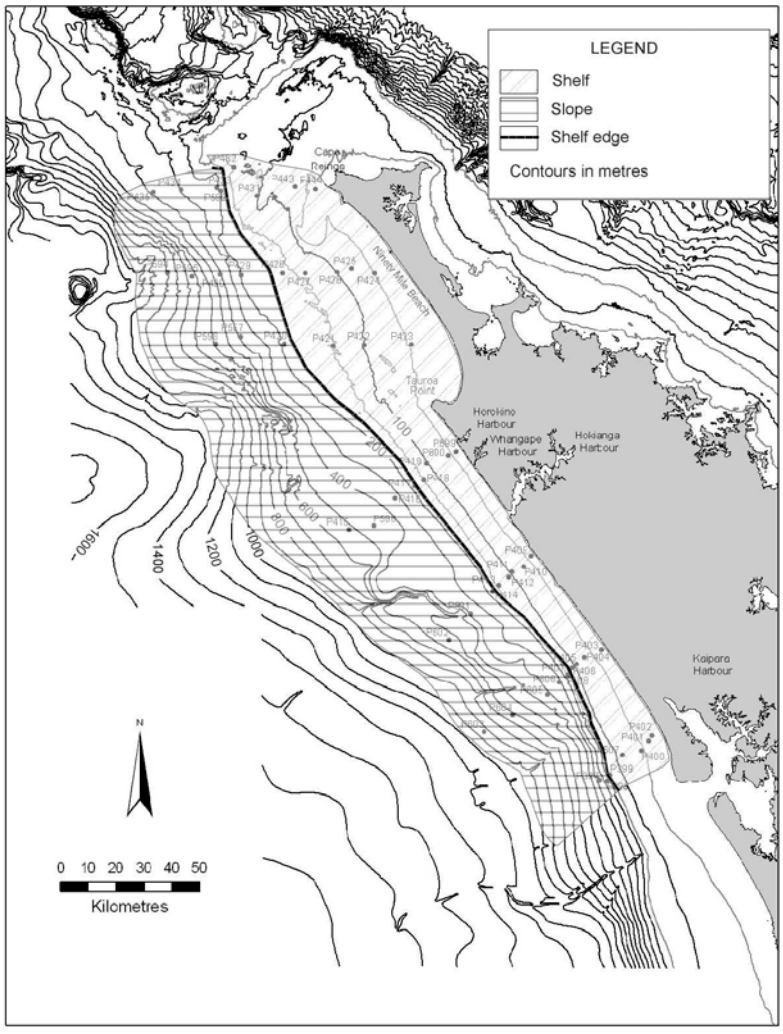

Figure 4-1. The shelf and slope area of the NKCM considered in this thesis study.

(Section 4.3), siliciclastic mineralogy (Section 4.4), calciclastic types (Section 4.5) and other components (Section 4.6) is discussed in detail in this chapter.

4.2 SEDIMENT TEXTURE

This section describes the weight percent distribution of the gravel, sand and mud fractions (4.2.1) in the NKCM sediments, followed by their textural categories (4.2.2) and the distribution of their sorting characteristics (4.2.3).

4.2.1 Gravel, sand and mud fractions

Over most of the NKCM the gravel fraction (>2 mm) of bottom sediments is less than 5% (Fig. 4-2). From 0-50 m water depth the sediment typically consists of <0.5% gravel. In the southern half of the NKCM this band increases to 1-5% gravel between 50-100 m water depth before decreasing to <0.5% gravel beyond 100 m depth. Along transect D there is an increase in the gravel fraction to 5-20% at 150 m water depth before decreasing to <0.5% gravel. In the northern half of the NKCM the trend is more complex with a significant increase from <0.5% gravel at <50 m water depth to between 0.5 and 75% gravel from 50-100 m water depth across transects E and F and 50-400 m depth along transect G.

The sand fraction (0.063-2 mm) completely dominates sediment from the NKCM, mainly comprising 90-100% of samples (Fig. 4-3A). As with the gravel fraction, the distribution varies considerably more in the northern half of the NKCM than in the south. 90-100% sand dominates the inshore area across the NKCM out to 80-100 m water depth with a second band between 200 and 700 m depth in the northern half. This band joins the inshore 90-100% sand band and extends out to c. 480 m water depth. In the southern half of the NKCM the sand fraction decreases rapidly to <30% beyond 500 m water depth. Along transect D the sand fraction varies more considerably with a decrease to between 50 and 90% sand between 100-150 m water depth before increasing to 90-100% sand at c. 180 m depth. After 400 m water depth the sand fraction decreases to 30-50% out to c. 550 m depth. Along transects E and F between 50 and 200 m water depth there is a significant decrease in the sand fraction to <30% at 100 m depth. Another area of <30% sand occurs at 65 m water depth along transect G.

The sand modal sizes across the NKCM are dominated by medium, fine and very fine sand sizes (Fig. 4-3B). Fine sand dominates the inshore area out to c. 80 m water depth in the north and c. 300 m depth in the south. The only exception is along transect C at <50 m water depth where the modal size decreases to very fine sand. The fine sand area grades into very fine sand with increasing depth in the southern half of the NKCM. A band of medium sand interrupts this transition along transect D between c. 180 and 350 m water depth and extends north between 100 and 200 m depth across transect E. The inshore fine sand band in the northern half of the NKCM grades into very fine sand which extends out to 1015 m water depth along transect F. Along transect G this very fine sand band passes into medium sand at c. 100 m water depth and then fine sand between 150 and 200 m depth. It increases again to medium sand from 300-400 m water depth.

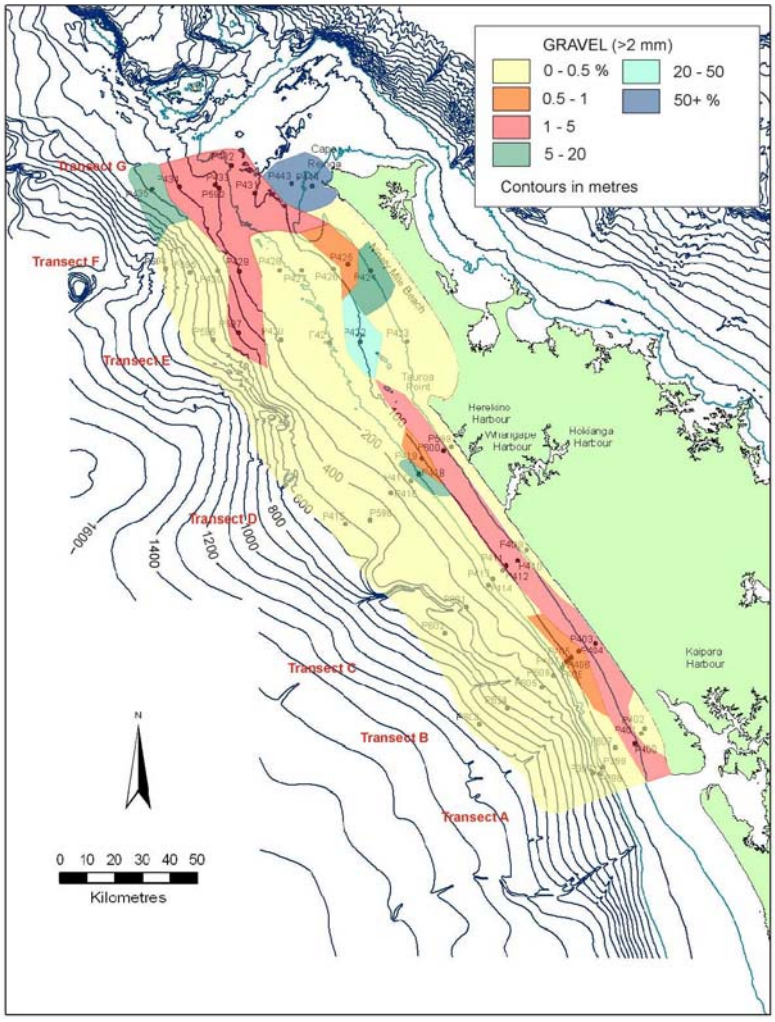

Figure 4-2. Distribution of gravel sized sediment (>2 mm) across the NKCM.

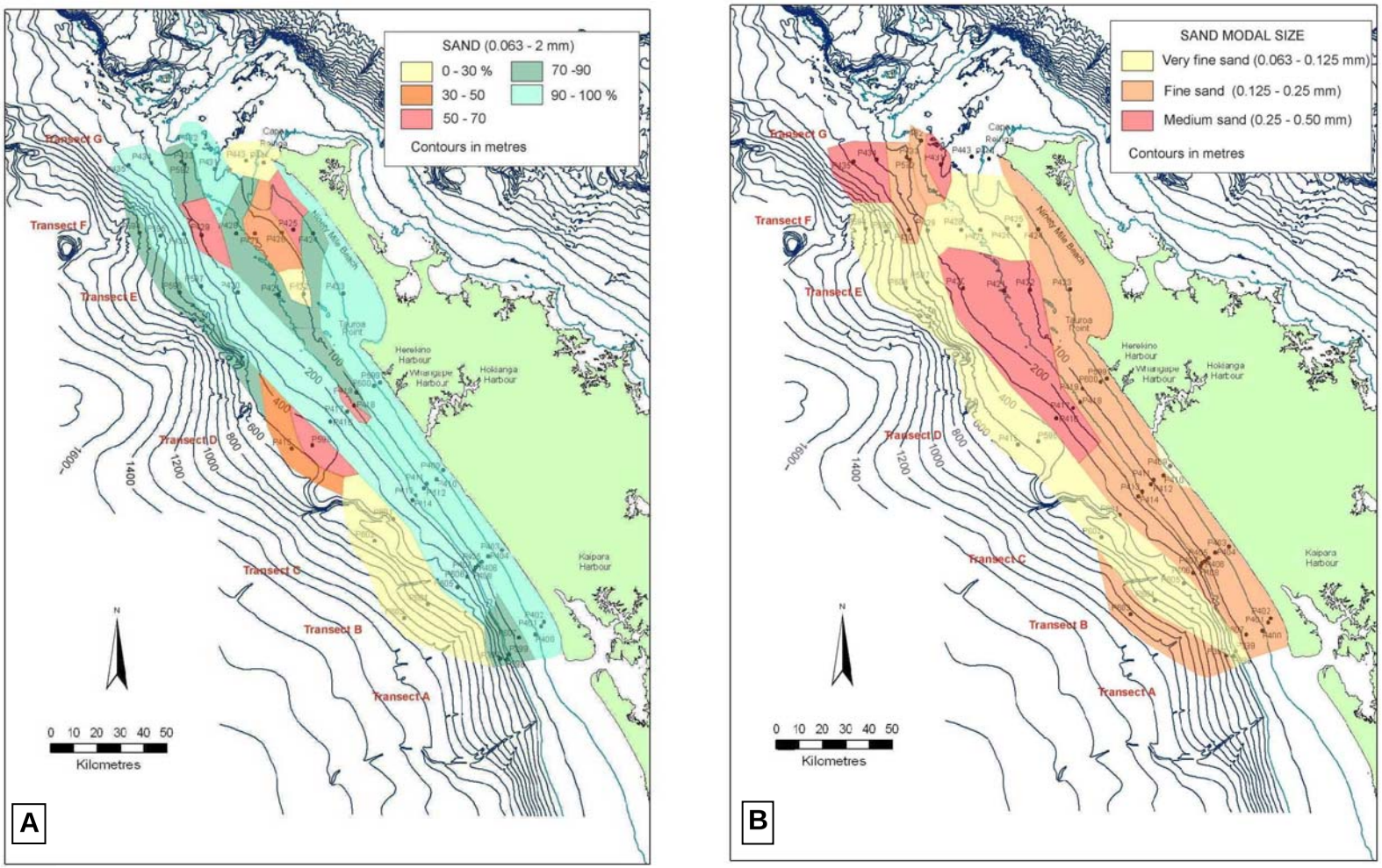

Figure 4-3 Distribution of (A) sand sized grains (0.063-2 mm) and (B) sand modal sizes in bottom sediments across the NKCM.

The percentage of mud-sized grains in bottom sediments varies considerably (from 0-90%) across the NKCM (Fig. 4-4). A band of <0.5% mud dominates the inshore area out to c. 80 m water depth across the length of the NKCM except for transect F where it increases to 0.5-5% mud. In the southern half of the NKCM the mud fraction gradually increases offshore to between 5 and 20% at 200 m water depth. This band continues out to c. 400 m water depth and extends into the northern half of the NKCM between 600 and 1015 m depth. In the southern half the 5-20% band then grades into >50% mud which extends over a large area up to transect D at depths of 400-1050 m. The distribution of the mud fraction in the northern half of the NKCM is more complex with a rapid increase to >50% mud out to 100-150 m water depth across transect F. It then decreases to 20-50% between c. 150 and 300 m and <0.5% between c. 300 and 500 m on transects F and G. The percentage of mud sized grains then increases to 5-20% out to 1015 m water depth.

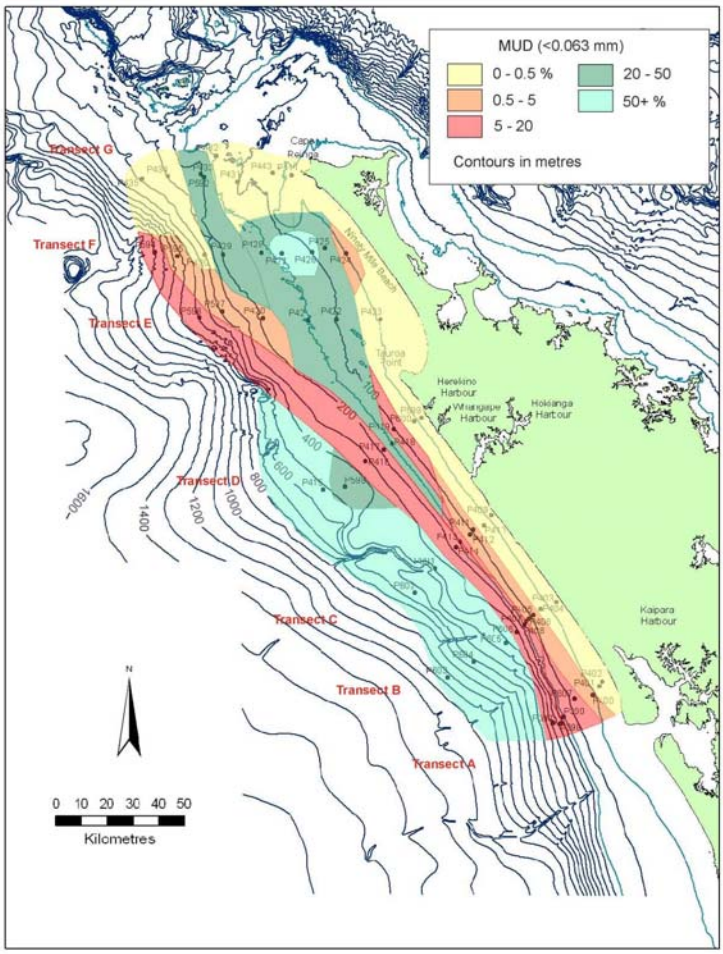

Figure 4-4. Distribution of mud sized material (<0.063 mm) in NKCM bottom sediments.

In Figure 4-5 the percentages of gravel, sand and mud are plotted against water depth to illustrate the trends across each transect. It is evident that the sand fraction dominates across the seven transects but decreases in this dominance towards the north. The gravel fraction shows an overall increase to the north with most of the gravel-sized grains found at inner to mid shelf depths (<100-150 m water depth). However, along transects F and G the gravel fraction extends off the shelf down to c. 400-1015 m water depth. Figure 4-5 also emphasises the overall increase in mud-sized grains offshore and especially along transects A-D. It also illustrates the area of very high mud content on the mid shelf along transects D, E and F as observed also on Figure 4-4. Another notable feature is the areas of both

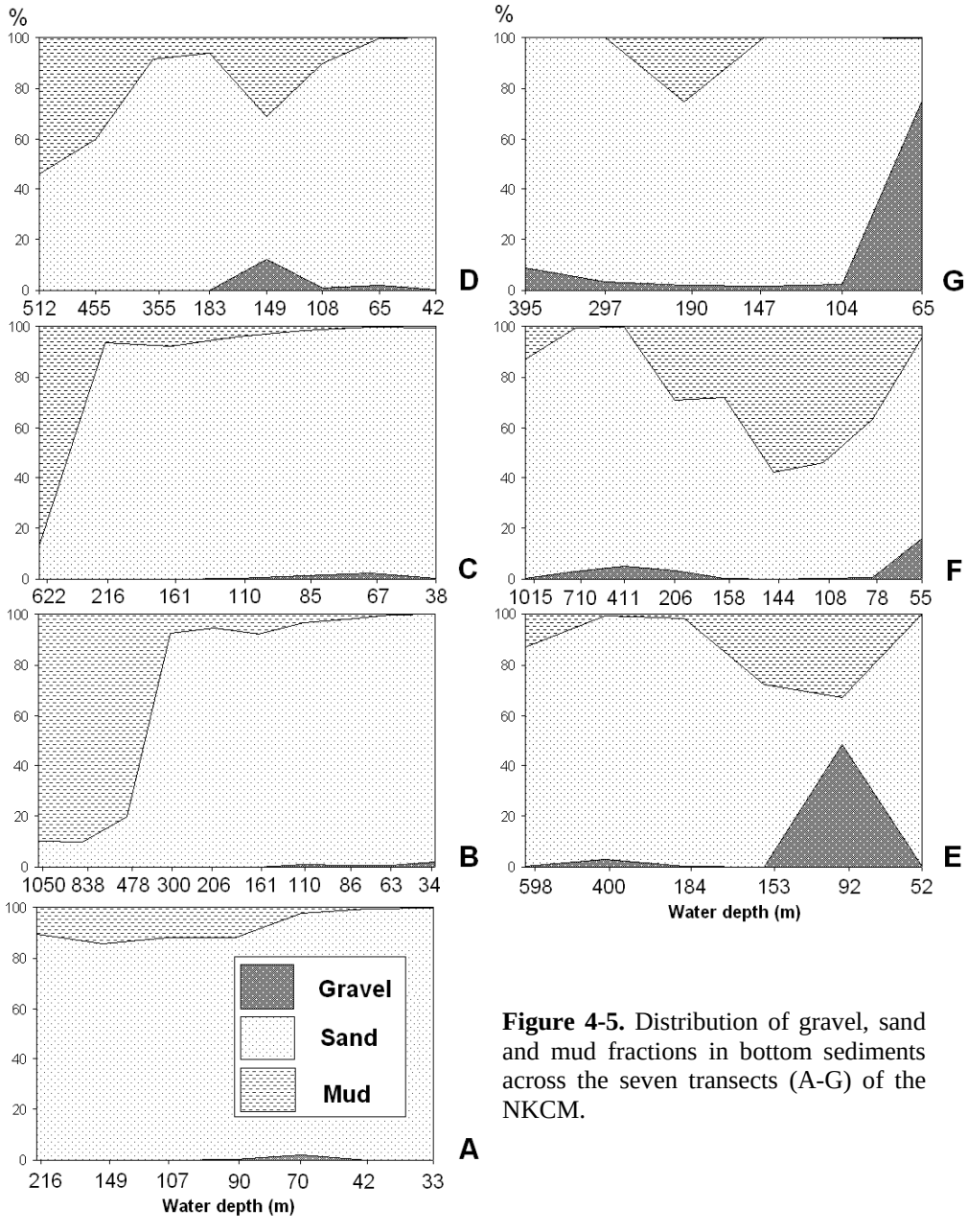

Figure 4-5. Distribution of gravel, sand and mud fractions in bottom sediments across the seven transects (A-G) of the NKCM.

higher gravel and mud content along transects D and E between c. 50-150 m water depth.

4.2.2 Sediment textural classification

The gravel, sand and mud fraction data are used to classify the NKCM bottom sediments on a textural triangle plot (Fig. 4-6, after Folk, 1968). The majority of samples fall in the sand section of the triangle and particularly within the slightly gravelly sand division [(g)S]. A small number of samples plot within the mud section and only two within the gravel section.

These textural classifications are mapped in Figure 4-7 to demonstrate their distribution across the NKCM. Slightly gravelly sand dominates, especially along the inshore region out to 100-150 m water depth with a second band between 200-400 m depth along transects D and E. Slightly gravelly muddy sand is the second most common texture but occurs mainly in the northern half of the NKCM. It extends from inshore out to greater than 1000 m water depth in the north. The mud textures predominantly occur in the southern half of the NKCM with three of

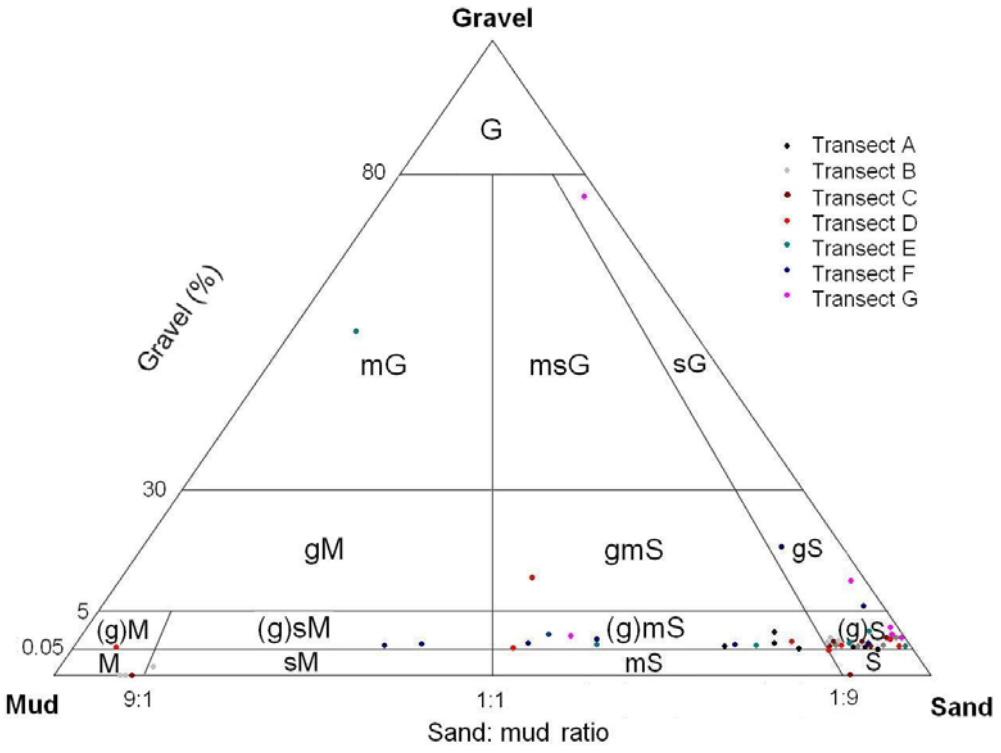

Figure 4-6. Textural classification (after Folk, 1968) of NKCM sediments. G=gravel, S=sand, M=mud, g=gravelly, s=sandy, m=muddy, (g)=slightly gravelly.

the four types (slightly gravelly mud, sandy mud and mud) occurring in this half at greater than c. 400 m water depth across transects B and C and greater than c. 500 m depth along transect D. The only occurrence of a mud texture (gravelly sandy mud) in the northern half of the NKCM occurs along transect F between 100 and 150 m water depth. The gravel textures are only found within the northern half of the NKCM (100 m water depth along transect E and 50-100 m along transect G), while a pure sand texture only occurs at 150-200 m water depth along transect C and <50 m depth along transect A.

4.2.3 Sediment sorting

Sorting of sediment across the NKCM (Figure 4-8) appears complex and lacks any consistent trends, although in the southern half of the NKCM there is a general tendency of decreasing sorting values with increasing depth. Very well

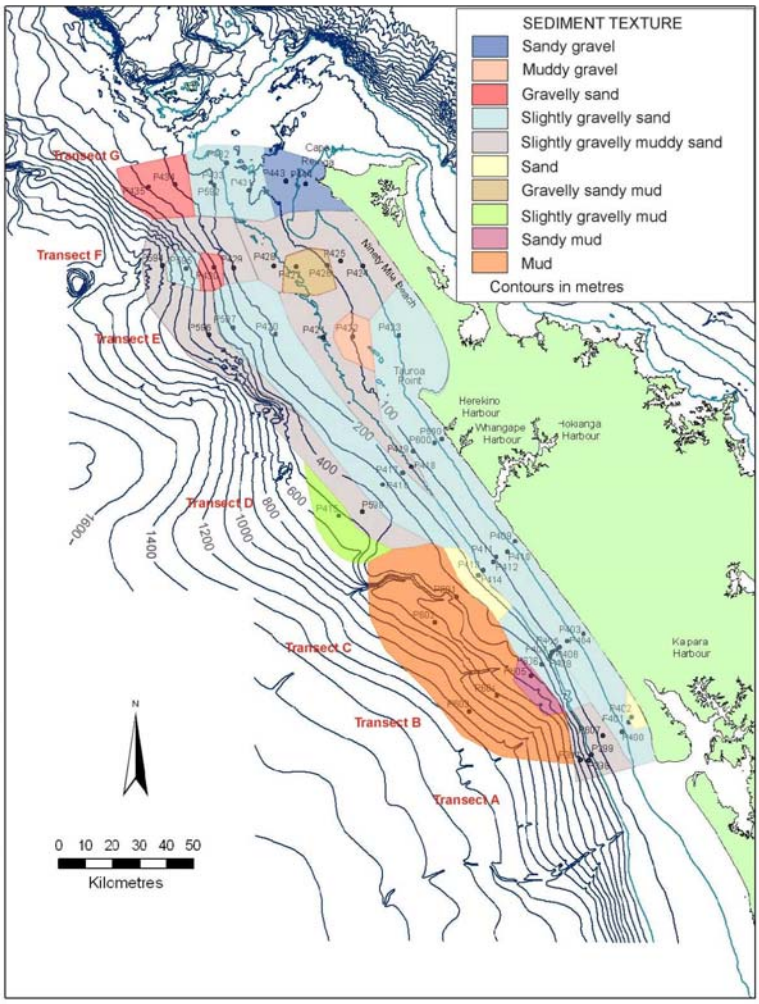

Figure 4-7. Textural classifications of surficial sediment from the NKCM (data from Figure 4-6).

sorted and well sorted sediments dominate the inshore region out to c. 100 m water depth across the NKCM except along transect G in the far north where the sediments are very poorly sorted. Very well sorted sediments also occur between c. 300 and 750 m water depth in the north and 500-550 m and 1050 m depth in the south along transects D and B, respectively. A band of moderately sorted sediment exists the length of the southern half of the NKCM between c. 100 and 350 m water depth and extends into the northern half along transect E at 150 m water depth. Very poorly sorted sediment also occurs at c. 100 m water depth along transect E, 150 m depth along transect D and c. 400-750 m water depth along transect B. A large area of moderately well sorted sediment occurs between c. 200 and 600 m water depth along transects D and E.

Well sorted and very well sorted sediment generally corresponds with very high percentages of sand sized (90-100%) or mud sized (>50%) grains, particularly along the inshore band at <100 m water depth and offshore at >500 m depth,

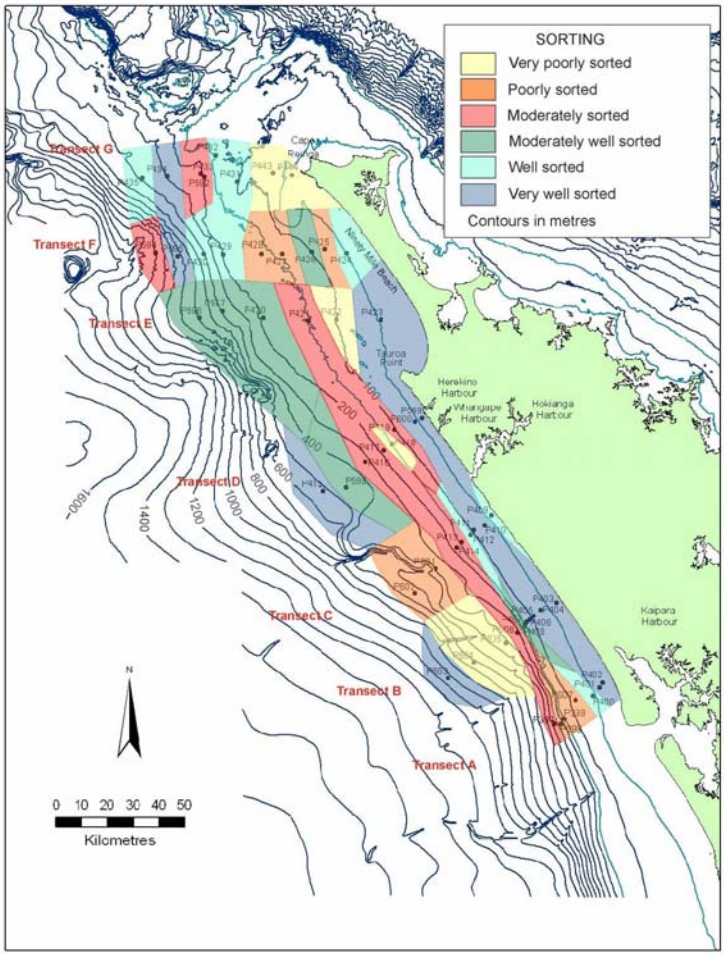

Figure 4-8. Distribution of surficial sediment sorting values across the NKCM.

respectively. The very well sorted band in the northern half of the NKCM also corresponds to an area of 90-100% sand while the very poorly sorted sediment along transects D and E corresponds to mixed sand and gravel sized grains (Fig. 4-5).

4.3 CARBONATE CONTENT

The calcium carbonate ($CaCO_3$) content of the NKCM sediment ranges from 3-91% with a clear increase in carbonate content offshore and to the north (Figure 4-9). Sediment containing <5% carbonate occurs at only 10 of 54 sample sites, mostly along the inshore area (<50 m water depth) in the southern half of the NKCM. These bands interfinger with areas of 5-10% carbonate out to c. 350 m water depth and extend into the northern half along transect E from inshore to c. 200 m water depth. In the southern half of the NKCM the carbonate content

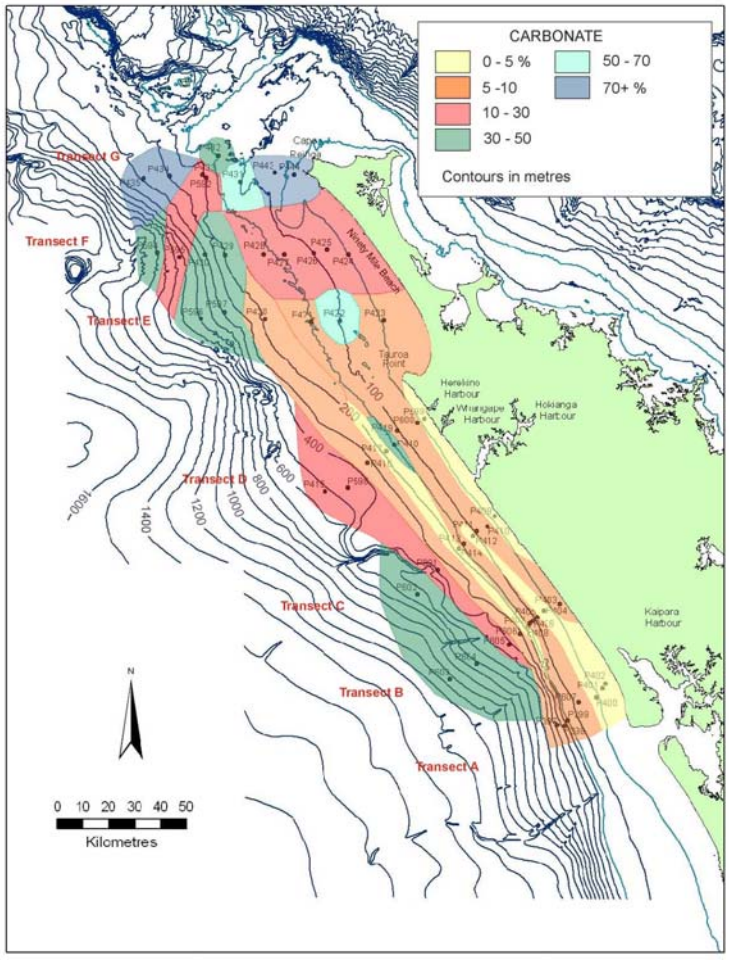

Figure 4-9. Distribution of calcium carbonate in NKCM bottom sediments.

continues to increase offshore with 10-30% carbonate between 400 and 500 m water depth and 30-50% carbonate at depths greater than c. 500 m. There is a small anomalous area of 30-50% carbonate at 150 m water depth along transect D which is bordered by 0-10% carbonate. In the northern half of the NKCM the carbonate content also increases offshore with 10-30% carbonate from inshore to c. 180 m water depth along transect F which increases to 30-50% carbonate from 200-600 m depth. There is another anomalous area of 50-70% carbonate within surrounding sediment of 5-30% carbonate content along transect E. The carbonate content increases to >70% along transect G at 50-100 m water depth and c. 300-400 m depth.

4.4 SILICICLASTIC MINERALOGY

The siliciclastic minerals in the shelf and slope sediments from the NKCM include quartz and feldspar (Section 4.4.1), non-opaque heavy minerals (Section 4.4.2), mica (Section 4.4.3), rock fragments (Section 4.4.4), opaques (Section 4.4.5) and clay minerals (Section 4.4.6).

4.4.1 Quartz and feldspar

In general, quartz and feldspar grains co-dominate the sediment across the NKCM with approximately equal amounts (less than 10% difference) in most of the samples and no sites recording less than 5% quartz or feldspar (Fig. 4-10A and B). Both quartz and feldspar grains are subrounded and well sorted (Plate 1 a-b) with a general decrease in percentage offshore (with depth) and to the north. Quartz grains have a dominant modal grain size of 0.15-0.20 mm (fine sand) while for feldspar grains the modal size is close to 0.20 mm (fine sand) (Plate 1 a-b). Many of the quartz and feldspar grains, particularly in the south, have a dirty appearance and include limonite staining of fractures and surfaces. Determining quartz from feldspar in thin section was difficult due to this degraded nature of the grains and their significant rounding. Consequently, XRD data (Appendix C, Table 5) were used together with petrography (Appendix C, Table 7) to help resolve this issue and estimate occurrence abundances.

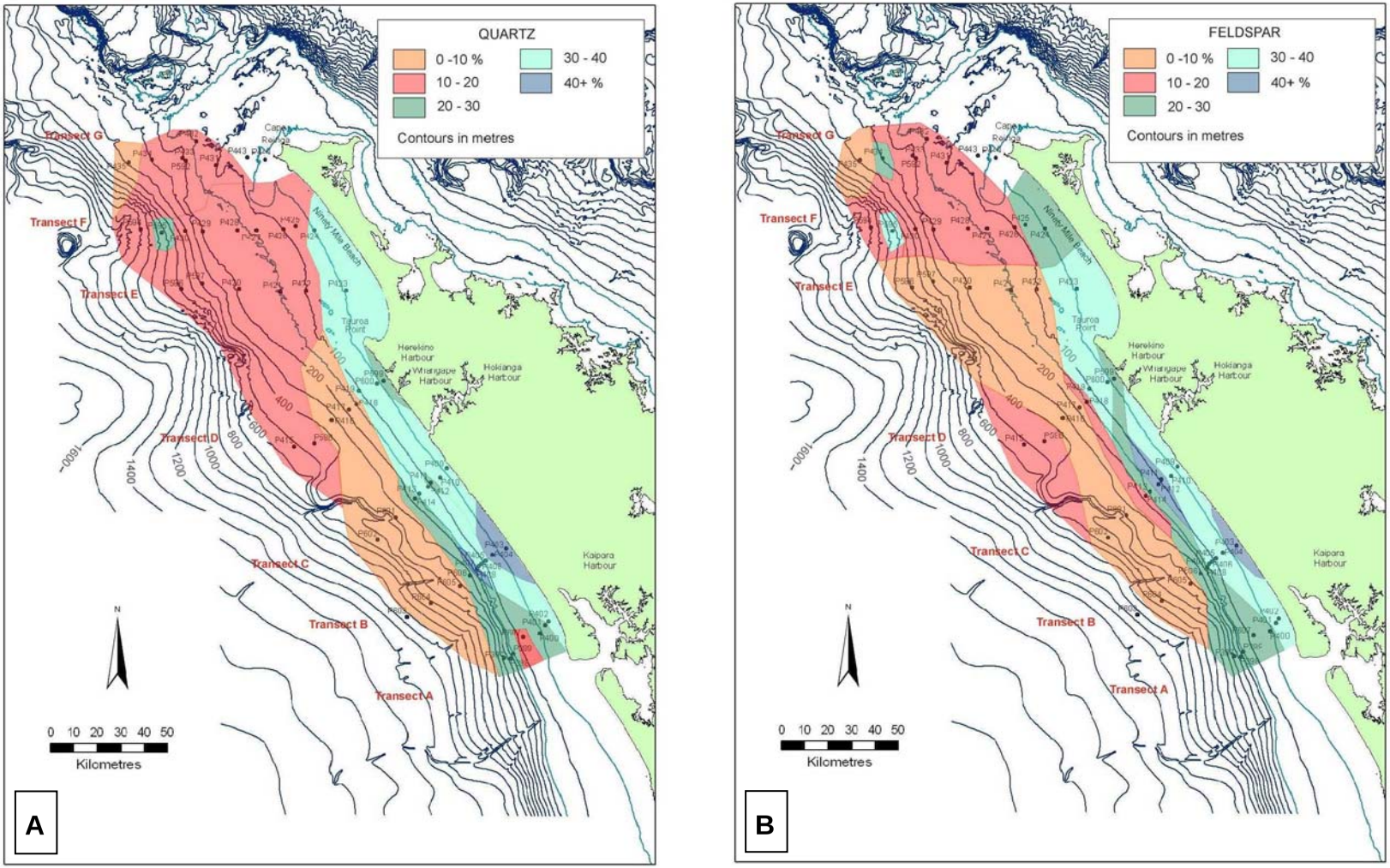

Figure 4-10. Distribution of (A) quartz and (B) feldspar in NKCM bottom sediments.

In the southern half of the NKCM the sediment consists of 30-40% quartz from inshore out to c. 100-150 m water depth except along transect B where it increases to 40-50% and transect D where it decreases to 20-30% (Fig. 4-10A). A band of 5-10% quartz occurs from c. 150 m water depth along transect D and >400 m water depth along transects B and C. Along transect D the quartz content increases again at >450 m water depth. The quartz distribution is less complex in the northern half of the NKCM and is dominated by 10-20% quartz; however, a small anomaly of 20-30% quartz exists at c. 700 m water depth along transect F.

The highest concentration of feldspar grains (40-50%) occurs at <40 m water depth along transect B and c. 30-130 m water depth along transect C (Fig. 4-10B). Along most of the inshore region at less than c. 100-150 m water depth there is a band of 30-40% feldspar which decreases offshore to 20-30% feldspar along transects A and B. At water depths greater than c. 200 m along transects B and C this grades into a band of 5-10% feldspar. Along transect D this 5-10% band increases to 10-20% feldspar from c. 400-550 m water depth. The band of 5-10% feldspar grains extends into the northern half of the NKCM between 100 and 600 m water depth along transect E. North of transect E, the percentage of feldspar grains increases to 10-20% between 100 and 1050 m water depth with the exception of three sample sites (Fig. 4-10B); the most significant of these is at c. 700 m water depth along transect F where 30-40% feldspar occurs within an area of otherwise 10-20% feldspar.

Cathodoluminescence microscopy (CL) was conducted on a selection of samples across two transects in an attempt to determine different species of quartz and feldspar (Boggs and Krinsley, 2006). Plate 1 shows CL results for two samples: one from transect B (c-f) and the other from transect F (g-j). In both samples, potassium (K) feldspar, or orthoclase (bright blue), and plagioclase feldspar (green/yellow) begin to luminesce first (Plate 1 d, h) before becoming overexposed (f and j). K feldspar appears to dominate all the samples analysed comprising c. 60-80% of the feldspar present with no apparent trends from north to south. Brown-lilac coloured quartz luminesces first in the southern sample (e) with the blue-violet quartz following this (f). Brown-lilac quartz is indicative of an ultimate metamorphic source (Boggs and Krinsley, 2006) and occurs in low

amounts (c. 2-20%) across the two transects with the exception of P408 and P409 where it increases to c. 70% of the quartz content. Blue-violet quartz is indicative of volcanic and plutonic sources (Boggs and Krinsley, 2006) and dominates both samples, but particularly the northern one where it comprises >90%. The other samples from the northern transect also have proportions of blue-violet quartz at >90%.

4.4.2 Heavy minerals

The heavy minerals are accessory minerals that have a specific gravity greater than 2.9 and the total percentages produced here are derived from the proportion of the heavy mineral fraction when separated from the total sample (Appendix C, Table 4). The percentage of heavy mineral grains in NKCM sediments does not show any significant trends either onshore to offshore or north to south (Figure 4-11A). Most of the sample sites contain less than 5% heavy minerals and only two have >30%. Both of these sites are in the inshore area (<50 m water depth) of the southern half of the NKCM with 30-50% heavy mineral grains recorded along transect D (Plate 2 a, b) and >50% along transect C. They are both surrounded by sediment that contains <10% heavy minerals. Along transect A the heavy mineral content increases to 10-30% at c. 40 and 90 m water depth. There are four areas of 10-30% heavy minerals within sediment containing only 0-1%. Three are in the northern half of the NKCM at 100 and 400 m water depth along transect E and 300 m depth along transect G. The fourth is in the southern half along transect D between 500 and 550 m water depth.

Table 4-1 lists the non-opaque heavy minerals identified and Figure 4-11B maps the main non-opaque heavy mineral(s) types across the NKCM. Overall, hornblende is the dominant heavy mineral with garnet, augite and hypersthene of secondary dominance. The dominant modal grain size for the heavy minerals as a whole is 0.18-0.21 mm (fine sand). Hornblende occurs usually as elongated grains with distinct brown to green pleochroism (Plate 2 c-d). Garnet comprises colourless, irregular grains with high relief, conchoidal fractures and pitted surfaces. The grains are characteristically isotropic and may have dark discoloured outer surfaces. Hypersthene consists of elongated prismatic crystals with distinct

Table 4-1. The heavy minerals found in the sediments of the NKCM and their most probable primary source rocks (Klein, 2002).

HEAVY MINERAL	ULTIMATE SOURCE
Hornblende Oxyhornblende Blue-green amphibole	Widespread in igneous and metamorphic rocks, common in medium grade metamorphics
Actinolite	Greenschist facies
Epidote Clinozoisite	Regional metamorphism, especially greenschist facies
Hypersthene	
Augite	Dark coloured igneous rocks, especially basalts and andesites
Garnet	Mica schist, hornblende schist, gneisses, granites and pegmatites
Chlorite	Greenschist facies
Zircon	Common in all igneous rocks, especially granite
Titanite	Granites, gneisses, chlorite schists
Monazite	Granites, gneisses, pegmatites

pink-green pleochroism. Augite grains are light green and irregular in shape, lacking clear cleavage and pleochroism. Zircons in the NKCM sediments occur as both small elongated prisms and rounded grains, commonly with a dark outer halo.

An association of hornblende and garnet dominates the inshore region (<50 m water depth) of the NKCM and extends out to 150 m depth along transects B and C (Fig. 4-11B). Hornblende dominates the northern half of the NKCM with a band extending into the southern half between 50 and 500 m water depth. The co-dominance of hornblende and augite is also common between 150 and 350 m water depth along transects B-E and from 500-550 m depth along transect D. Garnet dominates in the southern half of the NKCM from 100-1000 m water depth across transects A and B. Several smaller areas of co-dominance occur between 100 and 150 m water depth along transects D, E and G (Fig. 4-11B).

In Figure 4-12 A and B the distributions of hornblende and garnet are mapped. Unlike the other diagrams presented in this chapter they are mapped as a percentage of the total heavy mineral content, not the total sediment. The distribution of both hornblende and garnet vary significantly across the NKCM

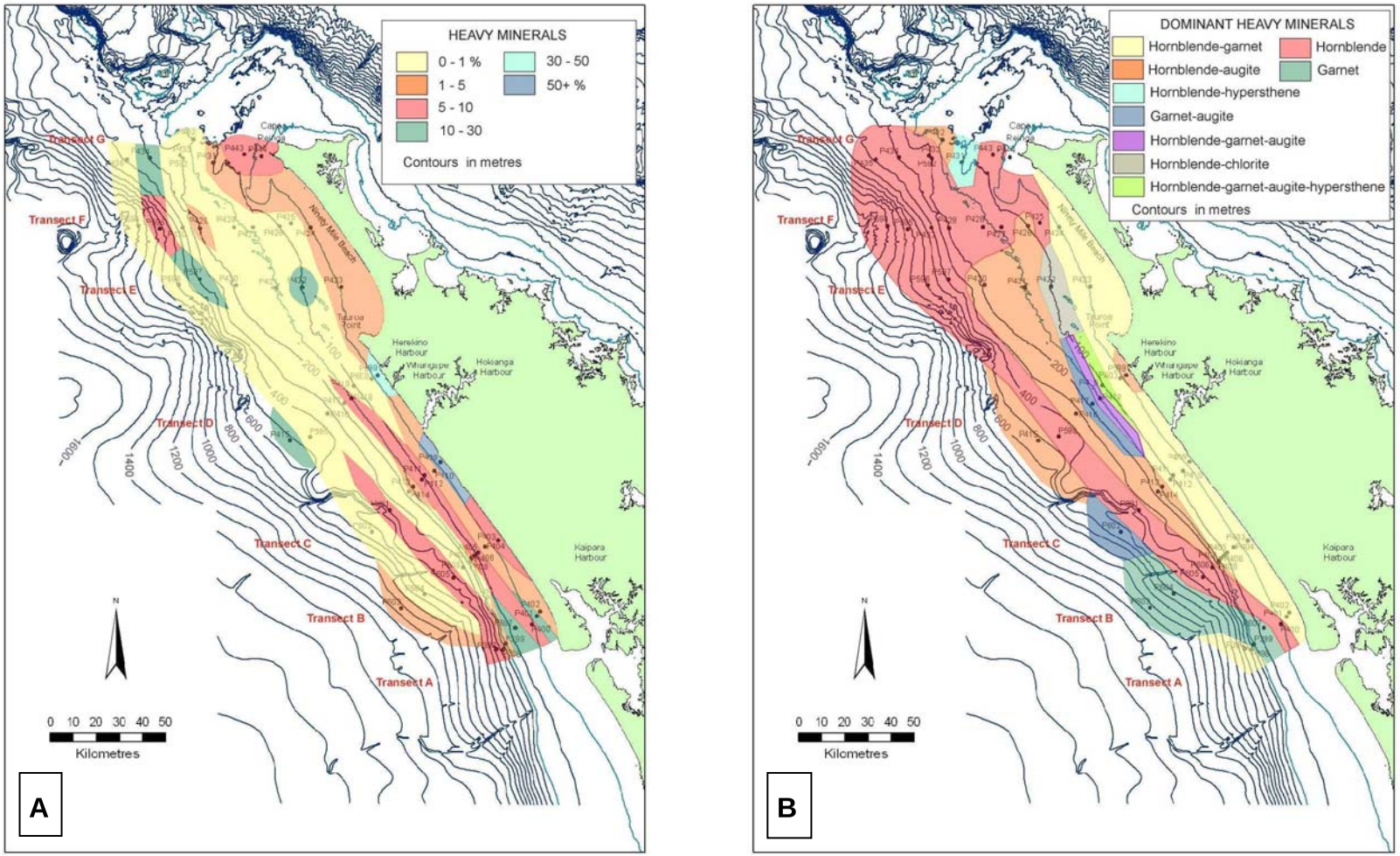

Figure 4-11. Distribution of (A) heavy minerals and (B) dominant non-opaque heavy mineral types in NKCM bottom sediments.

with the highest values for both generally occurring at less than 200 m water depth.

The highest concentration of hornblende grains occurs in the inshore area (<50 m water depth) along transects A and D and at c. 150 m water depth along transect G where hornblende comprises >50% of the heavy mineral component (Fig. 4-12A). In the southern half of the NKCM the hornblende percentage decreases offshore with a band of 30-40% hornblende along the mid to outer shelf (c. 80-200 m water depth) which decreases to 20-30% along transects C-F from the outer shelf to c. 400 m water depth. In the south, the hornblende percentage decreases to 5-10% across the mud dominated sample sites of transects B and C at > 600 m water depth but does not fall below 5%. In the northern half of the NKCM the hornblende percentage increases to 40-50% out to c. 1000 m water depth.

The overall distribution of garnet within the heavy mineral fraction decreases to the north with the highest percentage (>50%) in the inshore region (<50 m water depth) across transects C and F, at c. 65 m depth along transect D and c. 100 m depth along transect A (Fig. 4-12B). In the southern half of the NKCM <5% garnet occurs inshore along transect D where the hornblende percentage is very high, but also at 300 m water depth along transects B and D. A band of 5-10% garnet extends the length of the NKCM between 50 and 500 m water depth. In the south this band grades into 20-30% garnet across transect C and 40-50% garnet along transect B. In the northern half of the NKCM the garnet percentage is predominantly <5%, especially at c. 80-150 m and 400-1000 m water depth.

Overall, hypersthene, augite and zircon occur in lesser amounts than hornblende and garnet. Hypersthene is common (10-30%) at 27 of the 54 samples sites while the same percentage range of augite occurs at 36 of the 54 sites. Augite is abundant (30-50%) at only 7 of the 54 sample sites. Only 10 of 54 sites contain more than 5% zircon with 8 of those sites in less than 150 m water depth. Chlorite, titanite and monazite occur sporadically at very low percentages (<5%) across the NKCM.

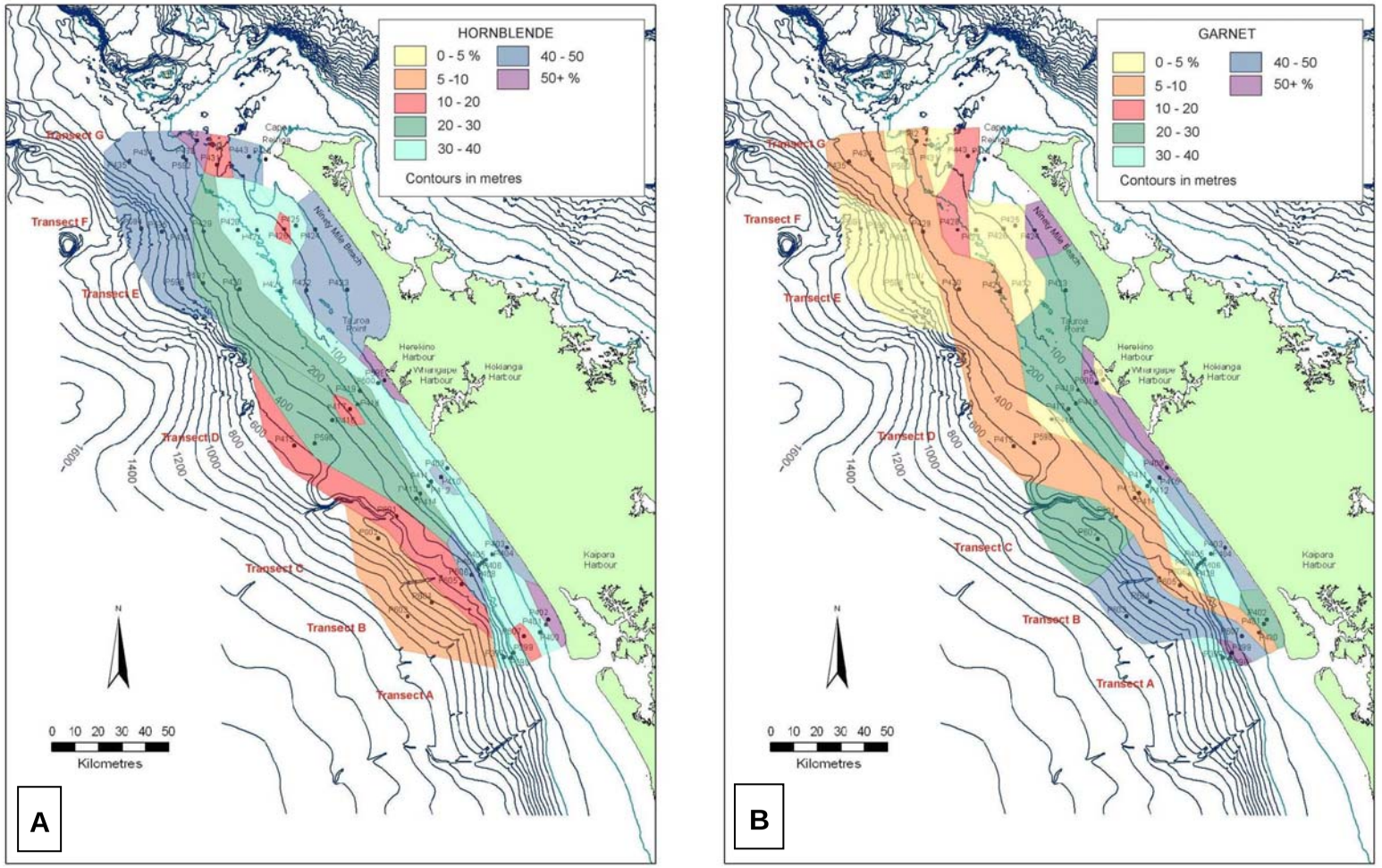

Figure 4-12. Distribution of (A) hornblende and (B) garnet across the NKCM. The percentages of each mineral are of the total heavy mineral fraction, not the total sediment fraction.

4.4.3 Mica

As for the other minerals, the mica content of NKCM sediments was determined from thin sections. However, this can lead to an under-representation of the mica content due to the hydrodynamic behaviour of mica flakes during settling in resin. In this study this effect was minimised by purposely mixing the sediment grains in the resin mounts rather than simply allowing them to settle out. Consequently, the mica contents are regarded to be reasonably accurate.

Mica grains occur primarily as thin elongated flakes with a dominant modal grain size of 0.15-0.25 mm (fine sand) (Plate 2 e-f). Across most of the NKCM the abundance of mica grains in the sediment is <5% with only a small number of isolated areas that have a greater quantity (Figure 4-13). 5-10% mica occurs at 70-150 m water depth along transect A, <50 m depth along transect C and c. 600 m

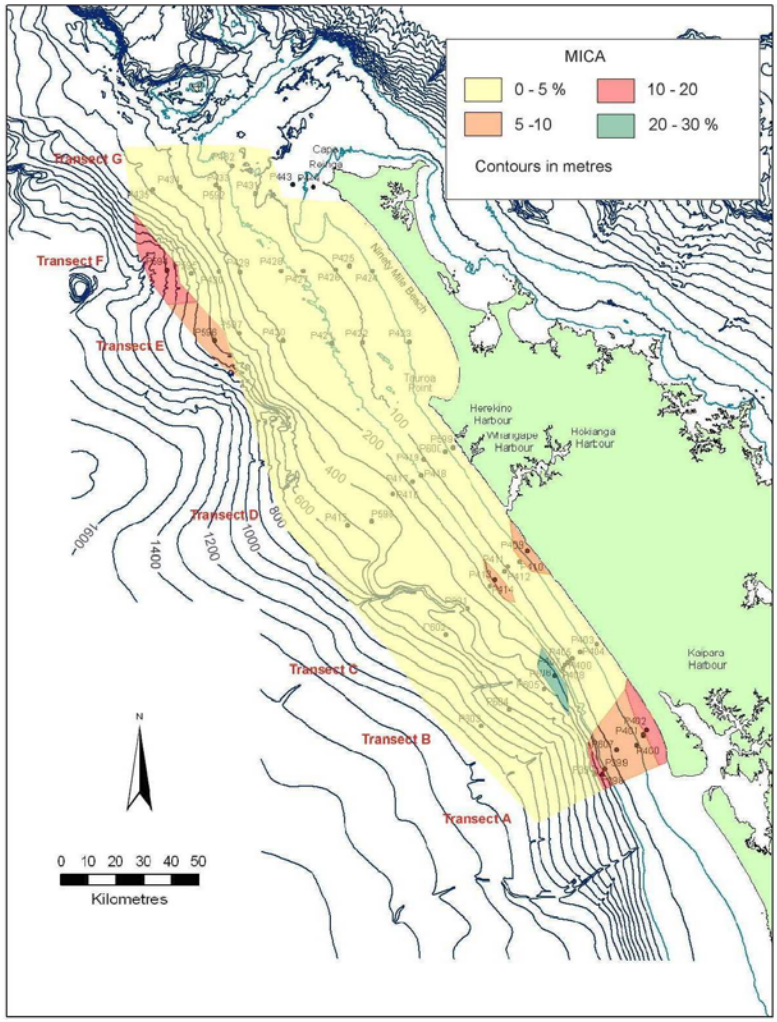

Figure 4-13. Distribution of mica grains in NKCM sediments.

water depth along transect E. 10-20% mica occurs at c. 30 and 150 m water depth along transect A and >1000 m depth along transect F. The only area where the mica content exceeds 20% is along transect B at c. 300 m water depth.

The colour of the mica (in loose sediment) was determined in 15 samples from transects A-F (Fig. 4-14). White (or clear) mica dominates the samples from the NKCM with 12 of the 15 samples recording more of this colour than black, brown or green varieties. White mica especially dominates sample sites P604, P602, P418 and P421. Brown mica only dominates two sample sites (P406 and P594), although it is usually the second most common colour type after white mica. Black mica varies considerably in content from 0 to c. 45% and only dominates one sample site (P401). The black and brown micas are probably biotite, while the white and green micas are muscovite and chlorite (not strictly a mica), respectively.

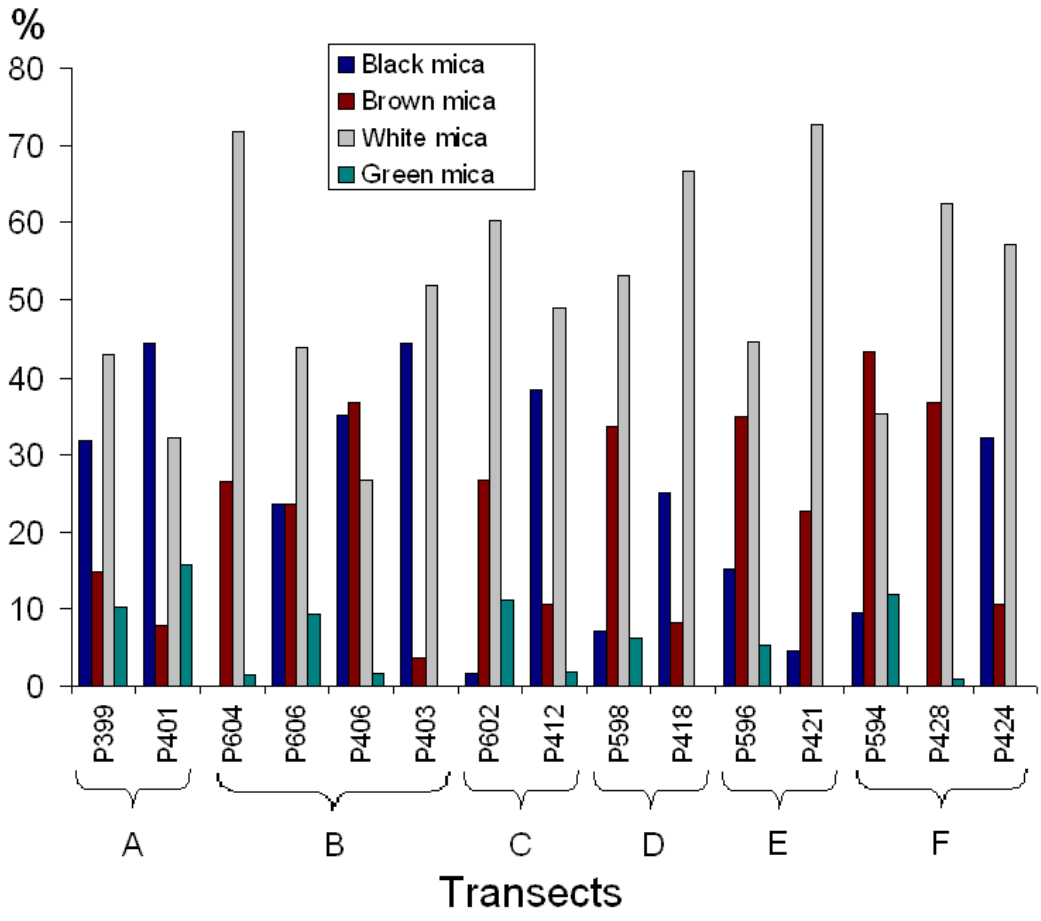

Figure 4-14. Contents of black, brown, white and green mica grains in 15 samples from transects A-F on NKCM.

4.4.4 Rock fragments

Rock fragments comprise only a small part (<30%) of the total sediment and, like the associated mineral grains, have a modal size in the fine sand grade. Their abundance decreases offshore (with depth) and towards the north, with a wide band of <5% rock fragments across the entire NKCM between 100 and 1000 m water depth (Fig. 4-15). The highest concentration of rock fragments (20-30%) occurs at less than 50-100 m water depth along transects B-F and decreases to 10-20% between c. 100 and 250 m depth in the southern half of the NKCM. In the northern half, the rock fragment percentage decreases to 5-10% between c. 80 and 180 m water depth although an area of 10-20% occurs at c. 100 m depth along transect G.

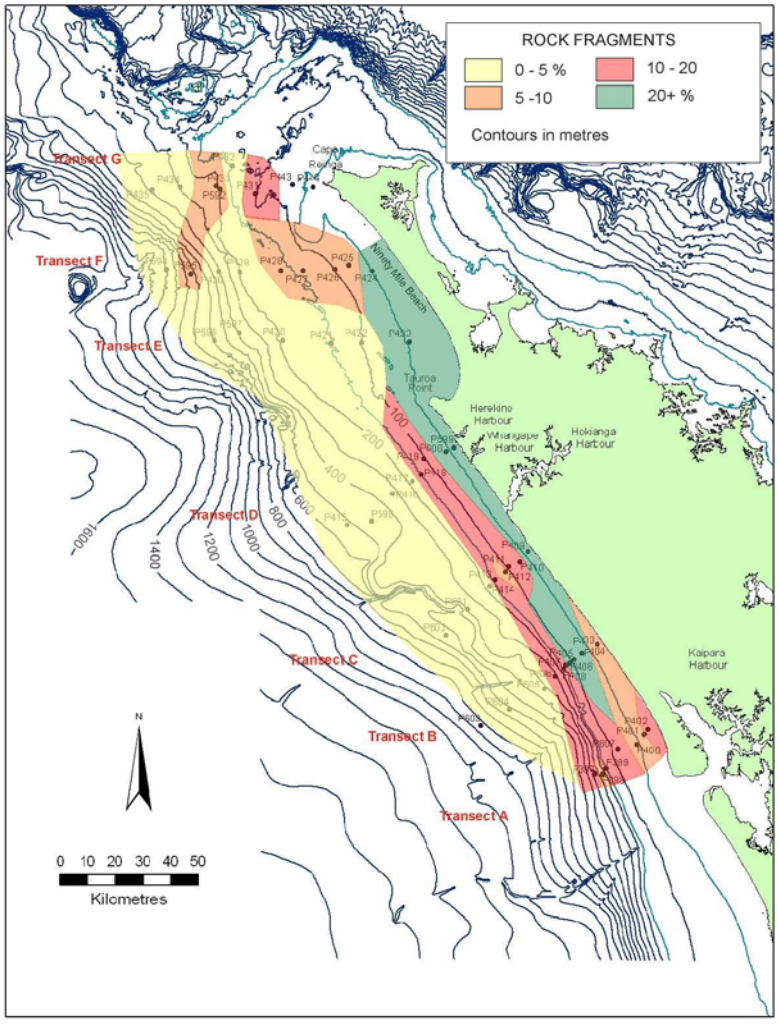

Figure 4-15. Distribution of rock fragments in NKCM bottom sediments.

The rock fragments range in type with the most common comprising elongated quartz and feldspar grains within a very fine-grained groundmass indicating they are volcanic rock fragments (Plate 3 b-e). The two other main types of rock fragments are those that consist of moderate sized crystals, mostly of the same size (Plate 3 c, brown grain above centre), and large uneven sized crystals with little matrix (Plate 3 a). Both these types of rock fragments are most probably sedimentary in origin.

4.4.5 Opaques

Compared to other mineral components the opaque fraction is relatively insignificant with the majority of NKCM samples containing less than 5% opaque grains. Only six of the 54 sites contain more than 5% opaques (5-10%) and nearly all of these occur along the southernmost transect A. The opaque grains are dominated by a 0.08-0.10 mm (very fine sand) modal grain size. The dominant opaque mineral is altered ilmenite, or leucoxene, with only minor amounts (<1%) of hematite and pyrite. Note that titanomagnetite, such a common opaque mineral on the Taranaki-Waikato shelf to the south (Carter, 1975), appears to be absent from all NKCM bottom sediment.

4.4.6 Clay minerals

The clay mineralogy of 41 samples was determined and roughly estimated using XRD (Appendix C, Table 6). The clay mineral fraction comprises only a small proportion of the NKCM samples (rarely exceeding 30%) and appears to have no consistent trend in its distribution. Montmorillite or smectite dominates the clay fraction of all the NKCM samples, with illite and chlorite+kaolinite of secondary importance (c. <30%). Mixed layer clays involving chlorite are recorded in only two samples (P426, P604) in very small amounts (c. <4%). Montmorillite/smectite only decreases to below c. 70% of the clay mineral fraction in five samples (P404, P417, P429, P596, P603) with illite comprising this deficit in three of the samples and chlorite+kaolinite in the other two samples.

4.5 CALCICLASTIC (SKELETAL) TYPES

The calciclastic content of the NKCM increases offshore with depth and towards the north (Fig. 4-16A). In the southern half of the NKCM the calciclastic content is 0-5% in <80 m water depth along transects C and D and this band extends out to 200 m water depth along transects A and B. A second smaller area of <5% occurs between 150 and 200 m water depth along transect C and D and grades into 5-10% calciclastics to a depth of 300 m along transects B-D. This band increases to >50% between 300 and c. 1000 m water depth and extends into the northern half of the NKCM to form a distinct wide band. A significant number of the sample sites within this band consist of >75% calciclastics. Another small area containing >50% calciclastics occurs between 100 and 150 m water depth along transects D and E and both of these comprise >75% calciclastics. In the northern half of NKCM the calciclastic content ranges mainly between 10 and 30% out to 200 m water depth where it increases to 40-50% skeletal material beyond this depth.

In Figure 4-16B the dominant skeletal type(s) are mapped. The calciclastic grains of the NKCM are typically highly fragmented and abraded making identification of the different skeletal types difficult; consequently this map mainly reflects the dominant skeletal types of whole or primarily whole taxa. Planktic foraminifera are the dominant type extending over most of the NKCM at >200 m water depth, but extending into shallower depths (c. 80 m) along transect F. Bivalve and bivalve/gastropod (Plate 4 a-d) skeletal fragments dominate the inshore area at <80 m water depth, with only small areas of other skeletal types present in this zone.

Bryozoan grains are more common in the northern half of the NKCM and become dominant at >250 m water depth along transect G (Plate 4 c, e-f).

Endolithic boring of the major skeletal grains (predominantly bivalve and gastropod) is common at some sample sites (particularly in the northern half of the NKCM) and these borings are usually filled with glauconite or limonite (Plate 4 d, g-h). Glauconite and limonite infills are also common within foraminiferal

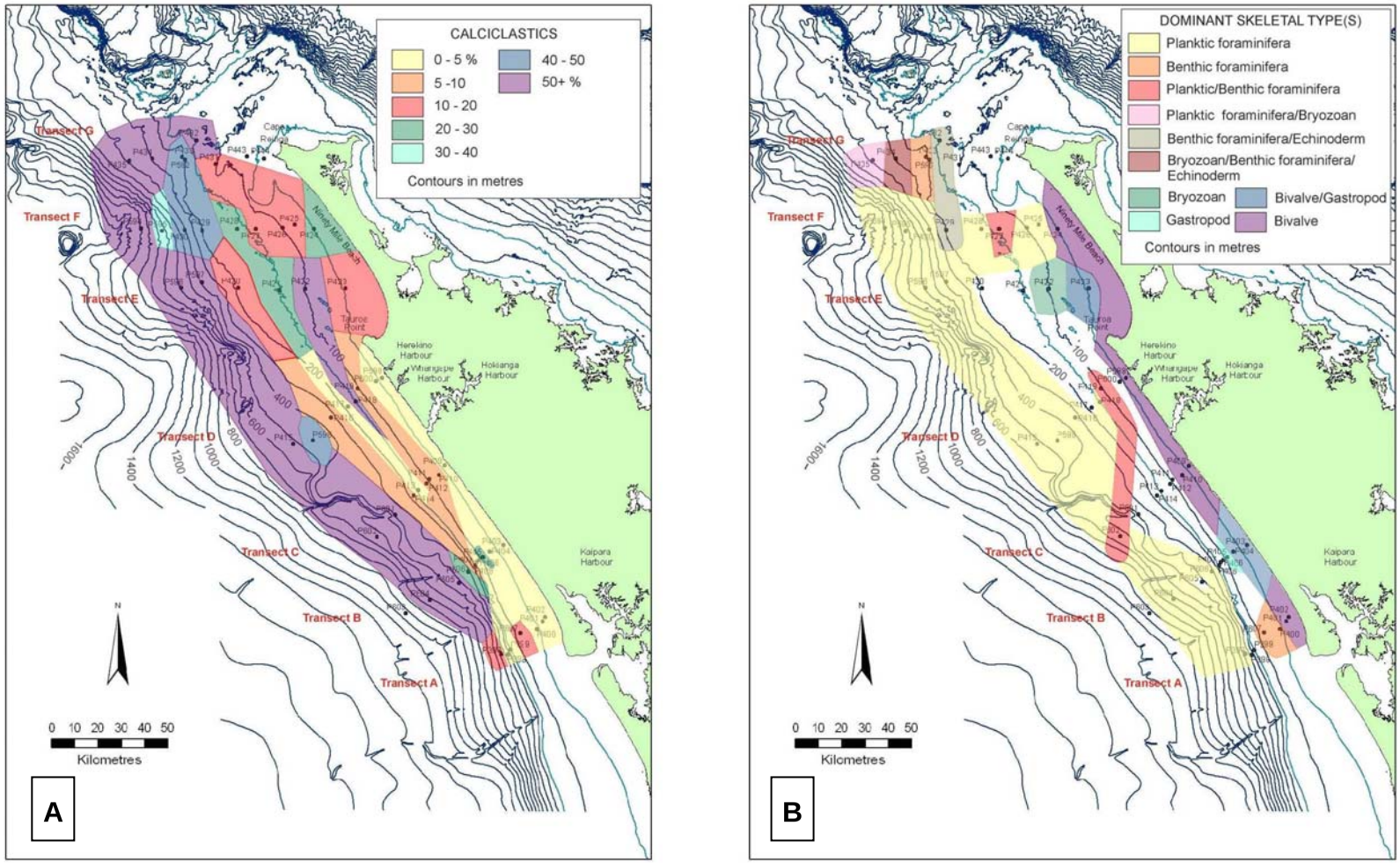

Figure 4-16. Distribution of (A) calciclastic fraction and (B) dominant skeletal types in NKCM bottom sediments.

tests, and mud/clay infills occur in two samples (P416, P598) in >400 m water depth along transect D.

Calcitic skeletons, such as foraminifera and bryozoans, display red-orange CL colours while aragonitic skeletons, often bivalves, appear dark blue-purple (Plate 4 i-j).

4.6 OTHER COMPONENTS

Bottom sediments of the NKCM contain other components, which include glauconite, mixed carbonate-siliciclastic pellets and phosphatic grains.

4.6.1 Glauconite

Glauconite grains are ubiquitous across the NKCM, being absent at only three of the 54 sample sites (P401, P409, P422). The glauconite content ranges from 0 to >75% but is predominantly <10% (Fig. 4-17A). The 0-5% glauconite range dominates the inshore region at <100 m water depth with two areas of 10-20% glauconite in the north and south. The northern band extends along most of transect F and is interrupted by 5-10% glauconite in the mud dominated area at 100-150 m water depth and at >900 m depth. The southern band of 10-20% glauconite occurs parallel to the shoreline from transects A-D at water depths between 50 and 400 m. A large area of very high glauconite concentration (>50%) occurs on the shelf edge in 150-400 m water depth along transects D and E. All four of these sample sites contain greater than 75% glauconite and are equivalent to modern greensands. The glauconite content decreases to 20-30% west (along transect E) and east (transect D) of this concentrated area. A small area of 30-40% glauconite occurs directly to the south of the concentrated area, suggesting possible southwards dispersal of grains.

The glauconite grains on the NKCM are generally well rounded, light to dark green pelletal grains, predominantly 0.15-0.25 mm (fine sand) in size, and include common limonitised dehydration cracks (Plate 3 f-h). The grains range from very

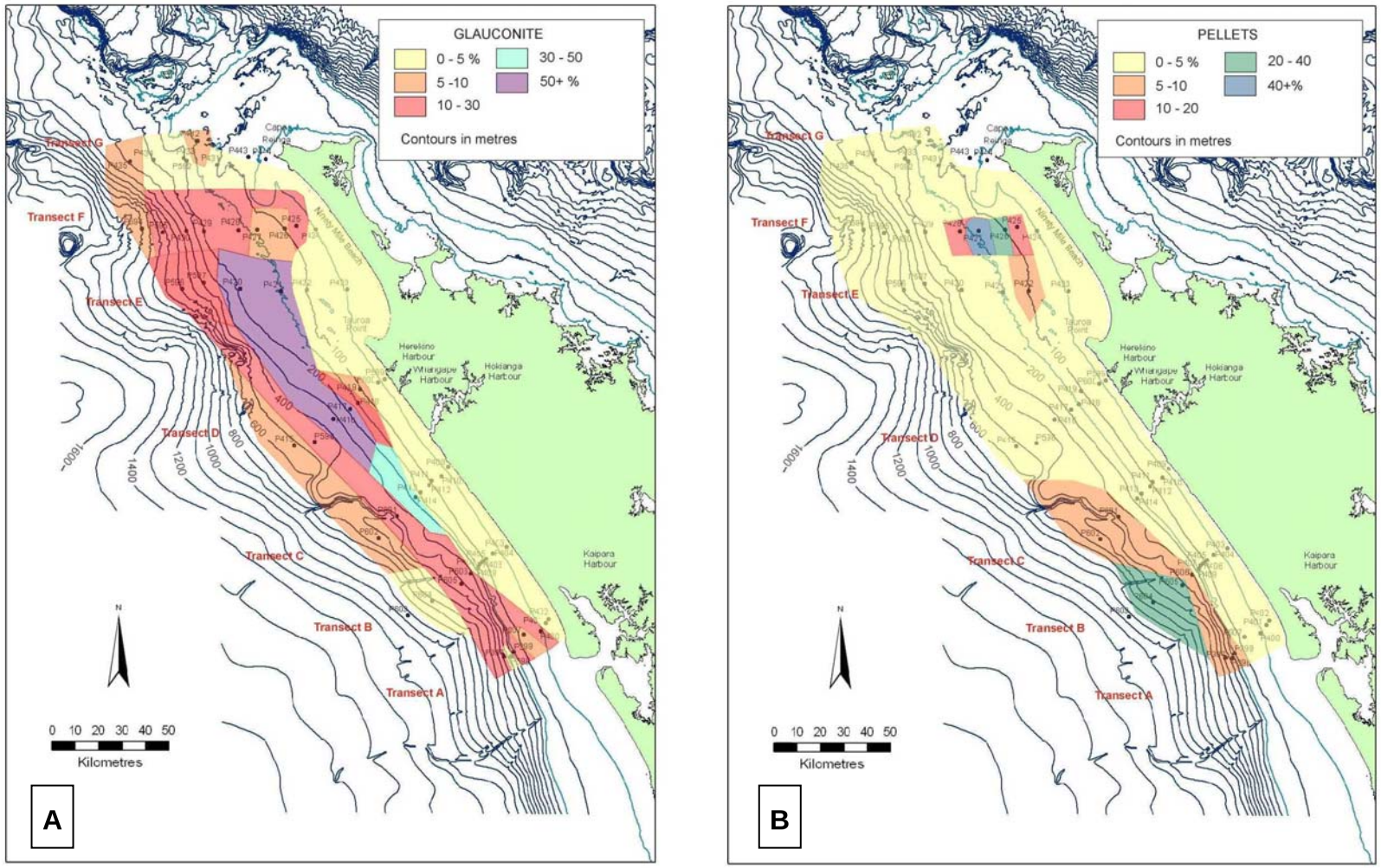

Figure 4-17. Distribution of (A) glauconite and (B) mixed carbonate-siliciclastic pellets in NKCM bottom sediments.

fresh (bright green, limited cracking), which are most common in the concentrated area, to highly degraded (brown, cracked and splitting), which are more common in the southernmost NKCM. The nature of these glauconite grains is discussed in more detail in Chapter 6.

4.6.2 Mixed carbonate-siliciclastic pellets

The mixed carbonate-siliciclastic pellets in the NKCM sediments are well rounded grains that vary considerably in size but with a dominant mode of 0.20-0.25 mm (fine sand). These grains are similar to glauconite in shape and form but they consist of very fine grained quartz, feldspar and heavy mineral grains as well as skeletal fragments contained within a tan to brown coloured micritic-argillaceous matrix (Plate 5 a, e). Some of these pellets have darker centres, similar to nuclei, which appear to range in size between different grains (Plate 5 a). Under CL, the quartz, feldspar and skeletal grains within the pellets luminesce readily (Plate 5 b-d, f-h) while the argillaceous matrix, heavy mineral grains and darker nuclei fail to luminesce even under high exposure times (Plate 5 h).

These pellets form 0-5% of most of the NKCM sediment although their content is higher at 12 sample sites (Fig. 4-17B). Two areas of sediment consist of >10% pellets, one in the northern half of NKCM and the other in the south. The northern area includes the highest concentration of pellets (up to 40-50%) between 140 and 150 m water depth which decreases inshore to 20-30% at c. 100 m depth and 10-20% at c. 80 m depth. There is also an area of 20-30% pellets in the southern portion of the NKCM between c. 400 and 800 m water depth along transect B. This decreases to 5-10% pellets in 300-700 m water depth along transects A-C.

Microprobe analysis was conducted on the matrix of eight pelletal grains (Appendix E) from P605 and P427 from transects B and F, respectively. The 11 analyses carried out produced totals between 44.48 and 58.76% with the dominant oxides present being SiO_2, CaO, Al_2O_3, FeO and MgO (Table 4-2) and only small amounts (<1%) of Na_2O, SO_3, Cl, K_2O, TiO_2 and P_2O_5. The southern pelletal matrix (P605) has a slightly different composition with c. 2% less Al_2O_3 and c.

6% less SiO_2. Analyses were also conducted on pellets containing nuclei to compare the nucleus composition with the surrounding matrix (Fig. 4-18). The compositional change from the central nucleus to the outside matrix varies between samples. Both the southern grains (P605b and c) contain less SiO_2 in the nucleus than the matrix, however there is little difference in SiO_2 in the northern sample. Al_2O_3 and FeO have higher concentrations in the nucleus than the outside matrix in P427 and P605c compared with P605b, where the opposite trend occurs. A similar trend occurs with CaO where P427 and P605c have a lower CaO content in the centre than the outside, while in P605b this is higher.

The low totals (i.e. c. 50% cf. ideal >90%) suggest the pelletal matrix comprises other elements not measured by the microprobe. When submerged in dilute hydrochloric acid the pellets effervesced suggesting this other component is CO_2 and the pelletal matrix comprises carbonate which was precipitated into the pore spaces of recently deposited faecal pellets. The compositional constituents discussed above are assumed to have been measured from only the pelletal matrix material but it is possible some contamination also occurs from detrital quartz, feldspar and skeletal grains within the pellet.

Table 4-2. Microprobe analyses for the six main oxides in the matrix of pellets in samples P605 and P427.

OXIDE	**P605**	**P427**
Al_2O_3	12.72	9.97
SiO_2	18.41	24.49
CaO	13.02	12.76
K_2O	0.82	0.69
FeO	3.05	3.16
MgO	1.41	1.28
TOTAL	51.01	53.45

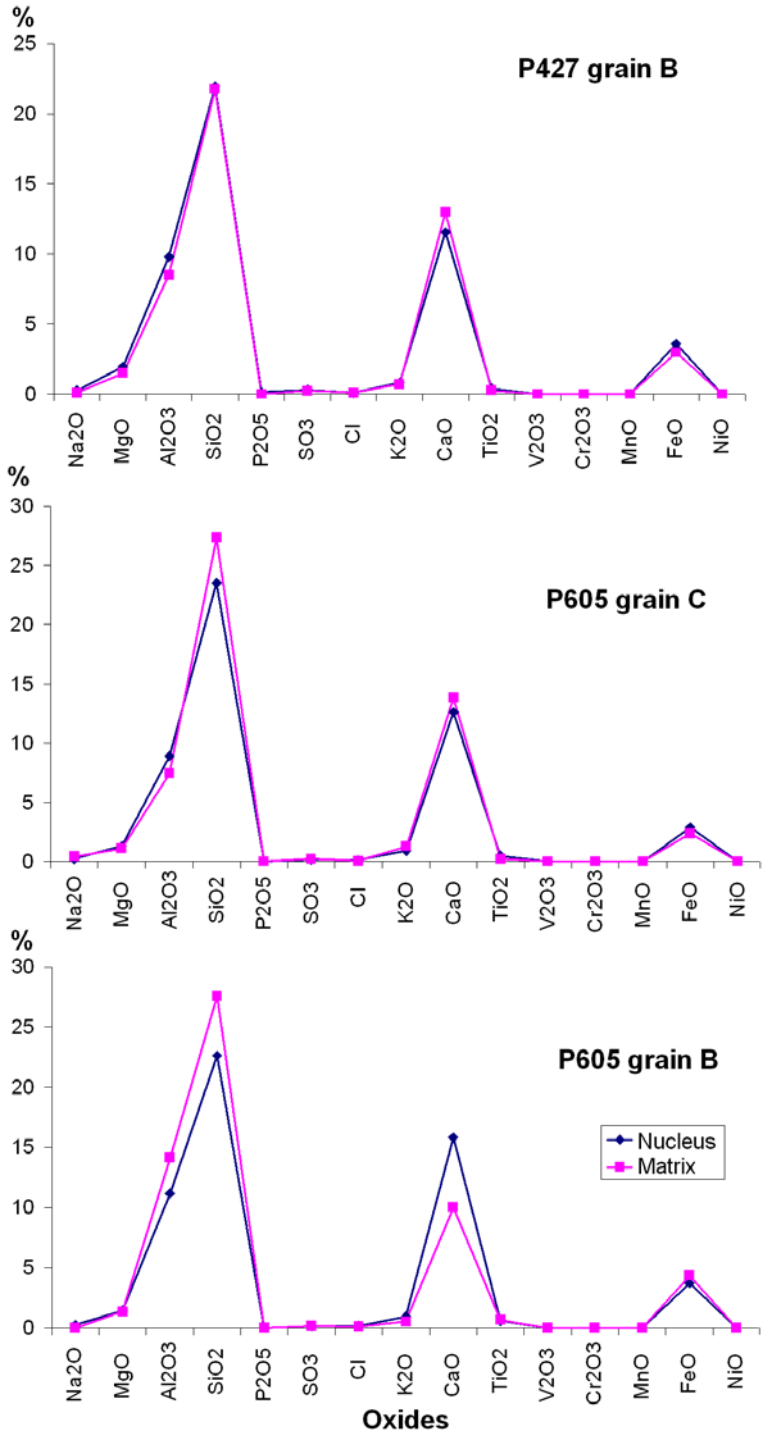

Figure 4-18. Graph comparing the oxide percentages (using microprobe) from the central and outer portion of three pelletal grains.

4.6.3 Phosphatic grains

The phosphatic component consists of skeletal fragments, mainly bivalve and gastropod, which have been phosphatised. These phosphatic fragments increase in content towards the north with 10-30% occurring between 100 and 200 m water

depth and at 400 m depth along transects E and F. This decreases to only 5-10% from c. 700-1000 m water depth along transect F and c. 150-400 m along transect G. The rest of the NKCM sediments comprise 0-5% phosphatic material, usually towards the lower value. The phosphatic component of the NKCM, including phosphate nodules and phosphatised slabs dredged from the Hokianga Terrace, is discussed in more detail in Chapter 6.

Chapter 5

SKELETAL TAXA, PRESERVATION AND MINERALOGY

5.1 INTRODUCTION

A split of the shell material greater than 0.5 mm, both whole and fragmented, was separated from the sand and gravel fraction from all the sample sites across the north Kaipara continental margin (NKCM). This shell material was then inspected and divided into the main taxonomic groups (Mollusca, Bryozoa, Foraminifera) before the individual species were picked out and identified primarily using Powell (1979), Keane (1986b) and A. Beu (pers. comm., 2007). Identification of the individual species was relatively difficult due to the prevalence of small specimens (especially micro-molluscs), the overall lack of adult specimens within the samples, their fragile thin-shelled nature and, at times, their variably degraded appearance. A full list of taxonomic groups, species present and their abundances can be found in Appendix D.

5.2 SKELETAL DISTRIBUTION

The skeletal fraction shows distinctive trends in distribution across the NKCM. The overall abundance of shell material in samples increases significantly to the north with very small amounts (<5%) of shell material recovered from the southernmost samples. There is also a corresponding decrease of shell material from inshore to offshore, especially beyond 100 m water depth.

The major skeletal groups present are Mollusca (primarily Bivalvia and Gastropoda, but also Pteropoda and Scaphopoda), Bryozoa and Foraminifera. The distribution of the dominant group(s) across the NKCM is illustrated in Figure 5-1. A common New Zealand situation in northern New Zealand is for a bivalve dominated inner shelf, passing into a bryozoan dominated mid to outer shelf and foraminifera dominated outer shelf and slope (Keane, 1986b). For the NKCM, the Bivalvia group dominates overall with a distinct band of bivalve dominance along

the inshore area from the northern to the southern extent of the NKCM. This band of bivalve dominance extends out to between 50 and 100 m water depth before grading into a combined bivalve-gastropod dominated band except along transect A where it passes directly into the foraminifera dominated band. There are also three smaller areas of bivalve dominance – one between 100 and 150 m depth on transect F, another at approximately 200 m depth along transect E and one at 150-200 m depth along transect B. The combined bivalve-gastropod dominated area extends from 50-200 m water depth with another significant band of bivalve-gastropod dominance between 150 and 1000 m depth in the northern part of the NKCM. The inner bivalve-gastropod band is broken by two small areas of gastropod dominance at approximately 100-150 m depth along transect B and C. Two larger areas of gastropod dominance are observed at about 150 m and

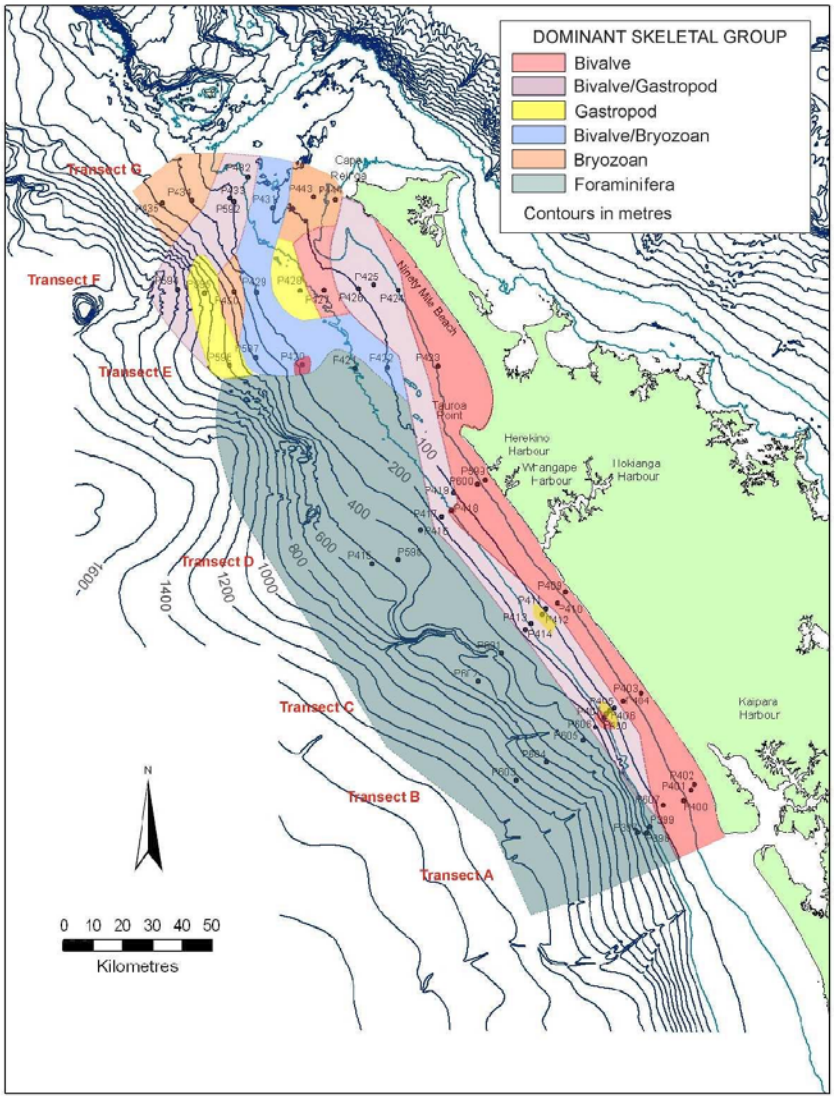

Figure 5-1. Distribution of dominant skeletal groups identified at each of the sample sites across the NKCM.

between 600 and 800 m in the northern third of the NKCM. A combined bivalve-bryozoan dominated band occurs between approximately 100 and 400 m depth across the three northernmost transects while three relatively small occurrences of solely bryozoan dominance are observed in the two northernmost transects at 50-100 m depth and 300-400 m water depth. A foraminifera dominated band occurs offshore and extends across three-quarters of the NKCM from 150-1050 m water depth; it likely extends deeper offshore.

Across the southern half of the NKCM (transects A-D) there is a relatively simple rapid transition offshore from bivalve to bivalve-gastropod and then foraminifera dominated sediment across only 200 m water depth. This offshore transition is considerably more complicated in the northern half of the NKCM (transects E-G) where, as described above, there is a larger range of dominating skeletal groups which extends much deeper offshore than those in the southern half (1000 m compared with 200 m).

5.2.1 Mollusca

5.2.1.1 Bivalvia

In Table 5-1 the bivalve species identified in skeletal samples from the NKCM are listed, while in Figure 5-2A the six most dominant species of Bivalvia have been mapped and, as with the dominant skeletal groups, there are distinctive trends evident from inshore to offshore. *Hiatella arctica* dominates only in the southern half of the NKCM from inshore to approximately 80 m water depth where *Scalpomactra scalpellum* then dominates out to c. 300 m depth. *Scalpomactra scalpellum* also extends into the northern half of the NKCM in less than c. 80 m water depth. There is also a small area of *Scalpomactra scalpellum* dominance at about 30 m water depth along transect B. *Saccella maxwelli* dominates in three locations but predominantly in the northern half between 150 and 200 m depth but also in smaller areas from 80-100 m depth. *Nucula nitidula* only dominates in the northern half of the NKCM between c. 100 and 200 m depth across transects E, F and G with two smaller areas along transect D at c. 60 and 200 m depth. *Pleuromeris zelandica* primarily dominates in the northern half between 100 and

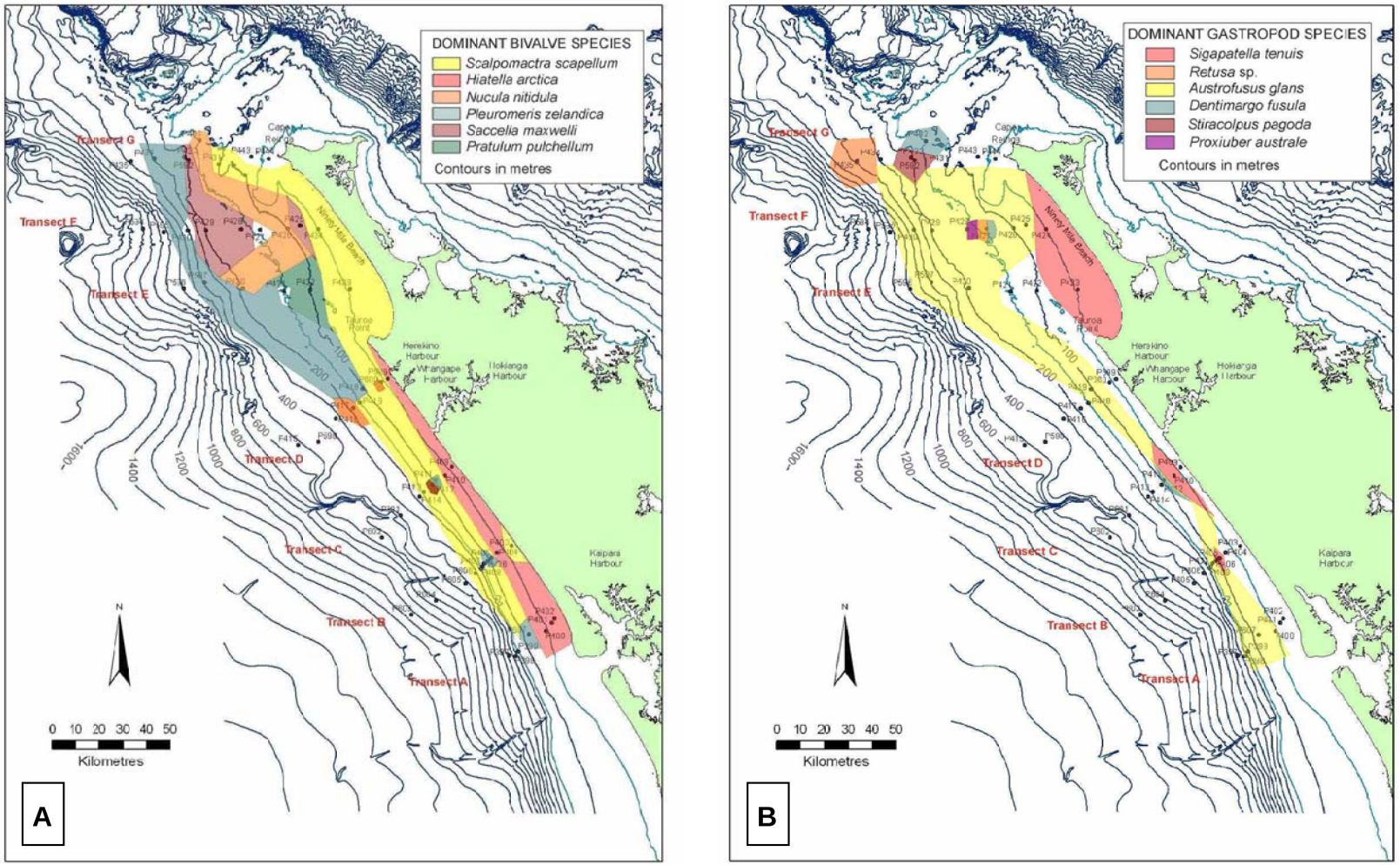

Figure 5-2. Distribution of the six dominant (A) Bivalvia and (B) Gastropoda species at each sample site across the NKCM.

400 m but also occurs at about 80 m along transect C, 80-110 m along transect B and 90 m along transect A. *Pratulum pulchellum* dominates in only one small location along transect E in the northern half of the NKCM at approximately 200 m water depth.

5.2.1.2 Gastropoda

In Table 5-2 the gastropod species identified in skeletal samples from the NKCM are listed, while in Figure 5-2B the six most dominant species of Gastropoda have been mapped across the NKCM. They do not appear to show any significant trends in distribution either inshore to offshore or north to south. *Sigapatella tenuis* dominates in shallower waters between 50 and 100 m water depth and is found across the entire NKCM. *Austrofusus glans* dominates between 50 and 200 m depth and was observed in every transect except transect C. *Retusa* sp.,

Table 5-1. Taxonomic list of the Bivalvia species identified in skeletal samples from the NKCM (using Powell, 1979 and A. Beu, pers. comm., 2007). Main species are illustrated in Plate 6.

MOLLUSCA	
Bivalvia	
Scalpomactra scalpellum	*Nuculidae* sp. unnamed
Nucula nitidula	*Neilo australis*
Pratulum pulchellum	*Serratina charlottae*
Hiatella arctica	*Zenatia acinaces*
Saccella maxwelli	*Barbatia novaezealandiae*
Pleuromeris zelandica	*Leptomya retiaria*
Cardita aoteana	*Caryocorbula zelandica*
Gonimyrtea concinna	*Thyasira* sp.
Pleuromeris sp.	*Austrovenus stutchburyi*
Talochlamys gemmulata	*Tawera spissa*
Melliteryx sp.	*Myllitella vivens*
Moerella huttoni	*Notocallista multistriata*
Poroleda lanceolata	*Divaricella huttoniana*
Limopsis lata	*Escalima regularis*
Purpurocardia purpurata	*Borniola reniformis*
Barythaerus caneatus	*Parvamussium* sp.
Gari lineolata	

Dentimargo fusula, *Stiracolpus pagoda* and *Proxiuber australe* all occur in small areas across the NKCM.

Three species of Pteropoda (Table 5-2) were identified across the NKCM: *Cavolina inflexa*, *Cavolina telemus* and *Clio pyramidata*. Pteropods were most common in the northern half of the NKCM (transects E-G) and at water depths greater than 100 m. They comprise between 0.3 and 21% of the total sample with the largest percentage (21%) observed at sample site P596 in 598 m water depth. The largest number of pteropods (25) was observed at sample site P425 in slightly shelly and sandy mud at 78 m water depth – the only site where pteropods occur in less than 100 m water depth.

Table 5-2. Taxonomic list of the Gastropoda species in skeletal samples from the NKCM (using Powell, 1979 and A. Beu, pers. comm., 2007). Main species are illustrated in Plate 7.

MOLLUSCA	
Gastropoda	
Austrofusus glans	*Antalis nana*
Proxiuber australe	*Solatisonax supraradiata*
Sigapatella tenuis	*Uberella denticulifera*
Stiracolpus pagoda	*Epitonium* sp.
Dentimargo fusula	Pyramidellidae
Almalda novaezelandiae	*Zemitrella* sp.
Antisolarium egenum	*Acteon cratericulatus*
Retusa sp.	*Balcis* sp.
Pupa affinis	*Alvinia (Linemea) gallinacea*
Antiguraleus sp.	*Philine constricta*
Syrnola crawfordi	*Solariella luteola*
Epitonium ?bucknilli	*Epitonium jukesianum*
Cancellariidae; unnamed	*Maoricrypta sodalis*
Emarginula striatula	*Pisinna* sp.
Mesoginella manawatawhia	*Notocrater craticulata*
Notoacmea sp.	*Atlanta peroni*
Tanea zelandica	*Almalda* sp.
Pervicacia tristis	
Pteropoda	*Clio pyramidata*
Cavolina inflexa	*Cavolina telemus*

5.2.2 Bryozoa

A broad range of bryozoan species was identified across the NKCM (Table 5-3) but only in significant numbers within the northern half. Keane (1986b) previously noted the bryozoan species in samples from the southwestern side of the Three Kings platform. Bryozoans comprise only 0.5-5.3% of the skeletal sample in the southern half of the NKCM (transects A-D), but this increases to between 0.3 and 80% in the northern half (transects E-G). *Cellaria immersa* and *Celleporaria tridenticulata* are the dominant species present with over three times the number of skeletal fragments observed compared to each of the other species. These two species are most common in Transect G where they dominate 5 out 7 sample sites; however, they are absent in samples from the southern half of the NKCM. *Steginoporella neozelandica* and *Galeopsis polyporus* are the next most dominant species and, like *Cellaria immersa* and *Celleporaria tridenticulata*, are only observed in the northern half of the NKCM. *Otionella symmetrica* is the only species of bryozoan identified within the southern half of the NKCM with four sample sites recording the species. The majority of the bryozoan skeletal fragments identified are highly abraded suggesting they have been reworked extensively by high-energy swell waves or transported long distances from source areas. The location of living carbonate communities 30 km to the north around Three Kings Islands (Nelson, 1982; Nelson et al., 1982) supports this, however a smaller carbonate producing area is present between Cape Maria Van Diemen and Cape Reinga. The lack of less abraded bryozoan material from this source may be the result of strong tidal currents around Cape Reinga that transport the material to the northeast.

Table 5-3. The bryozoan species identified in skeletal samples from the NKCM (using Keane, 1986b).

BRYOZOA	
Cellaria immersa	Free living Conescharellinidae
Celleporaria tridenticulata	*Otionella symmetrica*
Steginoporella neozelandica	*Hippellozoon novazelandiae*
Galeopsis polyporus	*Notocyathus* sp.
Steginoporella sp.	

5.2.3 Foraminifera

Foraminifera were identified in 75% of the sample sites across the NKCM, comprise between 0.1 and 95% of the skeletal fraction and predominantly occur within the deeper water sediment samples (>100 m). Foraminifera are identified in all the sample sites in transect E and all but the shallowest sample sites in transects C and D; however, they are less common in transects F and G.

The content of foraminifera present within the skeletal fraction shows an increase with water depth with the six sample sites that have a percentage greater than 55% occurring in approximately 400 m water depth or greater. However, there are significant exceptions with only a single foraminifera identified within the two deepest sample sites at 710 and 1015 m which comprise only 1.9 and 3.1% of the total skeletal sample, respectively. Benthic foraminifera dominate the macro-skeletal samples analysed here (>0.5 mm) with over 70% of the foraminifera identified being benthic.

Foraminifera from the 0.063-1 mm fraction were picked and identified in ten samples across two transects (B and F) (Table 5-4). An eleventh sample was investigated (P403, 34 m water depth) but no foraminifera were found. Species of benthic foraminifera dominated overall with 87 benthic species identified compared to only 14 planktic species. As a result, a very wide range of benthic species occur on the NKCM with *Cibicides corticatus*, *Hoeglundina elegans*, *Quinqueloculina auberiana*, *Saidovina karreriana* and *Uvigerina peregrina* the most dominant (Plate 8 a-h, m). *Quinqueloculina auberiana* was more common in the north (transect F) while *Cibicides corticatus* was more common in the southern transect. *Evolvocassidulina orientalis* and *Bulimina marginata* f. *marginata* (Plate 8 k-l, n) were also common across both transects. Agglutinated benthic foraminifera were relatively rare although several species were identified (Table 5-4). As with the molluscan species, the other benthic foraminifera species often occur in very small numbers. The ratio of planktic to benthic foraminifera increases with depth as expected and the planktic species occur over a wider depth range than most of the benthic species. *Globorotalia inflata* (Plate 8 i-j), *Globigerina bulloides* and *Orbulina universa* are the dominant planktic species

and these three species are also the only ones to occur in every sample site where the identification of foraminifera took place.

Table 5-4. Species of benthic and planktic foraminifera identified in ten NKCM samples.

FORAMINIFERA	
Benthic species	
Cibicides corticatus	*Pyrgo anomala*
Cibicides marlboroughensis	*Pyrgo depressa*
Cibicides sp.	*Notorotalia* sp.
Dyocibicides sp.	*Notorotalia* ?*zelandica*
Hoeglundina elegans	*Notorotalia* af. *finlayi*
Evolvocassidulina orientalis	*Notorotalia depressa*
Quinqueloculina auberiana	*Notorotalia* af. *depressa*
Quinqueloculina af. *delicatula*	*Bolivina* sp.
Quinqueloculina af. *cooki*	*Bolivina* ?*cacozela*
Quinqueloculina suborbicularis	*Bolivina* cf. *hornbrooki*
Quinqueloculina sp.	*Bolivina* af. *neocompacta*
Bulimina sp.	*Bolivina spathulata*
Bulimina (hispid)	*Saidovina karreriana*
Bulimina marginata f. *marginata*	*Zeaflorilus parri*
Discorbinella bertheloti	*Neouvigerina proboscidea*
Lenticulina ?*australis*	*Uvigerina* (hispid)
Lenticulina af. *suborbicularis*	*Uvigerina peregrina*
Lenticulina subgibba	*Uvigerina* ?*rodleyi*
Lenticulina sp.	*Uvigerina* sp.
Lenticulina sp. 2	*Astrononion* sp.
Lenticulina sp. 3	*Astrononion novozealandicum*
Lagena sp.	*Oridorsalis umbonatus*
Lagena striata	*Pullenia bulloides*
Lagena ?*spicata*	*Pullenia subcarinata*
Lagena (hispid)	*Sphaeroidina bulloides*
Cassidulina carinata	*Oolina* af. *melo*
?*Nonionellina flemingi*	*Elphidium* sp.
Nonionella magnalingua	*Bolivinta* sp.
Saracenaria italica	*Haynesina depressula*
Chilostomella sp.	*Trioculina* ?*tricarinata*
Globobulimina sp.	*Trifarina angulosa*
Fursenkoina schreibersiana	*Gyroidina* sp.
Reussella spinulosa	*Amphicoryna hirsuta*
Laevidentalina sp.	*Ammonia* sp.
Stilostomella sp.	*Laticarrinina pauperata*
Gyroidinoides sp.	*Anomalinoides sphericus*
Savacenarid ?*latifrons*	*Globocassidulina canalisuturata*
Globocassidulina subglobossa	*Ehrenbergina* af. *willetti*
Unknown sp.1	*Planularia australis*
Unknown sp.2	*Sigmoilopsis* ?*elliptica*
Sigmoilopsis schlumbergeri	*Sigmoilopsis* sp. 2
Sigmoilopsis sp. 1	*Textularia* sp.
Semivulvulina sp.	*Agglutinated* sp. (int)
Siphotextularia?	

Table 5-4 cont. Species of benthic and planktic foraminifera identified in ten NKCM samples.

Planktic species	
Globorotalia inflata	*Globigerinoides aequilateralis*
Globorotalia crassaformis "keeled"	*Globigerinoides ruber*
Globorotalia crassaformis "unkeeled"	*Globigerinoides* ?*ruber*
Globorotalia crassula	*Globigerina bulloides*
Globorotalia truncatulinoides	*Neogloboquadrina pachyderma*
Globorotalia ?*puncticuloides*	*Neogloboquadrina dutertrei*
Orbulina universa	*Globigerina quinquloba*

5.3 RELATION OF SKELETAL TYPES TO BATHYMETRY

Bivalvia and Gastropoda

The depth ranges of the Bivalvia and Gastropoda species recorded from the NKCM are illustrated in Figures 5-3 and 5-4, respectively. It is evident in Figure 5-3 that the majority of bivalve species live between 0 and 200 m water depth with only *Limopsis lata*, *Neilo australis*, *Thyasira* sp. and *Parvamussium* sp. inhabiting deeper water. *Limopsis lata* covers the largest depth range from 100-1200 m and only *Parvamussium* sp. has its expected depth range starting beyond 200 m (at 420 m). The gastropod species depth ranges follow a similar but less accentuated trend (Fig. 5-4) with 22 of the 36 species (cf. 25 of 31 bivalve species) found at less than 200 m. *Austrofusus glans* covers the largest depth range from low tide to 550 m and, like the bivalve species, only one gastropod species, *Waipaoa marwicki*, has its expected depth range minimum at greater than 200 m. The gastropod species show considerable variety in their depth ranges when compared to the bivalve species with both very narrow (35 m) and very wide (550 m) depth ranges shown.

Assessment of the Bivalvia and Gastropoda specimens was carried out to determine if they were recovered from the expected depth range (m) for each of the species. The species found outside of their expected ranges are listed in Table 5-5 and 5-6 for Bivalvia and Gastropoda, respectively. The depth the specimens were found, their expected depth range and the overall condition of the skeletal fragments are also noted.

Sixteen bivalve species were found outside their normal expected depth range by

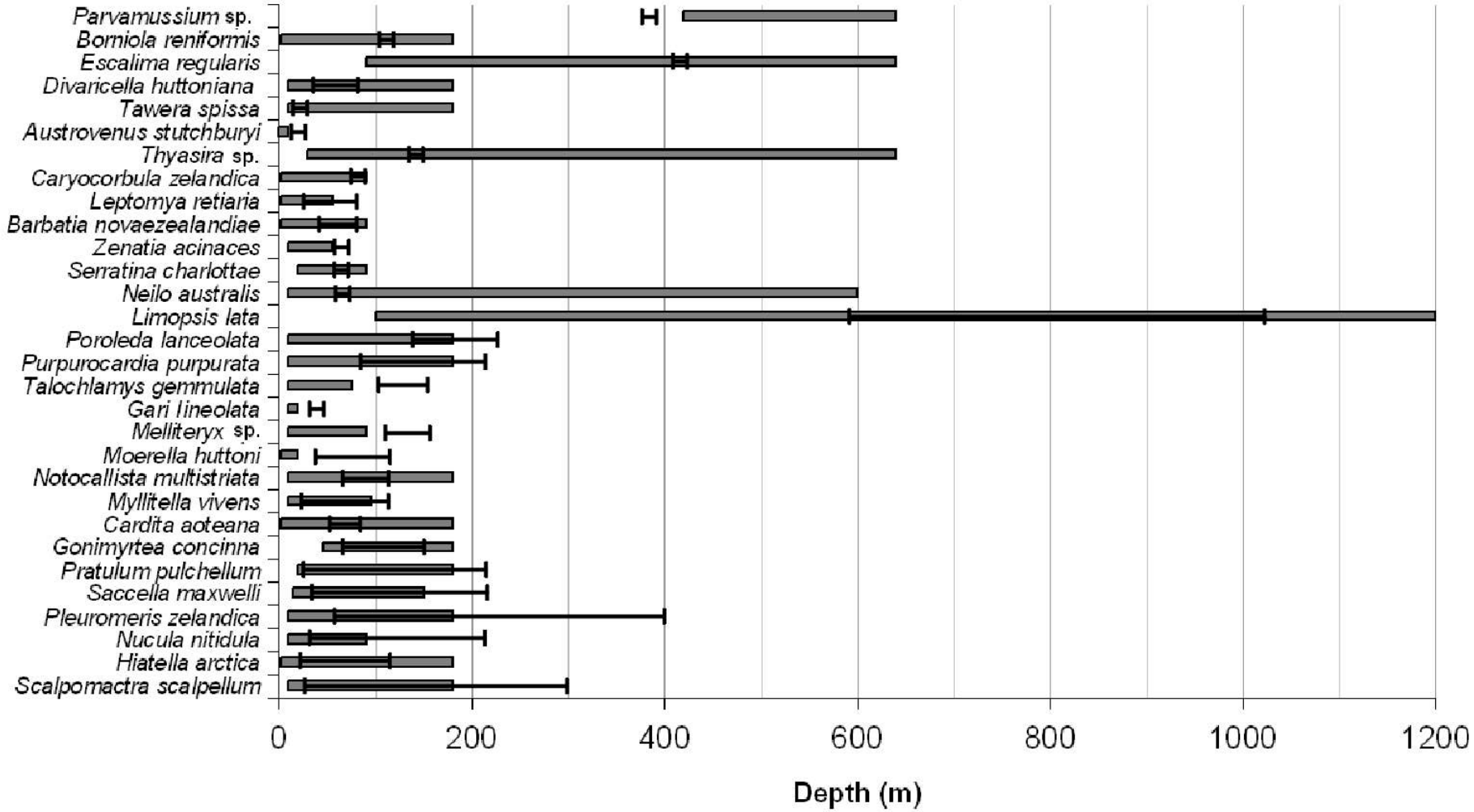

Figure 5-3. The expected depth range (m) of the Bivalvia species found within skeletal samples from the NKCM (depth ranges based on Powell, 1979). The species are listed from least abundant at the top to most abundant at the bottom. Grey bars are expected depths, black bars are depths species were found at.

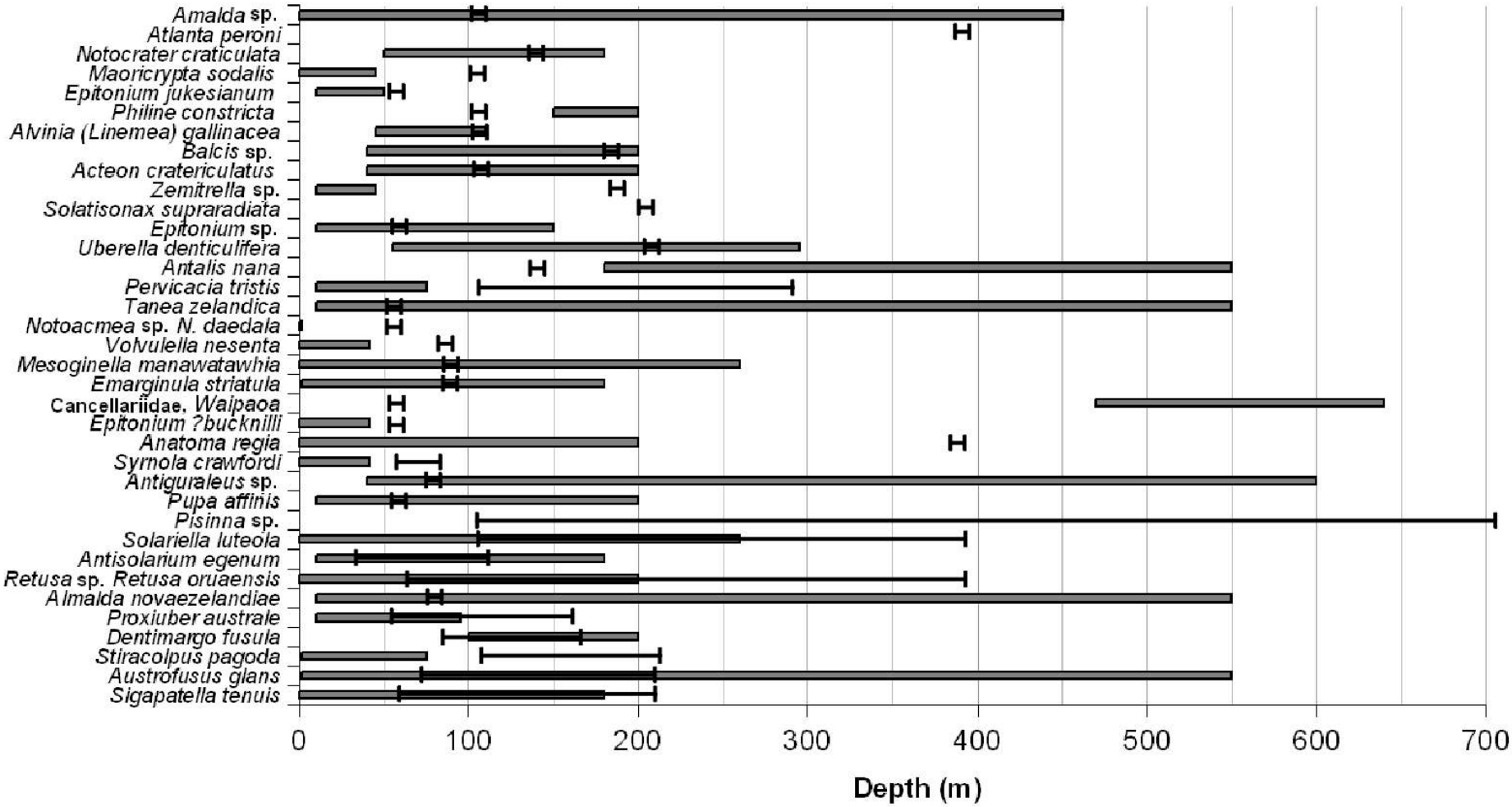

Figure 5-4. The expected depth range (m) of the Gastropoda species found within skeletal samples from the NKCM (depth ranges based on Powell, 1979). The species are listed from least abundant at the top to most abundant at the bottom. Grey bars are expected depths, black bars are depths species were found at.

as much as 9-120 m, but mainly by between c. 18 and 37 m. The majority (15 out of 16) of these species were found at depths greater than their expected range with only one species, *Parvamussium* sp., found at a shallower depth. These apparently anomalous depth ranges could be due to (a) the species having a greater depth range than has previously been recorded in the literature, or (b) the shells having been reworked and transported by tide, storm wave or coastal currents, or (c) shell deposition being associated with times of lower sea level. Nine out of the twelve recorded species occur in skeletal samples classified as relict or mixed fresh-relict, with only three graded as fresh. This dominance of degraded skeletal material supports association with lowered sea levels and/or shell reworking.

The gastropod species found out of place vary considerably with 13 species between 15 and 312 m outside of their expected depth ranges. The majority of

Table 5-5. The Bivalvia species found outside their expected depth range showing the depth they were found, their expected depth ranges (from Powell, 1979) and the condition of skeletal fragments from the samples in which they were found. F = fresh, M = mixed fresh–relict and R = relict.

Species	Depth (m) found	Depth range (m)	Preservation (no.)
Scalpomactra scapellum	34-300	Shallow-180	M
Nucula nitidula	34-206	Shallow-90	R (8)
Pleuromeris zelandica	65-400	Shallow-180	R (2)
Saccella maxwelli	42-206	15-150	R (3)
Pratulum pulchellum	33-206	20-180	R
Myllitella vivens	34-104	Shallow-95	F
Moerella huttoni	52-108	Low tide-20	F
Melliteryx sp.	108-158	Shallow-90	R (3)
Gari lineolata	42	Shallow-20	F
Talochlamys gemmulata	104-158	Shallow-75	R (4)
Purpurocardia purpurata	92-206	Shallow-180	R
Poroleda lanceolata	144-216	10-180	F
Zenatia acinaces	78	Shallow-55	M
Leptomya retiaria	42-92	Low tide-55	M – R
Austrovenus stutchburyi	34	Tidal	F
Parvamussium sp.	395	c. 420-640	R

species occur only some 15-60 m outside of their range with only four of the 13 species found at a shallower depth than expected. Nine of the thirteen species were found in skeletal samples graded relict or mixed fresh-relict with three species found in fresh samples and one species, *Pervicacia tristis*, found in both relict and fresh samples. The fresh sample that contained *Pervicacia tristis* is located 30 m deeper than the expected depth range for that species while the relict sample was over 220 m deeper. The other two species found in fresh samples are *Notoacmea* sp. and *Maoricrypta sodalis*, both of which are over 50 m outside their expected depth ranges. *Waipaoa marwicki* was found the furthest outside its expected depth range (312 m) and is one of the four species recorded at shallower depths than expected. As with the bivalve species, the dominance of degraded skeletal material suggests displaced shells were deposited during lower sea level and/or transported by tides, storm waves or coastal currents to their present

Table 5-6. The Gastropoda species found outside their expected depth range showing the depth they were found, their expected depth ranges (from Powell, 1979) and the condition of skeletal fragments from the samples in which they were found. F = fresh, M = mixed fresh–relict and R = relict.

Species	Depth (m) found	Depth range (m)	Preservation (no.)
Stiracolpus pagoda	108-206	Low water-75	R (4)
Sigapatella tenuis	52-206	Intertidal-180	R
Proxiuber australe	55-158	10-95	M, R (3)
Dentimargo fusula	85-158	100-200	M
Retusa sp.	67-395	200	R
Syrnola crawfordi	65-78	42	F-M
Anatoma regia	395	200	R
Epitonium ?bucknilli	52	42	F
Waipaoa marwicki	158	470-640	R
Volvulella nesenta	92	42	M-R
Notoacmea sp.	52	Splash zone	F
Pervicacia tristis	104-297	Shallow-75	F, R (3)
Antalis nana	144	180-550	M
Zemitrella sp.	183	Shallow-45	M
Philine constricta	108	c. 150-200	R
Maoricrypta sodalis	104	Intertidal-45	F

position. In the case of the three species found within fresh samples all were within 120 m water depth where sediment transport between the beach or nearshore and middle to outer shelf is active.

A few of the bivalve and gastropod species identified are of special interest. A stained and abraded adult specimen of *Austrovenus stutchburyi* was identified in sample P403 (A. Beu, pers. comm., 2007) – a grab of fine sand at 34 m water depth. *Austrovenus stutchburyi* is generally found on tidal mud and sand flats within estuaries and harbours (Powell, 1979) suggesting this specimen has been transported a significant distance (as P403 is located c. 60 km from both the Hokianga and Kaipara Harbour mouths) or it represents a shell deposited during the last glaciation when the sea level was significantly lower (A. Beu, pers. comm., 2007). An adult specimen of the rare *Solatisonax supraradiata* was observed in sample P429 in glauconitic very fine sand at 206 m water depth.

Bryozoa

The expected depth range for *Galeopsis polyporus* is from 100 to greater than 1000 m water depth while *Celleporaria tridenticulata* occurs at generally less than 300 m depth. The only bryozoan species in the southern half of the NKCM, *Otionella symmetrica*, generally occurs at depths of less than 100 m but may be found out to 300 m water depth (Keane, 1986b). *Galeopsis polyporus* was identified in nine sample sites with seven of these sites within the expected depth range of the species. The two sites outside of this range were shallower and within 50 m depth of the expected range. Seven of the ten sample sites containing *Celleporaria tridenticulata* were within the expected depth range with three other samples considerably deeper (between 95 and 715 m). These samples are relict in nature suggesting the bryozoan fragments were transported to deeper water through storm, tide or coastal current processes. The eight sample sites that recorded *Otionella symmetrica* were within the expected depth range for the species with four of these sites in less than 100 m water depth.

Benthic Foraminifera

Only 59 of 87 benthic foraminiferal species had adequate depth range information available with 40 species identified in sample sites outside of their expected depth ranges (Fig. 5-5). Of these 40 species, 15 were found just outside of their expected range (within 10-50 m). Most of the species were found at depths greater than expected (>70%) with only eight species found at shallower depths (Fig. 5-5). Of these eight species only three, *Stilostomella* sp., *Uvigerina peregrina* and *Amphicoryna hirsuta*, occur completely outside of their expected depth range. Of the other 25 foraminiferal species most are only outside of their expected depth range by between 100 and 200 m water depth, although the maximum depth difference is 430 m. Both *Cibicides corticatus* and *Cibicides marlboroughensis* occur between 50 and 420 m deeper than expected with both species identified in six of the ten samples (Fig. 5-5). The *Cibicides corticatus* specimens were generally more abraded, pitted and bored than *Cibicides marlboroughensis*. *Ammonia* sp. is identified in two samples (P426, P428) between 100 and 160 m water depth. This species is typically found in estuaries and enclosed harbours suggesting a considerable distance of transport has occurred to deposit it at this depth.

5.4 PRESERVATION

The level of disintegration of shell material and the amount of bleaching and boring and break down of the shell surfaces were assessed for each of the samples using the grading system outlined in Table 5-7 and Plate 9. Relict vs. fresh

Table 5-7. Description of the three grades of preservation used for the skeletal samples from the NKCM.

GRADE	DESCRIPTION	NAME
1	Shells brightly coloured, shiny, mostly whole	Fresh
2	Shells mostly broken, faded appearance/colour	Mixed fresh-relict
3	Shells all broken, bleached, grey colour, some boring and breakdown of shell surface	Relict

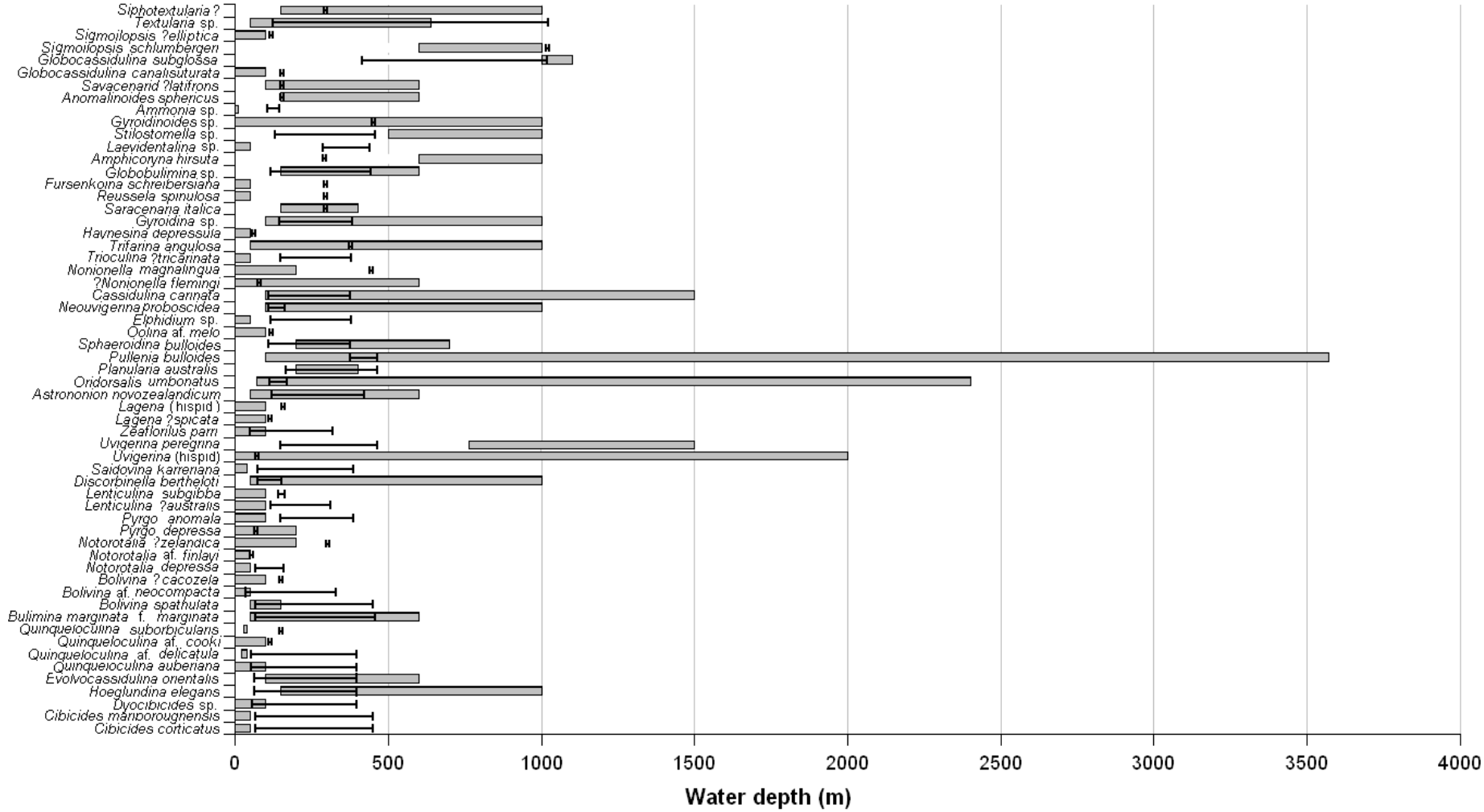

Figure 5-5. The expected depth range (m) of the benthic foraminifera species identified in ten samples from the NKCM (depth ranges based on Hayward et al., 1999). Grey bars are expected depths, black bars are depths species were found at.

skeletal material is considered important as the relict material may represent skeletal fragments deposited during lowered sea levels accompanying last glacial and post-glacial times. However, this is not always accurate and relict appearing skeletal fragments may in reality be modern but have been subjected to environmental factors such as a higher hydrodynamic regime that has led to the fragments degraded appearance (Nelson et al., 1982).

In Figure 5-6 the level of degradation of the skeletal fragments is mapped and shows a general trend of increasing skeletal degradation with depth, with fresh skeletal material in the inshore area grading to mixed fresh-relict and then relict

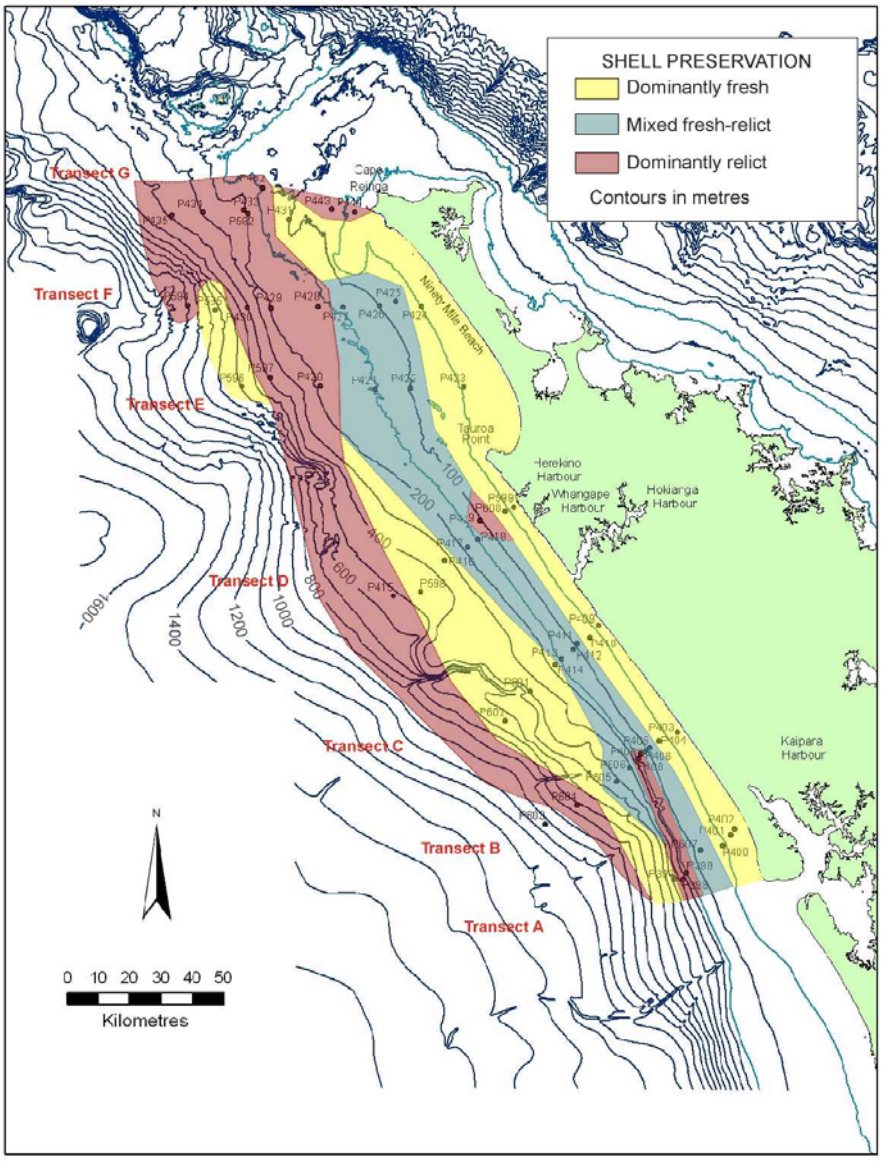

Figure 5-6. Distribution of fresh, mixed fresh-relict and relict skeletal fragments at each sample site across the NKCM (see Plate 9).

material further offshore. The fresh inshore band extends to a depth of 50-100 m across the entire NKCM and represents an area of high bivalve production, and as a result, fresh bivalve-dominated shell material. The mixed fresh-relict band generally occurs between 50 and 100 m out to 150-200 m across the length of the NKCM; however, it extends out to 450 m depth along transect B due to the presence of high contents of foraminifera which have a bright fresh appearance. Relict skeletal material is primarily observed between 150 and 1000 m water depth, although smaller areas occur within the mixed fresh-relict band at 100 m depth along transect D and 150-250 m depth along transects A and B. In the northern half of the NKCM the relict material occurs on the outer shelf and upper slope where modern sedimentation rates are low due to the lack of rivers supplying terrigenous sediment to the system from Northland. In the southern half of the NKCM this relict band is pushed further offshore due to the presence of more coastal rivers and discharge of sediment from the Hokianga, Whangape and Herekino Harbours. Fresh skeletal material is also found seaward of the mixed fresh-relict band between 200 and 650 m depth in the southern half of the NKCM and between 400 and 600 m in the northern half. This secondary fresh band represents mostly foraminifera-dominated skeletal material. However, P596 along transect E is dominated by pteropod skeletons which are deposited by settling from the water column and are usually less degraded as a result. Sample P432 is unusual in that it consists of approximately half relict and half fresh skeletal material suggesting transportation of relict bryozoan material to an area of modern bivalve and gastropod production.

5.5 MINERALOGY

Skeletal Carbonate Mineralogy

Aragonite and calcite are the two major carbonate minerals that comprise skeletal grains and the calcite minerals may be separated into low Mg-calcite (<5 wt% $MgCO_3$) and high Mg-calcite (>5 wt% $MgCO_3$) (Keane, 1986b). Bivalve skeletal grains may consist of aragonite or calcite with most infaunal bivalves aragonitic and most epifaunal bivalves calcitic. Gastropod skeletal grains (including

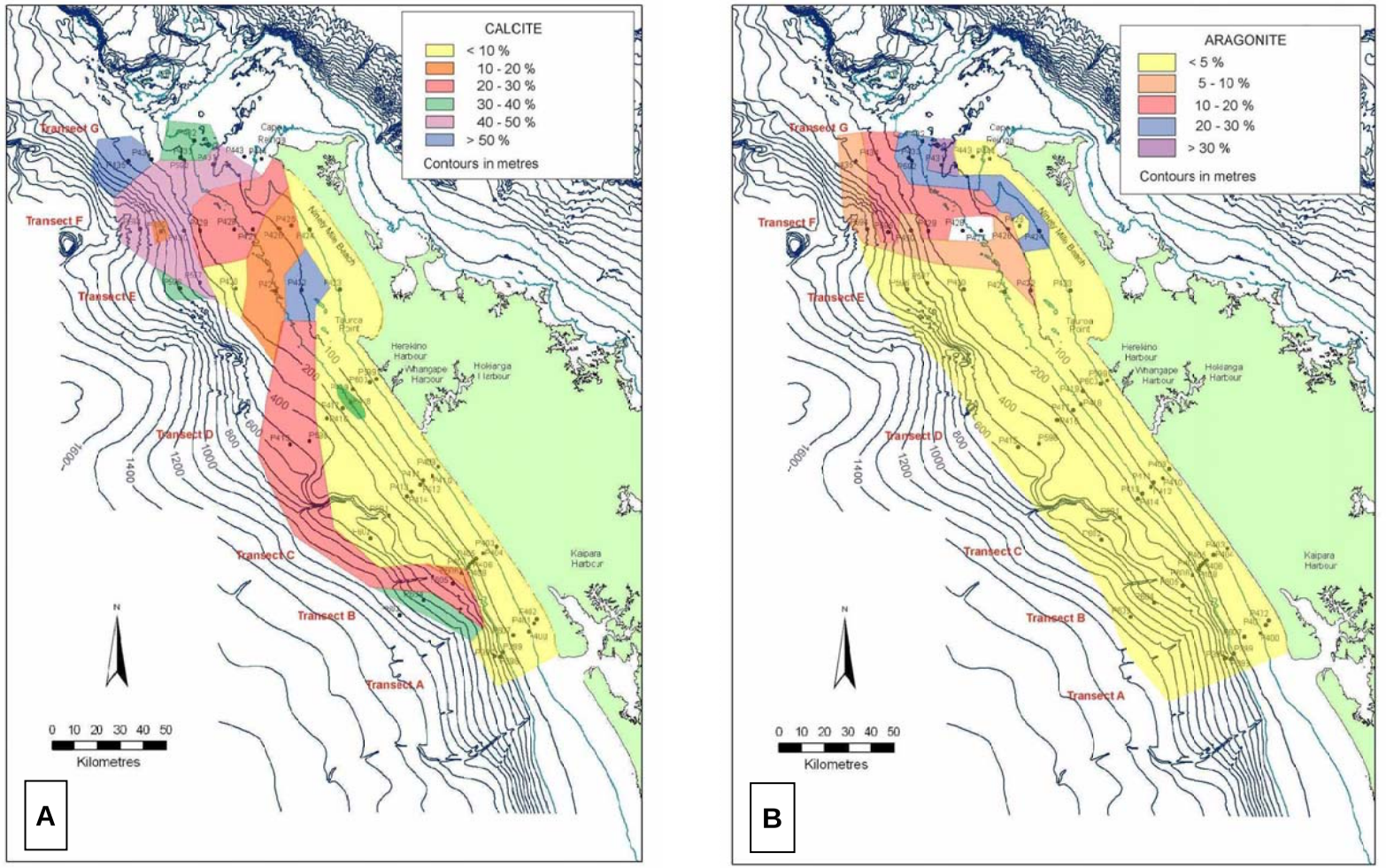

Figure 5-7. Distribution of (A) calcite and (B) aragonite at each of the sample sites across the NKCM.

pteropods) are aragonitic and with bivalves often dominate the aragonitic fraction of carbonate sediments in New Zealand. Bryozoan skeletal grains may be composed of either mineral but are dominated by high Mg-calcite (Keane, 1986b). *Steginoporella* sp. fragments consist of low Mg-calcite or low/high Mg-calcite while *Hippellozoon novaezelandiae*, *Cellaria immersa*, *Galeopsis polyporus* and *Celleporaria tridenticulata* are also calcitic (Keane, 1986b). Foraminifera (both planktic and benthic) predominantly consist of low Mg-calcite, although the encrusting benthic *Homotrema* sp. is composed of high Mg-calcite. Echinoderm skeletal fragments have high Mg-calcite skeletons (Keane, 1986b).

Bulk Sediment Carbonate Mineralogy

The mineralogy of the bulk sediment varies considerably across the NKCM but, overall, is dominated by calcite. Calcite occurs at every sample site and shows a general increase in abundance with water depth (Fig. 5-7A). Calcite contents range between 3 and 82% with the highest values in the northern half of the NKCM, reflecting the higher proportion of skeletal material within these samples. Areas of lower or higher calcite concentrations break this trend in only a small number of places. There are two areas of lower concentrations: the first at about 750 m water depth in transect F where an area of 10-20% calcite occurs in otherwise 40-50% calcite; the second occurs at 200 m depth in transect E where an area of <10% calcite occurs in normally 20-30% calcite. The high levels of glauconite and phosphate in the second are the likely cause of the lowered calcite percentage. There are also two areas of higher calcite concentrations compared to the surrounding sediment. The first occurs at about 100 m water depth in transect E where an area of >50% calcite occurs within otherwise 30-40% calcite, and the second is in 150 m water depth along transect D where 10-20% calcite is found within <10% calcite band.

Aragonite also occurs across the NKCM but is only significant in the northern half (Fig. 5-7B). It shows a decrease in percentage with depth with the lowest abundances between 150 and 1000 m water depth. The highest concentration of aragonite in a sample occurs in P431 at 100 m water depth with 34% of the skeletal material comprised of aragonite. There is a small area of lower concentration at about 80 m water depth along transect F.

In Figure 5-8 the calcite and aragonite percentages are plotted against depth for the seven transects (A-G). Overall these graphs show a decrease in the aragonite percentage offshore and an increase in both aragonite and calcite to the north. The graphs show the same basic trends of overall increase in calcite percentage with water depth. In more detail, calcite increases with water depth from c. 50 to 100-150 m before decreasing from 100-150 to 200 m depth. Between 200 and 400 m depth there is an increase in calcite again followed by a decrease out to 600-700 m. Transect F is the only transect to extend beyond 700 m where the calcite percentage shows an increase out to 1000 m water depth. Transects A and C show different trends in calcite percentage: transect A shows minor variation across 0-200 m when compared to other transects with the maximum change in calcite percentage only 8% (34-42%), while transect C shows the opposite trend with a considerable decrease in calcite percentage between 50 and 100 m depth before increasing sharply again out to 200 m depth. The calcite percentage along transect C then decreases from 200-600 m depth compared to the other transects which show an increase to 400 m and then decrease to 600 m depth.

The aragonite percentage varies considerably between the four transects D to G with transect D recording the southernmost occurrence of aragonite above trace levels at 150 m water depth. The aragonite percentage in transect E also increases out to 100 m (from trace-10%) before decreasing out to 150 m (from 10-3%). From 400-600 m water depth the aragonite percentage decreases to trace amounts. A more complicated trend in aragonite percentage is observed across Transect F with aragonite decreasing offshore from 23% to trace amounts between 50 and 150 m water depth followed by a small increase (trace-11%) from 150-200 m before the aragonite concentration then fluctuates between 5 and 11% from 200-1000 m water depth. Transect G shows a very simple decrease in aragonite percentage from 100-400 m water depth.

5.6 SKELETAL COMPARISONS WITH ADJACENT AREAS

Located to the north of the NKCM is the Three Kings platform and to the south is the West Auckland (includes NKCM), Waikato and Taranaki shelves. This

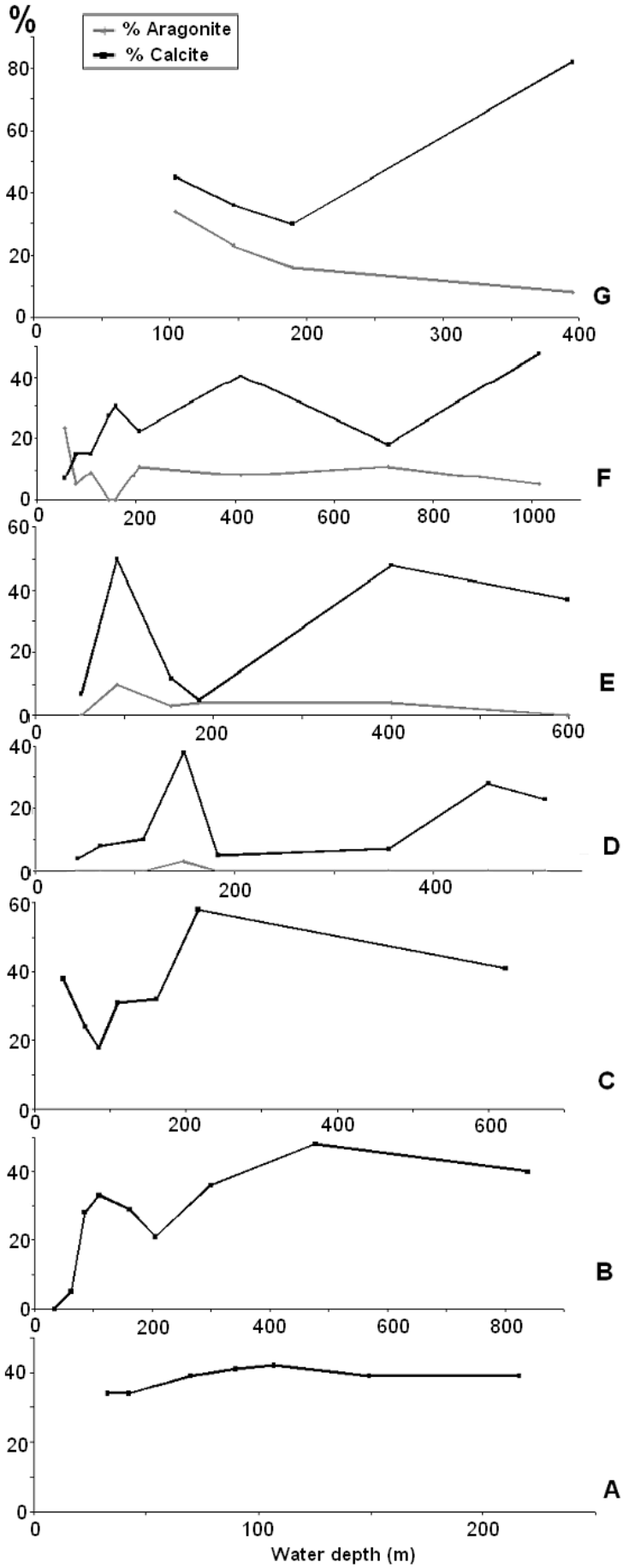

Figure 5-8. Distribution of calcite and aragonite inshore to offshore across the seven transects.

section briefly compares the skeletal components of these adjacent margins with those presented here for the north Kaipara continental margin (NKCM).

5.6.1 Three Kings platform

The Three Kings platform has a significantly greater range of skeletal material than the NKCM as a result of less terrigenous sediment input and warmer waters (Carter, 1975; Nelson, 1982; Nelson et al., 1988). A bryozoan skeletal lithofacies dominates the Three Kings platform (Fig. 5-9) (Nelson, 1982; Keane, 1986b) compared with only bivalve dominating on the NKCM. The bivalve-bryozoan and bivalve-gastropod associations observed on northern and northwestern NKCM, respectively (Fig. 5-1), extend into the Three Kings platform as far north as the Three Kings Islands but quickly grade into bryozoan and bryozoan-bivalve associations (Fig. 5-9).

Bryozoan (45.5%) and molluscan (16.7%) skeletal material dominate the Three Kings platform sediments with only 7% of foraminiferal material present (Nelson, 1982; Keane, 1986b). This compares to the NKCM, which is dominated by molluscan (54.5%) and foraminiferal (15.7%) material and only 11.4% bryozoan material. Within the molluscan skeletal material on Three Kings platform the bivalves dominate with 7.6% followed by gastropods (5.9%) and pteropods (3.2%). On the NKCM there is a similar trend with bivalves (37.8%) dominating and lesser amounts of gastropods (14.8%) and pteropods (2%).

The eight species of bryozoans found in NKCM sediments are the most common in the Three Kings platform area, occurring at over 20% of sample sites (Keane, 1986b). Relatively high abundances of *Tawera spissa*, *Scalpomactra scapellum* and *Saccella maxwelli* occur in the Three Kings platform area with only moderate abundances of *Pratulum pulchellum*, *Purpurocardia purpurata*, *Pleuromeris zelandica* and *Nucula nitidula* (Keane, 1986b). The NKCM has similar bivalve quantities, however *Scalpomactra scapellum*, *Saccella maxwelli*, *Hiatella arctica* and *Nucula nitidula* have the highest abundances and *Tawera spissa* only occurs in low abundances on the NKCM. *Parvamussium* sp., *Escalima regularis*,

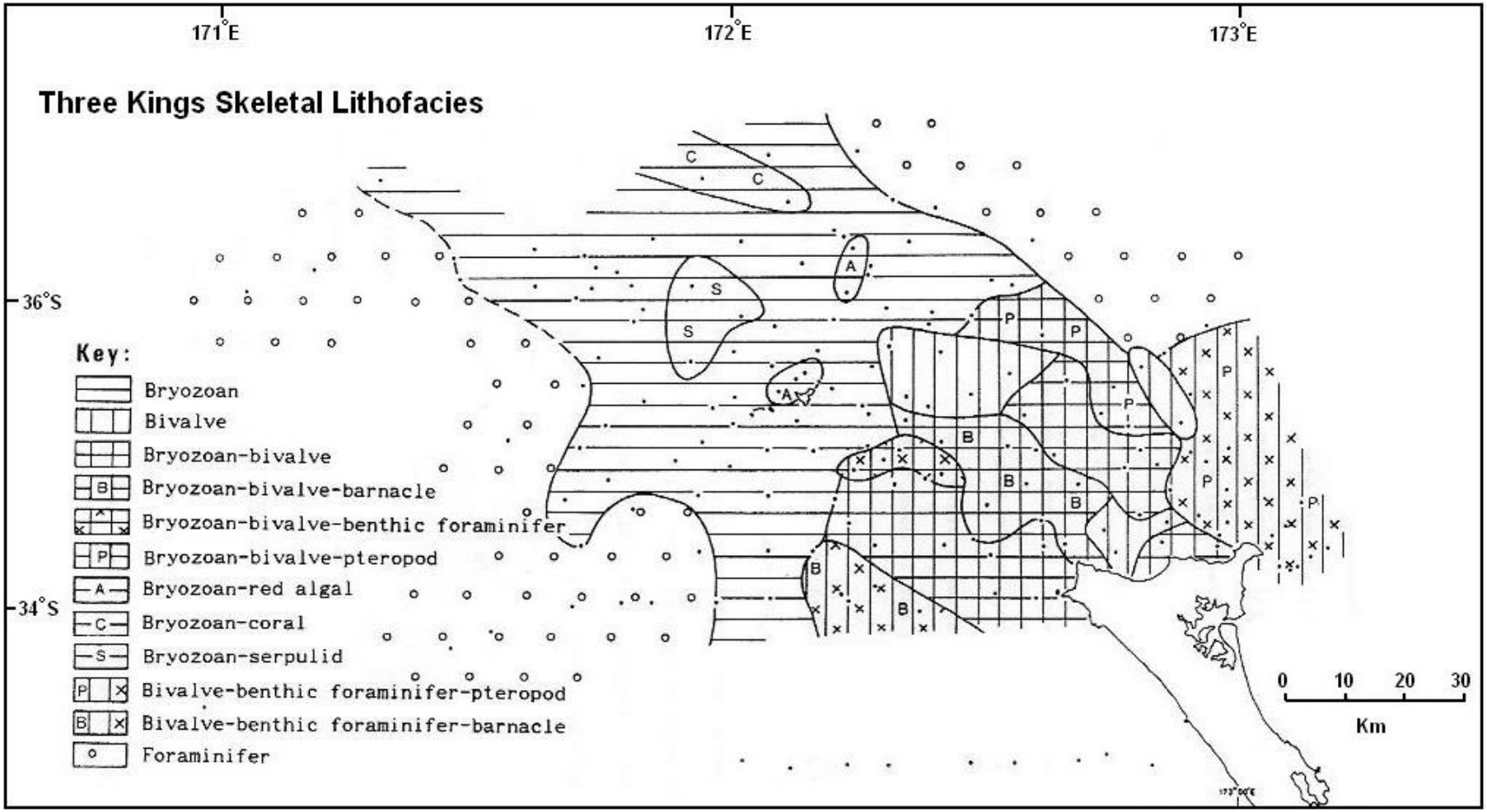

Figure 5-9. Distribution of skeletal lithofacies on the Three Kings platform (from Keane, 1986b).

G*onimyrtea concinna*, *Myllitella vivens* and *Cardita aoteana* have much lower abundances in the Three Kings platform region (Keane, 1986) as well as the NKCM. Gastropod species vary significantly between sample sites in the Three Kings platform area with only *Emarginula striatula* and *Sigapatella tenuis* the dominant gastropods at more than 10% of sample sites (Keane, 1986).

Austrofusus glans is the third most widespread gastropod species and is common with *Sigapatella tenuis*. This compares with the NKCM, which is dominated by *Austrofusus glans* and *Sigapatella tenuis*, and with the third dominant species *Proxiuber australe*. *Clio pyramidata* is the most common pteropod present within the Three Kings platform area and the NKCM, followed by *Cavolina telemus* and *Clio inflexa*.

Calcite and aragonite show the same basic trends on the Three Kings platform as observed on the NKCM with calcite increasing offshore, aragonite decreasing with depth and both increasing to the north (Nelson, 1982). Aragonite on the Three Kings platform predominantly varies from 0-20%, like the NKCM, however, higher percentages occur with over 50% aragonite in some locations (cf. maximum of 35% in NKCM).

5.6.2 West Auckland, Waikato and Taranaki shelves

The skeletal material on the West Auckland, Waikato and Taranaki shelves has not been as well documented as the Three Kings platform or the NKCM as presented in this chapter. Simple distributions of the main skeletal groups are provided in the literature. Along the West Auckland and Waikato shelves the proportion of skeletal fragments increases with depth. Bryozoan fragments dominate the inner and middle shelf with foraminifera, molluscan and bryozoan fragments dominating on the shelf edge (Carter, 1975). Molluscs, echinoid spines, serpulid tubes, foraminifera and coccolith fragments dominate the upper slope (McDougall, 1972; Keane, 1986b).

The Taranaki shelf skeletal material is dominated by coarse grained molluscs, bryozoans and benthic foraminifera (Carter, 1975). The benthic foraminifera on the inner Taranaki shelf at less than 50 m water depth are dominated by *Rosalina irregularis* and *Zeaflorilus parri*. *Bulimina marginata* s.s. and *Discorbinella bertheloti*, as well as *Cassidulina carinata*, dominate the sediment between 50 and 550 m water depth (outer shelf to upper bathyal), while *Cassidulina carinata-Alabaminella weddellensis-Abditodentrix pseudothalmmanni* dominate middle to lower bathyal depths (500-1500 m) (Hayward et al., 2003). *Neouvigerina proboscidea* and *Trifarina angulosa* have their peak abundance at mid shelf to upper bathyal depths. At lower bathyal to upper abyssal depths between 1400 and 2150 m *Bulimina marginata* f. *aculeata* and *Globocassidulina subglobossa* are the primary benthic foraminifera while *Uvigerina peregrina* and *Oridorsalis umbonatus* dominate the >150 um fraction (Hayward et al., 2003).

Zeaflorilus parri is widespread around New Zealand on exposed coasts on the inner shelf (predominantly less than 25 m depth) in clean sand. *Rosalina irregularis*, *Bulimina marginata*, *Discorbinella bertheloti* and *Cassidulina carinata* are also all widespread around New Zealand (Hayward et al., 1999). The dominant benthic foraminiferal species on the Taranaki shelf vary considerably from those identified in NKCM sediments. The inner NKCM shelf (0-55 m) is dominated by *Quinqueloculina auberiana*, with *Zeaflorilus parri* and *Haynesina depressula* also important species. The mid shelf to upper bathyal depths primarily comprises *Cibicides corticatus*, *Hoeglundina elegans*, *Uvigerina peregrina* and *Saidovina karreriana*, while middle to lower bathyal depths are dominated by *Globocassidulina subglobossa* and *Lagena* sp.

Chapter 6

GLAUCONITE-PHOSPHATE ASSOCIATION

6.1 INTRODUCTION

Glauconitic and phosphatic minerals occur in varying quantities in sediment across the north Kaipara continental margin (NKCM), as mentioned in Chapter Four. Glauconite, in particular, comprises a significant component of the siliciclastic-rich sediments with only three of the 54 sample sites seemingly lacking glauconite (P401, P409, P422). It may be authigenic (formed more or less *in situ*) or allogenic (transported after formation), modes that can often be inferred from grain morphology and mineralogy (McRae, 1972). Glauconite-phosphate associations are common features in marine environments with many examples known from continental margins in the rock record (e.g. Shublik Formation, Arctic Alaska (Parrish et al., 2001); Helvetic Shelf, north Africa (Notholt and Jarvis, 1990)) and in the modern (e.g. East Australian continental margin, (James et al., 2004); outer continental shelf, Cape Canyon, South Africa, (Compton et al., 2004)).

This chapter investigates the composition and morphology of glauconite grains in some detail (Section 6.2) as well as the occurrence of phosphate on the NKCM (Section 6.3). The modern glauconite-phosphate association is discussed in Section 6.4 and then compared briefly to some similar associations in New Zealand's Tertiary rock record (Section 6.5).

6.2 GLAUCONITE

Glauconite occurs mainly in small (<10%) but ubiquitous quantities across the NKCM but increases to concentrations of 75-95% glauconite between 150 and 400 m water depth along transects D and E either side of Tauroa Point (Fig. 4-17A). Glauconite grains from this concentrated area (P414, P416, P420, P421) were analysed for composition (Section 6.2.1) and morphology (Section 6.2.2)

along with a sample from each of transect A (P399) and transect F (P430) for comparison.

6.2.1 Glauconite composition

Average composition of glauconite grains

Microprobe analysis was conducted on 35 glauconite grains from seven sample sites across the NKCM (Appendix E). 43 analyses were carried out in total with over half of these on the glauconite-rich sediments along transects D and E. The measurements produced reasonable totals between 83.80 and 90.74% with the bulk of the remainder to 100% inferred to be water.

Table 6-1 shows the average percentage of the major components of the glauconite grains from each site measured. SiO_2 expectedly dominates the glauconite composition with total Fe next common (total Fe = $FeO+Fe_2O_3$) and the other elements each comprising much less than 10%. The samples from the glauconite-rich region (P414, P416, P417, P420, P421) have very similar compositions (Fig. 6-1A) with only minor differences in MgO, Al_2O_3 and total Fe. When compared with the northern (P430) and southern (P399) samples (Fig. 6-1B) the major components show some considerable differences. MgO is slightly higher in P399 than the glauconite-rich area and P430. Al_2O_3 is also greater in P399 and P430, although this is more significant in P399 where it is over 3% higher than the glauconite-rich area. SiO_2 and K_2O are lower in both P399 and P430 compared to the glauconite-rich samples by 3-4% and 1-4%, respectively. The CaO content in the glauconite-rich area and P399 is very similar (0.12-

Table 6-1. Average percentage of the major oxide components of glauconite from each of the seven sites analysed. These results are averaged across all points from all grains for each sample. Total Fe = $FeO+Fe_2O_3$. The totals of all the oxides measured are also noted at the bottom. Difference from 100% equates mainly to water.

OXIDE	P399	P414	P416	P417	P420	P421	P430
MgO	5.81	3.84	4.72	4.91	5.54	4.24	4.55
Al_2O_3	7.79	2.99	2.99	2.22	2.34	3.43	4.01
SiO_2	45.14	48.22	50.25	48.78	49.85	48.42	44.96
K_2O	3.24	7.04	7.86	8.00	8.08	7.40	6.79
CaO	0.58	0.27	0.15	0.17	0.12	0.26	4.77
Total Fe	23.05	24.78	23.27	24.85	23.94	24.88	21.20
Total	85.85	87.16	89.38	88.97	89.88	88.75	89.57

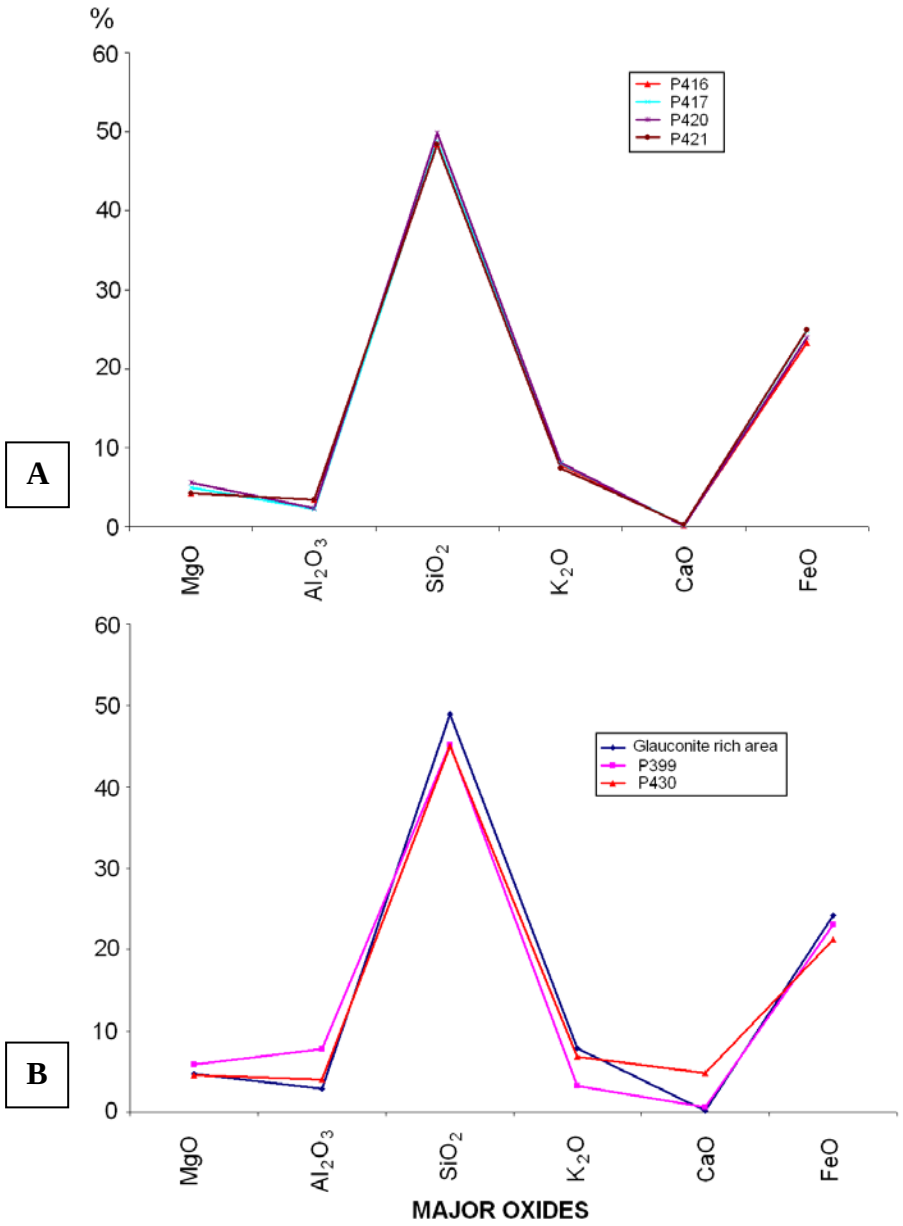

Figure 6-1. (A) A comparison of the main oxides in the four concentrated glauconite samples from the NKCM. (B) A comparison of the major oxides between the glauconitic-rich area and the two samples to the north (P430) and south (P399). FeO = FeO+Fe_2O_3.

0.58%), but in P430 it is more than 4% higher. Total Fe differs only slighter between the sample sites with P399 and P430 both having a slightly lower total Fe content than the glauconite-rich samples. The typical range in major oxide abundances for glauconite universally is SiO_2 43-53%, Fe_2O_3 8-25%, Al_2O_3 3-14%, K_2O 4-7%, MgO 2-5% and FeO 1-6% (McRae, 1972; Nelson, 1973), with New Zealand glauconite oxide abundances in the order SiO_2>Fe_2O_3>Al_2O_3>K_2O>MgO>FeO (Nelson, 1973). Glauconites in the Oligocene Te Kuiti Group generally comprise <1% CaO, 2.3-5% MgO, 5-8%

K_2O, 13-30% total Fe and a low Na_2O content (Nelson, 1973; Nelson and Hume, 1987). The NKCM glauconites are within the standard compositional range for mainly SiO_2 and MgO. Al_2O_3 is slightly lower than expected in four of the seven samples and all these four samples are within the glauconite-rich region of the NKCM. The fifth glauconite-rich sample is just within the expected Al_2O_3 content at 3.43%. K_2O is slightly greater than the expected range in five of the seven samples with the sixth sample falling below (3.24%) and the other sample within the range. The total Fe content in NKCM glauconite is between 21 and 25% and within the expected range of 13-30%. The oxide abundance of NKCM glauconite occurs in order of SiO_2> total Fe> K_2O> MgO >Al_2O_3> CaO which is different to the general glauconite composition given in the literature. A similar CaO content to Te Kuiti Group glauconites is observed in NKCM glauconite (<1%), however TiO_2 and Na_2O are rare. Al_2O_3 is significantly lower than in Te Kuiti Group glauconites (>10%) with six of the seven samples containing less than 4.5% Al_2O_3 and the seventh comprising only 7.79%.

Compositional differences across glauconite grains

During the course of microprobe analysis it was observed, as expected, that the glauconite grains do not always comprise the same composition across the grain. Secondary precipitation of glauconite has occurred around grains and within previous dehydration cracks. 11 points were analysed across five grains to determine the changes in composition with three analyses around the edge of the grains and three in veins or dehydration cracks (Table 6-2a,b). The edge or vein compositions have similar or lower MgO, SiO_2 and CaO contents than the centres

Table 6-2a. Comparison between the major oxide constituents of glauconite in the centre of a grain (I) and the edge of the grain (E) or a vein/crack (V). A, B, C infers the location of the grain on the slide and A2 infers grain 2 in location A.

	P414 B		P414 C			P416 A2		P421 A2	
OXIDE	I	E	I	V1	V2	I	E	I	V
MgO	3.96	4.13	4.11	3.3	3.57	5.96	4.73	4.22	4.01
Al_2O_3	1.73	6.05	2.47	4.24	2.64	2.51	7.83	1.18	7.33
SiO_2	48.27	48.91	47.95	48.68	47.83	50.71	51.8	48.29	45.3
K_2O	7.75	6.59	7.67	4.68	6.41	8.48	4.91	7.57	5.48
CaO	0.18	0.37	0.26	0.57	0.30	0.00	0.49	0.22	0.71
Total Fe	25.33	21.23	24.72	23.32	25.34	22.28	17.86	26.95	23.45
Total	87.20	87.28	87.18	85.08	86.09	89.95	88.16	88.42	86.93

Table 6-2b. Comparison between the major oxide constituents of glauconite in the centre of a grain (I) and the edge of the grain (E) or a vein/crack (V). A, B, C infers the location of the grain on the slide and A2 infers grain 2 in location A.

OXIDE	P421 E	
	I	E
MgO	4.52	4.51
Al_2O_3	2.76	5.69
SiO_2	48.78	49.54
K_2O	7.91	7.06
CaO	0.09	0.37
Total Fe	25.00	22.39
Total	89.06	89.81

(Fig. 6-2). Al_2O_3 is greater in all the veins and edges (average of 4.2% higher) when compared to the centres while K_2O and total Fe are lower. K_2O is between 1 and 4% lower in the edges and veins compared to the centres while total Fe is 1-5% lower (Fig. 6-2). In sample P414 the composition of an infilled dehydration crack (Appendix E, P414 grain C) was measured towards the edge and closer to the centre. The centre vein measurement (red line) has a more comparable composition to the centre of the grain with the exception of a lower MgO and K_2O content by c. 1% (Fig. 6-2). TiO_2 occurs in three of the edge or vein analyses (<0.5%) while Cl, Cr_2O_3, MnO and Na_2O occur in a single measurement each (<0.3%).

Comparison to Hokianga Terrace glauconite

Glauconite grains occur within Oligocene to Miocene aged phosphate nodules and phosphatised conglomeratic slabs dredged from the southern flank of the Hokianga Terrace (Fig. 2-6B) (Phillip, 1986). The composition of the glauconite grains was determined using microprobe analysis and is presented in Table 6-3. Type I glauconite comprises oxidised, green-brown to brown grains with a random microcrystalline internal texture. Types II and III glauconite consist of grass green to yellow-green grains with random to patch-orientated microcrystalline texture and frequently lighter coloured rims. When compared to the modern NKCM glauconite, these glauconite grains have similar MgO, SiO_2 and iron contents. Al_2O_3 is slightly higher in the Oligocene to Miocene glauconite by c. 1% with the oxidised Type I glauconite somewhat similar to that in P399.

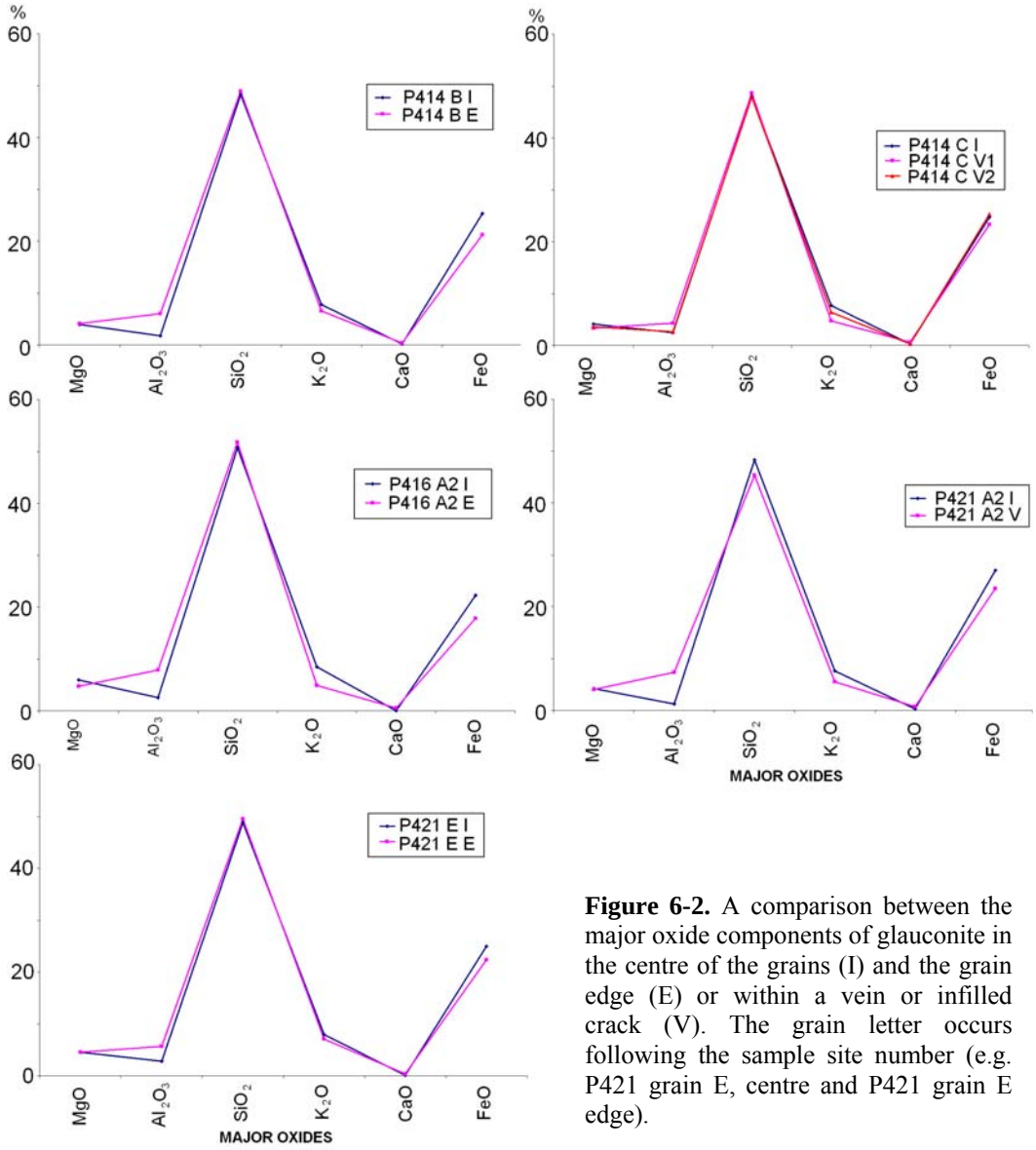

Figure 6-2. A comparison between the major oxide components of glauconite in the centre of the grains (I) and the grain edge (E) or within a vein or infilled crack (V). The grain letter occurs following the sample site number (e.g. P421 grain E, centre and P421 grain E edge).

The K_2O content of this glauconite is comparable to highly evolved glauconite on the NKCM, while the CaO content varies considerably between the three types, as it does on the NKCM.

6.2.2 Glauconite morphology

The seven main glauconite morphologies are ovoidal or spheroidal, tabular or discoidal, lobate, vermicular, fossil casts and internal moulds, fragmentary and composite. The glauconite morphology on the NKCM was quantified by classifying between 580 and 630 grains per sample. Ovoidal or spheroidal grains completely dominate (84-96%) all the samples while tabular or discoidal grains (0-6.4%) and fossil casts and internal moulds (1.8-11.8%) are of secondary

Table 6-3. The percentages of the main oxides of three types of glauconite found in Oligocene to Miocene aged phosphate nodules and phosphatised conglomeritic slabs from Hokianga Terrace (from Phillip, 1986).

OXIDE	Type I	Type II	Type III
MgO	4.69	4.79	4.97
Al_2O_3	6.04	3.80	3.63
SiO_2	40.81	51.23	48.83
K_2O	6.09	8.41	8.01
CaO	5.22	0.36	1.13
Total Fe	23.41	26.11	25.50

importance (Table 6-4). Very small amounts of vermicular and lobate grains occur while composite grains are relatively rare and fragmentary grains absent. Both ovoidal or spheroidal and tabular or discoidal glauconite may have simple or mammillated surfaces. Simple surfaces are smooth and lustrous with minor or absent external suturing, while mammillated surfaces are irregular with shallow sutures infilled with pale green to white crystalline material which may be iron stained (Nelson, 1973).

Ovoidal or spheroidal grains are generally dark green to black with a simple rounded shape and NKCM glauconites have several variations. In samples P420 and P421 the grains are dark green to black and have mostly mammillated surfaces with iron stained sutures common (Plate 10, b-c). In P416 the light to dark green grains also have mostly mammillated surfaces but the sutures are predominantly infilled by white crystalline material and iron staining is absent. In P417 the irregular grains are brown to black and have a mix of simple and mammillated surfaces with both white and iron stained sutures. Most of the grains with simple surfaces in P417 are mammillated grains with iron stained sutures that have been polished until the grains are smooth and round. In P430 all the grains have mammillated surfaces with well-developed sutures infilled with white crystalline material and minor iron staining. The majority of the glauconite grains in P430 are light green to brown with rare dark green to black grains. P399 ovoidal or spheroidal glauconite grains are very similar to P430 but are very irregular in shape and have large numbers of small sutures (as opposed to a small number of large sutures e.g. P420).

Tabular or discoidal glauconite grains are usually flattened, plate- or disc-like and pale to medium green in colour (Nelson, 1973; Compton, 1989). The tabular glauconite grains in the NKCM samples (e.g. P416, P420, P421) comprise dark green to black grains with mostly simple surfaces that appear polished (Plate 10, d). Lobate grains are irregular in shape with pale and dark green zones similar in form to popcorn. NKCM lobate morphologies are usually light green with well-developed sutures infilled by mostly white crystalline material (e.g. P420; Plate 10, e). Vermicular grains are elongate with a curved concertina appearance while fossil casts and internal moulds (also known as steinkerns) comprise glauconite grains shaped like the shell cavity they infilled, such as foraminiferal tests (Nelson, 1973; Compton, 1989). Vermicular grains in the NKCM sediments are dark green to black with very common iron staining in the sutures (Plate 10, f). These grains have smooth surfaces and appear polished (e.g. P421, P430). The grains comprising fossil casts and internal moulds in NKCM glauconite are mostly light green and are predominantly shaped in the form of foraminiferal tests (both benthic and planktic) with lesser amounts of bryozoan shaped grains (P416, P417, P420, P430; Plate 11, a-d). Fragmentary grains consist of broken glauconite grains while composite grains comprise two or more distinct mineral species cemented by a glauconitised matrix (Nelson, 1973; Compton, 1989). Fragmentary grains are not seen in NKCM sediments but occasional composite grains are and consist primarily of multiple glauconite grains within a white crystalline matrix (e.g. P420; Plate 11, e-f).

Table 6-4. The percentage of the different morphological types of glauconite in the six samples analysed from the NKCM.

Type	P399	P416	P417	P420	P421	P430
Ovoidal/ spheroidal	93.5	96	94	84	91	87
Tabular/discoidal	0.2	0.7	3.4	6.4	4.3	0
Lobate	0	0	0.2	4.7	1.0	0.8
Vermicular	2.1	1.2	0.3	0.3	0.7	0.5
Casts/internal moulds	3.5	1.8	1.9	3.3	2.3	11.8
Composite	1.0	0.2	0.2	0.9	0.5	0

6.2.3 Internal structure of glauconite

The internal structure of the glauconite from NKCM samples is dominated by randomly oriented microcrystalline material which is characterised by aggregate polarisation and mottled extinction in grains. Orientated microcrystalline structures occur predominantly in vermicular glauconite. The NKCM glauconites also contain inclusions of quartz, feldspar and calcite in some grains. These inclusions can be single large grains or multiple small grains but all are well incorporated into the glauconite grain.

6.2.4 Glauconite formation

The ideal conditions for glauconite formation occur between 65˚S and 80˚N on continental shelves (<500 m water depth) with pH conditions that are slightly alkaline (7-8 pH) and a water temperature between 15 and 20˚C (McRae, 1972). A slightly reducing environment with bacterial decomposition of organic matter is favoured and on modern shelves glauconite formation is often associated with areas of reduced sedimentation and relict sediment (McRae, 1972).

The most common methods of glauconite formation are internal moulds, faecal pellets, replacement of carbonate skeletal fragments and the coating and replacement of mineral or rock grains (Odin and Fullagar, 1988). Foraminiferal tests are the dominant host for internal moulds and the glauconite is precipitated directly into the test or replaces clay-sized material previously deposited in the test. This form is relatively common (second most important morphology) in NKCM sediments with only two samples (>500 m along transect D) containing foraminiferal tests infilled by non-glauconitised clay material. Faecal pellets are also common, particularly in modern sediments, and are produced by filter feeding or soft-bodied organisms which consume mud. Glauconite appears to form in the pores of these pellets and slowly replaces the muddy material within the pellet (Odin and Fullagar, 1988). There are two main ways carbonate skeletal fragments can be replaced: (1) the glauconite mineral infills pores (either framework pores or boring or dissolution pores) within the skeletal fragment and (2) the carbonate mineral is completely replaced by glauconite preserving the

original structure of the skeletal fragment. In the NKCM bryozoan fragments are the most common skeletal fragments to be replaced. Glauconitisation of mineral grains or rock fragments can occur with quartz, feldspar, mica, calcite, phosphate and volcanic glass common minerals to be replaced or coated by glauconite. Replacement of the mineral grain occurs along fissures or cleavage planes and tends to produce vermicular morphology (Odin and Fullagar, 1988). Replaced mica grains are present in all of the samples where morphology was analysed and glauconite coatings and rims are common on quartz and feldspar grains in the southern half of the NKCM.

There are four main stages of glauconite formation: nascent, slightly evolved, evolved and highly evolved (Odin and Fullagar, 1988). At the nascent stage the glauconite is just beginning to form and is iron rich with K_2O contents of 2-4%. Slightly evolved glauconite has K_2O contents of 4-6% and most of the original grain (mineral, faecal pellet, clay) has been replaced (Odin and Fullagar, 1988). Glauconite grains reach the evolved stage when their K_2O contents are 6-8% and all of the original grains structure and texture have been lost. In highly evolved grains of glauconite any cracking of the grains is infilled to produce smooth surfaces and the K_2O content is greater than 8% (Odin and Fullagar, 1988). The glauconite infilling the cracks has less K_2O and is less evolved as a result. Based on K_2O content, most of the NKCM glauconite falls within the evolved stage (five out of seven samples) with one sample (P420) within the highly evolved stage. P399 falls in the nascent class (K_2O 3.24%) although it is possible the reduced K_2O content is the result of oxidation and weathering of the glauconite grains during transport from the concentrated area as opposed to these grains forming at this location.

6.3 PHOSPHATE

6.3.1 Occurrence

Phosphatic material from sediment samples considered within this study occurs in the form of phosphatised skeletal fragments, as mentioned in Chapter Four. These

fragments are broken rounded grains that in thin section are brown in plane light and isotropic under cross-polarised light.

Samples previously dredged in 1983 from the southern flank of the Hokianga Terrace from 505-600 m water depth recovered phosphatised conglomeratic slabs and phosphate nodules with only a small amount of phosphatised bivalve and brachiopod fragments (Phillip, 1986). The conglomeratic slabs are between 2 and several cm in thickness and have irregular, pitted and bored surfaces. These slabs consist of phosphatic nodular material, some brachiopod casts and phosphatic ooze in a calcareous glauconitic phosphatic matrix. Borings and burrows are lined or partially infilled by phosphatic ooze and the glauconite can comprise up to 45% of the matrix material (Phillip, 1986). Glauconite-rich sediment may also infill burrows and borings into the phosphatic material. Carbonate-apatite dominates the composition of these slabs with lesser amounts of calcite, glauconitic smectite and glauconitic illite. The phosphatic nodules comprise 50-60% of the dredge haul and consist of dense, relatively homogenous nodules between 2 and 16 cm in size (Phillip, 1986). The surface of the nodules may be glauconitised and glauconite and/or phosphatic ooze may infill borings. The nodules have an average carbonate content of 61.5% and may have two matrix types: (1) yellow-brown finely crystalline calcite and collophane and (2) late stage non-phosphatic mud (Phillip, 1986). Calcite dominates the composition of the nodules with lesser amounts of carbonate-apatite and glauconitic smectite. The deposition of this glauconite and phosphate was considered by Phillip (1986) to have occurred during the early Miocene which coincides with deposition of most of New Zealand's marine phosphate deposits (e.g. Chatham Rise; Cullen, 1989).

6.3.2 Phosphate formation

In the oceanic environment, phosphorus is relatively rare with an average of only 70 ppb in both organic and inorganic forms and surface water is further depleted of inorganic phosphorus by phytoplankton activity (Phillip, 1986). Phosphate-enriched water is mainly introduced to the shelf and slope through upwelling which increases the surface water concentration and, as a result, phytoplankton activity. Phosphate is incorporated into the sediment through the introduction of

phytoplankton remains, which through decomposition result in the accumulation and concentration of inorganic phosphate in oxygen-poor sediments. Phosphate accumulation predominantly occurs in areas of upwelling currents, which often arise along the western margins of continents, while the optimum water depth for phosphate formation is from 30-200 m (Phillip, 1986; Parrish et al., 2001; Coles et al., 2002).

In the case of the phosphatised slabs and nodules dredged from Hokianga Terrace, the most likely source of the high levels of phosphorus required to produce such features is upwelling onto a subtropical continental shelf followed by Miocene or Plio-Pleistocene reworking and concentration of the nodules as a result of sea level changes (Phillip, 1986). Phosphate in sediments from the Alpine Helvetic Shelf on the Tethyan Margin of North Africa developed through condensation with very low rates of accumulation on the order of 2-10 m per million years (Notholt and Jarvis, 1990). Comparable kinds of conditions are envisaged for the formation of phosphatic nodules and phosphatised slabs on the NKCM.

6.4 GLAUCONITE-PHOSPHATE ASSOCIATION ON NKCM

Glauconite is commonly associated with phosphate (McRae, 1972; Odin and Fullagar, 1988), as is the case in samples dredged from the Hokianga Terrace. These samples imply low sedimentation rates, which allowed a glauconite-phosphate association to form on the upper slope during the Miocene (Phillip, 1986). In terms of the modern NKCM, the area of highest phosphatic material (10-30%) overlaps with >30% glauconite north of Tauroa Point. However, this overlap does not extend south of Tauroa Point where the percentage of glauconite reaches >95% in samples along transect D (Fig. 6-3). Seven glauconite microprobe analyses recorded P_2O_5 contents between 0.01 and 0.3%, while one glauconite grain in sample P430 contained a P_2O_5 content of c. 8-9%. Phillip (1986) reported glauconite grains in phosphatised slabs near the Hokianga Terrace which also contained P_2O_5 contents of 4.15% prior to phosphatisation of the sediments. Both phosphate and glauconite require slightly reducing conditions and organic decomposition and along with these analyses this indicates that phosphate and glauconite are being precipitated simultaneously on the NKCM.

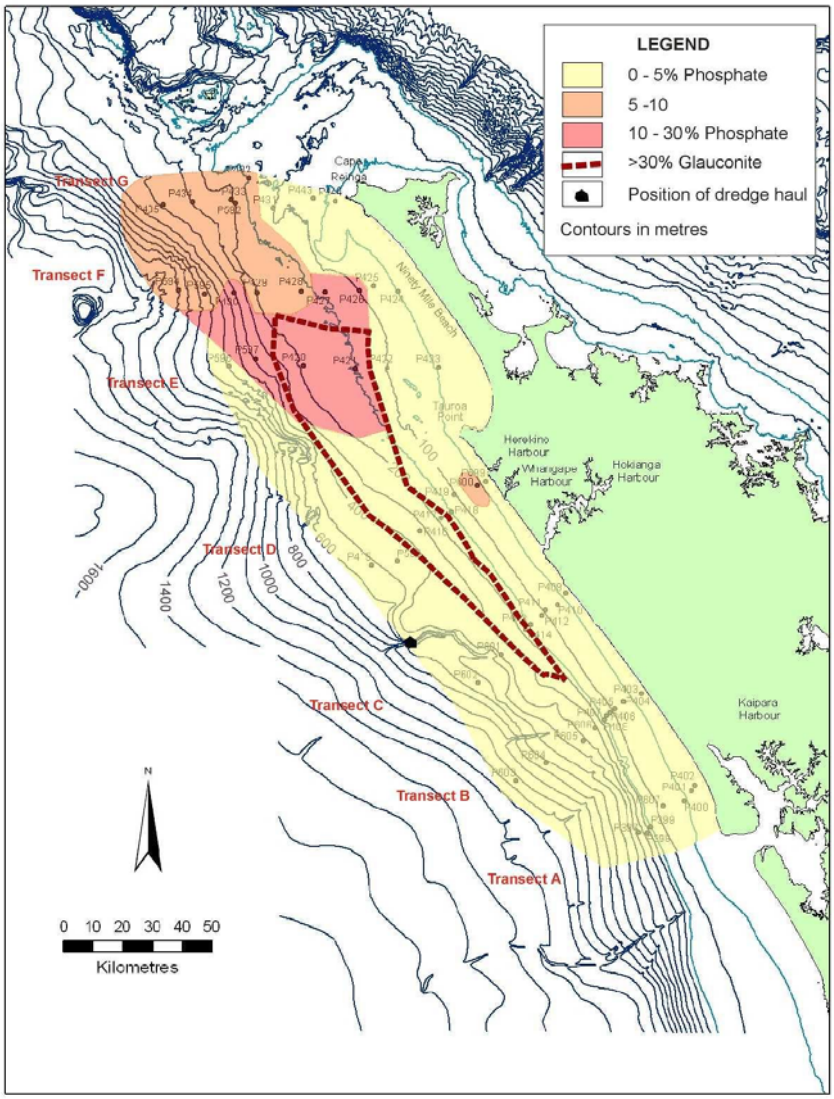

Figure 6-3. Distribution of phosphatised skeletal fragments, the location of >30% glauconite content and the location of the dredge haul (Phillip, 1986) on the Hokianga Terrace.

Slow deposition of phosphate and glauconite in condensed sections is common and is often associated with sea level rise (Compton, 1989).

6.5 EXAMPLES FROM NEW ZEALAND TERTIARY ROCK RECORD

The Tertiary rock record in New Zealand comprises marine sedimentary and coastal plain or deltaic (e.g. coal measures) rocks deposited in response to a tectonically driven transgressive-regressive cycle (Fig. 6-4). The cycle was primarily caused by subsidence following rifting and drifting from Gondwanaland during and following the Late Cretaceous and then uplift and deformation

associated with the formation of the convergent plate boundary through New Zealand in the Early Miocene (Fig. 6-4) (Dodd and Nelson, 1998). During the maximum period of subsidence in the Oligocene and earliest Miocene the development and deposition of limestone was widespread throughout New Zealand (Fig. 6-4). The formation and deposition of glauconite also occurred during this time (Fig. 6-4) and was at least locally associated with phosphate precipitation. These glauconite-phosphate associations are usually developed in the vicinity of major unconformities. Three examples of glauconite-phosphate associations in the Tertiary rock record have been examined and catalogued from Port Waikato, from Waitomo and from Gees Point near Oamaru. All of these associations also involve limestone in the stratigraphy.

6.5.1 Port Waikato

At Port Waikato (G.R. R13/653175) the stratigraphic level of interest here is the boundary zone between the Waimai Limestone and the Carter Siltstone of the Oligocene aged Te Kuiti Group (Fig. 6-5). The Waimai Limestone is a 2.5 m

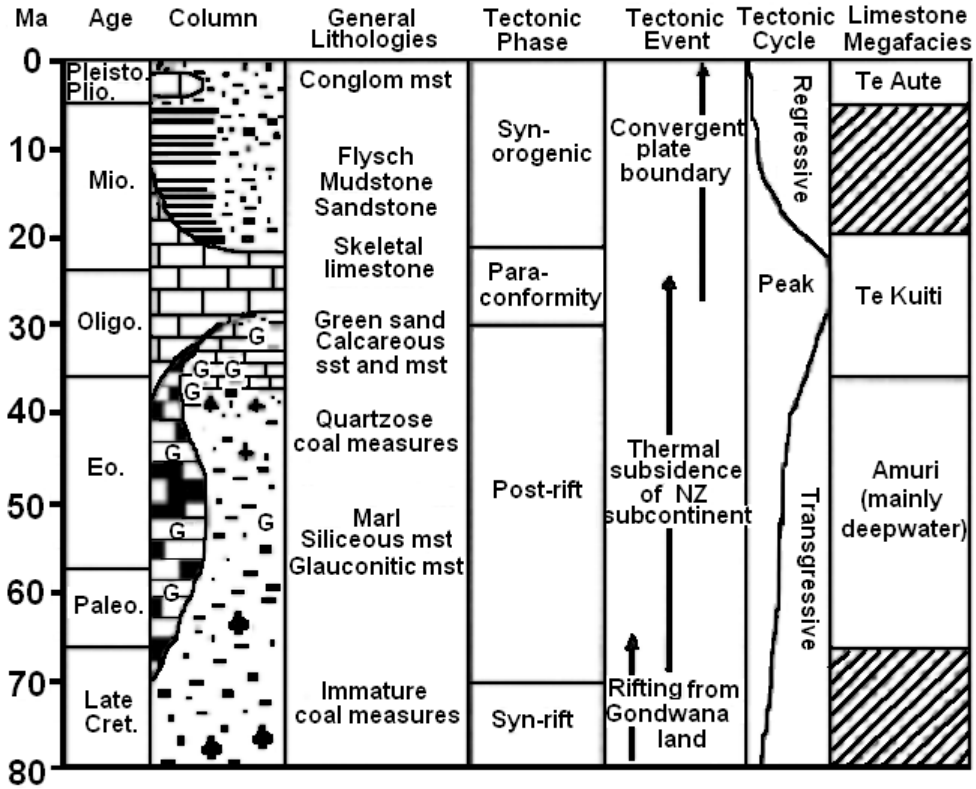

Figure 6-4. Idealised New Zealand sedimentary sequence from the Late Cretaceous to Pleistocene emphasising at right the shelfal Te Aute and Te Kuiti limestone megafacies and the deeper water Amuri limestone megafacies. The mid-Tertiary Te Kuiti carbonates and associated calcareous facies are conspiciously glauconitic. G = glauconite, ♠ = carbonaceous (from Dodd and Neslon, 1998).

thick flaggy limestone with well developed cross bedding present at this site. It seemingly grades upwards into a massive sandy limestone and calcareous glauconitic sandstone approximately 3 m thick that includes occasional muddier interbeds. Within the glauconitic sandstone, phosphate nodules and clasts occur in varying sizes (c. 2-6 cm) and amounts. Two different types of phosphate clasts were thin sectioned and analysed using cathodoluminescence petrography (CL) to provide information about their composition and structure. The two clasts were (1) a large flat crumbly phosphatised fragment (Pk1, Fig. 6-6A) and (2) a well-developed and lithified rounded phosphate nodule (Pk2, Fig. 6-6B,C). The phosphatised fragment under plane polarised light comprises a brown irregular framework filled with clear-white and black-brown material. The framework under CL produces a dark blue luminescence indicative of a phosphatic (whale) bone fragment while the clear-white material luminesces bright orange and is

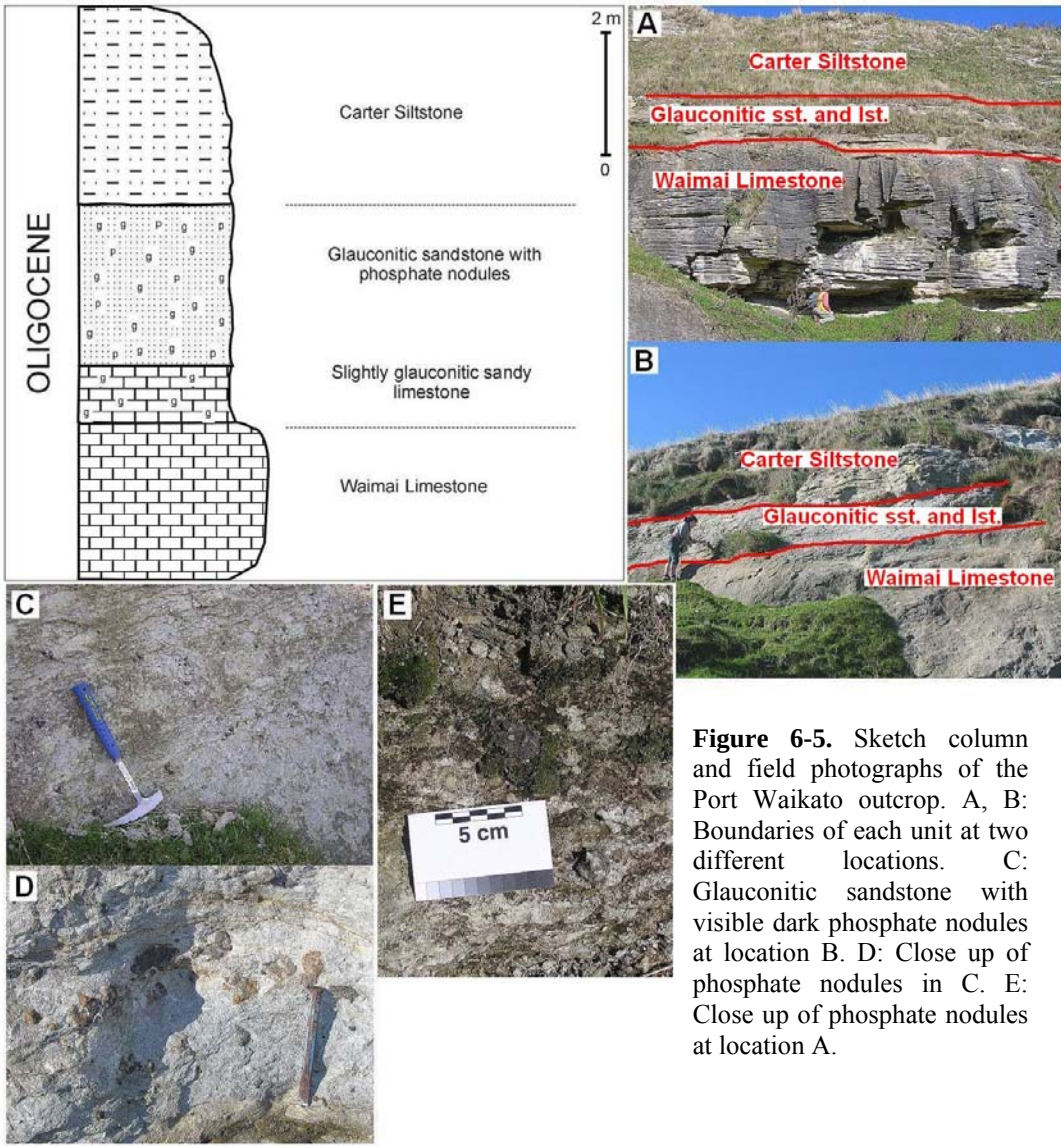

Figure 6-5. Sketch column and field photographs of the Port Waikato outcrop. A, B: Boundaries of each unit at two different locations. C: Glauconitic sandstone with visible dark phosphate nodules at location B. D: Close up of phosphate nodules in C. E: Close up of phosphate nodules at location A.

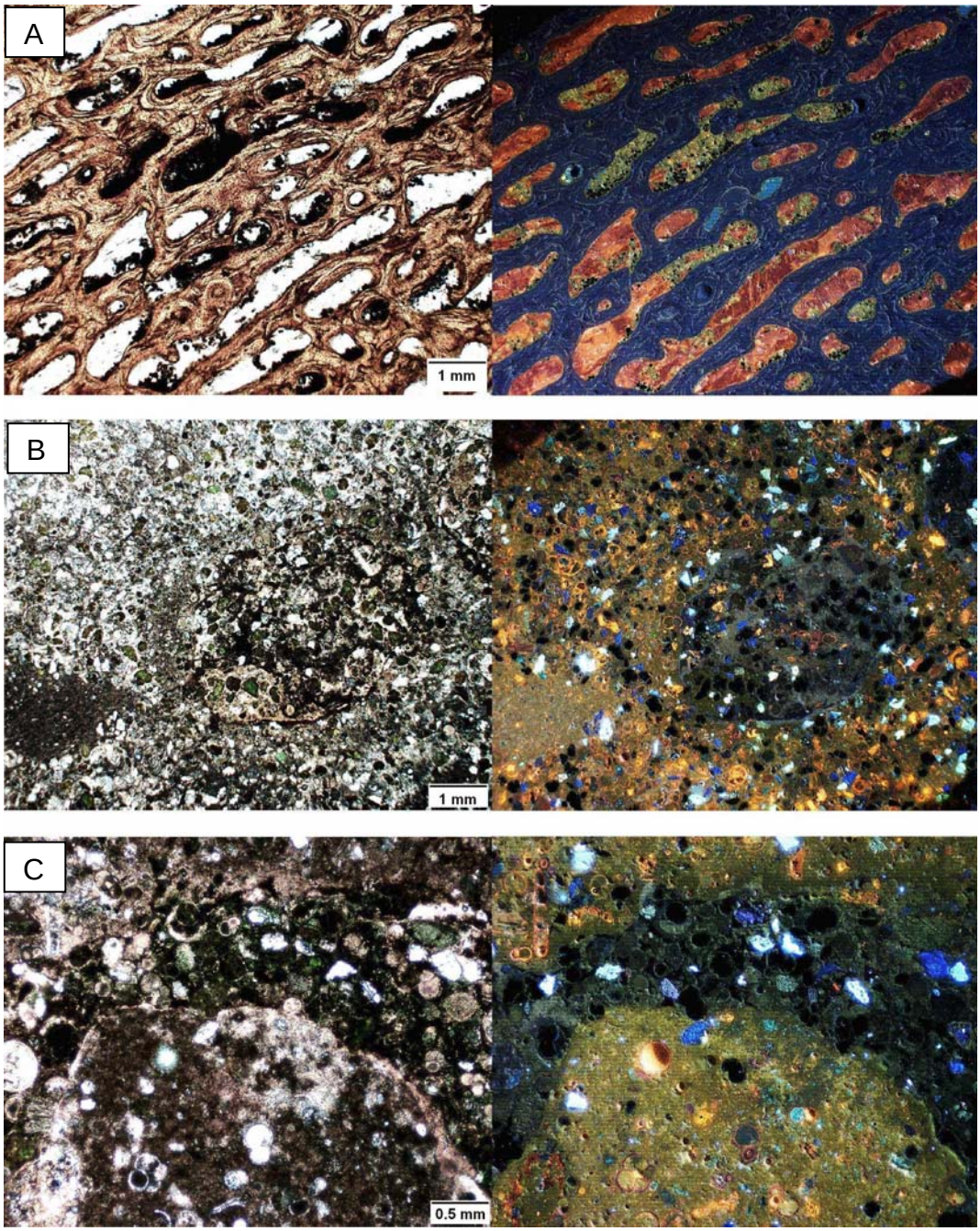

Figure 6-6. Plane polarised light (left) and cathodoluminescence (right) photomicrographs of two phosphate nodules. A: large flat crumbly phosphatised fragment (from outcrop in Fig. 6-5C). B: well-developed and lithified rounded phosphate nodule (from outcrop in Fig. 6-5E). C: phosphate nodule in B at higher magnification (from outcrop in Fig. 6-5E).

indicative of calcite. Bright blue possibly K-feldspar grains are present in small amounts while other CL colours produced include small yellow grains, a green matrix like material and non-luminescent rounded clasts of unknown composition or origin. The phosphate nodule under plane polarised light comprises glauconite grains, colourless minerals, skeletal fragments and muddy brown matrix materials. Most of the skeletal fragments consist of bright orange calcite and the mineral

grains are predominantly feldspar and quartz. The glauconite grains do not luminesce, but the muddy brown matrix luminesces a grey to green colour. This matrix produces a range of distinctive colours that appear to suggest multiple episodes of phosphatisation or production of this matrix.

6.5.2 Waitomo

The outcrop at Waitomo (G.R. S16/963292) is also within the Oligocene age Te Kuiti Group with the boundary between the Aotea Formation and the Orahiri Limestone being of interest here (Fig. 6-7B). The top of the Aotea Formation in this area comprises the Kihi Sandstone Member, which is a friable, soft, massive, calcareous sandstone that is highly glauconitic in places, sufficiently so that at Waitomo it forms a greensand (White and Waterhouse, 1993). This greensand

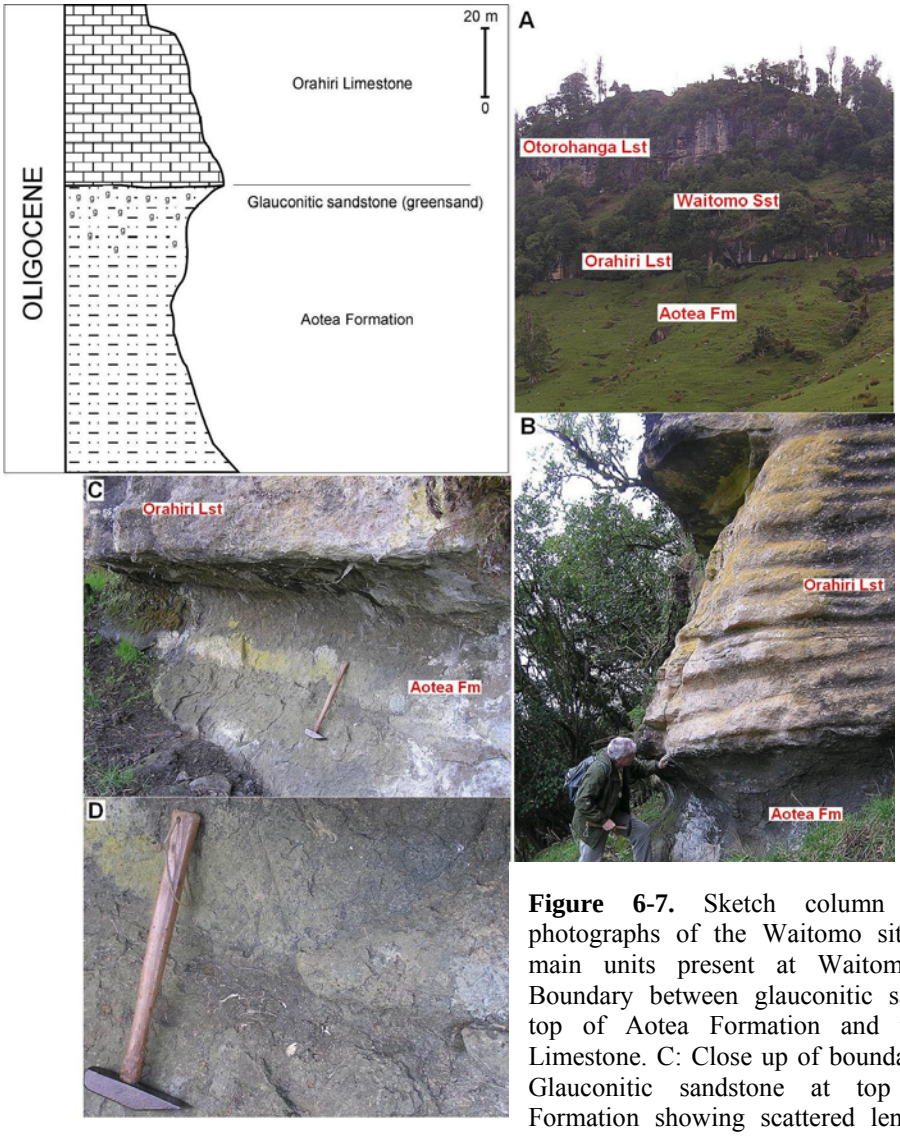

Figure 6-7. Sketch column and field photographs of the Waitomo site. A: Four main units present at Waitomo site. B: Boundary between glauconitic sandstone at top of Aotea Formation and the Orahiri Limestone. C: Close up of boundary in B. D: Glauconitic sandstone at top of Aotea Formation showing scattered lenses of fine shell debris.

includes scattered fossiliferous layers with common pectinid shells. Burrows down into the Aotea Formation are infilled by the overlying Orahiri Limestone, which is flaggy, sandy, pebbly and noticeably glauconitic in its basal portions (White and Waterhouse, 1993).

6.5.3 Gees Point, Oamaru

At Gees Point (G.R. J42/456580) near Oamaru the late Eocene-Oligocene Ototara Limestone forms the bulk of the outcrop of interest with beds of basaltic Deborah and Waiareka Volcanics (not observed) at the base of the limestone (Fig. 6-8) (Edwards, 1991). The majority of the Ototara Limestone comprises yellow-brown to cream, massive, fossiliferous, bryozoan-dominated limestone with lesser amounts of brachiopod valves, echinoid spines, echinoderm plates, foraminiferal tests, coralline algae and molluscan fragments (Chappell, 1995). The upper part of the Ototara Limestone has been extensively burrowed and phosphatised before being infilled by the glauconitic-rich Oligocene aged Otekaike Limestone. The Otekaike limestone may include octocorals, shell fragments, phosphatised fragments of Ototara Limestone and reworked Kakanui Mineral Breccia, with some areas very rich in this lithic material (Chappell, 1995). The Miocene Gee Greensand comprises >50% glauconite and overlies the Otekaike Limestone and phosphatised Ototara Limestone. Fragments of phosphatised limestone occur throughout the greensand and may be up to 2 cm in size (Chappell, 1995). Fossil rich layers are present in the greensand, particularly at its base. In places the Gee Greensand infills burrowed surfaces in the underlying limestone to produce an irregular boundary between the units.

6.6 PALEOENVIRONMENTAL IMPLICATIONS OF THESE GLAUCONITE-PHOSPHATE ASSOCIATIONS

The three examples presented here from the New Zealand Tertiary rock record primarily exhibit overall deepening upwards sequences. The sequence stratigraphic implications of the glauconite-phosphate associations remain to be studied in detail, but some general comments are offered here. According to Amorosi (1995), glauconite can occur in most depositional sequences but is

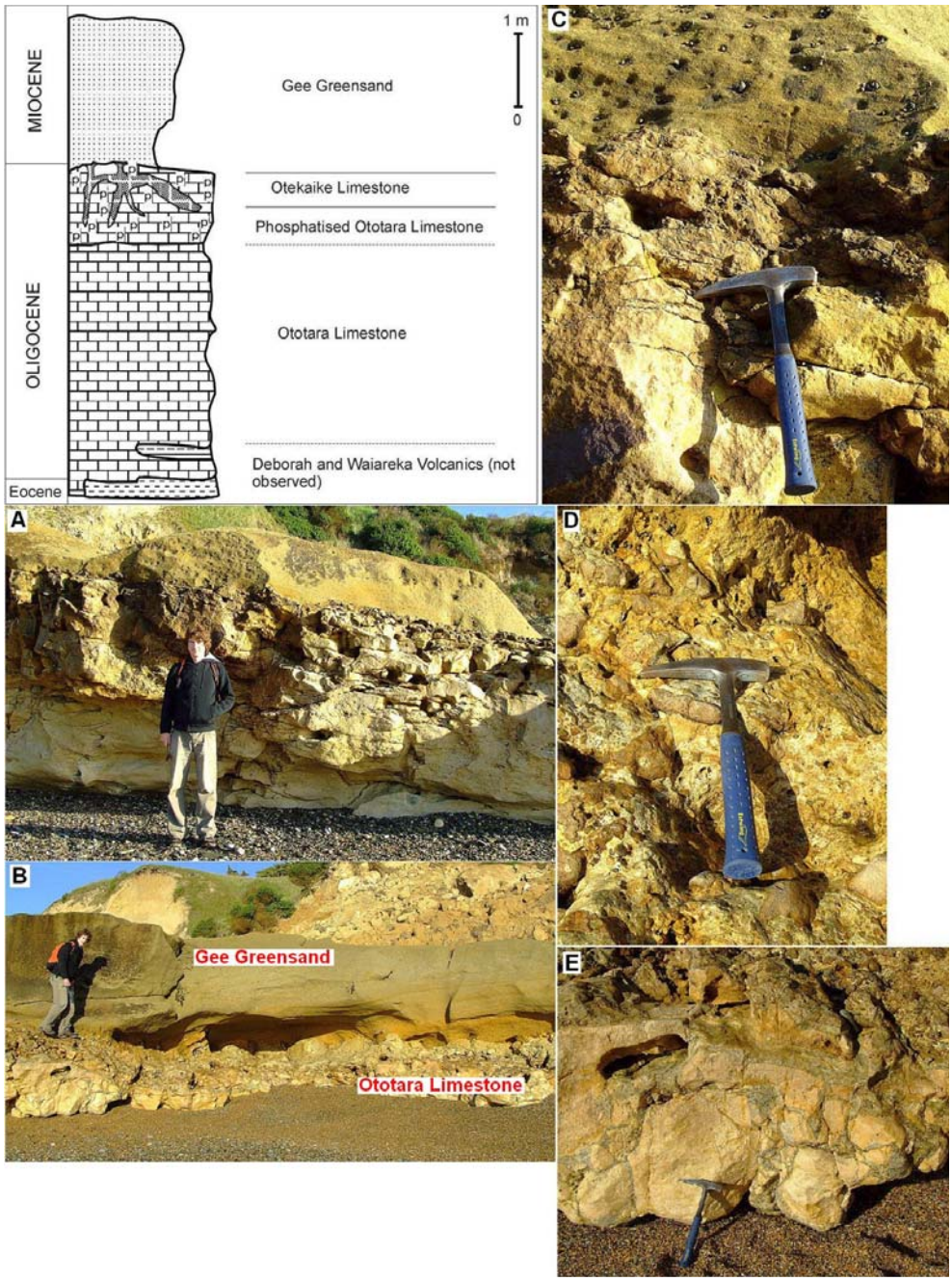

Figure 6-8. Sketch column and field photographs of the Gees Point outcrop. A, B: General view of outcrop at Gees Point. The thick cream-brown Ototara Limestone is evident with phosphatised top (dark brown) overlain by thin Gee Greensand. C: Close up of boundary between limestone and greensand. Dark phosphatised limestone evident. D: Close up of Otekaike Limestone. E: Otekaike Limestone infilling burrows in Ototara Limestone.

generally most common in the deposits of the transgressive systems tract (TST) where it tends to show an upwards increase in concentration and compositional maturity. The glauconite content decreases in the highstand systems tract (HST) and is generally of low to moderate compositional maturity. In condensed sections very high concentrations of glauconite occur compared to the over- and

underlying deposits. The glauconite in condensed sections is also usually of high compositional maturity (Amorosi, 1995). Differing rates of supply of siliciclastic sediment is the primary control on the presence of glauconite in depositional sequences and, as such, glauconite is considered one of the most reliable indicators of low sedimentation rates (Amorosi, 1995).

The simplest sequence of sedimentary deposits within the three examples studied occurs at Port Waikato where limestone is overlain by glauconitic sandstone and then siltstone. This sequence infers significant overall relative sea level rise and the subsequent landward shift of finer grained outer shelf and possibly deeper sediments following deposition of the transgressive Waimai Limestone at inner to mid shelf depths**.** Glauconite in the Te Kuiti Group is considered to have been transported from nearby deeper water sites and consists of slightly evolved to evolved grains (4-7% K_2O) (Nelson and Hume, 1987). The glauconitic sandstone likely equates to a condensed section, with the fine-grained calcareous Carter Siltstone representing a TST to early HST. Rising sea level probably involved considerable transport and reworking of glauconite on the shelf until it was flooded by mud-sized sediment forming the Carter Siltstone. Phosphate nodules were also deposited in association with glauconite in the TST, suggesting the transport of these nodules from other sites in close proximity. Phosphate grains, with abundant skeletal material, are common in condensed sections where the glauconite concentration and compositional maturity is greatest with dark green, evolved and highly evolved glauconite grains widespread.

The Waitomo outcrop consists of a basal limestone (Waimai Limestone) overlain by calcareous muddy sandstone (Aotea Sandstone) and then another limestone unit (Orahiri Limestone). This depositional sequence is slightly more complicated than at Port Waikato, although it still infers relative sea level rise with subsequent landward migration of finer grained outer shelf and upper slope deposits following the deposition of the Waimai Limestone (TST). However, the relative sea level rise and creation of accommodation space is not as significant as at Port Waikato as very fine-grained units, such as the Carter Siltstone, are absent. The Aotea Formation at Waitomo comprises a glauconitic sandstone and marks the initiation of early HST deposition (A. Tripathi, pers. comm., 2007). The

glauconite content increases up the unit to sufficiently high concentrations at the top to form greensand and the maximum flooding surface. The greensand forms a condensed section as it contains significantly higher concentrations of glauconite than the over and underlying sediments (as defined by Amorosi, 1995). As with the Port Waikato glauconitic sandstone, glauconite in the Aotea Formation is probably sourced from deeper water as relative sea level rose and it was transported inshore. However the greensand at the top is more likely to be autochthonous or formed *in situ* (Amorosi, 1995) due to the very high concentrations present and its position at the base of the Orahiri Limestone. Following the deposition of the Aotea Formation, rates of relative sea level rise decreased (eventually reaching stillstand) reducing the sediment input to the shelf and allowing the deposition of a TST (Orahiri Limestone), as coastal and marginal marine sediments migrated offshore (Amorosi, 1995; Catuneanu, 2006).

The Gees Point section is the most complicated depositional sequence of the three examples and comprises a basal limestone with phosphatised top overlain by greensand. This depositional sequence also indicates relative sea level rise and the subsequent landward shift of finer grained outer shelf and upper slope deposits. The Ototara Limestone was deposited possibly as part of a HST before relative sea level dropped resulting in the burrowing of the limestone deposit before it was lithified by calcite and phosphate (Chappell, 1995). This chemical precipitation and replacement phase likely corresponds to a lowstand systems tract (LST) situation. The limestone formed a basal hardground and the overlying patchy Otekaike Limestone was deposited during and following this sea level low (Chappell, 1995), so that it may be recording mainly TST conditions. Fragments of phosphatised Ototara Limestone occur within the Otekaike Limestone suggesting sea floor erosion was significant and widespread throughout the LST-TST period. Relative sea level must have increased significantly to deposit the Gee Greensand, which could mark either the TST-HST transition as a condensed sequence or the HST proper under conditions of no or little siliciclastic sediment supply. Whichever, the relative sea level rise must have been rapid to promote the very low sedimentation rates conducive to glauconite formation (Amorosi, 1995). It is favoured that the Gee Greensand probably represents a condensed section, as the glauconite concentration is significantly higher in the unit compared to both

the underlying Otekaike Limestone and the overlying blue-grey siltstone of the Rifle Butts Formation (observed at Cape Wanbrow, north of Gees Point), and that the latter corresponds to the true HST in the section.

Chapter 7

ONSHORE COASTAL BEACH AND DUNE SEDIMENTS

7.1 INTRODUCTION

The north Kaipara continental margin (NKCM) coastline is characterised by widespread beach and dune features, which are major areas of sand storage along the coast. Most of the NKCM coastline is prograding and active dunes are common in western Northland, particularly at Te Paki, Hokianga Harbour mouth and Pouto Point (Fig. 7-1) (Hayward, 2006). These active dunes usually have sparse vegetation cover with continuous aeolian sedimentation resulting in the formation of large dune fields extending up to 80 km along the coastline and 5 km inland (Hilton, 2006). The beach and dune features formed mainly since the Last Glaciation 20 000 years ago when sea level rose and large amounts of sand were

Figure 7-1. Active dunes at (A) Hokianga Harbour mouth and (B) Te Paki Stream.

transported onshore by waves and wind to form the coastal dune fields and beaches (Hume et al., 2003). Western Northland is a high-energy open coast where sediment transport is driven by waves and tides, which move large volumes of sediment through littoral drift acting within the surf zone. The primary sediment supply is from this gross littoral drift from south to north with c. 175 000 m^3 of sand transported north at least as far as Kaipara Harbour every year (Hume et al., 2003).

The aim of this chapter is to consider the composition and grain size of the beach and dune sands so as to compare them with the sediments out on the NKCM and to see if it is feasible for sediment exchange processes to be occurring between the shelf and beach zones (covered in Chapter 8). Previous studies have found the western Northland peninsula beach and dune sands are comprised primarily of quartz (65-75%) with a mean grain size of 0.15-0.18 mm (Kasper-Zubillaga et al., 2005). Laurent (2000) studied beach samples from south of Cape Egmont to Cape Maria van Diemen and his samples, collected onshore from the seven NKCM offshore transects in this study (Fig. 3-1), are investigated here. In addition, five dune samples were collected inland from these transects in the course of this study.

7.2 BEACH SEDIMENTS

Seven beach samples collected by Laurent (2000), namely sample sites 96, 104, 113, 122, 133, 139 and 146 (Fig. 7-2), were examined to determine their sediment components using the same petrography methods as the NKCM samples (Appendix F, Table 1). The mean grain size of these beach samples ranges between 0.19 and 0.29 mm (fine and medium sand) with well to very well sorted and rounded to well rounded grains dominating the sediment.

Quartz and feldspar co-dominate the beach samples overall with similar quantities adjacent to transects D-G, but greater amounts of feldspar occur in the beach samples on transects A-C and particularly on transect B. The quartz content

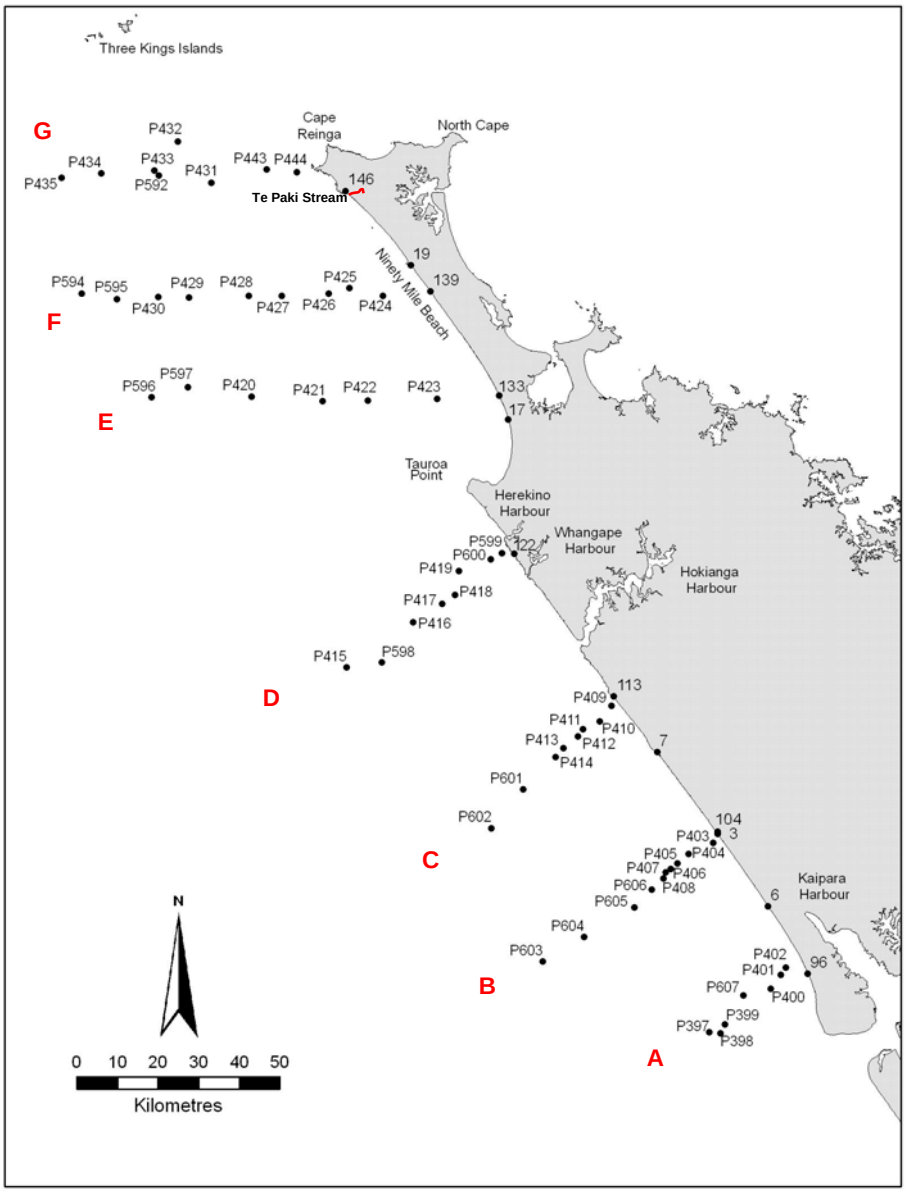

Figure 7-2. Location of beach and dune samples. Beach = 96, 104, 113, 122, 133, 139, 146. Dune = 3, 6, 7, 17, 19.

ranges between c. 10 and 50%, but is most commonly 30-40% (four out of seven transects). The feldspar content of the beach samples ranges between 30 and >50%, with 30-40% feldspar in the three northern transects (E-G) and higher percentages (40-50% and >50%) in the four southern transects (A-D). Plagioclase dominates the feldspar content, ranging predominantly between 20 and 40%, but may reach up to 40-50% of the total sediment. Orthoclase feldspar also occurs comprising between 5 and 20% of the sediment, with 10-20% orthoclase being common. XRD analysis by Laurent (2000) shows that the orthoclase content of the beach sand increases to 55% at The Bluff (near Transect F) with 35% and 30% occurring 5 km either side of this. Rock fragments are also very common and

were found in all the beach samples, mostly comprising 10-20% of the total sediment. The transect G beach sample contained the highest content (30-40%) of rock fragments. The rock fragments are volcanic with a porphyritic texture and plagioclase the most common phenocryst.

Other sediment components comprise a much smaller proportion of the beach sediments. Glauconite occurs in four of the seven beach samples (transects B-C, E-F), but only a total of ten glauconite grains were identified. These grains are very fine grained and weathered. Single biotite grains were found in samples from transects D and F, while minor quantities of shell material are recorded at five of the seven sample sites. Opaque mineral grains are very rare and occur in only three of the seven samples at less than 5% abundance. Non-opaque heavy minerals occur at all the sample sites, generally comprising less than 5% of the total sediment; however, transect B has a higher heavy mineral content at 10-20%. The heavy mineral fraction is dominated by hornblende and oxyhornblende, which occur at all the sample sites.

Laurent (2000) found a number of alongshore trends in the composition of the beach samples. These include the quartz content, which increases north of Port Waikato with a significant increase from North Head (<10% to >20%), and the orthoclase feldspar content, which increases north of Muriwai by up to 10%. The plagioclase feldspar content increases north of South Head by between 10 and 20%. However, the non-opaque heavy mineral and opaque mineral contents decrease significantly north of North Head. Augite is an example of this, decreasing from between 20 and 30% south of North Head to less than 1% (Laurent, 2000).

7.3 DUNE SEDIMENTS

Dune samples were collected from only five of the seven transects due to issues with accessibility along transects D and G. The mean grain size of these dune samples ranges between 0.18 and 0.23 mm (fine sand) with well to very well

sorted and subrounded to rounded grains dominating the sediment (Appendix F, Table 2).

Quartz and feldspar also dominate the dune sediments, although feldspar is the more abundant in these samples. Quartz comprises typically 10-20% of the sediment (four of five samples) with an increase to 20-30% along transect B. Feldspar dominates the sediment, ranging between 30 and 50%, with 40-50% feldspar occurring in three of the five dune samples. As with the beach samples, plagioclase feldspar dominates comprising between 20 and 30% in four of the five samples. Along transect C the plagioclase feldspar content increases to between 30 and 40%. Orthoclase feldspar also occurs and ranges between c. 10 and 20% of the sediment. Rock fragments are also an important component of the dune sediment forming between 10 and 30% in four of the five samples. Along transect C the rock fragment content is slightly lower, between 5 and 10%.

Six weathered grains of glauconite occur in two dune samples (transects A and F) with shell material found in only one sample along transect F. Opaque minerals are also rare in the dune sediments, occurring in only three samples and comprising between 0 and 5%. Non-opaque heavy minerals occur in every sample studied and range between 5 and 20% of the sediment. Hornblende dominates the heavy mineral component while oxyhornblende and augite occur in four of the five samples.

7.4 COMPARISON TO NKCM SEDIMENTS

The NKCM sediments are compared to the beach and dune samples discussed above to determine any differences in grain size and sediment composition. This is important as the dunes, beach and shelf are typically considered to be interacting environments which exchange sediment regularly during large storm events.

7.4.1 Grain size

Figure 7-3 shows the mean grain size of the beach and dune sands as well as the inshore shelf samples from each of the seven transects (between 33 and 65 m water depth). As expected, the beach samples are slightly coarser grained than the dune samples and have mean grain sizes mostly between 0.19 and 0.22 mm (fine sand). However, along transects C and D the grain size increases to 0.29 and 0.24 mm, respectively. The dune sample along transect C also shows the same trend increasing from between 0.18 and 0.20 mm to 0.23 mm. The inner shelf samples vary significantly from south to north (A-G) and compared to the beach and dune samples. The inner shelf sediments do not fine considerably offshore from the beach as would normally be anticipated, with three of the seven transects (B, F, G) showing the shelf deposits to be coarser than the corresponding beach samples. In the case of transects F and G this probably reflects the presence of shell material in the offshore sediment which is otherwise absent in beach samples. Along transect B the quartz and feldspar grains are slightly coarser (by 0.05-0.10 mm) than the samples to the north and south producing a larger mean grain size overall as quartz and feldspar both comprise between 40 and 50% of the sample.

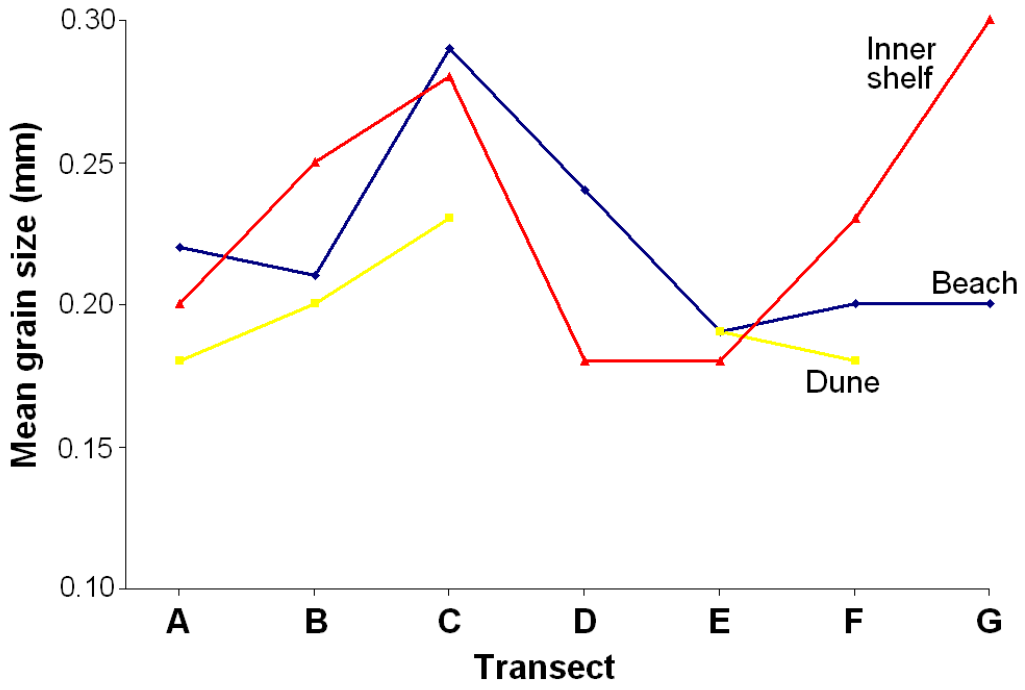

Figure 7-3. Comparison of mean grain size between beach (blue), dune (yellow) and inner shelf (red) sediments.

7.4.2 Sediment composition

Quartz and feldspar

The quartz content varies considerably in the offshore NKCM samples across the seven transects, although this variation tends to lessen to the north. The quartz content increases onshore across all transects except transect B while four of the five dune samples show a decrease in quartz from the beach samples (Fig. 7-4). Along the southernmost transect A, the quartz content increases from c. 20-30% on the shelf to 30-40% on the beach before a significant decrease into the dunes (30-40% to 10-20%). The opposite trend occurs along transect B with a decrease in the quartz content from the shelf to the beach (40-50% to 5-10%) followed by a small increase to c. 20-30% in the dune sample. Transect C shows a considerable increase in quartz from the outermost sample (5-10% quartz) at 622 m water depth to 160 m depth (30-40% quartz). The quartz content then decreases onshore to 20-30% on the beach and 10-20% in the dunes. Along transect D the quartz content also increases significantly onshore, from 5-20% on the outer shelf to 30-40% in c. 60-100 m water depth. A slight decrease then occurs in the heavy mineral rich inner shelf sample (P599) followed by an increase onshore to the beach from 20-30% to 30-40%. The quartz content along transect E also increases from the outer shelf (5-10%) to the innermost sample (30-40%). The beach sample has a similar quartz content to the inner shelf (c. 30-40%), however the quartz component decreases into the dunes by 10-20%. The quartz content along transect F increases onshore from 10-20% at outer shelf depths to 30-40% on the beach before decreasing to 10-20% to the dune. Along transect G the quartz content increases significantly onshore from 10-20% on the inner shelf to 30-40% on the beach.

The feldspar content increases shoreward overall with the beach and dune samples having higher percentages of feldspar than the NKCM sediments (Fig. 7-4). Along transect A, the feldspar percentage increases onshore from 20-30% on the outer shelf to 40-50% in the beach and dune sediments. The feldspar content also increases onshore along transect B from 20-30% at greater than c. 200 m water depth to 50-60% feldspar on the beach. However, this decreases to 30-40%

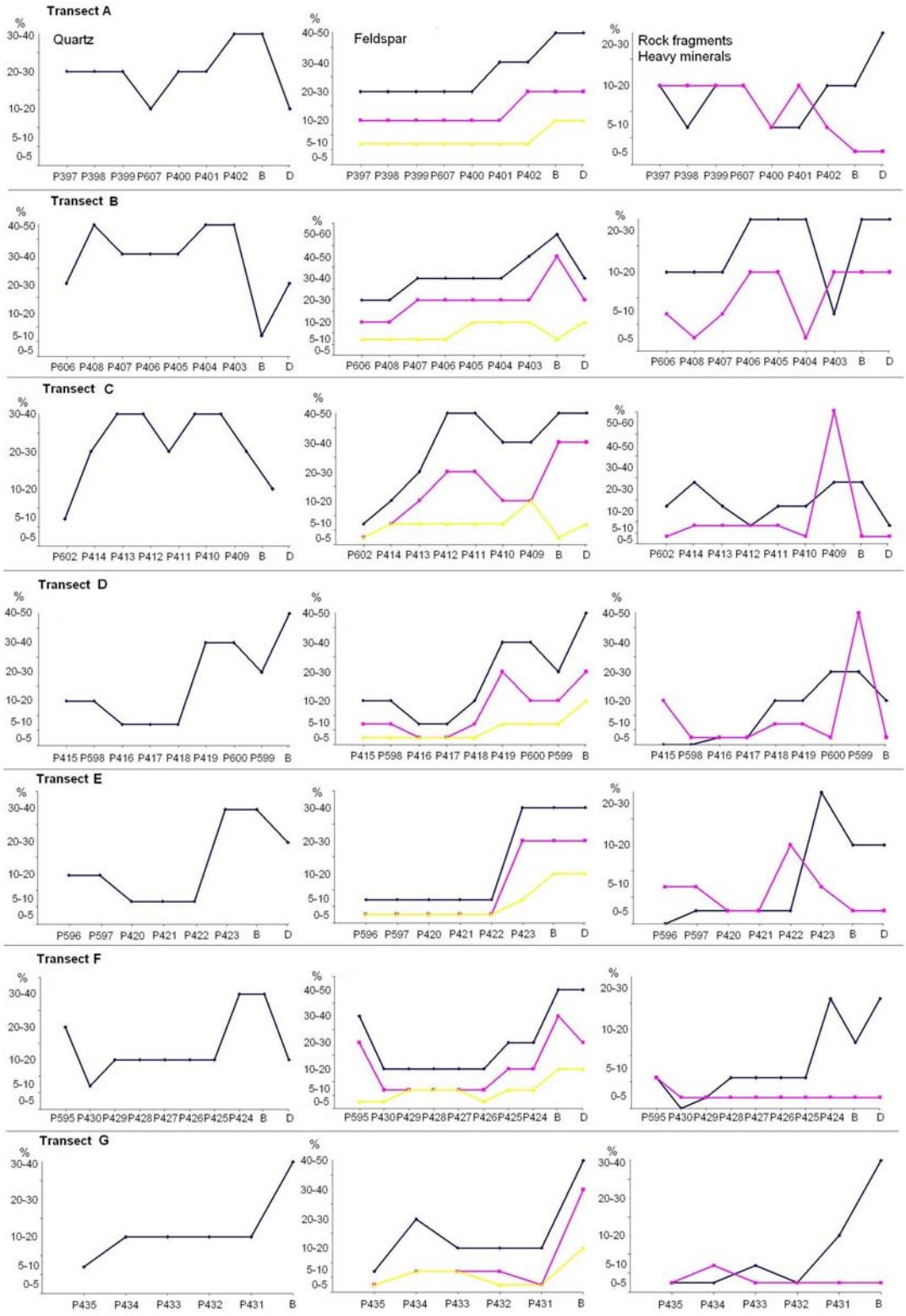

Figure 7-4. Distribution of quartz, feldspar, rock fragments and heavy minerals across each of the seven transects (A-G)and onto the adjacent beach (B) and dune (D). Feldspar column: blue = total feldspar, pink = plagioclase feldspar, yellow = orthoclase feldspar. Rock fragment and heavy mineral column: blue = rock fragments, pink= heavy minerals.

feldspar in the dune sample. Transect C shows an overall increase shorewards from 5-10% feldspar at greater than 600 m water depth to 40-50% feldspar at c. 80 m water depth. Between c. 30 and 70 m water depth this decreases to 30-40% feldspar as the quartz and heavy mineral components increase at this depth. The feldspar content then increases to 40-50% in the beach and dune samples. Along transect D the feldspar percentage increases from 5-20% at greater than c. 150 m water depth to 30-40% feldspar at c. 60 m water depth. A small decrease occurs in the heavy mineral rich sample at c. 40 m water depth before increasing to 40-50% feldspar on the beach. The feldspar content along transect E increases significantly from 5-10% at greater than 90 m water depth to 30-40% feldspar at c. 50 m water depth and in the beach and dune sediments. Along transect F feldspar increases from 10-20% between c. 100 and 400 m water depth to 40-50% in the beach and dune samples, while the feldspar content in transect G increases significantly onshore from c. 10-30% at greater than c. 100 m water depth to 40-50% feldspar on the beach.

The difference between plagioclase and orthoclase feldspars was distinguished in thin section for both the beach and dune samples, however XRD traces were used in the NKCM samples. This method was only used to allow a basic comparison, as the analysis of the XRD traces was only semi-quantitative and considered bulk feldspar (including rock fragments which are dominated by plagioclase feldspar) as opposed to only singular feldspar grains, which has likely lead to an overestimate of plagioclase feldspar. Both plagioclase and orthoclase feldspars have similar trends to total feldspar, increasing shorewards from the outer shelf and upper slope to the beach and dune sediments (Fig. 7-4). Plagioclase feldspar follows the total feldspar trend closely along all seven transects, increasing onshore, and comprising 10-30% along transect A, 10-50% along transect B, c. 5-40% along transects C and G, c. 5-30% along transects D and E and 10-40% along transect F. The orthoclase feldspar component is more variable in comparison to total feldspar, comprising between c. 5 and 20% of every sample.

Rock fragments and non-opaque heavy minerals

The amount of rock fragments generally increases shorewards, but the trend from inner shelf to beach and dune varies considerably across the seven transects (Fig. 7-4). Along transect A the rock fragment sediment component increases onshore from 5-10% at inner-mid shelf depths to 10-20% on the beach. The rock fragment content also increases from the beach (10-20%) to the dune (20-30%). The rock fragment percentage along transect B also shows an overall increase towards shore, but decreases significantly from 20-30% at c. 60 m water depth to 5-10% at c. 30 m water depth. The rock fragment component then increases considerably in the beach and dune samples (20-30%). Along transect C the rock fragment percentage does not show a strong trend, with a slight decrease from 10-30% to 5-10% between c. 600 and c. 100 m water depth which then increases to 20-30% on to the beach and decreases to 5-10% in the dunes. Along transect D the content of rock fragments also increases shorewards to the inner shelf, however they show a slight decrease on to the beach from 20-30% to 10-20%. Along transect E the rock fragment component increases significantly from c. 90 to c. 50 m water depth (0-5% to 20-30%) followed by a slight decrease into the beach and dune samples (10-20%). The rock fragments along transect F show an increase onshore from 0-10% at greater than c. 80 m water depth to 20-30% at c. 50 m water depth. This is followed by a decrease to the beach (10-20%) and increase into the dunes (20-30%). Along transect G the percentage of rock fragments increases significantly onshore from less than 10% at greater than c. 150 m water depth to 30-40% on the beach.

The non-opaque heavy minerals generally show a decrease from the outermost continental margin samples to the onshore beach and dune samples (Fig. 7-4). Along transect A the heavy mineral content decreases significantly onshore from 10-20% at greater than c. 40 m water depth to 0-5% in the beach and dune samples. Along transect B the heavy mineral component shows the opposite trend with an increase shorewards from 0-10% between 160 and 300 m water depth to 10-20% between c. 80 and 110 m depth. There is a sharp decrease in heavy minerals from c. 80 to 60 m water depth followed by considerable increase back to 10-20% in the beach and dune samples. Along transect C, heavy minerals

comprise only 0-10% of the total sediment at greater than c. 60 m water depth but increase significantly to between 50 and 60% at c. 30 m water depth. Despite this, the beach and dune samples are relatively depleted in heavy minerals, comprising only 0-5%. Transect D shows a very similar trend with less than 20% heavy minerals at greater than c. 60 m water depth and a significant increase to 40-50% at c. 40 m water depth. This is followed by a decrease to between 0 and 5% heavy minerals on the beach and dune. Along transect E the heavy mineral content varies considerably but decreases overall to the beach and dune (between 5 and 20% to 0-5%). Along transects F and G the heavy mineral percentage is stable with 0-5% heavy minerals at all sites except P595 and P434, respectively.

The trends in grain size and sediment composition observed between the NKCM and beach and dune sediments are indicative of sediment exchange between the shelf and beach. The extent of this sediment exchange is discussed further in Section 8.2.7.

Chapter 8

THE SEDIMENTARY REGIME - PROVENANCE, FACIES AND SEDIMENTATION MODELS

8.1 INTRODUCTION

The data presented in chapters Four, Five, Six and Seven can be combined to produce an overall picture of the sedimentary regime on the north Kaipara continental margin (NKCM). This chapter first aims to determine the provenance of each of the main sediment components present on the NKCM (Section 8.2) followed by the development of facies based on regionally important sediment types (Section 8.3) and the interpretation of these facies (Section 8.4). In Section 8.5, the NKCM is compared to four published sedimentation models developed for wave-dominated continental shelves.

8.2 PROVENANCE OF MAIN SEDIMENT COMPONENTS

The provenance of each main sediment component is discussed firstly in terms of possible rock sources (i.e. metamorphic, plutonic, etc.) and then in terms of some more specific sources most likely for the component on the NKCM, summarised in Table 8.1. In Section 8.2.6 the likely provenance of the NKCM sediments is reviewed as a whole. This section (8.2) does not attempt to cover all the rock units in western North Island and South Island but rather includes those rock units where sufficient data are available in the literature to allow a simple comparison of composition between the source rock and NKCM sediments.

8.2.1 Quartz and feldspar

Quartz and feldspar grains dominate much of the sediment across the NKCM (Fig. 4-10). However, determining their provenance can be challenging, because quartz and feldspar are common in a wide range of rock types. Quartz may have both igneous (volcanic/plutonic) and metamorphic sources, with monocrystalline

quartz (blue-violet under CL) being dominantly of volcanic or plutonic origin and polycrystalline quartz (brown-lilac under CL) generally metamorphic. Potash feldspar (orthoclase) is an important component of silicic plutonic rocks and is abundant in granites, while plagioclase feldspar is the most abundant mineral in the majority of basaltic and andesitic rocks (Deer et al., 1992).

Quartz

The CL analysis of quartz in NKCM samples (Plate 1, c-j) suggests that volcanic or plutonic sourced (generally monocrystalline) quartz dominates with smaller amounts of metamorphic sourced quartz. This suggests the Taupo Volcanic Zone (TVZ) is the probable source of the majority of volcanic quartz grains in NKCM sediment as it has erupted large volumes (16000-20000 km^3) of quartz-rich rhyolitic/silicic volcanic material during the last 1.6 Ma (Fig. 8-1) (Houghton et al., 1995). Other sources include the North Island greywackes, South Island granites, Moeatoa Conglomerate and Northland and Waikato sedimentary and volcanic rocks. North Island greywackes include both Torlesse and Murihiku terranes consisting primarily of north to south trending ranges in central to southern North Island (Fig. 8-1). Quartz is common in the Permian-Jurassic Torlesse Terrane greywackes, comprising 15-25% monocrystalline quartz. Triassic-Jurassic Murihiku Terrane rocks crop out on the west coast between Awakino and Port Waikato and comprise 20-35% quartz with monocrystalline quartz dominant (Fig. 8-1) (Stokes and Nelson, 1991; Hudson, 1996; Briggs et al., 2004). Another potential source of monocrystalline quartz to the NKCM is the South Island granites, which consist of three belts comprising the Paleozoic-Cretaceous Separation Point Granite, Karamea Granite and an undifferentiated granite south of this (Fig. 8-1). Quartz is common forming between 30 and 50% in each of these belts (Hudson, 1996). In western Northland, moderate to high amounts of monocrystalline quartz also occur in the Oligocene-Miocene Ruatangata Sandstone (Te Kuiti Group) and Late Cretaceous Punakitere Sandstone (Northland Allochthon), from 20-28% and 26-41% quartz, respectively (Fig. 8-1) (Gilbert et al., 1989). The Late Triassic Moeatoa Conglomerate includes large granitoid clasts comprising between 21 and 46% monocrystalline quartz (Keane 1986a), while quartz is also present in minor quantities in the Tangihua

Table 8-1. Potential source rocks of mineral components in NKCM sediments. In most cases percentage ranges are used, otherwise D = dominant, P = present but quantity not reported in literature, ? = not known if present and - = absent. Literature sources for data referred to in text. Mono=monocrystalline. Poly=polycrystalline.

	Quartz		Feldspar		Micas		Heavy minerals				
Source rocks	Mono	Poly	Plagioclase	Orthoclase	Biotite	Muscovite	Hornblende	Garnet	Augite	Hypersthene	Opaques
TVZ andesites	P	?	25-50	–	<5	–	<1	–	D	D	
TVZ rhyolites	D	?	P	–	<5	–	<1	–	D	D	<1
Taranaki andesites	<1		25-50	–	<5	–	D	–	D	<5	<5
NI Murihiku Terrane	30-50	15-25	25-35	3-12	1-5	1-5	1-5	<1	1-5	1-5	?
NI Torlesse Terrane	15-25	?	1-5	30-40	<5	–	–	–	<1	–	?
SI granites	30-50	–	15-25	25-50	P	P	<5	<5	–	–	<5
SI schists	–	50-75	15-25	–	P	P	–	P	–	–	<5
Ruatangata Sandstone	20-28	5-8	15-26	?	<1	<1	?	?	?	?	<5
Punakitere Sandstone	26-41	3-16	9-42	?	1	1-5	?	?	?	?	<5
Waipapa Terrane	–	D	D	–	?	P	?	?	?	?	?
Waitakere arc volcanics	?	?	33-63	–	?	?	<1	–	25-40	P	P
Tangihua Complex	<5		D	–	–	–	<5	–	P	<5	–
Kaihu Group	15-50 D	?	5-20	5-15	?	?	P	–	P	P	<5
Moeatoa Conglomerate	21-46	?	7-41	20-46	1-5	1-5	?	?	?	?	P

Complex rocks of the Ahipara Massif in western Northland (Fig. 8-1) (Larsen and Parker, 1989). The Pliocene-Quaternary Kaihu Group rocks which outcrop on the west coast of the North Island contain between 15 and 50% quartz (primarily monocrystalline) in the Kaawa-Ohuka and Awhitu Peninsula formations (Fig. 8-1) (Stokes and Nelson, 1991).

Metamorphic (generally polycrystalline) quartz is rare in NKCM sediments. Possible sources of polycrystalline quartz include the Waipapa and Murihiku terranes, South Island schists, and Te Kuiti Group and Northland Allochthon rocks. The Permian-Jurassic Waipapa Terrane block near Omahuta (northeastern Hokianga Harbour) comprises sandstones metamorphosed to prehnite-pumpellyite-epidote and pumpellyite-stilpnomelane-actinolite-epidote grade which are both dominated by polycrystalline quartz (Fig. 8-1) (Jennings, 1989). Polycrystalline quartz also occurs in Murihiku Terrane greywackes (15-25%) (Hudson, 1996) and is very common in Permian-Jurassic South Island schists where it comprises between 50 and 75% of the chlorite, biotite and garnet-oligoclase zones in the Marlborough Sounds and Southern Alps (Hudson, 1996). Minor amounts of polycrystalline quartz also occur in the Ruatangata (Te Kuiti Group) and Punakitere (Northland Allochthon) sandstones, from 5-8% and 3-16%, respectively (Gilbert et al., 1989).

Feldspar

Feldspar in NKCM sediments (Fig. 4-10B) could be derived from an extremely wide range of sources in both the North and South Islands. The CL analysis of feldspar suggests potash feldspar (orthoclase) often just dominates the sediment with slightly lesser amounts of plagioclase feldspar, however, XRD analysis suggests plagioclase feldspar dominates. As discussed in Chapter 7 the XRD results consider the bulk mineralogy of the sediment, which provides a less accurate semi-quantification of the discrete plagioclase feldspar mineral content because it also includes plagioclase feldspar in rock fragments (which are dominantly volcanic with plagioclase phenocrysts).

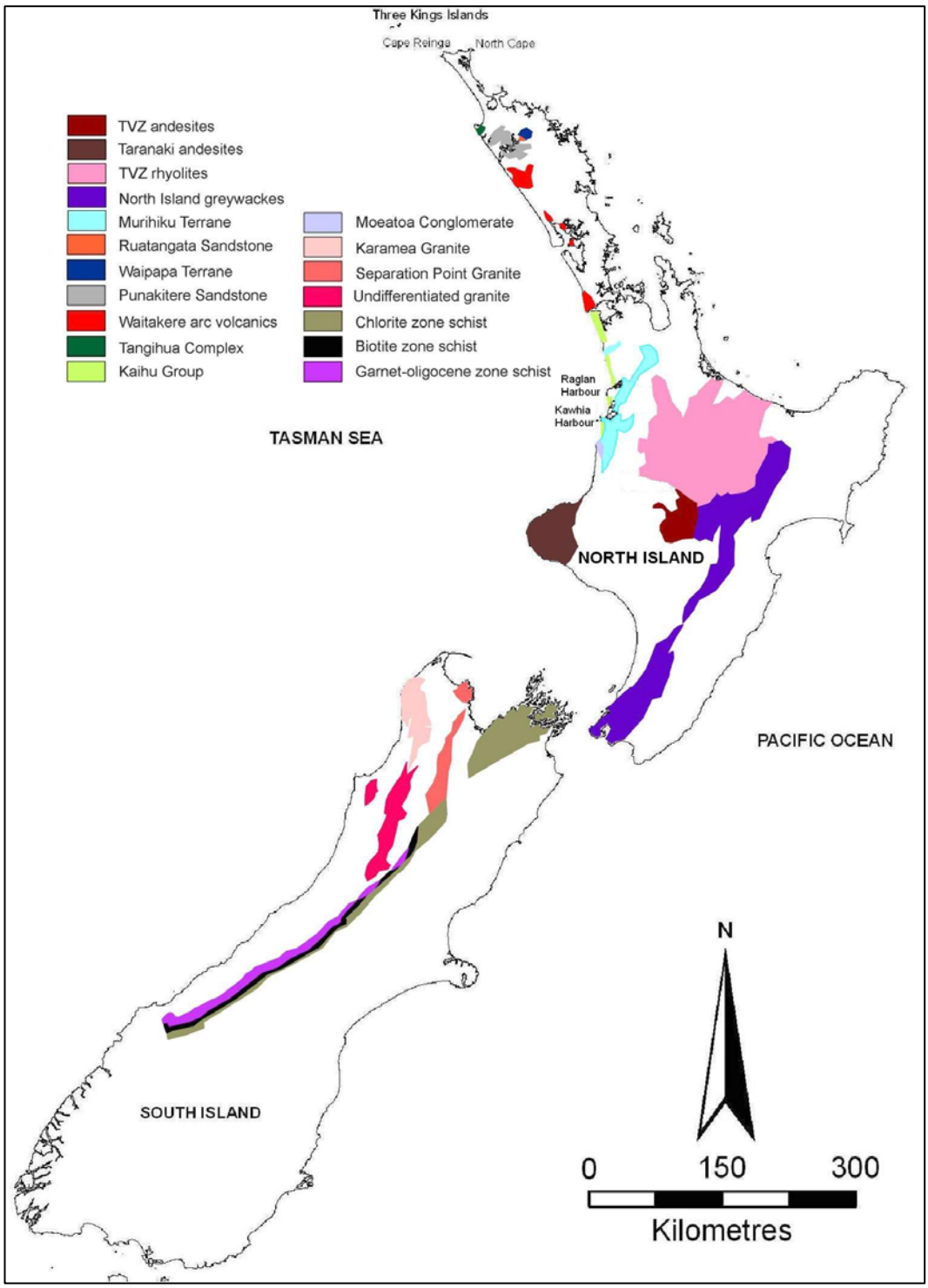

Figure 8-1. Location of the potential source rocks mentioned in the text. Location of South Island granites sourced from Hudson (1996). South Island schists = Hudson (1996) and Grapes, (1995). Moeatoa Conglomerate = Keane (1986a). North Island greywackes = Hudson (1996) and Stokes and Nelson (1991). Kaihu Group = Stokes and Nelson (1991). TVZ and Taranaki volcanics = Hudson (1996). Tangihua Complex = Larsen and Parker (1989). Ruatangata Sandstone and Punakitere Sandstone = Gilbert et al. (1989). Waipapa Terrane = Jennings (1989). Waitakere arc volcanics = Issac (1996). The location of each group is only approximate.

NKCM plagioclase feldspar has many potential sources, including central North Island volcanics, basement rocks, Northland volcanic and sedimentary rocks and South Island schists and granites. Plagioclase feldspar dominates the mineral assemblages of both the TVZ (Ruapehu and Tongariro) and Taranaki andesites (25-50%), comprising both phenocrysts and groundmass (Stokes and Nelson, 1991), while the rhyolites from the TVZ also include plagioclase (Fig. 8-1) (Hudson, 1996). Plagioclase feldspar generally occurs in small amounts in both the Torlesse and Murihiku terranes (1-5%) (Hudson, 1996), but may reach 25-35% in some Murihiku Terrane rocks (Stokes and Nelson, 1991). Plagioclase feldspar comprises 15-25% of both the South Island granites and schists. Both metamorphic zones of the Omahuta Waipapa Terrane block are also dominated by plagioclase feldspar, particularly in vein systems (Jennings, 1989). Plagioclase feldspar is present in the Tangihua Complex rocks of the Ahipara Massif where it occurs as the dominant phenocryst (Larsen and Parker, 1989), while plagioclase forms between 15 and 26% of the Ruatangata Sandstone and 9-42% of the Punakitere Sandstone (Gilbert et al., 1989). The Moeatoa Conglomerate comprises between 7 and 41% plagioclase feldspar, while the Kaihu Group sediments generally consist of 5-20% plagioclase (Stokes and Nelson, 1991). The Miocene age basaltic to basaltic andesite rocks of the Waitakere volcanic arc contain plagioclase as the dominant phenocryst phase (Smith et al., 1989) with the Waipoua Basalt, the largest onland outcrop of Waitakere arc rocks, comprising plagioclase-augite-olivine basalt (Fig. 8-1) (Wright, 1980; Issac, 1996). Plagioclase is the dominant phenocryst phase (33-63%) and also occurs in the groundmass of these rocks (Wright, 1980; Smith et al., 1989).

The K feldspar (orthoclase) identified in NKCM sediments also has a range of potential sources, including the North Island greywackes, Moeatoa Conglomerate, Kaihu Group, and South Island granites. The North Island greywackes comprise between 25 and 50% orthoclase feldspar overall, with up to 30-40% present in Torlesse Terrane rocks (Hudson, 1996). Murihiku Terrane rocks generally consist of between 3 and 12% orthoclase feldspar (Stokes and Nelson, 1991; Briggs et al., 2004), while the granitoid rocks of the Moeatoa Conglomerate generally comprise between 20 and 46% (Keane, 1986a). The Kaihu Group also includes 5-15% orthoclase feldspar (Stokes and Nelson, 1991). However, the largest potential

source of orthoclase is the South Island granites which consist of between 25 and 50% orthoclase (Hudson, 1996).

8.2.2 Heavy minerals

Igneous rocks are the predominant (ultimate) source of heavy mineral types in NKCM sediments (Deer et al., 1992; Mange and Maurer, 1992). Hornblende, hypersthene and augite are typically abundant in andesitic and basaltic rocks (Deer et al., 1992). Titanite, monazite, and zircon are common accessory minerals in silicic plutonic rocks such as granites, although zircons may also occur in volcanic silicic rocks (Deer et al., 1992). Actinolite, garnet, epidote and chlorite are predominantly found in metamorphic rocks, particularly those of greenschist facies (Deer et al., 1992). Garnet is characteristic of metamorphic rocks and particularly in mica and hornblende schists.

The heavy mineral suite in NKCM sediments (Fig. 4-11A) has a wide range of potential source rocks across both the North and South Islands. The Taranaki andesites include common augite and hornblende, with titanomagnetite, olivine and hypersthene as accessory heavy minerals (Stokes and Nelson, 1991; Hudson, 1996). Hypersthene and augite are the dominant heavy minerals in both the TVZ rhyolites and andesites, with rare hornblende, zircon and opaque minerals (Stokes and Nelson, 1991; Hudson, 1996). The Torlesse Terrane contains minor chlorite and rare augite (Hudson, 1996), while Murihiku Terrane rocks comprise minor chlorite, epidote, augite, hypersthene, hornblende (c. 1-5%) and rare zircon and garnet (<1%) (Stokes and Nelson, 1991; Hudson, 1996; Briggs et al., 2004). Heavy minerals may also be sourced from the South Island schists with the chlorite and garnet-oligoclase zones of the Alpine Schist providing a potential source of chlorite, epidote and garnet minerals with ilmenite and titanite as accessory constituents (Mortimer, 2000). The garnet-oligoclase zone of the Haast Schist is the closest exposed zone to the Alpine Fault resulting in high erosion rates and transport to the coast via rivers such as the Haast River. The South Island granites in northwest Nelson contain accessory heavy minerals including zircon, hornblende, titanite, magnetite and garnet (Hudson, 1996; Mortimer et al., 1997). Epidote and titanite are present in both metamorphic zones of the Waipapa

Terrane, with chlorite and actinolite also present in the higher-grade pumpellyite-stilpnomelane-actinolite-epidote zone (Jennings, 1989). The Waitakere arc volcanics contain augite in basaltic and basaltic andesite rocks and augite, hypersthene and titanomagnetite in andesitic and dacitic rocks. The groundmass of these rocks usually consists of augite, titanomagnetite and hypersthene. Hornblende is rare in the andesitic rocks of the Waitakere volcanic arc except at Tokatoka in northern Kaipara Harbour (Smith et al., 1989). The Waipoua Basalt exposed on the coastline south of Hokianga Harbour (Fig. 2-1) contains primarily augite (25-40%) but also titanomagnetite (4-9%) (Wright, 1980; Issac, 1996). The heavy minerals in the Kaihu Group primarily consist of augite, hypersthene, hornblende, oxyhornblende and actinolite, with accessory titanite and chlorite, while the opaque minerals are dominated by titanomagnetite (Stokes and Nelson, 1991). In general, the Te Kuiti Group rocks contain epidote, zircon, garnet, titanite, opaques and hornblende, while the Mohakatino Group comprises hornblende, augite, opaques and epidote (Stokes and Nelson, 1991). The Tangihua Complex rocks in the Ahipara Massif involve a range of heavy minerals with augite, opaques and minor hypersthene common in oceanic andesite and tholeiitic lavas and dikes. Minor amounts of hypersthene, opaques and amphibole also occur in the groundmass of these rocks (Larsen and Parker, 1989). Augite, red-brown hornblende and minor opaque minerals dominate the alkaline gabbros in the Ahipara Massif, while augite, hypersthene, olivine, brown hornblende and opaque minerals occur in the cumulitic gabbros (Larsen and Parker, 1989).

8.2.3 Mica

Biotite occurs in many igneous rocks but is particularly common in granites and granitic pegmatites. It also occurs in volcanic and metamorphic rocks such as rhyolite, andesite, gneiss, greenschist and amphibolite facies rocks. Muscovite is common in mainly metamorphic rocks and particularly schists and gneisses but also occurs in granites, pegmatites and hydrothermal veins (Mange and Maurer, 1992).

The mica fraction is relatively minor across the NKCM with only a small area of high abundance along transects A, B and F (Fig. 4-13). Potential source rocks are

relatively limited. They include central North Island volcanics, North Island greywackes, South Island schists and granites, Waipapa Terrane and Northland and Waikato sedimentary rocks. Biotite occurs as an accessory mineral in the TVZ (both rhyolites and andesites) and Taranaki volcanic rocks (Hudson, 1996), as well as in the Kaihu Group sandstones (Stokes and Nelson, 1991). The Torlesse Terrane contains minor biotite (Hudson, 1996), while the Murihiku Terrane rocks comprise c. 1-5% biotite and muscovite (Briggs et al., 2004). Biotite and muscovite also occur in minor amounts (1-5%) in the Moeatoa Conglomerate, with biotite more common than muscovite (Keane, 1986a). Biotite and muscovite are rare (<1%) in the Ruatangata Sandstone but reach c. 1% muscovite and c. 1-5% biotite in the Punakitere Sandstone (Gilbert et al., 1989). Muscovite is also present in the metamorphic zones of the Waipapa Terrane (Jennings, 1989). Both biotite and muscovite occur in the biotite schists of the South Island while muscovite only occurs in the chlorite schists (Hudson, 1996). Muscovite is abundant in the Alpine Schist with flakes of biotite greater than 1 mm long also included (Mortimer, 2000). The South Island granites comprise biotite granites and granodiorites (Mortimer et al., 1997) that contain both biotite and muscovite flakes (Hudson, 1996). Mica also occurs in the Mohakatino (Stokes and Nelson, 1991), Mokau and Mount Messenger groups in the Taranaki Basin with mica in the Mokau and Mount Messenger groups sourced from low grade schists and phyllites of southern North Island and South Island (King and Thrasher, 1996).

8.2.4 Rock fragments

Rock fragments can be sourced from any of igneous (especially volcanic), sedimentary or metamorphic rocks. The NKCM rock fragments comprise mainly volcanic rock fragments dominated by plagioclase feldspar phenocrysts, but sedimentary rock fragments also occur. Volcanic rock fragments are commonly derived from the erosion of TVZ and Taranaki andesites, which contain large quantities of plagioclase feldspar. They can also be sourced from erosion of TVZ rhyolites and ignimbrites, Waitakere arc volcanics, Tangihua Complex rocks and the Kaihu Group deposits (Stokes and Nelson, 1991). Andesite dominated volcanic rock fragments are common (up to 80%) in Murihiku Terrane rocks

where they are dominated by plagioclase feldspar with minor hornblende, augite, hypersthene and biotite (Briggs et al., 2004). Sedimentary rock fragments may also be present in small amounts (Hudson, 1996). The Torlesse Terrane contains between 15 and 25% rock fragments, which are dominated by fine grained sedimentary sandstones/siltstones with rare rhyolite and andesite rock fragments (Hudson, 1996). Volcanic rock fragments are also present in the Ruatangata (1-5%) and Punakitere (1-11%) sandstones, which also contain sedimentary rock fragments, from 4-9% and 2-12% in each, respectively (Gilbert et al., 1989).

8.2.5 Clay minerals

The clay minerals in NKCM sediments may be sourced from a wide range of rocks, including Murihiku Terrane and Te Kuiti, Mokau, Mahoenui, Mohakatino and Kaihu group rocks that crop out on the coast and catchment areas in the Waikato-King Country region (Hume and Nelson, 1986). Murihiku Terrane rocks comprise 30-40% clay minerals dominated by chlorite, but also include mixed layer and smectite clays (Stokes and Nelson, 1991). Te Kuiti Group rocks contain between 10 and 90% clay minerals dominated by smectite and with important amounts of illite, kaolinite and chlorite clay minerals (Hume and Nelson, 1986; Stokes and Nelson, 1991). Clay minerals comprise between 5 and 50% of the Mokau Group with smectite, illite, chlorite and mixed layer clays present. Illite, smectite, chlorite, mixed layer and kaolinite clays also occur in the Mahoenui Group which includes 30-40% clay minerals (Stokes and Nelson, 1991). Both the Mohakatino and Kaihu groups contain less than 5% clay minerals with illite, smectite, chlorite, mixed layer and kaolinite clays occurring in the Mohakatino Group and halloysite, illite, mixed layer and smectite clays in the Kaihu Group (Stokes and Nelson, 1991).

The most likely source rocks for smectite, the dominant clay mineral in the mud fraction of NKCM sediments, are the Oligocene and Miocene age mudstones that occur along on the coastline and in the catchment areas in the Waikato-King Country region (Hume and Nelson, 1986) and western Northland. The clay mineralogy of these mudstones reaches 80-90% smectite providing a potentially significant source of detrital smectite to the western North Island shelf (Hume and

Nelson, 1986). Kaolinite is most likely to be sourced from soils on Murihiku Terrane rocks as well as erosion of the Te Kuiti Group coal measures, while illite and chlorite are probably sourced ultimately from the schists and granites of northwest Nelson and the Southern Alps.

8.2.6 Likely provenance for NKCM sediment

The provenance of NKCM sediments is complex due to both local and distal sources combining to produce the sediment distributions observed. This makes it difficult to determine the precise source of each component and therefore the total sediment. This section aims to infer the major sources of the NKCM sediment obtained from combining the sources of each sediment component.

The TVZ rhyolites provide probably the largest volume of quartz-rich sediment transported by the Waikato River to the coastline at Port Waikato. The same silicic volcanics are also possible sources of minor amounts of plagioclase feldspar, hypersthene and augite and rare biotite and hornblende. The TVZ andesites are probably a source of plagioclase feldspar, augite and hypersthene, with rare biotite and moderate amounts of volcanic rock fragments also provided to the marine sedimentary system by the Waikato River.

The Taranaki andesites are also potentially major sources of plagioclase feldspar and for the NKCM are possibly more significant than the TVZ andesites due to the large mass of Mount Taranaki and its ancestral cones (Kaitake and Pouaki) in a readily erodible coastal setting. The Taranaki andesites are a potential major source of augite and hornblende heavy minerals and volcanic rock fragments to the NKCM, with minor titanomagnetite and hypersthene also supplied.

The Torlesse and Murihiku terrane rocks are dominated by quartz and may supply minor to moderate amounts of polycrystalline and monocrystalline quartz, respectively to the NKCM. These rocks are likely to be less significant sources of quartz compared to the TVZ rhyolites due their location in central to southern North Island and the greater difficulty in transporting the eroded material to the NKCM. Potash feldspar (orthoclase) forms a major constituent of the Torlesse

Terrane and therefore the low to moderate quantities (5-20%) in NKCM sediments is probably, at least partially, sourced from these rocks. Both the Torlesse and Murihiku terranes are possibly minor sources of chlorite, augite, epidote, hornblende, mica, and garnet, while the Torlesse Terrane may be a relatively important source of sedimentary rock fragments.

The South Island granites are dominated by quartz but they probably provide only a minor to moderate contribution of quartz to the NKCM sediments due to the relatively low uplift and erosion rates (0-1.5 mm/year) in the Nelson region (Wellman, 1979) and the relatively small volume and areal extent of the granites. It is also likely that a significant amount of the eroded granitic material is swept into Cook Strait before it can be transported north due to the presence of strong tidal currents acting this area (Carter and Heath, 1975). The South Island granites are also probably a sizeable source of orthoclase feldspar and moderate source of plagioclase feldspar and mica (biotite and muscovite), potentially providing small amounts of these minerals to the NKCM. Zircon, hornblende, titanite and garnet are only minor components of the South Island granites and so are unlikely to be the source of these minerals in NKCM sediments.

The South Island schists are dominated by polycrystalline quartz grains and as such are probably one of the major sources of this form of quartz to the NKCM as a result of the high uplift and erosion rates (c. 7-10 mm/year) in the Southern Alps (Wellman, 1979). Moderate amounts of chlorite, epidote, mica (both biotite and muscovite) and garnet, as well as minor ilmenite and titanite, are also supplied to the marine sedimentary system from the erosion of primarily garnet-oligoclase, biotite and chlorite zone schist along the Southern Alps.

The Kaihu Group, Ruatangata Sandstone (Te Kuiti Group) and Punakitere Sandstone (Northland Allochthon) rocks probably supply small quantities of quartz and plagioclase and orthoclase feldspar to the western North Island margin. While each of these groups may comprise moderate to high concentrations of quartz (30+%), their overall volume and areal extent is small compared to other source rocks. Consequently, these units are likely to be only minor sources of sediment to the NKCM. Most of the Northland Allochthon rocks are not

considered here due to the predominance of mudstones, which do not supply sand sized mineral grains to the NKCM, but are probably important sources of clay minerals. The Punakitere Sandstone is the only widespread sandstone in the Northland Allochthon along western Northland. The block of Waipapa Terrane near Omahuta also possibly provides a relatively small quantity of mineral grains to the NKCM. These rocks are dominated by polycrystalline quartz and plagioclase feldspar with moderate amounts of epidote and minor titanite, chlorite and actinolite. To be deposited on the NKCM these mineral grains must be transported by river into the Hokianga Harbour and then flushed out of the harbour onto the shelf.

The Waitakere volcanic arc and Tangihua Complex rocks cropping out along the western Northland coastline may provide significant quantities of plagioclase feldspar to the beach and inner shelf sediments of the NKCM. Moderate amounts of augite and minor quartz, hypersthene and titanomagnetite are also present in these rocks. Hornblende is common in the Tokatoka volcanics inside northern Kaipara Harbour and may be the source of the higher levels of hornblende along transect B. The heavy mineral percentage reaches >30% along transects C and D at 38 and 42 m water depth, respectively (Fig. 4-11A), directly offshore from outcrops of Waipoua Basalt (transect C) and the Ahipara massif of the Tangihua Complex (transect D). Augite and hornblende co-dominate the heavy mineral fraction along transect D, which corresponds with the augite-dominated nature of these Tangihua Complex rocks. The planed peaks of the basaltic Herekino, Whangape and Hokianga massifs of the Waitakere volcanic arc are exposed offshore (Fig. 8-2) and are another potential source of mineral grains in NKCM sediments. Augite co-dominates the heavy mineral fraction with hornblende (Fig. 4-11B) in the proximity of all the massifs and the feldspar content (Fig. 4-10B) increases from 5-10% to 10-20% in the vicinity of these partially buried volcanoes.

In terms of the major source of sediment to the NKCM it may be concluded that the Taranaki andesites and TVZ rhyolites probably supply the dominant minerals in NKCM sediments (quartz and feldspar). The TVZ andesites are characterised by hypersthene and plagioclase with rare or absent hornblende, which suggests

they are not as significant contributors due to the large hornblende signature of the NKCM sediments (Stokes and Nelson, 1991) which can primarily be attributed to the Taranaki andesites. The North Island greywackes (Torlesse and Murihiku terranes), South Island schists and granites and sedimentary and volcanic rocks of Northland, Waikato, King Country and Taranaki are probably important secondary sources to the NKCM, but likely supply relatively small amounts of sediment to the overall system.

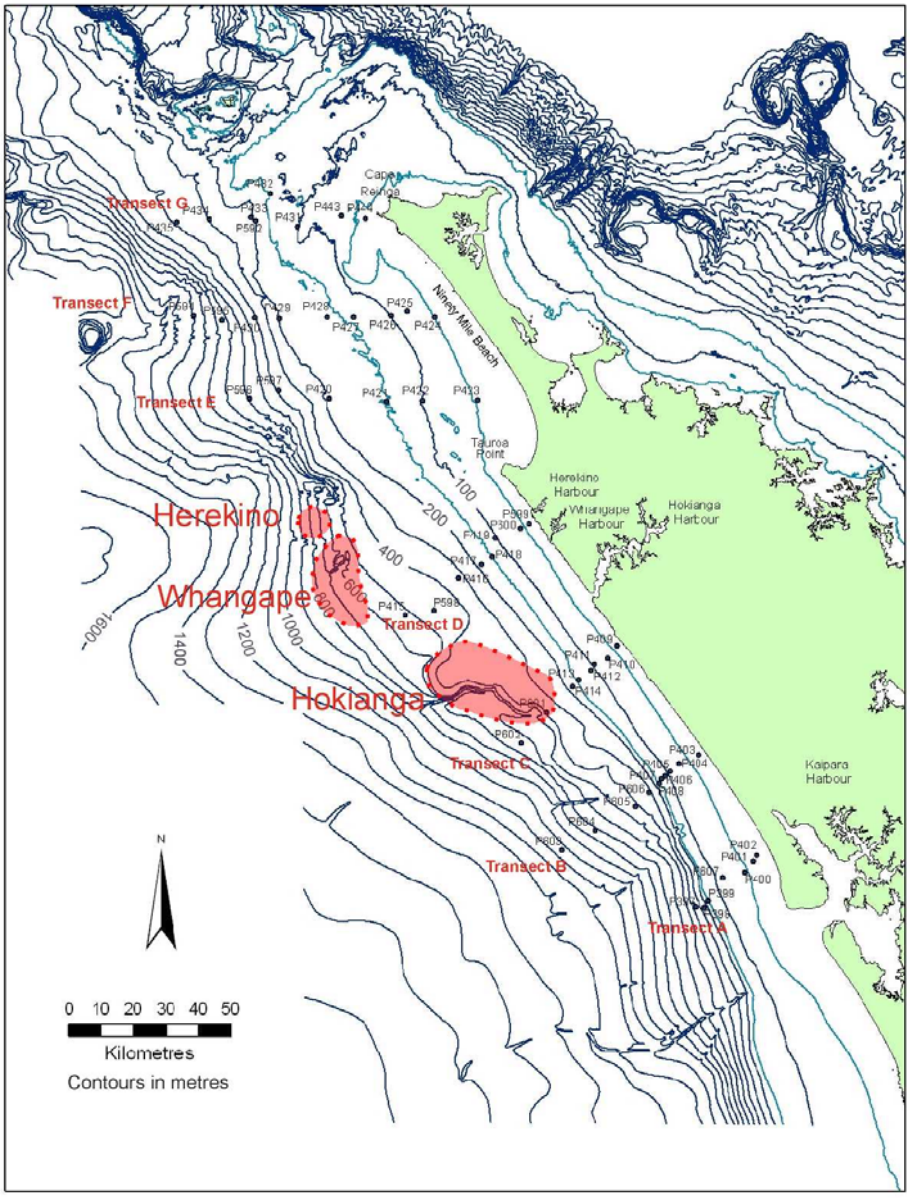

Figure 8-2. Location of the exposed Waitakere arc massifs on the NKCM.

8.2.7 Sediment pathways to the NKCM

Many of the potential source rocks discussed in Section 8.2.6 occur significant distances from the NKCM (e.g. South Island schists). In order to deposit the minerals observed in these sediments they first must be eroded and transported to the coastline via rivers. Griffiths and Glasby (1985) have estimated the sediment arriving at the coast to consist of both bedload and suspended sediment where the bedload component can be estimated to be only 2-4% of the total measured suspended sediment. The west coast rivers of the South Island, north of Haast (including the Haast River), have significant erosional power with suspended sediment yields of 120-130 million tonnes per year (Fig. 8-3) (Griffiths and Glasby, 1985). This is compared to the north coast South Island rivers, which contribute only 4-5 million tonnes of suspended sediment to the coastline each year (Fig. 8-3). The suspended sediment supply to the western North Island coast is also relatively small with 13-14 million tonnes delivered per year (Griffiths and Glasby, 1985). In addition to river transport, sediment is also directly supplied to the western coastline through the erosion of coastal cliffs by wave action (Fig. 8-3).

Once sediment is delivered to the coastline other oceanographic processes occur which result in the transport of sediment to the NKCM. The most important process is that of littoral or longshore drift within the surf zone which primarily occurs to the north (from Cape Egmont) with c. 175 000 m^3 of sand transported in this direction every year to western Northland (Fig. 8-3) (Hume et al., 2003). Schofield (1975) first discussed the northwards transport of sediment along western North Island through the Egmont-Kaipara sand system. This littoral drift is particularly evident between Mount Taranaki and the NKCM. There is also an estimated 3.8 million m^3 of sediment transported every year by net northwards littoral drift along the northern half of the west coast of the South Island (Probert and Swanson, 1985). The northerly net littoral drift component of sediment transport is a constant process caused by waves from the south and southwest breaking onshore at an oblique angle. This littoral drift has been actively modifying the current coastline since sea level reached its present height about 6500 years ago (Gibb, 1986).

On the NKCM waves are predominantly sourced from the southwest with 1-2 m waves occurring c. 20% of the time, 2-3 m waves occurring 10% of the time and >3 m waves c. 8% of the time. 1-2 m waves are also sourced from between the west and southwest (c. 15% of the time) along with 2-3 m (10%) and >3 m (5%) waves (R. Gorman, pers comm., 2007). The mean wave period is 9-13 s with a maximum wave period of 21 s. 1-3 m waves (10-14 s wave period) on the middle Taranaki shelf (75-110 m water depth) produce surface current speeds of between 24 and 112 cms^{-1}, but this reduces to bottom current speeds of only 2.3-11 cms^{-1}

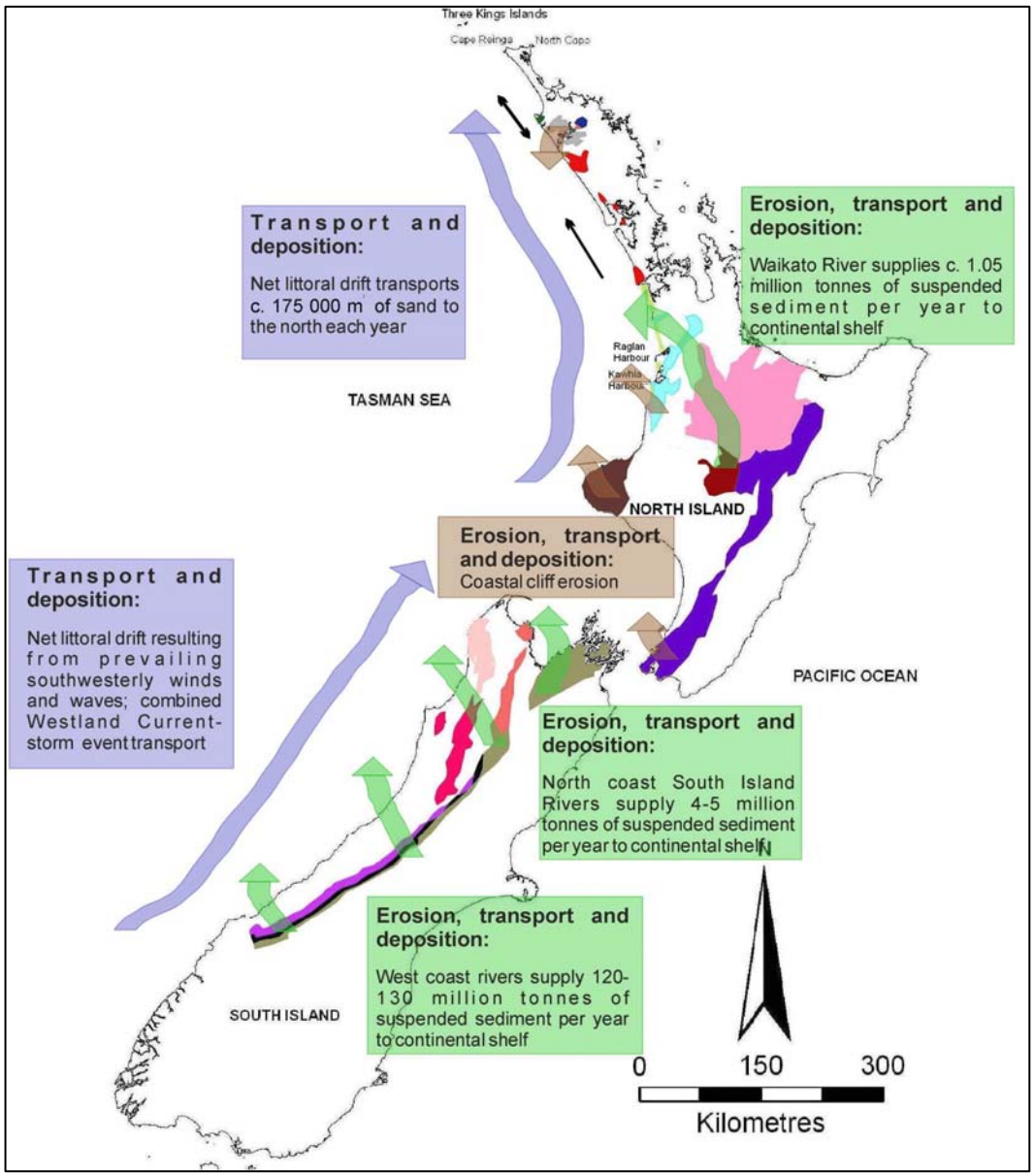

Figure 8-3. Dominant pathways of sediment transport and deposition to the NKCM. Source rock colours are defined in Fig. 8-1.

(Carter and Heath, 1975). 6-7 m waves (8-9 s wave period) produce much larger surface current speeds of 211-235 cms^{-1}, but considerably lower bottom current speeds of 0.08-4.5 cms^{-1} at 90-120 m water depth as the wave periods are shorter (Carter and Heath, 1975). The wave conditions on the NKCM are similar to the 1-3 m waves on the Taranaki shelf and as such probably produce similar bottom current speeds at 75-110 m water depth. Near bottom current speeds must reach greater than 35-40 cms^{-1} to suspend fine and medium sand sized sediment (Carter and Heath, 1975) and therefore waves on their own do not transport significant quantities of sediment on the NKCM outside of the surf zone.

Surface oceanic currents along western New Zealand (primarily the Westland Current) are capable of transporting sediment at most shelf depths when combined with storm waves and tidal currents and are therefore another sediment transport mechanism important for the NKCM (Fig. 8-3). For northernmost North Island, Schofield (1975) discussed possible southerly transport of sediment by the West Auckland Current to the entrance of the Kaipara Harbour. However, the West Auckland Current is described as weak and variable by Stanton (1973) who found that during parts of the year it actually flowed in the opposite direction. A recent study by NIWA suggests that the West Auckland Current is negligible (P. Sutton, pers. comm., 2007) and so would have an insignificant influence on sediment transport along the NKCM. In comparison to the constancy of the littoral drift process, combined storm and current sediment transport only occurs at less than 70 m water depth during annual storms and across much of the shelf (<130 m water depth) during a 25-year storm event (Carter and Heath, 1975). While such storm-assisted events provide the dominant transport mechanisms on the shelf as a whole they likely result in significantly slower northwards transport on the shelf compared to that in the coastal environment. If c. 175 000 m^3 of sand is transported north every year through littoral drift this accounts for c. 4.3 million m^3 of sand transport over 25 years. In order to move the same amount of sediment, a storm would have to suspend the top 4 mm of sediment across a 62 500 km^2 section of shelf at less than 150 m water depth. Probert and Swanson (1985) estimate 45 000 tonnes of bedload sediment is transported on the outer shelf off northwest Nelson every year. This equates to c. 37 000 m^3 (using density

of quartz sand = 1201 kg per m^3) of sediment transport on the outer shelf, which is significantly less than the 175 000 m^3 transport via littoral drift.

In Chapter 7, a comparison of the main sediment components between the NKCM and the bordering beach and dune environments was made. In general, the content of quartz, feldspar and rock fragments increases from the shelf to the beach by between 10 and 40%. The disparity could be explained by invoking the above uneven rate of sediment transportation across the margin with the most active transport of quartz rich sediment from the Waikato River mouth and of plagioclase feldspar and rock fragment rich sediment from the Mount Taranaki region occurring in the nearshore littoral system. Exchange between the beach and inner shelf samples would expectedly result in identical sediment compositions at less than 50 m water depth (Schofield, 1975), but this is generally not the case on the NKCM. For example, the inner shelf samples along transects C and D are considerably enriched in heavy minerals (>30%) however the corresponding beach samples comprise less than 5% abundance. Relatively regular reworking of the sediment must occur at less than 100 m water depth in the northern half and 150 m depth in the southern half of the NKCM as, firstly, glauconite grains occur in both beach and dune sediments (requiring sediment transport onshore) and, secondly, beyond these depths the quartz and feldspar components decrease significantly (c. >30% to c. <10%).

Another factor affecting sediment deposition and distribution on the NKCM is the strong tidal currents around Cape Reinga. The water displacement caused by these tidal currents probably extends down Aupouri Peninsula to the vicinity of Tauroa Point (P. Sutton, pers. comm., 2007) and appears to drag quartz and feldspar rich sediment northwards as the percentage of these components decreases along the inshore zone to the north. Tidal current speeds of c. 150 cms^{-1} moving southeastwards on the flood tide and c. 100 cms^{-1} northeastwards on ebb tide have been recorded between Cape Reinga and halfway down Ninety Mile Beach (Nelson et al., 1982) suggesting this may be the case.

8.3 FACIES DEVELOPED FROM NKCM SEDIMENTS

Five distinctive surficial sediment facies may be developed from the distribution of the NKCM sediment components based on their compositional and textural characteristics (Table 8-2). These facies are:

- Facies 1 (siliciclastic sand) - siliciclastic dominated slightly gravelly sand and slightly gravelly muddy sand.
- Facies 2 (glauconitic sand) - glauconite dominated slightly gravelly sand and slightly gravelly muddy sand.
- Facies 3 (mixed bryozoan-siliciclastic sand) - coarse bryozoan dominated sandy and muddy gravel, slightly gravelly sand and slightly gravelly muddy sand.
- Facies 4 (pelletal mud) - pellet dominated gravelly sandy mud.
- Facies 5 (foraminiferal sand and mud) - foraminifera dominated muddy and sandy sediments.

The siliciclastic sand facies (Facies 1) comprises at least 80% siliciclastic material with minor bivalve and gastropod skeletal material (dominated by *Scalpomactra scalpellum* and *Austrofusus glans*). Facies 1 can be divided into three subfacies based on the dominant siliciclastic minerals present.

The first subfacies (1a) is a well to very well sorted quartzofeldspathic sand facies, which generally consists of greater than 30% of both quartz and feldspar but may reach between 40 and 50% of each (Fig. 8-4, Plate 12). The facies has a heavy mineral fraction of less than 10% and a relatively high rock fragment content between 5 and 30%. It comprises fine sand and is restricted to shelf depths of less than 100 m in the northern half of the NKCM and generally less than c. 200 m in the southern half.

The second subfacies (1b) is a well to very well sorted heavy mineral dominated facies which contains heavy mineral concentrations greater than 30% and up to between 50 and 75% (Fig. 8-4, Plate 12). The heavy mineral fraction is dominated by hornblende, garnet and augite, with hypersthene and oxyhornblende also common. The facies occurs in less than 50 m water depth and has a quartz and

feldspar content which does not exceed 40% each and a rock fragment component over 20%.

The third subfacies (1c) is dominated by moderately sorted fine grained quartz, feldspar and mica (c. 20-30% each) with less than 20% glauconite and rock

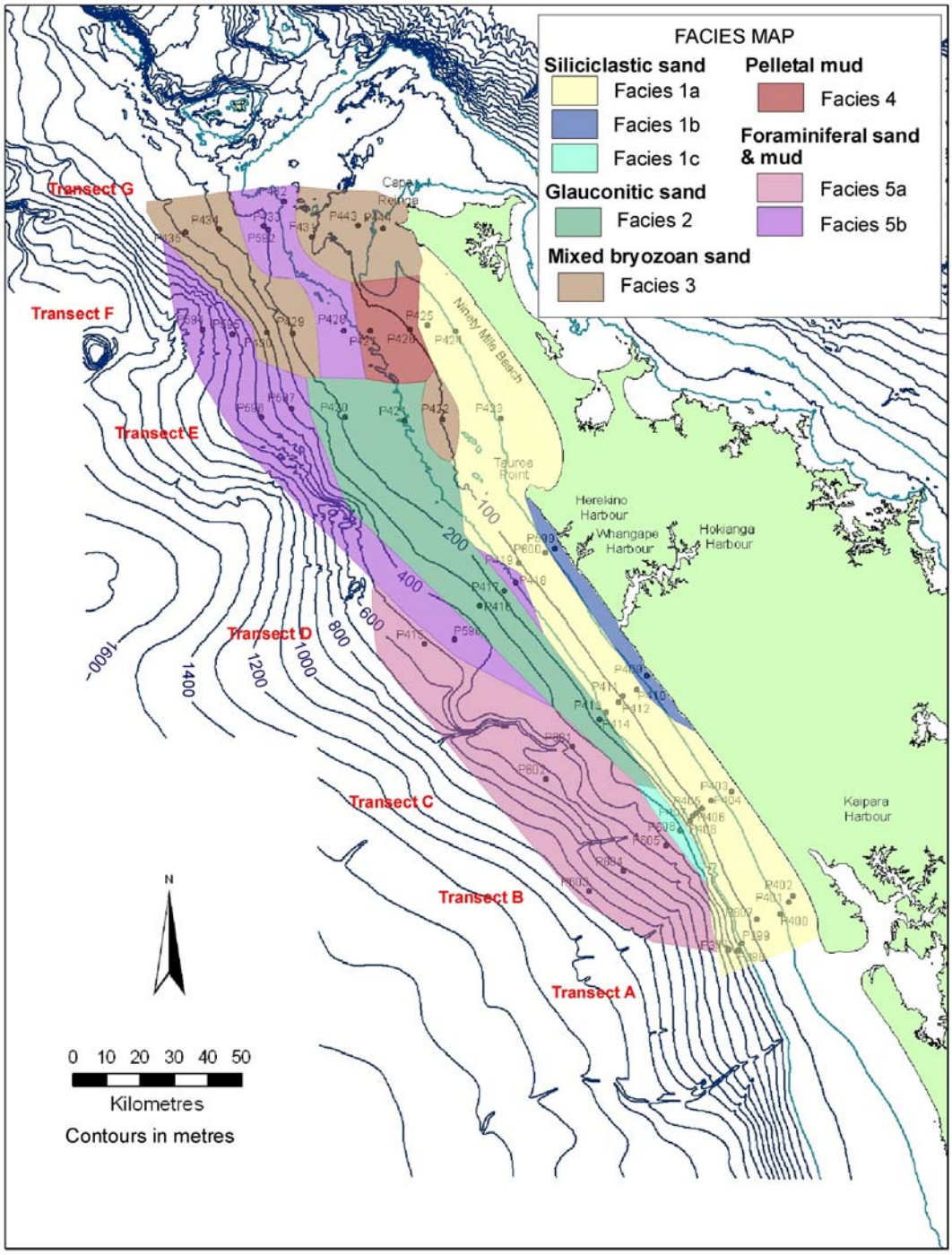

Figure 8-4. Distribution of the surficial sediment facies along the NKCM. See Table 8-2 for main attributes of each facies.

Table 8-2. Summary of essential properties of the five facies defined for the NKCM.

Facies	Sediment texture	Sorting	Siliciclastic minerals	Authigenic mineral	Skeletal %	Skeletal type
1	Sand	Well	>80%	<20% glauconite	<10%	Bivalve
2	Sand	Mod	<10%	>30% glauconite	<5%	Planktic forams
3	Gravel, sand	Well	<20%	<20% glauconite	>40%	Bryozoa
4	Mud	Mod	<20%	>30% pellets	<10%	Forams, spicules
5	Mud, sand	-	<20%	<20%	>30%	Forams

fragments and minor heavy minerals, opaques and mixed carbonate-siliciclastic pellets (0-10%, Plate 12). This subfacies only occurs at 300 m water depth along transect B (Fig. 8-4).

The glauconitic sand facies (Facies 2) comprises moderately to moderately well sorted, medium to fine sand with over 30% and up to as much as 75% glauconite grains (Plate 13). Minor quantities of the quartz, feldspar, rock fragments and heavy mineral fractions occur and rare planktic foraminifera are also present. This facies occurs between 150 and 400 m water depth in central NKCM, offshore from Tauroa Point (Fig. 8-4). Facies 2 provides glauconite grains to the rest of the NKCM with glauconite concentrations decreasing rapidly away from this facies. The glauconite also becomes rather stained and degraded with distance from this facies.

The mixed bryozoan-siliciclastic sand facies (Facies 3) comprises generally well to very well sorted abundant bryozoan skeletal material greater than 0.5 mm in size (Plate 13). The samples in this facies contain greater than 40% bryozoan material overall with most samples consisting of greater than 70%. Two samples co-dominate with bivalve fragments, which may reach up to 30%. Quartz, feldspar and glauconite is generally less than 20% in this facies, with minor heavy mineral, mica and opaque grains also present and rare siliciclastic pellets. The facies only occurs in the northern half of the NKCM at 30-150 and 190-300 m water depth along transect G, 200-400 m depth along transect F and at c. 90 m water depth along transect E (Fig. 8-4).

The pelletal mud facies (Facies 4) comprises muddy sediment dominated by greater than c. 30% mixed carbonate-siliciclastic pellets with minor foraminifera and opaline silica spicules (Plate 13). The sediment in this facies consists of moderately well sorted to poorly sorted very fine sand and mud, the latter exceeding 50%. This facies contains less than 20% quartz and feldspar grains and minor glauconite, rock fragments, opaques and heavy minerals. The facies occurs in a small area of 100-150 m water depth in the northern half of the NKCM (Fig. 8-4).

The foraminiferal sand and mud facies (Facies 5) comprises at least 30% foraminiferal tests with minor echinoderm fragments, opaline sponge spicules and mixed carbonate-siliciclastic pellets. Planktic foraminifera dominate the majority of samples within this facies (>30%), while benthic foraminifera generally comprise between 5 and 30%. The facies can be divided into two subfacies based on the texture and grain size of the sediment. Facies 5a consists of foraminifera dominated slightly gravelly mud, sandy mud and mud, while Facies 5b comprises foraminifera dominated slightly gravelly sand and slightly gravelly muddy sand. Facies 5a comprises greater than 50% mud sized sediment with most samples containing greater than 80% mud (Plate 14). It occurs at greater than 400 m water depth covering most of the slope in the southern half of the NKCM (Fig. 8-4). This subfacies consists of less than 20% quartz, feldspar, glauconite and heavy minerals and less than 5% mica, with opaque minerals and rock fragments absent. Subfacies 5b generally contains greater than 70% sand sized sediment which is predominantly moderately well sorted but ranges from very poorly sorted to very well sorted (Plate 14). Quartz, feldspar and glauconite comprise less than 20% of the sediment with minor mica and heavy mineral and rare opaque minerals and rock fragments. The facies occurs in two separate depth ranges across both northern and southern NKCM (Fig. 8-4): a deeper water band at slope depths occurs between 400 and 500 m depth along transect D, greater than 400 m depth along transect E and greater than 700 m depth along transect F, while a shallower band occurs at mid to outer shelf depths between c. 150 and 200 m water depth along transects D, F and G.

8.4 INTERPRETATION OF NKCM FACIES

Environmental conditions mainly control patterns of sediment distribution and as such the source, location and environment of each of the five NKCM facies (and subfacies) is discussed below.

Facies 1: Siliciclastic sand

Facies 1 is complex with three different siliciclastic minerals dominating and different potential sources for each dominant mineral type. The sediment in all three subfacies forms a modern sand prism, which extends from inner shelf to outer shelf depths (c. 200 m) and is where active sedimentation and sediment transport is occurring as a result of a high-energy environment. This high-energy sediment transport produces the predominantly well to very well sorted sediment that occurs throughout this facies by reworking and removing mud-sized particles. The distribution of siliciclastic sediment in this facies is controlled by the large flux of sediment from the south as a result of northwards littoral drift. This is seen in the decreasing width of Facies 1 from c. 200 m water depth in the southern half of the NKCM to c. 100 m depth in the north. Skeletal material in this facies is relatively rare (<10%) and generally comprises broken, shallow water bivalve and gastropod shells of dominantly *Scalpomactra scalpellum*, *Nucula nitidula*, *Austrofusus glans*, *Stiracolpus pagoda* and *Sigapatella tenuis*. Benthic foraminifera are unusually rare in less than 50 m water depth with none found in the transect B sample studied and only small amounts (<10%) in the transect F sample.

The sediment in Facies 1a (quartzofeldspathic sand) is probably sourced primarily from North Island volcanics (TVZ, Taranaki) and basement rocks. Littoral drift and the inshore coastal processes of shelf-beach sediment exchange as result of storm wave agitation likely control the distribution of this subfacies. The influx of quartz and feldspar rich sediment from the south significantly overwhelms other sediment sources to the inner and mid shelf except where Facies 1b (heavy mineral dominated sand) occurs. The erosion of basaltic to basaltic andesite coastal outcrops onshore from Facies 1b appears to exceed the supply of

quartzofeldspathic sediment to this area resulting in heavy mineral rich sediment and the presence of abundant rock fragments.

Facies 1c (mica rich sand) forms an unusual anomaly along transect B, as the surrounding NKCM samples only comprise low quantities (<5%) of mica grains. However, samples along transect A reach up to 10-20% mica suggesting mica, probably sourced from the South Island schists, has been transported northwards as far as these transects. Mica occurs as thin flakes that aid water transport through the grains being easier to suspend in the water column. The mica-rich sample P606 may be the result of sedimentation of these mica flakes due to a sudden increase in water depth (and corresponding decrease in energy) from c. 110 m water depth along transect A to 300 m depth along transect B at the same distance from the coastline (Fig. 2-7). Sediment may be flushed off the shelf edge and down the steep break during storm events resulting in deposition at c. 300 m water depth. This water depth is below the expected wave base during a 25 year storm and therefore the sediment deposited here is unlikely to move much potentially allowing the concentration of mica here.

Facies 2: Glauconitic sand

Facies 2 forms a widespread deposit of glauconitic sediment at mid shelf to upper slope depths. The period of time required to form evolved to highly evolved (K enriched) glauconite is c. 100 000 to 1 million years (Odin and Fullagar, 1988). This suggests that Facies 2 is an ‘old’ deposit, which has been concentrated and evolved on the outer shelf of the NKCM over a significant period of the margins history. The formation of this facies at outer shelf and upper slope depths suggests sediment bypassing must occur as the surrounding facies all contain moderate to high quantities of siliciclastic material. Glauconite only forms in areas of low sediment input, which suggests that this area of the NKCM has not been supplied with significant quantities of sediment over at least the last 100 000 years. Another important factor of glauconite (and associated phosphate) formation is the supply of nutrient rich water to the outer shelf through upwelling. The hydrodynamics of the NKCM are poorly understood. Upwelling is not considered a regular feature due to the lack of strong currents and suitable wind conditions

(which would need to be predominantly easterly and northeasterly winds c.f. Fig. 2-8) to produce wind-induced upwelling. However, such winds do occur during parts of the year (c. 20-30% of the time) and may result in minor upwelling. Easterly and northeasterly winds will also occur during storm events generated from north of New Zealand and so during these events could be associated with significant upwelling on the north Kaipara margin. The relatively minor siliciclastic fraction (generally <20%) is probably sourced from Facies 1 through offshore sediment transport during storm events. The supply of sediment through this process is considerably small and suggests bottom transport only occurs during extreme storm events.

The glauconite grains in this facies are well polished and have had depressions in the grain surfaces infilled with less evolved glauconite (Plate 3). This suggests that the grains have been subjected to reworking in a higher energy environment during lower sea levels and that multiple periods of glauconite formation have occurred.

Facies 3: Bryozoan-siliciclastic sand

Facies 3 is less extensive than the previous two facies, with tighter environment controls on its distribution. The facies occurs predominantly at mid to outer shelf depths, but it extends inshore along transect G. Facies 3 has formed as a result of low sediment input to the northern half of the NKCM due to the absence of large rivers discharging onto the shelf in this area. In addition, the strong tidal currents that occur around Cape Reinga produce a higher energy environment, which prevents significant sediment deposition and transports sediment to the east around Cape Reinga (Nelson et al., 1982). This allows bryozoan production at inner shelf depths along transect G as the skeletal material is not smothered by siliciclastics. Much of the bryozoan material in the outer shelf and upper slope band has probably been sourced from the bryozoan rich sediment on the Three Kings platform (or possibly inner shelf transect G) as all the samples in this band are degraded and relict looking. Bryozoan material extends to at least c. 400 m water depth in this band, which is beyond the depth of active bryozoan production. This suggests that the skeletal material in these samples has probably been transported a considerable distance off the shelf edge. This process is

common on the Three Kings platform with large quantities of coarse bryozoan material occurring at significant distances from bryozoan production areas (Nelson et al., 1982). The small area of Facies 3 along transect E is also an unusual anomaly as most of the surrounding sediments are siliciclastic rich. However, rocks were collected from this sample site and rocky outcrops were recorded on the depth sounder (Appendix B). These rock outcrops form a very suitable substrate for bryozoan colonisation by providing locations for attachment and extending above the sea floor and therefore preventing siliciclastic sediment from burying the skeletons.

Facies 4: Pelletal mud

Facies 4 is the most restricted facies on the NKCM occurring at only two sample sites. The mixed carbonate-siliciclastic pelletal material, which dominates this facies, also occurs at other sample sites (particularly in mud dominated sediment along transect B) but in less significant amounts. These pellets have formed from faecal pellets deposited by fish and soft-bodied organisms which have been cemented by carbonate before they could be broken down thus preserving the original shape and content of the pelletal material. Facies 4 is relatively poorly sorted due to the sediment comprising the coarser grained pellets (modal size of 0.22-0.24 mm) within much finer mud sized (<0.063 mm) siliciclastic material. The mud content of these samples exceeds 50% at mid shelf depths despite the surrounding sediment containing generally less than 30% mud sized sediment. Such high concentrations of mud (>50%) only occur elsewhere on the NKCM at greater than 400 m water depth in the southern half of the NKCM. This mud-dominated facies may be the result of several environmental conditions. The first is that lower wave energy conditions occur in this mid shelf area due to the very wide shelf (compared to the southern half of the NKCM), which causes wave energy dissipation over a larger area allowing for the deposition of mud. The surrounding sediment comprises between 20 and 30% mud suggesting these conditions are probably highly likely. A second possible explanation for this anomaly is the presence of a bathymetric depression, which has been infilled with mud-sized material, as the wave energy within this depression will be less than the surrounding sea floor. The available bathymetric data are not as detailed between

100 and 150 m water depth as they are in shallower waters, but it appears that the sea floor surface is relatively flat in this area. The third potential explanation is that the mud within these sample sites is relict and was deposited under different hydrodynamic conditions than those that are active on the NKCM at present.

Facies 5: Foraminiferal mud and sand

Facies 5 is one of the most widespread facies, extending along the entire NKCM at greater than 400 m water depth. This facies represents a deep-water deposit where wave energy, sedimentation and sediment transport are low or generally absent. Planktic foraminifera dominate over benthic foraminifera, which is indicative of the facies occurring at upper to mid slope depths. The predominance of planktic foraminifera occurs as a result of the environmental constraints on benthic foraminifera that prevent large quantities of these organisms accumulating at these depths. The mud content is the only difference between the two subfacies and is most probably the result of different sediment inputs to both the northern and southern halves of the NKCM.

Facies 5a comprises five samples which are all dominated by planktic foraminifera, with four of the five samples containing >80% mud. These samples occur in the southern half of the NKCM on the relatively steep slope (Fig. 2-7) where larger quantities of mud are supplied to the continental margin (compared to the northern half) through the harbours (Hokianga, Whangape, Herekino) and streams which discharge directly onto the shelf. The mud on the upper and mid slope is probably sourced from Facies 1 through transport of the reworked mud from shallower depths which is then actively deposited offshore at greater than 400 m water depth.

Facies 5b contains significantly less mud-sized material (generally <30%) than Facies 5a, probably as a result of the very wide shelf and absence of sources of mud in the northern half of the NKCM. The wide shelf may help prevent mud transport to the outer shelf and upper slope resulting in the more mud-dominated band, which occurs in Facies 4. The four shallower samples in Facies 5b (P418, P429, P432, P433) differ in that benthic foraminifera dominate over planktic

foraminifera. This is indicative of the much shallower mid to outer shelf depths (150-200 m water depth), a more suitable environment for increased numbers of benthic foraminifera.

8.5 SEDIMENTATION MODELS

The distribution of sediment types on the NKCM is extremely complex with a wide range of different components that dominate the sediment composition in different areas. The NKCM sediments vary significantly in texture as well as sediment composition and generalised textural trends applicable to the entire margin are difficult to assign. As a result, the production of a single integrated continental margin sedimentation model (textural and/or compositional) for the NKCM appears unfeasible. Sedimentation models have been published for wave-dominated shelves elsewhere and this section discusses these models in relation to the patterns observed on the NKCM.

8.5.1 Comparison to textbook sedimentation model

A large number of sedimentation models exist in the literature for the wave/weather-dominated continental shelf environment, and most of these exhibit a general trend of decreasing grain size offshore in response to decreasing wave energy with increasing water depth. A modern sand prism occurs in the nearshore zone at generally less than 10 m water depth with a modern mud blanket or area of mixed sand and mud between 10 and 50 m water depth. A relict sand blanket deposited during previous sea level lows may occur on the outer shelf, otherwise mud dominates at greater than 50 m water depth. The sedimentation model portrayed in Allen (1977) is of this sort and shows cross-bedded inshore sands at less than 2.5-10 m water depth with interbedded sand, silt and mud (clay) between 10 and 20-50 m water depth (Fig. 8-5). At greater than 20-50 m water depth the sediment is dominated by burrowed mud. This trend of fining offshore from the beach environment does not occur in NKCM sediments (Fig. 4-5, 4-6 and 4-7).

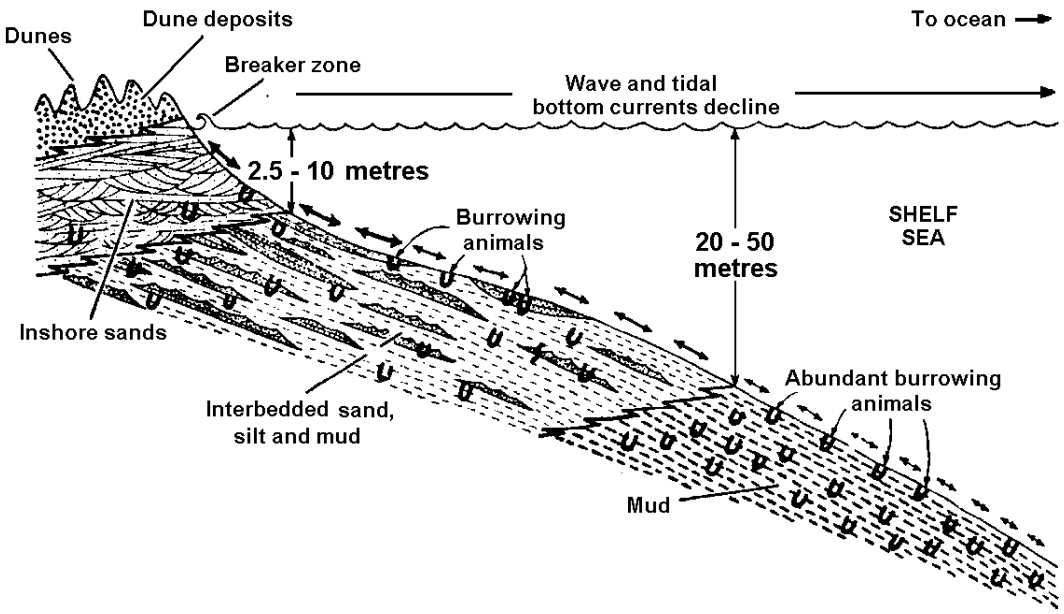

Figure 8-5. Sedimentation model for a wave-dominated shelf (Allen, 1977).

Figure 8-6 shows the modal grain size of the sand fraction (determined from thin section) from the beach (at 0 m water depth) across the shelf and upper slope along transects B and F. The grain size of the sediment varies significantly with depth and may become finer in certain parts of the shelf (e.g. c. 50-150 m along transect B) before coarsening again (e.g. c. 200 and 450 m water depth along transect B).

Several factors cause this deviation from the textbook model of shelf sedimentation. The presence of skeletal material (particularly bivalve and gastropod fragments) coarsens the sediment in the shallower shelf (c. <100 m water depth), while the presence of abundant foraminiferal tests causes the coarsening trend along transect F at greater than 400 m water depth. Other sediment components also increase the grain size, including the mixed carbonate-siliciclastic pellets between 100 and 150 m water depth along transect F and the glauconite grains between 150 and 400 m water depth along transect D and E (not shown here). Mud is not a significant component in NKCM sediments (>50%) until 400 m water depth in the southern half and between 100 and 150 m water depth in the northern half. This is considerably deeper than the 20-50 m water depth suggested by Allen's (1977) model to be the start of mud dominance on the

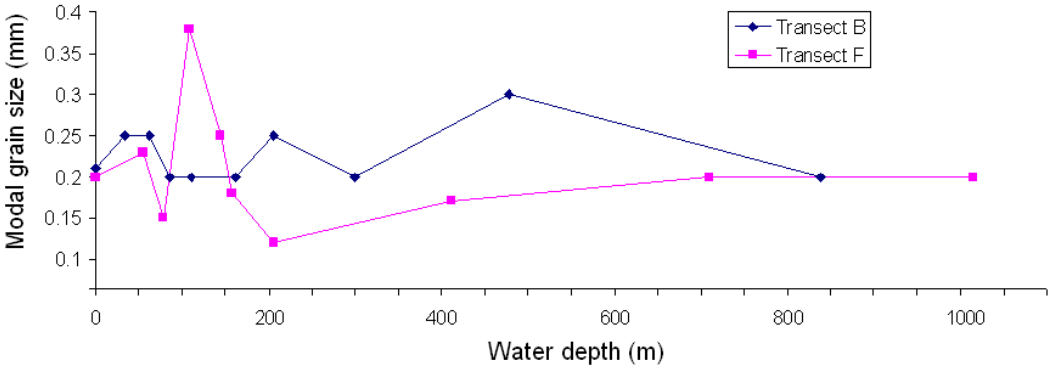

Figure 8-6. Modal grain size of the sand fraction across transects B and F showing the absence of fining offshore.

shelf. Relict sediment deposited during previous sea level lows also causes coarser sediment to occur in deeper water than expected on the NKCM and therefore the mixing of modern and relict sediment produces an offshore textural trend which differs significantly from that of the textbook model.

8.5.2 Comparison to textural sedimentation model for Manawatu coast, western North Island

The standard model of marine sedimentation for a wave-dominated continental shelf such as the NKCM suggests that sediment fines offshore as a result of decreasing wave-induced shear stress on the sea floor with increasing water depth (Dunbar and Barrett, 2005). Dunbar and Barrett (2005) developed a basic sedimentation model based on percent mud measurements from off the Manawatu coastline in southwestern North Island out to a water depth of c. 70 m (Fig. 8-7). This model has three main zones: (1) a high energy, shallow water zone where shear stress on the sea floor regularly exceeds the erosion threshold for mud; (2) a moderate energy zone where the shear stress periodically exceeds the mud erosion threshold; and (3) a low energy, deep water zone where the shear stress is below the mud erosion threshold and mud deposition occurs (Dunbar and Barrett, 2005). The resulting sediments are: (1) well sorted fine to very fine sand with 3-10% mud between 5 and 20 m water depth; (2) less well sorted interbedded mud and very fine sand with frequent shell fragments and 50-70% mud between c. 25 and 40 m water depth; and (3) poorly sorted very fine sandy mud with 60-85% mud at greater than c. 40 m water depth (Fig. 8-7). Further offshore the mud dominated

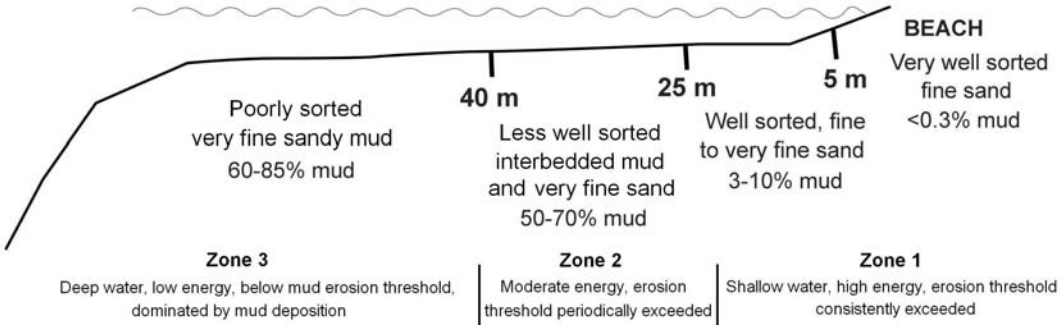

Figure 8-7. Sedimentation model for Manawatu coast (developed here from data in Dunbar and Barrett, 2005). Not drawn to scale.

area of zone 3 grades into gravelly sands and carbonates of relict and palimpsest nature (Dunbar and Barrett, 2005). The Manawatu coastline is exposed to westerly winds and swell waves similar to the NKCM but is generally a lower energy environment due to the sheltering effect of northwestern South Island.

The moderate to high energy coastline of Monterey Bay, California, was similarly considered by Dunbar and Barrett (2005) to determine if the same trends in grain size occurred with depth. In this higher energy environment well sorted fine sand occurs in the nearshore area and moderately sorted very fine sandy mud occurs between 25 and 50 m water depth. The 50% mud transition generally occurs at between 40 and 50 m water depth with the mud percentage greater than 80% at 70-80 m water depth.

In the southern half of the NKCM this model does not appear to hold with the >50% mud transition not occurring until 350-400 m water depth (cf. 25-50 m) and less than 20% mud present at depths shallower than this. Less well sorted sediment (moderately to poorly sorted) does not occur until c. 100 m water depth as the very well sorted and well sorted band of sediment (predominantly 90-100% sand) extends well beyond the nearshore area. Potential explanations suggested by Dunbar and Barrett (2005) for the absence of significant fining of sediment offshore include very low sediment supply, sediment bypassing the shelf, and relict or palimpsest sediment deposited during periods of lower sea level.

When compared to the Manawatu coastline, the southern half of the NKCM is a higher energy environment exposed to greater swell and storm wave activity that is likely to exceed the mud erosion threshold more regularly and to greater depths. The sources of river-derived sediment are also much lower in mud along the NKCM compared to the Manawatu coastline, which is well known for the extensive tracts of Tertiary mudstone rocks onshore (Hume and Nelson, 1986). The other important component of the coastal system affecting sediment deposition and distribution is longshore drift within the nearshore region. The mean longshore drift moves northward (Hume et al., 2003) from Cape Egmont and provides a greater sediment input to the NKCM than river-derived sediment thus resulting in a wider fine sand band and greatly reduced mud content.

In the northern half of the NKCM the mud percentage varies more significantly with the >50% mud transition occurring at 100-150 m water depth (still deeper than 40 m stated in model). However, the mud content does not continue to increase to >80% beyond this depth and instead decreases to between 0.5 and 20% down to c. 1000 m water depth. No major rivers discharge onto the coast between Tauroa Point and Cape Reinga implying very little sediment input onto the shelf. This is supported by a high concentration of skeletal material and glauconite grains, which require lower sedimentation rates to become abundant. Despite this low sediment input c. 55% mud occurs at mid-shelfal depths, possibly as a result of the wider shelf producing lower energy conditions (cf. southern half).

8.5.3 Comparison to cool water, temperate carbonate textural sedimentation model for wave-dominated shelf

A basic sedimentation model has been created for the cool water, temperate carbonate deposits on wave-dominated shelves based on the grain size of the skeletal material and the processes acting across the shelf and slope (Fig. 8-8) (James, 1997). This sedimentation model is divided into inner, middle, and outer shelf and slope sections. The inner shelf comprises gravel-dominated sediments and hard substrates, which are the result of constant wave agitation in this relatively shallow area reworking and removing sand and mud sized particles. The inner and middle shelves are areas of active sediment transport with the middle

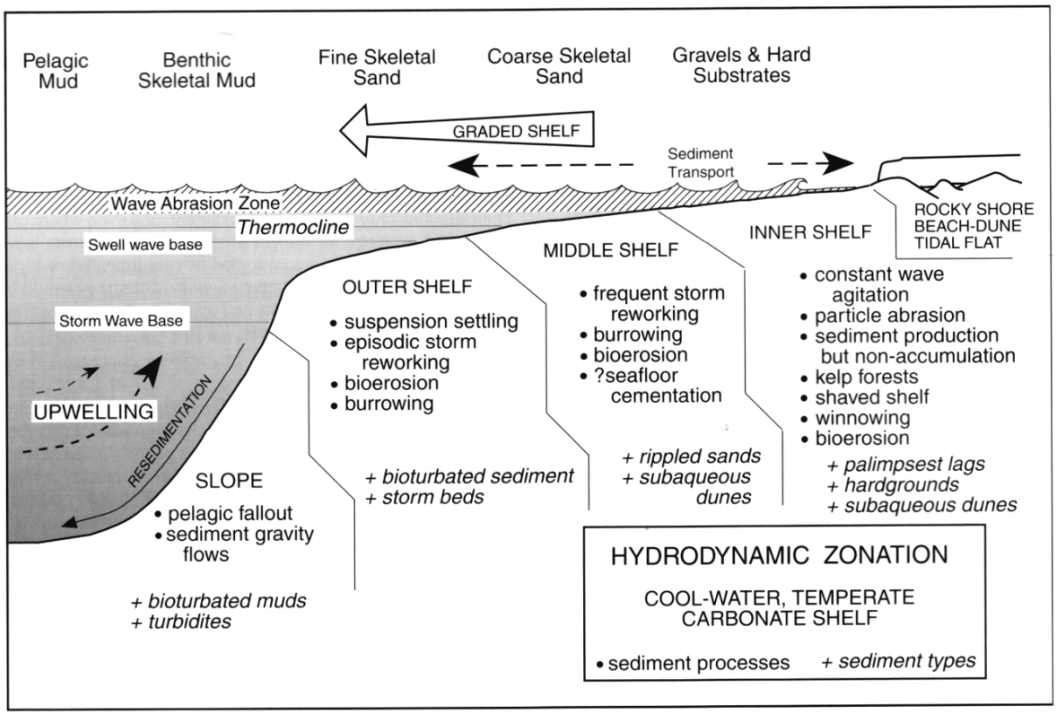

Figure 8-8. Textural sedimentation model for a carbonate wave-dominated shelf (From James, 1997). Base of the wave abrasion zone is between 30 and 70 m water depth. The swell wave base can be up to 120 m deep and storm wave base up to 250 m water depth.

shelf consisting of coarse skeletal sands, which are shaped by frequent storm reworking. The outer shelf sediments comprise fine skeletal sands, which are exposed to episodic storm reworking and bioturbation. The slope sediments consist of benthic skeletal muds formed from pelagic fallout and mass sediment flows such as turbidity currents. These muds are usually highly bioturbated.

Some aspects of this textural sedimentation model apply to the northern half of the NKCM and particularly the northernmost transect (G). Gravel sized skeletal grains (>50% gravel) dominate the inner shelf along transect G (<70 m water depth) with rocky outcrops and bryozoan encrusted cobbles common at less than 50 m water depth. Gravelly skeletal dominated sand occurs between 100 and 200 m water depth along transect G and this grades in deeper water into finer grained skeletal material. Skeletal dominated (>50%) slightly gravelly muddy sand and mud occurs at slope depths (>400 m) in the northern and southern halves of the NKCM, respectively. However, gravel size skeletal material also dominates at greater than 300 m water depth along transect D and at 100 m depth on transect E. The three sample sites at greater than 300 m water depth are dominated by coarse

skeletal material however occur outside the expected inner shelf depth range. The skeletal material in the two deep water samples along transect G (P434, P435) is most likely transported from skeletal rich areas on the Three Kings platform while the sample on transect E is probably an area of active bryozoan production. Well-developed skeletal mud has formed at slope depths in the southern half of the NKCM and is dominated by planktic foraminifera (Facies 5a).

8.5.4 Comparison to textural sedimentation model for west coast shelf and upper slope, South Island

The sediment off the west coast of the South Island is dominated by sand and mud sized material similar to the NKCM sediments. The shelf consists of an inshore sand dominated band which grades into sandy mud and mud at mid shelf depths and sandy mud or muddy sand on the outer shelf (Fig. 8-9) (Probert and Swanson, 1985). The inshore band comprises sand dominated sediment with minor mud (<10%) sized material and covers the inner shelf out to a depth of 30-40 m. Between 50 and 75 m water depth the sediment grades from muddy sand with 10-50% mud to sandy mud with 50-90% mud (Probert and Swanson, 1985). The mud content increases to greater than 90% from 90 to 140 m water depth (Fig. 8-9). Gravel occurs in very small amounts on the outer shelf and the carbonate content increases with water depth from c. 15% at 200 m to 70% at 650-700 m water depth (Probert and Swanson, 1985).

As discussed in Section 8.5.2, the mud content for NKCM sediments varies considerably and cannot easily be constrained by depth range. At less than 70 m water depth in both the northern and southern halves of the NKCM the mud content is considerably lower than on the west coast shelf with less than 0.5% mud present (cf. 10-90%). The mud content increases to between 0.5 and 5% at 70-100 m water depth in the southern half of the NKCM and to 20-50% mud at the same depth in the northern half (cf. 50-90%). At 100-400 m water depth, the mud content increases to 5-20% in the southern half of the NKCM before increasing significantly to 50-90% at greater than 400 m water depth. This increase to similar mud contents as the west coast South Island shelf sediments occurs at over 300 m deeper. In the northern half of the NKCM mud increases to

53-57% at 100-150 m water depth before decreasing to 20-50% from 150-200 m and less than 20% at greater than 200 m water depth. The NKCM is exposed to similar oceanographic conditions as the shelf and slope of the west coast of the South Island with dominant southerly and southwesterly swell waves producing a very high-energy environment. Despite this, significant differences in the onshore-offshore trend of mud occur between these two regions. The west coast receives significantly higher river derived suspended sediment yields (120-130 million tonnes per year cf. 13-14 million tonnes/yr) much of which is sourced from the erosion of schist in the Southern Alps. The high mud supply, along with possibly less common bypassing of the shelf, may have resulted in the considerably different textural trend here despite similar oceanographic conditions to the NKCM.

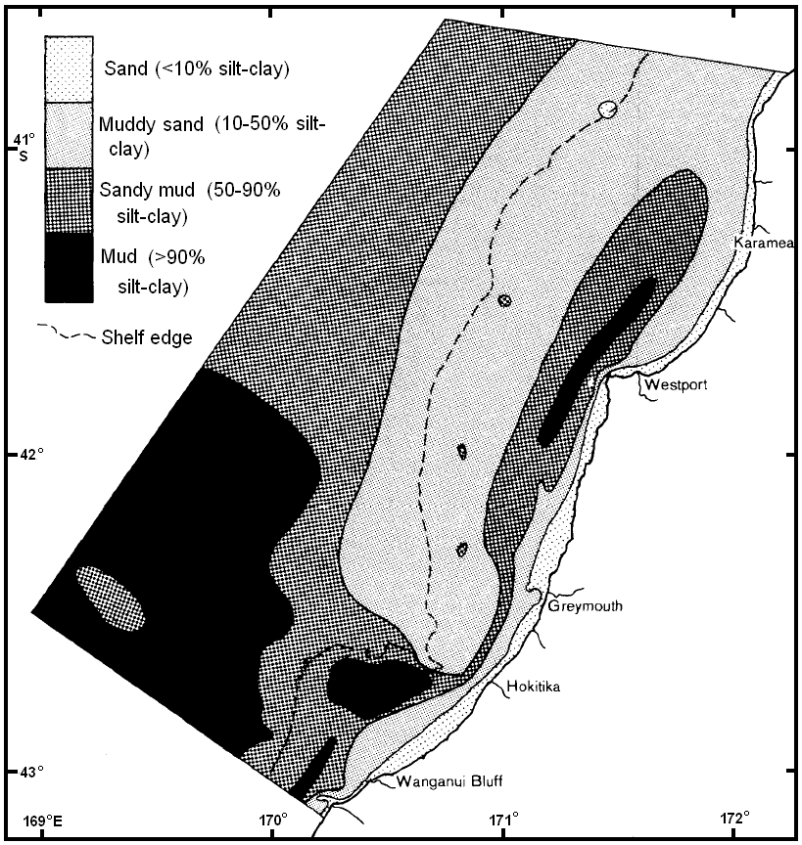

Figure 8-9. Distribution of sediment across the west coast South Island shelf and slope (Probert and Swanson, 1985).

8.5.5 Textural trends on the NKCM

A similar diagram to that produced by Probert and Swanson (1985) (Fig. 8-9) has been created for the NKCM (Fig. 8-10). As with the west coast South Island shelf and slope, the trend in mud content of NKCM sediments shows considerable variation across the study area. In the northern half the mud content increases to between 10 and 50% on the mid shelf before decreasing out to the shelf edge and upper slope (0-10%). In the southern half of the NKCM mud increases significantly from 0-10% to 50-90% at greater than 400 m water depth. While this latter textural trend is similar to that identified by Probert and Swanson (1985)

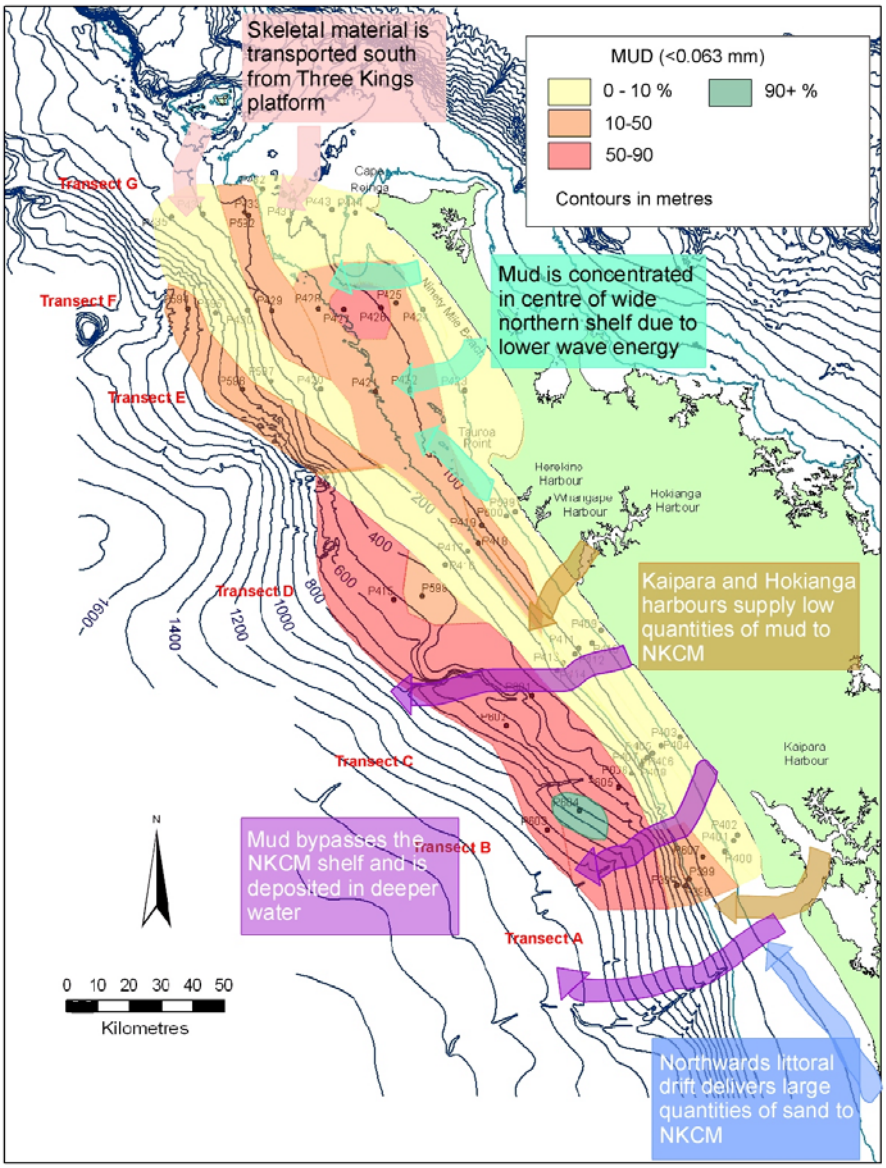

Figure 8-10. Distribution of mud across the NKCM and the processes acting to produce this distribution.

and the models shown in Sections 8.5.1 and 8.5.2, the water depths at which the mud percentage changes occur are significantly deeper. This is likely a consequence of the low mud input to the shelf from the adjacent hinterland, which is practically non-existent except from the Hokianga and especially Kaipara harbours (Fig. 8-10). The Wairoa River supplies c. 490 000 tonnes of suspended sediment to the Kaipara Harbour each year (Griffiths and Glasby, 1985), but most of this sediment becomes trapped within the harbour resulting in a low mud supply to the NKCM. In contrast, northwards littoral drift transports large volumes of primarily sand sized sediment along the coastal region which effectively drowns the low volume shelf mud supply so that (relict and) modern sand facies dominate the NKCM shelf (Fig. 8-10).

In addition to an inherently low mud supply, the absence of large quantities of mud at less than 100-200 m water depth is probably also a result of mud bypassing the shelf, particularly during times of lower sea level, coupled with the high energy environment which characterises the west coast of New Zealand (Fig. 8-10). The large swell and storm waves that occur relatively frequently on the NKCM rework any mud deposited on the shelf and transport it offshore where it is deposited at greater than 400 m water depth in the southern half of the NKCM (Fig. 8-10). In the northern half, a moderate amount of mud (10-50%) has been deposited at mid shelf depths, as swell and storm wave energy is dissipated across the wide shelf allowing mud deposition (Fig. 8-10).

Chapter 9

CORE STRATIGRAPHY AND LATE QUATERNARY SHELF HISTORY

9.1 INTRODUCTION

Short piston cores were obtained at three sample sites on the north Kaipara continental margin (NKCM). Two sample sites occur in the southern half of the NKCM (P600, P601) and one in the northern half (P592) (Fig. 3-1). The sediment recovered from these cores varies considerably and is described in Section 9.2. Some core data is summarised in Table 9-1. In Section 9.3 these cores and reconstructed sea level maps at 20 000, 16 000, 11 500 and 8000 years ago are used to develop a basic Late Quaternary shelf history for the NKCM sediments.

9.2 CORE STRATIGRAPHY

Description of cores

The three cores comprise a mix of grain sizes ranging from fine gravel to mud. P601: The shortest core, P601, is only 0.395 m long and was collected from 405 m water depth. It consists of a 21 cm thick lower unit of yellow to green brown gravelly sand, a 11.5 cm thick middle unit of white to pale green brown sand and an upper 7 cm thick dark green brown to yellow brown sand (Fig. 9-1 and 9-2). The lower unit contains c. 40% skeletal material which is dominated by foraminiferal tests, although other unidentified skeletal fragments are also present. The shells in this skeletal material are up to 1 cm in size with an average of 0.71-1.0 mm (coarse sand). The non-skeletal material in the basal unit is well sorted with an average grain size of 0.62-0.125 mm (very fine sand), although ranging up to 0.71-1.0 mm in size. The overlying middle unit comprises 50% skeletal material, which is also dominated by fragmented unidentified skeletal grains and foraminiferal tests (Fig. 9-1). The skeletal material has an average grain size 0.25-

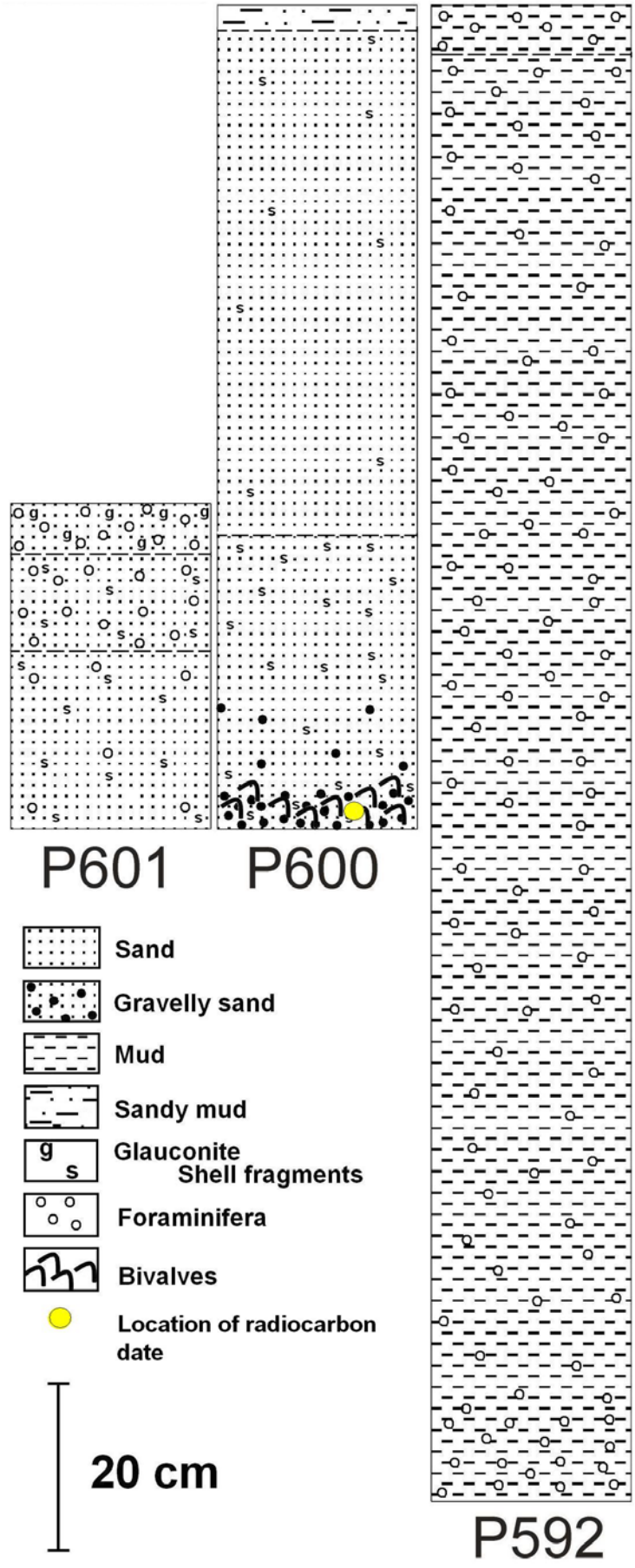

Figure 9-1. Description of three cores (P592, P600, P601) collected from the NKCM.

Table 9-1. Water depth, location and thickness of the three piston cores obtained from the NKCM. The transect each core was sampled from and the radiocarbon date obtained from P600 are also noted.

Core No.	Water depth (m)	Location	Thickness (m)	Transect	C_{14} date (yrs ago)
P592	204	34 29.5, 172 13.6	1.82	G	-
P600	68	35 20.8, 173 07.2	1.02	D	11 500
P601	405	35 51.5, 173 12.7	0.395	C	-

0.35 mm (medium sand) but may be up to 1.41-2.0 mm in size. The siliciclastic fraction (50%) in this unit is well sorted with an average grain size of 0.088-0.125 mm (very fine sand). The boundary between the lower and middle unit appears distinctive based on the internal consistency of the sediment types. The upper unit is a glauconite rich sediment dominated by the skeletal fraction (60%), which comprises foraminiferal tests (Fig. 9-1). This fraction has an average grain size of 0.35-0.50 mm (medium sand) but may be up to 1.41-2.0 mm in size. The non-skeletal fraction is well sorted with an average grain size of 0.062-0.088 mm (very fine sand) and a maximum grain size of 0.125-0.177 mm. The boundary between the middle and upper unit is also distinct and seemingly slightly irregular.

P600: The other core from the southern half of the NKCM, P600, is 1.02 m long and collected from 68 m water depth. It also comprises three different units. The lower unit (35 cm thick) consists of a graded yellow-brown gravelly sand to sandy gravel with abundant skeletal material especially near its base (Fig. 9-1 and 9-2). The amount and size of this skeletal material upwards from c. 70% at the bottom to c. 30% at the top. Bivalve fragments dominate the skeletal material and are on average 1.5 by 1 cm in size at the base and 0.5 by 0.5 cm in the centre of this unit. The main bivalve types include *Scalpomactra scalpellum, Nucula nitidula, Pratulum pulchellum, Saccella maxwelli* and *Purpurocardia purpurata*. These bivalve species occur at shallow water depths out to c. 180 m water depth. The top of this basal unit has an average skeletal grain size of 0.35-0.5 mm (medium sand) with a maximum grain size of 1.41-2.0 mm. The siliciclastic component comprises quartzofeldspathic sand, which is well sorted with an average grain size of 0.177-0.25 mm (fine sand) throughout the unit. The sorting of the lower unit improves upwards, from very poorly sorted at the base to well sorted at the top. The middle unit of core P600 is 65 cm thick and consists of a yellow-brown

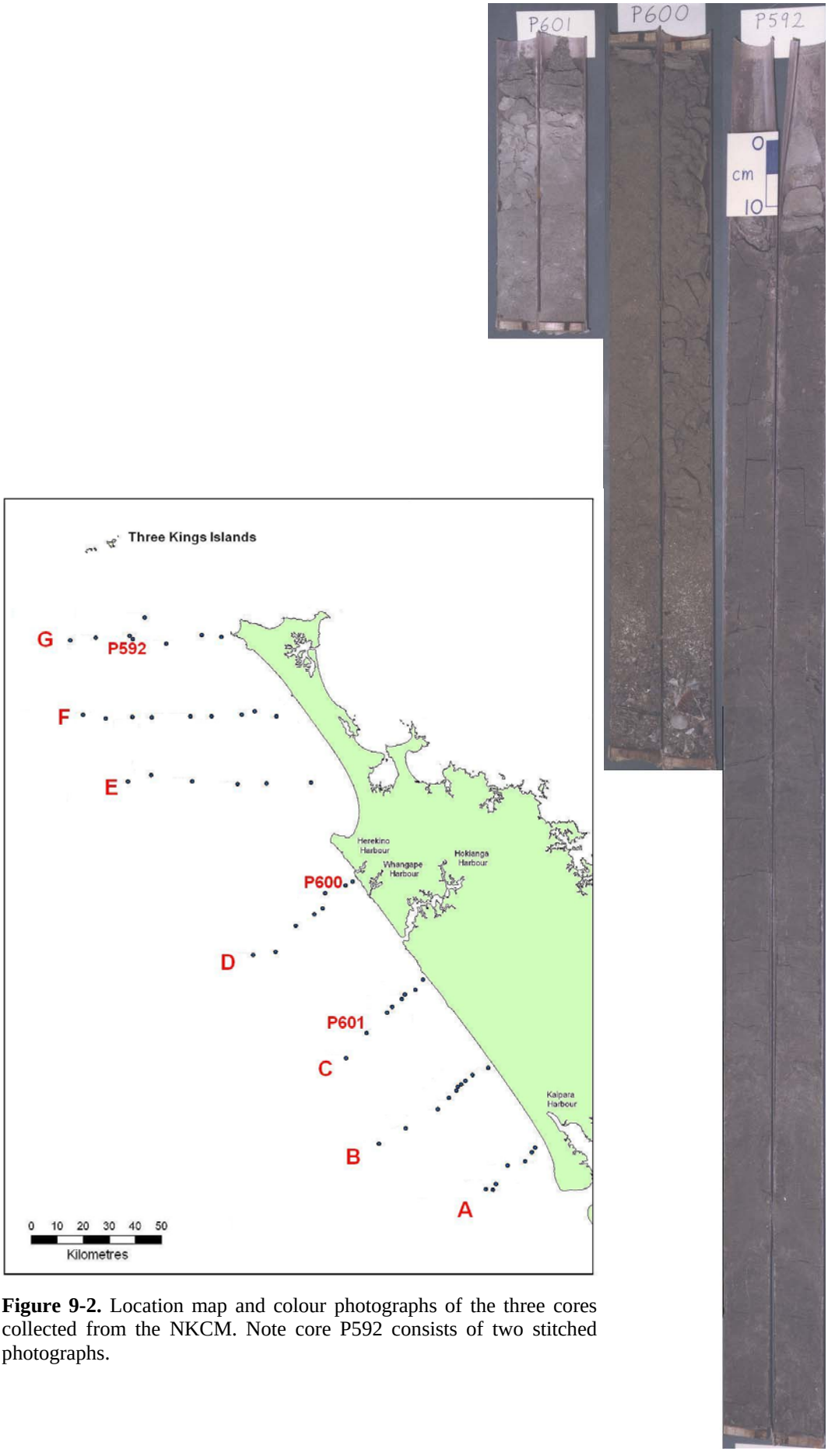

Figure 9-2. Location map and colour photographs of the three cores collected from the NKCM. Note core P592 consists of two stitched photographs.

siliciclastic rich sand (Fig. 9-1). The base of this middle unit has a skeletal content of 20%, which is dominated by unidentified skeletal fragments. The skeletal fraction has an average grain size of 0.35-0.50 mm (medium sand) with shells up to 1.41-2.0 mm in size. The dominant siliciclastic fraction is very well sorted with an average grain size of 0.177-0.25 mm (fine to medium sand) but may be up to 0.25-0.50 mm in size. The top of this middle unit has a much lower skeletal content (10%) with a finer average grain size of 0.177-0.25 mm (fine sand) and maximum grain size of 0.50-0.71 mm. The siliciclastic fraction at top of this middle unit is slightly finer with an average grain size of 0.088-0.125 mm (fine sand). The boundary between the lower and middle unit is indistinct. The upper unit of core P600 is very thin (2 cm) and comprises compacted yellow-brown sandy mud to muddy sand with an average grain size of 0.177-0.25 mm (fine sand).

A radiocarbon date (Wk-397) was obtained on shell material from the base of the lower unit in core P600 (Fig. 9-1 and 9-2). This gave a true age of 11 500 ± 120 years BP. The age can be used to determine a basic sedimentation rate for the inner to mid shelf of the NKCM. The basal skeletal rich (c. 70%) subunit is about 5 cm thick, which means approximately 97 cm of sand has been deposited since 11 500 years ago. This gives a sedimentation rate of 0.08 mm per year or 80 mm per 1000 years. The rate is only approximate as the period of time the dated shell fragments were exposed on the sea floor before burial is unknown. However, the shell fragments appear fresh suggesting they were not exposed for extremely long periods of time. This sedimentation rate is unlikely to apply to the whole of the NKCM as rates of sediment supply to the margin vary significantly both north to south and onshore to offshore.

P592: The core collected from the northern half of the NKCM, P592, is the longest at 1.82 m and was collected from 204 m water depth. It consists of a 175 cm thick dark green lower unit and an overlying 7 cm thick pale green-brown mud (Fig. 9-1 and 9-2). The lower unit comprises homogeneous very fine silt and clay sized sediment dominated by foraminiferal tests. The skeletal fraction forms c. 90% of the sediment at the base of this unit and decreases to c. 70% at the top (Fig. 9-1). The much thinner upper layer comprises very fine sediment with an

average grain size of 0.062-0.088 mm (very fine sand). The skeletal material is indistinguishable from the siliciclastic component but is also dominated by foraminifera. The boundary between the two units is distinct.

Comparison to surface sediments

P601: A surficial sample was not collected in the vicinity of core P601 (405 m water depth) and so P414 (216 m) and P602 (622 m) are used in this comparison. Sample P414 consists of moderately sorted fine sand sized sediment which is dominated by 30-40% glauconite. Mud comprises only c. 6% of the sediment with sand making up 93%. Skeletal material also occurs but in relatively low amounts (10%). P602 is much deeper and as such is dominated by poorly sorted mud sized sediment (86%). Skeletal material dominates comprising >75% of the sediment, 30-40% of this being benthic foraminifera and 40-50% planktic foraminifera. Core P601 appears to include a mix of these two surficial sediment samples with the upper glauconitic foraminifera rich unit (7 cm) comprising glauconite, which is abundant in P414 (but low in P602), and foraminifera, which is abundant in P602 (rare to absent in P414). The water depth of the core site (405 m) indicates that foraminiferal tests should be considerable components of the sediment. The sedimentation rate calculated for core P600 would suggest that this core accumulated over approximately 4 700 years and the glauconite rich unit over only the last 875 years. This would then imply that glauconite has only become significant at this sample site in the last 1000 years. As mentioned above, the calculated sedimentation rate in core P600 is unlikely to be the case over much of the NKCM, and particularly so for these deeper samples where the sediment input is considerably less. However, this core (P601) does show that glauconite has only comprised an important sediment component at this site for a relatively short period of geological time.

P600: A surficial sample was collected within 3 m water depth of the core P600. This sample (also labelled P600, 65 m) consists of very well sorted fine sand sized sediment (97% sand) which is dominated by quartz and feldspar (30-40% each). Rock fragments are also common (20-30%) with skeletal grains comprising less than 10% and dominated by bivalve fragments. This surficial sediment sample is

very similar to the middle unit of core P600 that is also a well sorted quartzofeldspathic sand. However the skeletal component in the surface sample is between 10 and 15% less. The upper unit in core P600 is dominated by mixed mud-sand sized sediment that contrasts with the surface sample which contains only 0.4% mud. This may simply reflect a degree of variability of the seabed sediment facies in different areas or perhaps that some of the mud content may have washed out during sample collection.

P592: The nearest surficial sample to core P592 is P433 (190 m water depth). This surface sample is dominated by moderately sorted fine sand sized sediment (72% sand) with only 25% mud present. Skeletal material comprises 40-50% of the sediment and is dominated by bivalve and gastropod hash in the coarse fraction (90%) and benthic foraminifera in the sand fraction (40-50%). The upper unit in core P592 comprises very fine sand sized sediment dominated by foraminiferal tests and is therefore slightly finer grained than P433. Core P592 is located 14 m deeper than P433, which may result in finer grained sediment dominating as energy decreases with water depth. The skeletal material in both the core and surficial samples is similar, although the presence of coarse bivalve and gastropod shells in P433 may indicate its shallower depth or the presence of relict skeletal material deposited during previous sea level lows.

9.3 LATE QUATERNARY SHELF HISTORY

Sea level has varied considerably over the last 20 000 years since the Last Glaciation. The distribution of sediment on NKCM and in cores can at least partly be attributed to this sea level change and the subsequent periods of sedimentation. Sea level rise since the Last Glaciation has occurred in a series of rapid transgressions (14-15 m per 1000 years) punctuated by at least six stillstands and reached present position c. 6500 years ago (Carter et al., 1986; Gibb, 1986). A series of sea level maps at 20 000, 16 000, 11 500 and 8 000 years ago have been created (using the regional sea level curve of Carter et al., 1986 in Fig. 9-3) to imply the position of the coastline and bathymetric features at each of these time intervals. However, much of the sediment and features of the present shelf are modern and would not have been present at greater than 6500 years ago. Changes

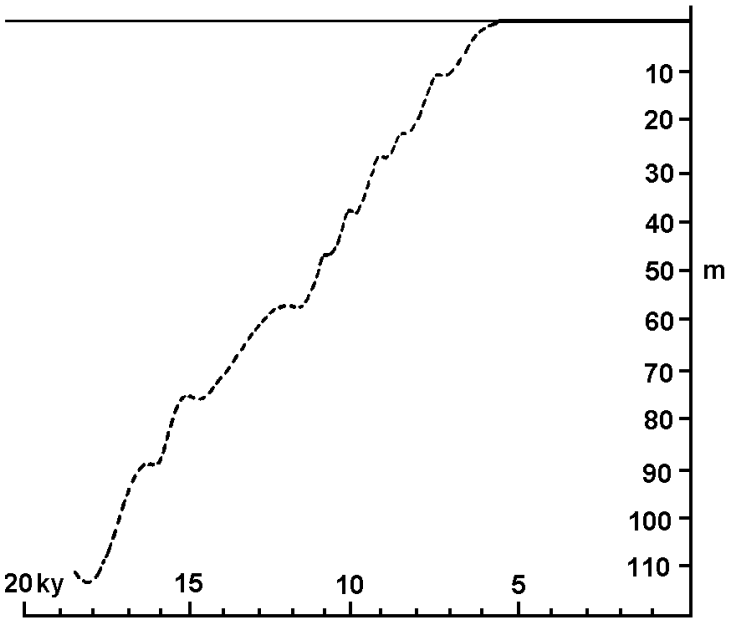

Figure 9-3. Regional sea level curve used to decide sea level position for each of the "time-slice" maps (adapted from Carter et al., 1986).

in sea level relating to tectonic uplift or subsidence were not considered in the creation of these maps. The absence of sufficient core data does not allow the development of an accurate shelf history.

9.3.1 20 000 years ago

At 20 000 years ago the relative sea level was c. 113-120 m below present sea level (Carter et al., 1986). Approximately half the present shelf area and 24 sample sites were subaerially exposed with another seven sites in the high-energy beach environment (Fig. 9-4). The climate during this time would have been cool and dry with high winds resulting in significant wind transport across the exposed shelf sands. Sharp changes in gradient at c. 120 m below present sea level are observed in the cross shore profiles along transects B, F and G (Fig 2-7), potentially inferring the position of this sea level low. A series of islands occurred along transect G near sample sites P431 and P432 (Fig. 9-4). These islands would have altered the movement of water and waves, most likely increasing the wave energy in the vicinity of these sample sites as the waves broke on and around the islands. In the southernmost NKCM (transects A and B) the waves would have been breaking more or less directly on the present day shelf edge resulting in the sand dominated sediment. The rivers which discharge into the four harbours in the NKCM (Kaipara, Hokianga, Whangape and Herekino) would have extended

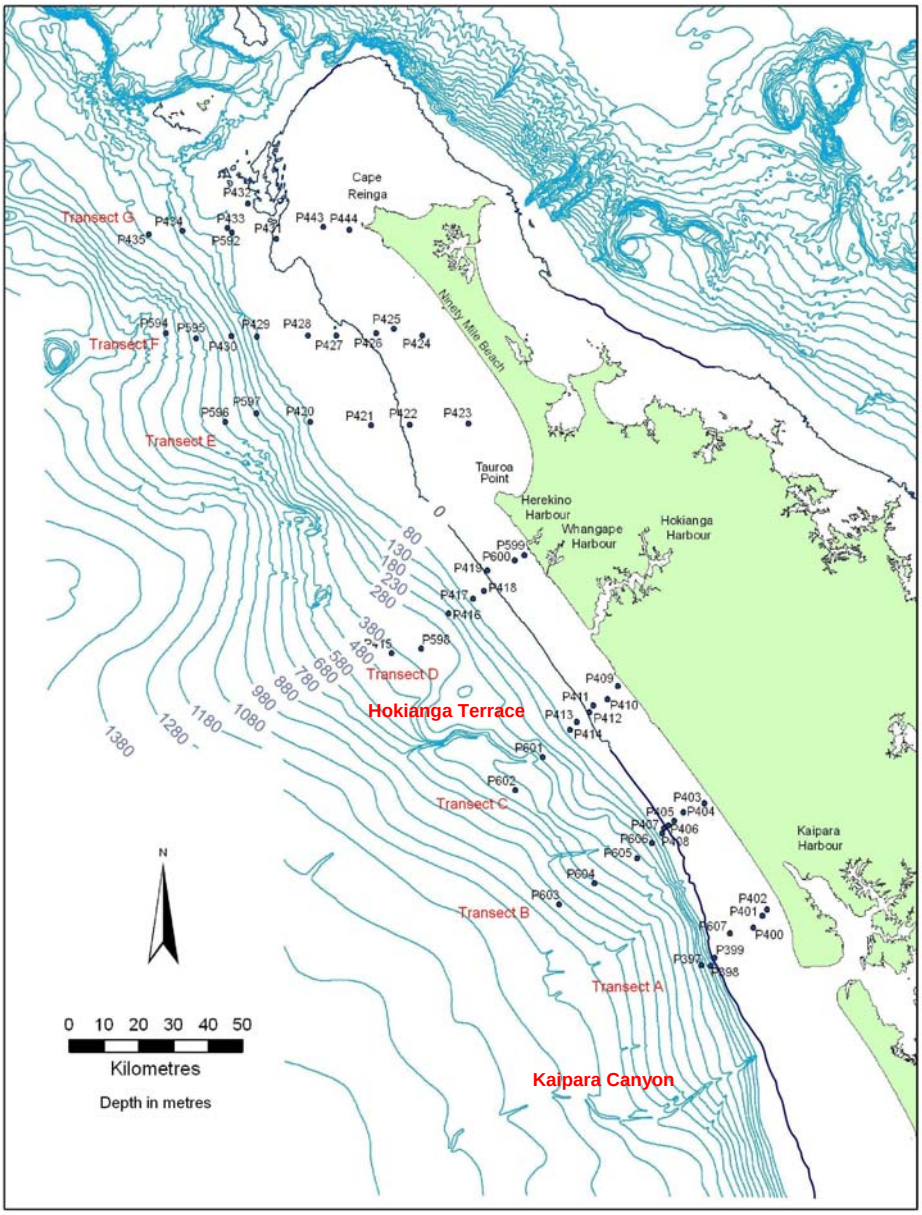

Figure 9-4. Bathymetry of the NKCM 20 000 years ago at the maximum sea level low (-c. 120 m).

across the shelf and may have formed the submarine canyons present south of Hokianga Terrace in the southern half of the NKCM (Fig. 2-6B). Kaipara Harbour (combined Wairoa, Otamatea, Arapaoa, Oruawharo, Kaipara rivers) probably discharged into the Kaipara Canyon and may have alternated between this canyon and the two smaller ones to the north, while the Hokianga Harbour rivers probably discharged across the shelf and along the southern side of the Hokianga Terrace (Fig. 2-6B). The presence of glauconite (and minor phosphate) in the centre of the NKCM suggests sediment must have bypassed the shelf in this manner during both the Last Glacial maximum and the subsequent sea level rise. Estuaries may

have also extended out onto the shelf resulting in mud deposition and the development of shell beds along the present day inner and mid shelf areas. All of the present-day outer shelf and upper slope area (<300 m water depth) would have been within 130 m water paleodepth and therefore exposed to wave action during large storm events. A large amount of sediment reworking would have occurred removing mud-sized sediment and depositing it in deeper water.

The glauconitic rich area in the centre of the NKCM was not exposed 20 000 years ago, although three of the sample sites (P417, P420, P421) were in less than 80 m water paleodepth (Fig. 9-4). This relatively shallow depth probably exposed the glauconite to reworking during storm events resulting in the very polished nature of the grains. The three shallower bryozoan rich sample sites (P422, P431, P443) were all exposed at this time (Fig. 9-4) suggesting the bryozoan material at these sites formed following sea level rise and submergence. The bryozoan rich samples P429 and P430 were in 80-280 m water paleodepth, while P434 and P435 occurred at 180-280 m water paleodepth. The mud dominated samples in the northern half of the NKCM between 100 and 150 m (present day) water depth (P426, P427) are on or above the shoreline (Fig. 9-4) suggesting the mud in this area must have been deposited following sea level rise as previously deposited mud sized sediment would have been quickly eroded in this environment. The mud dominated samples in the southern half of the NKCM (e.g. P415, P598) were not exposed (Fig. 9-4) and were always at greater than 300 m water depth.

Two of the three cores sites (P592, P601) remained beneath seawater 2 0000 years ago with only core P600 exposed above the shoreline (Fig. 9-4). P592 comprises mud-sized sediment dominated by foraminiferal tests, despite its relatively shallow paleodepth of only c. 80 m (Fig. 9-1 and 9-4). There are several possible reasons for this including: (1) the entire 1.8 m core was deposited in the last 20 000 years or (2) the sediment in this core is relict and had been deposited prior to the 20 000 year sea level low. All the sediment in this core is unlikely to have been deposited over the last 20 000 years as this requires a significant mud input to the shelf which does not exist in the northern half of the NKCM or in the Three Kings areas directly to the north.

Relative sea level rose c. 32 m between 20 000 and c. 17 000 years ago to 88 m below present sea level (Carter et al., 1986). A stillstand occurred at this time for approximately 500 years (Carter et al., 1986) and can possibly be seen in the cross-shore profiles of transects A, D and G. Along transect A this sea level would have occurred in the vicinity of P607 (Fig. 2-7). At this depth the shelf gradient steepens considerably down to the present day shelf edge. Along transect D and G a sharp change in gradient is also evident at 88 m below present sea level (Fig. 2-7).

9.3.2 16 000 years ago

16 000 years ago the sea level was 80 m below the present sea level with 14 sample sites exposed and two on the shoreline (Fig. 9-5). A much smaller area of the shelf was above sea level and the islands north of P431 and P432 are now submerged in 40 m of water (Fig. 9-5). These islands may be a significant source of sediment to the area due to their position in a shallow high-energy environment. Assuming they are rocky, they are the likely source of the comparatively high rock fragment content in P431 (10-20%). If on the other hand the islands are composed of shelf sediments they could be the supply of mud to core P592. With the 40 m rise in sea level, a series of small islands have formed around P443 while a large shelf bulge has formed between transects F and G (Fig. 9-5). The rivers formerly discharging across the shelf began to be submerged under the rising sea water and therefore exposed to a high-energy beach or nearshore environment resulting in significant reworking of any riverine deposits. Muddy sediment would have been resuspended and transported offshore and possibly deposited in the mud rich section of the southern half of the NKCM which is presently at >200 m water depth.

The glauconite rich area on the NKCM is now in greater than 70 m water paleodepth. This is deeper than the ‘modern’ annual storm wave base but still within a water depth that may be affected by a 25 year storm (Fig. 9-5). All of the bryozoan rich sample sites except P443 are now submerged (Fig. 9-5) with bryozoan establishment and growth at P422 and P431 (c. 20 m water paleodepth) likely to have begun from this time onwards. The mud dominated samples, P426

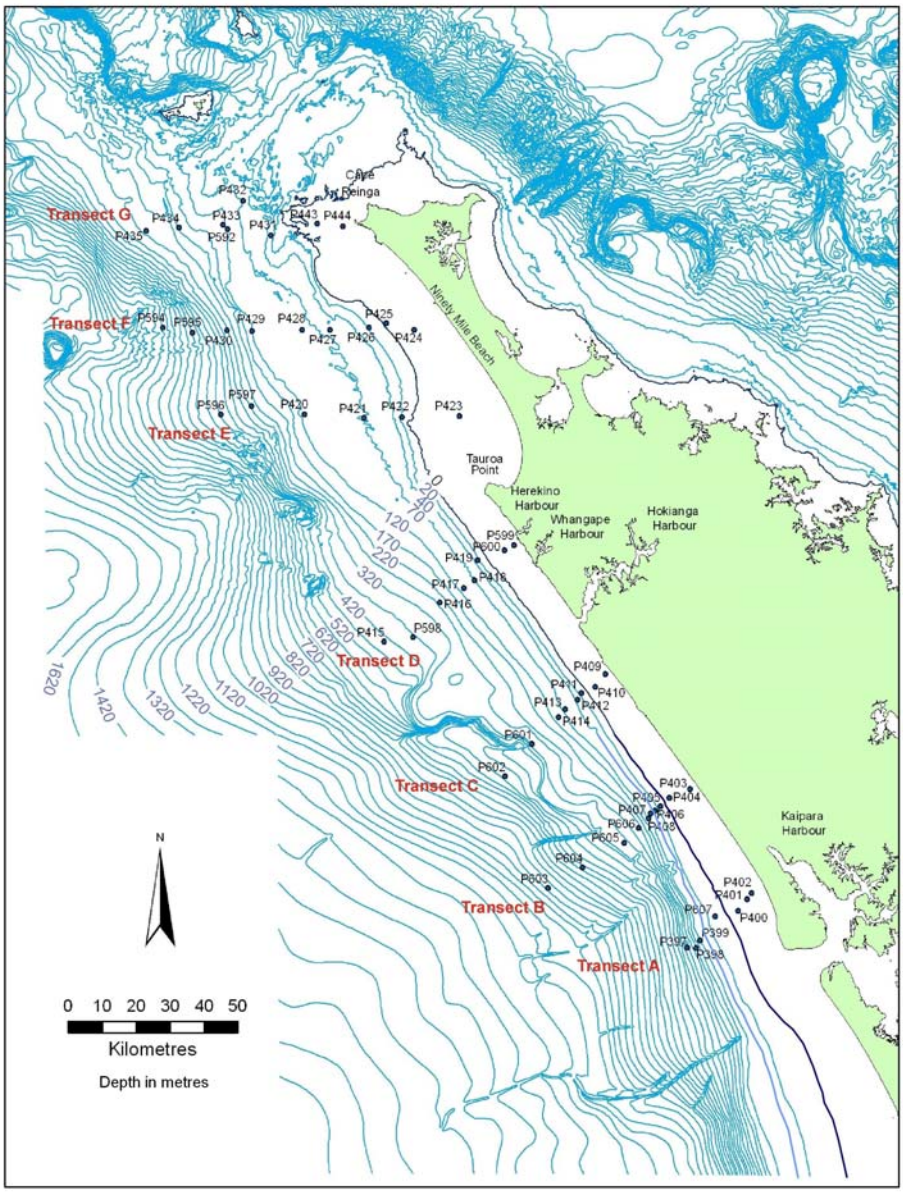

Figure 9-5. Bathymetry of the NKCM 16 000 years ago when sea level was c. 80 m below present sea level.

and P427, are now in 20-70 m water paleodepth (Fig. 9-5) which is still within the wave base of most annual storms so that mud deposition at these sites is still unlikely. The increase in sea level has allowed alongshore sediment transport to deposit quartz and feldspar rich sand on the present day mid shelf widening this inshore well-sorted quartzofeldspathic sand band. The absence of quartz and feldspar rich sediment beyond 200 m water depth (below present sea level) in the southern half of the NKCM is probably the result of the maximum sea level low not extending off the edge of the shelf and depositing this sediment at greater depths.

Relative sea level rose approximately 24 m between 16 000 and 12 000 years ago to 56 m below present sea level (Carter et al., 1986). A stillstand developed c. 12 000 years ago and lasted for up to 2 000 years (Carter et al., 1986). Features suggestive of this stillstand period are not evident in the bathymetric profiles across each transect on the NKCM.

9.3.3 11 500 years ago

11 500 years ago relative sea level was approximately 50 m below the present day sea level and only six metres above the stillstand period at c. 12 000 years ago. Only six NKCM sample sites remain above sea level with three located on the shoreline (Fig. 9-6). 14 samples occur within 50 m water paleodepth and the sediments at these sample sites would have been regularly reworked by storm events. It is likely that river derived sediment was flushed off the shelf at greater rates due to the higher energy environment in the present day mid shelf area. Any mud that was previously deposited in rivers and estuaries on the shelf would have been reworked and deposited offshore as sea level rose. The island near P443 in the northern reaches of the NKCM is now completely submerged although the shelf bulge south of this sample site is more developed and has extended further offshore (Fig. 9-6). This bulge would have affected the inshore wave conditions causing wave refraction and the concentration of wave energy on either side of the bulge. New islands have appeared along transect E and coincide with the location of the North Ahipara Bank (Fig. 2-6B and 9-6). These would have also altered the waves in the nearshore zone.

The glauconite rich area is now in greater than 100 m water depth and well below the expected sediment transport base during annual storms (c. 70 m water depth). It is still, however, within the 130 m water depth affected by 25 year storms. All of the bryozoan rich samples are now submerged, although P444 is still above sea level (Fig. 9-6). This is possibly why, along with a low sediment supply, this sample site comprises mostly rocks with very little sediment. The bivalve rich sample, P424, is now located in the beach zone (Fig. 9-6) suggesting the fresh colourful bivalve shells which characterise this sample site are younger than 11 500 years. This is because shell material is rare in modern beach sediments

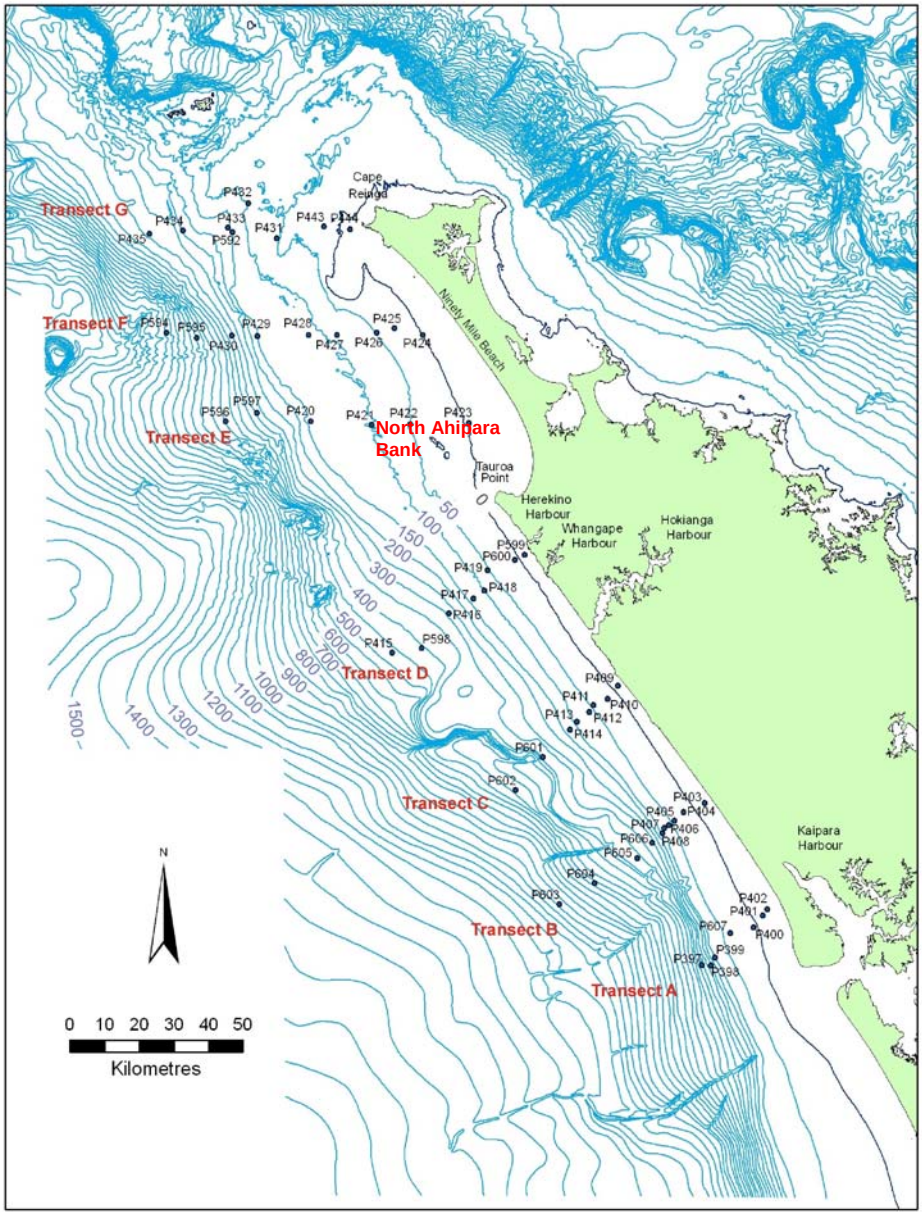

Figure 9-6. Bathymetry of the NKCM 11 500 years ago when sea level was c. 50 m below present sea level.

(Chapter 7) and it is unlikely that an estuarine environment developed in this area during periods of lower sea level due to a lack of rivers discharging from land. Core P600 is now located on the shoreline and would have been exposed to a high-energy environment. The shell material at the base of this core (probably deposited in a beach or estuarine environment), dating at about this time (11 500 ± 120 years BP), would have been extensively reworked. Relative sea level rose 10 m from 50 m below present level at 11 500 years ago to 40 m below present level at c. 11 000 years ago (Carter et al., 1986). This considerable increase in sea level would have allowed sediment transported from outside the NKCM to be deposited

over previously exposed samples (such as the shell material at the base of P600), building up thick shelf sand deposits.

At c. 11 000 years ago another stillstand developed at 40 m below present sea level (Carter et al., 1986) and is evident particularly along transect G between P443 and P444 where a large nick in the shelf surface results in a significant change in surface gradient (Fig. 2-7) and is indicative of shoreline erosion. The position of the shoreline at this stillstand is unlikely to be visible along most transects due to the large volumes of sediment which has been deposited with subsequent sea level rise. However, along transect G in the far north the sediment supply is very low and thus this change in gradient has not been buried by sediment. Another stillstand occurred at c. 9 000 years ago following 16 m of sea level rise to 24 m below present sea level (Carter et al., 1986). This period of stillstand is not evident along any of the transects due to significant sediment deposition on the inner shelf (Gibb, 1986).

9.3.4 8 000 years ago

8 000 years ago relative sea level had risen to 20 m below present sea level (Carter et al., 1986) and all the sample sites on the NKCM were submerged beneath seawater with the three innermost sample sites on transects B, C and D lying within the high energy beach environment (Fig. 9-7). The area of shelf below sea level has increased considerably and the bulge south of P443 and P444 is now a large island (Fig. 9-7). This island would have significantly affected the local wave processes, likely resulting in concentrated erosion in the vicinity of samples P443 and P444. These processes may have also affected the sample sites at less than 70 m water depth along transect F. Core P600 is now submerged in less than 50 m of water (Fig. 9-7) and was probably exposed to regular reworking due to storm events which resulted in deposition of the well sorted quartzofeldspathic sands forming the thick middle unit (Fig. 9-1).

The mud dominated samples, P426 and P427, are now in 70-110 m water paleodepth (Fig. 9-7) which is beyond the wave base of most annual storms but still within the erosive effects of a 25 year storm event. This suggests mud

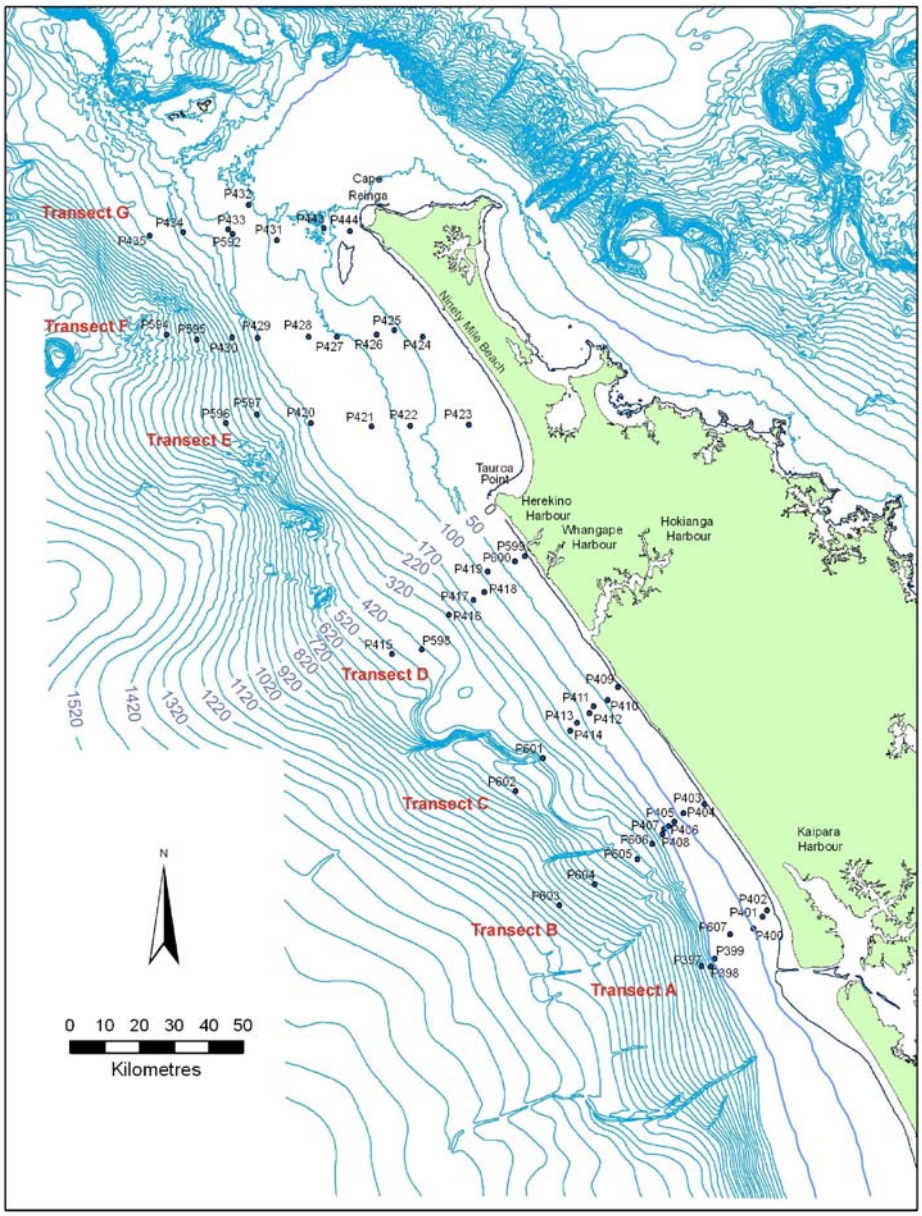

Figure 9-7. Bathymetry of the NKCM 8 000 years ago when sea level was c. 20 m below present sea level.

deposition may have begun at this location between 9 000 and 8 000 years ago. The mixed carbonate-siliciclastic pellets within these two samples are therefore more likely to have been formed once sea level reached water depths conducive to mud deposition. Deeper water would have also been important in reducing the break down of the pellets due to wave energy. The bulge located outside the mouth of the Kaipara Harbour comprises the tidal delta (Fig. 9-7) which is a modern feature that would not have been present 8 000 years ago as observed in Fig. 9-7.

A stillstand at 9 m below present sea level is suggested by Carter et al. (1986) to have developed between 7 500 and 7 300 years ago. Morphologic evidence for such a stillstand does not exist on the NKCM, perhaps because of burial beneath modern sand sedimentation on the inner self.

Chapter 10

POTENTIAL ECONOMIC RESOURCES

10.1 INTRODUCTION

Continental margins are potentially good sources of industrial and ore minerals such as quartz, feldspar, manganese, iron and phosphate with their relatively shallow depths often making extraction economic. As land based mineral resources are utilised, minerals on the sea floor will become more valuable and it is important that these resources are mapped and defined to allow for potential future exploitation. Quartzofeldspathic sand, glauconite and phosphate are the three components in the north Kaipara continental margin (NKCM) sediments that form potential economic mineral resources. The potential uses of these components are discussed briefly in this chapter as well as estimates of their volume and distribution.

10.2 POTENTIAL SAND RESOURCE

Sand has a wide range of uses in industry, including for abrasives, sand blasting, ceramics, ready mix concrete, foundry moulds, fibreglass manufacture, plastering and bedding sand (Associates, 1982). Feldspar-rich sand is used for glazes and within enamels in the ceramics industry and should ideally contain a calcium, sodium or potassium feldspar content of at least 50%, with both heavy minerals and quartz grains being undesirable components. The sand used for concrete must be clean and lack clay coatings, salt, sulphides and organic contaminants. Foundry sand must comprise grains evenly coated with non-reactive clay and be able to withstand high heat (Associates, 1982). Coated silica sands are preferred, but feldspar and iron sands are often used due to their significantly lower cost. In fibreglass manufacture, rounded to subrounded quartz sand of 0.15-0.25 mm (fine sand) grain size is favoured and can include up to 50% feldspar and should have at least 15% alumina. Iron, titanium and other heavy minerals are contaminants and the iron content must be less than 1.7%. Bedding sand for the building

industry requires well sorted sand with a median grain size of 0.15-0.20 mm (fine sand) (Associates, 1982).

Extraction of sand has occurred from inside Kaipara Harbour, primarily for use in ready mix concrete manufacture but also for builders mix, plastering sand and concrete block manufacture (Associates, 1982; Christie and Barker, 2007). The west coast of Northland is less sensitive to the extraction of sand mineral resources compared to the east coast as a result of higher rates of unhindered longshore transport of sediment to the north on the west coast. Ninety Mile Beach and the North Kaipara Barrier are considered depositional environments that are not especially sensitive to mineral extraction. This contrasts with the Hokianga coastline, which is graded stable to depositional and the level of sand extraction is limited by the volume and rate of the net longshore transport of sand to the coastline (Associates, 1982; Christie and Barker, 2007).

The NKCM sediments at less than 100 m water depth comprise the most suitable sand for extraction purposes, and particularly so in the southern half of the NKCM where there are high volumes of quartzofeldspathic fine sands (Fig. 4-3). The area at less than 100 m water depth in the southern half of the NKCM is c. 277 km^2 and this equates to c. 269 million m^3 (c. 323 million tonnes using quartz density of 1201 kg per m^3) of quartz and feldspar rich sediment to a depth of approximately 0.97 m (depth of sand in core P600). This estimate of the sand resource on the NKCM is most probably an overestimate as 97 cm of sand is unlikely to have been deposited across the entire margin at less than 100 m water depth. However, it may be likely that the higher amount of sediment deposited in the southern transects (particularly A and B) compensates for the lower amount of sediment deposited in the northern half of the NKCM. The mineral price of sand for industry is currently about $13 per tonne (Christie and Barker, 2007) suggesting a potential resource worth of $4199 million. Bedding sand and fibreglass manufacture are likely the most ideal uses of NKCM sands, the quartz and feldspar rich sand being of suitable grain size (0.15-0.25 mm) and sorting (very well to well sorted). Use of the inshore band of sand (<100 m water depth) for concrete manufacture could also be advantageous as these sediments are very low in clay minerals (0-5%), although it would be necessary to avoid sample sites rich

in heavy minerals (P599 and P409). Sand extraction for these purposes along transects A and B could be particularly economic, with higher rates of deposition occurring along this coastline, which is less sensitive to sand extraction compared to other areas in the NKCM (Hume et al., 2003). The volume of quartz and feldspar rich sediment to a water depth of 100 m (and 0.97 m sediment depth) between transects A and B is c. 75 million m^3.

The Pliocene to Holocene age beach and dune sands along western Northland are also potential sand resources. Silica and feldspar may be extracted from beach and dune sand across the west coast and particularly large dune systems such as North Kaipara Barrier. The composition and extent of these west coast deposits are unknown and, as such, detailed investigation of them is required (Christie and Barker, 2007). The beach and dune sand samples discussed in Chapter 7 suggest the beach and seaward face of the dunes are co-dominated by quartz and feldspar with relatively low heavy mineral content (<5%). These samples are probably most suitable for concrete and bedding sand for building industry and fibreglass manufacture due to their very good sorting and grain size (fine sand), however development of onland sand resources is difficult due to the aesthetic and environmental impacts of such activities.

Silica rich sand for use in glass making has also been identified in the dune sediments at Hokianga Harbour mouth (northern side) and Kaipara Harbour. The sand in Hokianga Harbour dunes has a suitable grain size for glass manufacture however has an iron contamination (due to heavy minerals) that is too high for economic extraction (Christie and Barker, 2007). Silica sand also occurs on the eastern shores of Kaipara Harbour in Early Quaternary dune sands. The lower grades of sand within these deposits are extracted as industrial sand for used in cement making and foundry sand. The extent of this sand resource is also unknown and requires quantification (Christie and Barker, 2007).

10.3 GLAUCONITE AND PHOSPHATE

The primary use of glauconite and phosphate for economic purposes is agricultural fertiliser with potassium (from glauconite) and phosphate (from

phosphatic sediments and rocks) being two of the three essential major plant nutrients (Coles et al., 2002).

Glauconite provides primarily a slow-acting source of potassium, particularly for depleted soils, and has been suggested for use in the northeastern United States, southern England, France, Belgium, Japan, Australia and New Zealand (Odin and Fullagar, 1988). Glauconite can also be a source of small quantities of magnesium and iron with trace amounts of calcium carbonate and phosphate often beneficially present as well. The sandy texture, uniform grain size, high density and magnetic susceptibility of glauconite grains allows for a straightforward method of extraction of modern seafloor deposits using suction dredging, although large grab samplers and normal dredges may also be used (Coles et al., 2002). Washing of the collected glauconite easily removes the mud fraction, but associated other sandy components such as quartz and carbonate (particularly foraminiferal tests) are more difficult to eliminate (Coles et al., 2002). In some cases this may not be an issue as small amounts of calcium and silica are also beneficial to plant growth. Coles et al. (2002) noted that shelf sediment off Denmark comprising c. 95% glauconite (of average composition), 2% quartz and 3% clay is valued at US$300 per tonne, making extraction viable. Summerhayes (1967) found that the sustained rate of potash release from Chatham Rise glauconite was about twice that of terrestrial sources of potassium and as such was a potentially economically viable source of potassium for New Zealand agricultural use. Glauconite may also be used as a water softener, a colouring agent in glass making and the paint industry, a sorbent for oils and an insulating material in the manufacture of slag wool (Dietrich and Skinner, 1979; Castro and Tourn, 2003). Glauconite on the NKCM, and primarily along transect D where the concentration reaches >95% (Fig. 4-17A), would be particularly suitable for extraction for fertiliser use. The glauconite resource on the NKCM comprises c. 82.5 million m^3 (165 km^2 glauconite concentrated area along transect D and E to a sediment depth of 0.5 m) while c. 41 million m^3 occurs along transect D alone. The NKCM glauconites would meet the requirements imposed on Denmark's shelf sediments for composition and their relatively shallow depth (150-400 m) and ease of extraction using a suction dredge (already common in sand extraction) would make this deposit viable to exploit.

Phosphatised rocks or nodules are primarily used to produce phosphate fertiliser (80% of phosphate reserves) including concentrated superphosphate, ammonium orthophosphate and ammonium polyphosphate (Kent, 1980; Coles et al., 2002). Coles et al. (2002) suggested that at least 30% of the unconsolidated sediment of interest must consist of phosphate nodules to be economically viable to extract. Phosphate is also used in detergents (12%), animal feeds (5%) and other applications (3%) such as food grade and metal treatment. Pelletal phosphate or phosphate nodules can be extracted from the seafloor using the same methods as glauconite (suction dredging), however the phosphorite rocks or phosphatised slabs must be fragmented by blasting or ripping before extraction can occur (Coles et al., 2002). The phosphatised shell fragments on the NKCM are by themselves clearly not economically viable sources of phosphate, but they would provide a phosphatic component to any glauconite that was extracted for fertiliser use. The phosphate nodules and phosphatised slabs on the southern flank of the Hokianga Terrace may be viable options for extraction for phosphate fertilisers as they are within reasonable water depths (c. <600 m), but the extent and reserves of the deposits first need evaluation. It is anticipated that the kind of phosphatic material dredged from the flanks of the Hokianga Terrace (Phillips, 1986) may also occur in association with rough topography elsewhere along the NKCM. Deposits of phosphorite nodules also occur on the Chatham Rise at water depths of c. 400 m and comprise Miocene aged phosphatised limestone. These deposits have high phosphate contents (21.5% P_2O_5) and are suitable for use as a fertiliser when finely crushed (Cullen, 1989). 100 million tonnes of phosphorite (total resource) is estimated to occur along the Chatham Rise within unconsolidated glauconitic sandy mud. Portions of the NKCM could well have similar future economic potential.

The phosphatic material in the two northern glauconite rich samples (P420, P421) equates to approximately 8-12 million m^3 of phosphate (at 20% of sample) potentially providing a considerable future source of this mineral. The difficulty in separating the phosphatic material from the glauconite may, however, preclude its extraction for high concentration phosphate fertilisers. Despite this, the combination of glauconite (potassium) and phosphatic material may make extraction of these sediments attractive for unrefined fertiliser use in the future.

Chapter 11

SUMMARY AND CONCLUSIONS

11.1 MARGIN SETTING

The seabed of the north Kaipara continental margin (NKCM) off the western side of Northland Peninsula is covered by siliciclastic and mixed carbonate-siliciclastic sediments together with significant areas of authigenic mineral deposits. The NKCM is a high energy environment exposed to predominantly westerly and southwesterly swell waves and northerly storm waves. The coastline bordering the NKCM comprises mostly sandy beach deposits (75%), which form prograding sand barriers in the south and north (North Kaipara Barrier and Aupouri Peninsula, respectively). The bathymetric nature of the sea floor varies considerably across the NKCM with a relatively narrow (c. 25 km wide) simple shelf and slope in the southern half and a wider (c. 50 km wide) more irregular shelf and slope in the northern half (Fig. 2-6 and 2-7). The textural and compositional characteristics of the NKCM sediments have been described and mapped from surficial sediment samples collected across seven transects from between 30 and 1015 m water depth.

11.2 SEDIMENT TEXTURE

A sand fraction (0.063-2 mm) completely dominates sediment from the NKCM, mainly comprising between 90 and 100% of samples, and comprises mainly medium, fine and very fine sand sizes (Fig. 4-3). Over most of the NKCM the gravel fraction (>2 mm) of bottom sediments is less than 5% but increases to 75% in some samples in the north (Fig. 4-2). The percentage of mud-sized grains varies considerably (from 0-90%) across the NKCM. In general, mud increases offshore in the southern half of the NKCM but only increases to mid-outer shelf depths in the northern half before decreasing further offshore (Fig. 4-4 and 4-5).

NKCM sediments are dominated by slightly gravelly sand and slightly gravelly muddy sand textures, particularly so across the shelf (Fig. 4-7). Mud textures

predominantly occur in the southern half of the NKCM, involving slightly gravelly mud, sandy mud and mud, largely beyond the shelf proper. In the northern half of the NKCM the only muddy texture, occupying a mid-shelf position, is a zone of gravelly sandy mud. Gravel textures are only found at three sample sites within the northern half of the NKCM.

11.3 SEDIMENT MINERALOGY

The siliciclastic sediments on the NKCM are, in general, co-dominated by quartz and feldspar with approximately equal amounts in most samples and no sites recording less than 5% quartz or feldspar. Both quartz and feldspar show a general decrease in abundance offshore (with depth) and to the north (Fig. 4-10). Other important sediment components include: heavy minerals, mica, rock fragments, opaques, clay minerals, glauconite and mixed carbonate-siliciclastic pellets. The percentage of heavy mineral grains in NKCM sediments does not show any significant trends either onshore to offshore or north to south (Fig. 4-11A). Most sample sites contain less than 5% heavy minerals and only two have concentrations of >30%. Overall, hornblende is the dominant heavy mineral with garnet, augite and hypersthene of secondary dominance (Fig. 4-11B). Across most of the NKCM the abundance of mica grains is <5% with only a small number of isolated areas having a greater quantity (Fig. 4-13). The only area where the mica content exceeds 20% is along transect B at c. 300 m water depth. Rock fragments comprise only a small proportion (<30%) of the total sediment with the highest concentration of rock fragments (20-30%) at less than 50-100 m water depth (Fig. 4-15). The rock fragments range in type with the most common comprising elongated quartz and feldspar grains within a very fine-grained groundmass indicating they are volcanic rock fragments. Opaque minerals are relatively insignificant with the majority of NKCM samples containing less than 5% opaque grains, mainly leucoxene (altered ilmenite). Titanomagnetite, such a common opaque mineral on the Taranaki-Waikato shelf to the south, appears to be absent from all NKCM bottom sediment. Clay minerals comprise only a relatively small proportion of the NKCM samples (rarely exceeding 30%) and appear to have no consistent trend in their distribution. Montmorillite or smectite dominates the clay

fraction of all the NKCM samples, with illite and chlorite+kaolinite of secondary importance.

11.4 SILICICLASTIC MINERAL PROVENANCE

In terms of the major source of siliciclastic minerals to the NKCM, the Taranaki andesites and TVZ rhyolites probably supply the dominant quartz and feldspar minerals in NKCM sediments (Fig. 8-1 and Table 8-1). TVZ andesites, having rare or absent hornblende, are unlikely to be significant sediment contributors to the hornblende content of the NKCM sediments, which can primarily be attributed to the Taranaki andesites. The North Island greywackes (Torlesse and Murihiku terranes) and sedimentary and volcanic rocks of Northland, Waikato, King Country and Taranaki are probably important secondary sources to the NKCM, but likely supply relatively small amounts of sediment to the overall system (Fig. 8-1 and Table 8-1). A South Island sediment source (particularly South Island schists and granites) is also implicated due to the relatively high quantities of mica and garnet in the NKCM sediments and for which few significant North Island sources exist.

11.5 SEDIMENT TRANSPORT

The above sources supplied minerals to mainly distant coastlines via rivers. Once at the coastline other oceanographic processes selectively sort, abrade and transport the minerals to the NKCM (Fig. 8-2). The most important process is regarded to be littoral or longshore drift within the surf zone off western North Island, which primarily occurs to the north beyond Cape Egmont. This littoral drift has been actively modifying the current coastline since sea level reached its present position c. 6500 years ago. On the shelf proper, combined storm and current sediment transport only occurs at less than 70 m water depth during annual storms and across much of the shelf (<130 m water depth) during a 25-year storm event. Another factor affecting sediment deposition and distribution on the NKCM is the strong tidal currents around Cape Reinga. The effects of these tidal currents probably extend down Aupouri Peninsula to Tauroa Point and appear to transport quartz and feldspar rich sediment northwards towards Cape Reinga.

11.6 CARBONATE CONTENT AND SKELETAL MATERIAL

The calcium carbonate ($CaCO_3$) content of the NKCM sediment ranges from 3-91% with a clear increase in carbonate content offshore and to the north (Figure 4-9). The areas of high $CaCO_3$ content in the northern half of the NKCM and >400 m water depth in the southern half coincide with areas of high skeletal abundance (bryozoan and foraminiferal skeletal material, respectively). Varying quantities of calciclastic material occur in NKCM sediments, generally increasing offshore with depth and to the north (Fig. 4-16A). The greater than 0.5 mm calciclastic fraction of the NKCM sediment is dominated by bivalve and gastropod molluscs, particularly so in less than 200 m water depth (Fig. 5-1). The dominant bivalve species are *Hiatella arctica*, *Scalpomactra scalpellum*, *Saccella maxwelli*, *Nucula nitidula*, and *Pleuromeris zelandica* (Fig. 5-2A), while the six main gastropod species are *Sigapatella tenuis*, *Austrofusus glans*, *Retusa* sp., *Dentimargo fusula*, *Stiracolpus pagoda* and *Proxiuber australe* (Fig. 5-2B). Bryozoan skeletal material is most common in the northern half of the NKCM (Fig. 5-1) and is dominated by *Cellaria immersa* and *Celleporaria tridenticulata*. The coarse skeletal material ranges between fresh and relict looking with fresh material most common at less than 100 m water depth and relict material at greater than 200-400 m water depth (Fig. 5-6). A large band of mixed fresh-relict material occurs predominantly between 100 and 200 m water depth.

In the sand fraction, planktic foraminifera are the dominant skeletal type extending over most of the NKCM at >200 m water depth (Fig. 4-16B). Bivalve and bivalve/gastropod skeletal fragments dominate at <80 m water depth, with only small areas of other skeletal types present in this zone. A wide variety of benthic foraminifera occur in the NKCM sediments with *Cibicides corticatus*, *Hoeglundina elegans* and *Quinqueloculina* common. *Globorotalia inflata*, *Globigerina bulloides* and *Orbulina universa* are the main planktic species (Table 5-4).

11.7 GLAUCONITE

Glauconite grains are ubiquitous across the NKCM, ranging in content from 0 to 95% but predominantly <10% (Fig. 4-17A). A large area of very high glauconite concentration (>75%) occurs near the shelf edge between 150 and 400 m water depth, forming a modern greensand deposit. The glauconite content significantly decreases away from this concentrated area. The NKCM glauconite composition is dominated by SiO_2 and total Fe (total Fe = $FeO+Fe_2O_3$) with the other elements each comprising much less than 10% (Table 6-1). Samples from the glauconite-rich region have very similar compositions with high K_2O contents (7-8%) indicative of evolved to highly evolved glauconite. Only minor differences in MgO, Al_2O_3 and total Fe occur (Table 6-1). Ovoidal or spheroidal morphologies completely dominate the NKCM glauconites while tabular or discoidal grains (0-6.4%) and fossil casts and internal moulds (1.8-11.8%) are of secondary importance (Table 6-3).

11.8 PHOSPHATE

The phosphatic component of NKCM sediments consists of skeletal fragments, mainly bivalve and gastropod, which have been phosphatised. These phosphatic fragments increase in abundance towards the north (Fig. 6-3). In addition to phosphatised skeletal fragments, samples previously dredged from the southern flank of the Hokianga Terrace recovered phosphatised conglomeratic slabs and phosphate nodules. These slabs consist of phosphatic nodular material, some brachiopod casts and phosphatic ooze in a calcareous glauconitic phosphatic matrix. On the NKCM, the area of highest phosphatic material (10-30%) overlaps with >30% glauconite on the outer shelf north of Tauroa Point (Fig. 6-3). However, this overlap does not extend south of Tauroa Point where the percentage of glauconite reaches >95%. Both phosphate and glauconite require slightly reducing conditions and organic decomposition and their overlap distribution is suggestive of coeval formation on the NKCM.

11.9 MIXED CARBONATE-SILICICLASTIC PELLETS

Unusual mixed carbonate-siliciclastic pellets identified in NKCM sediments are well rounded grains which are similar to glauconite in shape and form but consist of very fine grained quartz, feldspar and heavy mineral grains as well as fine skeletal fragments contained within a tan to brown coloured micritic-argillaceous matrix (Plate 5). Some of these pellets have darker centres, similar to nuclei, which appear to range in size between different grains. Their occurrence is limited to two areas of sediment consisting of >10% pellets, one in the northern half of NKCM and the other in the south (Fig. 4-17B).

11.10 OFFSHORE SEDIMENTATION RATES

Glauconite, phosphatic material and mixed carbonate-siliciclastic pellets are sedimentary components that typically require low sedimentation rates to develop. The association suggests that areas of the NKCM have been sediment starved for reasonably long periods of geological time. Low sedimentation rates must have characterised central NKCM for at least the last 100 000 years – this being the minimum period of time required to form evolved to highly evolved glauconite – but probably much longer, perhaps over several cyclical changes in Quaternary sea level. The implication is that much of the present NKCM (and onland Northland) must have remained stable, and in the case of the glauconitic occurrences below sea level, for possibly up to the past 1-1.5 million years. The presence of glauconite and phosphate on the NKCM is also suggestive of past, and possibly present, shelf margin upwelling as high nutrient levels foster the formation of both minerals.

11.11 BEACH AND DUNE SEDIMENTS

In addition to the shelf and slope sediments, onshore beach and dune sediments bordering the NKCM were also investigated. Overall, quartz and feldspar completely dominate these deposits (Fig. 7-4). Rock fragments constitute 10-30% of the coastal sediments and there are small amounts of glauconite, opaque

minerals and skeletal fragments. Non-opaque heavy minerals are dominated by hornblende and oxyhornblende, forming <5% of samples (Fig. 7-4).

11.12 SHELF TO BEACH SEDIMENT EXCHANGE

In general, the content of quartz, feldspar and rock fragments increases from the shelf to the beach (Fig. 7-4). The disparity in composition between the shelf and beach deposits could be explained by uneven rates of sediment transport across the margin. The most active transport occurs in the nearshore littoral system affecting the composition of beach and dune sediments by transporting quartz and plagioclase feldspar rich sediment north at a much faster rate than the much slower, storm dominated, northwards transport of sediment on the shelf. Relatively regular reworking and exchange of the sediment in the beach and shelf environment must occur at less than 150 m water depth as, firstly, glauconite grains occur in both beach and dune sediments and, secondly, beyond these depths the quartz and feldspar components decrease significantly (Fig. 7-4).

11.13 SURFICIAL SEDIMENT FACIES

Five distinctive surficial sediment facies have been developed from the distribution of the NKCM sediment components based on their compositional and textural characteristics (Fig. 8-4 and Table 8-2). The major control on the distribution of these facies is the siliciclastic mineral input to the NKCM.

Facies 1 (siliciclastic sand) comprises at least 80% siliciclastic material with minor bivalve and gastropod skeletal material (dominated by *Scalpomactra scalpellum* and *Austrofusus glans*). It contains three subfacies. Subfacies 1a comprises quartzofeldspathic sands, generally involving >30% of both quartz and feldspar, that are restricted to shelf depths of <100 m in the northern half of the NKCM and generally <200 m in the southern half (Fig. 8-4). Subfacies 1b comprises heavy mineral dominated sands, which contain heavy mineral concentrations >30% and up to 75%. The heavy mineral fraction is dominated by hornblende, garnet and augite and occurs in less than 50 m water depth along transects C and D (Fig. 8-4). Subfacies 1c is dominated by fine grained quartz,

feldspar and mica (c. 20-30% each) grains and only occurs near 300 m water depth along transect B (Fig. 8-4). The sediment in Facies 1 forms a modern sand prism, extending out to outer shelf depths where active sedimentation and sediment transport is occurring as a result of a high-energy environment. The sediment in Facies 1a is probably sourced primarily from North Island volcanics (TVZ, Taranaki) and basement rocks, and the influx of quartz and feldspar rich sediment from the south significantly overwhelms other sediment sources to the inner-mid shelf except where Facies 1b occurs. The erosion of basaltic to basaltic andesite coastal outcrops onshore from Facies 1b appears to exceed the supply of quartzofeldspathic sediment to this area, resulting in heavy mineral rich sediment. The sediment in Subfacies 1c probably has at least a partial South Island source resulting in the mica rich character of this facies.

Facies 2 (glauconitic sand) comprises medium to fine grained sand with over 30% and up to as much as 75% glauconite grains. This facies occurs between 150 and 400 m water depth in central NKCM, offshore from Tauroa Point (Fig. 8-4). The formation of this facies at outer shelf and upper slope depths suggests sediment bypassing must occur as the surrounding facies all contain moderate to high quantities of siliciclastic material. The low sedimentation rates required for glauconite to form suggests that Facies 2 is an ‘old’ deposit, which has been concentrated and evolved on the outer shelf of the NKCM over a significant period of the margin’s history.

Facies 3 (mixed bryozoan-siliciclastic sand) comprises >40% bryozoan skeletal material. The facies only occurs in the northern half of the NKCM (Fig. 8-4) and has formed as a result of low sediment input to the northern half of the NKCM and the strong tidal currents around Cape Reinga which prevent significant sediment deposition on the northern NKCM. This allows bryozoan production at inner shelf depths as the skeletal material is not smothered by siliciclastics. However, it is acknowledged that a significant proportion of the bryozoan material on the outer shelf and upper slope has probably been reworked from the bryozoan rich sediment on the Three Kings platform immediately to the north.

Facies 4 (pelletal mud) comprises muddy sediment dominated by >30% mixed carbonate-siliciclastic pellets which include minor foraminifera and opaline silica spicules. The host sediment consists of very fine sand and mud, the latter exceeding 50%. The facies occurs in a small area of 100-150 m water depth in the northern half of the NKCM (Fig. 8-4). This facies likely represents an area of lower wave energy conditions in the mid shelf area due to the very wide shelf (compared to the southern half of the NKCM), which causes wave energy dissipation over a larger area.

Facies 5 (foraminiferal sand and mud) comprises at least 30% foraminiferal tests and contains two subfacies. Subfacies 5a is dominated by planktic foraminifera and contains >50% mud sized sediment. The facies occurs at greater than 400 m water depth in the southern half of the NKCM (Fig. 8-4). Subfacies 5b generally contains >70% sand sized sediment and occurs both as a deeper water band at slope depths and as a shallower band at mid to outer shelf depths (Fig. 8-4). Planktic foraminifera dominate the deeper water band while benthic foraminifera dominate the mid to outer shelf band.

11.14 SEDIMENTATION MODELS

Sedimentation models developed in the literature for wave-dominated siliciclastic shelves (e.g. Fig. 8-5, 8-7 and 8-8) generally do not appear to apply well to the NKCM sediments due to their complex textural characteristics, primarily as a result of variable sediment input to the margin and changes in sea level which have mixed relict and modern sediments. As such, the NKCM sediments do not show the expected fining offshore trends associated with most models (Fig. 8-6). The highly complicated nature of the textural and compositional trends in NKCM sediments makes it difficult to develop an integrated sedimentation model (sixth aim of thesis) that applies to both the northern and southern halves of the NKCM and, as such, one has not been developed here. The sediments in the northern half of the NKCM more closely follow a temperate carbonate textural model (Section 8.5.3 and Fig. 8-8), while the sediment in the southern half tends to be more similar to a standard siliciclastic sediment model based on mud percent (e.g. Section 8.5.4).

11.15 LATE QUATERNARY SEDIMENTARY HISTORY

The Late Quaternary history of the NKCM has been considered using the stratigraphy of three short piston cores and reconstructed sea level maps produced for the last 20 000 years. The three cores range in thickness from c. 0.4-1.8 m (Fig. 9-1) and comprise sandy and muddy sediments dominated by foraminifera and other skeletal fragments (e.g. bivalves). A radiocarbon date was obtained on shell material from the base of core P600. This gave a true age of 11 500 ± 120 years BP and a sedimentation rate of 0.08 mm per year or 80 mm per 1000 years for the inner-mid shelf of the NKCM. Between 20 000 and 16 000 years ago much of the NKCM (and the sample sites) was subaerially exposed and the rivers which discharge into the four harbours bordering the NKCM would have extended across the shelf (Fig. 9-4 and 9-5). The glauconitic rich area in the centre of the NKCM was not exposed but is within 100 m water paleodepth. The abundance of glauconite (and minor phosphate) suggests sediment must have bypassed the shelf in this area during both the Last Glacial maximum and the subsequent sea level rise. The mud (and pellet) dominated samples in the northern half of the NKCM are on or above the shoreline suggesting the mud in this area must have been deposited following sea level rise, as it is envisaged that any previously deposited mud sized sediment would have been quickly eroded in this environment. At 11 500 years ago most of the NKCM was submerged in seawater and any mud that was previously deposited in subaerial or marginal marine settings on the shelf would have been reworked and deposited offshore as sea level rose (Fig. 9-6). The continued rise in sea level between 11 500 and 6500 years ago would have allowed the deposition of sediment over previously exposed shelf samples, building up thick sand deposits (Fig. 9-7). Sea level reached its present position c. 6500 years ago and the present sediment distribution on the NKCM would have developed over this time with only small (<50 cm) fluctuations in sea level.

11.16 POTENTIAL ECONOMIC RESOURCES

The sediments on the NKCM may form potentially economic resources, particularly in the case of sand, glauconite and phosphate. The NKCM sediments at <100 m water depth comprise the most suitable sand for extraction purposes,

and particularly so in the southern half of the NKCM where there are high volumes of quartzofeldspathic fine sands (Fig. 4-3). Bedding sand and fibreglass manufacture are probably the most ideal uses of NKCM sands, the quartz and feldspar rich sand being of suitable grain size (0.15-0.25 mm) and sorting (very well to well sorted). Use of the inshore band of sand (<100 m water depth) for concrete manufacture could also be advantageous as these sediments are very low in clay minerals (0-5%). The area at <100 m water depth in the southern half of the NKCM equates to c. 269 million m^3 of quartz and feldspar rich sediment to a depth of approximately 0.97 m (depth of sand in core P600), providing a potentially significant sand resource.

The primary use of glauconite and phosphate for economic purposes is agricultural fertiliser with potassium (from glauconite) and phosphate (from phosphatic sediments and rocks) being two of the three essential major plant nutrients. Glauconite on the NKCM, and primarily along transect D where the concentration reaches >95% (Fig. 4-17A), would be particularly suitable for extraction for fertiliser use. The glauconite resource on the NKCM comprises c. 82.5 million m^3 (165 km^2 glauconite concentrated area along transect D and E to a sediment depth of 0.5 m) while c. 41 million m^3 occurs along transect D alone. The NKCM glauconites would meet the requirements imposed on Denmark's shelf sediments for chemical composition and their relatively shallow depth (150-400 m) and ease of extraction using a suction dredge (already common in sand extraction) would make this deposit viable to exploit.

11.17 FURTHER RESEARCH

The hydrodynamic regime operating over the NKCM is poorly known and much further research is required on the wave, oceanic and tidal currents in the area before a better picture can emerge as to their effects on reworking and distributing the NKCM sediments. In particular, research defining the existence, extent and strength of the West Auckland and Westland Currents is needed. The hydrodynamic data should be supplemented by SWATH bathymetry, side scan sonar imagery and bottom photography, all unavailable in the present study.

Further sediment samples and cores are also required to identify the extent and depth of the glauconite rich deposits (Facies 2) on the NKCM and the phosphatic deposits on the Hokianga Terrace and possibly elsewhere along the shelf margin. More cores and radiocarbon dates are also required to better constrain the Late Quaternary shelf history of the NKCM along with additional sea floor sampling between transects C and D (across Hokianga Terrace) and D and E to help more closely define the distribution of the contrasting sediment facies present.

Allen, J.R.L., 1977. Physical processes of sedimentation. George Allen and Unwin Ltd.

Amorosi, A., 1995. Glaucony and sequence stratigraphy: a conceptual framework of distribution in siliciclastic sequences. Journal of Sedimentary Research, B65: 419-425.

Associates, A.G., 1982. Coastal sand and shingle resources of Auckland and Northland, Applied Geology Associates.

Boggs, S. and Krinsley, D., 2006. Application of cathodoluminescence imaging to the study of sedimentary rocks. Cambridge University Press.

Bradford, J.M. and Roberts, P.E., 1978. Distribution of reactive phosphorus and plankton in relation to upwelling and surface circulation around New Zealand. New Zealand Journal of Marine and Freshwater Research, 12: 1-15.

Briggs, R.M., Middleton, M.P. and Nelson, C.S., 2004. Provenance history of a Late Triassic-Jurassic Gondwana margin forearc basin, Murihiku Terrane, North Island, New Zealand: petrographic and geochemical constraints. New Zealand Journal of Geology and Geophysics, 47: 589-602.

Brodie, J.W., 1960. Coastal surface currents around New Zealand. New Zealand Journal of Geology and Geophysics, 3: 235-252.

Carter, L., 1975. Sedimentation on the continental terrace around New Zealand: a review. Marine Geology, 19: 209-237.

Carter, L. and Heath, R.A., 1975. Role of mean circulation, tides, and waves in the transport of bottom sediment on the New Zealand continental shelf. New Zealand Journal of Marine and Freshwater Research, 9: 423-448.

Carter, R.M., Carter, L. and Johnson, D.P., 1986. Submergent shorelines in the SW Pacific: evidence for an episodic post-glacial transgression. Sedimentology, 33: 629-649.

Castro, L. and Tourn, S., 2003. Direct application of phosphate rocks and glauconite as alternative sources of fertiliser in Argentina. Exploration and Mining Geology, 12: 71-78.

Catuneanu, O., 2006. Principles of Sequence Stratigraphy. Elsevier.

Chappell, D.A., 1995. Gees Bay (North Otago): stratigraphy, paleontology and geochemistry. Unpublished BSc (Hons) Thesis, University of Otago.

Chiswell, S.M., 1994. Variability in sea surface temperature around New Zealand from AVHRR images. New Zealand Journal of Marine and Freshwater Research, 28: 179-192.

Christie, A.B. and Barker, R.G., 2007. Mineral resource assessment of the Northland region, New Zealand, GNS Science Report 2007/06.

Churchman, G.J., Hunt, J.L., Glasby, G.P., Renner, G.A. and Griffiths, G.A., 1988. Input of river-derived sediment to the New Zealand continental shelf: II. Mineralogy and composition. Estuarine, Coastal and Shelf Science, 27: 397-411.

Coles, S.K.P., Wright, C.I., Sinclair, D.A. and Van den Bossche, P., 2002. The potential for environmentally sound development of marine deposits of potassic and phosphatic minerals offshore, Southern Africa. Marine Georesources and Geotechnology, 20: 87-110.

Compton, J.S., Wigley, R. and McMillan, I.K., 2004. Late Cenozoic phosphogenesis on the western shelf of South Africa in the vicinity of the Cape Canyon. Marine Geology, 206: 19-40.

Compton, M.S., 1989. Morphology and geochemistry of glauconite from the Te Kuiti Group, South Auckland region, New Zealand. Unpublished MSc Thesis, University of Waikato.

Cullen, D.J., 1989. The submarine phosphorite deposits of central Chatham Rise, east of New Zealand. In: Kear, D. (Ed), Mineral Deposits of New Zealand Monograph 13, pp. 201-206.

Deer, W.A., Howie, R.A. and Zussman, J., 1992. An introduction to the rock forming minerals, 2nd Edition. Prentice Hall.

Dietrich, R.V. and Skinner, B.J. 1979. Rocks and rock minerals. John Wiley and Sons.

Dodd, J.R. and Nelson, C.S., 1998. Diagenetic comparisons between non-tropical Cenozoic limestones of New Zealand and tropical limestones from Indiana, USA: Is the non-tropical model better than the tropical model? Sedimentary Geology, 121: 1-21.

Dunbar, G.B. and Barrett, P.J., 2005. Estimating palaeobathymetry of wave-graded continental shelves from sediment texture. Sedimentology, 52: 253-269.

Edbrooke, S.W., 2001. Geology of the Auckland Area. Institute of Geological and Nuclear Sciences 1:250 000 geological map 3. Institute of Geological and Nuclear Sciences Ltd., 74 pp.

Edwards, A.R., 1991. The Oamaru Diatomite. New Zealand Geological Survey Paleontological Bulletin 64.

Folk, R.L., 1968. Petrology of sedimentary rocks. Hemphill Publishing, U.S.A.

Garner, D.M., 1969. The seasonal range of sea temperature on the New Zealand Shelf. New Zealand Journal of Marine and Freshwater Research, 3: 201-208.

Gibb, J.G., 1986. A New Zealand regional Holocene eustatic sea-level curve and its application to determination of vertical tectonic movements. Royal Society of New Zealand Bulletin, 24: 377-395.

Gilbert, D.B., Ballance, P.F. and Spörli, K.B., 1989. Te Kuiti Group and Northland Allochthon rocks on the north flank of the Omahuta Basement Block, Northland, New Zealand. In: Spörli, K.B. and Kear, D. (Ed), Geology of Northland accretion, allochthons and arcs at the edge of the New Zealand micro-continent. The Royal Society of New Zealand Bulletin 26.

Gillespie, J.L. and Nelson, C.S., 1996. Distribution and control of mixed terrigenous-carbonate surficial sediment facies, Wanganui shelf, New Zealand. New Zealand Journal of Geology and Geophysics, 39: 533-549.

Gillespie, J.L. and Nelson, C.S., 1997. Mixed siliciclastic-skeletal carbonate facies on Wanganui Shelf, New Zealand: a contribution to the temperate carbonate model. In: James, N.P. and Clarke, J.D.A. (Ed), Cool-Water Carbonates. Society of Economic and Petroleum Mineralogists Special Publication, pp. 127-140.

Gillespie, J.L., Nelson, C.S. and Nodder, S.D., 1998. Post-glacial sea-level control and sequence stratigraphy of carbonate-terrigenous sediments, Wanganui Shelf, New Zealand. Sedimentary Geology, 122: 245-266.

Grapes, R.H., 1995. Uplift and exhumation of Alpine Schist, Southern Alps, New Zealand: thermobarometric constraints. New Zealand Journal of Geology and Geophysics, 38: 525-533.

Griffiths, G.A. and Glasby, G.P., 1985. Input of river-derived sediment to the New Zealand continental shelf: I. Mass. Estuarine, Coastal and Shelf Science, 21: 773-787.

Hayward, B.W., 1993. The tempestuous 10 million year life of a double arc and intra-arc basin, New Zealand's Northland basin in the early Miocene. In: Ballance, P.F. (Ed), 1993. South Pacific Sedimentary Basins. Sedimentary Basins of the World 2: 113-142.

Hayward, B.W., 2006. Northland dunes. Geological Society of New Zealand Newsletter, 139: 39-43.

Hayward, B.W., Grenfell, H.R., Reid, C.M. and Hayward, K.A., 1999. Recent New Zealand shallow-water benthic foraminifera: taxonomy, ecologic distribution, biogeography, and use in paleoenvironmental assessment. Institute of Geological and Nuclear Sciences monograph 21.

Hayward, B.W., Grenfell, H.R., Sabaa, A. and Hayward, J.J., 2003. Recent benthic foraminifera from offshore Taranaki, New Zealand. New Zealand Journal of Geology and Geophysics, 46: 489-518.

Heath, R.A., 1982. What drives the mean circulation on the New Zealand west coast continental shelf? New Zealand Journal of Marine and Freshwater Research, 16: 215-226.

Heath, R.A., 1985. A review of physical oceanography of the seas around New Zealand - 1982. New Zealand Journal of Marine and Freshwater Research, 19: 79-124.

Herzer, R.H., 1995. Seismic stratigraphy of a buried volcanic arc, Northland, New Zealand and implications for Neogene subduction. Marine and Petroleum Geology, 12: 511-531.

Herzer, R.H., Chaproniere, G.C.H., Edwards, A.R., Hollis, C.J., Pelletier, B., Raine, J.I., Scott, G.H., Stagpoole, V., Strong, C.P., Symonds, P. and Wilson, G.J., 1997. Seismic stratigraphy and structural history of the Reinga Basin and its margins, southern Norfolk Ridge system. New Zealand Journal of Geology and Geophysics, 40: 425-451.

Hicks, D. and Hume, T.M., 1996. Morphology and size of ebb tidal deltas at natural inlets on open-sea and pocket-bay coasts, North Island, New Zealand. Journal of Coastal Research, 12: 47-63.

Hilton, M.J., 2006. The loss of New Zealand's active dunes and the spread of marram grass (*Ammophila arenaria*). New Zealand Geographer, 62: 105-120.

Houghton, B.F. et al., 1995. Chronology and dynamics of a large silicic magmatic system: central Taupo Volcanic Zone, New Zealand. Geology, 23: 13-16.

Hudson, D.S., 1996. Provenance of Miocene to Recent sands and sandstones of the Taranaki-Wanganui region, New Zealand. Unpublished MSc Thesis, University of Waikato.

Hume, T.M. and Nelson, C.S., 1986. Distribution and origin of clay minerals in surficial shelf sediments, western North Island, New Zealand. Marine Geology, 69: 289-308.

Hume, T.M., Green, M., Nichol, S. and Parnell, K., 2003. Kaipara sand study final report: sand movement, storage and extraction in the Kaipara tidal inlet. NIWA Report HAM2002-064.

Irwin, J. and Eade, J.V., 1984a. Hokianga Bathymetry, Coastal Chart Series 1:200 000. New Zealand Oceanographic Institute.

Irwin, J. and Eade, J.V., 1984b. Kaipara Bathymetry, Coastal Chart Series 1:200 000. New Zealand Oceanographic Institute.

Issac, M.J., 1996. Geology of the Kaitaia Area, Institute of Geological and Nuclear Sciences 1:250 000 geological map 1. Institute of Geological and Nuclear Sciences Ltd., pp. 44.

Issac, M.J., Herzer, R.H., Brook, F.J. and Hayward, B.W., 1994. Cretaceous and Cenozoic Sedimentary Basins of Northland, New Zealand, Institute of Geological and Nuclear Sciences Monograph 8. Institute of Geological and Nuclear Sciences Ltd., pp. 203.

James, N.P., 1997. The cool-water carbonate depositional realm. In: James, N.P. and Clarke, J.A.D. (Ed), Cool-water carbonates. SEPM Special Publication No. 56: 1-20.

James, N.P., Bone, Y., Kyser, T.K., Dix, G.R. and Collins, L.B., 2004. The importance of changing oceanography in controlling late Quaternary carbonate sedimentation on a high energy, tropical, oceanic ramp: northwestern Australia. Sedimentology, 51: 1-27.

Jennings, W.L., 1989. Metamorphism in the Waipapa Terrane, Omahuta and Puketi Forests, Northland, New Zealand. In: Spörli, K.B. and Kear, D. (Ed), Geology of Northland accretion, allochthons and arcs at the edge of the New Zealand micro-continent. The Royal Society of New Zealand Bulletin 26.

Jones, N.W. and Bloss, F.P., 1980. Laboratory manual for optical mineralogy. Burgess Publishing Company.

Kasper-Zubillaga, J.J., Dickinson, W.W., Carranza-Edwards, A. and Hornelas-Orozco, Y., 2005. Petrography of quartz grains in beach and dune sands of Northland, North Island, New Zealand. New Zealand Journal of Geology and Geophysics, 48: 649-660.

Keane, H.F.X., 1986a. Sedimentology and petrography of the Late Triassic Moeatoa Conglomerate. Unpublished MSc Thesis, University of Waikato.

Keane, S.L., 1986b. Temperate skeletal carbonate deposits on the New Zealand continental margin with particular reference to the Three Kings Region, Unpublished PhD Thesis, University of Waikato, 242 pp.

Kent, P., 1980. Minerals from the marine environment. Resource and Environmental Series. Edward Arnold.

King, P.R. and Thrasher, G.P., 1996. Cretaceous-Cenozoic geology and petroleum systems of the Taranaki Basin, New Zealand. Institute of Geological and Nuclear Sciences monograph 13.

Klein, C., 2002. The 22nd edition of the manual of mineral science. John Wiley and Sons, Inc.

Larsen, J.M. and Parker, R.J., 1989. Petrology and tectonic significance of igneous rocks from the Ahipara Tangihua Massif, Northland, New Zealand. In: Spörli, K.B. and Kear, D. (Ed), Geology of Northland accretion, allochthons and arcs at the edge of the New Zealand micro-continent. The Royal Society of New Zealand Bulletin 26.

Laurent, J.C., 2000. The provenance and dispersal of beach sands on the West Coast of the North Island, New Zealand. Unpublished MSc (Tech) Thesis, University of Waikato.

Mange, A. and Maurer, H.F.W., 1992. Heavy minerals in colour. Chapman and Hall.

McRae, S.G., 1972. Glauconite. Earth-Science Reviews, 8: 397-440.

McDougall, J.C., 1972. Carbonate variations in slope sediments, Kaipara, New Zealand. New Zealand Journal of Geology and Geophysics, 15: 558-571.

McDougall, J.C. and Brodie, J.W., 1967. Sediments of the western shelf, North Island, New Zealand. New Zealand Oceanographic Institute Memoir No. 40.

Mortimer, N., 2000. Metamorphic discontinuities in orogenic belts: examples of the garnet-biotite-albite zone in the Otago Schist, New Zealand. International Journal of Earth Sciences, 89: 292-306.

Mortimer, N., Tulloch, A.J. and Ireland, T.R., 1997. Basement geology of Taranaki and Wanganui Basins, New Zealand. New Zealand Journal of Geology and Geophysics, 40: 223-236.

Nelson, C.S., 1973. Stratigraphy and sedimentology of the Te Kuiti Group, Waitomo County, South Auckland. Unpublished PhD Thesis, University of Auckland.

Nelson, C.S., 1982. Compendium of sample data for temperate carbonate sediments Three Kings Region, Northern New Zealand. University of Waikato Occasional report No.7, 95 pp.

Nelson, C.S. and Cochrane, R.H.A., 1970. A rapid X-ray method for the quantitative determination of selected minerals in fine-grained and altered rocks. Tane, 16: 151-162.

Nelson, C.S. and Hume, T.M., 1987. Paleoenvironmental controls on mineral assemblages in a shelf sequence: Te Kuiti Group, South Auckland, New Zealand. New Zealand Journal of Geology and Geophysics, 30: 343-362.

Nelson, C.S., Hancock, G.E. and Kamp, P.J.J., 1982. Shelf to basin, temperate skeletal carbonate sediments, Three Kings Plateau, New Zealand. Journal of Sedimentary Petrology, 52: 717-732.

Nelson, C.S., Keane, S.L. and Head, P.S., 1988. Non-tropical carbonate deposits on the modern New Zealand shelf. Sedimentary Geology, 60: 71-94.

Norris, R.M., 1972. Shell and gravel layers, western continental shelf, New Zealand. New Zealand Journal of Geology and Geophysics, 15: 572-589.

Notholt, A.J.G. and Jarvis, I., 1990. Phosphorite research and development. Geological Society Special Publication No. 52.

Odin, G.S. and Fullagar, P.D., 1988. Geological significance of the glaucony facies. In: Odin, G.S. (Ed), Green marine clays: oolitic ironstone facies, verdine facies, glaucony facies and celadonite-bearing facies - a comparative study. Developments in Sedimentology 45. Elsevier.

Parrish, J.T., Droser, M.L. and Bottjer, D.J., 2001. A Triassic upwelling zone: the Shublik Formation, Arctic Alaska, USA. Journal of Sedimentary Research, 71: 272-285.

Phillip, D.M., 1986. Continental slope dredgings from the southern flank of the Hokianga Terrace, West Coast, North Island, New Zealand. Unpublished MSc Thesis, University of Auckland.

Powell, A.W.B., 1979. New Zealand Mollusca. William Collins Publishers Ltd.

Powers, M.C., 1953. A new roundness scale for sedimentary particles. Journal of Sedimentary Research, 23: 117-119.

Probert, P.K. and Swanson, K.M., 1985. Sediment texture of the continental shelf and upper slope off the west coast of South Island, New Zealand. New Zealand Journal of Marine and Freshwater Research, 19: 563-573.

Prothero, D.R. and Schwab, F., 1996. Sedimentary geology. W.H. Freeman & Co. U.S.A.

Rait, G.J., 2000. Thrust transport directions in the Northland Allochthon, New Zealand. New Zealand Journal of Geology and Geophysics, 43: 271-288.

Schofield, J.C., 1970. Coastal sands of Northland and Auckland. New Zealand Journal of Geology and Geophysics, 13: 767-824.

Schofield, J.C., 1975. Sea level fluctuations cause periodic, post-glacial progradation, South Kaipara Barrier, North Island, New Zealand. New Zealand Journal of Geology and Geophysics, 18: 295-316.

Smith, I.E.M., Ruddock, R.S. and Day, R.A., 1989. Miocene arc-type volcanic/plutonic complexes of the Northland Peninsula, New Zealand. In: Spörli, K.B. and Kear, D. (Ed), Geology of Northland accretion, allochthons and arcs at the edge of the New Zealand micro-continent. The Royal Society of New Zealand Bulletin 26.

Spörli, K.B. and Harrison, R.E., 2004. Northland Allochthon infolded into basement, Whangarei area, northern New Zealand. New Zealand Journal of Geology and Geophysics, 47: 391-398.

Stanton, B.R., 1969. Hydrological observations across the tropical convergence north of New Zealand. New Zealand Journal of Marine and Freshwater Research, 3: 124-146.

Stanton, B.R., 1972. Circulation along the eastern boundary of the Tasman Sea, Oceanography of the South Pacific, pp. 141-147.

Stanton, B.R., 1973. Hydrological investigations around northern New Zealand. New Zealand Journal of Marine and Freshwater Research, 7: 85-110.

Stokes, S. and Nelson, C.S., 1991. Tectono-volcanic implications of provenance changes in the late Neogene coastal sand deposits of Kaihu Group, South Auckland, New Zealand. New Zealand Journal of Geology and Geophysics, 34: 51-59.

Summerhayes, C.P., 1967. Marine environments of economic mineral deposition around New Zealand: a review. New Zealand Journal of Marine and Freshwater Research, 1: 267-282.

Summerhayes, C.P., 1969. Recent sedimentation around northernmost New Zealand. New Zealand Journal of Geology and Geophysics, 12: 172-207.

Wellman, H.W., 1979. An uplift map for the South Island of New Zealand, and a model for uplift of the Southern Alps. In: Cresswell, M.M. (Ed), The origin of the Southern Alps. The Royal Society of New Zealand Bulletin 18, pp. 13-20

White, P.J. and Waterhouse, B.C., 1993. Lithostratigraphy of the Te Kuiti Group: a revision. New Zealand Journal of Geology and Geophysics, 36: 255-266.

Wright, A.C., 1980. Volcanic geology of the Waipoua area, Northland, New Zealand. New Zealand Journal of Geology and Geophysics, 23: 83-91.

Wright, A.C. and Black, P.M., 1981. Petrology and geochemistry of Waitakere Group, North Auckland, New Zealand. New Zealand Journal of Geology and Geophysics, 24: 155-165.

PLATE 1

Photomicrographs of quartz and feldspar-rich NKCM sediments

a Quartz and feldspar rich sample P407 (transect B). The well sorted, subrounded nature of the sediment is evident. Most of the dusty-looking grains are variably limonite stained quartz or feldspar, but also include heavy minerals (particularly hornblende and augite), shell fragments and mica grains.

b Quartz and feldspar rich sample P408 (transect B). The subrounded nature of the grains and their dusty appearance is again evident. Surface fractures are very clear at higher magnification. This sample also includes shell material (planktic foraminifera, lower right), rock fragments (top and bottom left), mica (top), and heavy minerals.

c Quartz and feldspar rich sample P403 (transect B) at low magnification. This sample consists of a mix of quartz, feldspar and heavy minerals although quartz and feldspar dominate comprising most of the darker dirty grains (as evident when exposed to cathodoluminescence (CL) in **d-f**). Elongate flaky hornblende grains are present in the centre.

d-f Sample P403 (in c) under CL light at increasing exposure times. **d** plagioclase and orthoclase feldspar appear first at low exposure (light blue and green), **e** followed by brown coloured quartz and **f** dark blue-violet quartz at long exposure times.

g Sample P430 (transect F) at low magnification. Low to moderate amounts of quartz and feldspar are present with common skeletal fragments (foraminifera, bryozoan). The dark more rounded grains are glauconite, which do not luminesce under CL light (**see j**).

h-j Sample P430 (in g) under CL light at increasing exposure times. **h** calcite (orange) and plagioclase and orthoclase feldspar appear first at low exposure (light blue and green) followed by dark blue-violet coloured quartz at longer exposure times (**i-j**).

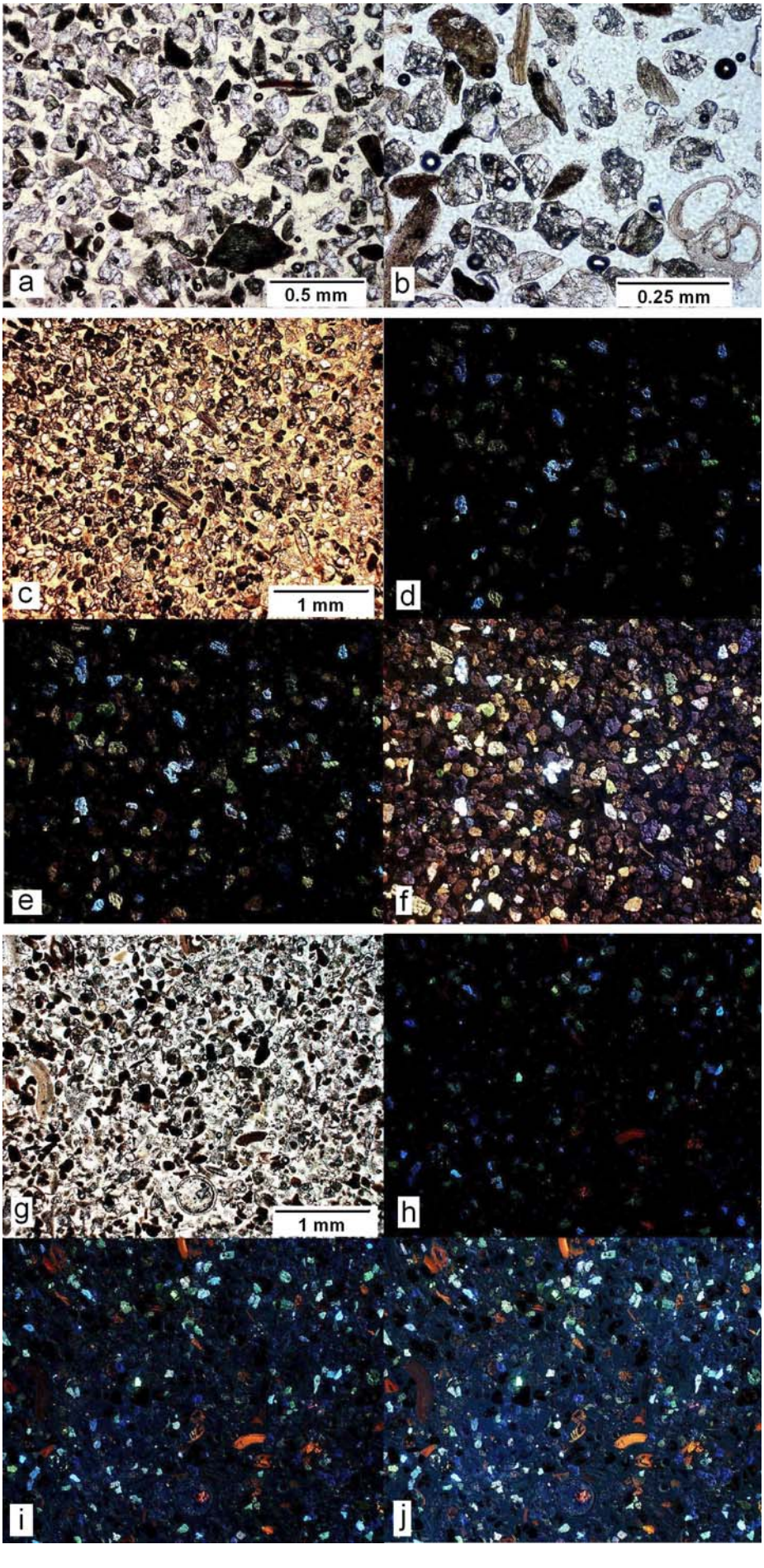
a
0.5 mm
b
0.25 mm
c
1 mm
d
e
f
g
1 mm
h
i
j

PLATE 2

Photomicrographs of some heavy mineral and mica grains in NKCM sediments

a Heavy mineral rich sample P599 (transect D). The dark heavy mineral fraction is obvious (40-50%) with abundant stubby to elongated brown-green hornblende grains and colourless to pale green augite grains. A moderate amount (c. 20-30%) of quartz and feldspar grains are also present with minor opaques, rock and skeletal fragments and oxyhornblende (red) grains.

b Heavy mineral rich sample P599 (in a) under cross polarised light. Where the original mineral colour does not obscure them, the green, pink, yellow and blue interference colours of augite and hornblende can be seen against the white to grey colours of quartz and feldspar.

c Heavy mineral rich sample P599 (transect D) at higher magnification. Brown-green stubby to elongate hornblende grains are obvious in the centre and right of the photomicrograph. Dirty or speckled quartz, feldspar and rock fragments are also present along with several colourless augite grains (see **d**).

d Heavy mineral rich sample P599 (in c) under cross polarised light. The higher interference colours (pink, yellow, green and dark blue) of the heavy mineral component and particularly the augite grains can be seen. The strong mineral colour of hornblende may obscure these interference colours. The quartz and feldspar grains show lower white to grey interference colours.

e Mica rich sample P594 (transect F). The long, thin elongated brown grains of biotite mica are clearly visible. This sample is also rich in skeletal grains, particularly planktic foraminifera and sponge spicules.

f High magnification photograph of a biotite grain in sample P409 (transect C). A sedimentary rock fragment is present to the left of the mica grain while the other grains are mainly dirty quartz or feldspar.

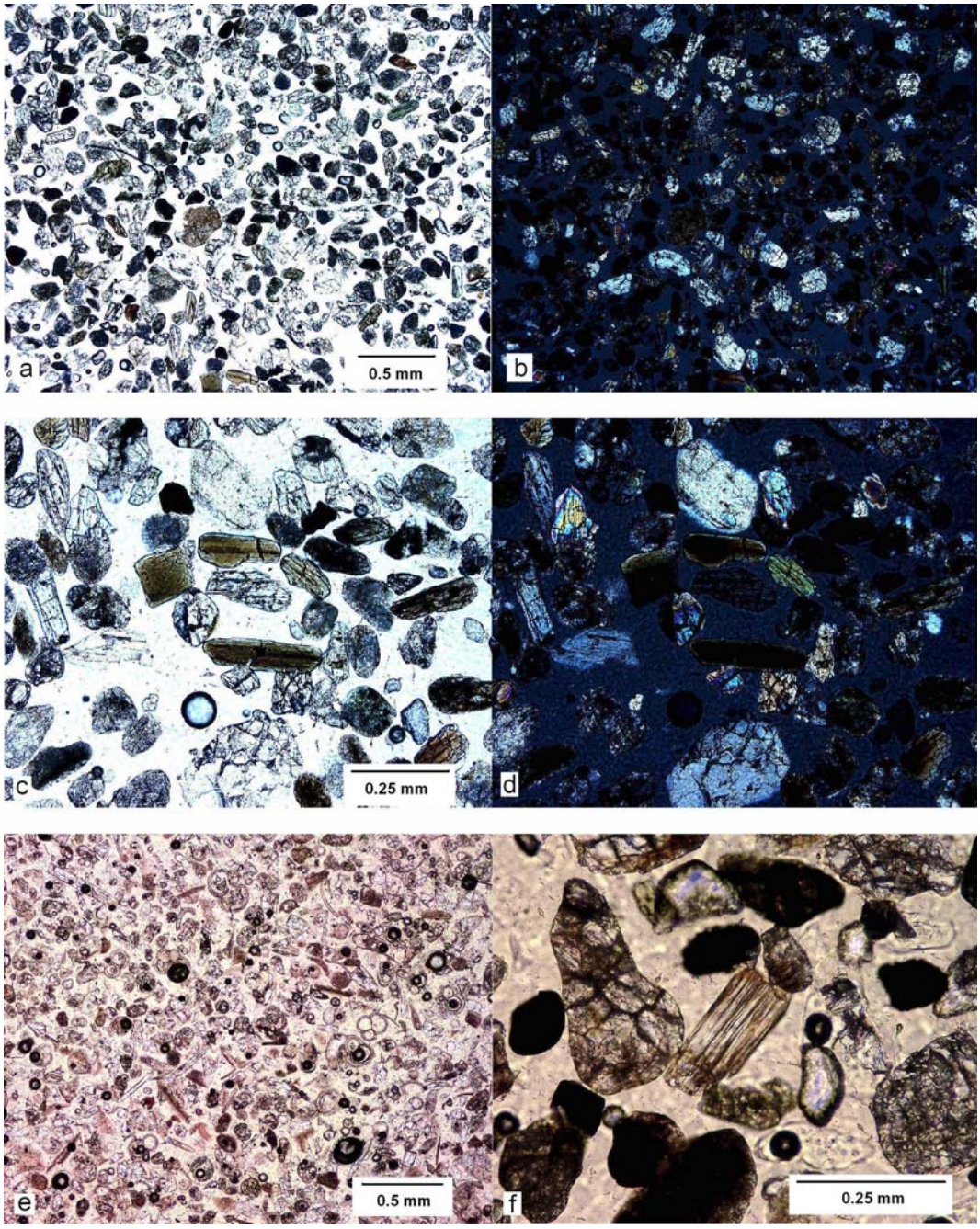
a
0.5 mm
b
c
0.25 mm
d
e
0.5 mm
f
0.25 mm

PLATE 3

Photomicrographs of rock fragments and glauconite in NKCM sediments

a Sedimentary rock fragment in sample P431 (transect G). The rock fragment comprises several large uneven sized crystals (quartz and/or feldspar) with little to no matrix or groundmass.

b-e Volcanic rock fragments in sample P431 (transect G). These fragments consist of numerous elongated feldspar crystals within a very fine-grained groundmass. The brown sedimentary rock fragment in **c** (top left) comprises moderately sized crystals mostly of the same size.

f Glauconite grains in sample P417 (transect D). Note the abundance of glauconite (>75%), its yellow to dark green colour and rounded pelletal texture with severe cracking and limonite staining.

g Glauconite grains in sample P421 (transect E). The glauconite in this sample is a brighter green and has less cracking and limonite staining than in P417 in **f**.

h Glauconite grains in **g** under cross polarised light showing the microcrystalline internal texture typical of glauconite.

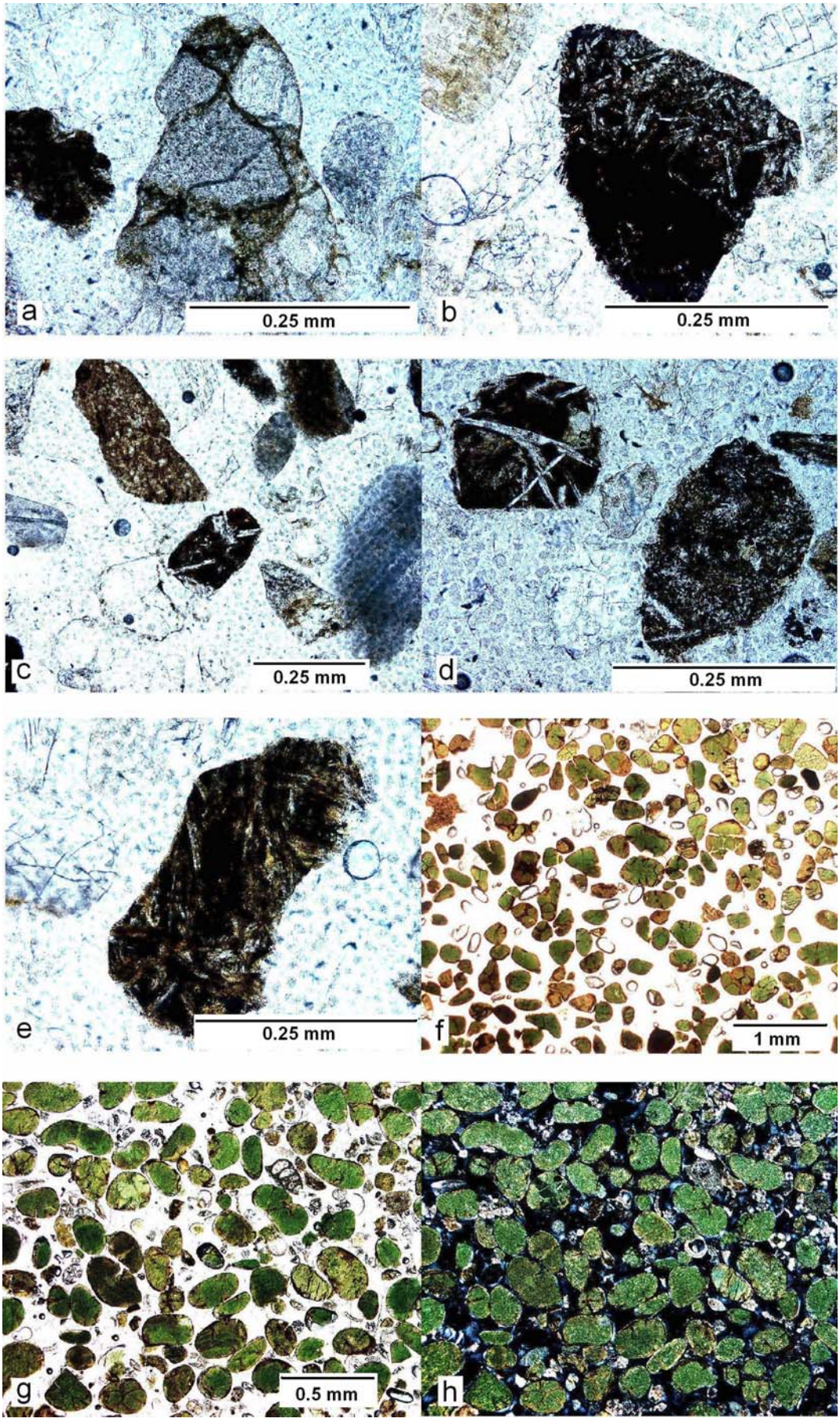
a
0.25 mm
b
0.25 mm
c
0.25 mm
d
0.25 mm
e
0.25 mm
f
1 mm
g
0.5 mm
h

PLATE 4

Photomicrographs of some skeletal fragments in NKCM sediments

a Large bivalve skeletal fragments within finer siliciclastic grains in sample P424 (transect F).

b A range of skeletal fragments in sample P422 (transect E). Bivalve and bryozoan fragments dominate with minor gastropod, foraminifera and serpulid skeletal grains.

c Bivalve, gastropod and bryozoan fragments in sample P422 (transect E).

d A highly degraded, limonite stained and endolith bored bivalve fragment in sample P422 (transect E).

e Bryozoan zooecia infilled with limonite or limonitised glauconite in sample P422 (transect E).

f A range of skeletal fragments including bryozoan and echinoderm in sample P434 (transect G). Note these fragments are less degraded than in sample P422 above (transect E).

g, h Endolithic borings in a bivalve or gastropod fragment in sample P422 (transect E). The borings are infilled with limonite.

i Mainly bivalve, bryozoan, foraminifera and sponge spicule fragments in sample P422 (transect E).

j Skeletal grains in sample P422 (in **i**) under CL light. The aragonitic bivalve fragments are blue while the calcitic bryozoan and foraminifera grains are orange. Note some foraminifera may comprise both calcite and aragonite and hence display both colours.

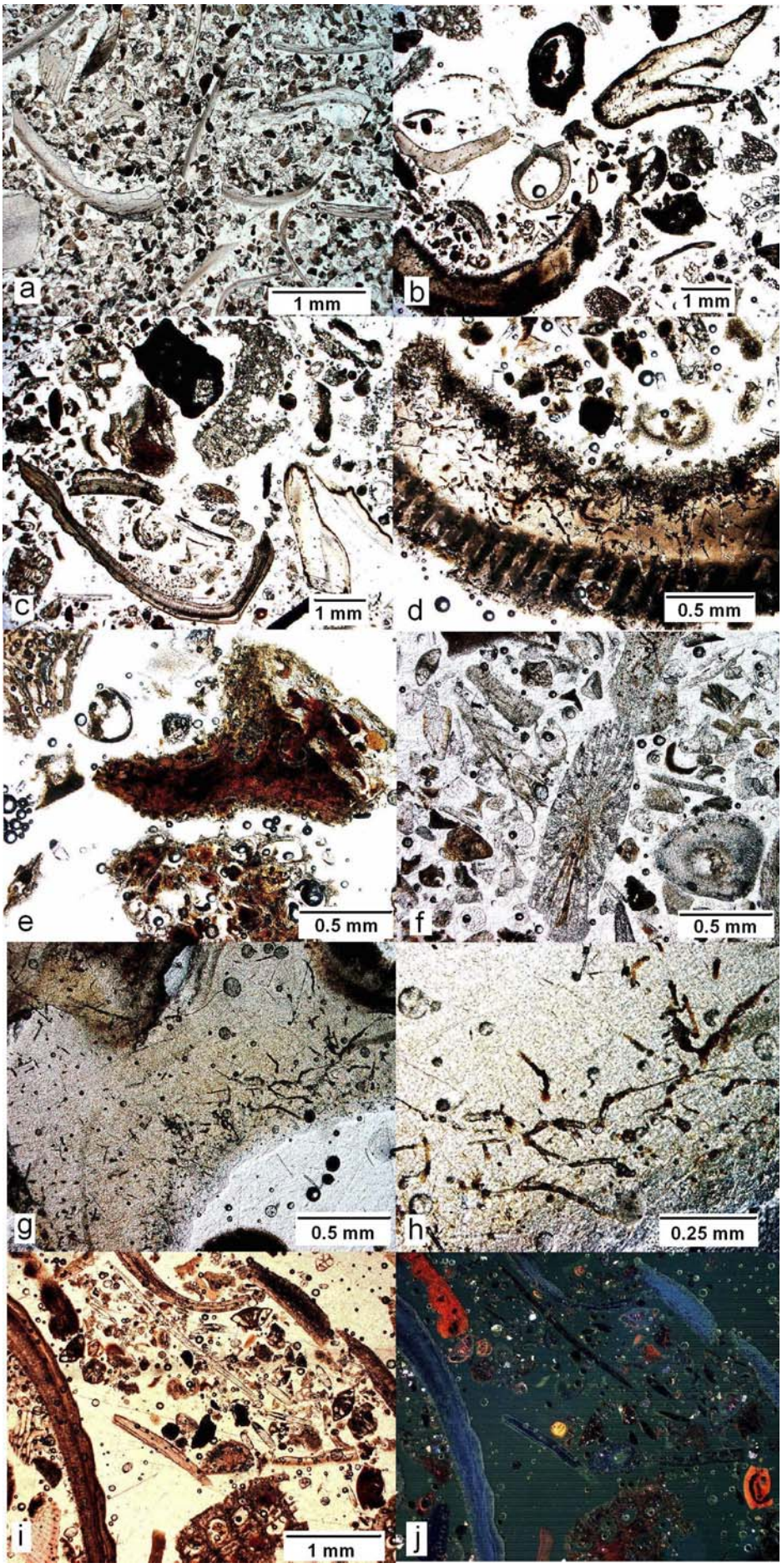
a
1 mm
b
1 mm
c
1 mm
d
0.5 mm
e
0.5 mm
f
0.5 mm
g
0.5 mm
h
0.25 mm
i
1 mm
j

PLATE 5

Photomicrographs of mixed carbonate-siliciclastic pellets in NKCM sediments

a Pelletal grains comprising quartz, feldspar, heavy mineral and skeletal grains in sample P427 (transect F). A darker coloured nucleus is apparent in five of these grains. The nuclei vary in size between grains.

b-d Pellets (as in **a**) under cathodoluminescence (CL) light at increasing exposure times. The quartz, feldspar and skeletal grains luminesce readily while the heavy minerals and matrix are non-luminescent.

e Pelletal grains lacking a significant nucleus in sample P427 (transect F).

f-h Pellets (in **e**) under CL light at increasing exposure times. As with the photographs above, the quartz, feldspar and skeletal grains luminesce readily while the heavy minerals and matrix do not even with long exposure times and consequent overexposure of other grain types (**h**).

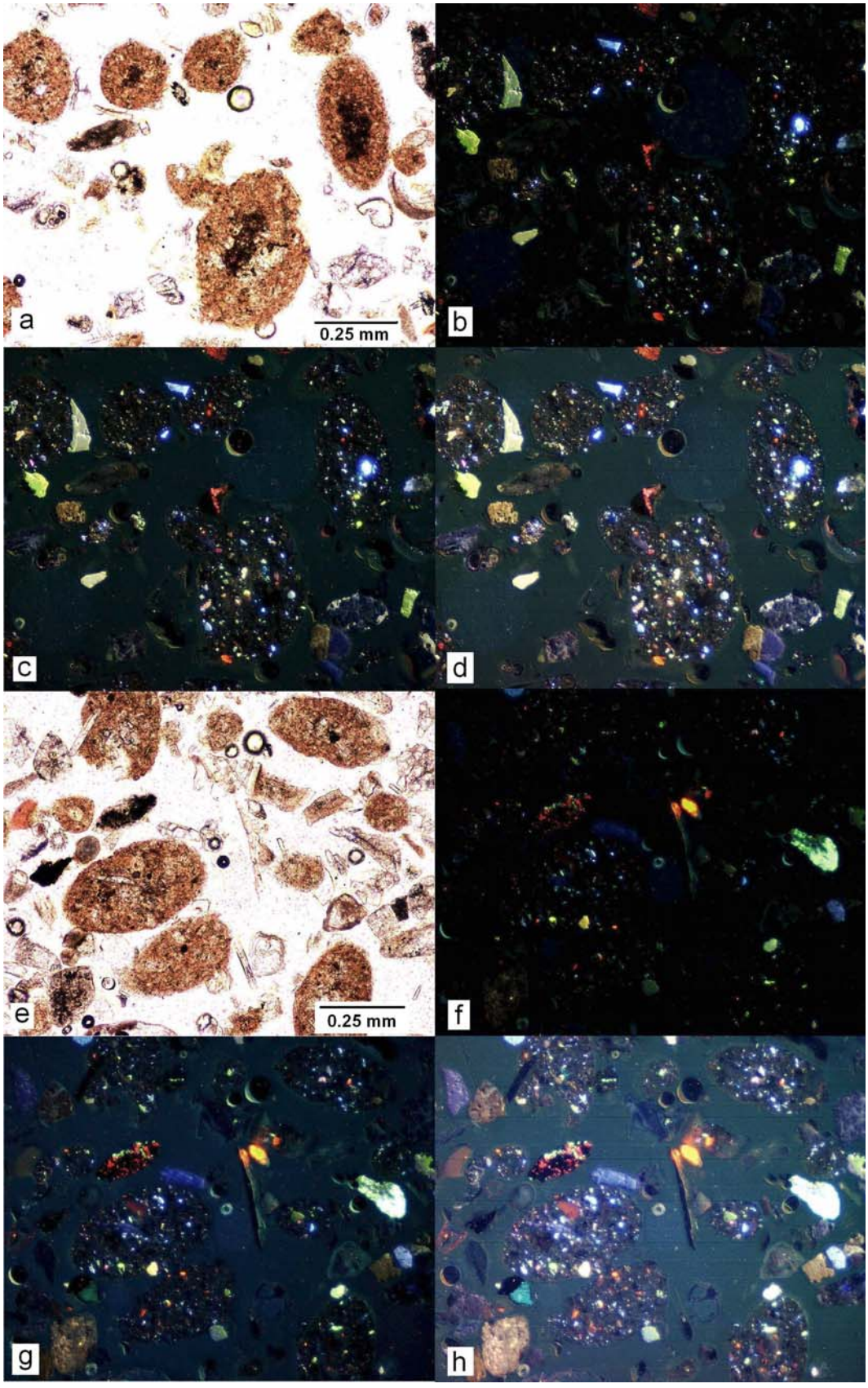
a
0.25 mm
b
c
d
e
0.25 mm
f
g
h

PLATE 6

Dominant bivalve species from NKCM sediments

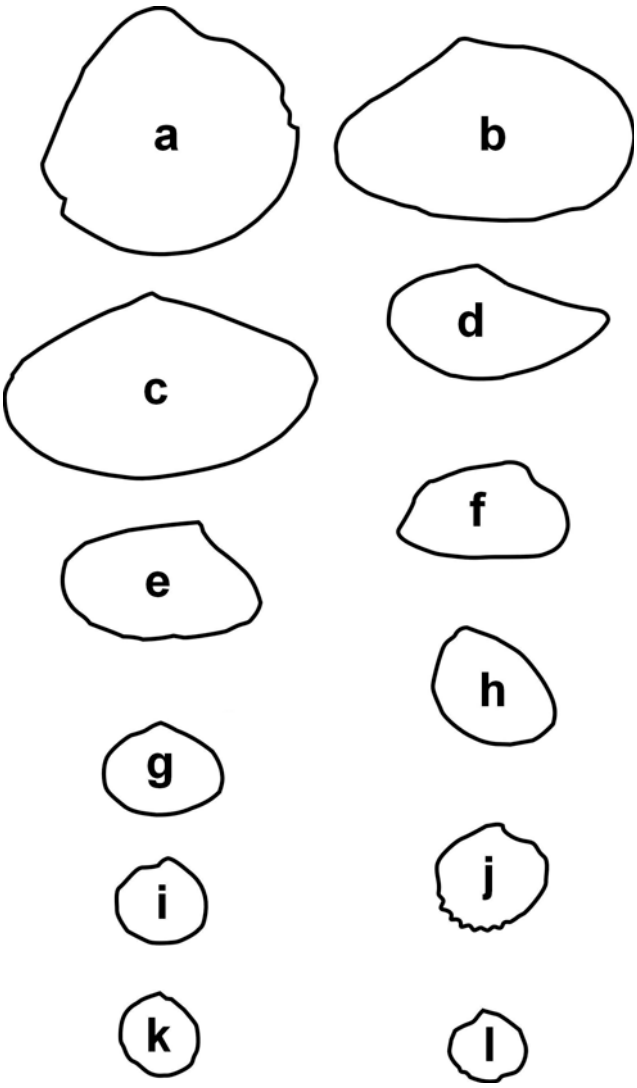

a *Pratulum pulchellum*
b *Serratina charlottae*
c *Scalpomactra scalpellum*
d *Saccella maxwelli*
e *Moerella huttoni*
f *Caryocorbula zelandica*
g *Leptomya retiaria Nucula nitidula*
h *Nucula nitidula*
i *Divaricella huttoniana*
j *Purpurocardia purpurata*
k *Limopsis lata*
l *Pleuromeris zelandica*


1 mm

PLATE 7

Selection of gastropod species from NKCM sediments

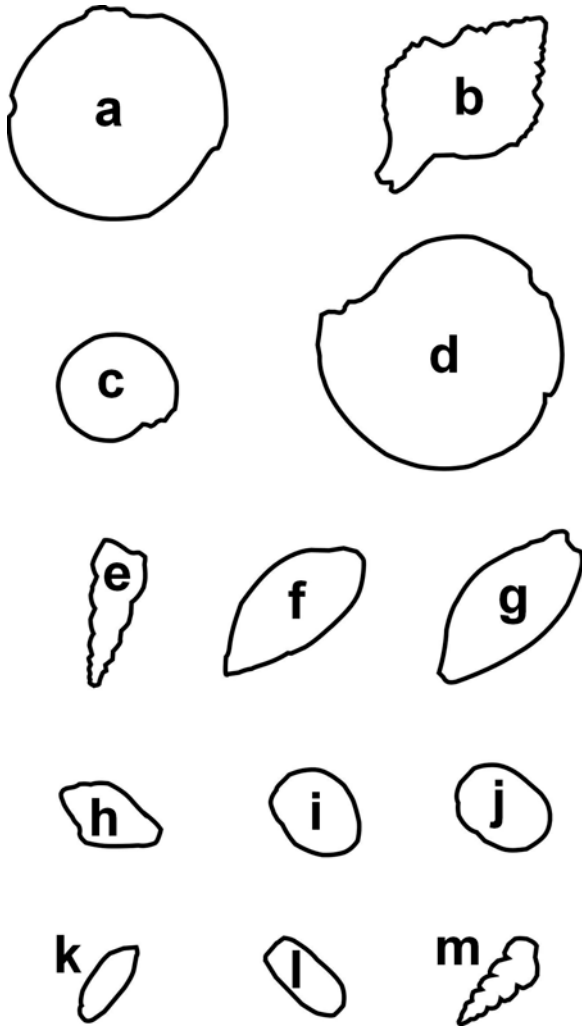

a *Sigapatella tenuis*
b *Austrofusus glans*
c *Antisolarium egenum*
d *Solatisonax supraradiata*
e *Stiracolpus pagoda*
f *Pupa affinis*
g *Amalda (Gracilispira) novaezelandiae*
h *Dentimargo fusula*
i *Uberella denticulifera*
j *Proxiuber australe*
k *Volvulella nesenta*
l *Retusa* sp.
m *Epitonium ?bucknilli*


1 mm

PLATE 8

SEM images of dominant benthic and planktic foraminifera in NKCM sediments

All scale bars = 0.1 mm

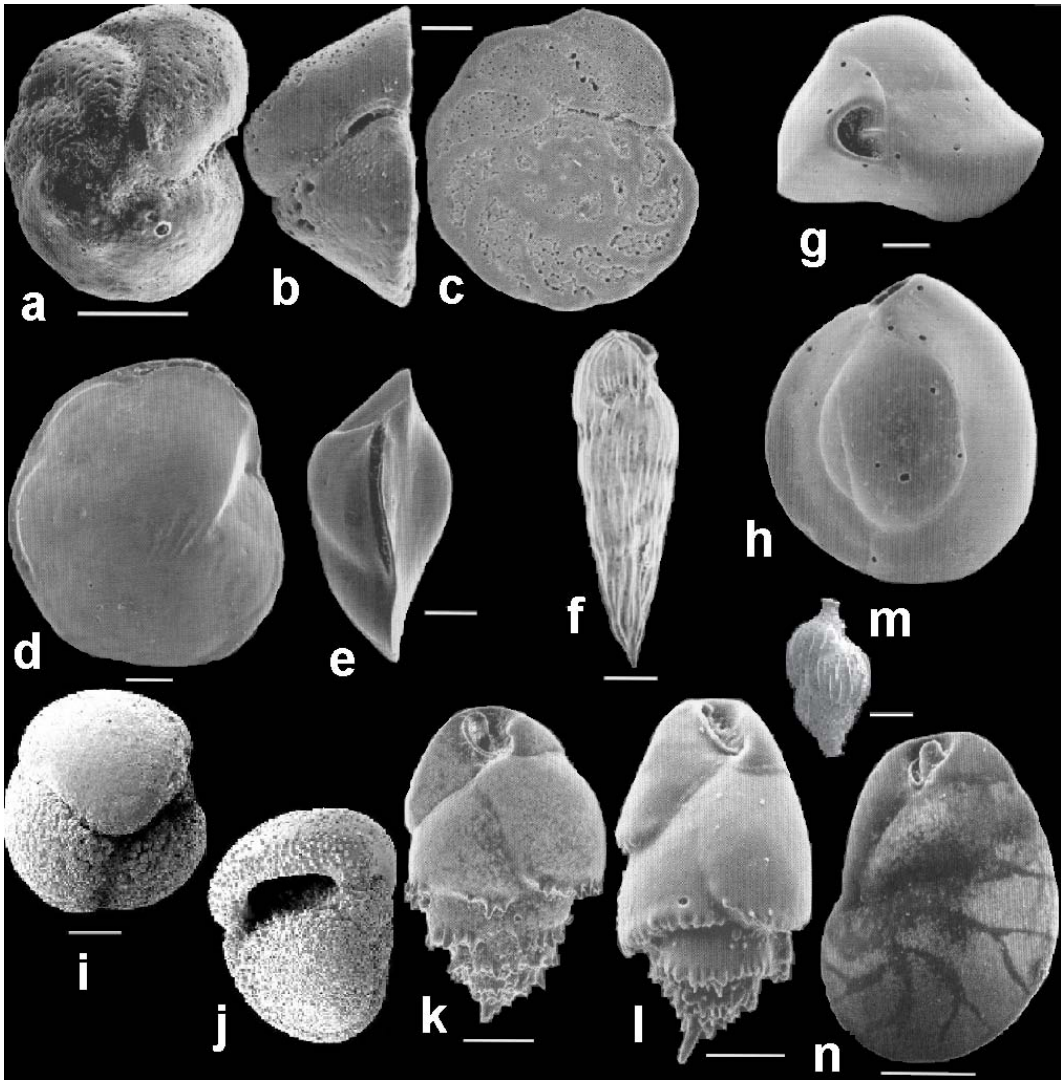

a, b, c	*Cibicides corticatus* (Hayward et al., 1999)
d, e	*Hoeglundina elegans* (Hayward et al., 1999)
f	*Saidovina karreriana* (Hayward et al., 1999)
g, h	*Quinqueloculina auberiana* (Hayward et al., 1999)
i, j	*Globorotalia inflata* (obtained from B.W. Hayward, Geomarine Research)
k, l	*Bulimina marginata* f. *marginata* (Hayward et al., 1999)
m	*Uvigerina peregrina* (Hayward et al., 2003)
n	*Evolvocassidulina orientalis* (from Hayward et al., 1999)

PLATE 9

Grades used to assess the preservation of skeletal material

a, b Grade 1: Fresh = shells brightly coloured, shiny, mostly whole. **a** = P423, **b** = P424

c, d Grade 2: Mixed fresh-relict = shells mostly broken, faded appearance/colour. **c** = P435 **d** = P433

e, f Grade 3: Relict = shells all broken, bleached, grey colour, some boring and breakdown of shell surface. **e, f** = P429

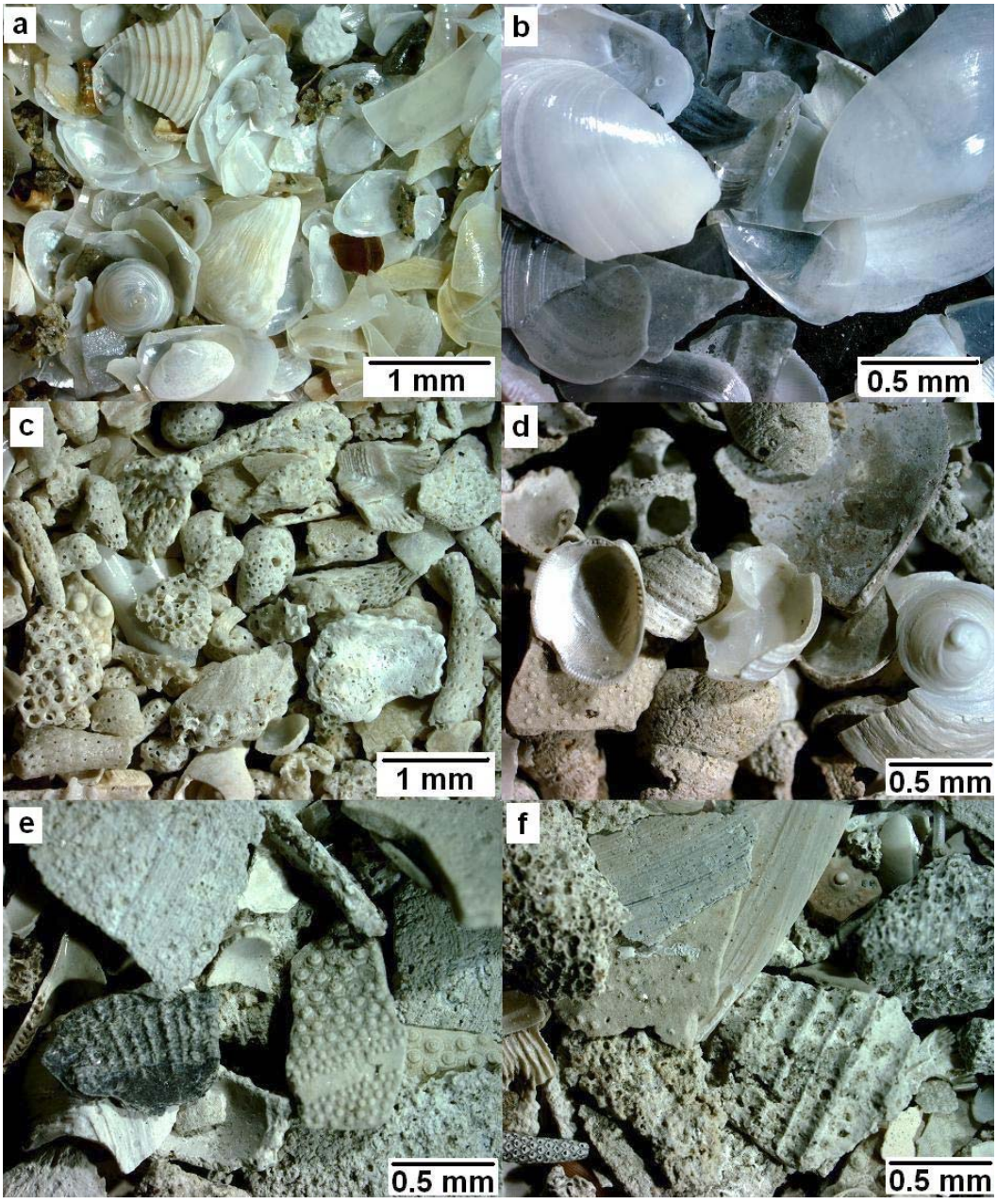
a
1 mm
b
0.5 mm
c
1 mm
d
0.5 mm
e
0.5 mm
f
0.5 mm

PLATE 10

Photomicrographs of glauconite morphology varieties observed on NKCM

a Bulk glauconite sample from P421 at 153 m water depth. Note the dominance of polished, highly evolved glauconite grains with common iron stained sutures. The glauconite is both well rounded and well sorted.

b, c Ovoidal or spheroidal glauconite grains from P421 (153 m water depth). The grains are predominantly dark green to black and have mostly mammillated surfaces with iron stained sutures common. This morphology dominates the NKCM glauconite.

d Tabular or discoidal glauconite grains from P421 (153 m water depth). The grains comprise dark green to black flattened disc-like grains with mostly simple surfaces that appear polished.

e A lobate glauconite grain from P420 (184 m water depth). The grains are irregular in shape, like popcorn, and usually light green in colour with well-developed sutures infilled by mostly white crystalline material.

f Vermicular glauconite grains from P421 (153 m water depth). These grains are dark green to black with a curved concertina appearance and iron staining in the sutures. They also have smooth surfaces and appear polished.

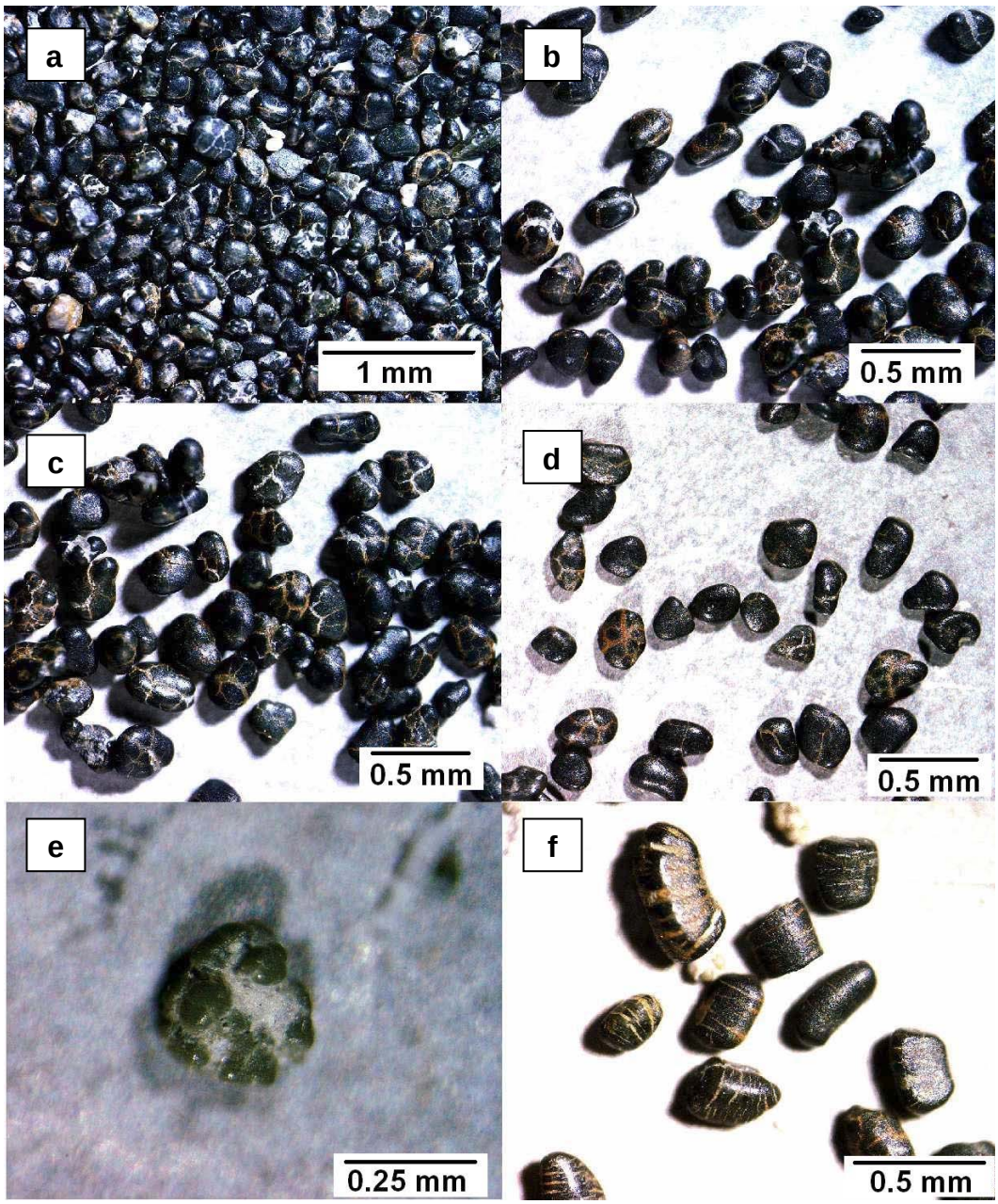
a
1 mm
b
0.5 mm
c
0.5 mm
d
0.5 mm
e
0.25 mm
f
0.5 mm

PLATE 11

Photomicrographs of glauconite morphology varieties observed on NKCM

a An internal mould of a benthic foraminifera from P420 (184 m water depth). These grains are mostly light green and are predominantly shaped in the form of foraminiferal tests (both benthic and planktic) with lesser amounts of bryozoan shaped grains. This particular example is more evolved and has developed a dark green colour.

b Internal moulds from P421 (153 m water depth). These grains are light brown and are shaped like planktic foraminifera with poorly developed sutures. The grains to the top left are of vermicular morphology.

c Internal mould of a benthic foraminifera from P421 (153 m water depth). This grain is also light brown and has some of the original test remaining.

d Internal mould of a planktic foraminifera (centre) from P421 (153 m water depth). Most of the original test shell is still present. The surrounding glauconite grains are all of vermicular morphology.

e Composite glauconite grain from P420 (184 m water depth). The grain comprises several large and small glauconite grains with a matrix of white crystalline material.

f Composite glauconite grain from P420 (184 m water depth). The grain comprises mostly matrix of white crystalline material with only a few small glauconite grains present.

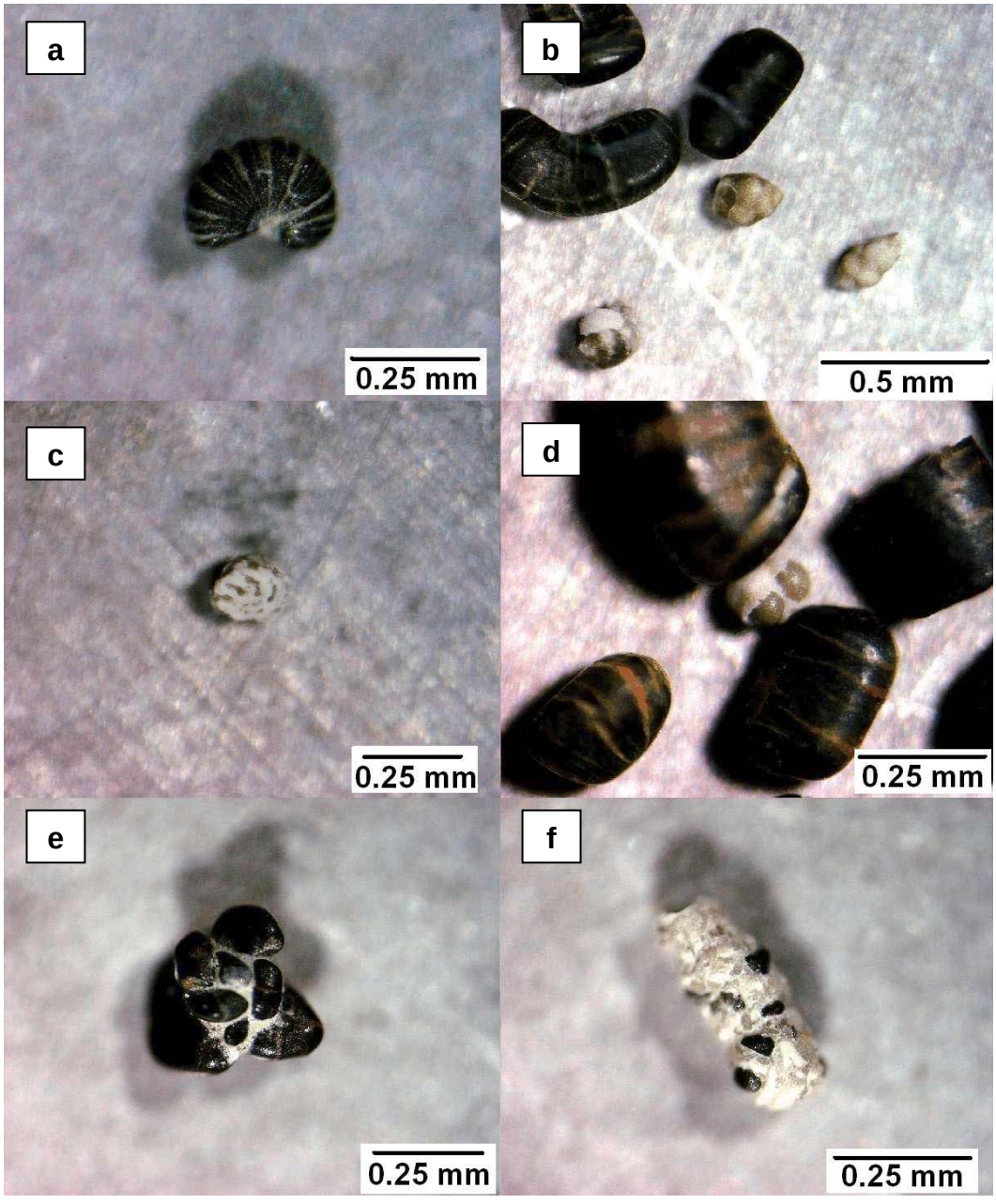
a
0.25 mm
b
0.5 mm
c
0.25 mm
d
0.25 mm
e
0.25 mm
f
0.25 mm

PLATE 12

Photomicrographs of Facies 1 (siliciclastic sand)-siliciclastic dominated slightly gravelly sand and slightly gravelly muddy sand

1a Well to very well sorted quartzofeldspathic sand facies. This facies generally consists of greater than 30% of both quartz and feldspar but may reach between 40 and 50% of each and is restricted to the shelf at less than 100 m water depth in the northern half of the NKCM and generally less than c. 200 m depth in the southern half. Examples are from P407, P408 and P405 (left to right).

1b Well to very well sorted heavy mineral dominated facies. This facies has a heavy mineral concentrations greater than 30% and up to between 50 and 75%. This facies occurs at less than 50 m water depth along transects C and D. Examples are from P409 and P599 (x2).

1c Moderately sorted mica rich facies. This facies consists of fine grained quartz, feldspar and mica (c. 20-30% each) and occurs at one sample site (P606) at 300 m water depth along transect B.

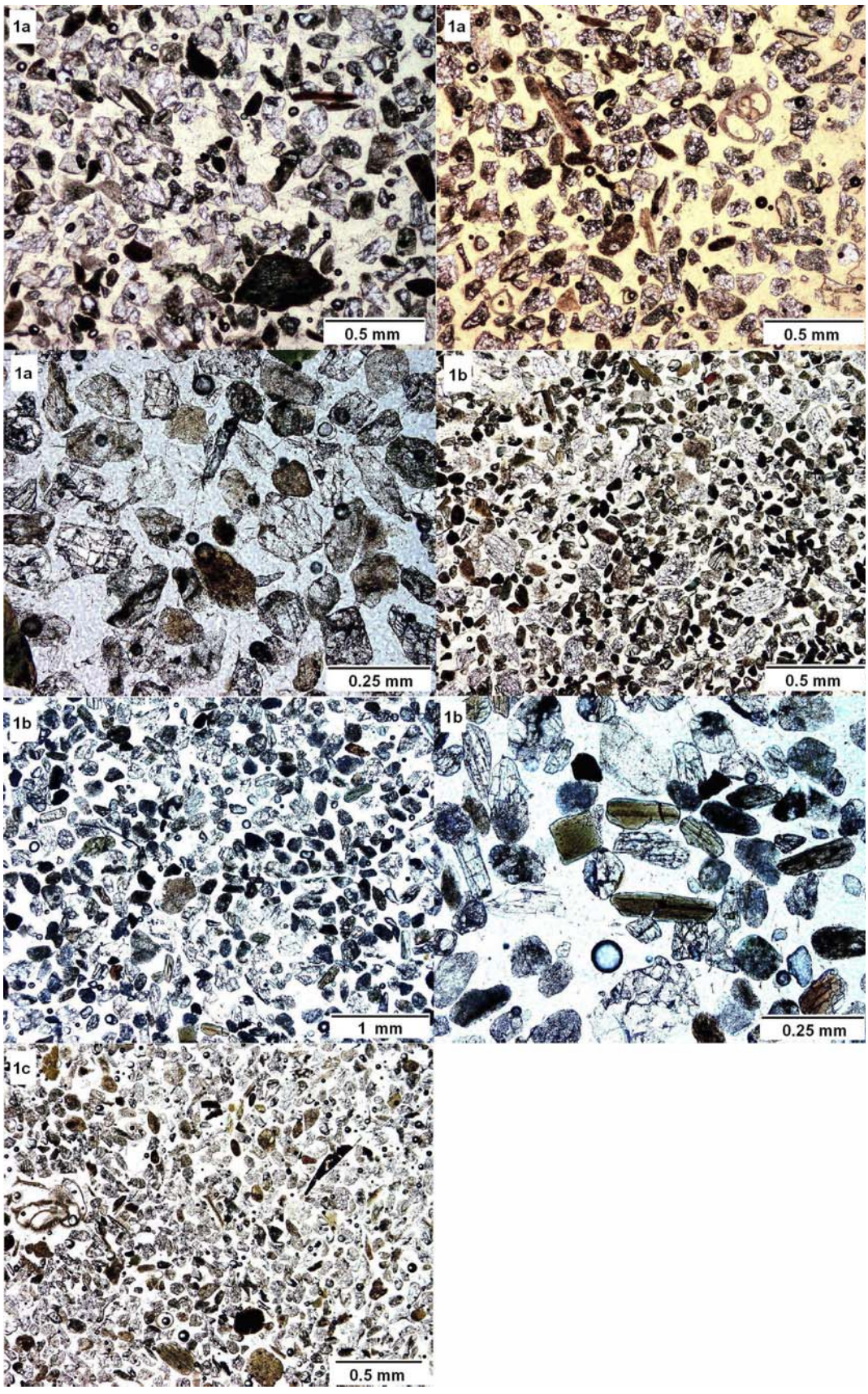
1a
0.5 mm
1a
0.5 mm
1a
0.25 mm
1b
0.5 mm
1b
1 mm
1b
0.25 mm
1c
0.5 mm

PLATE 13

Photomicrographs of Facies 2, 3 and 4

2 Glauconite dominated slightly gravelly sand and slightly gravelly muddy sand facies. This facies consists of moderately to moderately well sorted, medium to fine sand containing greater than 30% glauconite grains with concentrations, which may exceed 75%. This facies occurs between 150 and 400 m water depth in central NKCM offshore from Tauroa Point. Examples are from P421 and P420 (left to right).

3 Coarse bryozoan dominated sandy and muddy gravels, slightly gravelly sand and slightly gravelly muddy sand facies. This facies generally consists of well to very well sorted abundant bryozoan skeletal material greater than 0.5 mm in size. The samples in this facies contain greater than 40% bryozoan material overall with most samples consisting of greater than 70%. This facies only occurs in the northern half of the NKCM at 30-150 and 190-300 m water depth along transect G, 200-400 m depth along transect F and c. 90 m water depth along transect E. Examples are from P435 and P422.

4 Pellet dominated gravelly sandy mud facies. muddy sediment dominated by greater than c. 30% mixed carbonate-siliciclastic pellets with minor foraminifera and opaline spines. The sediment in this facies consists of moderately well sorted to poorly sorted very fine sand and mud with the mud content exceeding 50%. This facies occurs in a small area of 100-150 m water depth in the northern half of the NKCM. Examples are from P427.

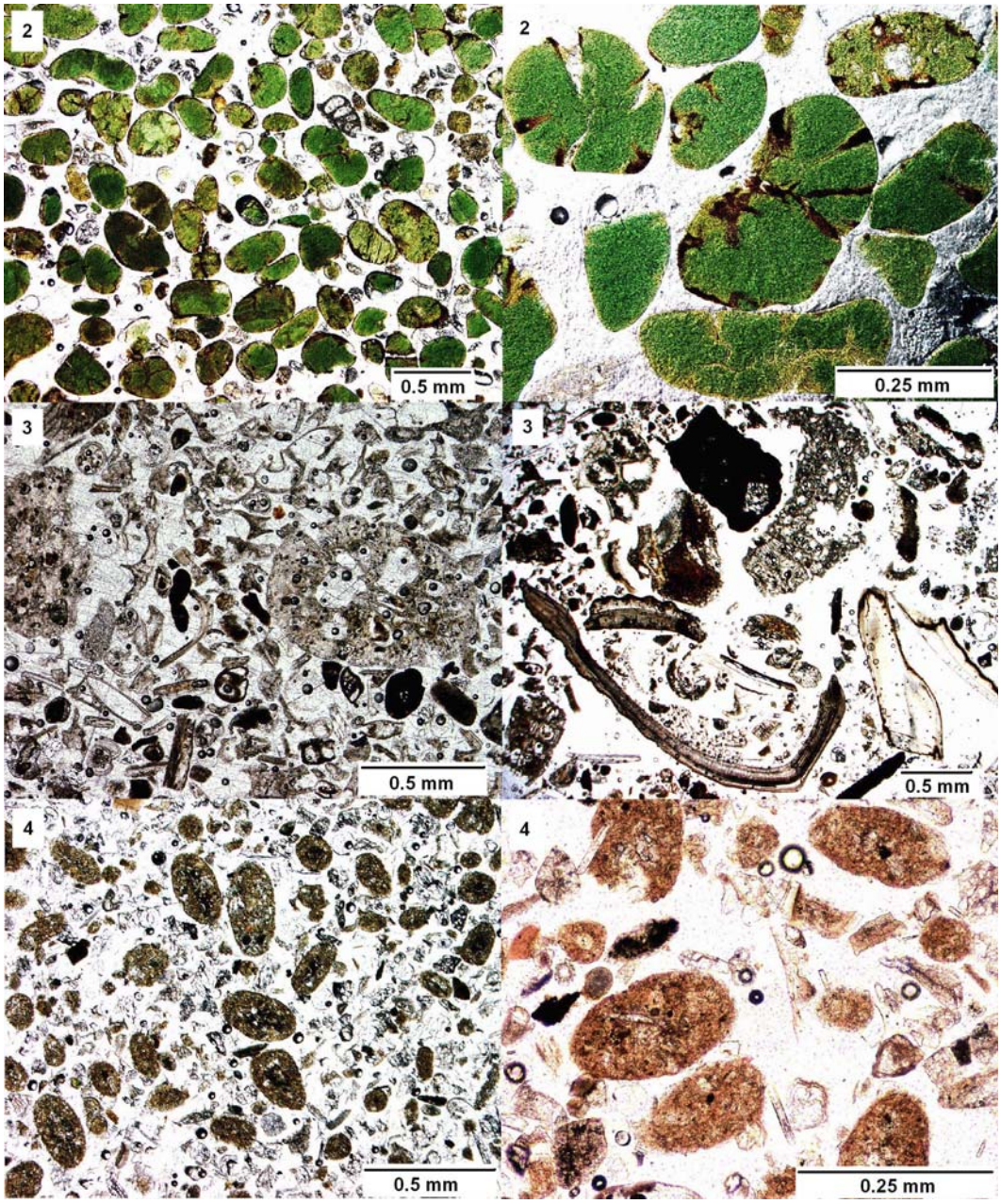
2
0.5 mm
2
0.25 mm
3
0.5 mm
3
0.5 mm
4
0.5 mm
4
0.25 mm

PLATE 14

Photomicrographs of Facies 5- foraminifera dominated muddy and sandy sediments

5a Foraminifera dominated mud facies. This facies consists of at least 30% foraminiferal tests (dominated by planktics) with minor echinoderm fragments, opaline spines and mixed carbonate-siliciclastic pellets. It also comprises greater than 50% mud sized sediment with most samples containing greater than 80% mud. It occurs at greater than 400 m water depth covering most of the slope in the southern half of the NKCM. Examples are from P602 and P605 (left to right).

5b Foraminifera dominated sand facies. This facies also consists of at least 30% foraminiferal tests with minor echinoderm fragments, opaline spines and mixed carbonate-siliciclastic pellets. It generally contains greater than 70% sand sized sediment. The facies occurs in two separate depth: a deeper water band at generally greater than 400 m depth along transects D, E and F, and a shallower band at mid to outer shelf depths between c. 150 and 200 m water depth along transects D, F and G. Planktic foraminifera dominates the deeper band while benthic foraminifera dominate the shallower band. Examples are from P594.

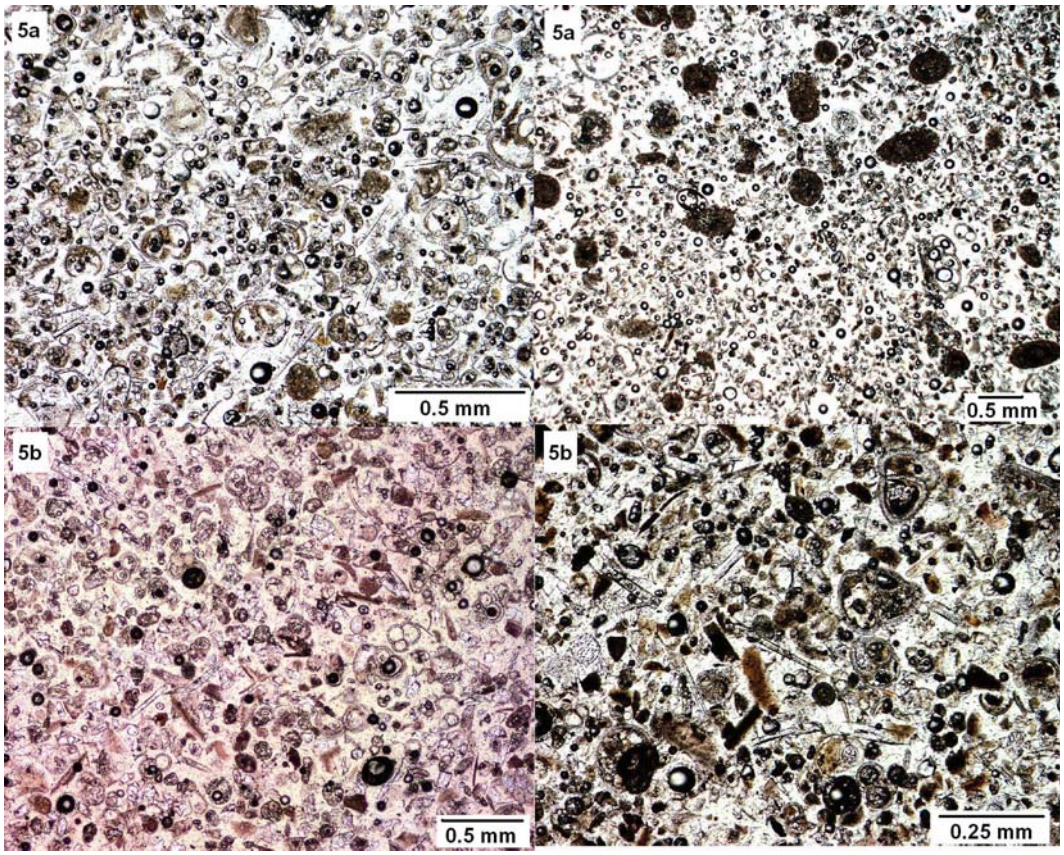
5a
0.5 mm
5a
0.5 mm
5b
0.5 mm
5b
0.25 mm

Appendix A: Localities maps

Map A: Localities in New Zealand mentioned in the text.

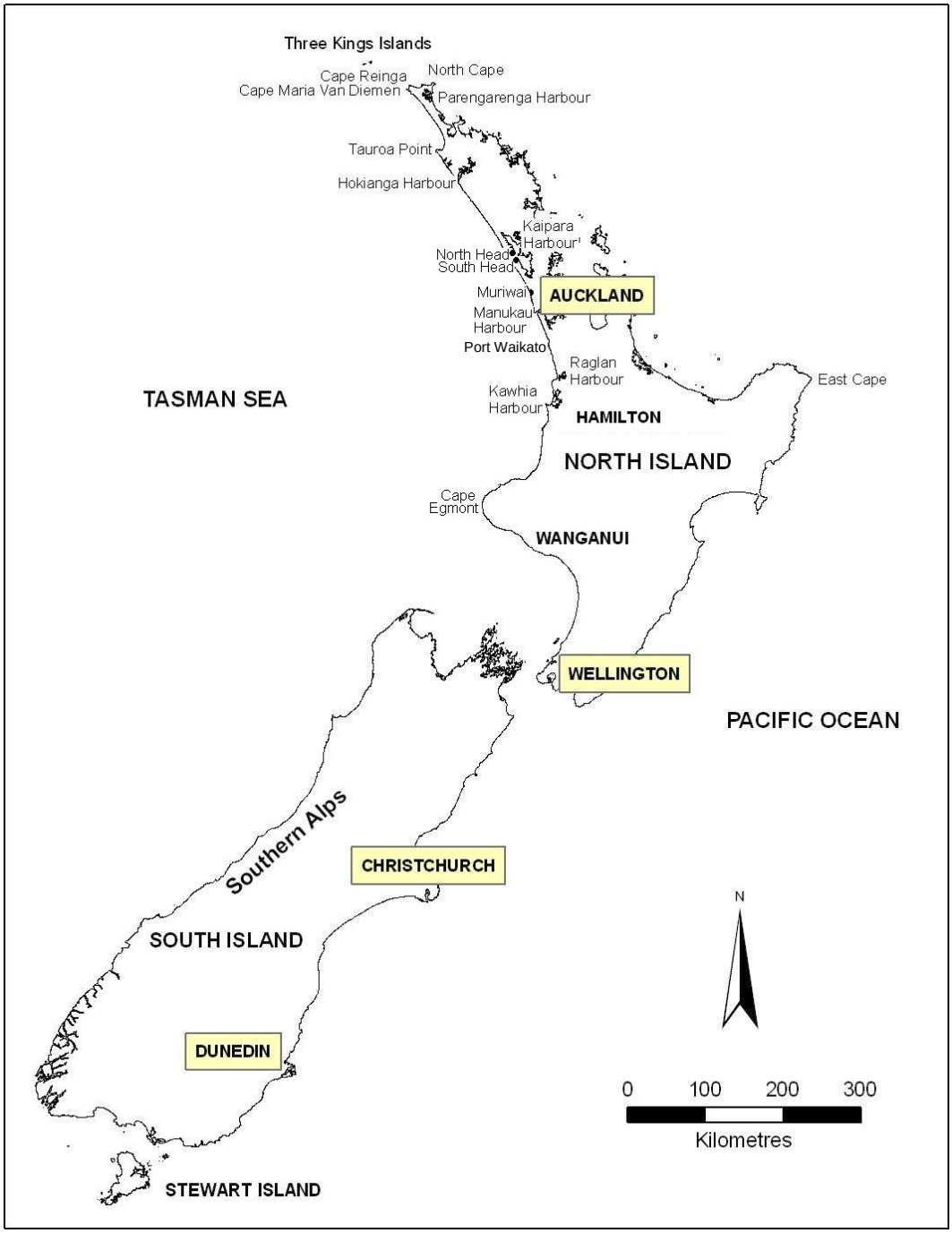

Map B: Localities in Northland mentioned in the text.

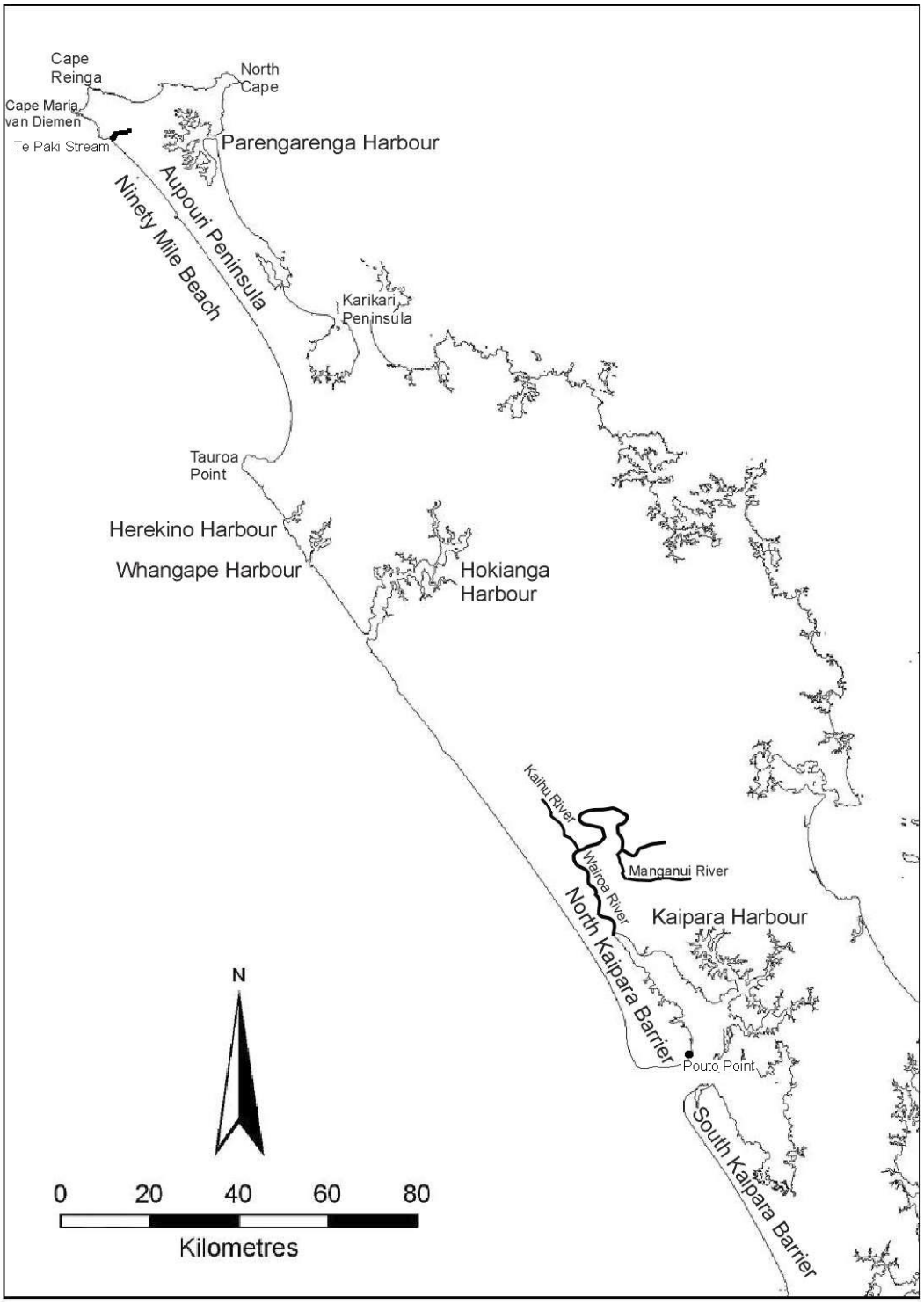

Appendix B: Sample locations

Note: Station sites are listed in running order.

Station No.	Lat.	Long.	Depth (m)	Remarks	Type
P397	36 23.8	173 43.5	216	slightly muddy and glauconitic very fine sand	O.P. Grab
P398	36 23.9	173 45.3	149	slightly muddy and glauconitic very fine sand	O.P. Grab
P399	36 22.7	173 46.1	107	glauconitic very fine sand	O.P. Grab
P400	36 17.9	173 53.5	70	slightly shelly and glauconitic fine sand	O.P. Grab
P401	36 16.0	173 55.2	42	fine sand	O.P. Grab
P402	36 15.0	173 56.0	33	fine sand	O.P. Grab
P403	35 58.5	173 43.8	34	fine sand	O.P. Grab
P404	36 00.0	173 39.8	63	slightly shelly very fine sand	O.P. Grab
P405	36 01.3	173 38.0	86	slightly shelly very fine sand	O.P. Grab
P406	36 02.0	173 36.9	110	slightly glauconitic and shelly very fine sand	O.P. Grab
P407	36 02.5	173 36.1	161	slightly glauconitic very fine sand	O.P. Grab
P408	36 03.3	173 35.7	206	slightly glauconitic fine sand	O.P. Grab
P409	35 40.3	173 27.0	38	fine sand	O.P. Grab
P410	35 42.4	173 25.1	67	slightly shelly very fine sand	O.P. Grab
P411	35 43.4	173 22.4	85	slightly shelly very fine sand	O.P. Grab
P412	35 44.4	173 21.6	110	slightly shelly glauconitic very fine sand	O.P. Grab
P413	35 46.0	173 19.2	161	glauconitic very fine sand	O.P. Grab
P414	35 47.2	173 17.9	216	glauconitic very fine sand	O.P. Grab
P415	35 35.3	172 43.8	512	cream clayey silt	Pipe Dredge
P416	35 29.2	172 54.6	355	fine glauconitic sand	O.P. Grab
P417	35 26.8	172 59.3	183	fine glauconitic sand, bioturbated "clods" included	Pipe Dredge
P418	35 25.6	173 01.4	149	slightly muddy and glauconitic very fine sand	Pipe Dredge
P419	35 22.4	173 02.0	108	slightly glauconitic very fine sand	O.P. Grab
P420	34 59.1	172 28.4	184	medium glauconitic sand	Pipe Dredge
P421	34 59.7	172 39.9	153	very muddy fine glauconitic sand	O.P. Grab
P422	34 59.6	172 47.2	92	gravelly shelly mud, rock outcrops on sounder	Pipe Dredge
P423	34 59.4	172 58.4	52	slightly shelly fine sand	O.P. Grab
P424	34 45.6	172 49.6	55	shelly very fine sand	O.P. Grab
P425	34 44.6	172 44.2	78	slightly shelly and sandy mud	O.P. Grab
P426	34 45.3	172 40.9	108	mud	O.P. Grab
P427	34 45.6	172 33.3	144	mud	O.P. Grab
P428	34 45.6	172 28.0	158	slightly glauconitic very muddy very fine sand	Pipe Dredge
P429	34 45.8	172 18.3	206	glauconitic very fine sand	Pipe Dredge
P430	34 45.7	172 13.4	411	shelly glauconitic fine sand	Pipe Dredge

Station No.	Lat.	Long.	Depth (m)	Remarks	Type
P431	34 30.5	172 22.0	104	medium shell sand	Pipe Dredge
P432	34 25.0	172 16.6	147	slightly shelly fine-medium sand	Pipe Dredge
P433	34 28.8	172 12.8	190	intermixed coarse shell sand and grey mud	Pipe Dredge
P434	34 29.2	172 04.3	297	very coarse shell sand	Pipe Dredge
P435	34 29.7	171 57.9	395	coarse shell sand	Pipe Dredge
P443	34 28.7	172 30.9	65	gravelly very coarse shell hash	Pipe Dredge
P444	34 29.1	172 35.8	30	some pebbles, coarse shell hash, sponge/seaweed	Pipe Dredge
P592	34 29.5	172 13.6	204	open later	Piston Corer
P594	34 45.2	172 01.0	1015	muddy very fine sand	Mod.Biol.Dredge*
P595	34 46.0	172 06.7	710	slightly muddy and glauconitic fine sand	Mod.Biol.Dredge
P596	34 59.1	172 12.2	598	muddy very fine sand	Mod.Biol.Dredge
P597	34 57.8	172 18.1	400	slightly shelly glauconitic medium sand	Mod.Biol.Dredge
P598	35 34.6	172 49.5	455	mud	Mod.Biol.Dredge
P599	35 20.0	173 09.0	42	fine sand	O.P. Grab
P600	35 20.8	173 07.2	65	fine sand, also 1.1 m core of sand over a basal shell layer at 68 m depth	Mod.Biol.Dredge & corer
P601	35 51.5	173 12.7	405	0.45 m core of glauconitic sand over mud	Piston Corer
P602	35 56.7	173 07.5	622	mud	Mod.Biol.Dredge
P603	36 14.5	173 16.0	1050	mud	Mod.Biol.Dredge
P604	36 11.2	173 22.8	838	mud	Mod.Biol.Dredge
P605	36 07.2	173 31.0	478	mud	Mod.Biol.Dredge
P606	36 04.8	173 33.8	300	muddy fine sand	Mod.Biol.Dredge
P607	36 18.8	173 49.0	90	very muddy fine sand	Mod.Biol.Dredge

* Modern biological dredge
O.P. grab = orange peel grab.

Appendix C: Description data

Table 1. Calculation of % gravel, % sand and % mud. Note: Samples are listed in running order.

Sample	wgt gravel	wgt sand	wgt mud	total wt	% gravel	% sand	% mud
P397	0.20	1215.20	143.90	1359.30	0.01	89.40	10.60
P398	1.32	1151.44	194.95	1347.71	0.10	85.44	14.47
P399	1.11	1358.88	184.05	1544.04	0.07	88.01	11.92
P400	32.58	1592.67	36.60	1661.85	1.96	95.84	2.20
P401	1.70	1757.25	14.15	1773.10	0.10	99.11	0.80
P402	0.22	1873.05	8.75	1882.02	0.01	99.52	0.46
P403	36.90	1796.90	-	1833.80	2.01	97.99	0.00
P404	9.90	1353.17	5.65	1368.72	0.72	98.86	0.41
P405	10.22	1611.66	33.40	1655.28	0.62	97.36	2.02
P406	13.97	1578.87	54.65	1647.49	0.85	95.83	3.32
P407	0.83	1386.13	112.30	1499.26	0.06	92.45	7.49
P408	0.73	1423.90	80.50	1505.13	0.05	94.60	5.35
P409	5.42	1639.76	8.00	1653.18	0.33	99.19	0.48
P410	43.81	1875.82	7.20	1926.83	2.27	97.35	0.37
P411	16.64	1445.32	22.00	1483.96	1.12	97.40	1.48
P412	7.40	1706.02	72.50	1785.92	0.41	95.53	4.06
P413	2.22	1551.76	126.45	1680.43	0.13	92.34	7.52
P414	-	1614.03	109.50	1723.53	-	93.65	6.35
P415	0.45	494.83	579.50	1074.78	0.04	46.04	53.92
P416	0.13	1166.50	109.50	1276.13	0.01	91.41	8.58
P417	0.82	1957.63	127.50	2085.95	0.04	93.85	6.12
P418	164.45	782.60	427.00	1374.05	11.97	56.96	31.00
P419	8.51	837.12	95.50	941.13	0.91	88.95	10.15
P420	5.28	1890.57	33.40	1929.25	0.27	98.00	1.73
P421	0.34	1126.81	434.40	1561.55	0.02	72.16	27.82
P422	667.30	257.43	450.00	1374.73	48.54	18.73	32.74
P423	7.13	1712.14	-	1719.27	0.42	99.59	-
P424	316.75	1564.90	89.00	1970.65	16.08	79.41	4.52
P425	7.90	696.30	404.50	1108.70	0.72	62.81	36.49
P426	1.60	425.10	499.50	926.20	0.18	45.90	53.93
P427	0.60	195.64	267.50	463.74	0.13	42.19	57.69
P428	3.35	933.21	363.50	1300.06	0.26	71.79	27.96
P429	50.78	1073.50	458.50	1582.78	3.21	67.83	28.97
P430	71.20	1297.45	6.00	1374.65	5.18	94.39	0.44
P431	43.00	1934.84	-	1977.84	2.18	97.83	-
P432	24.32	1615.33	-	1639.65	1.49	98.52	-
P433	27.30	1123.10	393.10	1543.50	1.77	72.77	25.47
P434	30.40	903.55	-	933.95	3.26	96.75	-
P435	92.11	935.59	-	1027.70	8.97	91.04	-
P443	951.38	306.42	6.00	1263.80	75.28	24.25	0.48
P444*	-	-	-	-	-	-	-
P594	0.50	570.77	92.00	663.27	0.08	86.05	13.87
P595	0.48	903.78	8.00	912.26	0.05	99.07	0.88
P596	0.95	487.44	74.00	562.39	0.17	86.67	13.16
P597	19.41	626.13	4.50	650.04	2.99	96.32	0.69
P598	0.18	462.15	311.50	773.83	0.02	59.72	40.25

Table 1 cont. Calculation of % gravel, % sand and % mud.

Sample	wgt gravel	wgt sand	wgt mud	total wt	% gravel	% sand	% mud
P599	1.79	975.55	-	977.34	0.18	99.82	-
P600	24.00	1180.80	5.00	1209.80	1.98	97.60	0.41
P602	-	70.04	452.00	522.04	-	13.42	86.58
P603	-	34.07	302.00	336.07	0.00	10.14	89.86
P604	-	87.00	784.00	871.00	0.00	9.99	90.01
P605	0.01	183.00	743.50	926.51	0.001	19.75	80.25
P606	0.18	700.40	54.50	755.08	0.024	92.76	7.22
P607	1.31	688.35	93.50	783.16	0.167	87.89	11.94

* Insufficient sample to measure

Table 2. Sediment parameters. Note: Samples are listed in running order.

Station No.	C	Median Md	Mean M_2	Sorting σ_I	Skewness Sk_I	Kurtosis K_G
P397	1.60	3.10	3.15	0.95	0.49	4.46
P398	2.40	3.10	3.22	1.27	0.65	4.10
P399	2.40	3.10	3.20	1.19	0.59	4.04
P400	1.40	2.90	2.93	0.37	0.11	1.33
P401	2.10	2.90	2.87	0.26	-0.04	1.23
P402	2.05	2.75	2.78	0.21	0.27	0.96
P403	1.35	2.60	2.62	0.30	0.04	2.56
P404	1.75	2.60	2.62	0.26	0.03	1.95
P405	2.00	2.80	2.83	0.31	0.27	1.97
P406	2.20	2.75	2.82	0.29	0.47	1.29
P407	1.90	2.50	2.57	0.61	0.58	4.17
P408	0.90	2.65	2.68	0.30	0.28	2.13
P409	1.40	3.00	3.00	0.44	-0.13	1.19
P410	1.80	2.60	2.63	0.20	0.29	1.64
P411	2.40	2.80	2.83	0.27	0.34	1.30
P412	2.40	2.90	2.57	0.49	-0.17	1.30
P413	2.40	2.90	2.90	0.66	0.42	5.62
P414	1.00	2.75	2.48	0.75	-0.33	1.64
P415	4.80	4.37	1.60	-0.30	1.05	1.35
P416	0.80	1.75	2.03	1.00	0.58	1.58
P417	0.90	1.80	1.83	0.75	0.34	2.57
P418	1.40	2.90	4.17	2.47	0.78	1.38
P419	2.40	2.80	2.87	0.89	0.71	8.52
P420	0.90	1.75	1.82	0.58	0.22	0.96
P421	1.95	3.25	2.60	0.87	1.86	1.25
P422	-2.10	4.90	5.88	3.02	0.38	1.00
P423	1.50	2.65	2.66	0.23	-0.02	2.05
P424	2.00	2.70	2.77	0.38	0.47	2.05
P425	2.70	3.80	4.37	1.53	0.84	1.84
P426	4.30	4.92	2.38	0.51	1.14	2.00
P427	2.10	4.30	4.47	2.00	0.38	1.81
P428	1.90	3.50	3.93	1.70	0.63	1.62
P429	3.60	4.07	1.74	0.45	1.15	1.70
P430	1.50	3.00	2.97	0.48	-0.17	1.39
P431	0.90	2.35	2.30	0.46	-0.15	0.95
P432	1.00	2.80	2.78	0.39	-0.39	2.46
P433	2.20	3.00	3.35	0.91	0.74	1.09
P434	1.30	2.60	2.57	0.33	-0.23	1.84
P435	2.40	3.10	3.17	0.38	0.21	0.98
P443	-4.20	2.45	0.65	2.52	-0.86	0.51
P592	core	core	core	core	core	core
P594	2.00	3.60	3.53	0.73	0.12	3.19
P595	2.20	3.20	3.20	0.29	-0.03	1.11
P596	1.90	3.70	3.58	0.54	-0.17	3.42
P597	1.40	3.10	3.03	0.54	-0.28	1.20
P598	3.90	4.35	1.06	0.56	1.20	2.00
P599	2.20	2.90	2.90	0.31	0.07	1.08
P600	1.70	2.60	2.62	0.24	0.03	1.74

Table 2 cont. Sediment parameters. Note: Samples are listed in running order.

Station No.	C	Median Md	Mean M_2	Sorting σ_I	Skewness Sk_I	Kurtosis K_G
P600	1.70	2.60	2.62	0.24	0.03	1.74
P601	core	core	core	core	core	core
P602	2.60	5.20	5.68	1.79	0.56	1.76
P603	2.00	4.29	4.27	0.15	-0.61	16.39
P604	2.40	6.30	7.13	2.06	0.50	0.84
P605	1.35	5.60	6.17	2.62	0.27	2.28
P606	1.40	2.85	2.88	0.72	0.47	6.72
P607	2.40	3.05	3.18	1.36	0.57	4.27

Table 3a. Calculation of carbonate ($CaCO_3$) content: sand and gravel. Note: Samples are listed in running order.

Sample	weight	large carbonates	weight put into acid	weight after acid	small carbonates	total $CaCO_3$	% $CaCO_3$ = weight/total $CaCO_3$
P397	78.00	0.01	77.99	72.28	5.71	5.72	7.33
P398	81.14	0.03	81.11	75.68	5.43	5.46	6.73
P399	81.73	0.27	81.46	76.66	4.80	5.07	6.20
P400	54.23	1.62	52.61	49.72	2.89	4.51	5.52
P401	69.08	0.26	68.82	66.30	2.52	2.78	4.02
P402	70.53	0.06	70.47	67.88	2.59	2.65	3.76
P403	59.62	3.69	55.93	54.36	1.57	5.26	8.82
P404	85.05	2.05	83.00	80.00	3.00	5.05	5.94
P405	77.11	1.29	75.82	72.38	3.44	4.73	6.13
P406	82.20	1.82	80.38	76.57	3.81	5.63	6.85
P407	94.10	0.13	93.97	89.35	4.62	4.75	5.05
P408	93.02	0.03	92.99	89.23	3.76	3.79	4.07
P409	91.26	0.29	90.97	88.24	2.73	3.02	3.30
P410	108.03	3.74	104.29	99.95	4.34	8.08	7.48
P411	80.32	1.94	78.38	74.61	3.77	5.71	7.11
P412	85.10	0.58	84.42	80.80	3.62	4.20	4.93
P413	78.34	0.30	78.04	74.56	3.48	3.78	4.82
P414	80.99	0.01	80.98	77.56	3.42	3.43	4.23
P415	46.79	0.25	46.54	32.73	13.81	14.06	30.05
P416	82.73	0.11	82.62	77.56	5.06	5.17	6.25
P417	93.57	-	93.57	90.38	3.19	3.19	3.41
P418	93.27	16.02	77.25	59.99	17.26	33.28	35.68
P419	82.55	2.12	80.43	75.68	4.76	6.88	8.33
P420	91.00	0.30	90.70	84.11	6.59	6.80	7.47
P421	98.10	0.03	98.07	96.78	1.29	1.32	1.35
P422	54.87	31.08	23.79	12.76	11.03	42.11	76.75
P423	91.55	2.23	89.32	85.43	3.89	6.12	6.68
P424	96.64	25.17	71.47	67.66	3.81	28.98	29.99
P425	64.45	1.06	63.39	50.22	13.17	14.23	22.08
P426	84.20	0.36	83.84	62.84	21.00	21.36	25.37
P427	70.40	0.19	70.21	51.97	18.24	18.43	26.18
P428	92.90	0.61	92.29	64.23	28.06	28.67	30.86
P429	61.55	5.32	56.23	36.12	20.11	25.43	41.32
P430	75.61	11.72	63.89	39.15	24.74	36.46	48.22
P431	105.16	2.73	102.43	46.76	55.67	58.40	55.53
P432	84.62	2.01	82.61	44.70	37.91	39.92	47.18
P433	94.70	6.24	88.46	62.95	25.51	31.75	33.57
P434a	93.04	10.47	82.57	25.34	57.23	67.70	72.76
P434b	91.23	25.15	66.08	24.62	41.46	66.61	73.01
P435	105.70	27.30	78.40	10.81	69.40	96.70	91.49
P443	89.60	60.45	29.15	19.24	9.91	70.36	78.53
P592	core	core	core	core	core	core	core
P594	52.46	0.05	52.41	27.00	25.41	25.46	48.53
P595	104.30	0.14	104.16	75.28	28.88	29.02	27.82
P596	46.78	0.08	46.70	31.81	14.89	14.97	32.00

Table 3a cont. Calculation of carbonate ($CaCO_3$) content: sand and gravel. Note: Samples are listed in running order.

Sample	weight	large carbonates	weight put into acid	weight after acid	small carbonates	total $CaCO_3$	% $CaCO_3$ = Weight/total $CaCO_3$
P597	65.00	8.28	56.72	34.09	22.63	30.91	47.55
P598	46.38	0.14	46.24	32.06	14.18	14.32	30.88
P599	90.45	0.76	89.69	86.90	2.79	3.55	3.92
P600	69.64	3.32	66.32	64.29	2.03	5.35	7.68
P601	core	core	core	core	core	core	core
P602	19.31	0.01	19.30	7.18	12.12	12.13	62.82
P603	26.19	-	26.19	8.52	17.67	17.67	67.68
P604	32.48	0.09	32.39	8.17	24.22	24.31	74.85
P605	66.40	0.10	66.30	44.28	22.02	22.12	33.31
P606	87.09	1.19	85.90	80.00	5.90	7.09	8.14
P607	82.88	0.28	82.60	77.90	4.70	4.98	6.00

Table 3b. Calculation of carbonate ($CaCO_3$) content: mud. Note: Samples are listed in running order.

Sample	mud weight (g)	filter weight (g)	filter + digested mud weight(g)	digested weight (g)	wt carbonate	% carbonate
P397	3.15	0.876	3.450	2.574	0.576	18.29
P398	2.51	0.892	2.941	2.049	0.461	18.37
P399	3.15	0.892	3.532	2.640	0.510	16.19
P400	2.86	0.854	3.354	2.500	0.360	12.59
P401	no mud	no mud	no mud	no mud	no mud	no mud
P402	no mud	no mud	no mud	no mud	no mud	no mud
P403	no mud	no mud	no mud	no mud	no mud	no mud
P404	no mud	no mud	no mud	no mud	no mud	no mud
P405	no mud	no mud	no mud	no mud	no mud	no mud
P406	3.37	0.851	3.574	2.723	0.647	19.20
P407	3.34	0.898	3.578	2.680	0.660	19.76
P408	3.71	0.885	3.737	2.852	0.858	23.13
P409	no mud	no mud	no mud	no mud	no mud	no mud
P410	no mud	no mud	no mud	no mud	no mud	no mud
P411	2.49	0.869	2.840	1.971	0.519	20.84
P412	3.08	0.874	3.285	2.411	0.669	21.72
P413	3.25	0.899	3.329	2.430	0.820	25.23
P414	3.26	0.872	3.369	2.497	0.763	23.40
P415	4.20	0.874	4.318	3.444	0.756	18.00
P416	3.49	0.871	3.678	2.807	0.683	19.57
P417	3.02	0.871	3.158	2.287	0.733	24.27
P418	3.89	0.906	2.886	1.980	1.910	49.10
P419	3.19	0.874	3.341	2.467	0.723	22.66
P420	3.17	0.863	2.924	2.061	1.109	34.98
P421	3.16	0.866	3.280	2.414	0.746	23.61
P422	3.60	0.872	3.655	2.783	0.817	22.69
P423	no mud	no mud	no mud	no mud	no mud	no mud
P424	3.26	0.863	3.300	2.437	0.823	25.25
P425	3.34	0.884	3.676	2.792	0.548	16.41
P426	3.09	0.893	3.324	2.431	0.659	21.33
P427	4.63	0.890	4.264	3.374	1.256	27.12
P428	3.61	0.870	3.456	2.586	1.024	28.37
P429	3.37	0.890	3.872	2.982	0.388	11.51
P430	no mud	no mud	no mud	no mud	no mud	no mud
P431	no mud	no mud	no mud	no mud	no mud	no mud
P432	no mud	no mud	no mud	no mud	no mud	no mud
P433 (a)	3.41	0.903	3.800	2.897	0.513	15.04
P433 (b)	2.22	0.873	2.149	1.276	0.944	42.52
P434	no mud	no mud	no mud	no mud	no mud	no mud
P435	no mud	no mud	no mud	no mud	no mud	no mud
P443	no mud	no mud	no mud	no mud	no mud	no mud
P592	core	core	core	core	core	core
P594	3.07	0.872	2.208	1.336	1.734	56.48
P595	no mud	no mud	no mud	no mud	no mud	no mud
P596	2.42	0.871	2.205	1.334	1.086	44.88
P597	no mud	no mud	no mud	no mud	no mud	no mud

Table 3b cont. Calculation of carbonate ($CaCO_3$) content: mud. Note: Samples are listed in running order.

Sample	mud weight (g)	filter weight (g)	filter + digested mud weight(g)	digested weight (g)	wt carbonate	% carbonate
P598	3.64	0.873	3.679	2.806	0.834	22.91
P599	no mud	no mud	no mud	no mud	no mud	no mud
P600	no mud	no mud	no mud	no mud	no mud	no mud
P601	core	core	core	core	core	core
P602	3.44	0.889	3.314	2.425	1.015	29.51
P603	3.07	0.876	2.653	1.777	1.293	42.12
P604	3.08	0.882	2.916	2.034	1.046	33.96
P605	3.52	0.900	3.616	2.716	0.804	22.84
P606	2.73	0.885	2.925	2.040	0.690	25.27
P607	3.04	0.864	3.442	2.578	0.462	15.20

Table 3c. Calculation of carbonate ($CaCO_3$) content: total sample. Note: Samples are listed in running order.

Sample	wt carbonate in orig. wt mud	wt carbonate in orig. wt s+g	total wt carbonate in sample	total wt of orig. sample	wt % carbonate in orig. sample
P397	26.32	89.09	115.41	1359.30	8.49
P398	35.81	77.58	113.39	1347.71	8.41
P399	29.80	84.32	114.12	1544.04	7.39
P400	4.61	89.71	94.32	1661.85	5.68
P401	1.27	70.71	71.98	1773.10	4.06
P402	0.79	70.43	71.22	1882.02	3.78
P403	-	161.74	161.74	1833.80	8.82
P404	0.90	80.97	81.87	1368.72	5.98
P405	6.35	99.42	105.77	1655.28	6.39
P406	10.49	109.11	119.60	1647.49	7.26
P407	22.19	70.04	92.23	1499.26	6.15
P408	18.62	57.98	76.60	1505.13	5.09
P409	0.72	54.29	55.01	1653.18	3.33
P410	0.15	143.59	144.74	1926.83	7.51
P411	4.58	103.95	108.53	1483.96	7.31
P412	15.75	84.47	100.22	1785.92	5.61
P413	31.90	74.90	106.80	1680.43	6.36
P414	25.62	68.27	93.89	1723.53	5.45
P415	104.31	148.83	253.14	1074.78	23.55
P416	21.43	72.91	94.34	1276.13	7.39
P417	30.94	66.78	97.72	2085.95	4.68
P418	209.66	337.91	547.57	1374.05	39.85
P419	21.64	70.44	92.08	941.13	9.78
P420	11.68	141.62	153.30	1929.25	7.95
P421	102.56	15.22	117.78	1561.55	7.54
P422	102.11	709.73	811.84	1374.73	59.05
P423	-	114.85	114.85	1719.27	6.68
P424	22.47	564.31	586.78	1970.65	29.78
P425	66.38	155.49	221.87	1108.70	20.01
P426	106.54	108.25	214.79	926.20	23.19
P427	72.55	51.38	123.93	463.74	26.72
P428	103.12	289.02	392.14	1300.06	30.16
P429	52.77	464.55	517.32	1582.78	32.68
P430	3.30	659.56	662.86	1374.65	48.22
P431	-	1098.29	1098.29	1977.84	55.53
P432	-	773.59	773.59	1639.65	47.18
P433	59.12	386.19	445.31	1543.50	28.85
P434	-	681.88	681.88	933.95	73.01
P435	-	940.24	940.24	1027.70	91.49
P443	2.25*	987.75	990.00	1263.80	78.34
P592	core	core	core	core	core
P594	51.96	277.24	329.20	663.27	49.63
P595	4.88	251.57	256.45	912.26	28.11
P596	33.21	156.28	189.49	563.27	33.64
P597	1.35	306.95	308.30	650.04	47.43
P598	71.36	131.65	203.01	773.83	26.23

Table 3c cont. Calculation of carbonate ($CaCO_3$) content: total sample. Note: Samples are listed in running order.

Sample	wt carbonate in orig. wt mud	wt carbonate in orig. wt s+g	total wt carbonate in sample	total wt of orig. sample	wt % carbonate in orig. sample
P599	-	38.31	38.31	977.34	3.92
P600	1.10	92.53	93.63	1209.80	7.74
P601	core	core	core	core	core
P602	133.39	44.00	177.39	522.04	33.98
P603	127.20	23.06	150.26	336.07	44.71
P604	266.25	65.12	331.37	871.00	38.04
P605	169.82	60.96	230.78	926.51	24.91
P606	13.77	57.03	70.80	755.08	9.38
P607	14.21	41.38	55.59	783.16	7.10

* Estimate only

Table 4. Calculation of heavy and light mineral percentages. Note: Samples are listed in running order.

Sample	Wgt Light	Wgt Heavy	Total wgt	Wgt % Light	Wgt % Heavy
P397	6.50	0.62	7.12	91.29	8.71
P398	4.95	0.49	5.44	90.99	9.01
P399	4.69	0.72	5.41	86.69	13.31
P400	5.74	0.44	6.18	92.88	7.12
P401	5.84	0.48	6.32	92.40	7.60
P402	8.30	0.41	8.71	95.29	4.71
P403	6.08	0.66	6.74	90.21	9.79
P404	5.02	0.16	5.18	96.91	3.09
P405	8.55	0.73	9.28	92.13	7.87
P406	5.96	0.70	6.66	89.49	10.51
P407	5.69	0.24	5.93	95.95	4.05
P408	6.46	0.01	6.47	99.84	0.16
P409	3.38	4.26	7.64	44.24	55.76
P410	6.28	0.19	6.47	97.06	2.94
P411	7.19	0.50	7.69	93.50	6.50
P412	6.14	0.45	6.59	93.17	6.83
P413	4.70	0.15	4.85	96.91	3.09
P414	6.51	0.09	6.60	98.64	1.36
P415	3.62	0.52	4.14	87.44	12.56
P416	6.83	0.01	6.84	99.85	0.15
P417	5.96	0.02	5.98	99.66	0.34
P418	6.30	0.53	6.83	92.24	7.76
P419	9.33	0.14	9.47	98.52	1.48
P420	4.27	0.05	4.32	98.84	1.16
P421	6.06	0.02	6.08	99.67	0.33
P422	3.55	0.61	4.16	85.34	14.66
P423	5.01	0.25	5.26	95.25	4.75
P424	3.96	0.12	4.08	97.06	2.94
P425	6.47	0.06	6.53	99.08	0.92
P426	5.69	0.01	5.70	99.82	0.14
P427	4.49	0.04	4.53	99.12	0.88
P428	6.58	0.10	6.68	98.50	1.50
P429	3.61	0.08	3.69	97.83	2.17
P430	7.44	0.15	7.59	98.02	1.98
P431	4.61	0.15	4.76	96.85	3.15
P432	6.95	0.14	7.09	98.02	1.98
P433	6.85	0.04	6.89	99.42	0.58
P434	5.63	0.70	6.33	88.94	11.06
P435	6.94	0.10	7.04	98.58	1.42
P443	5.58	0.42	6.00	93.00	7.00
P444*	-	-	-	-	-
P594	5.12	0.07	5.19	98.65	1.35
P595	8.74	0.46	9.20	95.00	5.00
P596	5.22	0.07	5.29	98.68	1.32
P597	7.21	0.99	8.20	87.93	12.07
P598	2.85	0.04	2.89	98.62	1.38
P599	3.80	1.99	5.79	65.63	34.37
P600	7.94	0.10	8.04	98.76	1.24

Table 4 cont. Calculation of heavy and light mineral percentages. Note: Samples are listed in running order.

Sample	Wgt Light	Wgt Heavy	Total wgt	Wgt % Light	Wgt % Heavy
P602	2.01	0.02	2.03	99.01	0.99
P603	2.13	0.05	2.18	97.71	2.29
P604	2.46	0.02	2.48	99.19	0.81
P605	4.3	0.35	4.65	92.47	7.53
P606	5.09	0.1	5.19	98.07	1.93
P607	5.88	1.22	7.1	82.28	17.18

Table 5a. Calculation of bulk mineralogy as determined by XRD: sand and gravel. Note: Samples are listed in running order.

	Height	Peak Heights														Revised values				
	background	Calcite	Aragonite	Quartz	Feldspar	Clay	Calcite	Feldpar	%	%	%	Aragonite:	%	%		%	%	% Clay	%	%
Sample	(about 25)	29.4-30	26.25	20.8	27.5-28.2	19.9	types	types	Quartz	Feldspar	Clay	calcite ratio	Aragonite	Calcite	Total	Quartz	Feldspar	+ others	Aragonite	Calcite
P397	12	2	-	18	10/19/6	1.5	HM	CaNa/K	27	7/13/4	>15	7	-	1	73	29	8/15/5	36	-	7
P398	11	4	-	20	30/5	3	HM	Ca/Na	30	21/4	30	7	-	2	92	31	22/5	35	-	7
P399	12	1	-	16	32/5	1	HM	Ca/Na	24	22/4	>>10	6	-	1	66	26	24/5	39	-	6
P400	10	2	-	17	28/6	3	HM	CaNa/K	25	20/5	30	6	-	1	86	27	22/6	39	-	6
P401	10	1	-	20	27/9	1	HM	CaNa/K	30	19/7	>10	4	-	1	70	33	21/8	34	-	4
P402	9	1	-	21	45/9	2	HM	Ca/NaK	31	35/7	20	4	-	1	97	33	36/7	20	-	4
P403	8	1	-	41	43/24	-	HM	Na/Ca	61	30/16	-	9	-	1	116	51	28/12	-	-	9
P404	8	3	-	34	39/14	-	HM	CaNa/K	51	28/10	-	6	-	2	95	51	28/10	5	-	6
P405	8	2	-	19	33/13	-	HM	CaNa/K	28	23/9	>>	6	-	1	66	32	25/10	27	-	6
P406	10	2	-	19	34/6	2	HM	CaNa/K	28	24/5	>20	7	-	1	84	30	26/5	32	-	7
P407	9	2	-	23	35/7	-	HM + LM	CaNa/K	34	25/5	>>	5	-	1	69	36	27/6	26	-	5
P408	8	2	-	30	29/9	1	A/LM	CaNa/K	45	20/7	>10	4	-	1	86	48	22/7	19	-	4
P409	12	7	-	15	23/17	1.5	HM	Na/Ca,Ca/Na	23	17/11	>>15	3	-	3	69	28	20/11	38	-	3
P410	8	3	-	23	33/12	2	HM + LM	CaNa/K	34	23/8	20	7	-	2	92	36	25/8	24	-	7
P411	9	3	-	21	58/9	2	HM + LM	CaNa/K	31	40/7	20	7	-	2	105	31	37/7	19	-	7
P412	10	2	-	22	36/6	3	HM + LM	CaNa/K	33	26/5	30	5	-	1	99	34	26/5	30	-	5
P413	10	3	-	28	28/6	3	HM + LM	Ca/Na/K	42	20/5	30	5	-	2	102	40	20/5	30	-	5
P414	20	2	-	16	16/4	6	LM	CaNa/K	24	11/3	60	4	-	1	102	24	11/3	58	-	4
P415	7	50	-	9	9/3	1.5	LM	CaNa/K	14	7/2	15	30	-	31	68	16	8/3	43	-	30
P416	22	7	-	4	4/2	8	LM	Ca/Na	6	3/2	80	6	-	3	97	7	4/2	81	-	6
P417	27	4	-	2	4/5/4	8.5	LM	Ca/Na/K	3	3/4/3	85	4	-	2	102	3	3/4/3	83	-	4
P418	11	32	-	9	11/4	4	LM	CaNa/K	14	8/3	40	36	-	20	101	14	8/3	39	-	36
P419	8	5	-	23	46/7	2.5	LM	CaNa/K	34	32/5	25	8	-	2	104	34	32/5	21	-	8
P420	21	9	2	4	4	8	LM	Ca/Na	6	3	80	8	5	5	97	8	4	80	4	4
P421	21	12	2	6	5/6	8	LM	CaNa/K	9	4/4	80	2+	4	7	99	9	4/4	72	4	7
P422	8	30	5	3	4/4	0.5	LM-HM	CaNa/K	4	3/3	5	77	12	45	92	5	3/3	12	15	62
P423	8	3	-	24	43/11	1.5	HM + LM	CaNa/K	35	30+/8	15	7	-	2	95	36	34/8	15	-	7
P424	7	3	9	22	33/10	1	HM + LM	CaNa/K	33	23/7	<10	30	24	2	103	33	23/7	7	24	6
P425	8	17	3	11	24/18/8	1.5	LM	CaNa/K	16	17/12/6	>15	22	5	10	88	17	17/12/6	26	7	15

Table 5a cont. Calculation of bulk mineralogy as determined by XRD: sand and gravel. Note: Samples are listed in running order.

Sample	Height background (about 25)	Peak Heights					Calcite types	Feldpar types	% Quartz	% Feldspar	% Clay	Aragonite: calcite ratio	% Aragonite	% Calcite	Total	Revised values				
		Calcite 29.4-30	Aragonite 26.25	Quartz 20.8	Feldspar 27.5-28.2	Clay 19.9										% Quartz	% Feldspar + others	% Clay	% Aragonite	% Calcite
P426	8	24	5	16	25/4	1	LM	CaNa/K	24	18/3	>>10	25	11	14	80	25	19/4	27	11	14
P427	8	23	-	11	19/10	1	LM	CaNa/K	16	14/7+	>10	26	-	13	86	17	20/8	29	-	26
P428	9	27	-	10	13/7	2.5	LM	CaNa/K	15	10/5	>>25	31	-	16	86	16	12/5	36	-	31
P429	10	17	6	9	10/8/7	3	LM	Ca/Na/K	14	7/5/5	30	41	15	25	102	14	7/5/5	28	15	26
P430	8	31	4	6	16/2	2	LM	CaNa/K	9	11/1+	20	48	8	45	89	10	14/2	26	8	40
P431	5	18/20	12	8	11/6/6	0.5	A/LM	Ca/Na/K	12	8/4/4	5	>56	34, 35	48, 10/1	89	12	7/2	-	34	45
P432	4	28/21	9	13	7/6/5	1.5	A/LM	Ca/Na/K	20	5/4/3	15	47	25	17/12	94	20	5/4/3	9	23	36
P433	5	15/14	9	14	15/8	2.5	A/LM	CaNa/K	21	11/6	25	34	24	9/8	97	21	11/6	15	22	25
P434																				
P435	4	38	4	2	2/4	0.5	HM/LM	CaNa/K	3	2/3	5	92	8	55/30	105	3	2/3	2	8	82
P443																				
P444																				
P592	core	core	core	core	core	core	core	core	core	core	core	core	core	core	core	core	core	core	core	core
P594	5	52	3	5	8/4	2.5	LM	CaNa/K	8	6/3	25	48	5	45	91	9	7/3	30	5	46
P595	7	19	4	15	47/4	1		CaNa/K	23	33/3	10	28	8	11+	97	23	33/3	12	11	18
P596	8	28	-	5	7/5	1.5	LM	CaNa/K	8	5/3	>>15	32	-	30+	63	10	6/3	46	-	35
P597	7	38	2	9	4	1.5	LM	CaNa	13	3	>15	49	4	50	79	15	5	28	4	48
P598	8	33	-	11	18	1.5	LM	CaNa	16	13	>>15	31	-	20	75	18	15	35	-	32
P599	11	2	-	12	15/4	3.5	A/LM	CaNa/K	17	11/3	>35	4	-	1	70	25	15/5	51	-	4
P600	8	-	-	32	31/8	2	-	CaNa/K	48	22/6	20	8	-	-	104	46	22/6	18	-	8
P601	core	core	core	core	core	core	core	core	core	core	core	core	core	core	core	core	core	core	core	core
P602	5	64	-	2	2/1	-	LM	CaNa/K	3	1/1	>>	63	-	44	68	5	2/1	27	-	65
P603																				
P604	5	67	-	1	1/1	1	LM	-	2	1/1	>10	75	-	48	90	4	2/1	18	-	75
P605	6	39	-	4	4/3	2	LM	CaNa/NaCa	6	3/2	>20	33	-	23	87	7	4/2	54	-	33
P606	12	5/7	-	20	24/9	3	A/LM	CaNa/K	30	18/8	>30	8	-	2/3	94	30	18/8	34	-	10
P607	10	5/4	-	15	28/9	2.5	HM/LM	CaNa/K	23	20/7	>25	6	-	2/2	81	25	22/7	38	-	8

Table 5b. Calculation of bulk mineralogy as determined by XRD: mud. Note: Samples are listed in running order.

Station	Height background (about 25)	Peak Heights				Calcite types	Feldpar types	% Quartz	% Feldspar	% Clay	Aragonite: calcite ratio	% Aragonite	% Calcite	Total	Revised values				
		Calcite 29.4-30	Aragonite 26.25	Quartz 20.8	Feldspar 27.5-28.2	Clay 19.9									% Quartz	% Feldspar	% Clay + others	% Aragonite	% Calcite
P397	10	20	-	9	9	4	LM	Ca/Na	13	6	40	18	-	11	77	13	6	63	-	18
P398	10	22	-	7	10	5	LM	Ca/Na	10	7	50	18	-	13	85	10	7	65	-	18
P399	10	16	-	9	13	4	LM	Ca/Na	13	9	40	16	-	9	78	13	9	62	-	16
P400	11	13	-	8	15	3	LM	Ca/Na	11	11	30	13	-	8	65	11	11	65	-	13
P401	11	7	-	10	16	3	LM	Ca/Na	15	12	30	9?	-	3	66	15	12	64	-	9
P402	10	7	-	11	16	2	LM	Ca/Na	17	12	20	9?	-	3	58	17	12	62	-	9
P403	-	-	-	-	-	-	-	-	-	-	-	-	-	-	-	-	-	-	-	-
P404	10	14	-	10	12/6	5	LM	Ca/Na	15	8/4	50	16?	-	9	93	15	8/4	57	-	16
P405	10	16	-	8	6/4	4.5	LM	all	11	4/3	45	19?	-	10	82	11	4/3	63	-	19
P406	10	17	-	8	9	4	LM	Ca/Na	11	6	40	19	-	10	76	11	6	64	-	19
P407	10	22	-	4	7	5	LM	Ca/Na	6	5	50	20	-	13	81	6	5	69	-	20
P408	10	25	-	7	7/7	4	LM	all	10	5/5	40	23	-	15	83	10	5/5	57	-	23
P409	10	8	-	12	15/14/6	2	LM	Ca/Na	18	11/10/4	20	9?	-	3	72	18	11/10/4	48	-	9
P410	10	15	-	8	10/11/5	4	LM	Na	11	7/8/3	40	16?	-	9	85	11	7/8/3	55	-	16
P411	10	21	-	9	9/8	4.5	LM	Ca/Na	13	6/5	45	21	-	12	91	13	6/5	55	-	21
P412	10	21	-	7	8/4	5	LM	Ca/Na	10	5/3	50	22	-	12	90	10	5/3	60	-	22
P413	10	29	-	8	6/5	4	LM	Ca/Na	11	4/3	40	25	-	17	83	11	4/3	57	-	25
P414	9	28	-	6	10/8	3	LM	Ca/Na	9	7/5	30	23	-	17	74	9	7/5	56	-	23
P415	6	24	-	22	19/4	2	LM	Ca/Na	33	14/3	20	18	-	15	88	33	14/3	33	-	18
P416	7.5	27	-	13	15/7	2	LM	Ca/Na/K	20	11/5	20	20	-	16	76	20	11/5	44	-	20
P417	9.5	32	-	8	9/9	4	LM	Ca/Na	11	6/6	40	24	-	20	87	11	6/6	53	-	24
P418	7	43	3	6	5	2	LM	all	9	4	20	49	5	28	87	9	4	37	8	42
P419	11	23	-	8	10/6	5	LM	Ca/Na	11	7/4	50	23	-	14	95	11	7/4	55	-	23
P420	8	37	-	6	6/4	3	LM	Ca/Na	9	4/3	30	35	-	23	81	9	4/3	49	-	35
P421	9	33	-	10	18/6	3	LM	Ca/Na	15	13/5	30	24	-	21	87	15	13/5	43	-	24
P422	9	26	-	10	16/8	5	LM	Ca/Na	15	12/7	50	23	-	16	107	15	12/7	43	-	23
P423	-	-	-	-	-	-	-	-	-	-	-	-	-	-	-	-	-	-	-	-
P424	10	25/10	-	8	11	2.5	HM + LM	Ca/Na	11	8	25	25	-	15/5	69	11	8	56	-	25
P425	9	18	-	13	20/15	3	LM	Ca/Na	20	15/11	30	16	-	10	92	20	15/11	38	-	16

Table 5b cont. Calculation of bulk mineralogy as determined by XRD: mud.
Note: Samples are listed in running order.

	Height	Peak Heights					Calcite	Feldpar	%	%	%	Aragonite:	%	%	%	Revised values					
Station	background (about 25)	Calcite 29.4-30	Aragonite 26.25	Quartz 20.8	Feldspar 27.5-28.2	Clay 19.9	types	types	Quartz	Feldspar	Clay	calcite ratio	Aragonite	Calcite	Total	%Quartz	%Feldspar	% Clay + others	%Aragonite	%Calcite
P426	9	24	3	10	13/18/7	2	LM	all	15	9/5/5	20	21	5	14	80	15	9/5/5	45	6	15
P427	8	30	-	8	11/8/5	3	LM	Ca/Na	11	8/6/4	30	27	-	18	86	11	8/6/4	44	-	27
P428	8	30	-	9	14/10	2.5	LM	Ca/Na	13	10/8	25	28	-	18	84	13	10/8	41	-	28
P429	9	9	-	18	10/27/5	2.5	A/LM	Na	28	8/19/4	25	12	-	4	96	28	8/19/4	29	-	12
P430	6	30/20	4	4	5	1.5	LM	all	6	4/4	15	27/18/**A10?**	8	18/11	92	6	4/4	31	10	45
P431	-	-	-	-	-	-	-	-	-	-	-	-	-	-	-	-	-	-	-	-
P432	-	-	-	-	-	-	-	-	-	-	-	-	-	-	-	-	-	-	-	-
P433a	9	12	-	14	16/12	3	LM	Ca/Na	22	12/9	30	15	-	7	88	22	12/9	42	-	15
P433b	7	41	-	7	5/4	2	LM	Ca/Na	10	4/3	20	43	-	25	80	10	4/3	40	-	43
P434	-	-	-	-	-	-	-	-	-	-	-	-	-	-	-	-	-	-	-	-
P435	-	-	-	-	-	-	-	-	-	-	-	-	-	-	-	-	-	-	-	-
P443																				
P444																				
P592	core	core	core	core	core	core	core	core	core	core	core	core	core	core	core	core	core	core	core	core
P594	5	63	3	4	5	-	LM	Ca/Na	6	4	-	56	5	45	71	6	4	30	6	54
P595	5	44	5	4	6	1.5	LM	Ca/Na	6	5	15	49/**A12?**	11	28	98	6	5	27	12	50
P596	5	43	-	8	9/6	2	LM	Ca/Na	11	6/5	20	45	-	27	87	11	6/5	33	-	45
P597	5	40	-	9	10/13	1.5	LM	all	13	8/9	15	**30?**	-	24	75	13	8/9	40	-	30
P598	8	30	-	13	23/5	1	LM	Na	20	17/4	10	23	-	18	74	20	17/4	36	-	23
P599																				
P600	12	17	-	9	9/3	4	LM	Ca/Na	13	6/2	40+	**22?**	-	10	83	13	6/2	57	-	22
P601	core	core	core	core	core	core	core	core	core	core	core	core	core	core	core	core	core	core	core	core
P602	7	41	-	11	14	2	LM	Ca/Na	17	10	20	30	-	24	77	17	10	43	-	30
P603	5.5	59	-	4	7	3.5	LM	Ca/Na	6	5	<35	42	-	40	88	6	5	47	-	42
P604	6	43	-	8	12/7	2	LM	Ca/Na	11	8/5	20	34	-	27	78	11	8/5	42	-	34
P605	7	32	-	10	12/10	2	LM	Ca/Na	15	8/7	20	23	-	20	73	15	8/7	47	-	23
P606	10	28	-	6	7/4	4	LM	Ca/Na	9	5/3	40	25	-	16	82	9	5/3	58	-	25
P607	11	14	-	8	8/8	4	LM	Ca/Na	11	5/5	40+	15	-	7	76	11	5/5	64	-	15

Table 5c. Calculation of bulk mineralogy as determined by XRD: total sediment. Note: Samples are listed in running order.

Sample	% Quartz	% Feldspar	% Clay + others	% Aragonite	% Calcite
P397	27	26	39	-	8
P398	28	24	39	-	9
P399	24	27	42	-	7
P400	27	28	39	-	6
P401	33	29	34	-	4
P402	33	29	34	-	4
P403	51	40	-	-	9
P404	51	38	5	-	6
P405	32	34	28	-	6
P406	29	30	33	-	8
P407	34	31	29	-	6
P408	46	28	21	-	5
P409	28	31	38	-	3
P410	36	33	24	-	7
P411	31	44	18	-	7
P412	33	30	31	-	6
P413	38	24	32	-	6
P414	23	14	58	-	5
P415	25	14	38	-	23
P416	8	7	78	-	7
P417	4	10	81	-	5
P418	12	9	38	3	38
P419	32	34	24	-	10
P420	8	4	79	4	5
P421	10	11	64	3	12
P422	8	10	22	10	50
P423	36	42	15	-	7
P424	32	29	9	23	7
P425	18	32	30	5	15
P426	20	19	37	9	15
P427	13	22	38	-	27
P428	15	17	38	-	30
P429	18	21	28	11	22
P430	10	16	26	8	40
P431	12	9	-	34	45
P432	20	12	9	23	36
P433	18	15	21	16	30
P434					
P435	3	5	2	8	82
P443					
P444					
P592	core	core	core	core	core
P594	9	9	30	5	47
P595	23	36	12	11	18
P596	10	9	44	-	37
P597	15	5	28	4	48
P598	19	18	35	-	28
P599	25	20	51	-	4
P600	46	28	18	-	8
P601	core	core	core	core	core
P602	16	9	41	-	28
P603					
P604	10	12	40	-	38
P605	14	13	48	-	25
P606	28	25	36	-	11
P607	23	27	41	-	9

Table 6. Calculation of clay mineral percentages. Note: Samples are listed in running order.

	Peak Height (µ)					Degree of crystallinity (µ)			Peak Area					% Clay minerals			
Sample	14	10	7	3.5	3.3	14	10	7	3.3 (µ)	3.5	10 (G)	17(G)	12(G)	Illite	C+K	C-I	M
P397	29	10	18	9	10	0.21	0.15	0.22	1.5	1.7	1.5	11.7	+	10.1	11.4	0	78.5
P398	15	6	13	7	6	0.33	0.25	0.38	1.2	1.2	0.9	10.8	0.0	7.1	7.1	0	85.8
P399	11	7	8	4	4	0.64	0.29	0.50	0.5	0.6	0.6	5.5	0.0	8.8	10.5	0	80.7
P400	10	4	10	7	5	0.50	0.50	0.40	1.0	0.8	0.5	4.9	0.0	8.6	6.9	0	84.5
P401	7	7	8	4	7	1.00	0.29	0.44	2.0	1.2	1.0	4.2	0.0	17.2	10.3	0	72.5
P402	-	-	-	-	-	-	-	-	-	-	-	-	-	-	-	-	-
P404	6	7	7	5	9	0.67	0.14	0.36	1.4	0.9	0.8	1.7	0.0	26.6	17.0	0	56.4
P405	19	12	11	5	13	0.26	0.08	0.23	1.9	1.0	0.8	8.3	0.0	8.4	4.5	0	87.1
P406	25	5	10	7	6	0.16	0.20	0.45	0.8	1.2	0.8	9.9	0.1+	6.7	10.1	0	83.2
P407	7	8	14	8	12	0.57	0.44	0.25	1.7	2.0	1.0	8.7	0.0	9.2	10.7	0	80.0
P408	34	4	11	8	7	0.12	0.38	0.45	1.8	1.6	1.2	15.0	0.0	6.9	6.2	0	86.9
P409	-	-	-	-	-	-	-	-	-	-	-	-	-	-	-	-	-
P410	10	4	9	3	6	0.80	0.30	0.61	0.5	0.3	0.3	6.4	+	4.4	2.6	0	93.0
P411	21	3	12	4	5	0.29	0.33	0.42	0.5	0.4	1.0	9.0	0.0	9.3	7.4	0	83.3
P413	29	6	10	6	8	0.24	0.33	0.30	1.2	1.7	0.5	8.8	0.1+	5.0	7.1	0	87.9
P414	19	10	16	10	14	0.26	0.15	0.50	1.8	1.5	1.2	10.0	+	9.8	8.2	0	82.0
P415A	18	11	17	9	12	0.28	0.14	0.18	1.8	1.3	1.8	8.9	0.1+	15.2	10.6	0	74.2
P415B	28	12	16	11	13	0.18	0.13	0.16	2.2	2.2	0.9	14.4	0.1+	5.6	5.6	0	88.8
P416	48	10	18	11	14	0.13	0.25	0.22	1.8	1.8	0.5	9.5	+	4.8	4.8	0	90.4
P417	27	6	15	8	10	0.15	0.42	0.20	2.5	2.5	1.0	8.6	0.1+	18.2	18.2	0	63.6
P418	17	7	8	6	7	0.29	0.36	0.22	1.2	1.0	1.0	8.6	0.1+	9.6	7.9	0	82.5
P419	24	4	13	9	8	0.17	0.38	0.31	2.3	2.0	0.9	8.8	+	8.6	7.5	0	83.9
P420	39	13	26	14	15	0.15	0.12	0.13	2.3	2.5	1.3	17.1	0.0	6.6	7.1	0	86.3
P421	12	8	13	10	11	0.33	0.25	0.27	1.6	1.3	1.0	6.2	0.1+	12.5	10.0	0	77.5
P422	24	11	20	13	14	0.21	0.32	0.25	1.8	2.7	1.4	12.0	+	9.0	13.6	0	77.4
P424	14	9	9	4	10	0.57	0.28	0.39	1.1	0.6	0.9	5.7	0.0	12.7	7.0	0	80.3
P425	28	7	13	7	9	0.18	0.21	0.27	1.5	1.5	0.5	5.4	0.0	7.8	7.8	0	84.4
P426	20	7	7.5	4	9	0.20	0.21	0.67	1.9	0.8	0.7	5.1	0.2	11.1	4.4	3.4	81.1
P427	24	11	15	7	11	0.17	0.18	0.27	1.7	1.5	1.5	10.0	0.1+	11.7	10.3	0	78.0
P428	17	9	13	7	8	0.29	0.17	0.31	1.3	1.0	0.6	8.4	0.1+	6.3	4.9	0	88.8
P429	18	25	31	21	29	0.39	0.08	0.06	4.7	3.7	3.0	9.0	0.1+	20.9	16.3	0	62.8
P430	9	12	13	5	9	0.44	0.13	0.15	1.5	0.9	1.3	3.0	0.0	25.6	15.3	0	59.1
P433	18	22	23	9	15	0.33	0.07	0.09	2.1	1.3	2.7	14.2	0.1+	14.5	9.0	0	76.5
P594	8	5	9	4	7	0.50	0.40	0.22	1.1	0.7	0.6	2.7	+	16.3	10.4	0	73.3
P595	9	12	9	5	10	0.33	0.13	0.17	1.4	0.8	0.5	3.4	0.0	11.9	7.1	0	81.0
P596	12	9	11	7	8	0.50	0.28	0.05	0.7	1.3	1.6	5.3	+	16.2	38.9	0	53.6
P597	-	-	-	-	-	-	-	-	-	-	-	-	-	-	-	-	-
P598	9	6	9	6	8	0.56	0.42	0.17	0.9	1.0	0.9	5.8	0.1+	11.8	12.9	0	75.3
P600	9	9	12	6	11	0.44	0.17	0.21	1.8	1.1	0.8	3.0	+	18.6	11.4	0	70.0
P602	21	15	19	10	15	0.24	0.13	0.13	2.0	2.0	1.2	11.6	0.0	8.6	8.6	0	82.9
P603	26	15	23	13	17	0.19	0.10	0.13	1.4	2.0	1.2	6.2	+	13.2	18.8	0	68.0
P604	30	12	21	7	10	0.13	0.13	0.17	1.3	1.0	1.4	14.4	0.2	8.2	6.3	1.1	84.3
P605	39	7	11	6	9	0.15	0.14	0.32	2.0	1.5	0.7	8.4	0.0	7.3	5.4	0	87.3
P606	29	6	12	8	10	0.14	0.50	0.33	1.8	0.9	0.8	9.6	0.0	7.4	3.7	0	88.9
P607	11	9	14	6	7	0.55	0.28	0.29	1.0	1.0	1.0	8.8	0.0	9.3	9.3	0	81.4

$$\% \text{ Illite} = \frac{\text{area 10Å (G)}}{\text{area 10Å (G)}} \qquad \% \text{ Montmorillite (M)} = \frac{\text{area 3.5Å (µ)}}{\text{area 3.3Å (µ)}}$$

$$\% \text{ Chlorite + kaolinite (C+K)} = \frac{\text{area 3.5Å (µ)}}{\text{area 3.3Å (µ)}}$$

$$\% \text{ Chlorite mixed layer clays (C-L)} = \frac{\text{area 12Å (G)}}{\text{area 10Å (G)}}$$

Table 7a. Petrography of NKCM sediments: P397-P409. Note: Samples are listed in running order with two pages per set of samples.

Sample Site	P397	P398	P399	P400	P401	P402	P403	P404	P405	P406	P407	P408	P409
Depth (m)	216	149	107	70	42	33	34	63	86	110	161	206	38
SILICICLASTIC MINERALS													
Quartz %	uC	uC	uC	uC	uC	lA	uA	uA	lA	lA	lA	uA	lA
Modal grain size - 1	0.18	0.15	0.20	0.24	0.15	0.20	0.30	0.25	0.20	0.15	0.20	0.20	0.20
Modal grain size - 2	0.20	0.18	0.18	0.15		0.15	0.23	0.20	0.25	0.21	0.15		0.30
Sorting	5	5	5	4	5	4	4	4	4	4	4	4	3
Roundness	2	3	2	3	3	3	3	3	3	2	3	3	2
Feldspar %	uC	uC	uC	uC	lA	lA	uA	lA	lA	lA	lA	uC	lA
Modal grain size - 1	0.20	0.15	0.17	0.22	0.22	0.20	0.25	0.35	0.25	0.15	0.20	0.14	0.20
Modal grain size - 2	0.18	0.20	0.14	0.15				0.20	0.20	0.20	0.15	0.22	0.34
Sorting	5	4	4	4	5	4	4	4	4	4	4	4	3
Roundness	2	2	2	3	3	3	3	3	3	2	3	3	2
Biotite/Muscovite %	uR	lC	uS	S	uS	lC	-	R	R	-	R	R	S
Modal grain size - 1	0.21	0.17	0.22	0.17	0.24	0.32		0.30	0.25		0.12	0.20	0.20
Modal grain size - 2	0.10	0.13		0.23									
Sorting	4	4	4	4	4	4		4	4		4	3	4
Roundness	2	2	3	2	2	4		4	4		3	3	3
CALCICLASTICS													
Total %	lC	lR	uR	uR	R	R	R	R	uC	R	R	S	R
Sorting	3	4	4	3	3	3	3	3	3	2	3	3	4
Roundness	2	2	3	2	3	3	3	3	4	3	3	2	4
Skeletal abrasion	High	High	High	High	High	High	High	High	High	M-H	High	High	High
Bivalve %	-	-	R	R	R	R	R	R	R	-	-	-	R
Modal grain size - 1			0.25	0.50	0.45	0.32	1.00	0.70	0.16				0.23
Modal grain size - 2				1.00									
Gastropod %	R	-	R	R	-	-	R	R	S	R	R	R	-
Modal grain size - 1	0.20		0.57	1.30			0.80	0.60	0.65		0.40	0.90	
Modal grain size - 2									1.2				
Bryozoan %	-	R	R	R	-	R	-	R	R	-	-	R	-
Modal grain size - 1		0.18	0.23	0.26		0.22		1.3	0.91			0.30	
Modal grain size - 2													
Foram - benthic %	uR	R	R	uR	-	-	-	-	R	R	R	R	-
Modal grain size - 1	0.27	0.35	0.24	0.35					0.25	0.20	0.30	0.30	
Modal grain size - 2	0.28	0.14	0.12						0.45				
Foram - planktic %	uS	R	R	R	-	-	-	-	R	-	R	R	-
Modal grain size - 1	0.18	0.10	0.20	0.10					0.25		0.18	0.2	
Modal grain size - 2	-	0.22	0.10	0.18									
Echinoderm %	R	R	-	-	R	R	R	-	-	-	-	-	-
Modal grain size	0.70	0.15			0.43	0.26	0.15						
Serpulid %	-	-	-	R	-	-	-	-	-	-	-	-	-
Modal grain size				0.56									
Algae %	-	-	-	-	R	-	-	-	-	-	-	-	-
Modal grain size													
Spicules %	-	-	-	-	-	-	-	-	-	-	-	-	-
Modal grain size													
Opaline spines %	-	-	-	-	-	-	-	-	-	-	-	-	-
Modal grain size													
Coral %	-	-	-	-	-	-	-	-	-	-	-	-	-
Modal grain size													
Barnacle %	-	-	-	-	-	-	-	-	-	-	-	-	-
Modal grain size													
GLAUCONITE %	lC	uR	lC	lC	-	R	R	R	R	R	R	R	-
Modal grain size - 1	0.25	0.13	0.23	0.25		0.18	0.13	0.30	0.21	0.25	0.20	0.30	
Modal grain size - 2		0.32	0.13	0.17				0.18		0.08		0.13	
Sorting	3	4	3	4		4	4	3	4	3	4	3	
Roundness	4	4	5	4		4	4	4	4	5	5	4	

Table 7a cont. Petrography of NKCM sediments. Note: Samples are listed in running order with two pages per set of samples.

Sample Site	P397	P398	P399	P400	P401	P402	P403	P404	P405	P406	P407	P408	P409
Depth (m)	216	149	107	70	42	33	34	63	86	110	161	206	38
ROCK FRAGMENTS %	lC	S	lC	S	S	lC	S	uC	uC	uC	lC	lC	uC
Modal grain size - 1	0.18	0.10	0.15	0.15	0.17	0.20	0.18	0.33	0.20	0.22	0.15	0.18	0.20
Modal grain size - 2		0.18		0.20	0.22	0.17		0.20			0.18	0.21	0.30
Sorting	4	4	3	4	4	4	4	4	4	4	4	4	4
Roundness	4	4	4	3	3	3	3	4	3	3	3	3	3
OPAQUES %	lS	uR	S	S	S	R	R	R	R	R	R	R	R
Modal grain size - 1	0.08	0.11	0.08	0.08	0.08	0.11	0.10	0.09	0.10	0.10	0.13	0.15	0.08
Modal grain size - 2	0.05				0.10	0.08							
Sorting	4	5	5	5	4	4	4	4	4	4	4	4	4
Roundness	3	3	2	3	4	4	4	4	4	4	4	4	3
HEAVY MINERALS %*	lC	lC	lC	S	lC	S	lC	R	lC	lC	S	R	lvA
Modal grain size - 1	0.16	0.18	0.18	0.16	0.24	0.21	0.20	0.21	0.20	0.18	0.17	0.25	0.18
Modal grain size - 2		0.15	0.13		0.18								0.25
Sorting	4	4	4	4	4	4	4	4	4	4	4	4	3
Roundness	3	3	2	3	3	3	4	4	3	3	3	3	2
Hornblende	lA	lA	lA	lA	lA	vA	uA	lA	lA	lA	lA	uA	lA
Oxyhornblende	S	S	S	S	S	lC	lC	S	S	lC	S	R	uC
Blue-green amphibole	S	lC	S	S	S	S	S	S	uC	S	S	S	S
Actinolite	R	R	-	R	-	R	R	-	-	S	S	S	R
Hypersthene	lC	lC	S	lC	S	S	lC	lC	uC	lC	uC	uC	lC
Epidote	R	S	S	R	S	S	S	R	S	S	S	R	S
Garnet	lA	lA	vA	S	uC	uC	uA	lA	lA	lA	lA	lA	vA
Chlorite	R	-	-	-	R	R	-	R	-	-	R	R	R
Zircon	R	R	S	R	R	S	S	-	R	R	R	R	S
Clinozoisite	-	-	-	-	-	-	-	-	-	R	-	R	R
Titanite	S	S	S	S	S	S	S	S	S	S	S	S	-
Augite	uC	uC	lA	uC	uC	uC	uC	lC	lC	lA	lA	A	lA
Monazite	-	-	-	-	-	-	-	-	-	-	-	R	-
LITHOCLAST/PELLET %	S	S	S	R	R	-	-	-	R	-	-	-	-
Modal grain size - 1	0.30	0.23	0.25	0.25	0.25				0.51				
Modal grain size - 2	0.70	0.15	0.31										
Sorting	3	4	4	4	4				4				
Roundness	3	4	4	4	5				5				
PHOSPHATE %	-	-	-	-	-	-	-	-	R	-	-	-	-
Modal grain size									0.25				
OVERALL													
Modal grain size - 1	0.20	0.15	0.15	0.25	0.18	0.20	0.25	0.25	0.20	0.20	0.20	0.25	0.30
Modal grain size - 2	0.33						0.18	0.20		1.75		0.18	0.15
Sorting	3	4	4	4	4	4	4	4	4	4	4	4	3
Roundness	2	2	3	3	3	3	3	3	3	3	3	3	2

Percentage range key:

R	=	0-5%	**uC**	=	20-30%	**vA**	= 50% +
S	=	5-10%	**lA**	=	30-40%	**uvA**	= 75% +
lC	=	10-20%	**uA**	=	40-50%		

Sorting		**Roundness**	
1	Very poorly sorted	1	Angular
2	Poorly sorted	2	Sub angular
3	Moderately sorted	3	Sub rounded
4	Well sorted	4	Rounded
5	Very well sorted	5	Well rounded

*** Note:** the heavy minerals proportions here are a percentage of the total heavy mineral content - not the total sediment.

P397 Limonite rims on Q/F. Forams have glauconite infills, glauconite is highly degraded brown-green, few fresh grains, pellets include Q/F, opaques, skeletal frags. Are heavily glauconitised

P399 Glauconite infills in forams, RF glauconitised, limonite stained Q/F

P404 Skeletal grains have endolithic borings filled with limonite

P405 Glauconite filled forams, endolithic borings phosphate = shell frag.

P408 Glauconite infills

Table 7b. Petrography of NKCM sediments: P410-P422. Note: Samples are listed in running order with two pages per set of samples.

Sample Site	P410	P411	P412	P413	P414	P415	P416	P417	P418	P419	P420	P421	P422
Depth (m)	67	85	110	161	216	512	355	183	149	108	184	153	92
SILICICLASTIC MINERALS													
Quartz %	lA	uC	lA	lA	uC	lC	uS	S	S	lA	S	S	S
Modal grain size - 1	0.20	0.15	0.20	0.20	0.12	0.05	0.10	0.15	0.20	0.18	0.10	0.10	0.08
Modal grain size - 2	0.30	0.20	0.16	0.15	0.20		0.08	0.20	0.15		0.15		
Sorting	4	4	4	4	4	4	4	4	4	4	4	4	4
Roundness	4	3	3	3	3	3	2	3	4	3	3	2	4
Feldspar %	lA	uA	uA	uC	lC	lC	uS	S	lC	lA	S	S	S
Modal grain size - 1	0.20	0.20	0.20	0.15	0.10	0.05	0.25	0.22	0.20	0.20	0.10	0.11	0.07
Modal grain size - 2	0.30		0.15	0.20	0.20		0.15	0.10	0.18		0.15		
Sorting	4	5	4	4	4	4	3	3	4	4	4	4	4
Roundness	4	2	3	2	3	3	3	3	4	3	3	2	4
Biotite/Muscovite %	R	R	R	S	R	R	R	R	R	R	R	R	R
Modal grain size - 1	0.30	0.15	0.23	0.18	0.14	0.1	0.20	0.30	0.20	0.27	0.13	0.15	0.08
Modal grain size - 2		0.30	0.30						0.08				
Sorting	4	3	4	4	4	4	4	4	4	4	4	4	4
Roundness	3	3	2	4	3	3	3	2	3	3	3	3	3
CALCICLASTICS													
Total %	S	S	S	R	S	vA	uS	R	uvA	S	lC	C	uvA
Sorting	1	3	3	3	4	4	4	4	4	2	3	2	2
Roundness	4	3	2	2	3	3	4	3	3	2	2	1	3
Skeletal abrasion	High	High	High	High	M-H	High	Mod	M-H	High	High	Mod	High	High
Bivalve %	R	R	R	R	-	-	R	-	-	-	R	R	C
Modal grain size - 1	0.88	0.75	0.98	0.32							0.38		3.50
Modal grain size - 2													
Gastropod %	-	R	-	-	R	-	R	R	-	R	R	S	C
Modal grain size - 1					0.32		0.20	0.20		0.85		0.10	0.70
Modal grain size - 2													
Bryozoan %	-	R	-	-	-	-	R	-	R	R	R	S	lA
Modal grain size - 1		0.40					0.35		0.24	1.05			1.37
Modal grain size - 2													0.70
Foram - benthic %	-	R	R	R	R	C	R	-	S	S	R	R	S
Modal grain size - 1		0.33	0.23	0.23	0.22	0.20	0.16		0.18	0.35			0.43
Modal grain size - 2		0.15		0.18									
Foram - planktic %	-	R	R	R	-	A	S	R	A	S	R	S	R
Modal grain size - 1		0.20	0.13	0.20		0.12	0.20	0.20	0.07	0.17		0.05	0.28
Modal grain size - 2				0.30			0.08		0.16				
Echinoderm %	R	-	R	-	-	-	-	-	-	R	R	-	S
Modal grain size	0.40		0.45							0.60			1.25
Serpulid %	-	-		-	-	R	-	-	-	-	-	-	R
Modal grain size						0.30							0.68
Algae %	-	-	-	-	-	-	-	-	-	-	-	-	-
Modal grain size													
Spicules %	-	-	-	-	-	uC	R	-	-	-	-	R	-
Modal grain size						0.10							
Opaline spines %	-	-	-	-	-	-	-	-	S	-	-	-	R
Modal grain size									0.21				0.15
Coral %	-	-	-	-	-	-	-	-	-	-	-	-	R
Modal grain size													
Barnacle %	-	-	-	-	-	-	-	-	-	-	-	-	-
Modal grain size													
GLAUCONITE %	R	R	R	S	lA	S	uvA	vA	lC	S	uvA	uvA	-
Modal grain size - 1	0.08	0.13	0.18	0.15	0.20	0.08	0.55	0.25	0.20	0.15	0.45	0.40	
Modal grain size - 2				0.30	0.30		0.28	0.38	0.25		0.20	0.20	
Sorting	4	4	4	3	3	4	2	4	4	4	2	4	
Roundness	4	5	4	5	3	4	4	3	3	3	5	5	

Table 7b cont. Petrography of NKCM sediments: P410-P422. Note: Samples are listed in running order with two pages per set of samples.

Sample Site	P410	P411	P412	P413	P414	P415	P416	P417	P418	P419	P420	P421	P422
Depth (m)	67	85	110	161	216	512	355	183	149	108	184	153	92
ROCK FRAGMENTS %	IC	IC	S	IC	uC	-	R	R	IC	IC	R	R	R
Modal grain size - 1	0.18	0.17	0.15	0.18	0.17		0.27	0.14	0.26	0.24	0.88	0.16	0.35
Modal grain size - 2					0.20				0.18	0.16			
Sorting	4	4	4	4	4		4	4	3	4	4	4	4
Roundness	3	3	3	3	3		3	3	3	3	3	3	3
OPAQUES %	R	S	R	R	-	-	R	-	R	R	-	R	-
Modal grain size - 1	0.15	0.15	0.10	0.09			0.10		0.15	0.06		0.10	
Modal grain size - 2				0.12									
Sorting	4	4	4	4			4		4	4		4	
Roundness	3	4	4	3			3		3	3		2	
HEAVY MINERALS %*	R	S	S	S	S	IC	R	R	S	S	R	R	IC
Modal grain size - 1	0.27	0.20	0.15	0.21	0.25	0.07	0.10	0.10	0.15	0.18	0.12	0.14	0.23
Modal grain size - 2			0.20	0.15					0.12				
Sorting	4	4	4	4	4	4	4	4	4	4	4	4	4
Roundness	4	4	4	2	2	3	4	3	3	4	3	3	3
Hornblende	uA	IA	IA	C	uC	IC	uC	IC	uC	uC	uC	IA	uA
Oxyhornblende	S	S	S	R	IC	R	S	R	R	S	R	S	S
Blue-green amphibole	S	R	S	S	S	S	S	S	S	IC	R	R	S
Actinolite	-	R	S	R	-	S	-	R	R	R	R	-	R
Hypersthene	S	IC	S	S	IC	S	S	IC	IC	uC	IC	IC	IC
Epidote	S	R	S	S	S	R	R	S	S	R	R	R	IC
Garnet	uA	IA	IA	S	S	S	R	uC	uC	uC	S	S	R
Chlorite	R	R	-	-	-	-	-	-	-	-	R	-	uC
Zircon	R	S	R	R	R	-	R	R	S	R	R	-	R
Clinozoisite	R	-	-	R	-	-	-	-	-	-	-	-	-
Titanite	S	S	S	IC	S	S	R	R	R	S	-	S	R
Augite	IC	uC	uC	IC	uC	IC	uC	uC	uC	uC	uC	uC	IC
Monazite	-	-	-	-	-	-	-	-	-	-	-	-	-
LITHOCLAST/PELLET %	-	-	R	-	-	-	-	-	R	S	-	R	S
Modal grain size - 1			0.28						1.29	0.30		1.65	0.63
Modal grain size - 2													
Sorting			4						4	4		4	4
Roundness			5						5	5		4	5
PHOSPHATE %	-	-	-	-	-	-	R	R	-	-	C	C	-
Modal grain size								0.22			0.25	0.10	
OVERALL													
Modal grain size - 1	0.20	0.20	0.18	0.18	0.30	0.07	0.50	0.25	0.20	0.18	0.15	0.38	1.30
Modal grain size - 2					0.18	0.20	0.25	0.38	0.18	0.20	0.45	0.10	0.08
Sorting	4	4	4	4	4	4	2	4	4	5	3	4	2
Roundness	3	3	3	3	2	3	4	3	4	3	3	3	3

Percentage range key:

R	=	0-5%	**uC**	=	20-30%	**vA**	= 50% +
S	=	5-10%	**IA**	=	30-40%	**uvA**	= 75% +
IC	=	10-20%	**uA**	=	40-50%		

Sorting			**Roundness**		
	1	Very poorly sorted		1	Angular
	2	Poorly sorted		2	Sub angular
	3	Moderately sorted		3	Sub rounded
	4	Well sorted		4	Rounded
	5	Very well sorted		5	Well rounded

*** Note:** the heavy minerals proportions here are a percentage of the total heavy mineral content - not the total sediment.

P410 Limonite rims/staining on Q/F, limonite borings in skeletal grains,

P414 Less fresh glauconite grains than 416, 420, 421

P415 Forams filled with clays/argilleous material, opaline silica

P416 Glauconite has less staining than 420, 421, finer fracturing

P418 4 large masses up to 3.8 mm consisting of skeletal fragments, glauconite, Q/F glued together, similar to pellets but less well rounded and significantly larger

P420 Glauconite has more fracturing compared to 421 but less alteration rims and limonite, 1x volcanic gl

P422 Extensive endolithic boring with limonite infill

Table 7c. Petrography of NKCM sediments: P423-P435. Note: Samples are listed in running order with two pages per set of samples.

Sample Site	P423	P424	P425	P426	P427	P428	P429	P430	P431	P432	P433	P434	P435
Depth (m)	52	55	78	108	144	158	206	411	104	147	190	297	395
SILICICLASTIC MINERALS													
Quartz %	IA	IA	IC	IC	IC	IC	IC	S	IC	IC	IC	IC	S
Modal grain size - 1	0.24	0.18	0.08	0.14	0.18	0.15	0.16	0.13	0.25	0.21	0.14	0.20	0.15
Modal grain size - 2	0.19	0.22						0.17			0.11	0.16	0.17
Sorting	4	4	5	4	5	5	4	4	4	4	4	4	4
Roundness	3	3	3	3	3	3	3	3	3	3	3	3	3
Feldspar %	IA	uC	uC	IC	IC	IC	IC	IC	IC	IC	IC	uC	S
Modal grain size - 1	0.18	0.18	0.10	0.17	0.21	0.20	0.18	0.18	0.30	0.21	0.15	0.28	0.17
Modal grain size - 2	0.24	0.22		0.14	0.18	0.16		0.14			0.18	0.25	0.21
Sorting	4	4	5	4	4	4	4	4	4	4	4	4	4
Roundness	3	3	3	3	3	3	3	3	3	3	3	3	3
Biotite/Muscovite %	-	R	R	R	R	R	R	R	R	R	R	R	-
Modal grain size - 1		0.13	0.09	0.10	0.13	0.20	0.16	0.18	0.30	0.25	0.25	0.19	
Modal grain size - 2													
Sorting		4	4	4	4	4	4	4	4	4	4	4	
Roundness		3	3	3	4	4	3	3	3	3	3	3	
CALCICLASTICS													
Total %	IC	uC	IC	IC	IC	uC	uA	uA	IC	vA	uA	uvA	uvA
Sorting	3	2	2	4	4	4	4	3	3	3	3	3	4
Roundness	3	3	3	3	3	3	3	3	4	3	3	3	3
Skeletal abrasion	High	High	High	High	High	High	High	High	High	High	High	High	High
Bivalve %	C	C	R	-	R	R	R	R	R	S	R	R	R
Modal grain size - 1	1.00	1.70	3.25		0.43	0.89			0.60	1.05	1.20	1.58	1.00
Modal grain size - 2													
Gastropod %	C	S	-	R	R	-	R	R	R	S	R	R	R
Modal grain size - 1	0.50	0.75		0.42	0.50			1.98	0.75		1.30	0.50	
Modal grain size - 2													
Bryozoan %	-	-	-	R	-	-	R	R	R	S	-	uC	IA
Modal grain size - 1				0.25				0.85	0.33	0.35		1.15	0.85
Modal grain size - 2													1.65
Foram - benthic %	-	-	R	R	S	IC	S	uC	R	uC	A	uC	uC
Modal grain size - 1			0.27	0.20	0.18	0.31	0.32	0.32	0.35	0.38	0.35	0.35	0.33
Modal grain size - 2					0.40			0.27		0.33		0.28	0.38
Foram - planktic %	-	-	IC	S	S	uC	R	A	R	R	S	S	IA
Modal grain size - 1			0.10	0.18	0.20	0.15	0.23	0.20	0.30	0.40	0.26	0.33	0.23
Modal grain size - 2			0.08	0.14	0.09	0.24		0.25				0.38	0.27
Echinoderm %	R	-	R	R	-	-	S	uC	-	uC	R	uC	IC
Modal grain size	0.60		0.31	0.50			0.85	1.02		0.26	0.23	0.63	0.80
Serpulid %	-	-	-	-	R	-	R	R	-	-	-	-	-
Modal grain size					0.34		0.22	0.35					
Algae %	-	-	-	-	-	-	-	-	R	S	-	-	R
Modal grain size									0.65				
Spicules %	-	-	-	-	-	-	-	-	-	R	-	-	-
Modal grain size													
Opaline spines %	-	-	S	R	R	-	R	-	-	-	R	-	R
Modal grain size			0.15	0.15	0.15		0.12				0.60		
Coral %	-	-	-	-	-	-	-	-	-	-	-	-	-
Modal grain size													
Barnacle %	-	R	-	-	-	-	-	-	-	R	-	-	-
Modal grain size		0.42								0.26			
GLAUCONITE %	R	R	IC	S	S	IC	IC	IC	R	S	R	R	S
Modal grain size - 1	0.14	0.10	0.10	0.11	0.20	0.16	0.21	0.17	0.30	0.22	0.13	0.10	0.12
Modal grain size - 2			0.15	0.19		0.20	0.16	0.10					0.17
Sorting	4	4	4	4	4	4	4	4	4	4	4	4	4
Roundness	3	5	4	4	3	4	3	4	4	4	3	4	3

Table 7c cont. Petrography of NKCM sediments: P423-P435. Note: Samples are listed in running order with two pages per set of samples.

Sample Site	P423	P424	P425	P426	P427	P428	P429	P430	P431	P432	P433	P434	P435
Depth (m)	52	55	78	108	144	158	206	411	104	147	190	297	395
ROCK FRAGMENTS %	uC	uC	S	S	S	S	R	-	IC	R	S	R	R
Modal grain size - 1	0.20	0.15	0.35	0.18	0.20	0.18	0.20		0.38	0.33	0.21	0.14	0.25
Modal grain size - 2	0.16	0.17	0.18	0.15					0.55				
Sorting	4	4	4	4	4	4	4		3	4	4	4	4
Roundness	3	3	3	3	3	3	3		2	2	3	3	3
OPAQUES %	R	R	R	R	R	R	R	-	R	R	-	R	-
Modal grain size - 1	0.12	0.12	0.05	0.04	0.10	0.08	0.20		0.20	0.15		0.26	
Modal grain size - 2	0.08		0.04										
Sorting	4	4	5	4	4	4	4		4	4		4	
Roundness	3	3	4	3	3	3	3		3	4		3	
HEAVY MINERALS %*	S	R	R	R	R	R	R	R	R	R	R	S	R
Modal grain size - 1	0.24	0.14	0.07	0.08	0.16	0.19	0.10	0.15	0.34	0.21	0.20	0.17	0.13
Modal grain size - 2		0.10	0.13	0.21	0.42	0.15				0.16			
Sorting	4	4	4	4	3	4	4	4	4	4	4	4	5
Roundness	3	3	3	3	3	3	3	3	3	3	3	3	4
Hornblende	A	uA	IA	IC	IA	IA	uC	A	IC	IvA	uA	uA	uA
Oxyhornblende	IC	IC	IC	S	S	S	S	S	S	IC	S	R	S
Blue-green amphibole	S	S	S	R	S	S	S	R	R	-	R	R	R
Actinolite	-	-	-	-	-	-	-	-	-	-	S	R	R
Hypersthene	IC	IC	S	S	S	IC	S	uC	IC	S	IC	IC	IC
Epidote	R	R	R	R	R	S	R	R	S	S	S	S	R
Garnet	uC	vA	R	R	R	IC	S	R	R	S	-	S	S
Chlorite	-	-	-	-	R	-	R	R	-	S	S	R	-
Zircon	R	R	-	R	-	-	R	R	R	S	S	S	-
Clinozoisite	-	-	-	-	-	-	-	-	-	R	-	-	-
Titanite	S	R	R	R	R	R	R	R	R	S	R	R	R
Augite	IC	IC	S	IC	S	IC	S	uC	S	IA	IC	IC	uC
Monazite	-	-	-	-	-	-	-	-	-	-	-	-	-
LITHOCLAST/PELLET %	-	-	IC	uC	uA	IC	R	-	R	R	-	-	-
Modal grain size - 1			0.21	0.24	0.22	0.21	0.43		0.41	0.18			
Modal grain size - 2					0.32	0.26							
Sorting			4	4	4	4	4		4	4			
Roundness			5	4	5	4	4		4	4			
PHOSPHATE %	R	-	-	IC	IC	S	S	IC	-	S	S	S	S
Modal grain size	0.45			0.30	0.35	0.22		0.33		0.26	0.24	0.35	0.50
OVERALL													
Modal grain size - 1	0.18	0.23	0.15	0.38	0.25	0.18	0.12	0.17	0.30	0.40	0.35	0.70	0.85
Modal grain size - 2	0.13	0.88		0.16	0.18	0.13	0.25	0.85	0.60	0.21	0.14	0.20	0.17
Sorting	5	3	5	3	3	4	4	2	4	3	2	2	2
Roundness	3	3	3	3	3	3	3	3	3	3	3	3	3

Percentage range key:

R	=	0-5%	**uC**	=	20-30%	**vA**	= 50% +
S	=	5-10%	**IA**	=	30-40%	**uvA**	= 75% +
IC	=	10-20%	**uA**	=	40-50%		

Sorting		**Roundness**	
1	Very poorly sorted	1	Angular
2	Poorly sorted	2	Sub angular
3	Moderately sorted	3	Sub rounded
4	Well sorted	4	Rounded
5	Very well sorted	5	Well rounded

*** Note:** the heavy minerals proportions here are a percentage of the total heavy mineral content - not the total sediment.

P434 Plagioclase common, endolithic borings and glauconite/limonite infills

P435 Potential redeposition from shallower water, Endolithic borings common

P427 2 grains of volcanic glass

Table 7d. Petrography of NKCM sediments: P443-P607. Note: Samples are listed in running order with two pages per set of samples.

Sample Site	P443	P594	P595	P596	P597	P598	P599	P600	P602	P603	P604	P605	P606	P607
Depth (m)	65	1015	710	598	400	455	42	65	622	1050	838	478	300	90
SILICICLASTIC MINERALS														
Quartz %		lC	uC	lC	lC	lC	uC	lA	S		S	S	uC	lC
Modal grain size - 1		0.10	0.16	0.08	0.15	0.09	0.25	0.21	0.08		0.10	0.08	0.19	0.14
Modal grain size - 2		0.18					0.19	0.30	0.10			0.05	0.15	0.17
Sorting		4	5	4	4	5	4	5	4		4	4	4	4
Roundness		3	3	3	3	4	4	3	3		3	4	3	4
Feldspar %		lC	lA	S	S	lC	uC	lA	S		S	S	uC	uC
Modal grain size - 1		0.12	0.17	0.07	0.13	0.10	0.21	0.21	0.08		0.11	0.06	0.21	0.20
Modal grain size - 2		0.15	0.15			0.07	0.14	0.32				0.08	0.11	0.18
Sorting		4	4	4	4	4	4	4	4		5	4	4	5
Roundness		3	3	3	3	4	4	3	3		3	4	3	4
Biotite/Muscovite %		lC	R	S	R	R	R	R	R		-	R	uC	S
Modal grain size - 1		0.25	0.24	0.20	0.25	0.15	0.19	0.36	0.15			0.11	0.24	0.20
Modal grain size - 2		0.15											0.29	
Sorting		4	4	4	4	4	4	4	4			4	4	4
Roundness		2	3	3	3	3	3	3	3			4	3	3
CALCICLASTICS														
Total %		uvA	lA	lvA	vA	uA	S	S	uvA		uvA	uvA	uC	lC
Sorting		4	4	4	3	4	3	3	4		4	4	3	4
Roundness		3	3	3	3	3	3	3	3		3	3	3	3
Skeletal abrasion		High	High	High	High	High	High	High	High		High	High	High	High
Bivalve %		-	-	-	S	-	S	S	-		-	-	R	S
Modal grain size - 1					1.20		1.10	1.26					0.37	2.00
Modal grain size - 2														
Gastropod %		-	-	-	R	-	R	R	-		-	-	R	R
Modal grain size - 1					1.50		0.60	0.20					0.54	1.25
Modal grain size - 2														
Bryozoan %		-	-	-	S	-	-	-	-		-	R	S	-
Modal grain size - 1					0.40							0.45	0.65	
Modal grain size - 2														
Foram - benthic %		S	lC	uC	uC	uC	-	-	lA		uC	uC	lC	S
Modal grain size - 1		0.10	0.16	0.14	0.37	0.19			0.31		0.42	0.30	0.32	0.22
Modal grain size - 2		0.15		0.20					0.45		0.20	0.20		0.17
Foram - planktic %		A	lA	A	A	A	-	-	uA		A	A	C	R
Modal grain size - 1		0.20	0.20	0.12	0.26	0.19			0.20		0.25	0.29	0.26	0.24
Modal grain size - 2		0.24		0.09					0.17		0.30	0.20		
Echinoderm %		-	R	R	A	-	-	-	-		R	R	R	-
Modal grain size			0.21	0.38	0.40						0.75	0.70	2.10	
Serpulid %		-	-	-	R	R	-	-	-		-	-	-	-
Modal grain size					0.50	0.20								
Algae %		-	-	-	-	-	-	-	-		-	-	-	-
Modal grain size														
Spicules %		-	-	-	R	-	-	-	-		S	A	-	-
Modal grain size												0.35		
Opaline spines %		R	-	R	-	lC	-	-	uA		-	S	-	-
Modal grain size		0.17		0.15		0.10			0.05			0.10		
Coral %		-	-	-	-	-	-	-	-		-	-	-	-
Modal grain size														
Barnacle %		-	-	-	-	R	-	-	-		-	-	-	-
Modal grain size						0.35								
GLAUCONITE %		S	lC	uC	uC	lC	R	R	S		R	lC	lC	S
Modal grain size - 1		0.10	0.10	0.11	0.12	0.07	0.15	0.09	0.06		0.06	0.10	0.18	0.11
Modal grain size - 2		0.14		0.08	0.16	0.11						0.13		
Sorting		4	4	4	4	4	4	4	4		4	4	4	4
Roundness		4	3	4	3	3	4	4	4		3	4	4	4

Table 7d cont. Petrography of NKCM sediments: P443-P607. Note: Samples are listed in running order with two pages per set of samples.

Sample Site	P443	P594	P595	P596	P597	P598	P599	P600	P602	P603	P604	P605	P606	P607
Depth (m)	65	1015	710	598	400	455	42	65	622	1050	838	478	300	90
ROCK FRAGMENTS %		-	S	-	R	-	uC	uC	-		-	-	IC	IC
Modal grain size - 1			0.16		0.18		0.20	0.20					0.15	0.45
Modal grain size - 2							0.26	0.23					0.18	
Sorting			4		4		4	4					4	4
Roundness			3		3		4	3					3	3
OPAQUES %		R	R	-	R	-	R	R	-		-	-	R	S
Modal grain size - 1		0.18	0.08		0.08		0.09	0.13					0.11	0.10
Modal grain size - 2							0.10							
Sorting		4	4		4		4	4					5	4
Roundness		3	2		3		3	3					3	3
HEAVY MINERALS %*	S	R	S	S	S	R	uA	R	R	R	R	S	S	IC
Modal grain size - 1		0.12	0.23	0.22	0.20	0.07	0.18	0.21	0.13		0.09	0.07	0.16	0.18
Modal grain size - 2		0.15	0.18	0.18			0.15	0.25			0.22	0.14	0.20	0.16
Sorting		4	4	4	4	4	4	4	4		4	4	4	4
Roundness		3	3	4	3	4	4	3	3		3	3	3	3
Hornblende	uA	uA	uA	uA	uC	uC	vA	IA	S	S	S	IC	uA	IC
Oxyhornblende	S	R	R	S	R	R	IC	S	R	R	R	S	R	R
Blue-green amphibole	R	R	R	R	-	R	uC	S	R	S	S	R	IC	S
Actinolite	R	-	R	-	R	-	R	-	-	-	-	-	-	-
Hypersthene	S	S	S	R	S	S	S	S	S	S	S	S	IC	S
Epidote	S	R	-	R	R	R	R	R	-	R	R	-	R	R
Garnet	IC	-	R	R	R	S	R	vA	uC	uA	uA	S	R	uA
Chlorite	-	-	S	S	R	R	-	-	-	R	-	S	R	-
Zircon	R	R	-	R	R	-	-	S	-	R	-	R	R	R
Clinozoisite	-	-	-	-	-	-	-	-	-	-	-	-	-	-
Titanite	S	R	-	R	R	-	R	S	R	-	S	R	R	R
Augite	uC	S	S	S	S	S	uA	uC	uC	IC	uC	S	IC	uC
Monazite	-	-	-	-	-	-	-	-	-	-	-	-	-	-
LITHOCLAST/PELLET %		-	-	-	-	-	-	-	S		uC	uC	S	R
Modal grain size - 1									0.25		0.20	0.45	0.35	0.47
Modal grain size - 2									0.23		0.33	0.50		
Sorting									3		4	3	3	4
Roundness									4		5	5	5	4
PHOSPHATE %		S	S	R	uC	-	-	S	-		-	-	R	R
		0.22	0.18	0.18	0.40			1.04					0.39	3.00
OVERALL														
Modal grain size - 1		0.20	0.20	0.12	0.26	0.20	0.15	0.21	0.20		0.20	0.30	0.20	0.18
Modal grain size - 2		0.10	0.17	0.08	0.13	0.10	0.20	1.26	0.08		0.10	0.10	0.24	0.20
Sorting		4	4	4	4	4	4	3	3		3	3	4	4
Roundness		3	3	3	3	3	4	3	3		3	4	3	4

Percentage range key:

R	=	0-5%	**uC**	=	20-30%	**vA**	=	50% +
S	=	5-10%	**IA**	=	30-40%	**uvA**	=	75% +
IC	=	10-20%	**uA**	=	40-50%			

Sorting		**Roundness**	
1	Very poorly sorted	1	Angular
2	Poorly sorted	2	Sub angular
3	Moderately sorted	3	Sub rounded
4	Well sorted	4	Rounded
5	Very well sorted	5	Well rounded

*** Note:** the heavy minerals proportions here are a percentage of the total heavy mineral content - not the total sediment.

P598 Glauconite and mud/clay infill of forams

P600 Plagioclase very common, endolithic borings present

Appendix D: Skeletal data

Table 1a. Coarse skeletal identifications (>0.5 mm): P397-P409. Note: samples are listed in running order with two pages per set of samples.

Sample Site	P397	P398	P399	P400	P401	P402	P403	P404	P405	P406	P407	P408	P409
Depth (m)	216	149	107	70	42	33	34	63	86	110	161	206	38
MOLLUSCA													
Gastropoda - Total	4	1	3	11	1	-	1	3	8	12	2	-	1
- Percentage	33	8.3	14	5.3	0.8	-	2.3	0.7	1.9	11	8.8	-	0.7
Austrofusus glans			1	1						3	1		
Proxiuber australe													
Sigapatella tenuis									1				
Stiracolpus pagoda													
Dentimargo fusula													
Almalda novaezelandiae													
Antisolarium egenum										1			~1
Retusa sp. *Retusa oruaensis*													
Pupa affinis													
Antiguraleus sp.													
Syrnola crawfordi													
Epitonium ?bucknilli													
Cancellariidae, unnamed													
Emarginula striatula													
Mesoginella manawatawhia													
Volvulella nesenta													
Notoacmea sp. *N. daedala*													
Tanea zelandica													
Pervicacia tristis													
Antalis nana													
Solatisonax supraradiata													
Uberella denticulifera													
Epitonium sp.													
Pyramidellidae							1		1				
Zemitrella sp.													
Acteon cratericulatus													
Balcis sp.													
Alvinia (Linemea) gallinacea													
Philine constricta													
Solariella luteola													
Epitonium jukesianum													
Maoricrypta sodalis													
Pisinna sp.													
Notocrater craticulata													
Anatoma regia													
Atlanta peroni													
Amalda sp.			1										
Bivalvia - Total	1	-	-	10	34	5	9	15	22	10	-	-	5
- Percentage	8.3	-	-	4.8	28	0.9	21	3.6	5.2	9	-	-	3.6
Scalpomactra scalpellum				1	2		5	4	1	1			1
Nucula nitidula					1		1						
Pratulum pulchellum				1		1							
Hiatella arctica				2	9	4		10	4				4
Saccella maxwelli					1								
Pleuromeris zelandica				1					13	2			
Cardita aoteana													
Gonimyrtea concinna													
Pleuromeris sp.													
Talochlamys gemmulata													
Melliteryx sp.													
Moerella huttoni								1					
Poroleda lanceolata	1												
Limopsis lata													
Purpurocardia purpurata													
Nuculidae sp. Unnamed													
Neilo australis													
Serratina charlottae													

Table 1a cont. Skeletal identifications: P397-P409. Note: samples are listed in running order with two pages per set of samples.

Sample Site	P397	P398	P399	P400	P401	P402	P403	P404	P405	P406	P407	P408	P409
Depth (m)	216	149	107	70	42	33	34	63	86	110	161	206	38
Bivalvia cont.													
Zenatia acinaces													
Barbatia novaezealandiae													
Leptomya retiaria					2								
Caryocorbula zelandica													
Thyasira sp.													
Austrovenus stutchburyi							1						
Tawera spissa							1						
Myllitella vivens							1						
Notocallista multistriata									2				
Divaricella huttoniana													
Escalima regularis													
Borniola reniformis													
Barythaerus caneatus													
Parvamussium sp.													
Gari lineolata					6								
Pteropoda - Total	-	-	-	-	-	-	-	-	-	2.7	-	-	-
- Percentage	-	-	-	-	-	-	-	-	-	3	-	-	-
Cavolina inflexa													
Cavolina telemus										3			
Clio pyrmidata													
Scaphopoda	-	-	-	-	-	-	-	-	-	-	-	-	-
BRYOZOA - Total	-	-	-	4	-	3	-	15	3	1	-	-	1
- Percentage	-	-	-	1.9	-	0.6	-	3.6	0.7	0.9	-	-	0.7
Cellaria immersa													
Celleporaria tridenticulata													
Branching cheilostomes													
Steginoporella neozelandica													
Galeopsis polyporus													
Steginoporella sp.													
Free living Coneschareliinidae													
Otionella symmetrica								2					
Hippellozoon novazelandiae													
Notocyathus sp.													
FORAMINFERA - Total	5	4	3	-	1	1	-	7	6	3	-	-	-
- Percentage	42	33	14	-	0.8	0.2	-	1.7	1.4	2.7	-	-	-
Planktic forams						1		7	5	1			
Benthic forams	5	4	3		1				1	2			
Homotrema sp. *Benthic foram*													
Unidenified Shell Hash (%)	-	50	50	45	50	95	65	80	85	60	65	100	90
- dominance	-	-	-	Bi	Bi	Bi	Bi	Bi	Bi/G	G	Sr/G	Bi	Bi
Serpulids - Total	1	-	5	-	-	1	-	2	3	10	5	-	-
- Percentage	8.3	-	23	-	-	1	-	0.5	0.7	9	22	-	-
Rock Fragments (%)	-	-	-	40	17	2.8	10	10	5	5	4.4	-	5
Other													
Echinoid spine	1	1	-	2	1	1	-	-	-	-	-	-	-
Echinoid ossicle	-	-	-	-	3	-	1	-	-	-	-	-	-
Echinoid/barnacle plate	-	-	-	3	3	2	-	-	-	-	-	-	-
Fish otolith	-	-	-	1	-	-	-	-	-	-	-	-	-
Fish tooth?	-	-	-	-	-	-	-	-	-	-	-	-	-
Crab claw	-	-	-	-	-	-	-	-	-	-	-	-	-
Coral	-	-	-	-	-	-	-	-	-	-	-	-	-
Fish vertebrae	-	-	-	-	-	-	-	-	-	-	-	-	-
Overall Condition of Sample	F	R	R	F-M	F	F-M	F	F	M	M	R	R	F

Bi = bivalve
G = gastropod
Sr = serpulid
Br = bryozoan
Pt = Pteropod

F = fresh
M = mixed fresh-relict
R = Relict

Table 1b. Coarse skeletal identifications (0.5 mm): P410-P422. Note: samples are listed in running order with two pages per set of samples.

Sample Site	P410	P411	P412	P413	P414	P415	P416	P417	P418	P419	P420	P421	P422
Depth (m)	67	85	110	161	216	512	355	183	149	108	184	153	92
MOLLUSCA													
Gastropoda - Total	10	7	6	4	-	-	-	6	-	20	1	1	27
- Percentage	1.7	1.6	3	9.4	-	-	-	16	-	5.3	0.4	6	4.9
Austrofusus glans										4	1		
Proxiuber australe													
Sigapatella tenuis	2									1			
Stiracolpus pagoda										1			
Dentimargo fusula		1											
Almalda novaezelandiae													
Antisolarium egenum													
Retusa sp. *Retusa oruaensis*	1									1			
Pupa affinis													
Antiguraleus sp.													
Syrnola crawfordi													
Epitonium ?bucknilli													
Cancellariidae, unnamed													
Emarginula striatula													1
Mesoginella manawatawhia													1
Volvulella nesenta													1
Notoacmea sp. *N. daedala*													
Tanea zelandica													
Pervicacia tristis													
Antalis nana													
Solatisonax supraradiata													
Uberella denticulifera													
Epitonium sp.													
Pyramidellidae								1		1			
Zemitrella sp.								1					
Acteon cratericulatus										1			
Balcis sp.								1					
Alvinia (Linemea) gallinacea										1			
Philine constricta										1			
Solariella luteola								1					
Epitonium jukesianum													
Maoricrypta sodalis													
Pisinna sp.													
Notocrater craticulata													
Anatoma regia													
Atlanta peroni													
Amalda sp.													
Bivalvia - Total	52	17	3	1	-	1	-	6	1	30	4	1	59
- Percentage	8.7	3.8	1.5	2.3	-	0.1	-	16	1.3	7.9	1.7	6	11
Scalpomactra scalpellum	15	2		1					1	1			
Nucula nitidula	11							2		1	2		1
Pratulum pulchellum		1											28
Hiatella arctica	15												
Saccella maxwelli	2	1	2					1		2			
Pleuromeris zelandica	4	10						1		9	2		
Cardita aoteana													10
Gonimyrtea concinna													
Pleuromeris sp.										2			
Talochlamys gemmulata										1			
Melliteryx sp.										2			
Moerella huttoni										1			
Poroleda lanceolata													
Limopsis lata													
Purpurocardia purpurata													1
Nuculidae sp. Unnamed													
Neilo australis													
Serratina charlottae													

Table 1b cont. Coarse skeletal identifications (0.5 mm): P410-P422. Note: samples are listed in running order with two pages per set of samples.

Sample Site	P410	P411	P412	P413	P414	P415	P416	P417	P418	P419	P420	P421	P422
Depth (m)	67	85	110	161	216	512	355	183	149	108	184	153	92
Bivalvia cont.													
Zenatia acinaces													
Barbatia novaezealandiae													1
Leptomya retiaria													1
Caryocorbula zelandica													1
Thyasira sp.													
Austrovenus stutchburyi													
Tawera spissa													
Myllitella vivens													
Notocallista multistriata										6			
Divaricella huttoniana	1	1											
Escalima regularis													
Borniola reniformis													
Barythaerus caneatus													
Parvamussium sp.													
Gari lineolata													
Pteropoda - Total	-	-	-	-	-	-	-	-	-	-	-	-	-
- Percentage	-	-	-	-	-	-	-	-	-	-	-	-	-
Cavolina inflexa													
Cavolina telemus													
Clio pyrmidata													
Scaphopoda	-	-	-	-	-	-	-	-	-	-	-	-	-
BRYOZOA - Total	15	9	-	-	-	-	-	-	-	2	-	1	133
- Percentage	2.6	2	-	-	-	-	-	-	-	0.5	-	6	24
Cellaria immersa													33
Celleporaria tridenticulata													23
Branching cheilostomes													51
Steginoporella neozelandica													12
Galeopsis polyporus													8
Steginoporella sp.													4
Free living Conescharellinidae													
Otionella symmetrica	1	5								2			
Hippellozoon novazelandiae													
Notocyathus sp.													
FORAMINFERA - Total	3	7	2	3	1	-	123	6	2	18	3	45	41
- Percentage	0.5	1.6	1	7	11	95	70	16	2.5	4.7	1.3	50	7.5
Planktic forams	3	4		1		25%				18	2		3
Benthic forams		3	2	2		70%	123	6	2		1	45	11
Homotrema sp. *Benthic foram*													27
Unidenified Shell Hash (%)	75	85	85	60	-	-	-	-	90	70	45	10	50
- dominance	Bi	Bi/G	G/Sr	Bi	-	-	-	-	Bi	Bi/G	Bi	Bi	Bi/Br
Serpulids - Total	6	3	11	1	-	-	-	2	2	24	4	2	4
- Percentage	1	0.7	5.5	2.3	-	-	-	5.2	2.5	6.3	1.7	12	0.7
Rock Fragments (%)	10	5	4	-	89	0.7	29	30	3.8	5	50	10	1.6
Other													
Echinoid spine	2	1	-	7	-	38	6	5	-	-	-	-	-
Echinoid ossicle	-	-	-	-	-	-	-	-	-	-	-	-	-
Echinoid/barnacle plate	-	1	-	1	-	-	-	-	-	1	-	-	-
Fish otolith	-	-	-	-	-	-	-	-	-	-	-	-	-
Fish tooth?	-	-	-	-	-	-	-	-	-	-	-	-	-
Crab claw	-	-	-	-	-	-	-	-	-	-	-	-	-
Coral	-	-	-	-	-	-	-	-	-	-	-	-	-
Fish vertebrae	-	-	-	-	-	-	-	-	-	-	-	-	-
Overall Condition of Sample	F	M	M	M	F	R	F	M	M	R	R	M	M-R

Bi = bivalve
G = gastropod
Sr = serpulid
Br = bryozoan
Pt = Pteropod

F = fresh
M = mixed fresh-relict
R = Relict

Table 1c. Coarse skeletal identifications (0.5 mm): P423-P435. Note: samples are listed in running order with two pages per set of samples.

Sample Site	P423	P424	P425	P426	P427	P428	P429	P430	P431	P432	P433	P434	P435
Depth (m)	52	55	78	108	144	158	206	411	104	147	190	297	395
MOLLUSCA													
Gastropoda - Total	24	14	70	13	8	40	7	3	19	19	13	2	7
- Percentage	6	2.9	25	14	8.3	9.8	3.2	0.2	9.7	6.6	3.4	0.1	2.2
Austrofusus glans		1	23	5		3	3						
Proxiuber australe		2	2	1		3				1			
Sigapatella tenuis	13	4	1				1						
Stiracolpus pagoda						2	1				12		
Dentimargo fusula					1	1				10			
Almalda novaezelandiae			9										
Antisolarium egenum	2	2							1				
Retusa sp. *Retusa oruaensis*					1	2				1			3
Pupa affinis	4												
Antiguraleus sp.			3										
Syrnola crawfordi			2										
Epitonium ?bucknilli	2												
Cancellariidae, unnamed						2							
Emarginula striatula													
Mesoginella manawatawhia													
Volvulella nesenta													
Notoacmea sp. *N. daedala*	1												
Tanea zelandica	1												
Pervicacia tristis			1						2	1		1	
Antalis nana					1								
Solatisonax supraradiata							1						
Uberella denticulifera							1						
Epitonium sp.													
Pyramidellidae													
Zemitrella sp.													
Acteon cratericulatus													
Balcis sp.													
Alvinia (Linemea) gallinacea													
Philine constricta													
Solariella luteola									3				1
Epitonium jukesianum		1											
Maoricrypta sodalis									1				
Pisinna sp.									2				
Notocrater craticulata										1			
Anatoma regia													2
Atlanta peroni													1
Amalda sp.													
Bivalvia - Total	83	65	47	11	14	31	22	4	30	50	7	3	1
- Percentage	21	14	17	12	15	7.6	10	0.3	15	17	1.9	0.1	0.3
Scalpomactra scalpellum	76	59	2						4				
Nucula nitidula	1			2			2		3	39	1		
Pratulum pulchellum							1						
Hiatella arctica	3	3							1				
Saccella maxwelli			12			6	3				2		
Pleuromeris zelandica			6			3					2	3	
Cardita aoteana													
Gonimyrtea concinna			7			8							
Pleuromeris sp.				5									
Talochlamys gemmulata				1		1			2				
Melliteryx sp.				1		3							
Moerella huttoni	3												
Poroleda lanceolata					3								
Limopsis lata													
Purpurocardia purpurata							3						
Nuculidae sp. Unnamed					3								
Neilo australis			2										
Serratina charlottae			2										

Table 1c cont. Coarse skeletal identifications (0.5 mm): P423-P435. Note: samples are listed in running order with two pages per set of samples.

Sample Site	P423	P424	P425	P426	P427	P428	P429	P430	P431	P432	P433	P434	P435
Depth (m)	52	55	78	108	144	158	206	411	104	147	190	297	395
Bivalvia cont.													
Zenatia acinaces			2										
Barbatia novaezealandiae													
Leptomya retiaria													
Caryocorbula zelandica													
Thyasira sp.					2								
Austrovenus stutchburyi													
Tawera spissa													
Myllitella vivens									7				
Notocallista multistriata													
Divaricella huttoniana													
Escalima regularis								1					
Borniola reniformis									3				
Barythaerus caneatus													1
Parvamussium sp.													1
Gari lineolata													
Pteropoda - Total	-	-	25	-	-	4	-	4	1	3	-	8	6
- Percentage	-	-	9.1	-	-	1	-	0.3	0.5	1	-	0.4	1.9
Cavolina inflexa													2
Cavolina telemus												1	
Clio pyrmidata													
Scaphopoda	1	-	-	-	6	20	4	-	-	-	-	-	-
BRYOZOA - Total	1	2	1	-	2	2	51	32	-	16	6	93	-
- Percentage	0.3	0.4	0.4	-	2.1	0.5	24	2.6	30	5.5	1.6	4.3	80
Cellaria immersa					1	2	29	24	5	6	2	~90	
Celleporaria tridenticulata	1		1				18		12				5
Branching cheilostomes													
Steginoporella neozelandica								2		1		1	32
Galeopsis polyporus								2	5	1	2	1	33
Steginoporella sp.													
Free living Conescharellinidae					1								
Otionella symmetrica									2	7		1	
Hippellozoon novazelandiae							1						5
Notocyathus sp.								4					
FORAMINFERA - Total	1	-	-	13	18	65	-	-	-	-	-	1	14
- Percentage	0.3	-	-	14	19	16	-	10	-	-	-	0.1	4.4
Planktic forams	1			13		65							3
Benthic forams					18								7
Homotrema sp. *Benthic foram*													4
Unidenified Shell Hash (%)	70	80	55	50	50	60	45	70	40	60	90	95	10
- dominance	Bi	Bi/G	Bi/G	G/Bi	Bi	G	Bi/Br	Br	Bi	Bi/G	G/Bi	Br	-
Serpulids - Total	-	9	-	6	-	-	-	8	1	2	2	1	-
- Percentage	-	1.9	-	6.4	-	-	-	0.7	0.5	0.7	0.5	0.1	-
Rock Fragments (%)	0.3	-	-	2.1	-	0.5	2.8	-	20	-	1	-	-
Other													
Echinoid spine	-	-	-	-	-	-	11	15%	-	-	2	-	4
Echinoid ossicle	-	-	-	-	-	-	-	-	-	-	-	-	-
Echinoid/barnacle plate	9	3	6	1	-	-	17	8	8	26	4	-	-
Fish otolith	-	1	-	-	-	-	-	2	-	-	-	-	-
Fish tooth?	-	-	-	-	-	-	-	-	-	-	-	-	-
Crab claw	-	1	-	-	-	-	-	-	-	-	-	-	-
Coral	-	-	-	-	-	-	1	-	-	-	-	-	-
Fish vertebrae	-	-	-	1	-	-	-	-	-	-	-	-	-
Overall Condition of Sample	F	F	M	M	M	R	R	R	F	F/R	R	R	R

Bi = bivalve
G = gastropod
Sr = serpulid
Br = bryozoan
Pt = Pteropod

F = fresh
M = mixed fresh-relict
R = Relict

Table 1d. Coarse skeletal identifications (0.5 mm): P443-P607. Note: samples are listed in running order with two pages per set of samples.

Sample Site	P443	P594	P595	P596	P597	P598	P599	P600	P602	P604	P605	P606	P607
Depth (m)	65	1015	710	598	400	455	42	65	622	838	478	300	90
MOLLUSCA													
Gastropoda - Total	-	6	5	1	1	1	6	6	-	-	-	-	3
- Percentage	-	11.1	15	3.5	0.5	1.4	3.4	2.5	-	-	-	-	5.8
Austrofusus glans													1
Proxiuber australe													
Sigapatella tenuis													
Stiracolpus pagoda													
Dentimargo fusula													
Almalda novaezelandiae													
Antisolarium egenum													
Retusa sp. *Retusa oruaensis*													
Pupa affinis													
Antiguraleus sp.													
Syrnola crawfordi								1					
Epitonium ?bucknilli													
Cancellariidae, unnamed													
Emarginula striatula													
Mesoginella manawatawhia													
Volvulella nesenta													
Notoacmea sp. *N. daedala*													
Tanea zelandica													
Pervicacia tristis													
Antalis nana													
Solatisonax supraradiata													
Uberella denticulifera													
Epitonium sp.								1					
Pyramidellidae													
Zemitrella sp.													
Acteon cratericulatus													
Balcis sp.													
Alvinia (Linemea) gallinacea													
Philine constricta													
Solariella luteola													
Epitonium jukesianum													
Maoricrypta sodalis													
Pisinna sp.			2										
Notocrater craticulata													
Anatoma regia													
Atlanta peroni													
Amalda sp.													
Bivalvia - Total	2	4	-	1	6	-	44	38	-	-	-	1	5
- Percentage	0.7	7.4	-	3.5	2.8	-	25	16	-	-	-	7.5	9.6
Scalpomactra scalpellum							16	7				1	
Nucula nitidula							3	7					
Pratulum pulchellum													
Hiatella arctica							21	3					
Saccella maxwelli								1					
Pleuromeris zelandica					1								2
Cardita aoteana	1												
Gonimyrtea concinna													
Pleuromeris sp.								11					
Talochlamys gemmulata													
Melliteryx sp.													
Moerella huttoni								2					
Poroleda lanceolata													
Limopsis lata		2		1									
Purpurocardia purpurata													
Nuculidae sp. Unnamed													
Neilo australis													
Serratina charlottae													

Table 1d cont. Coarse skeletal identifications (0.5 mm): P443-P607. Note: samples are listed in running order with two pages per set of samples.

Sample Site	P443	P594	P595	P596	P597	P598	P599	P600	P602	P604	P605	P606	P607
Depth (m)	65	1015	710	598	400	455	42	65	622	838	478	300	90
Bivalvia cont.													
Zenatia acinaces													
Barbatia novaezealandiae	1												
Leptomya retiaria													
Caryocorbula zelandica													
Thyasira sp.													
Austrovenus stutchburyi													
Tawera spissa													
Myllitella vivens													
Notocallista multistriata													
Divaricella huttoniana							1						
Escalima regularis													
Borniola reniformis													
Barythaerus caneatus													
Parvamussium sp.													
Gari lineolata													
Pteropoda - Total	-	3	2	6	5	-	-	-	-	-	-	-	-
- Percentage	-	5.6	6.2	21	2.3	-	-	-	-	-	-	-	-
Cavolina inflexa													
Cavolina telemus													
Clio pyrmidata					1								
Scaphopoda	-	-	-	1	3	-	-	3	-	-	-	-	-
BRYOZOA - Total	177	9	2	4	33	1	2	7	-	1	4	-	1
- Percentage	66	16.7	6.2	14	15	1.4	1.1	2.9	-	2.6	5.3	-	1.9
Cellaria immersa	38			1	20								
Celleporaria tridenticulata	75	5		3				1					
Branching cheilostomes													
Steginoporella neozelandica		1											
Galeopsis polyporus	5	1											
Steginoporella sp.	37	2											
Free living Coneschar ellinidae					13								
Otionella symmetrica								6					
Hippellozoon novazelandiae	2												
Notocyathus sp.													
FORAMINFERA - Total	20	1	1	6	-	51	-	6	7	29	43	-	-
- Percentage	7.5	1.9	3.1	21	30	71	-	2.5	64	76	57	55	-
Planktic forams				1				6					
Benthic forams		1	1	5		51			7	29			
Homotrema sp. *Benthic foram*	20												
Unidenified Shell Hash (%)	20	40	60	30	40	-	70	60	-	-	5.3	-	75
- dominance	Br	G/Bi	-	Pt	Bi/Br	-	Bi	Bi	-	-	Bi	-	Bi
Serpulids - Total	-	-	1	-	2		-	-	-	-	-	-	4
- Percentage	-	-	3.1	-	0.9		-	15	-	-	-	-	7.7
Rock Fragments (%)	5	-	-	-	-		-	-	-	-	-	10	-
Other													
Echinoid spine	-	-	-	1	2%	16	3	-	4	8	24	20%	-
Echinoid ossicle	-	-	-	-	-	-	4	-	-	-	-	-	-
Echinoid/barnacle plate	2	2	-	-	6	1	-	-	-	-	-	-	-
Fish otolith	-	2	2	-	4	2	-	-	-	-	-	1	-
Fish tooth?	-	-	-	-	-	-	-	-	-	-	-	-	-
Crab claw	-	-	-	-	-	-	-	-	-	-	-	-	-
Coral	-	-	-	-	-	-	-	-	-	-	-	-	-
Fish vertebrae	-	-	-	-	-	-	-	-	-	-	-	-	-
Overall Condition of Sample	R	M-R	F	F	R	F	F	F	F	R	M	M	M

Bi = bivalve
G = gastropod
Sr = serpulid
Br = bryozoan
Pt = Pteropod

F = fresh
M = mixed fresh-relict
R = Relict

Table 2. Foraminifera identifications (0.063-1 mm): P443-P607. Note: samples are listed in running order with two pages per set of samples.

Sample Site	P405	P406	P407	P606	P605	P424	P426	P428	P430	P594
Depth (m)	86	110	161	300	478	55	108	158	411	1015
BENTHIC										
Cibicides corticatus	M-C	S-M	C	-	S	-	S-M	S-M	-	-
Cibicides marlboroughensis	S-M	R-S	R	-	S	-	R	R	R	-
Cibicides sp.	-	-	-	M	-	R	-	-	R	-
Dyocibicides sp.	R	R	-	-	-	R	-	R	R	-
Hoeglundina elegans	R-S	R	R	R	-	-	R-S	S-C	R	-
Evolvocassidulina orientalis	M	S	R	R	-	-	S	R	R	-
Quinqueloculina auberiana	S-M	R	-	-	-	A	S-M	-	S	-
Quinqueloculina af. *delicatula*	-	-	-	-	-	S-M	R	-	R	-
Quinqueloculina af. *cooki*	-	-	-	-	-	-	S	-	-	-
Quinqueloculina suborbicularis	-	-	-	-	-	-	-	R	-	-
Quinqueloculina sp.	-	-	-	-	-	-	-	-	R	-
Bulimina marginata f. *marginata*	R	R-S	R	R	S	-	S	M	-	-
Bulimina (hispid)	-	R	-	-	-	-	-	-	-	-
Bulimina sp.	-	-	-	-	-	-	-	-	R	-
Bolivina spathulata	R	-	-	R-S	S	R	S	-	-	-
Bolivina af. *neocompacta*	-	R	-	R-S	-	-	-	-	-	-
Bolivina cf. *hornbrooki*	-	-	R	-	-	-	-	-	-	-
Bolivina ?cacozela	-	-	S	-	-	-	-	-	-	-
Bolivina sp.	-	S	-	-	-	R	-	R	-	-
Notorotalia af. *depressa*	S	-	-	-	-	-	-	-	-	-
Notorotalia depressa	-	-	R	-	-	-	R	-	-	-
Notorotalia af. *finlayi*	-	-	-	-	-	R	-	-	-	-
Notorotalia ?zelandica	-	-	-	R	-	-	-	-	-	-
Notorotalia sp.	-	R-S	-	-	-	-	-	R-S	R	-
Pyrgo depressa	R	-	-	-	-	-	-	-		-
Pyrgo anomala	-	-	R	-	-	-	-	-	R	-
Lenticulina ?australis	-	R		S	-	-	-	-	-	-
Lenticulina af. *suborbicularis*	-	-	R	-	-	-	-	-	-	-
Lenticulina subgibba	-	-	R	-	-	-	-	R	-	-
Lenticulina sp.	-	-	R	-	R	-	R	R	-	-
Lenticulina sp. 2	-	-	-	-	R	-	-	-	-	-
Lenticulina sp. 3	-	-	-	-	R	-	-	-	-	-
Discorbinella bertheloti	R-S	R	-	-	-	-	-	R	-	-
Saidovina karreriana	R	-	S	R	-	-	S-M	M-C	R	-
Uvigerina (hispid)	R	-	-	-	-	-	-	-	-	-
Uvigerina peregrina	-	-	S	M-C	C	-	-	S-M	-	-
Uvigerina sp.	-	R	-	-	-	-	-	-	-	-
Uvigerina ?rodleyi	-	-	-	-	-	-	-	-	R	-
Zeaflorilus parri	R	-	-	R	-	C	R	R	-	-
Lagena sp.	R	-	-	-	-	-	-	-	-	R
Lagena striata	-	-	R	-	-	-	-	-	-	-
Lagena ?spicata	-	-	-	-	-	-	R	-	-	-
Lagena (hispid)	-	-	-	-	-	-	-	R	-	-
Astrononion novozealandicum	-	-	R	-	-	-	R	M	S	-
Astrononion sp.	-	R	-	-	-	-	-	-	-	-
Oridorsalis umbonatus	-	R	R	-	-	-	R	R-S	-	-
Planularia australis	-	-	-	-	R	-	-	R	-	-
Pullenia bulloides	-	-	-	-	R	-	-	-	R	-
Pullenia subcarinata	-	-	-	-	R	-	-	-		-
Sphaeroidina bulloides	-	R	R	-	-	-	S	R	R	-
Oolina af. *melo*	-	R	-	-	-	-	-	-	-	-
Elphidium sp.	-	R	-	-	-	-	-	-	R	-
Neouvigerina proboscidea	-	-	S	-	-	-	R	R	-	-
Cassidulina carinata	-	-	R	-	-	-	R	-	R	-
?Nonionellina flemingi	R	-	-	-	-	-	-	-	-	-
Nonionella magnalingua	-	-	-	-	R	-	-	-	-	-
Bolivinta sp.	-	R	-	-	-	-	-	-	-	-
Trioculina ?tricarinata	-	-	R	-	-	-	-	-	R	-
Trifarina angulosa	-	-		-	-	-	-	-	S-M	-
Chilostomella sp.	-	-	R	-	-	-	-	-	-	-

Table 2 cont. Foraminifera identifications (0.063-1 mm): P443-P607. Note: samples are listed in running order with two pages per set of samples.

Sample Site	P405	P406	P407	P606	P605	P424	P426	P428	P430	P594
Depth (m)	86	110	161	300	478	55	108	158	411	1015
BENTHIC cont.										
Haynesina depressula	-	-	-	-	-	S	-	-	-	-
Gyroidina sp.	-	-	-	-	-	-	-	R	R	-
Saracenaria italica	-	-	-	R	-	-	-	-	-	-
Reussella spinulosa	-	-	-	R	-	-	-	-	-	-
Fursenkoina schreibersiana	-	-	-	R	-	-	-	-	-	-
Globobulimina sp.	-	-	-	-	R	-	R	R	-	-
Amphicoryna hirsuta	-	-	-	R	-	-	-	-	-	-
Laevidentalina sp.	-	-	-	R	R	-	-	-	-	-
Stilostomella sp.	-	-	-	-	R	-	-	R	-	-
Gyroidinoides sp.	-	-	-	-	R	-	-	-	-	-
Ammonia sp.	-	-	-	-	-	-	S-M	R	-	-
Laticarrinina pauperata	-	-	-	-	-	-	-	R	-	-
Anomalinoides sphericus	-	-	-	-	-	-	-	R	-	-
Savacenarid ?latifrons	-	-	-	-	-	-	-	R	-	-
Globocassidulina canalisuturata	-	-	-	-	-	-	-	R-S	-	-
Globocassidulina subglobossa	-	-	-	-	-	-	-	-	R	R
Ehrenbergina af. *willetti*	-	-	-	-	-	-	-	-	-	-
Unknown sp. 1	-	R	S	-	-	R	R	R	-	-
Unknown sp. 2	-	R-S	-	-	-	-	-	-	-	-
Sigmoilopsis schlumbergeri	-	-	-	-	-	-	-	-	-	R
Sigmoilopsis ?elliptica	-	-	-	-	-	-	R	-	-	-
Sigmoilopsis sp. 1	-	-	-	-	-	-	R	-	-	-
Sigmoilopsis sp. 2	-	-	-	-	-	-	R	-	-	-
Semivulvulina sp.	R	-	-	-	-	-	-	-	-	-
Textularia sp.	-	-	R	-	-	-	R	R	R	R
Siphotextularia ?	-	-	-	R	-	-	-	-	-	-
Agglutinated sp. (int)	-	-	-	-	-	-	R	R	-	R
PLANKTIC										
Globorotalia inflata	S	S	M	M	C	R	R	R-S	C-A	A
Globorotalia crassaformis "keeled"	R	-	-	R	S	-	-	-	-	-
Globorotalia crassaformis "unkeeled"	R	R	-	-	-	-	-	-	-	-
Globorotalia crassula	-	-	-	-	R	-	-	R	-	-
Globorotalia truncatulinoides	-	R	R	R-S	S	-	-	R-S	S	S
Globorotalia ?puncticuloides	-	-	-	-	-	-	-	-	R	-
Globigerinoides aequilateralis	-	R	-	R	-	-	R	-	R	S
Globigerinoides ruber	-	-	R	-	R	R	R	R	-	S-M
Globigerinoides ?ruber	-	-	-	-	-	-	-	-	R	-
Globigerina bulloides	R	M	S	S	S-M	S	M	R-S	M-C	S
Neogloboquadrina pachyderma	-	-	R	-	-	R	R	-	S	R
Neogloboquadrina dutertrei	-	-	-	-	-	-	-	-	-	R
Orbulina universa	R	R	R	S	S	R	R	R-S	R	C-A
Globigerina quinquloba	-	-	-	-	R	-	-	-	-	-
PLANKTIC:BENTHIC RATIO	30:70	30:70	30:70	50:50	50:50	10:90	10:90	60:40	70:30	95:5

Unknown sp. 1 — Moderately small and transulcent, spiral side can see al the chambers (convolute), involute ventral side, sutures sweep out to periphery on ventral side, flat spiral side, slightly ventroconical

Unknown sp. 2 — Small to moderate in size, biconvex, sharp periphery, perforate, spiral

R	Rare	<5%
S	Some	5-10%
M	Many	10-30%
C	Common	30-50%
A	Abundant	>50%

Appendix E: Microprobe images and data

Backscatter electron image (BEI) of glauconite grain A in sample P399. Black dot shows location of sample point.

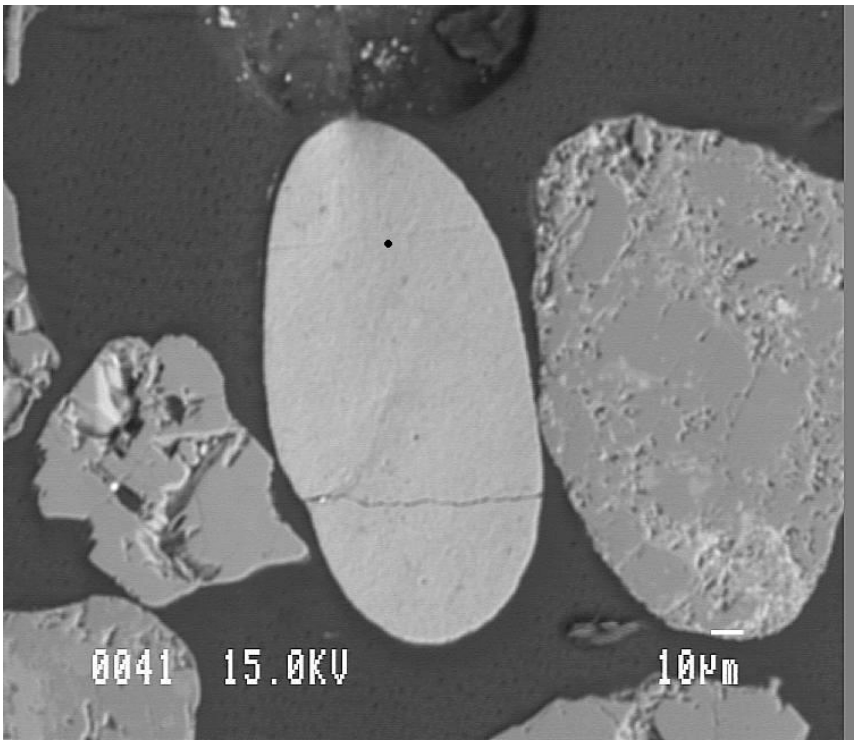

BEI of glauconite grain A2 in sample P399. Black dot shows location of sample points.

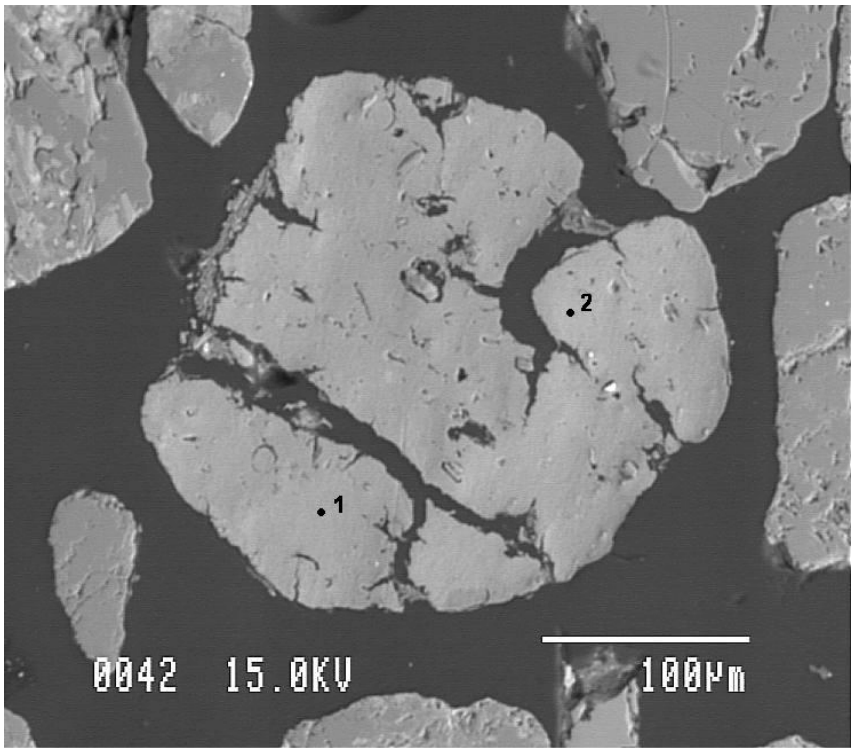

BEI of glauconite grain C in sample P399. Black dot shows location of sample point.

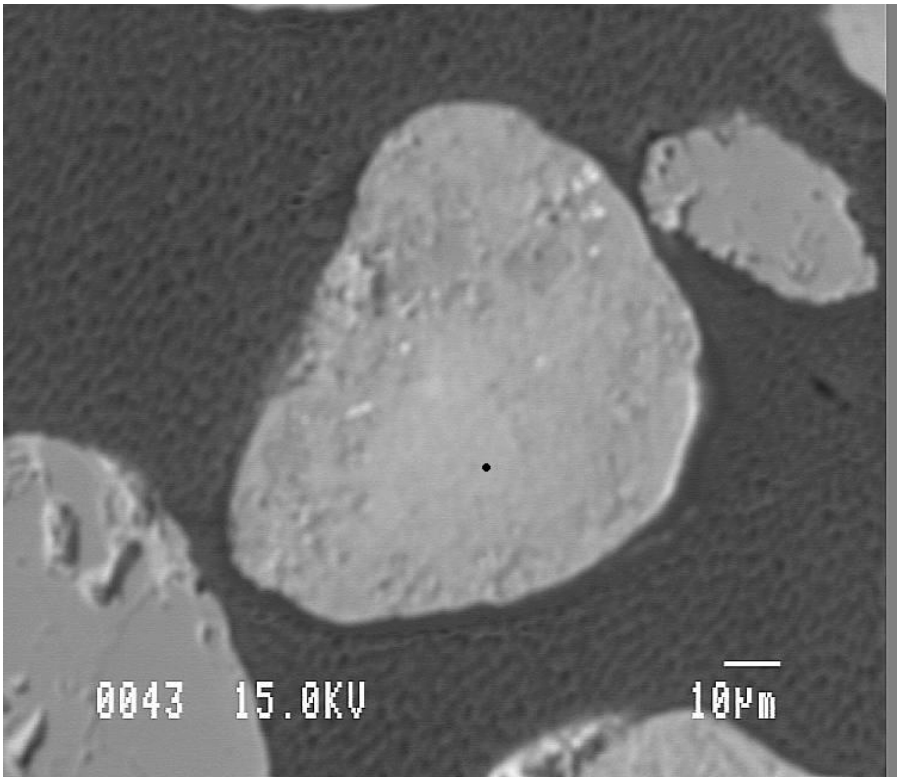

BEI of glauconite grain A in sample P414. Black dot shows location of sample point.

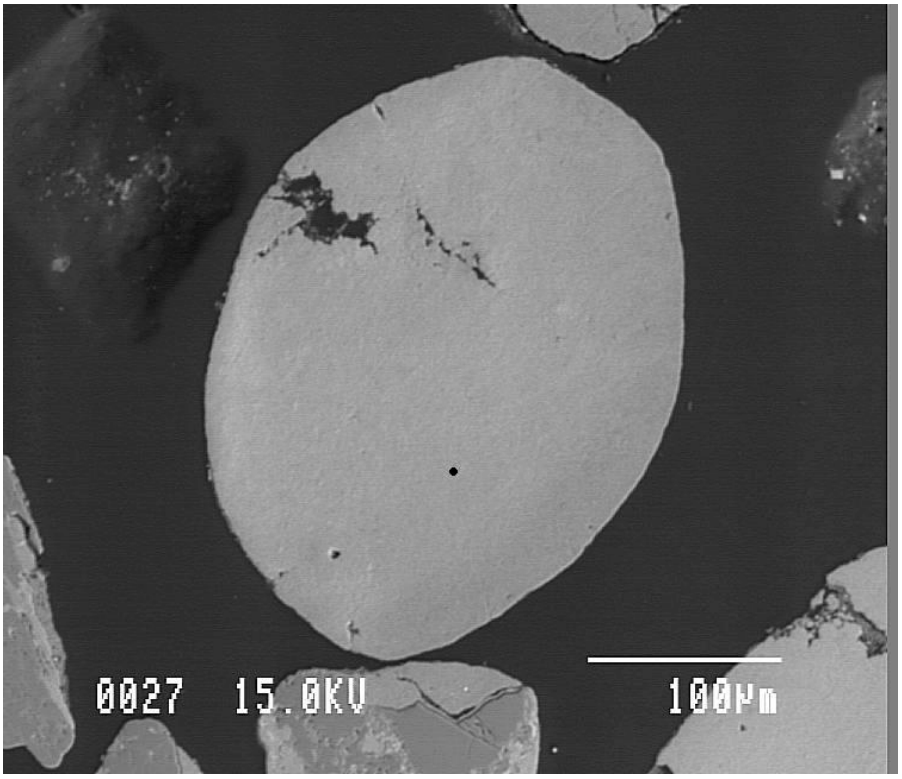

BEI of glauconite grain B in sample P414. Black dot shows location of sample points.

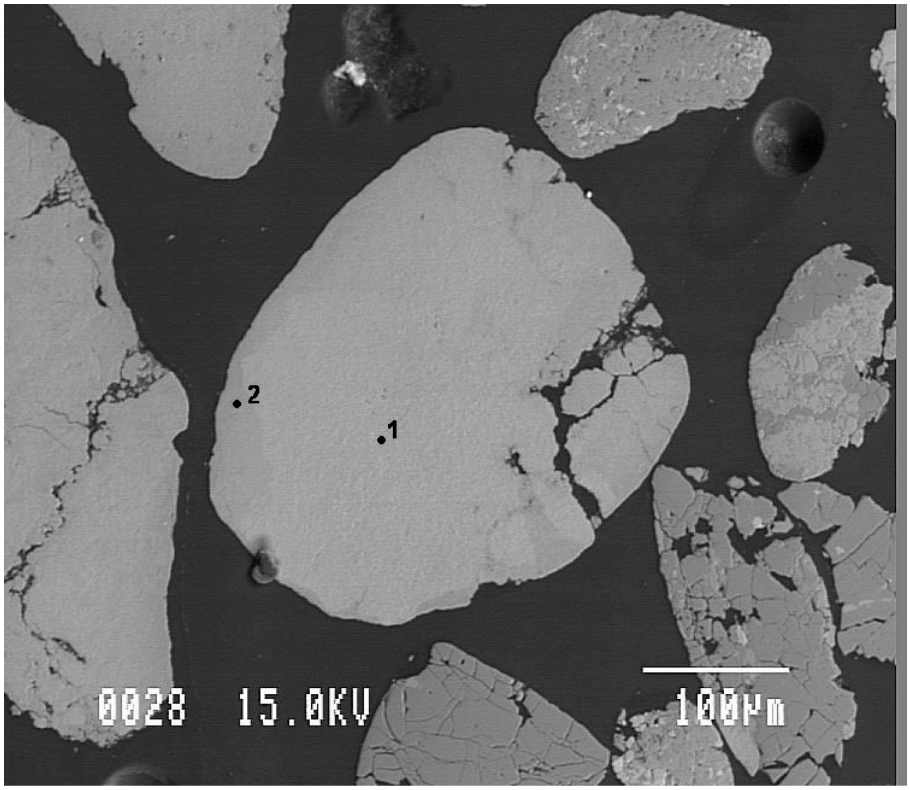

BEI of glauconite grain C in sample P414. Black dot shows location of sample points.

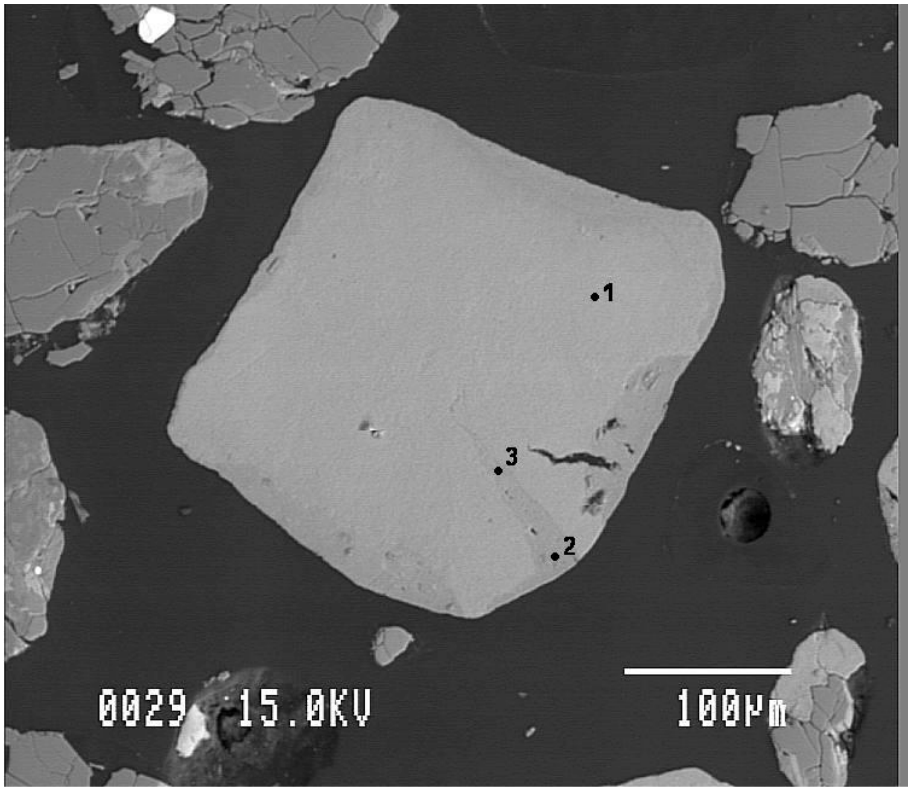

Microprobe images and data

BEI of glauconite grain D in sample P414. Black dot shows location of sample point.

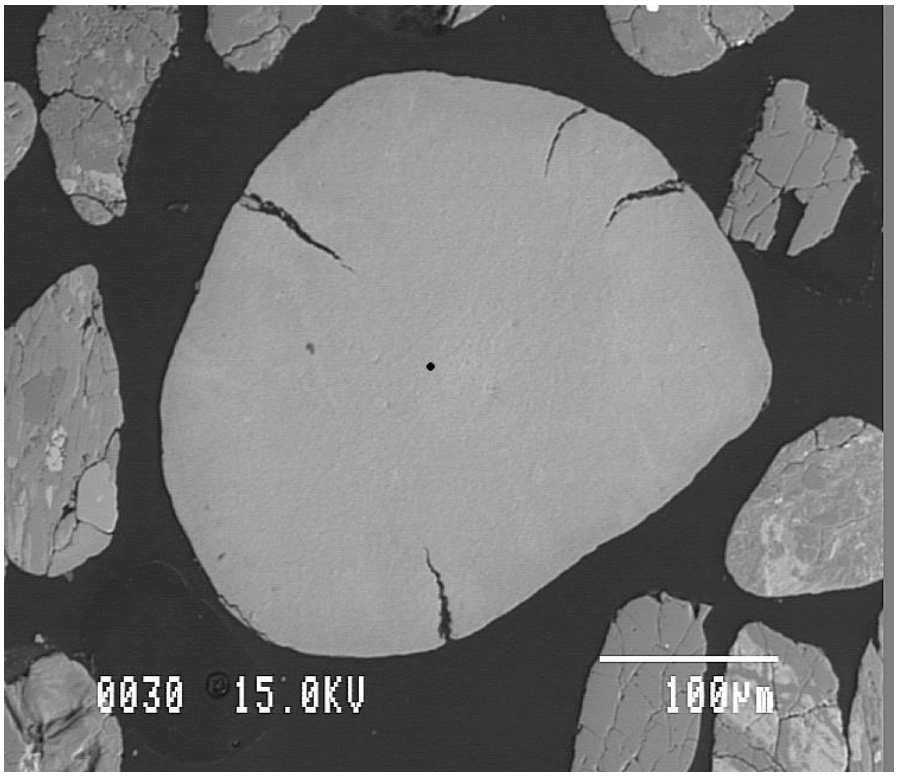

BEI of glauconite grain E in sample P414. Black dot shows location of sample point.

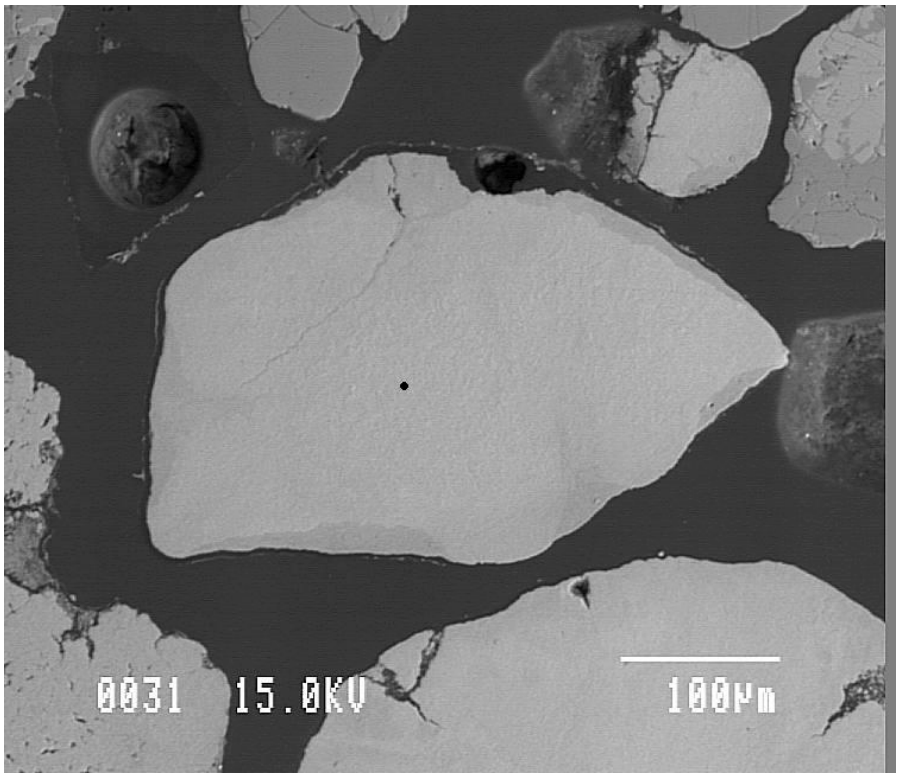

BEI of glauconite grain A1 and A2 in sample P416. Black dot shows location of sample points.

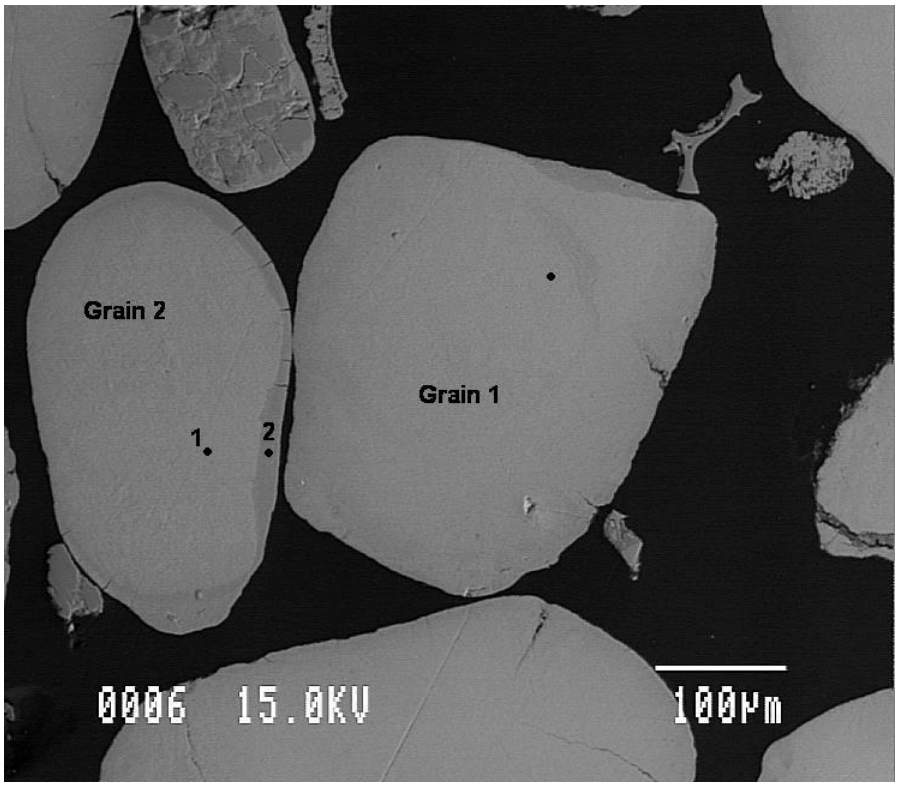

BEI of glauconite grain B in sample P416. Black dot shows location of sample point.

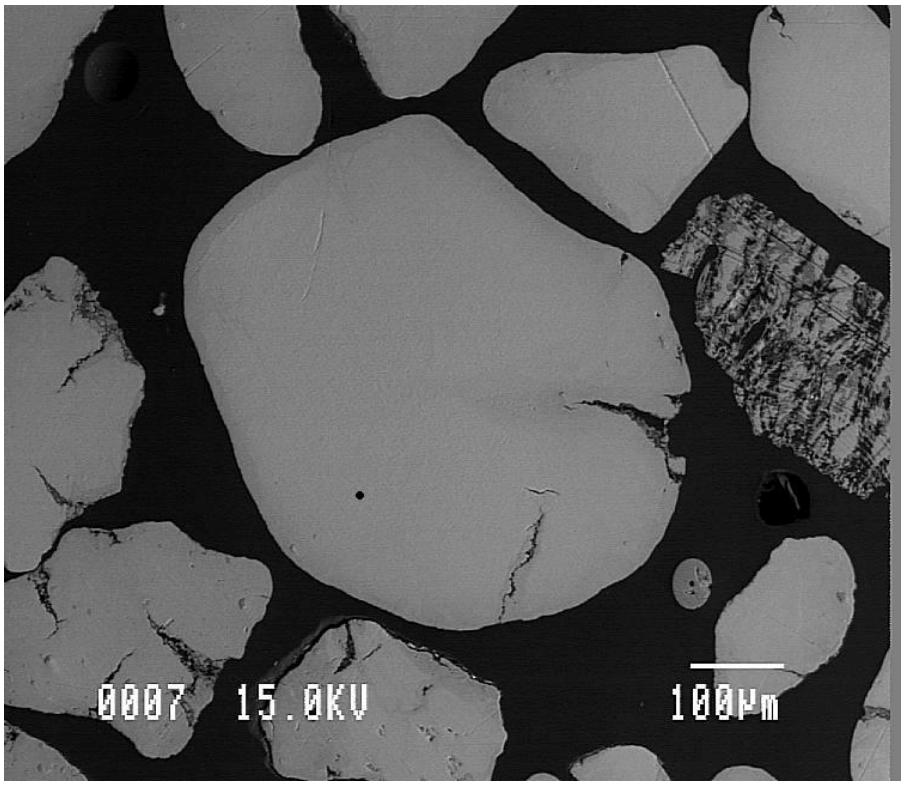

Microprobe images and data

BEI of glauconite grain C in sample P416. Black dot shows location of sample point.

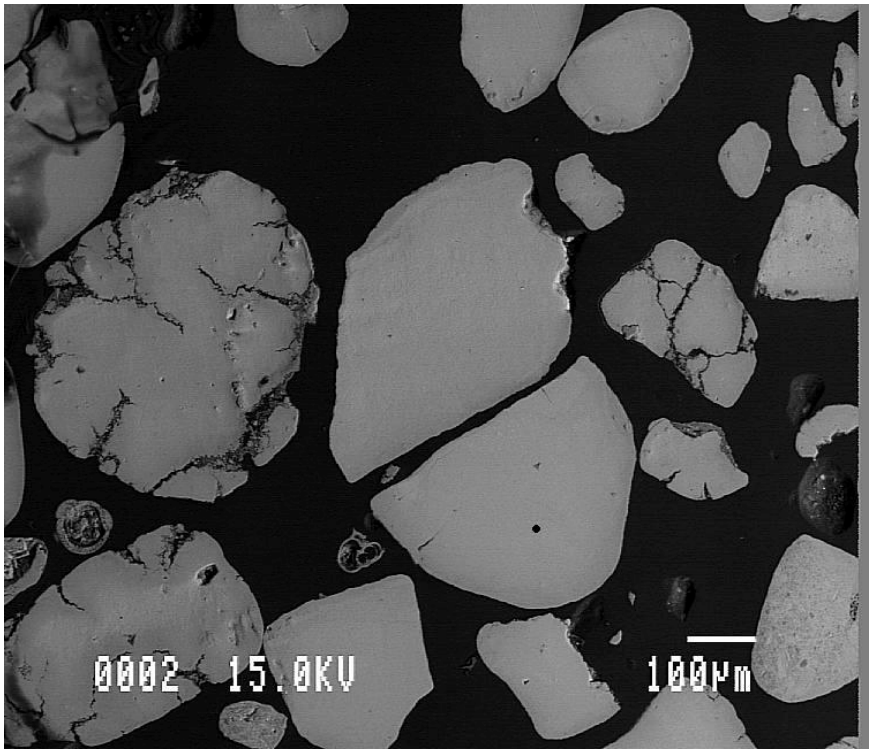

BEI of glauconite grain D in sample P416. Black dot shows location of sample point.

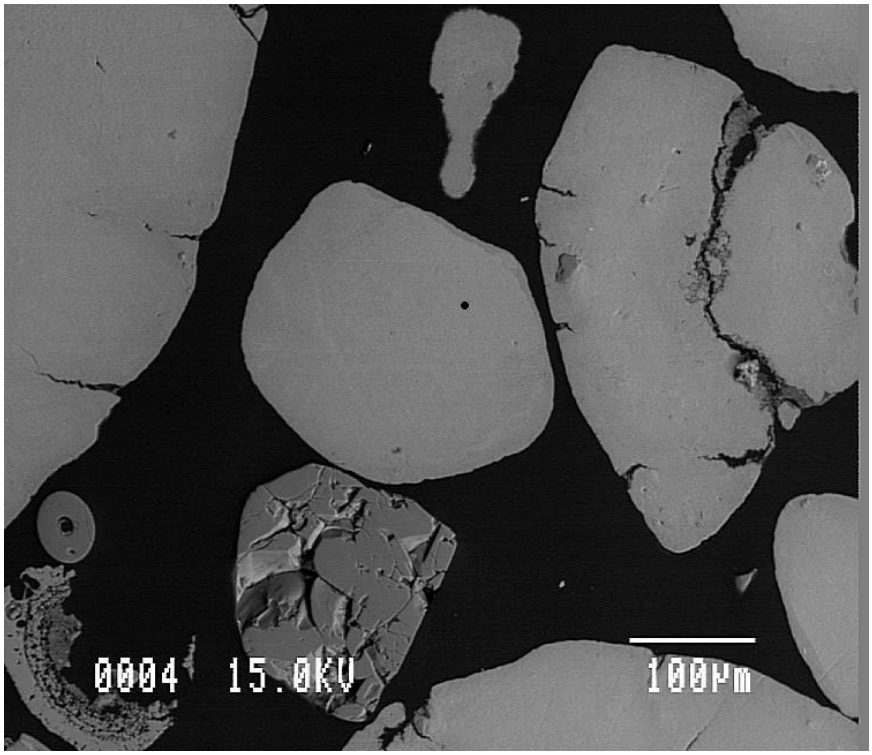

BEI of glauconite grain E in sample P416. Black dot shows location of sample point.

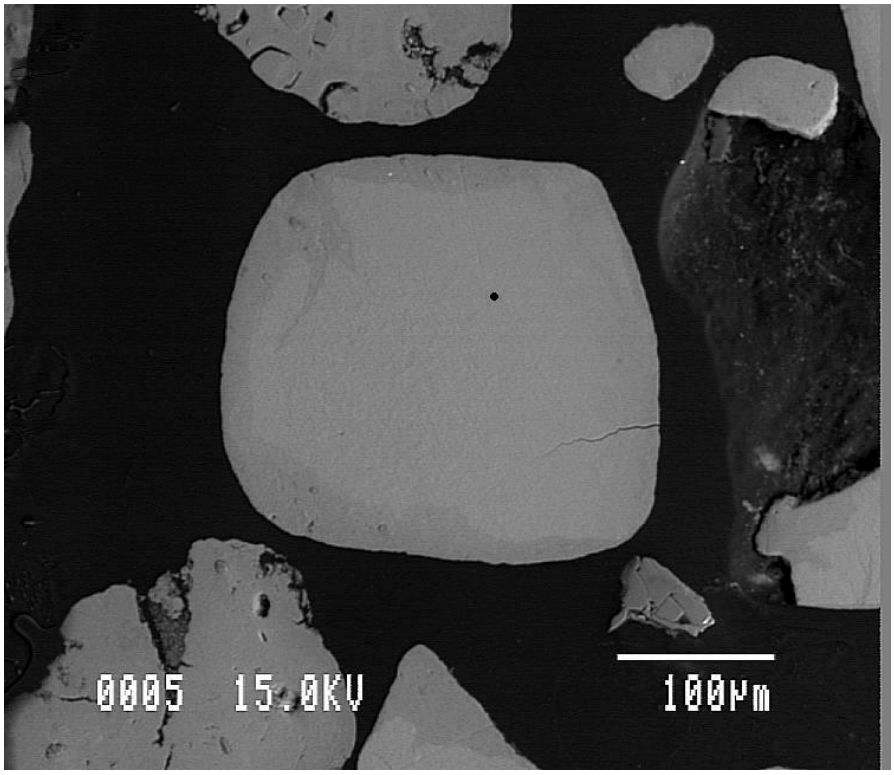

BEI of glauconite grain A in sample P417. Black dot shows location of sample point.

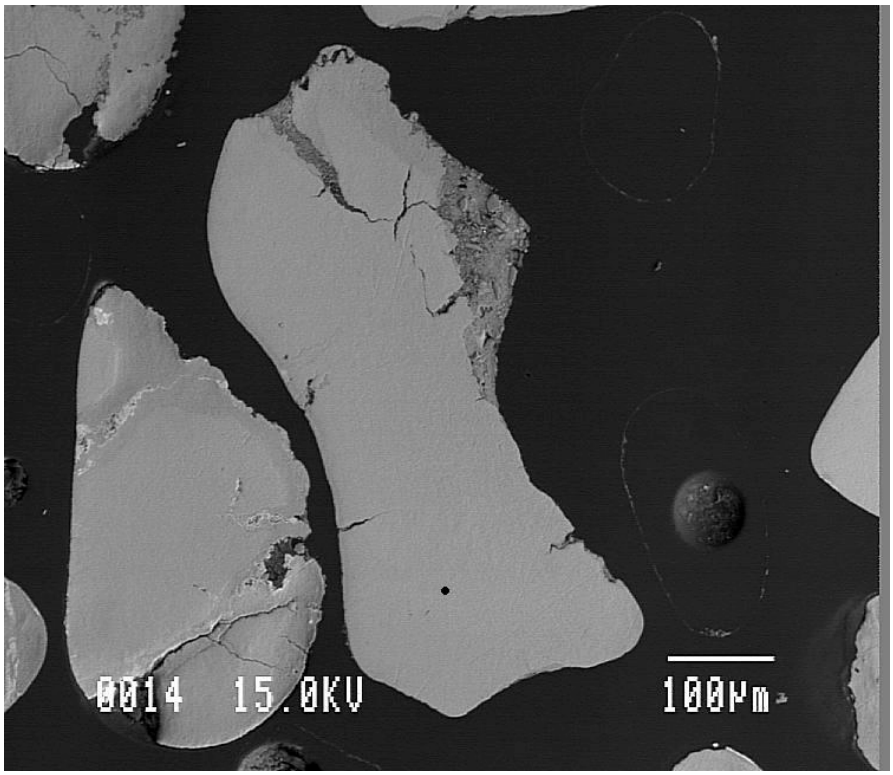

Microprobe images and data

BEI of glauconite grain B in sample P417. Black dot shows location of sample point.

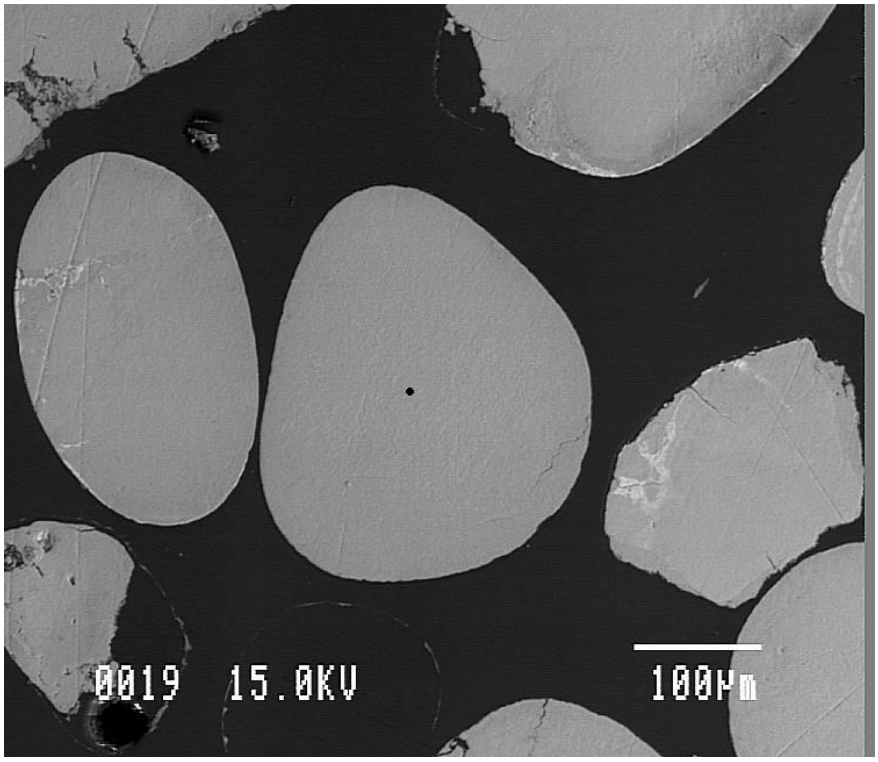

BEI of glauconite grain C in sample P417. Black dot shows location of sample point.

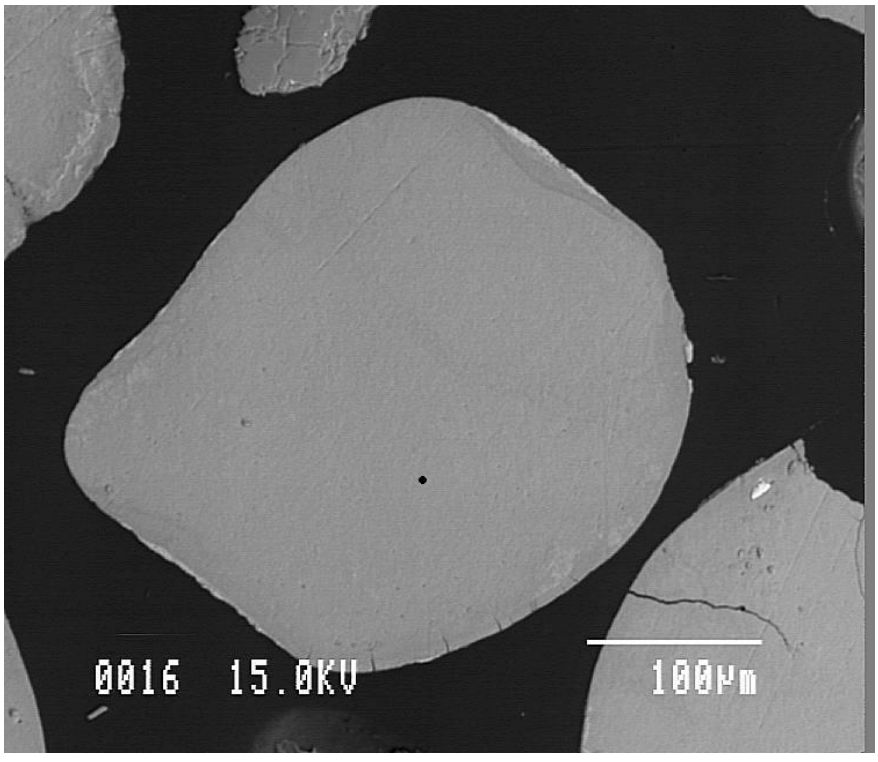

BEI of glauconite grain D in sample P417. Black dot shows location of sample point.

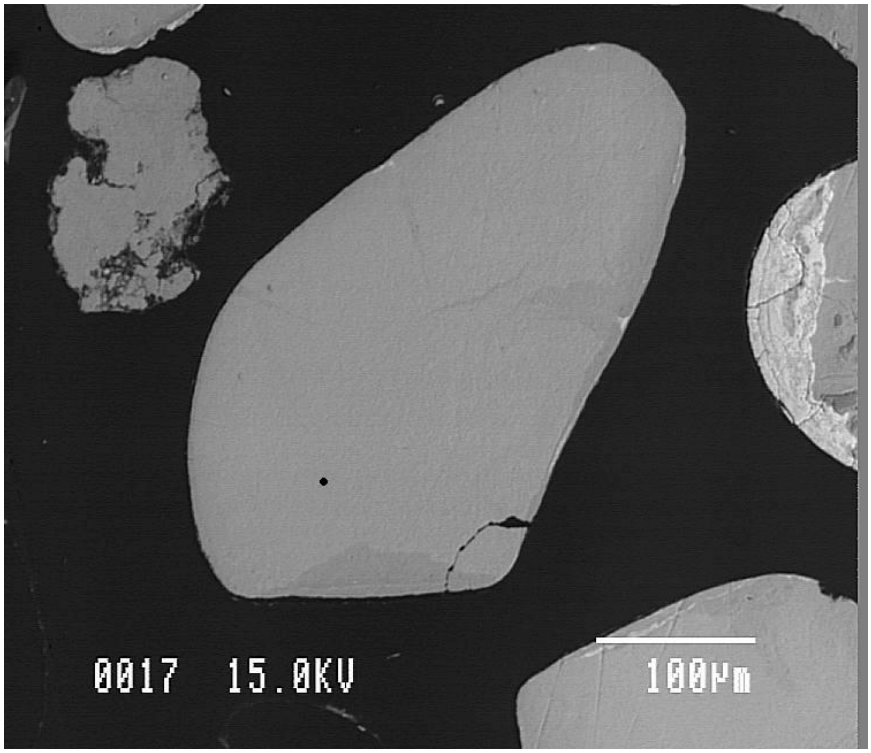

BEI of glauconite grain E in sample P417. Black dot shows location of sample point.

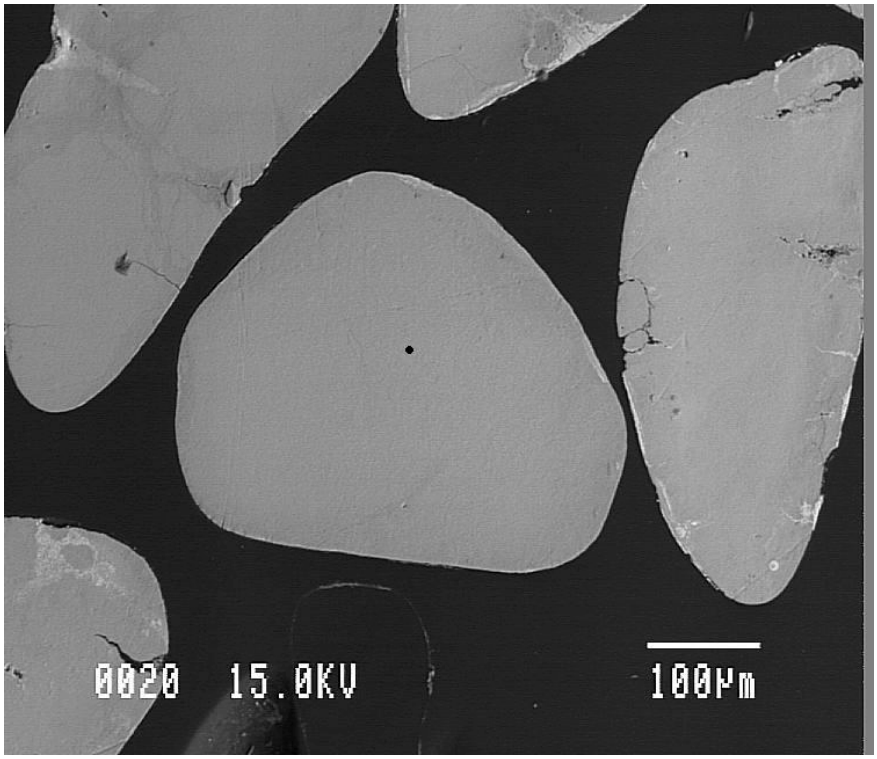

Microprobe images and data

BEI of glauconite grain A in sample P420. Black dot shows location of sample point.

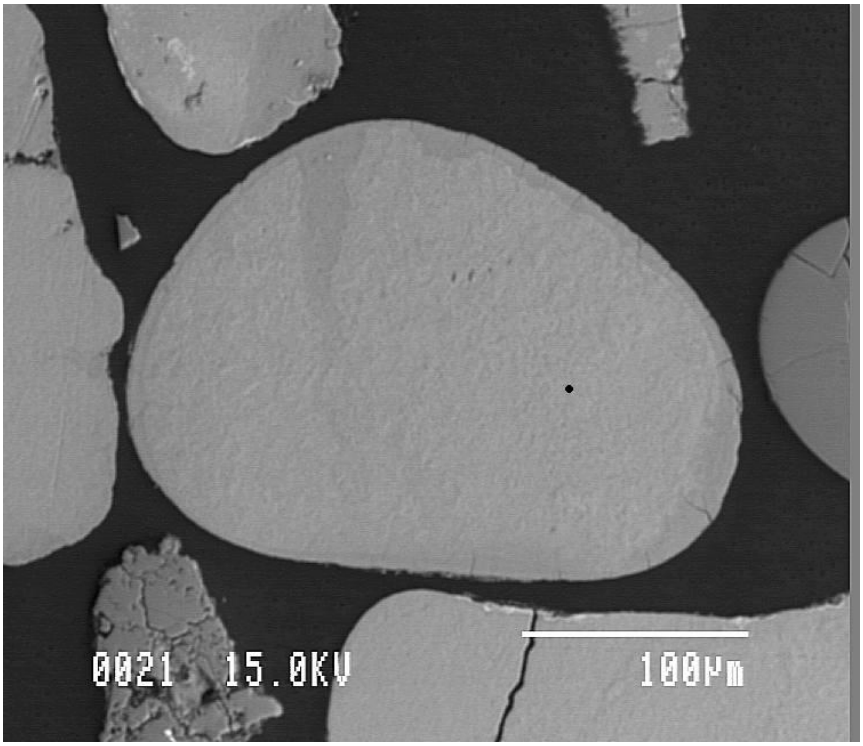

BEI of glauconite grain B in sample P420. Black dot shows location of sample point.

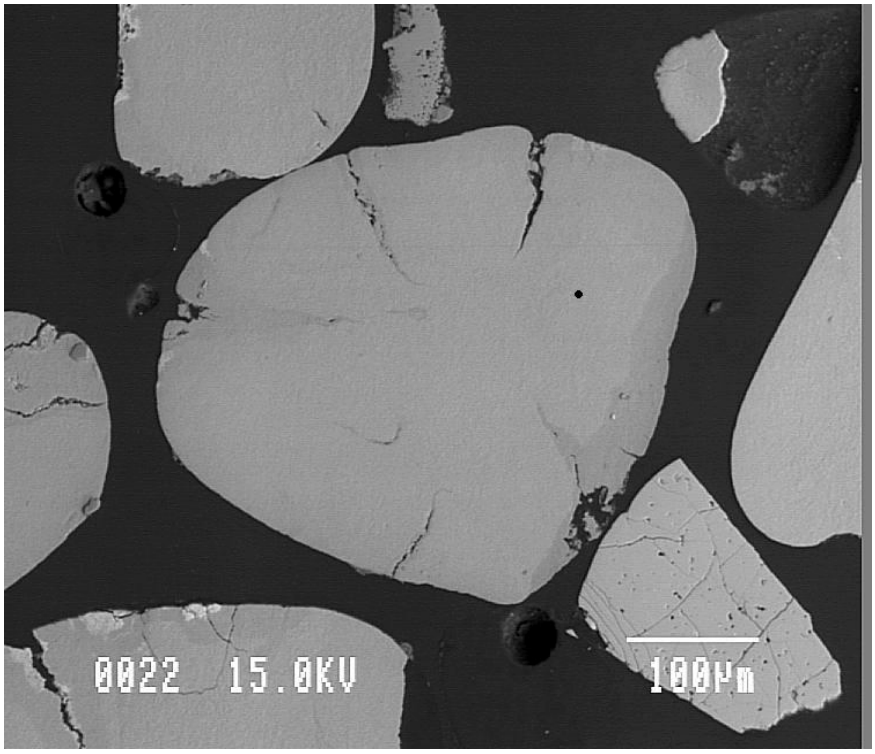

BEI of glauconite grain C in sample P420. Black dot shows location of sample point.

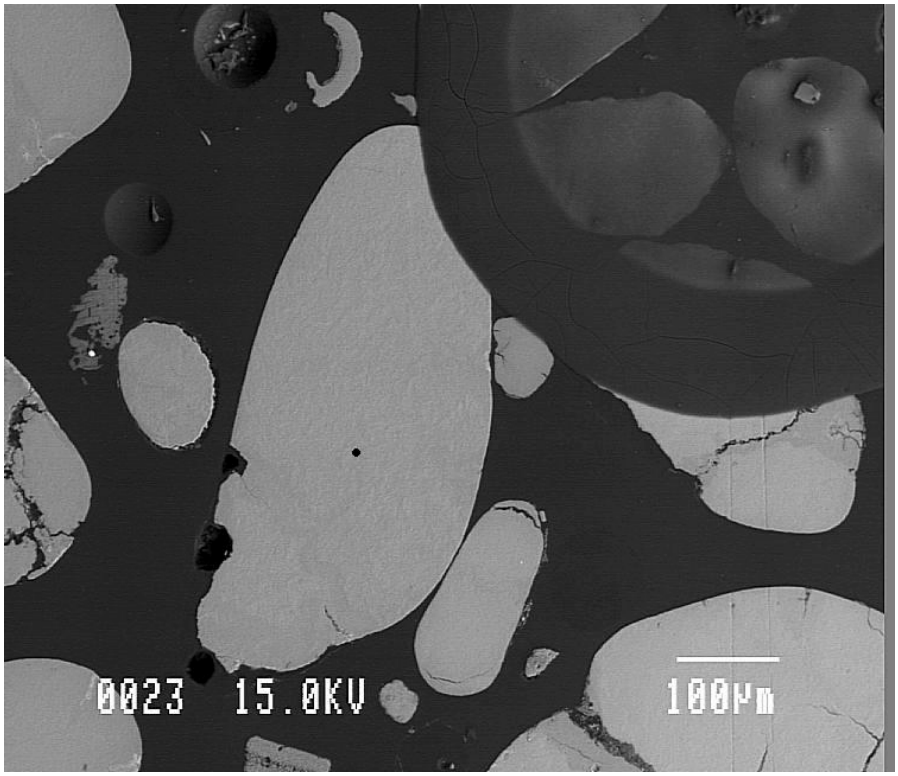

BEI of glauconite grain D in sample P420. Black dot shows location of sample point.

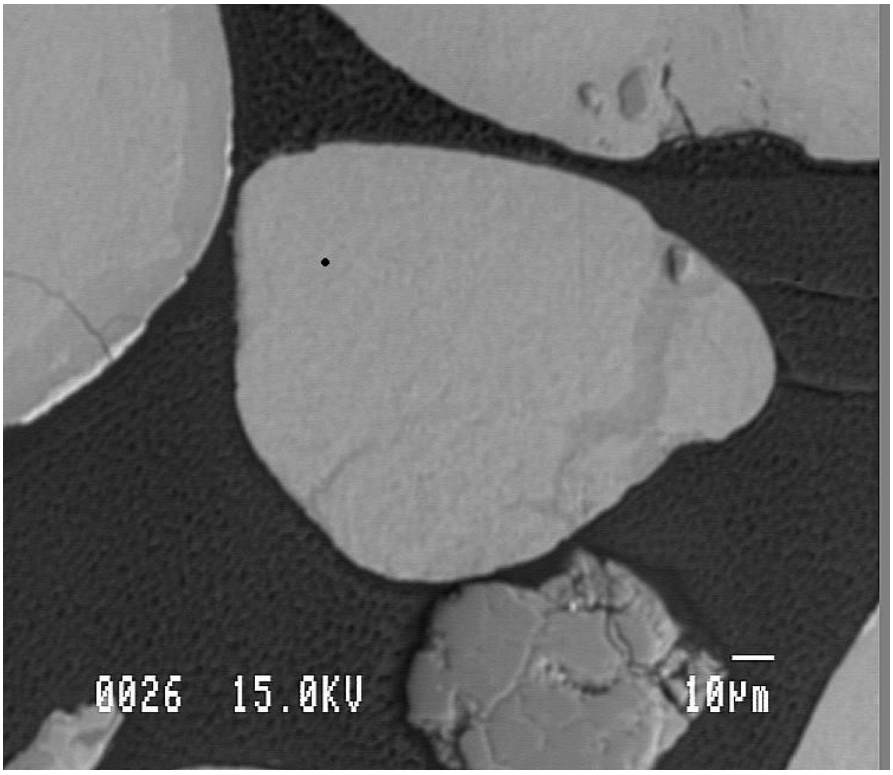

Microprobe images and data

BEI of glauconite grain E in sample P420. Black dot shows location of sample point.

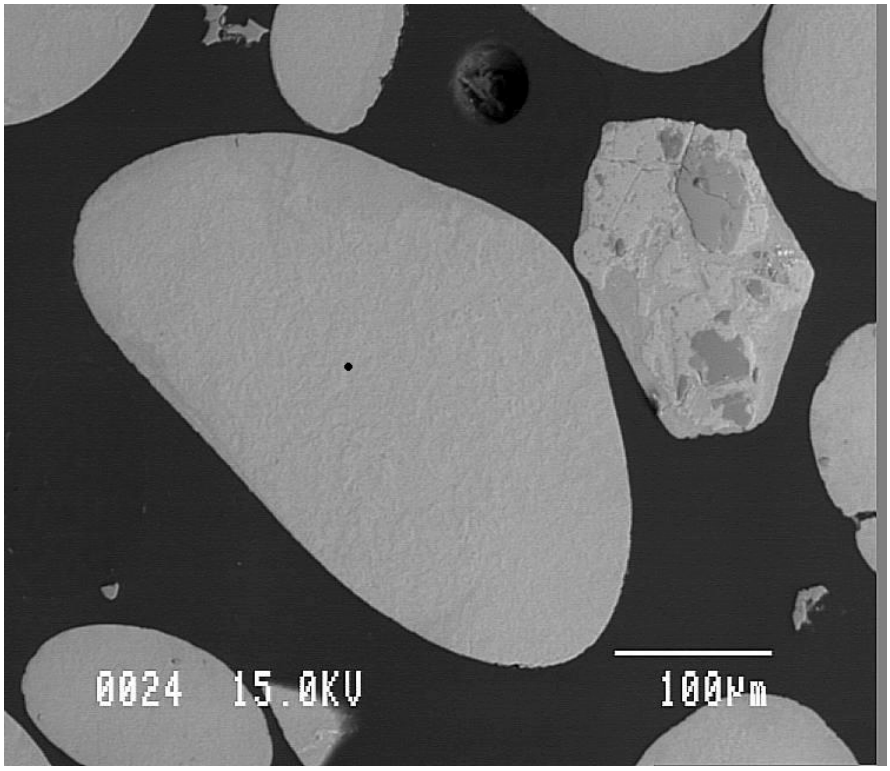

BEI of glauconite grain A1 and A2 in sample P421. Black dot shows location of sample points.

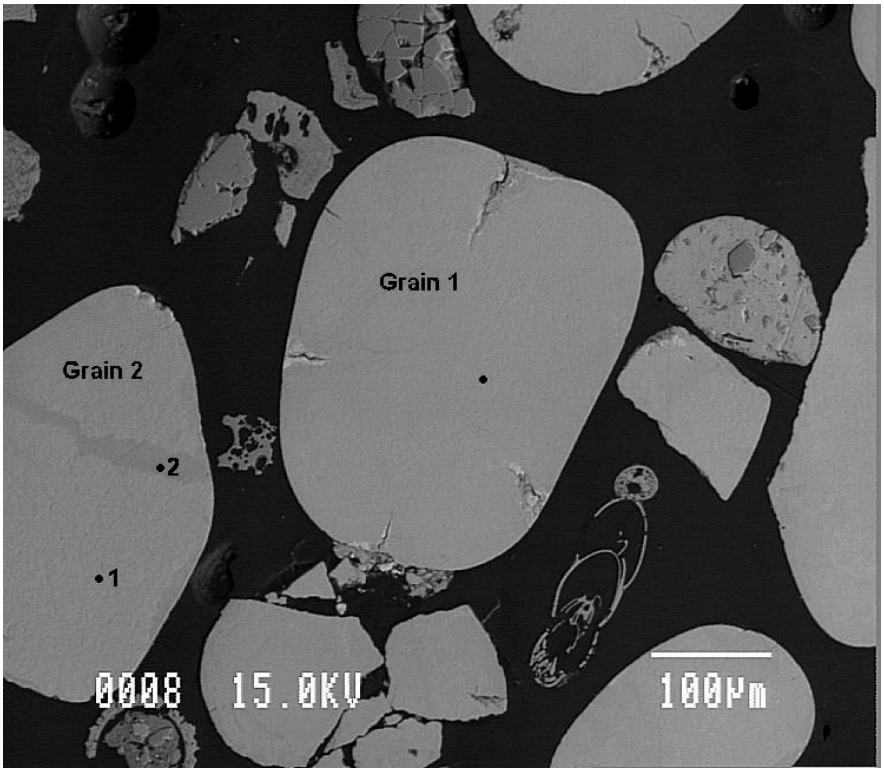

Backscatter image (BEI) of glauconite grain B in sample P421. Black dot shows location of sample point.

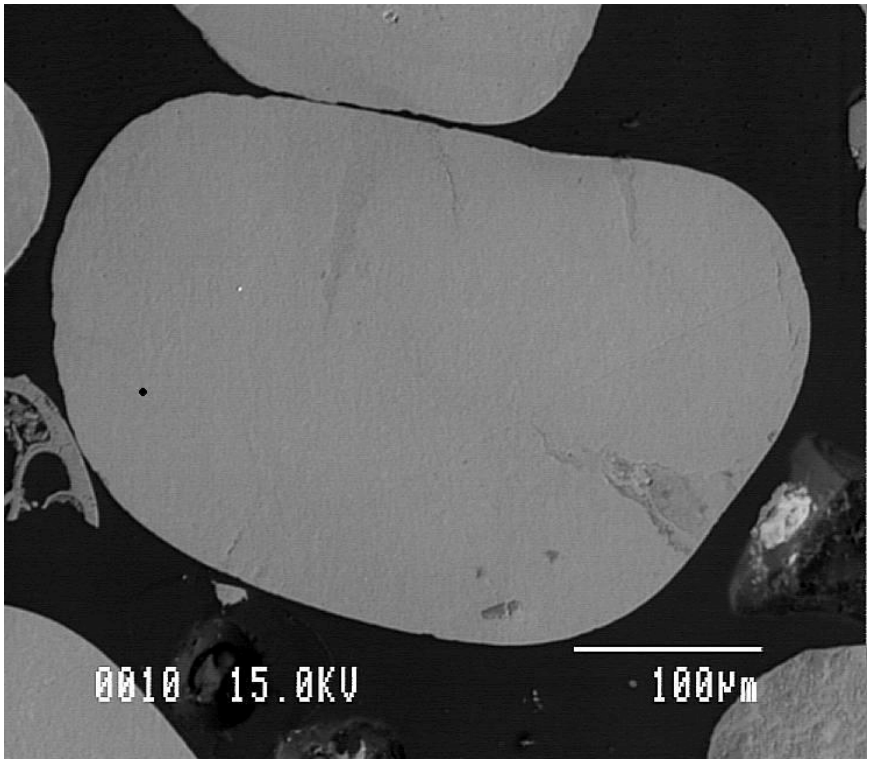

BEI of glauconite grain C in sample P421. Black dot shows location of sample point.

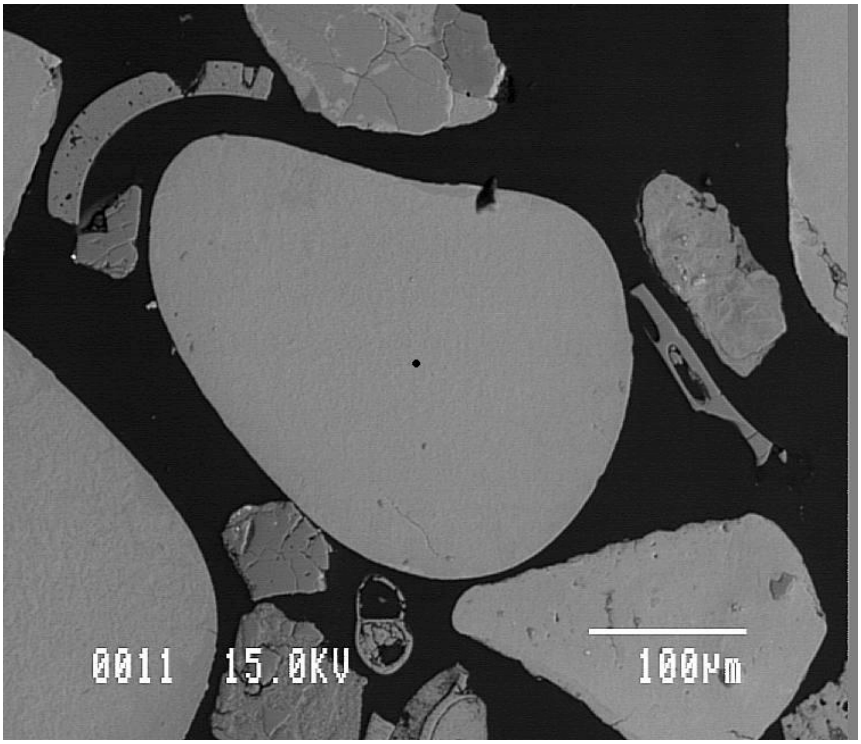

Microprobe images and data

BEI of glauconite grain D in sample P421. Black dot shows location of sample point.

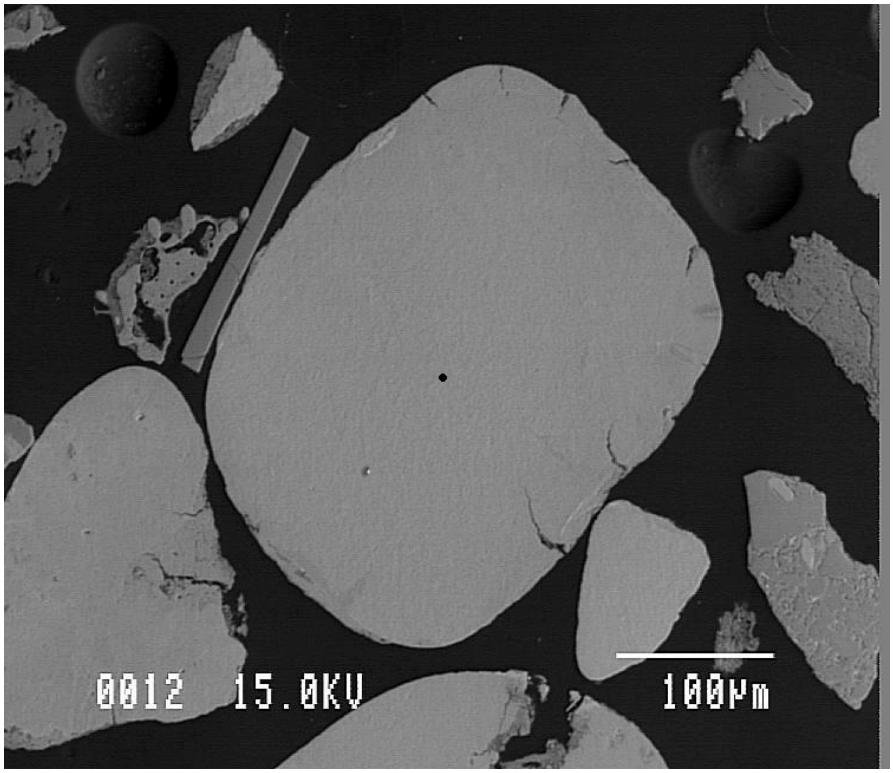

BEI of glauconite grain E in sample P421. Black dot shows location of sample points.

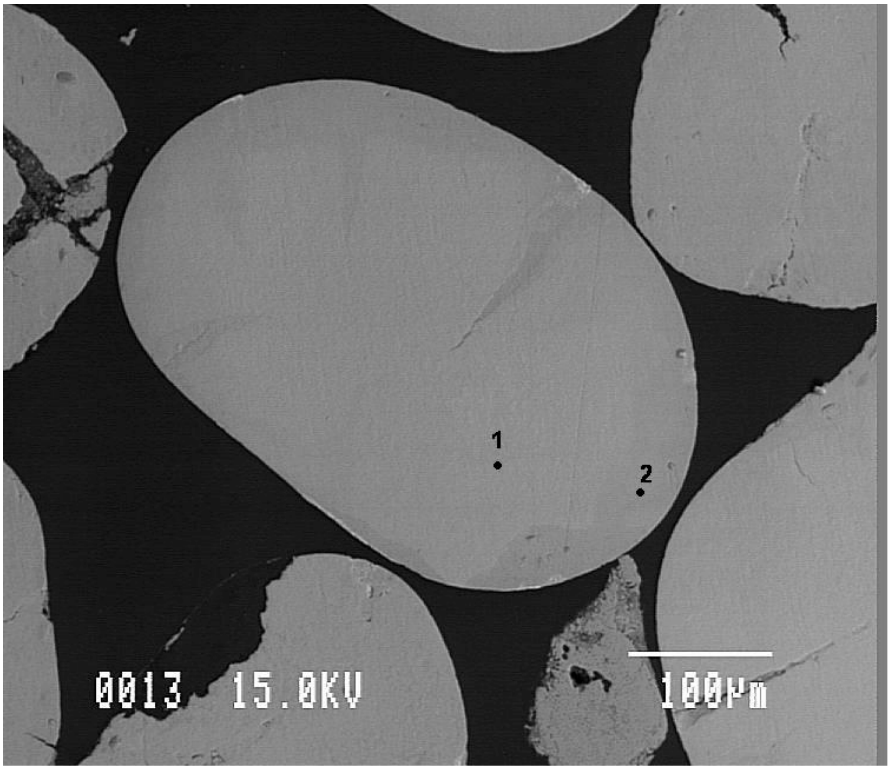

BEI of glauconite grain A in sample P430. Black dot shows location of sample points.

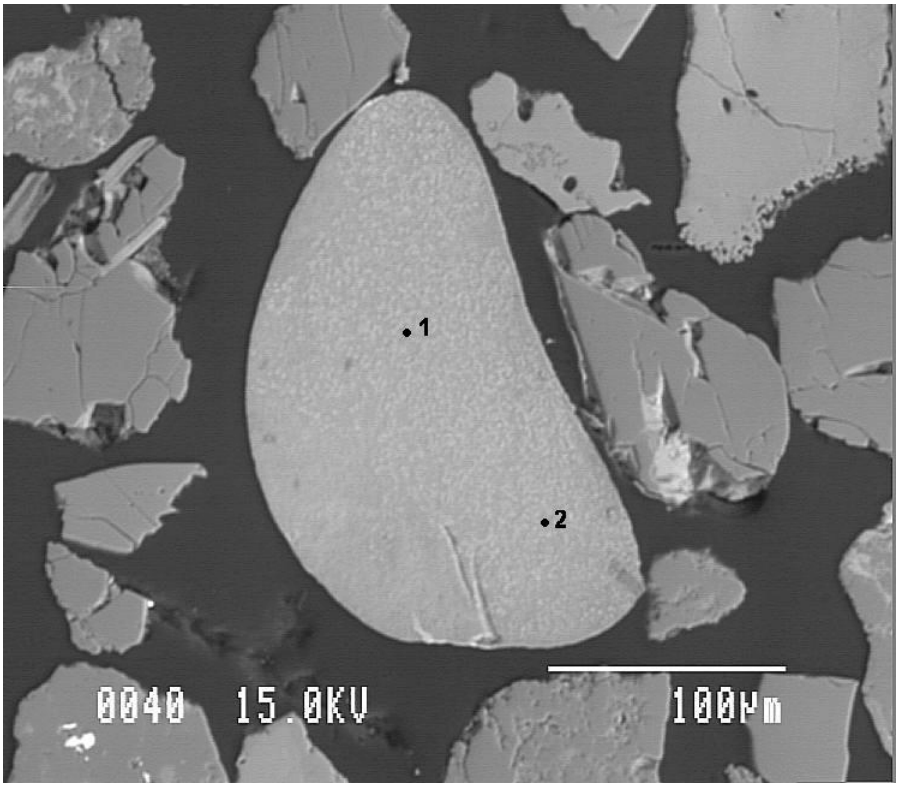

BEI of glauconite grain B in sample P430. Black dot shows location of sample point.

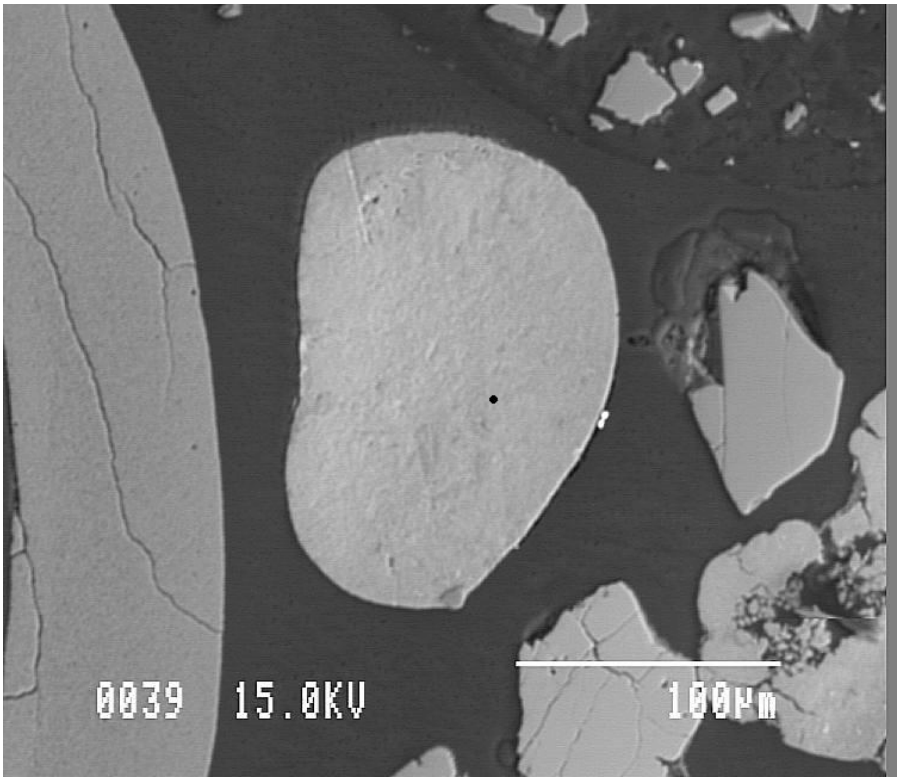

Microprobe images and data

BEI of glauconite grain C in sample P430. Black dot shows location of sample point.

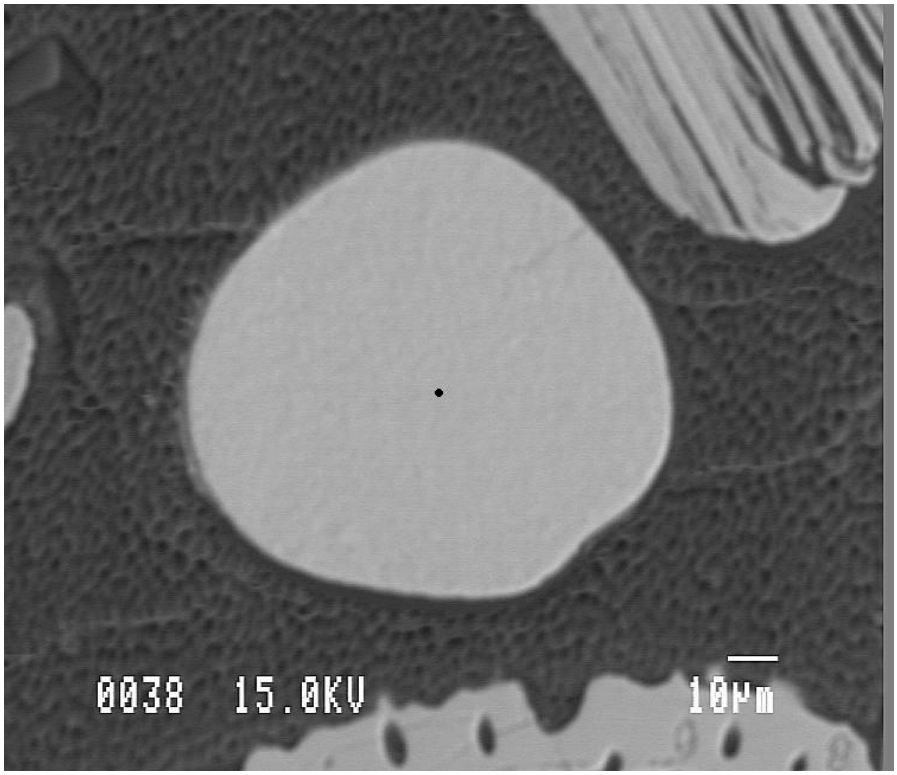

BEI of glauconite grain D in sample P430. Black dot shows location of sample point.

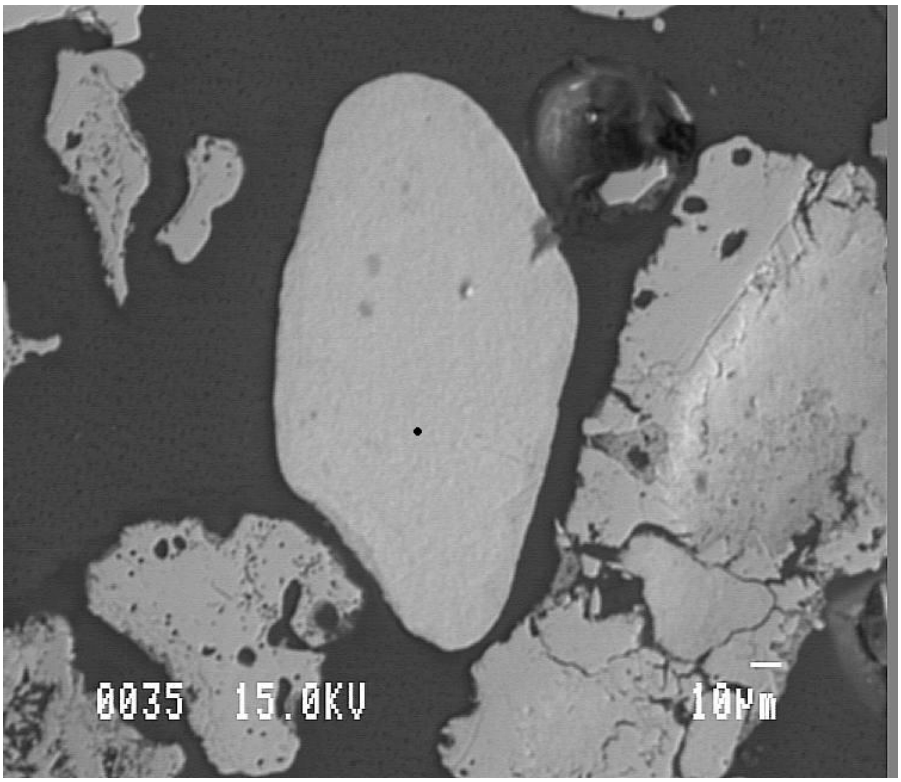

BEI of glauconite grain E in sample P430. Black dot shows location of sample point.

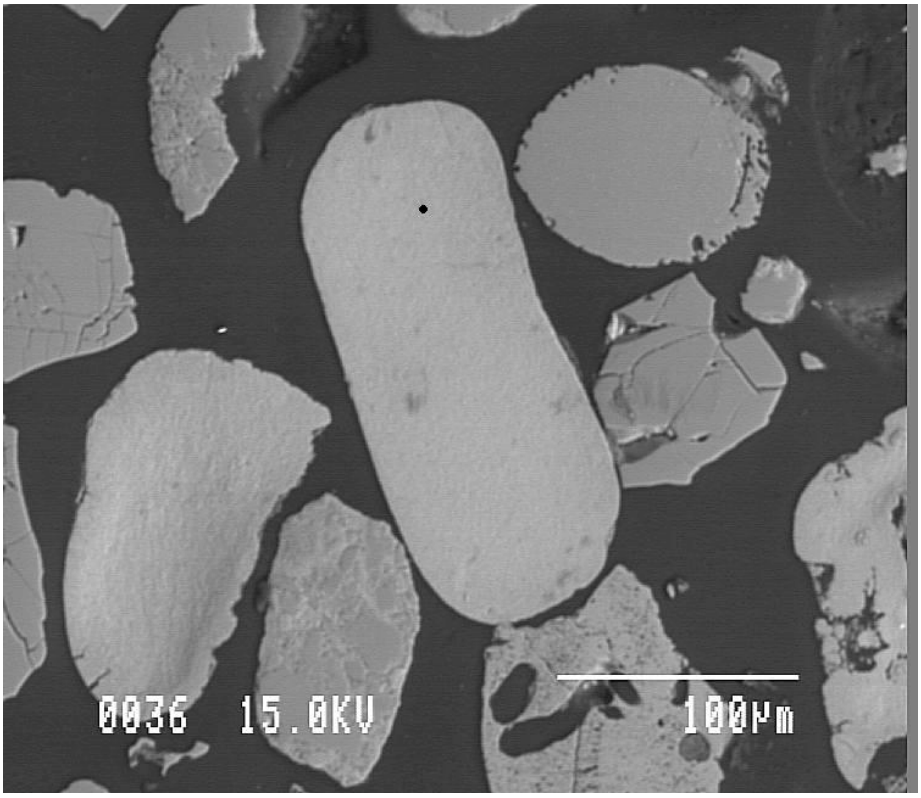

BEI of pelletal grain A in sample P605. Black dot shows location of sample point.

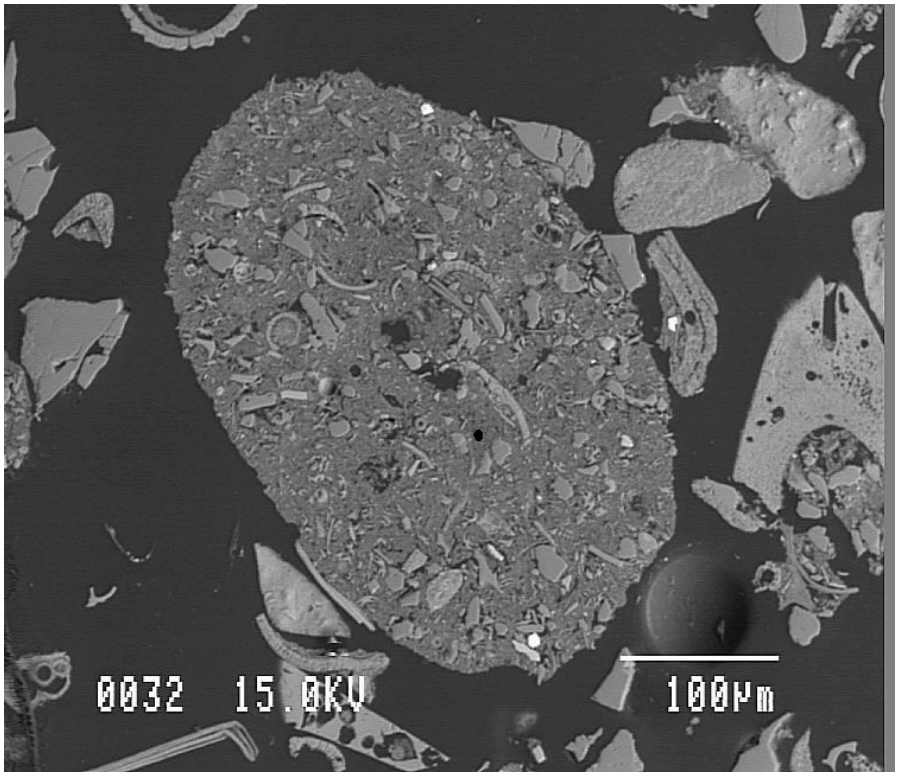

Microprobe images and data

BEI of pelletal grain B in sample P605. Black dot shows location of sample points.

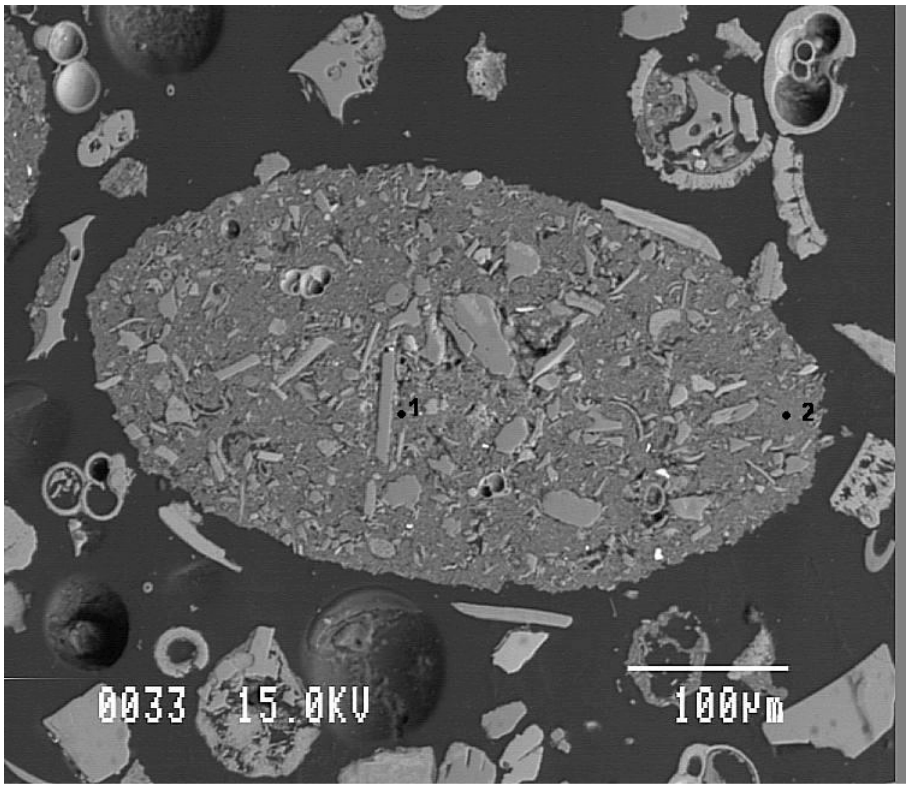

BEI of pelletal grain C in sample P605. Black dot shows location of sample points.

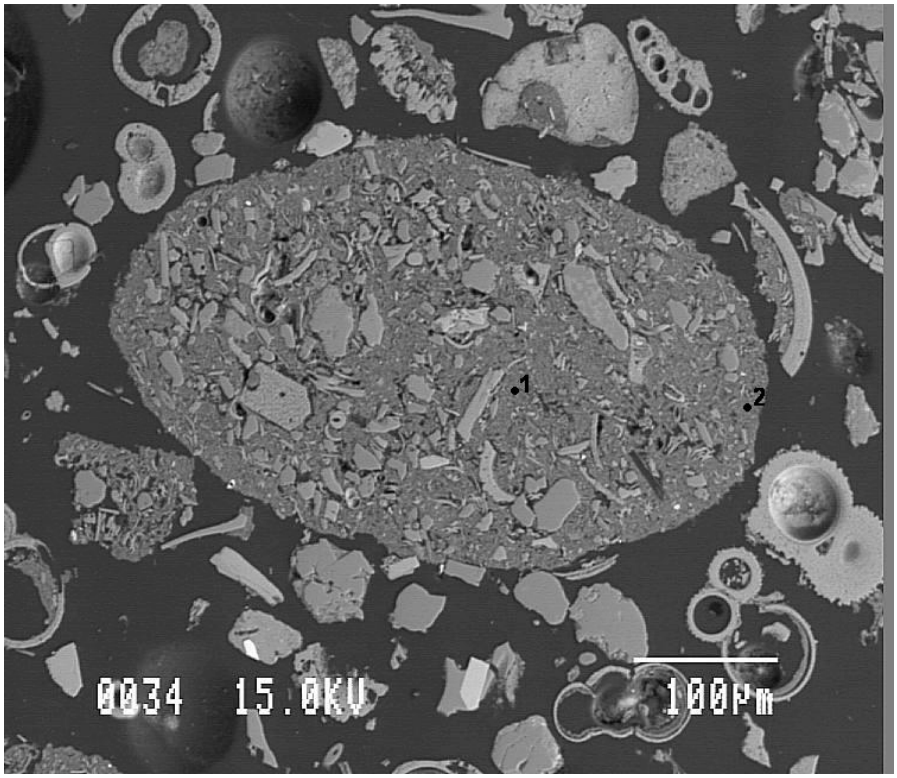

Table 1. Microprobe data for P399: glauconite.

ID = P399 A grain1 spot1					
Livetime = Bulk STDS.					
kV= 15	Angle= 40	B.C.= 1.			
OXIDE	WEIGHT %	+/- 2 SIGMA	11 OXYGENS	K RATIO	MDL
Na2O	0.15	0	0.02	0.0004	0.082
MgO	5.04	0.08	0.63	0.0167	0.058
Al2O3	7.57	0.08	0.74	0.0257	0.06
SiO2	42.38	0.22	3.54	0.1464	0.144
P2O5	0	0	0	0	0.117
SO3	0	0	0	0	0.09
Cl	0	0	0	0	0.056
K2O	5.19	0.06	0.55	0.0382	0.034
CaO	0.35	0.01	0.03	0.0023	0.088
TiO2	0	0	0	0.0006	0.193
V2O3	0	0	0	0	0.147
Cr2O3	0	0	0	0.0004	0.211
MnO	0	0	0	0.0001	0.181
FeO	26.65	0.28	1.86	0.1756	0.087
NiO	0	0	0	0.0005	0.253
TOTAL	87.33		7.38		
ID = P399 A2 grain1 spot2					
Livetime = Bulk STDS.					
kV= 15	Angle= 40	B.C.= 1.			
OXIDE	WEIGHT %	+/- 2 SIGMA	11 OXYGENS	K RATIO	MDL
Na2O	0	0	0	0	0.082
MgO	6.45	0.09	0.78	0.0218	0.058
Al2O3	5.03	0.06	0.48	0.0171	0.06
SiO2	47.62	0.24	3.88	0.1667	0.144
P2O5	0	0	0	0.0001	0.117
SO3	0	0	0	0.0002	0.09
Cl	0	0	0	0	0.056
K2O	2.28	0.03	0.24	0.0166	0.034
CaO	0.81	0.02	0.07	0.0053	0.088
TiO2	0	0	0	0.0004	0.193
V2O3	0	0	0	0	0.147
Cr2O3	0	0	0	0	0.211
MnO	0	0	0	0.001	0.181
FeO	22.7	0.26	1.55	0.1486	0.087
NiO	0	0	0	0	0.253
TOTAL	84.9		7		
ID = P399 C grain1 spot1					
Livetime = Bulk STDS.					
kV= 15	Angle= 40	B.C.= 1.			
OXIDE	WEIGHT %	+/- 2 SIGMA	11 OXYGENS	K RATIO	MDL
Na2O	0.23	0.01	0.03	0.0007	0.082
MgO	5.12	0.07	0.6	0.0177	0.058
Al2O3	13.86	0.12	1.28	0.0484	0.06
SiO2	43.6	0.23	3.43	0.1489	0.144
P2O5	0	0	0	0	0.117
SO3	0	0	0	0.0003	0.09
Cl	0	0	0	0.0002	0.056
K2O	3.45	0.05	0.35	0.0251	0.034
CaO	0.37	0.01	0.03	0.0024	0.088
TiO2	0.5	0.01	0.03	0.0026	0.193
V2O3	0	0	0	0	0.147
Cr2O3	0	0	0	0	0.211
MnO	0	0	0	0.0003	0.181
FeO	20.24	0.24	1.33	0.1323	0.087
NiO	0	0	0	0.0008	0.253
TOTAL	87.37		7.09		

Microprobe images and data

Table 2. Microprobe data for P414: glauconite.

ID = P414 A grain1 spot1					
Livetime =	Bulk STDS.				
kV= 15	Angle= 40	B.C.= 1.			
OXIDE	WEIGHT %	+/- 2 SIGMA	11 OXYGENS	K RATIO	MDL
Na2O	0	0	0	0	0.082
MgO	3.83	0.06	0.47	0.0127	0.058
Al2O3	2.77	0.04	0.27	0.0095	0.06
SiO2	48.25	0.24	3.98	0.1721	0.144
P2O5	0	0	0	0	0.117
SO3	0	0	0	0	0.09
Cl	0	0	0	0.0001	0.056
K2O	7.29	0.07	0.77	0.0535	0.034
CaO	0.32	0.01	0.03	0.0021	0.088
TiO2	0	0	0	0.0001	0.193
V2O3	0	0	0	0	0.147
Cr2O3	0	0	0	0	0.211
MnO	0	0	0	0.0005	0.181
FeO	25.37	0.27	1.75	0.1668	0.087
NiO	0	0	0	0	0.253
TOTAL	87.83		7.27		
ID = P414 B grain1 spot1					
Livetime =	Bulk STDS.				
kV= 15	Angle= 40	B.C.= 1.			
OXIDE	WEIGHT %	+/- 2 SIGMA	11 OXYGENS	K RATIO	MDL
Na2O	0	0	0	0	0.082
MgO	3.96	0.06	0.49	0.0132	0.058
Al2O3	1.73	0.03	0.17	0.0059	0.06
SiO2	48.27	0.24	4.03	0.1728	0.144
P2O5	0	0	0	0	0.117
SO3	0	0	0	0	0.09
Cl	0	0	0	0.0001	0.056
K2O	7.75	0.08	0.83	0.057	0.034
CaO	0.18	0	0.02	0.0011	0.088
TiO2	0	0	0	0.0005	0.193
V2O3	0	0	0	0.0001	0.147
Cr2O3	0	0	0	0	0.211
MnO	0	0	0	0	0.181
FeO	25.33	0.27	1.77	0.1665	0.087
NiO	0	0	0	0	0.253
TOTAL	87.2		7.3		
ID = P414 B grain1 spot2					
Livetime =	Bulk STDS.				
kV= 15	Angle= 40	B.C.= 1.			
OXIDE	WEIGHT %	+/- 2 SIGMA	11 OXYGENS	K RATIO	MDL
Na2O	0	0	0	0	0.082
MgO	4.13	0.06	0.49	0.0141	0.058
Al2O3	6.05	0.07	0.57	0.0211	0.06
SiO2	48.91	0.24	3.93	0.1736	0.144
P2O5	0	0	0	0.0001	0.117
SO3	0	0	0	0	0.09
Cl	0	0	0	0.0001	0.056
K2O	6.59	0.07	0.67	0.048	0.034
CaO	0.37	0.01	0.03	0.0024	0.088
TiO2	0	0	0	0.0003	0.193
V2O3	0	0	0	0	0.147
Cr2O3	0	0	0	0.0001	0.211
MnO	0	0	0	0	0.181
FeO	21.23	0.25	1.42	0.1388	0.087
NiO	0	0	0	0	0.253
TOTAL	87.28		7.12		

Table 2 cont. Microprobe data for P414: glauconite.

ID = P414 C grain1 spot1					
Livetime =	Bulk STDS.				
kV= 15	Angle= 40	B.C.= 1.			
OXIDE	WEIGHT %	+/- 2 SIGMA	11 OXYGENS	K RATIO	MDL
Na2O	0	0	0	0	0.082
MgO	4.11	0.06	0.51	0.0137	0.058
Al2O3	2.47	0.04	0.24	0.0085	0.06
SiO2	47.95	0.24	3.99	0.1712	0.144
P2O5	0	0	0	0	0.117
SO3	0	0	0	0	0.09
Cl	0	0	0	0	0.056
K2O	7.67	0.08	0.81	0.0563	0.034
CaO	0.26	0	0.02	0.0017	0.088
TiO2	0	0	0	0.0002	0.193
V2O3	0	0	0	0.0002	0.147
Cr2O3	0	0	0	0.0002	0.211
MnO	0	0	0	0	0.181
FeO	24.72	0.27	1.72	0.1624	0.087
NiO	0	0	0	0	0.253
TOTAL	87.18		7.3		

ID = P414 C grain1 spot2					
Livetime =	Bulk STDS.				
kV= 15	Angle= 40	B.C.= 1.			
OXIDE	WEIGHT %	+/- 2 SIGMA	11 OXYGENS	K RATIO	MDL
Na2O	0.28	0.01	0.05	0.0008	0.082
MgO	3.3	0.05	0.41	0.0111	0.058
Al2O3	4.24	0.05	0.41	0.0147	0.06
SiO2	48.68	0.24	4.02	0.173	0.144
P2O5	0	0	0	0	0.117
SO3	0	0	0	0	0.09
Cl	0	0	0	0	0.056
K2O	4.68	0.06	0.49	0.0342	0.034
CaO	0.57	0.01	0.05	0.0037	0.088
TiO2	0	0	0	0.0008	0.193
V2O3	0	0	0	0.0001	0.147
Cr2O3	0	0	0	0.0002	0.211
MnO	0	0	0	0.0004	0.181
FeO	23.32	0.26	1.61	0.1529	0.087
NiO	0	0	0	0.0001	0.253
TOTAL	85.08		7.04		

ID = P414 C grain1 spot3					
Livetime =	Bulk STDS.				
kV= 15	Angle= 40	B.C.= 1.			
OXIDE	WEIGHT %	+/- 2 SIGMA	11 OXYGENS	K RATIO	MDL
Na2O	0	0	0	0	0.082
MgO	3.57	0.06	0.45	0.0119	0.058
Al2O3	2.64	0.04	0.26	0.009	0.06
SiO2	47.83	0.24	4.01	0.1704	0.144
P2O5	0	0	0	0.0001	0.117
SO3	0	0	0	0	0.09
Cl	0	0	0	0.0001	0.056
K2O	6.41	0.07	0.68	0.0471	0.034
CaO	0.3	0.01	0.03	0.0019	0.088
TiO2	0	0	0	0.0009	0.193
V2O3	0	0	0	0	0.147
Cr2O3	0	0	0	0.0004	0.211
MnO	0	0	0	0	0.181
FeO	25.34	0.27	1.78	0.1667	0.087
NiO	0	0	0	0.0007	0.253
TOTAL	86.09		7.2		

Microprobe images and data

Table 2 cont. Microprobe data for P414: glauconite.

ID = P414 D grain1 spot1					
Livetime =	Bulk STDS.				
kV= 15	Angle= 40	B.C.= 1.			
OXIDE	WEIGHT %	+/- 2 SIGMA	11 OXYGENS	K RATIO	MDL
Na2O	0	0	0	0	0.082
MgO	3.79	0.06	0.47	0.0126	0.058
Al2O3	2.31	0.03	0.23	0.0079	0.06
SiO2	47.27	0.24	3.95	0.1685	0.144
P2O5	0	0	0	0	0.117
SO3	0	0	0	0	0.09
Cl	0	0	0	0.0002	0.056
K2O	8.05	0.08	0.86	0.0592	0.034
CaO	0	0	0	0.0004	0.088
TiO2	0	0	0	0	0.193
V2O3	0	0	0	0	0.147
Cr2O3	0	0	0	0	0.211
MnO	0	0	0	0.0001	0.181
FeO	26.41	0.28	1.85	0.1739	0.087
NiO	0	0	0	0	0.253
TOTAL	87.83		7.36		

ID = P414 E grain1 spot1					
Livetime =	Bulk STDS.				
kV= 15	Angle= 40	B.C.= 1.			
OXIDE	WEIGHT %	+/- 2 SIGMA	11 OXYGENS	K RATIO	MDL
Na2O	0	0	0	0	0.082
MgO	4	0.06	0.49	0.0133	0.058
Al2O3	1.69	0.03	0.16	0.0058	0.06
SiO2	48.61	0.24	4.01	0.1737	0.144
P2O5	0	0	0	0.0002	0.117
SO3	0	0	0	0	0.09
Cl	0	0	0	0	0.056
K2O	7.87	0.08	0.83	0.0579	0.034
CaO	0.13	0	0.01	0.0009	0.088
TiO2	0	0	0	0	0.193
V2O3	0	0	0	0.0001	0.147
Cr2O3	0	0	0	0.0004	0.211
MnO	0	0	0	0.0001	0.181
FeO	26.53	0.28	1.83	0.1747	0.087
NiO	0	0	0	0	0.253
TOTAL	88.82		7.33		

Table 3. Microprobe data for P416: glauconite.

ID = P416 A grain1 spot1					
Livetime = Bulk STDS.					
kV= 15	Angle= 40	B.C.= 1.			
OXIDE	WEIGHT %	+/- 2 SIGMA	11 OXYGENS	K RATIO	MDL
Na2O	0	0	0	0	0.082
MgO	4.57	0.07	0.55	0.0154	0.058
Al2O3	2	0.03	0.19	0.0069	0.06
SiO2	49.73	0.24	4.03	0.1784	0.144
P2O5	0	0	0	0.0001	0.117
SO3	0.1	0	0.01	0.0003	0.09
Cl	0	0	0	0.0004	0.056
K2O	8.46	0.08	0.87	0.062	0.034
CaO	0.23	0	0.02	0.0015	0.088
TiO2	0	0	0	0.0001	0.193
V2O3	0	0	0	0	0.147
Cr2O3	0	0	0	0	0.211
MnO	0	0	0	0.0006	0.181
FeO	23.97	0.27	1.62	0.1573	0.087
NiO	0	0	0	0	0.253
TOTAL	89.06		7.3		

ID = P416 A grain2 spot1					
Livetime = Bulk STDS.					
kV= 15	Angle= 40	B.C.= 1.			
OXIDE	WEIGHT %	+/- 2 SIGMA	11 OXYGENS	K RATIO	MDL
Na2O	0	0	0	0	0.082
MgO	5.96	0.08	0.7	0.0204	0.058
Al2O3	2.51	0.04	0.23	0.0087	0.06
SiO2	50.71	0.24	4.02	0.1815	0.144
P2O5	0	0	0	0	0.117
SO3	0	0	0	0	0.09
Cl	0	0	0	0.0003	0.056
K2O	8.48	0.08	0.86	0.0619	0.034
CaO	0	0	0	0.0004	0.088
TiO2	0	0	0	0	0.193
V2O3	0	0	0	0.0004	0.147
Cr2O3	0	0	0	0	0.211
MnO	0	0	0	0	0.181
FeO	22.28	0.26	1.48	0.1459	0.087
NiO	0	0	0	0.0006	0.253
TOTAL	89.95		7.29		

ID = P416 A grain2 spot2					
Livetime = Bulk STDS.					
kV= 15	Angle= 40	B.C.= 1.			
OXIDE	WEIGHT %	+/- 2 SIGMA	11 OXYGENS	K RATIO	MDL
Na2O	0	0	0	0	0.082
MgO	4.73	0.07	0.54	0.0166	0.058
Al2O3	7.83	0.08	0.71	0.0277	0.06
SiO2	51.8	0.25	3.96	0.1837	0.144
P2O5	0.01	0	0	0	0.117
SO3	0	0	0	0	0.09
Cl	0.03	0	0	0.0003	0.056
K2O	4.91	0.06	0.48	0.0355	0.034
CaO	0.49	0.01	0.04	0.0032	0.088
TiO2	0.33	0.01	0.02	0.0017	0.193
V2O3	0	0	0	0	0.147
Cr2O3	0.11	0	0.01	0.0007	0.211
MnO	0.04	0	0	0.0003	0.181
FeO	17.86	0.23	1.14	0.1162	0.087
NiO	0	0	0	0	0.253
TOTAL	88.16		6.9		

Microprobe images and data

Table 3 cont. Microprobe data for P416: glauconite.

ID = P416 B grain1 spot1					
Livetime =	Bulk STDS.				
kV= 15	Angle= 40	B.C.= 1.			
OXIDE	WEIGHT %	+/- 2 SIGMA	11 OXYGENS	K RATIO	MDL
Na2O	0	0	0	0	0.082
MgO	4.76	0.07	0.57	0.016	0.058
Al2O3	1.79	0.03	0.17	0.0062	0.06
SiO2	49.85	0.24	4.02	0.1785	0.144
P2O5	0.02	0	0	0.0001	0.117
SO3	0	0	0	0	0.09
Cl	0	0	0	0	0.056
K2O	8.42	0.08	0.87	0.0617	0.034
CaO	0.02	0	0	0.0001	0.088
TiO2	0.02	0	0	0.0001	0.193
V2O3	0.01	0	0	0.0001	0.147
Cr2O3	0	0	0	0	0.211
MnO	0.01	0	0	0.0001	0.181
FeO	25.12	0.27	1.69	0.1651	0.087
NiO	0.03	0	0	0.0002	0.253
TOTAL	90.06		7.33		

ID = P416 C grain1 spot1					
Livetime =	Bulk STDS.				
kV= 15	Angle= 40	B.C.= 1.			
OXIDE	WEIGHT %	+/- 2 SIGMA	11 OXYGENS	K RATIO	MDL
Na2O	0	0	0	0	0.082
MgO	4.49	0.07	0.54	0.015	0.058
Al2O3	1.8	0.03	0.17	0.0062	0.06
SiO2	49.8	0.24	4.03	0.1785	0.144
P2O5	0	0	0	0	0.117
SO3	0	0	0	0	0.09
Cl	0	0	0	0	0.056
K2O	8.35	0.08	0.86	0.0612	0.034
CaO	0.06	0	0.01	0.0004	0.088
TiO2	0.08	0	0	0.0004	0.193
V2O3	0	0	0	0	0.147
Cr2O3	0.04	0	0	0.0003	0.211
MnO	0	0	0	0	0.181
FeO	24.91	0.27	1.69	0.1637	0.087
NiO	0	0	0	0	0.253
TOTAL	89.53		7.31		

Table 3 cont. Microprobe data for P416: glauconite.

ID = P416 D grain1 spot1					
Livetime =	Bulk STDS.				
kV= 15	Angle= 40	B.C.= 1.			
OXIDE	WEIGHT %	+/- 2 SIGMA	11 OXYGENS	K RATIO	MDL
Na2O	0.01	0	0	0.0001	0.082
MgO	4.44	0.07	0.52	0.0152	0.058
Al2O3	3.96	0.05	0.37	0.0138	0.06
SiO2	50.7	0.24	4.01	0.1814	0.144
P2O5	0	0	0	0	0.117
SO3	0	0	0	0	0.09
Cl	0	0	0	0	0.056
K2O	8.29	0.08	0.84	0.0605	0.034
CaO	0.13	0	0.01	0.0008	0.088
TiO2	0	0	0	0	0.193
V2O3	0	0	0	0	0.147
Cr2O3	0.04	0	0	0.0003	0.211
MnO	0.01	0	0	0.0001	0.181
FeO	22.36	0.26	1.48	0.1464	0.087
NiO	0	0	0	0	0.253
TOTAL	89.94		7.23		

ID = P416 E grain1 spot1					
Livetime =	Bulk STDS.				
kV= 15	Angle= 40	B.C.= 1.			
OXIDE	WEIGHT %	+/- 2 SIGMA	11 OXYGENS	K RATIO	MDL
Na2O	0	0	0	0	0.082
MgO	4.08	0.06	0.5	0.0135	0.058
Al2O3	1.03	0.02	0.1	0.0035	0.06
SiO2	49.15	0.24	4.04	0.1762	0.144
P2O5	0	0	0	0	0.117
SO3	0	0	0	0	0.09
Cl	0.01	0	0	0.0001	0.056
K2O	8.11	0.08	0.85	0.0596	0.034
CaO	0.11	0	0.01	0.0007	0.088
TiO2	0.03	0	0	0.0001	0.193
V2O3	0	0	0	0	0.147
Cr2O3	0.06	0	0	0.0004	0.211
MnO	0	0	0	0	0.181
FeO	26.4	0.28	1.82	0.1739	0.087
NiO	0	0	0	0	0.253
TOTAL	88.97		7.33		

Table 4. Microprobe data for P417: glauconite.

ID = P417 A grain1 spot1					
Livetime =	Bulk STDS.				
kV= 15	Angle= 40	B.C.= 1.			
OXIDE	WEIGHT %	+/- 2 SIGMA	11 OXYGENS	K RATIO	MDL
Na2O	0	0	0	0	0.082
MgO	3.95	0.06	0.49	0.013	0.058
Al2O3	1.34	0.02	0.13	0.0046	0.06
SiO2	48	0.24	4.01	0.1715	0.144
P2O5	0	0	0	0	0.117
SO3	0	0	0	0.0001	0.09
Cl	0	0	0	0.0002	0.056
K2O	7.55	0.08	0.8	0.0556	0.034
CaO	0.23	0	0.02	0.0015	0.088
TiO2	0	0	0	0	0.193
V2O3	0	0	0	0.0001	0.147
Cr2O3	0	0	0	0	0.211
MnO	0	0	0	0	0.181
FeO	26.75	0.28	1.87	0.1762	0.087
NiO	0	0	0	0.0002	0.253
TOTAL	87.83		7.33		

ID = P417 B grain1 spot1					
Livetime =	Bulk STDS.				
kV= 15	Angle= 40	B.C.= 1.			
OXIDE	WEIGHT %	+/- 2 SIGMA	11 OXYGENS	K RATIO	MDL
Na2O	0	0	0	0	0.082
MgO	4.8	0.07	0.58	0.0161	0.058
Al2O3	2.3	0.03	0.22	0.0079	0.06
SiO2	48.99	0.24	4	0.175	0.144
P2O5	0	0	0	0.0001	0.117
SO3	0	0	0	0	0.09
Cl	0	0	0	0.0001	0.056
K2O	7.93	0.08	0.83	0.0581	0.034
CaO	0.14	0	0.01	0.0009	0.088
TiO2	0	0	0	0	0.193
V2O3	0	0	0	0	0.147
Cr2O3	0	0	0	0	0.211
MnO	0	0	0	0.0001	0.181
FeO	24.33	0.27	1.66	0.1598	0.087
NiO	0	0	0	0.0011	0.253
TOTAL	88.49		7.3		

ID = P417 C grain1 spot1					
Livetime =	Bulk STDS.				
kV= 15	Angle= 40	B.C.= 1.			
OXIDE	WEIGHT %	+/- 2 SIGMA	11 OXYGENS	K RATIO	MDL
Na2O	0	0	0	0	0.082
MgO	5.81	0.08	0.7	0.0196	0.058
Al2O3	2.33	0.03	0.22	0.008	0.06
SiO2	48.58	0.24	3.95	0.1731	0.144
P2O5	0	0	0	0	0.117
SO3	0	0	0	0	0.09
Cl	0	0	0	0	0.056
K2O	8.34	0.08	0.86	0.0611	0.034
CaO	0.11	0	0.01	0.0007	0.088
TiO2	0	0	0	0	0.193
V2O3	0	0	0	0.0002	0.147
Cr2O3	0	0	0	0	0.211
MnO	0	0	0	0.0003	0.181
FeO	23.89	0.27	1.62	0.1568	0.087
NiO	0	0	0	0	0.253
TOTAL	89.06		7.37		

Table 4 cont. Microprobe data for P417: glauconite.

ID = P417 D grain1 spot1					
Livetime =	Bulk STDS.				
kV= 15	Angle= 40	B.C.= 1.			
OXIDE	WEIGHT %	+/- 2 SIGMA	11 OXYGENS	K RATIO	MDL
Na2O	0	0	0	0	0.082
MgO	4.49	0.07	0.54	0.015	0.058
Al2O3	2.77	0.04	0.27	0.0095	0.06
SiO2	48.57	0.24	3.95	0.1731	0.144
P2O5	0	0	0	0	0.117
SO3	0	0	0	0	0.09
Cl	0	0	0	0.0004	0.056
K2O	7.93	0.08	0.82	0.0582	0.034
CaO	0.21	0	0.02	0.0014	0.088
TiO2	0.23	0.01	0.01	0.0012	0.193
V2O3	0	0	0	0	0.147
Cr2O3	0	0	0	0.0004	0.211
MnO	0	0	0	0	0.181
FeO	25.04	0.27	1.7	0.1647	0.087
NiO	0	0	0	0.0009	0.253
TOTAL	89.24		7.32		

ID = P417 E grain1 spot1					
Livetime =	Bulk STDS.				
kV= 15	Angle= 40	B.C.= 1.			
OXIDE	WEIGHT %	+/- 2 SIGMA	11 OXYGENS	K RATIO	MDL
Na2O	0	0	0	0	0.082
MgO	5.48	0.08	0.65	0.0185	0.058
Al2O3	2.38	0.03	0.22	0.0082	0.06
SiO2	49.77	0.24	3.98	0.1776	0.144
P2O5	0	0	0	0	0.117
SO3	0	0	0	0	0.09
Cl	0	0	0	0.0001	0.056
K2O	8.24	0.08	0.84	0.0603	0.034
CaO	0.14	0	0.01	0.0009	0.088
TiO2	0	0	0	0.0002	0.193
V2O3	0	0	0	0	0.147
Cr2O3	0	0	0	0.0006	0.211
MnO	0	0	0	0	0.181
FeO	24.22	0.27	1.62	0.159	0.087
NiO	0	0	0	0	0.253
TOTAL	90.22		7.33		

Table 5. Microprobe data for P420: glauconite.

ID = P420 A grain1 spot1					
Livetime =	Bulk STDS.				
kV= 15	Angle= 40	B.C.= 1.			
OXIDE	WEIGHT %	+/- 2 SIGMA	11 OXYGENS	K RATIO	MDL
Na2O	0	0	0	0	0.082
MgO	5.64	0.08	0.67	0.0192	0.058
Al2O3	2.06	0.03	0.19	0.0071	0.06
SiO2	50.57	0.24	4.03	0.1811	0.144
P2O5	0	0	0	0	0.117
SO3	0	0	0	0.0001	0.09
Cl	0	0	0	0.0001	0.056
K2O	8.45	0.08	0.86	0.0618	0.034
CaO	0.13	0	0.01	0.0008	0.088
TiO2	0	0	0	0.0002	0.193
V2O3	0	0	0	0.0002	0.147
Cr2O3	0	0	0	0	0.211
MnO	0	0	0	0	0.181
FeO	23.29	0.26	1.55	0.1527	0.087
NiO	0	0	0	0	0.253
TOTAL	90.14		7.31		

ID = P420 B grain1 spot1					
Livetime =	Bulk STDS.				
kV= 15	Angle= 40	B.C.= 1.			
OXIDE	WEIGHT %	+/- 2 SIGMA	11 OXYGENS	K RATIO	MDL
Na2O	0	0	0	0	0.082
MgO	4.39	0.07	0.54	0.0146	0.058
Al2O3	2.6	0.04	0.25	0.0089	0.06
SiO2	48.11	0.24	3.95	0.1713	0.144
P2O5	0	0	0	0	0.117
SO3	0	0	0	0	0.09
Cl	0	0	0	0.0002	0.056
K2O	7.56	0.08	0.79	0.0555	0.034
CaO	0.19	0	0.02	0.0012	0.088
TiO2	0	0	0	0	0.193
V2O3	0	0	0	0.0003	0.147
Cr2O3	0	0	0	0.0006	0.211
MnO	0	0	0	0.0002	0.181
FeO	25.76	0.28	1.77	0.1695	0.087
NiO	0	0	0	0	0.253
TOTAL	88.62		7.32		

Table 5 cont. Microprobe data for P420: glauconite.

ID = P420 C grain1 spot1					
Livetime =	Bulk STDS.				
kV= 15	Angle= 40	B.C.= 1.			
OXIDE	WEIGHT %	+/- 2 SIGMA	11 OXYGENS	K RATIO	MDL
Na2O	0	0	0	0	0.082
MgO	5.68	0.08	0.67	0.0193	0.058
Al2O3	3.01	0.04	0.28	0.0104	0.06
SiO2	50.24	0.24	3.98	0.1793	0.144
P2O5	0	0	0	0	0.117
SO3	0	0	0	0	0.09
Cl	0	0	0	0	0.056
K2O	8.26	0.08	0.83	0.0604	0.034
CaO	0.16	0	0.01	0.001	0.088
TiO2	0	0	0	0	0.193
V2O3	0	0	0	0	0.147
Cr2O3	0	0	0	0.0007	0.211
MnO	0	0	0	0	0.181
FeO	22.88	0.26	1.52	0.15	0.087
NiO	0	0	0	0.0009	0.253
TOTAL	90.23		7.3		

ID = P420 D grain1 spot1					
Livetime =	Bulk STDS.				
kV= 15	Angle= 40	B.C.= 1.			
OXIDE	WEIGHT %	+/- 2 SIGMA	11 OXYGENS	K RATIO	MDL
Na2O	0	0	0	0.0001	0.082
MgO	6.27	0.09	0.74	0.0213	0.058
Al2O3	2.56	0.04	0.24	0.0088	0.06
SiO2	50.01	0.24	3.97	0.1782	0.144
P2O5	0	0	0	0	0.117
SO3	0	0	0	0	0.09
Cl	0	0	0	0.0001	0.056
K2O	7.72	0.08	0.78	0.0564	0.034
CaO	0.13	0	0.01	0.0008	0.088
TiO2	0	0	0	0.0002	0.193
V2O3	0	0	0	0	0.147
Cr2O3	0	0	0	0.0001	0.211
MnO	0	0	0	0.0001	0.181
FeO	23.27	0.26	1.55	0.1525	0.087
NiO	0	0	0	0	0.253
TOTAL	89.96		7.3		

ID = P420 E grain1 spot1					
Livetime =	Bulk STDS.				
kV= 15	Angle= 40	B.C.= 1.			
OXIDE	WEIGHT %	+/- 2 SIGMA	11 OXYGENS	K RATIO	MDL
Na2O	0	0	0	0	0.082
MgO	5.74	0.08	0.68	0.0194	0.058
Al2O3	1.45	0.02	0.14	0.005	0.06
SiO2	50.34	0.24	4.02	0.1802	0.144
P2O5	0	0	0	0	0.117
SO3	0	0	0	0.0002	0.09
Cl	0	0	0	0	0.056
K2O	8.4	0.08	0.86	0.0615	0.034
CaO	0	0	0	0.0002	0.088
TiO2	0	0	0	0	0.193
V2O3	0	0	0	0.0006	0.147
Cr2O3	0	0	0	0	0.211
MnO	0	0	0	0	0.181
FeO	24.51	0.27	1.64	0.161	0.087
NiO	0	0	0	0	0.253
TOTAL	90.44		7.34		

Table 6. Microprobe data for P421: glauconite.

ID = P421 A grain1 spot1

Livetime = Bulk STDS.

kV= 15 Angle= 40 B.C.= 1.

OXIDE	WEIGHT %	+/- 2 SIGMA	11 OXYGENS	K RATIO	MDL
Na2O	0	0	0	0	0.082
MgO	3.88	0.06	0.48	0.0129	0.058
Al2O3	2.49	0.04	0.24	0.0085	0.06
SiO2	48.39	0.24	3.99	0.1726	0.144
P2O5	0	0	0	0	0.117
SO3	0	0	0	0	0.09
Cl	0	0	0	0	0.056
K2O	7.58	0.08	0.8	0.0557	0.034
CaO	0.19	0	0.02	0.0012	0.088
TiO2	0	0	0	0.0003	0.193
V2O3	0	0	0	0.0004	0.147
Cr2O3	0	0	0	0	0.211
MnO	0	0	0	0	0.181
FeO	25.74	0.28	1.77	0.1694	0.087
NiO	0	0	0	0.0006	0.253
TOTAL	88.28		7.29		

ID = P421 A grain2 spot1

Livetime = Bulk STDS.

kV= 15 Angle= 40 B.C.= 1.

OXIDE	WEIGHT %	+/- 2 SIGMA	11 OXYGENS	K RATIO	MDL
Na2O	0	0	0	0	0.082
MgO	4.22	0.07	0.52	0.0139	0.058
Al2O3	1.18	0.02	0.11	0.004	0.06
SiO2	48.29	0.24	4.01	0.1725	0.144
P2O5	0	0	0	0	0.117
SO3	0	0	0	0.0001	0.09
Cl	0	0	0	0	0.056
K2O	7.57	0.08	0.8	0.0557	0.034
CaO	0.22	0	0.02	0.0015	0.088
TiO2	0	0	0	0	0.193
V2O3	0	0	0	0.0003	0.147
Cr2O3	0	0	0	0	0.211
MnO	0	0	0	0	0.181
FeO	26.95	0.28	1.87	0.1776	0.087
NiO	0	0	0	0	0.253
TOTAL	88.42		7.34		

ID = P421 A grain2 spot2

Livetime = Bulk STDS.

kV= 15 Angle= 40 B.C.= 1.

OXIDE	WEIGHT %	+/- 2 SIGMA	11 OXYGENS	K RATIO	MDL
Na2O	0	0	0	0.0002	0.082
MgO	4.01	0.06	0.49	0.0135	0.058
Al2O3	7.33	0.08	0.71	0.0253	0.06
SiO2	45.3	0.23	3.71	0.1586	0.144
P2O5	0.16	0	0.01	0.0005	0.117
SO3	0	0	0	0	0.09
Cl	0	0	0	0	0.056
K2O	5.48	0.06	0.57	0.0402	0.034
CaO	0.71	0.01	0.06	0.0046	0.088
TiO2	0.49	0.01	0.03	0.0025	0.193
V2O3	0	0	0	0	0.147
Cr2O3	0	0	0	0.0009	0.211
MnO	0	0	0	0	0.181
FeO	23.45	0.26	1.6	0.1538	0.087
NiO	0	0	0	0.0004	0.253
TOTAL	86.93		7.18		

Table 6 cont. Microprobe data for P421: glauconite.

ID = P421 B grain1 spot1					
Livetime =	Bulk STDS.				
kV= 15	Angle= 40	B.C.= 1.			
OXIDE	WEIGHT %	+/- 2 SIGMA	11 OXYGENS	K RATIO	MDL
Na2O	0	0	0	0	0.082
MgO	4.14	0.06	0.5	0.0139	0.058
Al2O3	3.18	0.04	0.3	0.011	0.06
SiO2	49.46	0.24	3.98	0.1765	0.144
P2O5	0	0	0	0	0.117
SO3	0	0	0	0	0.09
Cl	0	0	0	0.0001	0.056
K2O	7.84	0.08	0.8	0.0575	0.034
CaO	0.24	0	0.02	0.0016	0.088
TiO2	0	0	0	0	0.193
V2O3	0	0	0	0	0.147
Cr2O3	0	0	0	0.0002	0.211
MnO	0	0	0	0.0002	0.181
FeO	24.76	0.27	1.67	0.1627	0.087
NiO	0	0	0	0	0.253
TOTAL	89.62		7.27		

ID = P421 D grain1 spot1					
Livetime =	Bulk STDS.				
kV= 15	Angle= 40	B.C.= 1.			
OXIDE	WEIGHT %	+/- 2 SIGMA	11 OXYGENS	K RATIO	MDL
Na2O	0	0	0	0	0.082
MgO	4.1	0.06	0.5	0.0137	0.058
Al2O3	2.4	0.03	0.23	0.0082	0.06
SiO2	48.45	0.24	3.99	0.1729	0.144
P2O5	0	0	0	0	0.117
SO3	0	0	0	0	0.09
Cl	0	0	0	0.0002	0.056
K2O	7.72	0.08	0.81	0.0567	0.034
CaO	0.13	0	0.01	0.0008	0.088
TiO2	0	0	0	0.0001	0.193
V2O3	0	0	0	0	0.147
Cr2O3	0	0	0	0.0002	0.211
MnO	0	0	0	0	0.181
FeO	25.56	0.28	1.76	0.1681	0.087
NiO	0	0	0	0.0004	0.253
TOTAL	88.35		7.3		

ID = P421 C grain1 spot1					
Livetime =	Bulk STDS.				
kV= 15	Angle= 40	B.C.= 1.			
OXIDE	WEIGHT %	+/- 2 SIGMA	11 OXYGENS	K RATIO	MDL
Na2O	0	0	0	0	0.082
MgO	4.57	0.07	0.55	0.0153	0.058
Al2O3	2.44	0.03	0.23	0.0084	0.06
SiO2	49.14	0.24	3.98	0.1754	0.144
P2O5	0	0	0	0	0.117
SO3	0	0	0	0	0.09
Cl	0	0	0	0.0002	0.056
K2O	8.03	0.08	0.83	0.0589	0.034
CaO	0.16	0	0.01	0.001	0.088
TiO2	0	0	0	0	0.193
V2O3	0	0	0	0	0.147
Cr2O3	0	0	0	0	0.211
MnO	0	0	0	0.0001	0.181
FeO	25.22	0.27	1.71	0.1658	0.087
NiO	0	0	0	0	0.253
TOTAL	89.56		7.32		

Table 6 cont. Microprobe data for P421: glauconite.

ID = P421 E grain1 spot1					
Livetime =	Bulk STDS.				
kV= 15	Angle= 40	B.C.= 1.			
OXIDE	WEIGHT %	+/- 2 SIGMA	11 OXYGENS	K RATIO	MDL
Na2O	0	0	0	0	0.082
MgO	4.52	0.07	0.55	0.0152	0.058
Al2O3	2.76	0.04	0.26	0.0095	0.06
SiO2	48.78	0.24	3.97	0.1739	0.144
P2O5	0	0	0	0	0.117
SO3	0	0	0	0	0.09
Cl	0	0	0	0	0.056
K2O	7.91	0.08	0.82	0.058	0.034
CaO	0.09	0	0.01	0.0006	0.088
TiO2	0	0	0	0	0.193
V2O3	0	0	0	0	0.147
Cr2O3	0	0	0	0	0.211
MnO	0	0	0	0	0.181
FeO	25	0.27	1.7	0.1643	0.087
NiO	0	0	0	0	0.253
TOTAL	89.06		7.31		

ID = P421 E grain1 spot2					
Livetime =	Bulk STDS.				
kV= 15	Angle= 40	B.C.= 1.			
OXIDE	WEIGHT %	+/- 2 SIGMA	11 OXYGENS	K RATIO	MDL
Na2O	0	0	0	0	0.082
MgO	4.51	0.07	0.53	0.0154	0.058
Al2O3	5.69	0.07	0.53	0.0198	0.06
SiO2	49.54	0.24	3.9	0.1756	0.144
P2O5	0	0	0	0	0.117
SO3	0	0	0	0	0.09
Cl	0	0	0	0.0002	0.056
K2O	7.06	0.07	0.71	0.0515	0.034
CaO	0.37	0.01	0.03	0.0024	0.088
TiO2	0.25	0.01	0.01	0.0013	0.193
V2O3	0	0	0	0	0.147
Cr2O3	0	0	0	0.0004	0.211
MnO	0	0	0	0	0.181
FeO	22.39	0.26	1.47	0.1468	0.087
NiO	0	0	0	0.0013	0.253
TOTAL	89.81		7.18		

Table 7. Microprobe data for P430: glauconite.

ID = P430 A grain1 spot1					
Livetime = Bulk STDS.					
kV= 15	Angle= 40	B.C.= 1.			
OXIDE	WEIGHT %	+/- 2 SIGMA	11 OXYGENS	K RATIO	MDL
Na2O	0.31	0.01	0.05	0.0009	0.082
MgO	3.82	0.06	0.46	0.0131	0.058
Al2O3	2.73	0.04	0.26	0.0096	0.06
SiO2	36.47	0.2	2.94	0.1323	0.144
P2O5	9.2	0.09	0.63	0.0289	0.117
SO3	0.4	0.01	0.02	0.0013	0.09
Cl	0	0	0	0.0002	0.056
K2O	5.57	0.06	0.57	0.0414	0.034
CaO	13.57	0.12	1.17	0.0883	0.088
TiO2	0	0	0	0	0.193
V2O3	0	0	0	0.0002	0.147
Cr2O3	0	0	0	0	0.211
MnO	0	0	0	0	0.181
FeO	17.17	0.22	1.16	0.1118	0.087
NiO	0	0	0	0.0005	0.253
TOTAL	89.24		7.25		
ID = P430 A grain1 spot2					
Livetime = Bulk STDS.					
kV= 15	Angle= 40	B.C.= 1.			
OXIDE	WEIGHT %	+/- 2 SIGMA	11 OXYGENS	K RATIO	MDL
Na2O	0.34	0.01	0.05	0.001	0.082
MgO	3.94	0.06	0.47	0.0136	0.058
Al2O3	3.83	0.05	0.36	0.0135	0.06
SiO2	37.09	0.2	2.96	0.1341	0.144
P2O5	8.83	0.09	0.6	0.0276	0.117
SO3	0.37	0.01	0.02	0.0012	0.09
Cl	0	0	0	0.0002	0.056
K2O	5.08	0.06	0.52	0.0377	0.034
CaO	13.4	0.12	1.15	0.0871	0.088
TiO2	0	0	0	0.0003	0.193
V2O3	0	0	0	0	0.147
Cr2O3	0	0	0	0.0003	0.211
MnO	0	0	0	0	0.181
FeO	16.25	0.22	1.08	0.1057	0.087
NiO	0	0	0	0.0005	0.253
TOTAL	89.11		7.21		
ID = P430 B grain1 spot1					
Livetime = Bulk STDS.					
kV= 15	Angle= 40	B.C.= 1.			
OXIDE	WEIGHT %	+/- 2 SIGMA	11 OXYGENS	K RATIO	MDL
Na2O	0	0	0	0	0.082
MgO	4.59	0.07	0.56	0.0154	0.058
Al2O3	2.99	0.04	0.29	0.0103	0.06
SiO2	48.24	0.24	3.93	0.1718	0.144
P2O5	0.3	0.01	0.02	0.0009	0.117
SO3	0	0	0	0.0001	0.09
Cl	0	0	0	0	0.056
K2O	7	0.07	0.73	0.0513	0.034
CaO	0.81	0.01	0.07	0.0053	0.088
TiO2	0	0	0	0	0.193
V2O3	0	0	0	0	0.147
Cr2O3	0	0	0	0.0003	0.211
MnO	0	0	0	0	0.181
FeO	24.43	0.27	1.66	0.1604	0.087
NiO	0	0	0	0	0.253
TOTAL	88.36		7.26		

Microprobe images and data

Table 7 cont. Microprobe data for P430: glauconite.

ID = P430 C grain1 spot1					
Livetime =	Bulk STDS.				
kV= 15	Angle= 40	B.C.= 1.			
OXIDE	WEIGHT %	+/- 2 SIGMA	11 OXYGENS	K RATIO	MDL
Na2O	0	0	0	0	0.082
MgO	5.68	0.08	0.66	0.0196	0.058
Al2O3	6.41	0.07	0.59	0.0223	0.06
SiO2	49.05	0.24	3.82	0.1732	0.144
P2O5	0	0	0	0	0.117
SO3	0	0	0	0	0.09
Cl	0	0	0	0	0.056
K2O	7.79	0.08	0.77	0.0568	0.034
CaO	0.23	0	0.02	0.0015	0.088
TiO2	0	0	0	0.0002	0.193
V2O3	0	0	0	0	0.147
Cr2O3	0	0	0	0	0.211
MnO	0	0	0	0.0004	0.181
FeO	21.58	0.25	1.41	0.1412	0.087
NiO	0	0	0	0	0.253
TOTAL	90.74		7.27		
ID = P430 D grain1 spot1					
Livetime =	Bulk STDS.				
kV= 15	Angle= 40	B.C.= 1.			
OXIDE	WEIGHT %	+/- 2 SIGMA	11 OXYGENS	K RATIO	MDL
Na2O	0	0	0	0	0.082
MgO	4.48	0.07	0.54	0.0151	0.058
Al2O3	3.35	0.04	0.32	0.0115	0.06
SiO2	49.14	0.24	3.95	0.175	0.144
P2O5	0	0	0	0	0.117
SO3	0	0	0	0	0.09
Cl	0	0	0	0.0001	0.056
K2O	7.9	0.08	0.81	0.0579	0.034
CaO	0.27	0.01	0.02	0.0018	0.088
TiO2	0	0	0	0	0.193
V2O3	0	0	0	0	0.147
Cr2O3	0	0	0	0	0.211
MnO	0	0	0	0	0.181
FeO	24.83	0.27	1.67	0.1631	0.087
NiO	0	0	0	0.0001	0.253
TOTAL	89.98		7.3		
ID = P430 E grain1 spot1					
Livetime =	Bulk STDS.				
kV= 15	Angle= 40	B.C.= 1.			
OXIDE	WEIGHT %	+/- 2 SIGMA	11 OXYGENS	K RATIO	MDL
Na2O	0	0	0	0	0.082
MgO	4.79	0.07	0.56	0.0163	0.058
Al2O3	4.74	0.06	0.44	0.0164	0.06
SiO2	49.75	0.24	3.93	0.1768	0.144
P2O5	0	0	0	0	0.117
SO3	0	0	0	0	0.09
Cl	0	0	0	0.0001	0.056
K2O	7.39	0.08	0.74	0.054	0.034
CaO	0.35	0.01	0.03	0.0023	0.088
TiO2	0	0	0	0.0004	0.193
V2O3	0	0	0	0.0003	0.147
Cr2O3	0	0	0	0.0003	0.211
MnO	0	0	0	0	0.181
FeO	22.96	0.26	1.52	0.1505	0.087
NiO	0	0	0	0.0002	0.253
TOTAL	89.97		7.22		

Table 8. Microprobe data for P427: pellet.

ID = P427 A grain1 spot1					
Livetime = Bulk STDS.					
kV= 15	Angle= 40	B.C.= 1.			
OXIDE	WEIGHT %	+/- 2 SIGMA	11 OXYGENS	K RATIO	MDL
Na2O	0.66	0.02	0.16	0.002	0.082
MgO	1.89	0.04	0.35	0.0065	0.058
Al2O3	9.2	0.1	1.35	0.0325	0.06
SiO2	22.21	0.15	2.77	0.0784	0.144
P2O5	0	0	0	0.0001	0.117
SO3	0.32	0.01	0.03	0.0011	0.09
Cl	0.11	0	0.02	0.0009	0.056
K2O	0.76	0.01	0.12	0.0057	0.034
CaO	12.67	0.12	1.69	0.0839	0.088
TiO2	3.49	0.07	0.33	0.0174	0.193
V2O3	0	0	0	0	0.147
Cr2O3	0	0	0	0.0001	0.211
MnO	0	0	0	0.0007	0.181
FeO	4.84	0.11	0.5	0.031	0.087
NiO	0	0	0	0	0.253
TOTAL	56.16		7.33		
ID = P427 A grain2 spot1					
Livetime = Bulk STDS.					
kV= 15	Angle= 40	B.C.= 1.			
OXIDE	WEIGHT %	+/- 2 SIGMA	11 OXYGENS	K RATIO	MDL
Na2O	0.2	0.01	0.07	0.0006	0.082
MgO	1.25	0.03	0.32	0.0042	0.058
Al2O3	6.33	0.08	1.27	0.0222	0.06
SiO2	13.77	0.12	2.34	0.0491	0.144
P2O5	0	0	0	0.0002	0.117
SO3	0.17	0	0.02	0.0006	0.09
Cl	0.12	0	0.04	0.0011	0.056
K2O	0.55	0.01	0.12	0.0043	0.034
CaO	19.15	0.14	3.49	0.1274	0.088
TiO2	0.3	0.01	0.04	0.0015	0.193
V2O3	0	0	0	0	0.147
Cr2O3	0	0	0	0	0.211
MnO	0	0	0	0	0.181
FeO	2.63	0.07	0.37	0.0168	0.087
NiO	0	0	0	0.0004	0.253
TOTAL	44.48		8.07		
ID = P427 A grain3 spot1					
Livetime = Bulk STDS.					
kV= 15	Angle= 40	B.C.= 1.			
OXIDE	WEIGHT %	+/- 2 SIGMA	11 OXYGENS	K RATIO	MDL
Na2O	0.31	0.01	0.09	0.0009	0.082
MgO	1.21	0.02	0.27	0.0041	0.058
Al2O3	8.27	0.09	1.45	0.0292	0.06
SiO2	16.56	0.13	2.47	0.0588	0.144
P2O5	0.12	0	0.02	0.0004	0.117
SO3	0.3	0.01	0.03	0.001	0.09
Cl	0.07	0	0.02	0.0006	0.056
K2O	0.68	0.01	0.13	0.0052	0.034
CaO	17.03	0.14	2.72	0.113	0.088
TiO2	1.34	0.03	0.15	0.0066	0.193
V2O3	0	0	0	0	0.147
Cr2O3	0	0	0	0	0.211
MnO	0	0	0	0	0.181
FeO	2.74	0.07	0.34	0.0175	0.087
NiO	0	0	0	0	0.253
TOTAL	48.64		7.69		

Microprobe images and data

Table 8 cont. Microprobe data for P427: pellet.

ID = P427 B grain1 spot1					
Livetime =	Bulk STDS.				
kV= 15	Angle= 40	B.C.= 1.			
OXIDE	WEIGHT %	+/- 2 SIGMA	11 OXYGENS	K RATIO	MDL
Na2O	0.26	0.01	0.07	0.0008	0.082
MgO	1.94	0.04	0.39	0.0067	0.058
Al2O3	9.77	0.1	1.55	0.0347	0.06
SiO2	21.96	0.15	2.96	0.0775	0.144
P2O5	0.12	0	0.01	0.0004	0.117
SO3	0.29	0.01	0.03	0.001	0.09
Cl	0.07	0	0.02	0.0006	0.056
K2O	0.78	0.02	0.13	0.0058	0.034
CaO	11.56	0.11	1.67	0.0761	0.088
TiO2	0.42	0.01	0.04	0.0021	0.193
V2O3	0	0	0	0.0003	0.147
Cr2O3	0	0	0	0.0003	0.211
MnO	0	0	0	0.0004	0.181
FeO	3.59	0.09	0.4	0.023	0.087
NiO	0	0	0	0	0.253
TOTAL	50.75		7.26		
ID = P427 B grain1 spot2					
Livetime =	Bulk STDS.				
kV= 15	Angle= 40	B.C.= 1.			
OXIDE	WEIGHT %	+/- 2 SIGMA	11 OXYGENS	K RATIO	MDL
Na2O	0.1	0	0.03	0.0003	0.082
MgO	1.52	0.03	0.32	0.0052	0.058
Al2O3	8.49	0.09	1.4	0.0302	0.06
SiO2	21.77	0.15	3.05	0.0774	0.144
P2O5	0	0	0	0.0002	0.117
SO3	0.2	0	0.02	0.0007	0.09
Cl	0.09	0	0.02	0.0008	0.056
K2O	0.69	0.01	0.12	0.0052	0.034
CaO	12.95	0.12	1.94	0.0853	0.088
TiO2	0.26	0.01	0.03	0.0013	0.193
V2O3	0	0	0	0	0.147
Cr2O3	0	0	0	0.0001	0.211
MnO	0	0	0	0	0.181
FeO	2.97	0.08	0.35	0.0189	0.087
NiO	0	0	0	0.0004	0.253
TOTAL	49.05		7.28		
ID = P427 C grain1 spot1					
Livetime =	Bulk STDS.				
kV= 15	Angle= 40	B.C.= 1.			
OXIDE	WEIGHT %	+/- 2 SIGMA	11 OXYGENS	K RATIO	MDL
Na2O	0.51	0.02	0.11	0.0017	0.082
MgO	0.64	0.01	0.11	0.0023	0.058
Al2O3	34.26	0.21	4.53	0.1279	0.06
SiO2	14.17	0.12	1.59	0.0457	0.144
P2O5	0.19	0	0.02	0.0006	0.117
SO3	0.25	0.01	0.02	0.0008	0.09
Cl	0.08	0	0.01	0.0006	0.056
K2O	0.65	0.01	0.09	0.0048	0.034
CaO	4.73	0.07	0.57	0.0308	0.088
TiO2	0	0	0	0.0008	0.193
V2O3	0	0	0	0.0001	0.147
Cr2O3	0	0	0	0	0.211
MnO	0	0	0	0	0.181
FeO	1.52	0.05	0.14	0.0097	0.087
NiO	0	0	0	0	0.253
TOTAL	57		7.19		

Table 9. Microprobe data for P605: pellet.

ID = P605 A grain1 spot1					
Livetime = Bulk STDS.					
kV= 15	Angle= 40	B.C.= 1.			
OXIDE	WEIGHT %	+/- 2 SIGMA	11 OXYGENS	K RATIO	MDL
Na2O	0.18	0.01	0.05	0.0006	0.082
MgO	1.18	0.02	0.26	0.004	0.058
Al2O3	8.17	0.09	1.41	0.0291	0.06
SiO2	21.44	0.15	3.14	0.0763	0.144
P2O5	0	0	0	0.0001	0.117
SO3	0.12	0	0.01	0.0004	0.09
Cl	0.07	0	0.02	0.0006	0.056
K2O	0.56	0.01	0.11	0.0042	0.034
CaO	11.53	0.11	1.81	0.076	0.088
TiO2	0.54	0.02	0.06	0.0027	0.193
V2O3	0	0	0	0	0.147
Cr2O3	0	0	0	0.0002	0.211
MnO	0	0	0	0	0.181
FeO	2.49	0.07	0.31	0.0159	0.087
NiO	0	0	0	0.0002	0.253
TOTAL	46.29		7.17		
ID = P605 B grain1 spot1					
Livetime = Bulk STDS.					
kV= 15	Angle= 40	B.C.= 1.			
OXIDE	WEIGHT %	+/- 2 SIGMA	11 OXYGENS	K RATIO	MDL
Na2O	0.27	0.01	0.06	0.0008	0.082
MgO	1.45	0.03	0.27	0.005	0.058
Al2O3	11.2	0.11	1.63	0.0401	0.06
SiO2	22.62	0.16	2.79	0.0797	0.144
P2O5	0	0	0	0	0.117
SO3	0.13	0	0.01	0.0004	0.09
Cl	0.17	0	0.04	0.0014	0.056
K2O	0.91	0.02	0.14	0.0069	0.034
CaO	15.85	0.13	2.09	0.1044	0.088
TiO2	0.55	0.02	0.05	0.0027	0.193
V2O3	0	0	0	0	0.147
Cr2O3	0	0	0	0.0004	0.211
MnO	0	0	0	0	0.181
FeO	3.72	0.09	0.38	0.0237	0.087
NiO	0	0	0	0.0001	0.253
TOTAL	56.86		7.46		
ID = P605 B grain1 spot2					
Livetime = Bulk STDS.					
kV= 15	Angle= 40	B.C.= 1.			
OXIDE	WEIGHT %	+/- 2 SIGMA	11 OXYGENS	K RATIO	MDL
Na2O	0	0	0	0.0002	0.082
MgO	1.36	0.03	0.23	0.0048	0.058
Al2O3	14.1	0.13	1.86	0.0511	0.06
SiO2	27.57	0.18	3.09	0.0964	0.144
P2O5	0	0	0	0.0002	0.117
SO3	0.13	0	0.01	0.0004	0.09
Cl	0.08	0	0.01	0.0006	0.056
K2O	0.5	0.01	0.07	0.0037	0.034
CaO	9.99	0.1	1.2	0.0654	0.088
TiO2	0.68	0.02	0.06	0.0034	0.193
V2O3	0	0	0	0	0.147
Cr2O3	0	0	0	0.0002	0.211
MnO	0	0	0	0	0.181
FeO	4.35	0.1	0.41	0.0278	0.087
NiO	0	0	0	0	0.253
TOTAL	58.76		6.95		

Microprobe images and data

Table 9 cont. Microprobe data for P605: pellet.

ID = P605 C grain1 spot1					
Livetime =	Bulk STDS.				
kV= 15	Angle= 40	B.C.= 1.			
OXIDE	WEIGHT %	+/- 2 SIGMA	11 OXYGENS	K RATIO	MDL
Na2O	0.23	0.01	0.06	0.0007	0.082
MgO	1.3	0.03	0.26	0.0045	0.058
Al2O3	8.92	0.09	1.4	0.0319	0.06
SiO2	23.49	0.16	3.13	0.0836	0.144
P2O5	0	0	0	0.0002	0.117
SO3	0.17	0	0.02	0.0006	0.09
Cl	0.1	0	0.02	0.0008	0.056
K2O	0.89	0.02	0.15	0.0067	0.034
CaO	12.63	0.12	1.8	0.083	0.088
TiO2	0.48	0.01	0.05	0.0024	0.193
V2O3	0	0	0	0	0.147
Cr2O3	0	0	0	0.0001	0.211
MnO	0	0	0	0	0.181
FeO	2.89	0.08	0.32	0.0185	0.087
NiO	0	0	0	0	0.253
TOTAL	51.12		7.22		

ID = P605 C grain1 spot2					
Livetime =	Bulk STDS.				
kV= 15	Angle= 40	B.C.= 1.			
OXIDE	WEIGHT %	+/- 2 SIGMA	11 OXYGENS	K RATIO	MDL
Na2O	0.4	0.01	0.1	0.0012	0.082
MgO	1.12	0.02	0.21	0.0039	0.058
Al2O3	7.46	0.08	1.1	0.0269	0.06
SiO2	27.33	0.17	3.41	0.0984	0.144
P2O5	0	0	0	0.0002	0.117
SO3	0.2	0	0.02	0.0007	0.09
Cl	0.07	0	0.01	0.0005	0.056
K2O	1.26	0.02	0.2	0.0094	0.034
CaO	13.81	0.12	1.84	0.0905	0.088
TiO2	0.23	0.01	0.02	0.0011	0.193
V2O3	0	0	0	0	0.147
Cr2O3	0	0	0	0.0001	0.211
MnO	0	0	0	0.0003	0.181
FeO	2.36	0.06	0.25	0.015	0.087
NiO	0	0	0	0	0.253
TOTAL	54.24		7.15		

Appendix F: Beach and dune data

Table 1. Petrography of beach samples.

Transect	**A**	**B**	**C**	**D**	**E**	**F**	**G**
Sample number	11	13	30	72	25	8	22
SILICICLASTIC MINERALS							
Quartz %	lA	S	uC	uA	lA	lA	lA
Feldspar %	uA	vA	uA	uA	lA	lA	lA
Plagioclase	uC	uA	lA	uC	uC	lA	lA
Orthoclase	lC	S	R	lC	lC	lC	lC
Biotite/Muscovite %	-	-	-	R	-	R	-
CALCICLASTICS							
Total %	R	R	R	-	R	R	-
GLAUCONITE %	-	R (3)	R (1)	-	R (5)	R (1)	-
ROCK FRAGMENTS %	lC	uC	uC	lC	lC	lC	lA
OPAQUES %	R	-	-	-	-	R	R
HEAVY MINERALS %	R	lC	R	R	R	R	R
Hornblende	R	lC	R	R	R	R	R
Oxyhornblende	R	S	R	R	R	R	R
Blue-green amphibole	-	-	-	-	-	-	R
Actinolite	-	-	-	-	-	-	-
Hypersthene	R	-	-	-	-	-	-
Augite	R	R	R	-	R	-	-
Chlorite	-	-	R	-	R	R	-
OVERALL							
Mean grain size	0.22	0.21	0.29	0.24	0.19	0.20	0.20
Sorting	5	5	4	4	5		
Roundness	4	4	5	3	4		

Percentage range key

R = 0-5% **S** = 5-10%
lC = 10-20% **uC** = 20-30%
lA = 30-40% **uA** = 40-50%
vA = 50+% **uvA** = 75+%

Sorting

1 Very poorly sorted
2 Poorly sorted
3 Moderately sorted
4 Well sorted
5 Very well sorted

Roundness

1 Angular
2 Sub angular
3 Sub rounded
4 Rounded
5 Well rounded

Table 2. Petrography of dune samples.

Transect	**A**	**B**	**C**	**D**	**E**	**F**	**G**
Sample number	N6	N3	N7	N/S	N17	N19	N/S
SILICICLASTIC MINERALS							
Quartz %	lC	uC	lC	N/S	lC	lC	N/S
Feldspar %	uA	lA	uA	N/S	lA	uA	N/S
Plagioclase	uC	uC	lA		uC	uC	
Orthoclase	lC	lC	S		lC	lC	
Biotite/Muscovite %	-	-	-	N/S	-	-	N/S
CALCICLASTICS							
Total %	-	-	-	N/S	-	R	N/S
GLAUCONITE %	R (4)	-	-	N/S	-	R (2)	N/S
ROCK FRAGMENTS %	uC	uC	S	N/S	lC	uC	N/S
OPAQUES %	-	R	R	N/S	R	-	N/S
HEAVY MINERALS %	R	lC	R	N/S	R	R	N/S
Hornblende	R	S	R		R	R	
Oxyhornblende	-	R	R		R	R	
Blue-green amphibole	-	-	-		-	-	
Actinolite	-	R	-		R	-	
Hypersthene	-	R	-		-	-	
Augite	R	R	R		R	-	
Chlorite	-	-	-		-	-	
Titanite	-	-	R		-	-	
OVERALL							
Mean grain size	0.18	0.20	0.23		0.19	0.18	
Sorting	5	4	4		5	5	
Roundness	4	3	4		3	4	

Percentage range key

R = 0-5% **S** = 5-10%
lC = 10-20% **uC** = 20-30%
lA = 30-40% **uA** = 40-50%
vA = 50+% **uvA** = 75+%

N/S = unable to sample

Sorting

1 Very poorly sorted
2 Poorly sorted
3 Moderately sorted
4 Well sorted
5 Very well sorted

Roundness

1 Angular
2 Sub angular
3 Sub rounded
4 Rounded
5 Well rounded